PhD-FSTC-2015-53
The Faculty of Sciences, Technology and Communication

# DISSERTATION

Defense held on 13/11/2015 in Luxembourg

to obtain the degree of

## DOCTEUR DE L'UNIVERSITÉ DU LUXEMBOURG

## EN SCIENCES DE L'INGENIEUR

by

Sebastian NELLINGER
Born on 26 August 1986 in Trier, (Germany)

# ON THE BEHAVIOUR OF SHEAR STUD CONNECTIONS IN COMPOSITE BEAMS WITH DEEP DECKING

## Dissertation defense committee

Dr.-Ing. Christoph ODENBREIT, dissertation supervisor
*Professor, Université du Luxembourg*

Dr.-Ing. Renata OBIALA
*Research associate, Université du Luxembourg*

Dr.-Ing. Markus SCHÄFER, Chairman
*Senior lecturer, Université du Luxembourg*

Dr.-Ing. Henning LUNGERSHAUSEN
*Professor, Hochschule Trier*

Dr.-Ing. Robert Mark LAWSON, Vice Chairman
*Professor, University of Surrey*

# Acknowledgements

The research leading to these results was part of the common research project 'Development of Improved Shear Connection rules in Composite beams (DISCCO)' of The Steel Construction Institute, University of Stuttgart, University of Luxembourg, University of Bradford and ArcelorMittal and has received funding from European Community's Research Fund for Coal and Steel (RFCS) under grant agreement no [RFCS-CT-2012-00030].

# Preface

This thesis was realised during my time as a research assistant at the ArcelorMittal Chair of Steel and Façade Engineering at the University of Luxembourg.

I would like to express my profound gratitude to my supervisor Prof. Dr.-Ing. Christoph Odenbreit, who offered me the opportunity to realize this thesis. His expertise in steel-concrete composite construction and his constructive criticism kept me pushing to successfully finish this thesis. Moreover, I thank him for the pleasant working environment and his open ear for personal concerns.

I want to express my sincere thanks to Prof. Dr.-Ing. Henning Lungershausen, my former Professor in steel and steel-concrete composite structures at Trier University of Applied Sciences and member of my Supervision committee (CET) and the dissertation defence committee. He investigated the very same research topic already in the 1980s. His expertise and the constructive discussions were a continuous source of inspiration and motivation.

My thanks are also due to Mark Lawson, Professor at the University of Surrey, member of The Steel Construction Institute and Deputy Chairman of my dissertation defence committee. He did a great job as the coordinator of DISCCO and the exchange of ideas on different mechanical design concepts for the shear stud resistance allowed me to see things from a different perspective. This was a major motivation during the development of my equations and pushed me to keep things as simple as I could.

Moreover, I express my thanks to Oliver Hechler, former Senior researcher at the ArcelorMittal Chair of Steel and Façade Engineering and former member of my supervision committee. His constructive contributions in discussions and meetings of the supervision committee were always a motivation. In addition, I thank him for his support and advise during the preparation and conduction of my very first laboratory tests, when this were uncharted waters to me.

In addition, I would like to express my thanks to Renata Obiala, Senior researcher at the ArcelorMittal Chair of Steel and Façade Engineering and member of my supervision committee and the dissertation defence committee. She was involved in DISCCO from early on, at first for ArcelorMittal and then for the University of Luxembourg. Her contributions always ensured that the research and all its scientific conclusions had the same weight as industrial interests.

I am deeply grateful to Dr.-Ing. Markus Schäfer, Senior lecturer at the University of Luxembourg, for his participation as Chairman in my dissertation defence committee.

The experimental part of this thesis would not have been possible without the marvellous support team in the laboratory of the University of Luxembourg. I am deeply grateful to the technicians Ed Weyer, Logan Freitas, Claude Collé and Vicente Adonis Reis for their tireless commitment. A special thanks is due to Logan Freitas for his extraordinary contribution to the assembly of the push-out tests and always being in good spirits. In addition, I would like to express my sincere thanks to engineers Marc Seil, Gilbert Klein and Ralph Reiter for their great support all around the matter of measurements.

I thank all my colleagues at the University of Luxembourg who accompanied me during my time there. Special thanks are to my colleagues Mike Tibolt, Vincent Dias, Yves Staudt, Job Duarte and Maciej Chrzanowski for the pleasant working spirit and their willingness to discuss

and help.

I express my gratitude to the whole staff of the University of Luxembourg for their administrative support, especially to Simone Drees.

I would like to thank Antoine Bielous and Luc Schenten for their contribution in the preparation and conduction of a large part of the experimental work, which was part of their Bachelors Thesis.

My profound gratitude is due to everyone who worked on DISCCO, especially Prof. Ulrike Kuhlmann, Prof. Dennis Lam, Florian Eggert, François Hanus and Eleftherios Aggelopoulos. It has been a privilege to work with them.

In the end, I thank my family for their commendable support and patience.

Luxembourg, in November 2015 Sebastian Nellinger

# Abstract

Steel-concrete composite construction has many advantages for the construction of multi-storey buildings. The use of composite beams acting compositely with the floor slab achieves longer spans and reduces the weight of the beams. The weight reduction can be further improved by replacing the solid concrete slab with a steel-concrete composite slab using steel decking.

However, using composite slabs reduces the shear forces that are transferred between the slab and the beam. This is because the number of studs in the span is limited by the deck geometry. In addition, the load-bearing behaviour of studs in the ribs of composite slabs is different to studs in solid slabs and shows typically a reduced resistance per stud.

Currently, [DIN EN 1994-1-1, 2010] applies an empirical reduction factor to the resistance of studs in solid slabs to analyse the resistance of studs in the ribs of composite slabs. A comparison to push-out test results shows that this formulae results in an unsatisfactory correlation. Furthermore, the reduction factor is unsafe in many cases with modern decking. The latest empirical reduction factors in [Konrad, 2011] are currently discussed as alternative to the rules of [DIN EN 1994-1-1, 2010]. They show a significantly improved correlation to test results and an increased field of application. A significantly higher correlation to test results is obtained with the mechanical model by [Lungershausen, 1988]. Because of the restrictive field of application and missing parameters, like the concrete strength, it is not discussed as replacement for the reduction factors.

A newly conducted series of push-out tests with modern deep steel decking shows the insufficiency of the presented analysis methods of the stud shear resistance, as the predictions were in general non-conservative. Furthermore, depending on the geometry of the shear connection, a new failure mode was observed: Rib pry-out failure. Investigation on concentric and eccentric transverse loading of push-out specimens, to consider the loading conditions of a real slab, show in general beneficial influences on the load-slip behaviour.

Based on the behaviour of the studs in push-out tests, equations for the shear connector resistance based on the failure modes are developed. A combined bending failure of the shear stud and the concrete rib is assumed. The observed failure modes in the tests are considered by different yield-lines of the shear stud. The shear resistance of the pure stud gives the upper bound for the shear connector resistance. The new equations show a good correlation to test results and are safe for modern types of steel decking. In comparison to [DIN EN 1994-1-1, 2010], the field of application is extended by the stud position, as in [Konrad, 2011], and deeper decking, as in [Lungershausen, 1988].

The analysis of the bending resistance of two accompanying beam tests confirms the accuracy of the new shear stud resistance. The beam tests have very low degrees of shear connection. The end-slip at ultimate load exceeds the limiting slip of 6mm, but at 95% of ultimate load the limiting slip is satisfied.

A numerical model for composite beams is verified against the test results. The model considers the shear studs as non-linear springs. A simplified load-displacement curve is presented and verified against real load-slip curves.

**Keywords:** Shear stud, deep decking, failure modes, mechanical model, transverse loading

# Contents

# 1 Introduction

Composite construction has many advantages in the construction of modern high rise and multi storey buildings. Considering especially the buildings slabs, it combines the advantages of skeletal steel structures with areal concrete structures.

Concrete has high strengths in compression, but it is weak in tension and so it must be reinforced. Concrete construction can be utilized in frameworks as well as flor slabs. The use of pre-cast elements allows a certain degree of prefabrication, but generally in-situ concrete is used. Because of this, concrete hardening has to be considered and temporary supports may be necessary. In addition, concrete members have larger cross sections than the equivalent steel members.

Steel is a very heavy but strong material. For the load bearing structure of a building, steel is typically used as a framework. Because of steels high strength, filigree members and light weight structures are possible. One of the biggest advantages of steel construction is the high degree of prefabrication. The mostly bolted connections between steel members allow a fast assembly. In addition, the bolted connections allow easy dismounting of the structure ones the buildings life span is exceeded. The dismounted steel members can be either reused in new constructions or recycled to make new products.

Typically, the slabs in a steel building are concrete slabs. In a pure concrete structure, a monolithic connection is achieved between the beam and the slab. This turns the beam into a tee-section and the slab contributes to the load-bearing capacity of the beam. To utilize this effect in an equivalent steel-concrete composite structure, it is necessary to establish a strong and stiff shear connection between steel beam and concrete slab.

Typically, the shear connection is achieved by welding headed stud shear connectors, cold formed steel bars with a pre-fabricated circular head, on top of the beam. The studs are then embedded in the concrete slab. This type of beam is called a composite beam. The concrete slab acts as the compression element and the steel section acts in tension. This is the ideal utilisation of each materials mechanical properties. In addition, the resulting tee-section requires a smaller steel profile than a beam without shear connection.

The beneficial potential of composite structures for the construction progress cannot be fully achieved when the slab consists of in-situ concrete, because temporary supports are still required. This creates dependencies between construction processes, which may slow down the overall progress.

In some cases, temporary supports of the slab can be avoided by using a composite slab, because the steel decking is used as a permanent formwork. In this case, a trapezoidal steel decking is placed on top of the beam and the concrete is cast on top of the steel sheet. The steel decking replaces the formwork during construction stages. If the type of decking and the spacing of the beams are chosen properly, the steel deck can support the concrete weight and working loads without any temporary supports. This makes construction progress less dependent on concrete hardening and may significantly speed up the overall progress. In addition, the decking replaces some or all of the bottom reinforcement in the slab, if it is not required for fire design. In addition, concrete consumption and structural weight are reduced, because of the trapezoidal shape of the steel decking.

However, the use of composite decks leads to an interrupted shear interface and the studs can only be welded in the deck ribs. In addition, the deck shape prevents the direct transfer of the shear force from the bottom of the stud into the compressed part of the concrete slab. This leads to a reduced shear resistance compared to shear connectors in solid slabs. In [DIN EN 1994-1-1, 2010] the reduction of the shear force is considered by the empirical reduction factor $k_t$. It considers the geometry of the stud and the steel decking. Because the factor $k_t$ is an empirical approach, there are important restrictions for its application. These restrictions are necessary, because the set of samples used for the development and calibration of the reduction factor covered only a certain range of parameters. The geometry of modern composite decks differs strongly from the ones used in the calibration of [DIN EN 1994-1-1, 2010, Roik et al., 1989] and is not sufficiently covered by the factor $k_t$. This is shown as the comparison with 261 tests reported in literature shows non-conservative results.

The reduced shar resistance of the studs in combination with the limited number of studs makes it in some cases impossible to satisfy the rules for the minimum degree of shear connection. The minimum degree of shear connection restricts the slip in the composite beam to a limiting value of 6 mm, which was used in the shear connection rules in [DIN EN 1994-1-1, 2010]. In combination with the required displacement capacity of the shear studs, the minimum degree of shear connection prevents a zip-like failure of the shear interface. However, the assumed limiting slip originally was obtained for solid slabs in propped construction. The current rules are too restrictive for un-propped construction or composite slabs, because the shear connectors typically reach a significantly larger slip.

To improve the rules of [DIN EN 1994-1-1, 2010], it is necessary to predict the shear connectors resistance more accurately than the factor $k_t$ does. A series of push-out tests was conducted to investigate the load-slip behaviour and failure modes of headed stud shear connectors. Because the standard push-out test according to [DIN EN 1994-1-1, 2010] is conservative compared to the load-slip behaviour of studs in beam tests, an improved test set-up is investigated. The improvement focuses on the consideration of transverse loading applied to the shear interface.

The results of the push-out tests are the base for a newly developed formulae of the shear connector resistance. The formulae is based on the observed failure modes and simple structural analysis. This leads to a significantly increased field of application and accuracy of the new formulae.

The predicted stud resistances represent the first maximum or failure load observed in a push-out test. In a real beam, there is a certain variability of the force per stud, because of the distributed slip along the span. The influence of the distributed slip on the shear force was assessed by composite beam tests and numerical analysis. Two composite beam tests with low degrees of shear connection were conducted. The tests showed that the plastic bending resistance could be reached without significantly exceeding the limiting slip of 6 mm.

The test results were also used to verify the FE-Model used in SOFiSTiK. With this model a parametric study was conducted to investigate the influence of the distribution of slip. It was found that the concrete compression force was about 15% smaller than the calculated value, which was the product of the stud shear resistance and number of studs. Comparing the results of beam tests with point loading and analytical results with distributed loading, it was concluded that the reduction is dependent on friction due to the loading of the beam as well as on the sensitivity of the shear connectors for transverse loading. Furthermore, it is shown that simplified load-slip curves could be used for parametric studies and the design of composite beams.

# 2 State of the art

## 2.1 General

To achieve composite action between steel beam and concrete slab, a reliable form of shear connection is needed. Typically, the shear connection is established by welding headed studs on top of the beam. The studs are then encased in the concrete. The common model describing the load-bearing behaviour of headed shear studs was given in [Lungershausen, 1988] and is presented in this section.

### 2.1.1 Load-bearing behaviour of studs in solid slabs

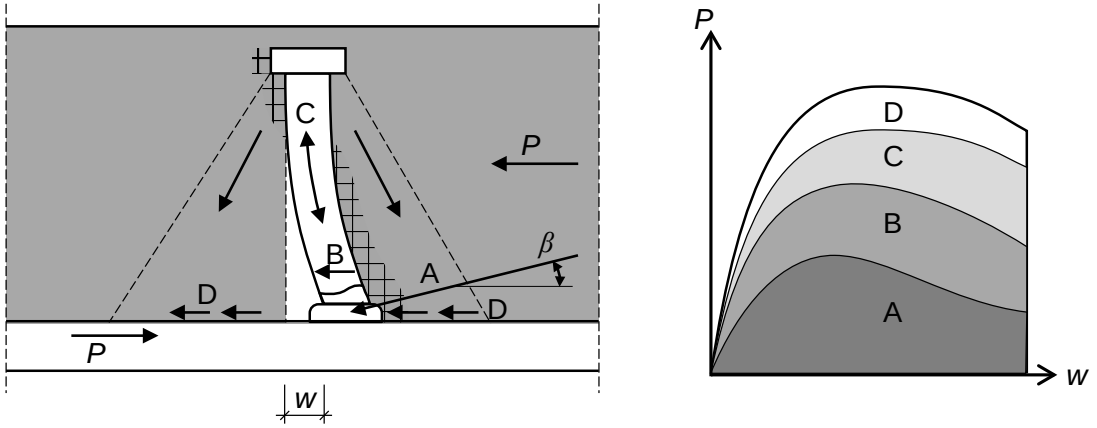


Figure 2.1: Load-bearing behaviour of headed shear studs in solid slabs according to [Lungershausen, 1988].

The load-bearing behaviour of studs in solid slabs (see Figure 2.1) can be described as follows:

A Initially the shear force, $P$, is applied to the concrete girder by a compression strut, $A$, acting on the weld collar at a shallow angle, $\beta$.

B With increasing load, the concrete at the base of the stud crushes. As a consequence, the shear force relocates to the lower stud shank, $B$. This results in plastic bending and shear deformations.

C The fixed support conditions of the head of the stud cause a tension force in the studs shank, $C$. The tension force is in equilibrium with compression forces in the concrete cone below the head of the stud.

D With increasing slip, the tension force in the studs shank increases disproportionately and the load component carried by bending effects decreases. Because the compression forces in the concrete cone increase, friction forces, $D$, between beam and slab are activated. Finally, failure occurs in the stud shank above the weld collar due to tension and shear.

Following parameters influence the resistance of the shear connector:

- The resistance of the stud for tension and shear.
- The concrete compressive strength has influence on the studs support conditions.
- Tension force in the stud shank because of geometric non-linearity.
- Geometry of the weld collar and quality of the weld.
- Friction between steel beam and concrete.

### 2.1.2 Load-bearing behaviour of studs in the ribs of composite slabs

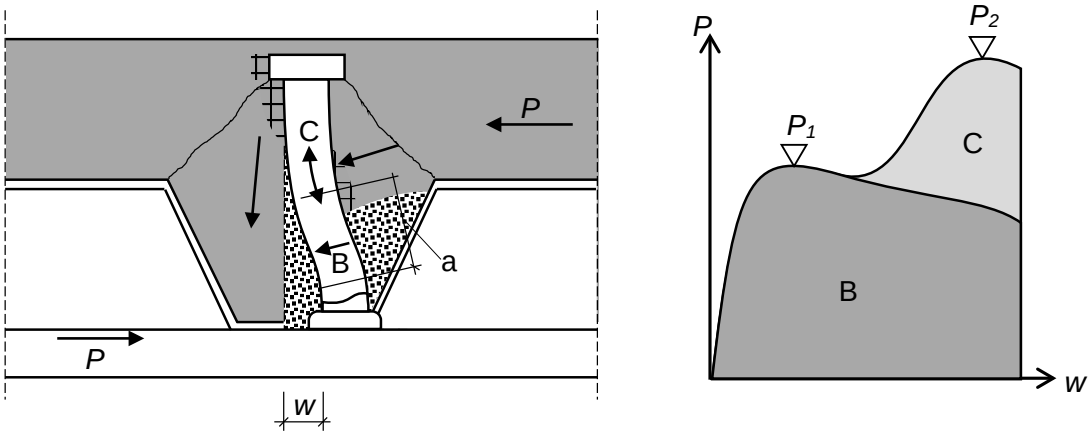


Figure 2.2: Load-bearing behaviour of headed shear studs in the ribs of composite slabs according to [Lungershausen, 1988].

The model describing the load-bearing behaviour of studs in the ribs of composite decks is shown in Figure 2.2. If the shear connector is placed in the rib of a composite slab, the ribs geometry has influence on the transfer of the shear force. In general, two loading stages can be defined:

B When the first peak load, $P_1$, is reached, the concrete in front of the stud fails and two yield hinges develop in the stud shank. The distance $a$ between the hinges is of major influence on the shear force that the stud can resist.

C At large slip, the vertical support conditions of the head of the stud lead to a back-anchorage effect. Thereby, the head of the stud introduces compression forces into the still intact concrete section and tension forces in the stud shank develop. This geometric non-linearity leads to the second peak load, $P_2$. Finally failure either occurs as concrete pull-out or stud rupture.

The following parameters have influence on the shear connectors resistance:

- Resistance of the stud for tension and shear.
- The concrete strength and the geometry of the rib influence the distance $a$ between the yield hinges.
- Tension force in the stud shank because of geometric non-linearity.
- Reinforcement pattern of the concrete girder.
- Embedment depth of the stud.

It can be concluded, that studs in solid slabs and studs in the ribs of composite slabs have different failure mechanisms:

In the case of a solid slab, stud failure occurs due to a combination of tension and shear in the stud shank.

In the case of composite slabs, the first peak load, $P_1$, is reached because of the behaviour of the stud in bending, whereat two yield hinges are develop. Further slip leads to back-anchorage effects of the head of the stud and because of the geometric non-linearity a second peak load, $P_2$, is reached.

### 2.1.3 Test set-ups to investigate the load-slip behaviour

The load-bearing behaviour of headed shear studs can be experimentally investigated by the conduction of push-out tests or full scale composite beam tests. The common approach is the conduction of push-out tests.

There are several reasons, why the push-out test is the preferred method to investigate the load-slip behaviour. The economic benefit of push-out specimen in comparison to a full scale beam is obvious. More important is the easy evaluation of the test results. The sum of the longitudinal shear forces and the slip are directly measured in a push-out specimen. In composite beam tests the shear forces must be back calculated from the applied bending moments or strain measurements. This means, that extensive strain and slip measurements are required, to consider the distributions along the span of the beam. Furthermore, simplified assumptions to consider the material properties and distributions of stresses, strains and slip are necessary to evaluate the load-slip behaviour of studs in composite beam tests.

The push-out test specimen for solid slabs, as proposed in [DIN EN 1994-1-1, 2010], Annex B2, is shown in Figure 2.3. The distribution of the shear forces in a push-out specimen, as assumed in [Roik and Hanswille, 1987], is suitable to reflect the behaviour in real beams with solid concrete slabs.

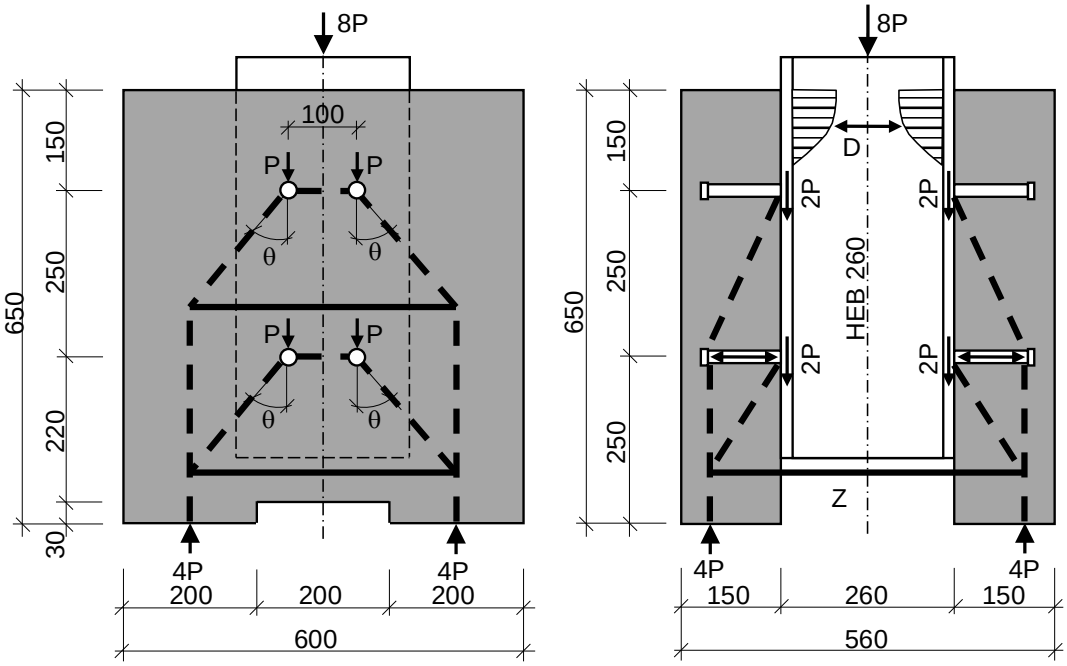


Figure 2.3: Dimensions of the push-out specimen according to [DIN EN 1994-1-1, 2010], Annex B, and force distribution according to [Roik and Hanswille, 1987].

According to [Hicks and Smith, 2014], the obtained load-slip behaviour from push-out tests

can result in up to 30% lower stud shear resistances and lower displacement capacities than in a composite beam test. The load-displacement behaviour of a push-out test is strongly dependent on the boundary conditions. Specimens with sliding bearings may underestimate the real resistance, whereas for example tension ties or any rigid horizontal restraints may lead to an overestimation of the resistance [Döinghaus, 2001, Ernst, 2006, Nellinger et al., 2014].

The differences in the behaviour of the shear connection between push-out test and beam test lead to the development of alternative test set-ups over recent years, like the single push-out test [Döinghaus, 2001] (see Figure 2.4) and the horizontal push-off test [Ernst, 2006, Lam, 1998] (see Figure 2.5).

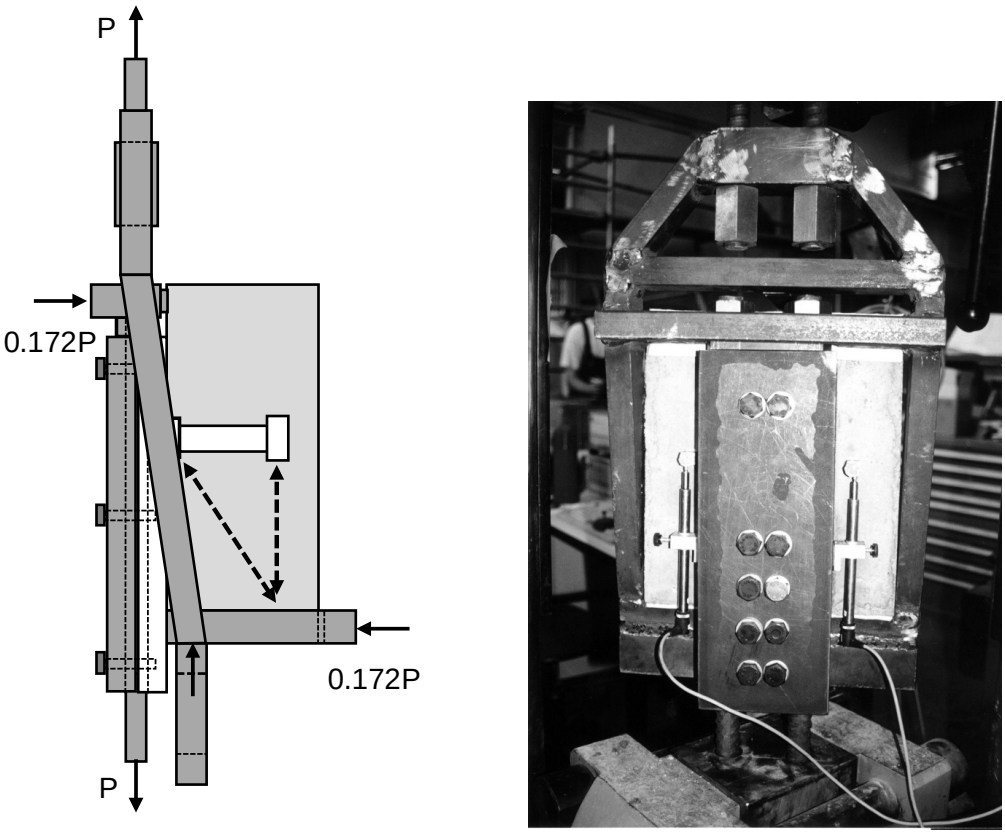


Figure 2.4: Single push-out test by [Döinghaus, 2001].

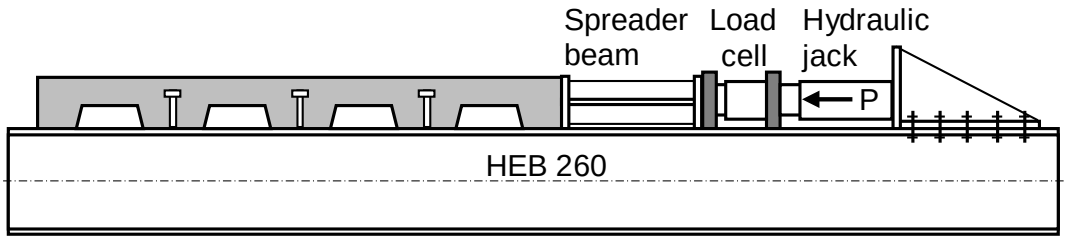


Figure 2.5: Horizontal push-off test by [Lam et al., 2011].

The single push-out test was developed for solid slabs and does not appear to be suitable to investigate cases with composite slabs. The horizontal push-off test represents a slight step towards the consideration of transverse loads, because the slabs self weight is taken into account. [Hicks and Smith, 2014] and [Rambo-Roddenberry, 2002] explicitly applied

transverse loads to typical push-out specimens (see Fig. 2.6). Thereby, concentric loading positions were used. Currently it is under discussion what amount of transverse load has to be applied. According to [Hicks and Smith, 2014], where values of 4 to 16% were investigated , a value of 12% of the longitudinal shear force is suitable to represent the behaviour of the shear studs in accompanying composite beam tests.

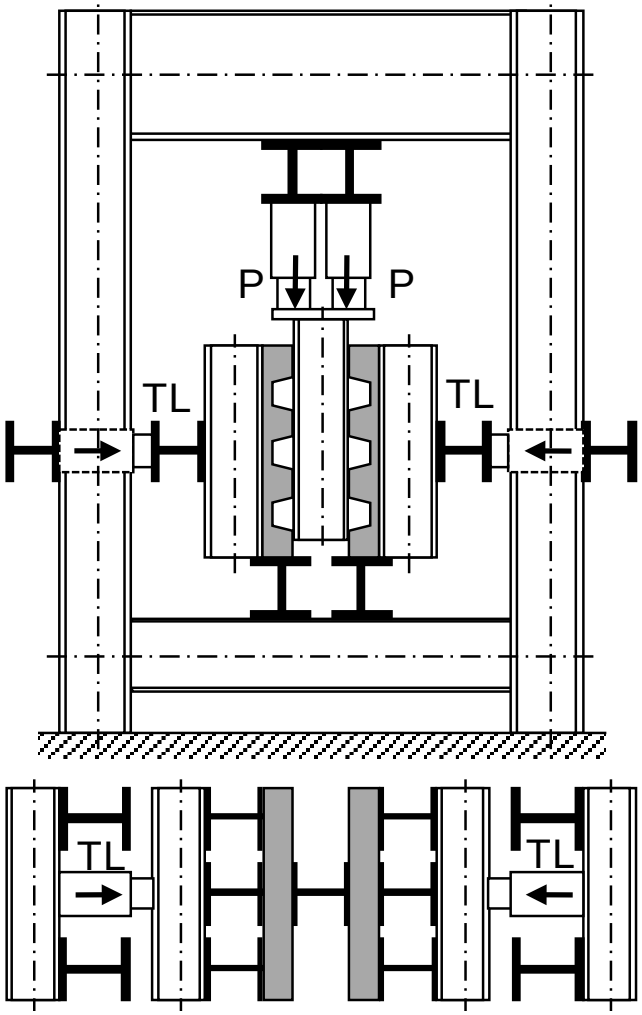


Figure 2.6: Transverse loaded push-out test by [Hicks and Smith, 2014].

## 2.2 Prediction of shear stud resistance

Considerable research has been carried out to investigate the load-bearing behaviour of shear connectors. The investigated parameters were mostly the geometry of the decking and stud as well as the stud position and number of studs per rib.

Many different methods exist to calculate the shear resistance of headed studs. Some of them are based on mechanical models, while others are based on statistical evaluation. Likewise, they focus on different aspects. Some are giving general reduction factors while others give predictions for several failure modes or pay special attention to the shear studs position in the ribs.

In the following sections, some methods to calculate the stud shear resistance are presented. Besides the prediction according to [DIN EN 1994-1-1, 2010, Roik et al., 1989], which is a

statistical approach, the model by [Lungershausen, 1988] was chosen as example for a simple mechanical procedure. The methods by [Rambo-Roddenberry, 2002] and [Konrad, 2011] paid special attention to the stud position. [Rambo-Roddenberry, 2002] represents a purely statistically based method while [Konrad, 2011] is an example for an statistical approach based on the correlation with tests and finite element analysis.

### 2.2.1 Resistance of shear studs according to EN 1994-1-1

[DIN EN 1994-1-1, 2010] suggests to calculate the resistance of shear studs in the ribs of composite slabs by reducing the resistance obtained for a solid slab. According to [Roik et al., 1989]. the mean shear resistance of shear studs in solid slabs is calculated by equations (2.1) and (2.2) in which equation (2.1) is the resistance of the stud shank for the combined tension-shear failure and equation (2.2) is the resistance for concrete crushing at the weld collar.

$$P_{Rm,s} = 1.0 \cdot f_{um} \cdot \pi \cdot d^2/4 \tag{2.1}$$

$$P_{Rm,c} = 0.374 \cdot \alpha \cdot d^2 \cdot \sqrt{f_{cm} \cdot E_{cm}} \tag{2.2}$$

where:

| | |
|---|---|
| $P_{Rm,s}$ | Resistance for steel failure (mean value) |
| $P_{Rm,c}$ | Resistance for concrete failure (mean value) |
| $f_{um}$ | Tensile strength of the stud (mean value) |
| $f_{cm}$ | Concrete compressive strength (mean value) |
| $E_{cm}$ | Young's-Modulus of concrete |
| $d$ | Stud diameter |
| $\alpha$ | for $h_{sc}/d > 4$: $\alpha = 1$ |
| | for $3 \leq h_{sc}/d \leq 4$: $0.2\left(\frac{h_{sc}}{d} + 1\right)$ |
| $h_{sc}$ | Stud height |

The statistically obtained factors 1.00 in equation (2.1) and 0.374 in equation (2.2) where verified by [Roik et al., 1989], [Konrad, 2011]. The evaluation against test results reported in literature (see Appendix A) confirmed the accuracy of the pre-factors, as shown in Figure 2.7. In many cases, the Young's-Modulus of the concrete was not reported. Therefore, it was calculated according to equation (2.3) [DIN 1045-1, 2008]. The resistance for concrete failure then is a function of the stud diameter and concrete strength.

$$E_{cm} = \alpha_i \cdot 9500 \cdot f_{cm}^{1/3} \tag{2.3}$$

where: $\alpha_i = (0.8 + 0.2 f_{cm}/88) \leq 1$

In addition to the verification of the pre-factors, the evaluation showed that equation (2.2) is also valid for concrete strengths higher than currently allowed in [DIN EN 1994-1-1, 2010]. This is shown by the comparison to the results of tests with high strength concrete reported in [Döinghaus, 2001] and [Feldmann et al., 2007].

The characteristic resistance of studs in solid slabs is obtained by equations (2.4) and (2.5). in [DIN EN 1994-1-1, 2010], the partial safety factor for design is 1.25. However, the german national annex requires a safety factor of 1.50 for concrete failure in equation (2.5).

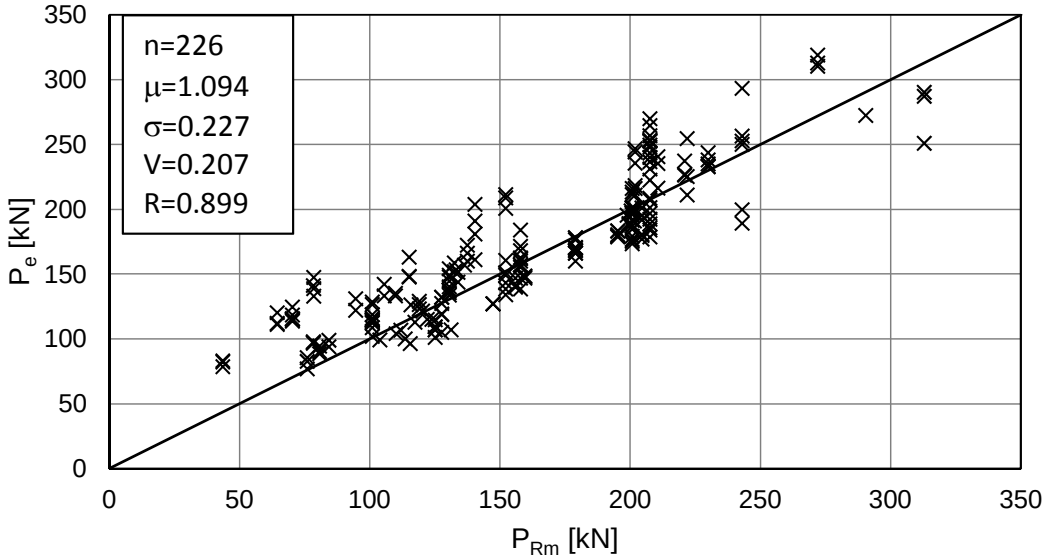


Figure 2.7: Comparison of the shear resistance according to [DIN EN 1994-1-1, 2010, Roik et al., 1989], $P_{Rm}$, with push-out test results for the case of solid slab specimens, $P_e$.

Furthermore, [DIN 18800-5, 1999] used the factor 0.25 instead of 0.29 in equation (2.5). This corresponded to a reduction of the resistance by the factor $\alpha_{cc} = 0.85$ to consider the long-term resistance of concrete, which is not considered in Eurocode 4.

$$P_{Rk,s} = 0.80 \cdot f_{uk} \cdot \pi \cdot d^2/4 \tag{2.4}$$

$$P_{Rk,c} = 0.29 \cdot \alpha \cdot d^2 \cdot \sqrt{f_{ck} \cdot E_{cm}} \tag{2.5}$$

where:

| | | |
|---|---|---|
| $P_{Rk,s}$ | Characteristic resistance for steel failure |
| $P_{Rk,c}$ | Characteristic resistance for concrete failure |
| $f_{uk}$ | Characteristic tensile strength of stud |
| $f_{ck}$ | Characteristic concrete compressive strength |

In the case of a composite slab with the ribs of the decking placed transversely to the beam, [DIN EN 1994-1-1, 2010] suggests to reduce the shear resistance calculated for solid slabs by the factor $k_t$. The reduction factor considers the geometry of the decking and the stud, as shown in equation (2.6). Thereby, $k_t$ is limited by the factor $k_{t,max}$ given in Table 2.1.

$$k_t = \frac{0.7}{\sqrt{n_r}} \cdot \frac{b_m}{h_p} \cdot \left( \frac{h_{sc}}{h_p} - 1 \right) \leq k_{t,max} \tag{2.6}$$

| | | |
|---|---|---|
| where: | $k_t$ | Reduction factor |
| | $k_{t,max}$ | Upper limit for $k_t$ |
| | $n_r$ | Number of studs per rib |
| | $b_m$ | Effective width of the deck rib |
| | $h_p$ | Height of the deck rib |
| | $h_{sc}$ | Height of the stud |

Table 2.1: Maximum reduction factors $k_{t,max}$ according to [DIN EN 1994-1-1, 2010]

| $n_r$ | $t$ [mm] | Through deck welded $d \leq 20$ mm | Welded through punched holes 19 mm $\leq d \leq 22$ mm |
|---|---|---|---|
| 1 | $\leq 1.00$ | 0.85 | 0.75 |
| | $> 1.00$ | 1.00 | 0.75 |
| 2 | $\leq 1.00$ | 0.70 | 0.60 |
| | $> 1.00$ | 0.80 | 0.60 |

$t$: Thickness of the steel decking

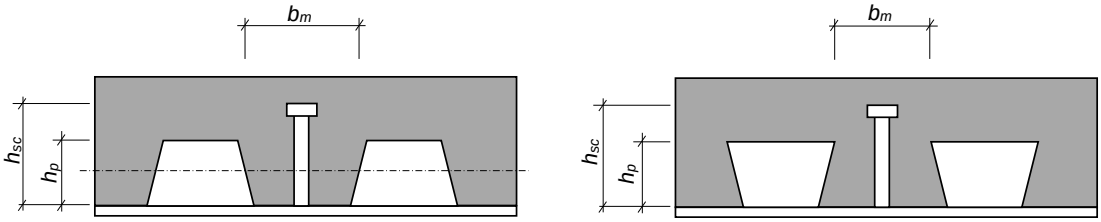


(a) Open deck shapes (b) Re-entrant deck shapes

Figure 2.8: Geometric parameters of the $k_t$-factor according to [DIN EN 1994-1-1, 2010].

In addition, the following restraints for the geometry of the decking, the stud and the stud position have to be considered:

- 19 mm $\leq d \leq$ 22 mm
- $h_p \leq 85$ mm
- $b_m \geq h_p$
- $b_{min} \geq 50$ mm
- $h_{sc} - h_p \geq 2 \cdot d$
- $h_{sc}/d \geq 4$
- $n_r \leq 2$
- studs in mid or staggert position
- $f_{uk} \leq 450$ N/mm$^2$

The comparison with 288 push-out tests with composite slabs (see Appendix B) is shown in Figure 2.9. No attention was paid to the mentioned limitations for the application of the reduction factor $k_t$. The comparison shows that with an average of the ratio $P_e/P_{Rm}$ of $\mu = 0.97$ the reduction factor $k_t$ is slightly non-conservative, but the coefficient of variation of $V = 0.38$ is quit large. The coefficient of correlation of only $R = 0.59$ shows that the formulae is not sufficiently covering all possible test parameters.

Comparing the push-out test results to the characteristic resistance, characteristic material properties are required. They were determined from the reported material properties according to equations (2.7) and (2.8).

$$f_{ck} = f_{cm} - 8 \tag{2.7}$$

$$f_{uk} = f_{um} \cdot (1 - k_\infty \cdot V_{fu}) \leq 450 \text{ N/mm}^2 \tag{2.8}$$

where: $k_\infty = 1.64$ Fractile factor, see [DIN EN 1990, 2002]
$V_{fu} = 0.05$ Variation of tensile strength, see [Roik et al., 1989]

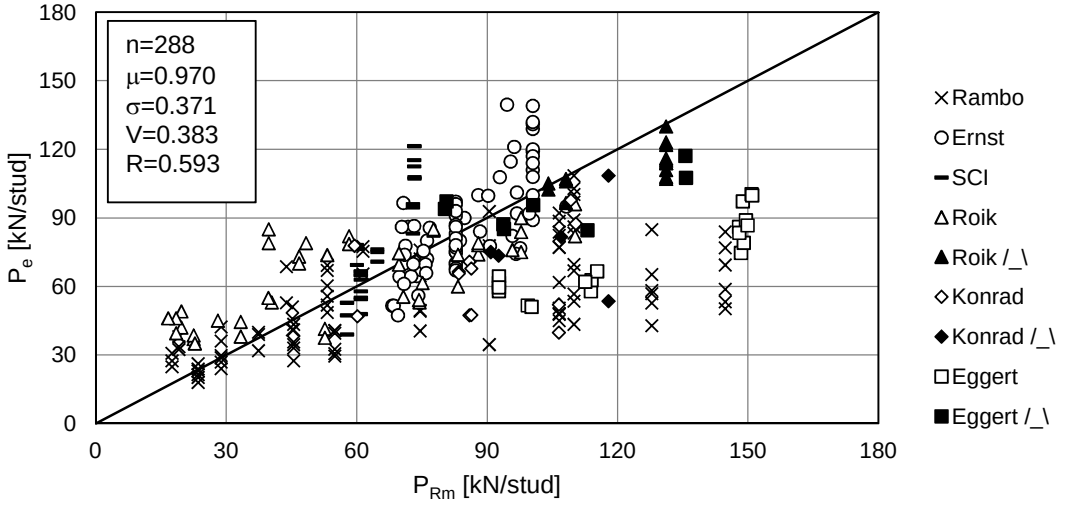


(a) Experimental resistance, $P_e$, vs. average resistance, $P_{Rm}$

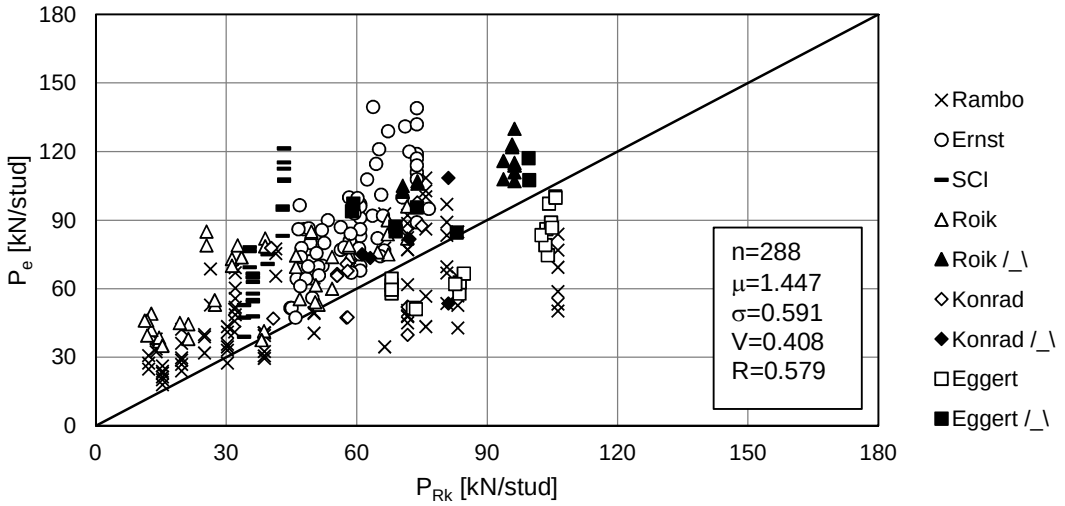


(b) Experimental resistance, $P_e$, vs. characteristic resistance, $P_{Rk}$

Figure 2.9: Comparison of the shear resistance according to [DIN EN 1994-1-1, 2010, Roik et al., 1989] with push-out test results when steel decking was used.

The average of the ratios $P_e/P_{Rk}$ of $\mu = 1.45$ is conservative. However, the coefficient of correlation, $R$, does not show a satisfactory correlation between the test results and the

calculated characteristic resistances. In addition, 55 out of 288 tests – i.e. 19% – have ratios $P_e/P_{Rk}$ of less than 1.0. This means that the calculated characteristic resistances do not satisfy the 5%-fractile as required in [DIN EN 1990, 2002], clause 4.2(1). Because the comparisons for solid slab specimens were satisfactory, the reduction factor $k_t$ must be too undifferentiated to consider the behaviour with composite slabs.

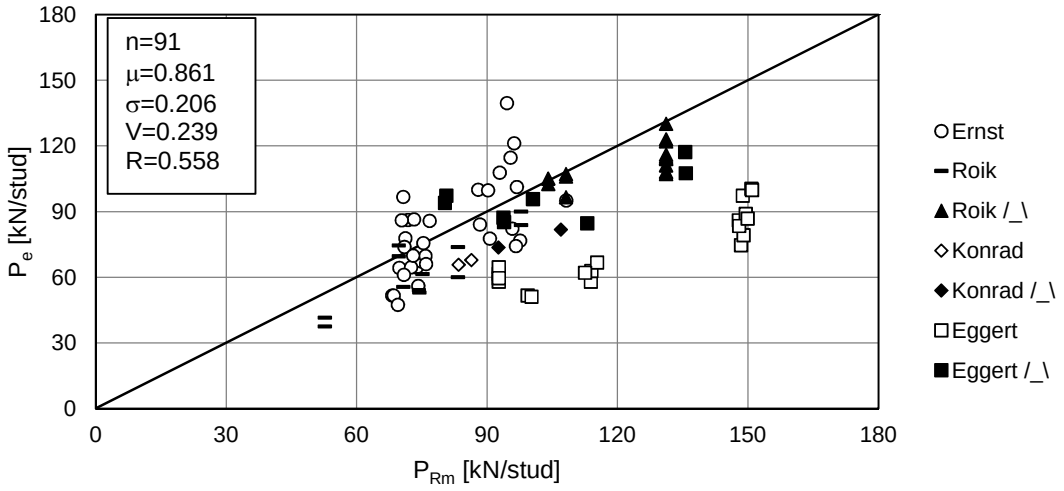


(a) Experimental resistance, $P_e$ vs. average resistance, $P_{Rm}$

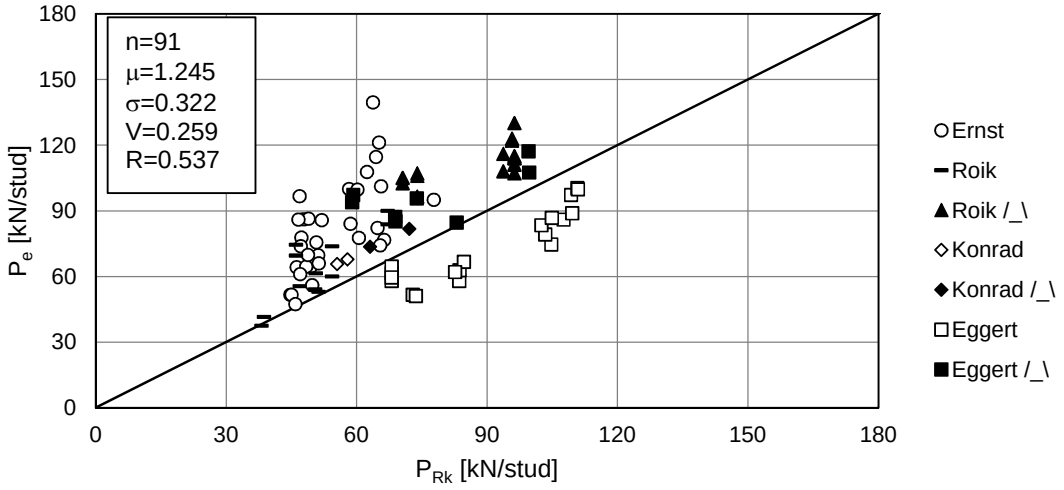


(b) Experimental resistance, $P_e$, vs. characteristic resistance, $P_{Rk}$

Figure 2.10: Comparison of the shear resistance according to [DIN EN 1994-1-1, 2010, Roik et al., 1989] with push-out test results of composite slab specimens, considering the restrictions.

Figure 2.10 shows the results of the evaluation, if the restrictions for the use of $k_t$ are considered. In this case, the predicted resistances were even more non-conservative. The experimental resistance, $P_e$, is in average 86% of the predicted resistance, $P_{Rm}$. The coefficient of variation strongly improved to $V = 0.24$, but the coefficient of correlation was slightly reduced to $R = 0.56$.

Comparing the test results to the characteristic resistance the ratio $P_e/P_{Rk}$ is in average $\mu =$

$1.25$. However, 20 out of 91 tests have smaller resistances than the predicted characteristic resistance, $P_{Rk}$. This are about 22% of the evaluated tests, so the formulae does not result in a 5%-fractile. Because of the limitations, the coefficient of variation did improve, but is still larger than for the comparison with average resistances $P_{Rm}$. The coefficient of correlation decreases compared to the evaluation with all 288 tests.

Considering the comparisons shown in Figure 2.10, especially the shear resistance of tests reported in [Odenbreit et al., 2015] are over-estimated. Many of these tests used a decking with very narrow ribs. The geometry satisfied all requirements of [DIN EN 1994-1-1, 2010], but because of the narrow ribs the studs were in an unfavourable position according to [Rambo-Roddenberry, 2002, Konrad, 2011]. According to the results of the comparison, this position is not covered by the current $k_t$-formulae. This means, that in addition to the current restrictions a minimum distance between the stud and the edge of the rib needs to be introduced to avoid studs in an unfavourable position. In this case, the results of the comparison would improve significantly, as shown in Figure 2.11 for the characteristic resistance, $P_{Rk}$.

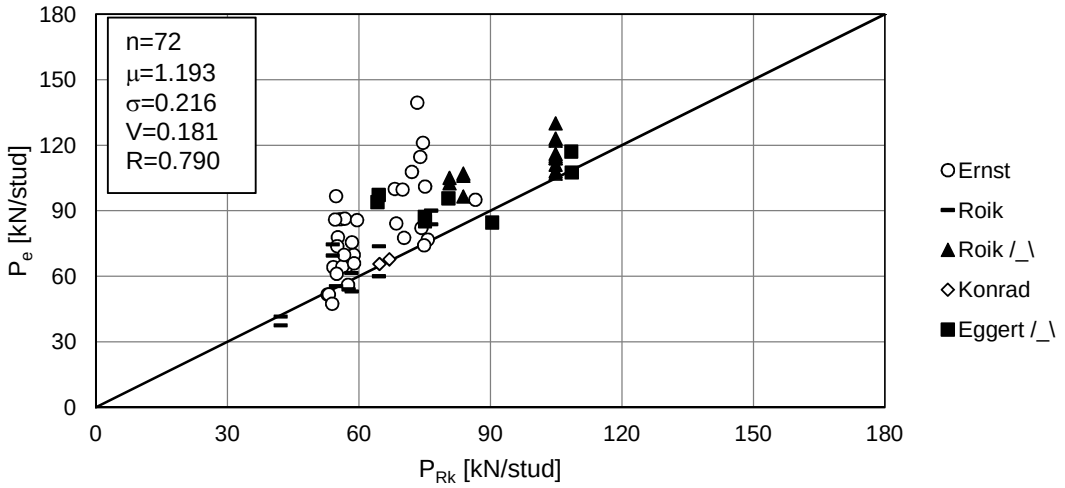


Figure 2.11: Comparison of the characteristic shear resistance, $P_{Rk}$ according to [DIN EN 1994-1-1, 2010, Roik et al., 1989] with push-out test results without studs in an unfavourable position.

A summary of the comparisons is given in Table 2.2. The comparisons showed that when the current restrictions of [DIN EN 1994-1-1, 2010] are used, the reduction factor $k_t$ results in non-conservative resistances, $P_{Rm}$, for studs in the ribs of composite slabs. Likewise, the comparison with characteristic values, $P_{Rk}$, showed that the formulae did not result in a 5%-fractile, which is the characteristic resistance defined in [DIN EN 1990, 2002].

Within the current restrictions of the formulae, the low coefficient of correlation of 0.53 to 0.56 showed that reducing the studs resistance in a solid slab with the factor $k_t$ treats the test parameters too undifferentiated. In addition, the formulae given in [DIN EN 1994-1-1, 2010] is already very restrictive concerning the geometry of the deck and stud as well as the stud position. If all current restriction are considered only one third of the tests in the database can be evaluated. Nevertheless, these restrictions are necessary, because the accuracy of the predicted resistances significantly worsened when they were not considered. Furthermore, additional restrictions need to be introduced to avoid an unfavourable position of the stud when the deck rib is very narrow. This would improve the accuracy significantly, but also

Table 2.2: Results of comparisons between experimental resistances, $P_e$, and theoretical resistance according to [DIN EN 1994-1-1, 2010, Roik et al., 1989].

| | Evaluation of the full test database | | Evaluation for tests in the field of application | |
|---|---|---|---|---|
| | $P_e$ vs. $P_{Rm}$ | $P_e$ vs. $P_{Rk}$ | $P_e$ vs. $P_{Rm}$ | $P_e$ vs. $P_{Rk}$ |
| $n$ | 288 | 288 | 91 | 91 |
| $\mu$ | 0.970 | 1.447 | 0.861 | 1.245 |
| $\sigma$ | 0.371 | 0.591 | 0.206 | 0.322 |
| $V$ | 0.383 | 0.408 | 0.239 | 0.259 |
| $R$ | 0.593 | 0.579 | 0.558 | 0.537 |

$n$: Number of tests
$\mu$: Average of ratios $P_e/P_{Rm}$ and $P_e/P_{Rk}$
$\sigma$: Standard deviation
$V$: Coefficient of Variation
$R$: Coefficient of correlation

result in an even stronger limitation of the field of application. This shows that there is a necessity to improve the prediction method as less strict restrictions are desirable.

### 2.2.2 Resistance of shear studs according to Lungershausen

[Lungershausen, 1988] suggested a formulae to calculate the mean shear resistance, $P_{Rm}$, for studs in the ribs of composite slabs according to equation (2.9). This is a semi-empirical approach based on the plastic bending resistance of the shear stud assuming two yield hinges, as shown in Figure 2.2. The spacing of the yield hinges, $\varkappa \cdot d$, was empirically determined from test results. The statistical evaluation according to [DIN EN 1990, 2002] lead to the characteristic resistance, $P_{Rk}$, according to equation (2.10). According to [Roik et al., 1989] the required partial safety factor is 1.30.

$$P_{Rm} = 1.006 \cdot \frac{\beta}{\sqrt{n_r}} \cdot \frac{2 \cdot M_{pl}}{\varkappa_m \cdot d} \tag{2.9}$$

$$P_{Rk} = 0.80 \cdot \frac{\beta}{\sqrt{n_r}} \cdot \frac{2 \cdot M_{pl}}{\varkappa_m \cdot d} \tag{2.10}$$

where:

| | | |
|---|---|---|
| $P_{Rm}$ | | Shear resistance of stud (mean value) |
| $P_{Rk}$ | | Characteristic shear resistance |
| $n_r$ | $\leq 3$ | Number of studs per rib |
| $\beta$ | $= \begin{cases} 1.0 & \text{for open deck shapes} \\ 1.1 & \text{for re-entrant deck shapes} \end{cases}$ | |
| $M_{pl}$ | $= f_{cal} \cdot d^3/6$ | Plastic bending resistance of stud |
| $f_{cal}$ | $= 500$ N/mm$^2$ | Calculative stress of stud |
| $\varkappa_m$ | $= 0.8 \cdot \left[\frac{h_p}{b_o}\right]^2 + 0.6$ | Relative distance of plastic hinges |
| $b_o$ | | Width of deck rib at top |

The following geometric limitations apply to the formula by [Lungershausen, 1988]:

- $h_p < 140$ mm
- $h_{sc}/d > 4$

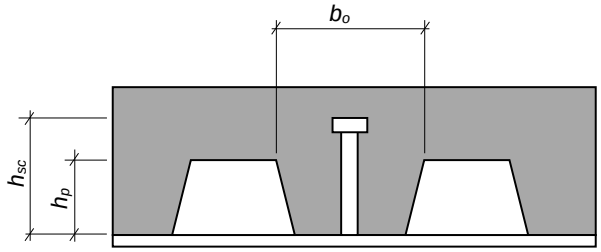


Figure 2.12: Geometric parameters for the calculation of the shear stud resistance in the ribs of composite slabs according to [Lungershausen, 1988].

- $h_{sc} - h_p > 2 \cdot d \cdot \sqrt{n_r}$
- $n_r \leq 3$

In addition, no load-bearing component for the concrete is considered. The tests considered by [Lungershausen, 1988] had concrete strengths between 19.6 and 41.9 N/mm$^2$ with an average value of 31.5 N/mm$^2$. One could argue that the model is not accurate for a concrete strength significantly different to 30 N/mm$^2$. Likewise, the position of the stud in the rib is not considered. It can be assumed that the predictions are calibrated for studs welded at the centre line of the rib.

In comparison with the database of push-out test results the formula by [Lungershausen, 1988] is conservative because the tests reach about 9% higher resistances than predicted. In comparison to [DIN EN 1994-1-1, 2010], the coefficient of variation of $V = 0.28$ and the coefficient of correlation of $R = 0.67$ significantly improved.

Comparing against the predicted characteristic resistance, $P_{Rk}$, using the characteristic tensile strength of the studs and considering its limitation to 500 N/mm$^2$, the ratios $P_e/P_{Rk}$ are even more conservative. The coefficients of variation and correlation do not show a significant change. However, about 10% of the evaluated tests have a resistance of less than $P_{Rk}$.

Considering the geometric restraints, the average resistance, $P_{Rm}$, is conservative by about 11%. The coefficient of variation improves to 0.20. The coefficient of correlation of 0.84 is a significant improvement compared to the formulae of [DIN EN 1994-1-1, 2010], where it was only 0.54.

The predicted characteristic resistances, $P_{Rk}$, is slightly more conservative. The coefficients of variation and correlation do not change. None of the tests shows a shear resistance that is smaller than $P_{Rk}$.

However, only 95 tests satisfy the geometric limitations so they are as restrictive as the ones in [DIN EN 1994-1-1, 2010].

A summary of the comparisons is given in Table 2.3. In general, this simple semi-emperical approach correlates better with the experimental resistances, as shown by the improved coefficients of variation, $V$, and correlation, $R$, than the formulae of [DIN EN 1994-1-1, 2010], even though important influence as concrete strength and stud position are not covered. The back draw is that the predictions are quite conservative.

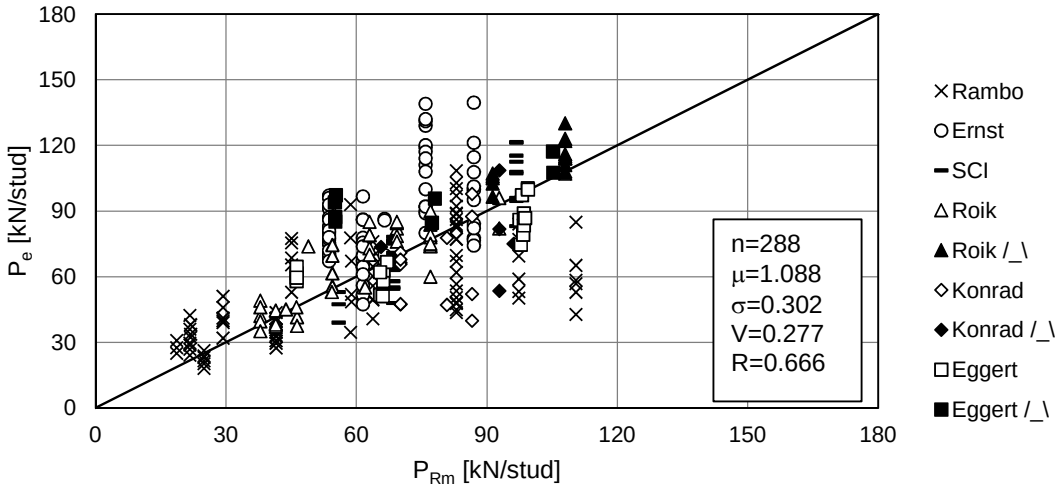


(a) Experimental resistance, $P_e$ vs. average resistance, $P_{Rm}$

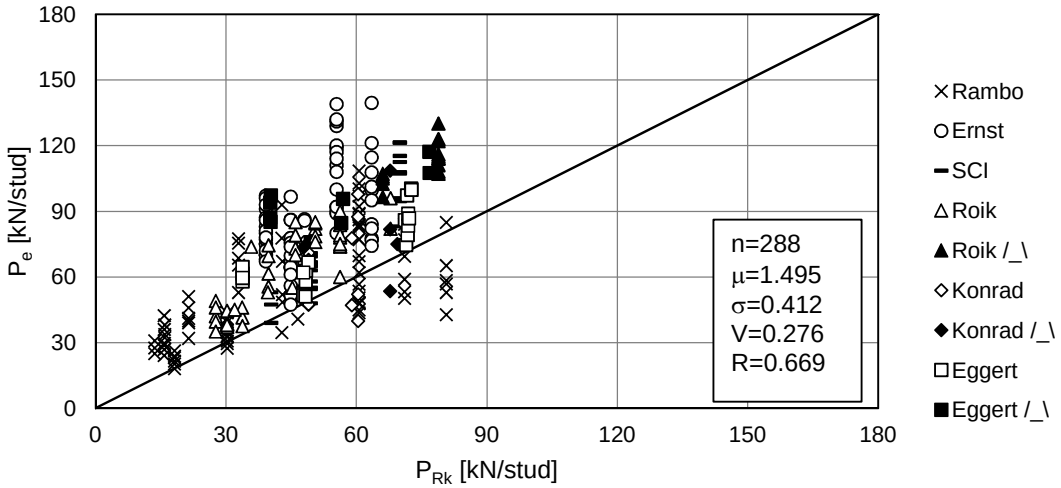


(b) Experimental resistance, $P_e$, vs. characteristic resistance, $P_{Rk}$

Figure 2.13: Comparison of the shear resistance according to [Lungershausen, 1988] with push-out test results.

Table 2.3: Results of comparisons between experimental resistances, $P_e$, and theoretical resistance according to [Lungershausen, 1988].

| | Evaluation of the full test database | | Evaluation for tests in the field of application | |
|---|---|---|---|---|
| | $P_e$ vs. $P_{Rm}$ | $P_e$ vs. $P_{Rk}$ | $P_e$ vs. $P_{Rm}$ | $P_e$ vs. $P_{Rk}$ |
| $n$ | 288 | 288 | 95 | 95 |
| $\mu$ | 1.088 | 1.495 | 1.108 | 1.410 |
| $\sigma$ | 0.302 | 0.412 | 0.224 | 0.306 |
| $V$ | 0.277 | 0.276 | 0.202 | 0.202 |
| $R$ | 0.666 | 0.669 | 0.841 | 0.841 |

$n$: Number of tests
$\mu$: Average of ratios $P_e/P_{Rm}$ and $P_e/P_{Rk}$
$\sigma$: Standard deviation
$V$: Coefficient of Variation
$R$: Coefficient of correlation

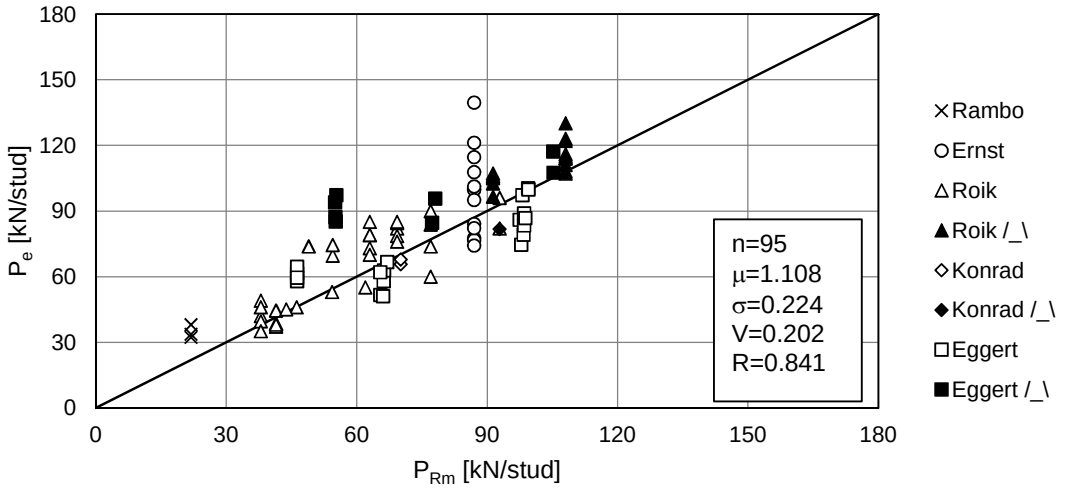


(a) Experimental resistance, $P_e$ vs. average resistance, $P_{Rm}$

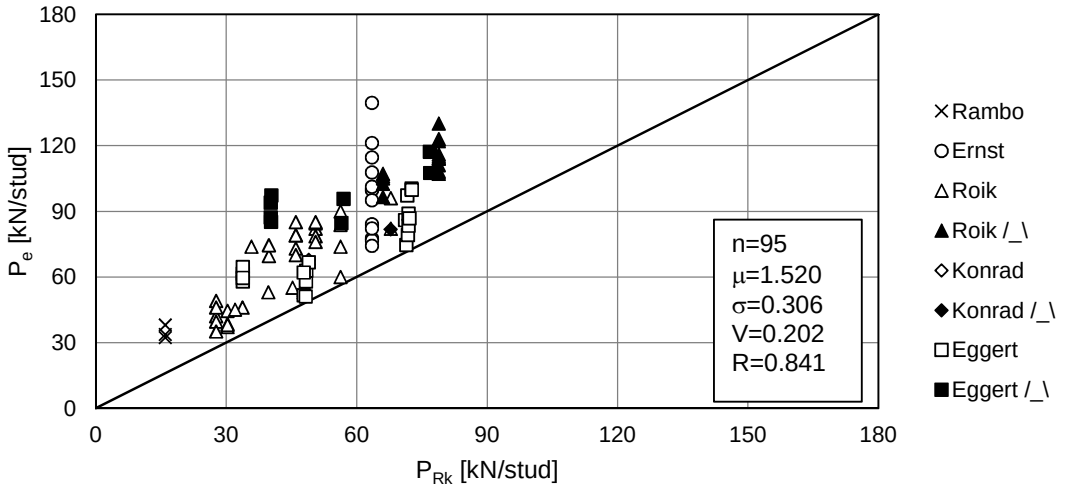


(b) Experimental resistance, $P_e$, vs. characteristic resistance, $P_{Rk}$

Figure 2.14: Comparison of shear resistances according to [Lungershausen, 1988] with push-out test results under consideration of geometric limitations.

### 2.2.3 Resistance of shear studs according to Rambo-Roddenberry

[Rambo-Roddenberry, 2002] conducted an extensive programme of push-out tests. To develop an approach for the calculation of the stud shear resistance, the test results were compared against the most important test parameters. This lead to correlation curves defining the studs resistance as a function of its tensile strength. The studs resistance is then calculated according to equations (2.11) to (2.14).

Each equation is only valid for certain deck heights and ratios of stud diameter, $d$, to flange thickness, $t_F$. Assuming typical dimensions of the steel section and the shear stud diameter it follows that equation (2.11) is the most relevant one in practice, because the other equations are for too low deck heights or lead to untypical ratios $d/t_F$. In addition, all equations were developed for through deck welded studs in open trapezoidal shaped decking.

Studs in 2 in. (51 mm) and 3 in. (76 mm) deck with $d/t_F \leq 2.7$:

$$P_{Rm} = R_p \cdot R_n \cdot R_d \cdot f_u \cdot \pi \cdot d^2/4 \tag{2.11}$$

Studs in 1 in. (25.4 mm) and 1.5 in. (38.1 mm) with $d/t_F \leq 2.7$:

$$P_{Rm} = R_n \cdot 3.08 \cdot e^{0.048 \cdot f_u \cdot \pi \cdot d^2/4} \tag{2.12}$$

Studs in 2 in. (50.8 mm) and 3 in. (76.2 mm) deck with $d/t_F > 2.7$:

$$P_{Rm} = R_p \cdot R_n \cdot R_d \cdot f_u \cdot \pi \cdot d^2/4 - 1.5 \cdot \left(\frac{d}{t_F} - 2.7\right) \tag{2.13}$$

Studs in 1 in. (25.4 mm) and 1.5 in. (38.1 mm) with $d/t_F \leq 2.7$:

$$P_{Rm} = R_n \cdot 3.08 \cdot e^{0.048 \cdot f_u \cdot \pi \cdot d^2/4} - 1.5 \cdot \left(\frac{d}{t_F} - 2.7\right) \tag{2.14}$$

where:

$P_{Rm}$ Average resistance of shear connector

$$R_p = \begin{cases} 0.68 & \text{for favourable position: } e_{mid-ht} \geq 2.2\text{”} = 55.9 \text{ mm} \\ 0.48 & \text{for unfavourable position: } e_{mid-ht} < 2.2\text{”} = 55.9 \text{ mm} \\ 0.52 & \text{for staggered position} \end{cases}$$

$$R_n = \begin{cases} 1.00 & \text{for single studs per rib or staggered position} \\ 0.85 & \text{for pairs of studs per rib} \end{cases}$$

$$R_d = \begin{cases} 1.00 & \text{studs in favourable position} \\ 0.88 & \text{studs in unfavourable position in 22 gauge deck} \\ 1.00 & \text{studs in unfavourable position in 20 gauge deck} \\ 1.05 & \text{studs in unfavourable position in 18 gauge deck} \\ 1.11 & \text{studs in unfavourable position in 16 gauge deck} \end{cases}$$

$t_F$ Thickness of steel flange

Table 2.4: Deck thickness according to gauge deck definition

| Gauge No. | Deck thickness in | |
|---|---|---|
| | [inch] | [mm] |
| 16 | 0.0625 | 1.59 |
| 18 | 0.0500 | 1.27 |
| 20 | 0.0375 | 0.95 |
| 22 | 0.0310 | 0.79 |

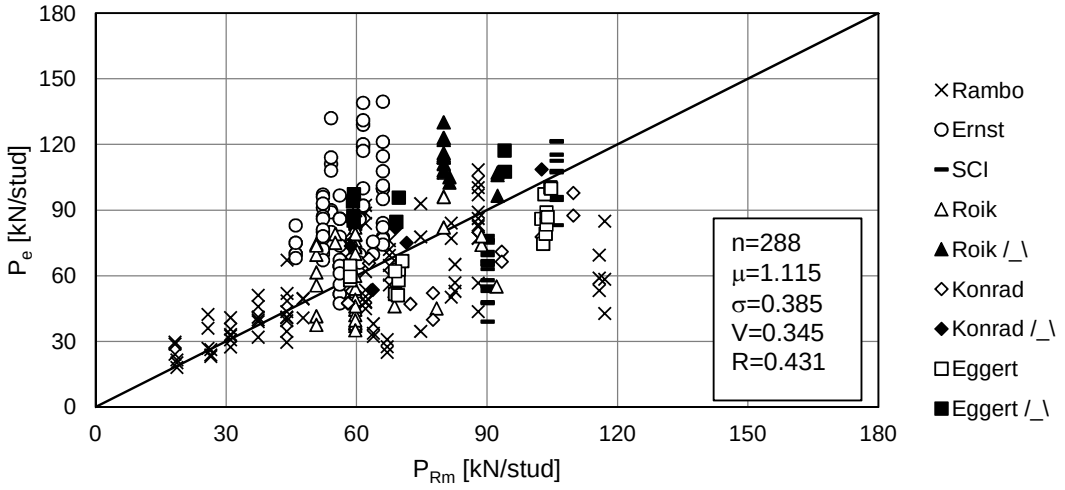


Figure 2.15: Comparison of shear resistances according to [Rambo-Roddenberry, 2002], $P_{Rm}$, with the full database of push-out test results, $P_e$.

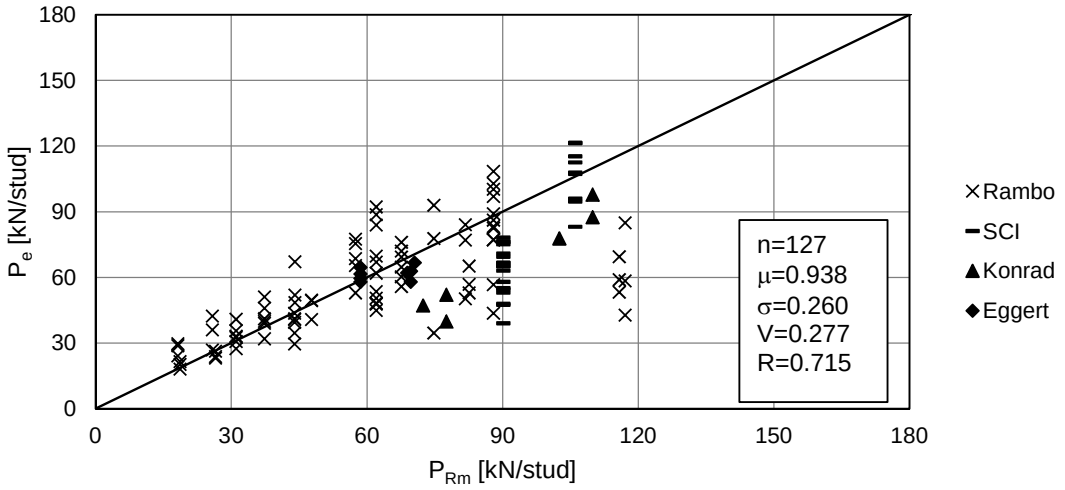


Figure 2.16: Comparison of shear resistances according to [Rambo-Roddenberry, 2002], $P_{Rm}$, with push-out test results under consideration of a limited field of application, $P_e$.

Using equation (2.11), the stud strength is calculated as a reduced tensile strength. Constant

reduction factors which depend on the stud position, the number of studs per rib and the thickness of the steel sheet are applied.

It is noted, that important influences as the geometry of the decking, the geometry of the stud and the concrete strength are not unconsidered, while the influence of the deck thickness is considered. For typical dimensions, this influence is relatively small [Konrad, 2011] and the decking only contributes to the resistance when the studs are through deck welded.

The comparison of the resistance according to equation (2.11) with the test database shows that the predictions results in good ratios $P_e/P_{Rm}$ because the model was statistical derived. However, because of the many unconsidered parameters the coefficient of correlation is very small with only $R = 0.43$.

To consider the limited field of application for equation (2.11), tests with a deck height of more than 85 mm and re-entrant deck shapes are removed from the evaluation. In addition, the number of studs is limited to no more than two studs per rib, only through deck welded studs are considered and test by Ernst [Ernst, 2006] with mixed stud positions are omitted. The resulting comparison is shown in Figure 2.16.

The comparison with the reduced database improves the coefficients of correlation and variation strongly. However, they are still not satisfactory and a large amount of tests with common parameters in practice was omitted. In addition, the results for the remaining tests tend to be non-conservative. Hence, the method developed by [Rambo-Roddenberry, 2002] appears to be too restrictive and undifferentiated to calculate the shear stud resistance.

### 2.2.4 Resistance of shear studs according to Konrad

Similar to [DIN EN 1994-1-1, 2010], [Konrad, 2011] suggests to calculate the resistance of studs in the ribs of composite slabs by reducing the resistance of studs in solid slabs. The new equations by [Konrad, 2011] are currently discussed as an alternative to the rules of [DIN EN 1994-1-1, 2010]. According to [Konrad, 2011] the average resistance of a shear stud in a solid slab is calculated according to equations (2.15) and (2.16). The characteristic resistance is obtained by equations (2.17) and (2.18):

$$P_{Rm,c} = 39.53 \cdot A_{Wulst,eff} \cdot f_{cm}^{2/3} + 3.72 \cdot d^2 \cdot f_{cm}^{1/3} \cdot f_{um}^{1/2} \tag{2.15}$$

$$P_{Rm,s} = 38.30 \cdot A_{Wulst,eff} \cdot f_{cm}^{2/3} + 0.57 \cdot f_{um} \cdot d^2 \tag{2.16}$$

$$P_{Rk,c} = 326 \cdot A_{Wulst,eff} \cdot \left(\frac{f_{ck}}{30}\right)^{2/3} + 220 \cdot d^2 \cdot \left(\frac{f_{ck}}{30}\right)^{1/3} \cdot \left(\frac{f_{uk}}{500}\right)^{1/2} \tag{2.17}$$

$$P_{Rk,s} = 313 \cdot A_{Wulst,eff} \cdot \left(\frac{f_{ck}}{30}\right)^{2/3} + 240 \cdot \left(\frac{f_{uk}}{500}\right) \cdot d^2 \tag{2.18}$$

| | | |
|---|---|---|
| where: | $A_{Wulst,eff} = 0.5 \cdot h_{Wulst} \cdot d_{Wulst}$ | Effective area of the weld collar |
| | $h_{Wulst}$ | Height of the weld collar |
| | $d_{Wulst}$ | Diameter of the weld collar |

The prediction of the stud shear resistance in solid slabs is calibrated for the following restrictions:

Table 2.5: Effective area of the weld collar according to [Konrad, 2011]

| $d$ [mm] | $h_{Wulst}$ [mm] | $d_{Wulst}$ [mm] | $A_{Wulst,eff}$ [mm$^2$] |
|---|---|---|---|
| 10 | 2.5 | 13.0 | 16.3 |
| 13 | 3.0 | 17.0 | 25.5 |
| 16 | 4.5 | 21.0 | 47.3 |
| 19 | 6.0 | 23.0 | 63.0 |
| 22 | 6.0 | 29.0 | 87.0 |
| 25 | 7.0 | 40.0 | 140.0 |

- $16 \text{ mm} \leq d \leq 25 \text{ mm}$
- $h_{sc}/d \geq 4$
- $20 \text{ N/mm}^2 \leq f_{ck} \leq 100 \text{ N/mm}^2$
- $f_{uk} \leq 740 \text{ N/mm}^2$

Because the accuracy of the predicted resistance of the stud in a solid slab is important to assess the accuracy of the reduction factors, equations (2.15) and (2.16) are verified against the test database (see Appendix A). The results of the verification are shown in Figure 2.17. It can be seen that the predictions correlate well with the test results. In addition, the accuracy is improved significantly in comparison to [Roik et al., 1989].

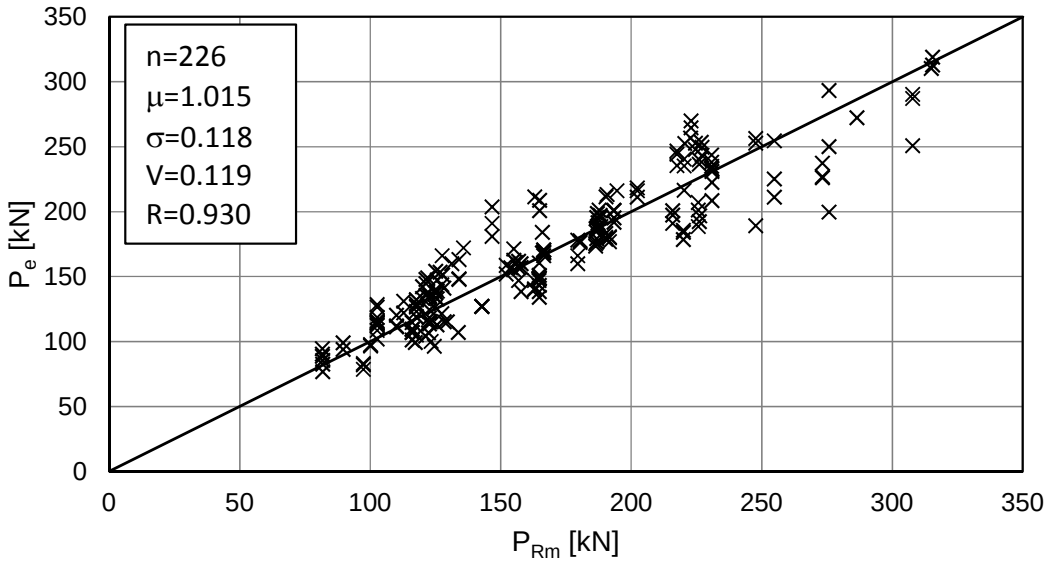


Figure 2.17: Verification of the shear stud resistance in solid slabs according to [Konrad, 2011].

[Konrad, 2011] developed his reduction factors from numerical analysis. The influence of parameter as the ratios $b_m/h_p$, $h_{sc}/h_p$ and the stud position were investigated, see Figure 2.18. Regression curves for these parameters were found and the resulting reduction factors were verified against 107 push-out test results. This procedure led to reduction factors for through deck welded studs in dependency of the stud position. For studs in the ribs of

composite slabs the stud position according to [Konrad, 2011] is defined as follows:

- unfavourable position: $e \leq 55$ mm
- mid-position: $55$ mm $< e \leq 100$ mm
- favourable position: $e > 100$ mm

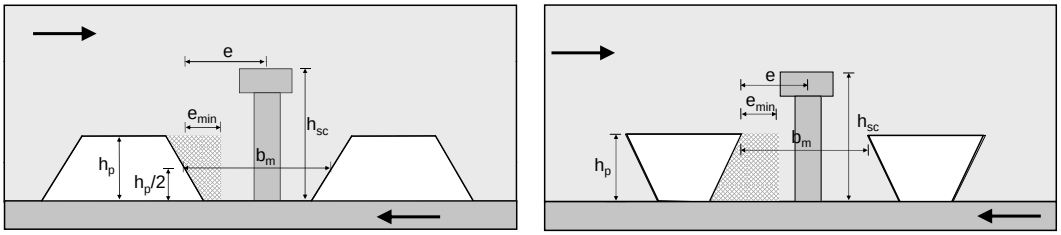


Figure 2.18: Geometric parameters of the shear connection used in [Konrad, 2011].

The obtained reduction factors for through deck welded shear connectors in open shaped composite decking are shown in equations (2.19) to (2.27).

For through deck welded shear connectors in mid-position, the reduction factors are:

For $h_{sc}/h_p \leq 1.56$:

$$k_{mid,1} = k_n \cdot \left[ 6.79 \cdot 10^{-4} \left( \frac{b_m}{h_p} \right)^2 + 0.170 \left( \frac{b_m}{h_p} \right) + 0.250 \left( \frac{h_{sc}}{h_p} \right) \right] \leq 1.0 \tag{2.19}$$

For $h_{sc}/h_p > 1.56$:

$$k_{mid,2} = k_n \cdot \left[ 5.34 \cdot 10^{-4} \left( \frac{b_m}{h_p} \right)^2 + 0.042 \left( \frac{b_m}{h_p} \right) + 6.83 \cdot 10^{-4} \left( \frac{h_{sc}}{h_p} \right) + 0,663 \right] \leq 1.0 \tag{2.20}$$

Equation (2.20) can be simplified to give:

$$k_{mid,3} = k_n \cdot \left[ 0.042 \left( \frac{b_m}{h_p} \right) + 0.663 \right] \leq 1,0 \tag{2.21}$$

For through deck welded shear connectors in favourable position, the reduction factors are:

For $h_{sc}/h_p \leq 1.56$:

$$k_{fav,1} = k_n \cdot \left[ 0.030 \left( \frac{b_m}{h_p} \right)^2 + 0.145 \left( \frac{b_m}{h_p} \right) + 0.240 \left( \frac{h_{sc}}{h_p} \right) \right] \leq 1.0 \tag{2.22}$$

For $h_{sc}/h_p > 1.56$:

$$k_{fav,2} = k_n \cdot \left[ 0.003 \left( \frac{b_m}{h_p} \right)^2 + 0.103 \left( \frac{b_m}{h_p} \right) + 0,318 \left( \frac{h_{sc}}{h_p} \right) \right] \leq 1.0 \tag{2.23}$$

Equation (2.23) can be simplified to give:

$$k_{fav,3} = k_n \cdot \left[0.084 \left(\frac{b_m}{h_p}\right) + 0.663\right] \leq 1.0 \tag{2.24}$$

For through deck welded shear connectors in unfavourable position, the reduction factors are:

For $h_{sc}/h_p \leq 1.56$:

$$k_{unfav,1} = k_n \cdot \left[0.036 \left(\frac{b_m}{h_p}\right)^2 + 0.004 \left(\frac{b_m}{h_p}\right) + 0.305 \left(\frac{h_{sc}}{h_p}\right) - 0,095\right] \leq 0.8 \tag{2.25}$$

For $h_{sc}/h_p > 1.56$:

$$k_{unfav,2} = k_n \cdot \left[0.029 \left(\frac{b_m}{h_p}\right)^2 + 0.266 \left(\frac{b_m}{h_p}\right) + 0.026 \left(\frac{h_{sc}}{h_p}\right)\right] \leq 0.8 \tag{2.26}$$

Equation (2.26) can be simplified to give:

$$k_{unfav,3} = k_n \cdot \left[0.317 \left(\frac{b_m}{h_p}\right) + 0.06\right] \leq 0.8 \tag{2.27}$$

Where: $k_n$ Factor to consider the number of shear connectors per rib

$$= \begin{cases} 1.00 & \text{for single studs} \\ 0.80 & \text{for pairs of studs} \end{cases}$$

Further modifications of the reduction factors to consider pre-punched and re-entrant decking then led to the reduction factors shown in equations (2.28) and (2.29). Thereby, shear studs in unfavourable position were excluded. A minimum embedment depth of the head of the stud is required by the ratio $h_{sc}/h_p$ of at least 1.56.

For shear connectors with $h_{sc}/h_p > 1.56$ welded directly to the flange of the beam in mid- and favourable position the reduction factor is:

$$k_{\perp} = k_n \cdot \left[k_e \cdot 0.038 \left(\frac{b_m}{h_p}\right) + 0.597\right] \leq 1.0 \tag{2.28}$$

Where: $k_e$ Factor to consider the position of shear connectors

$$= \begin{cases} 1 & \text{for } 55 \text{ mm} < e \leq 100 \text{ mm} \\ 2 & \text{for } e > 100 \text{ mm} \end{cases}$$

For through deck welded shear connectors with $h_{sc}/h_p > 1.56$ in mid- and favourable position the reduction factor is:

$$k_\perp = k_n \cdot k_{Tr} \left[ k_e \cdot 0.042 \left( \frac{b_m}{h_p} \right) + 0.663 \right] \leq 1.0 \tag{2.29}$$

Where: $k_{Tr}$ Factor to consider the deck shape

$$= \begin{cases} 1.25 & \text{for re-entrant deck shapes} \\ 1.00 & \text{for open deck shapes} \end{cases}$$

For shear connectors in composite slabs following additional restrictions are given:

- 16 mm $\leq d \leq$ $\begin{cases} 20 \text{ mm} & \text{for studs welded through the decking} \\ 22 \text{ mm} & \text{for studs welded through punched holes} \end{cases}$
- $n_r \leq 2$

A comparison of the predictions according to equations (2.28) and (2.29) to the test database is shown in Figure 2.19. The ratios $P_e/P_{Rm}$ are more unconservative than in the comparison to [DIN EN 1994-1-1, 2010]. Compared to [DIN EN 1994-1-1, 2010], the coefficient of variation strongly improves from $V = 0.371$ to $V = 0.288$, but the coefficient of correlation of $R = 0.56$ is still not satisfactory. While the comparison is unconservative for the mean shear resistance $P_{Rm}$, the characteristic resistance has a ratio $P_e/P_{Rk}$ of in average $\mu = 1.23$. These results are more accurate than for [DIN EN 1994-1-1, 2010], but the coefficient of correlation remains unsatisfactory. In addition, 28% of the tests did not reach the predicted characteristic resistance.

Considering that the reduction factors according to equations (2.28) and (2.29) are only valid for studs with a ratio $h_{sc}/h_p$ of at least 1.56 and only mid and favourable position are allowed, the results of the comparison improve significantly, as shown in Figure 2.20. Concerning the characteristic resistance, 15 out of 143 tests are over-estimated. It is noted, that especially the tests reported by [Rambo-Roddenberry, 2002] are over-predicted, although they should be covered because the studs were welded in favourable position. It is questionable if these results indicate some yet insufficiently considered influence.

In general, the reduction factors according to equations (2.28) and (2.29) show a better correlation with test results than [DIN EN 1994-1-1, 2010]. In addition, the number of tests that can be considered within the limitations is larger than for [DIN EN 1994-1-1, 2010]. A summary of the comparisons is given in Table 2.6.

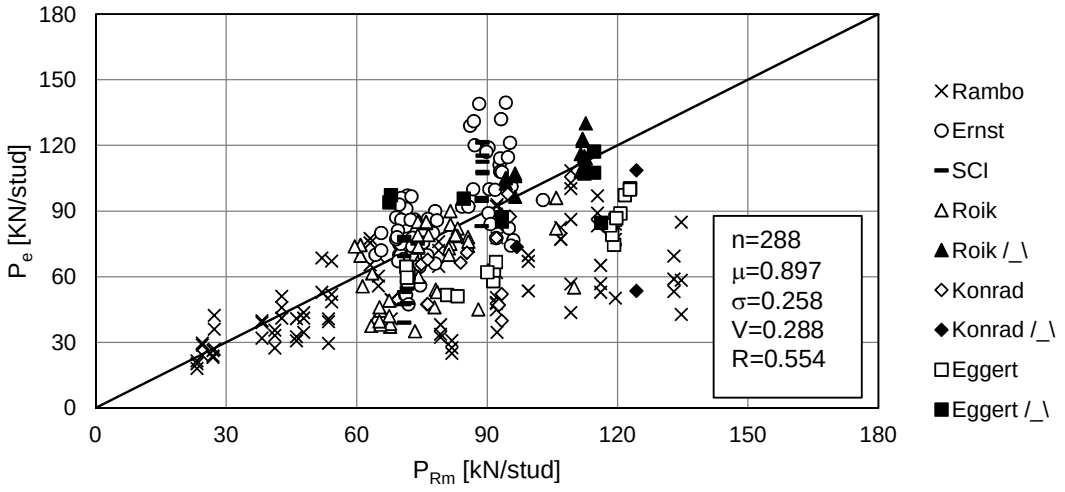


(a) [Experimental resistance, $P_e$ vs. average resistance, $P_{Rm}$

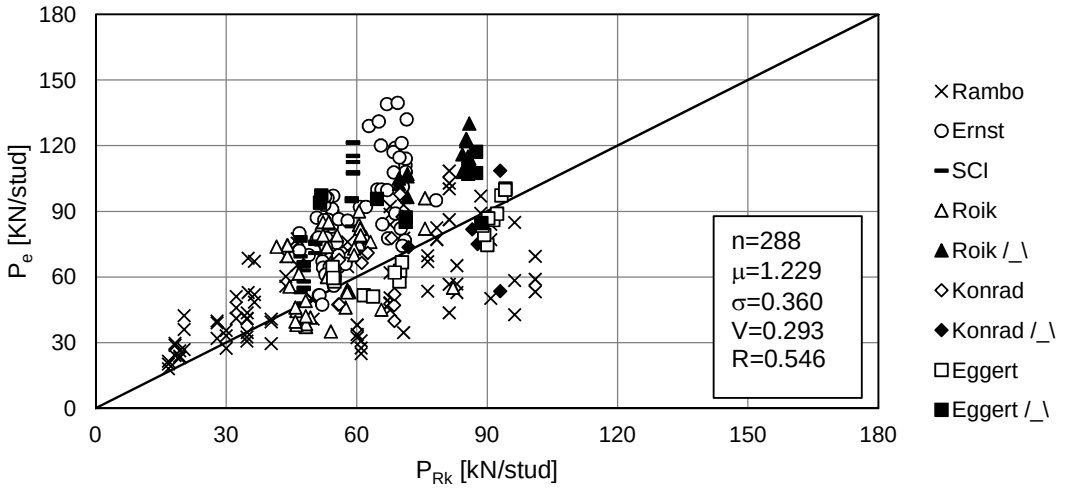


(b) Experimental resistance, $P_e$, vs. characteristic resistance, $P_{Rk}$

Figure 2.19: Comparison of shear resistances according to [Konrad, 2011] with push-out test results.

Table 2.6: Results of comparisons between experimental resistances, $P_e$, and theoretical resistance according to [Konrad, 2011].

| | Evaluation of the full test database | | Evaluation for tests in the field of application | |
|---|---|---|---|---|
| | $P_e$ vs. $P_{Rm}$ | $P_e$ vs. $P_{Rk}$ | $P_e$ vs. $P_{Rm}$ | $P_e$ vs. $P_{Rk}$ |
| $n$ | 288 | 288 | 143 | 143 |
| $\mu$ | 0.897 | 1.229 | 0.958 | 1.327 |
| $\sigma$ | 0.258 | 0.360 | 0.200 | 0.294 |
| $V$ | 0.288 | 0.293 | 0.209 | 0.222 |
| $R$ | 0.554 | 0.546 | 0.777 | 0.747 |

$n$: Number of tests
$\mu$: Average of ratios $P_e/P_{Rm}$ and $P_e/P_{Rk}$
$\sigma$: Standard deviation
$V$: Coefficient of Variation
$R$: Coefficient of correlation

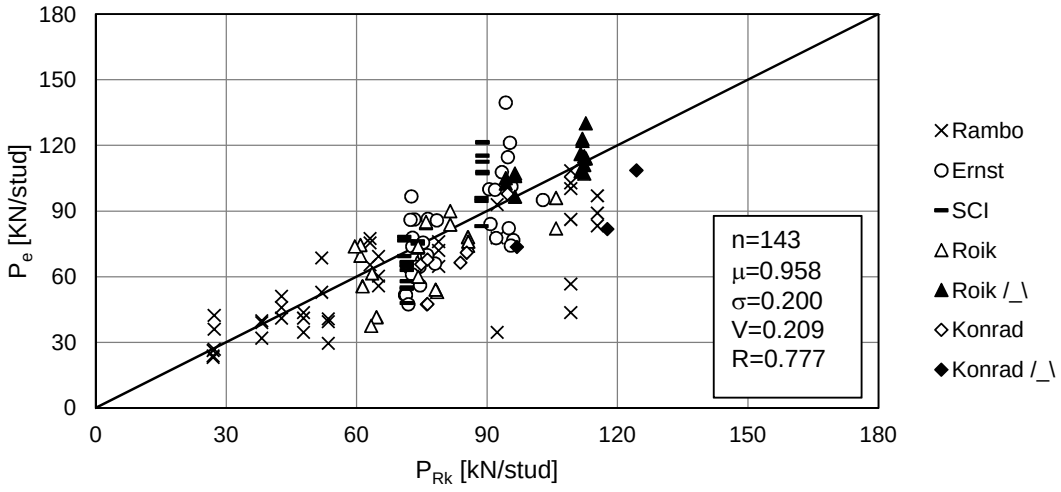


(a) [Experimental resistance, $P_e$ vs. average resistance, $P_{Rm}$

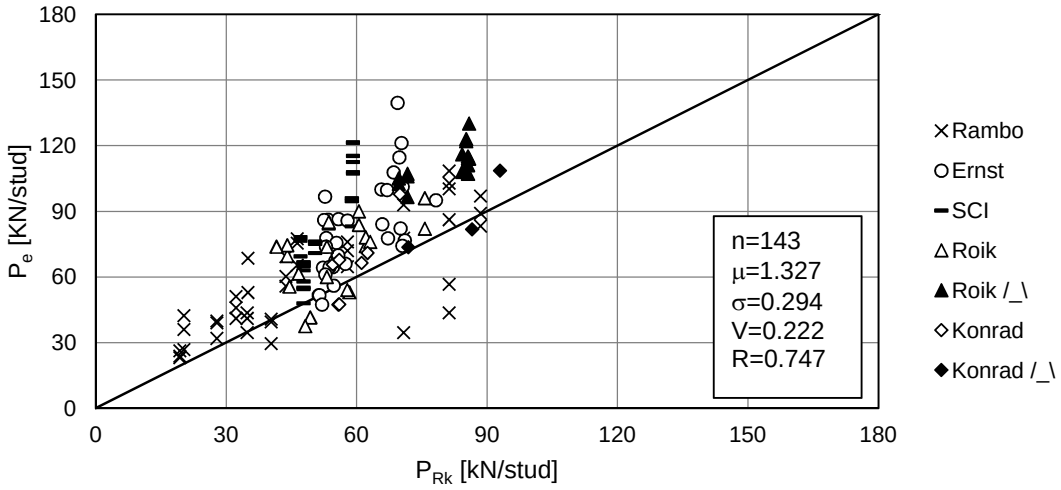


(b) Experimental resistance, $P_e$, vs. characteristic resistance, $P_{Rk}$

Figure 2.20: Comparison of shear resistances according to [Konrad, 2011] with push-out test results under consideration of geometric restraints.

### 2.2.5 Summary of the comparisons

Table 2.7 summarises the results of the previous evaluations. It can be concluded that none of the presented methods shows satisfactory results for the prediction of the shear resistance of studs in the ribs of composite slabs or they have strong limitations..

Table 2.7: Comparison of the evaluation of the shear resistance between the presented methods.

| Mean shear resistance, $P_{Rm}$, for the full database | | | | |
|---|---|---|---|---|
| | EUROCODE 4 | LUNGERSHAUSEN | RODDENBERRY | KONRAD |
| $n$ | 288 | 288 | 288 | 288 |
| $\mu$ | 0.970 | 1.088 | 1.115 | 0.897 |
| $\sigma$ | 0.371 | 0.302 | 0.385 | 0.258 |
| $V$ | 0.383 | 0.277 | 0.345 | 0.288 |
| $R$ | 0.593 | 0.666 | 0.431 | 0.554 |
| Mean shear resistance, $P_{Rm}$, in the respective field of application | | | | |
| | EUROCODE 4 | LUNGERSHAUSEN | RODDENBERRY | KONRAD |
| $n$ | 91 | 95 | 127 | 143 |
| $\mu$ | 0.861 | 1.108 | 0.938 | 0.958 |
| $\sigma$ | 0.206 | 0.224 | 0.260 | 0.200 |
| $V$ | 0.239 | 0.202 | 0.277 | 0.209 |
| $R$ | 0.558 | 0.841 | 0.715 | 0.777 |
| Characteristic shear resistance, $P_{Rk}$, for the full database | | | | |
| | EUROCODE 4 | LUNGERSHAUSEN | RODDENBERRY | KONRAD |
| $n$ | 288 | 288 | n.a. | 288 |
| $\mu$ | 1.447 | 1.495 | n.a. | 1.229 |
| $\sigma$ | 0.591 | 0.412 | n.a. | 0.360 |
| $V$ | 0.408 | 0.276 | n.a. | 0.293 |
| $R$ | 0.579 | 0.669 | n.a. | 0.546 |
| Characteristic shear resistance, $P_{Rk}$, in the respective field of application | | | | |
| | EUROCODE 4 | LUNGERSHAUSEN | RODDENBERRY | KONRAD |
| $n$ | 91 | 95 | n.a. | 143 |
| $\mu$ | 1.245 | 1.410 | n.a. | 1.327 |
| $\sigma$ | 0.322 | 0.306 | n.a. | 0.294 |
| $V$ | 0.259 | 0.202 | n.a. | 0.222 |
| $R$ | 0.537 | 0.841 | n.a. | 0.747 |

The method in [DIN EN 1994-1-1, 2010] gave satisfactory results for studs in solid slabs. However, the $k_t$-formulae showed non-conservative results for studs in the ribs of composite slabs. In addition, the limitations are very restrictive. The consideration of these restrictions improved the results, but the coefficients of variation and correlation were not satisfactory. This was because the position of the shear stud is currently not considered sufficiently. Considering the restrictions of each method, the formulae of [DIN EN 1994-1-1, 2010] shows the smallest correlation to the experimental results.

The very simple mechanical model in [Lungershausen, 1988] gave very conservative results. The given limitations are almost as restrictive as for [DIN EN 1994-1-1, 2010]. Nevertheless, this model showed the smallest variation and the largest correlation to experimental resistances in all conducted comparisons, even though important parameters as concrete strength or stud position are not explicitly considered.

The method in [Rambo-Roddenberry, 2002] did not show a satisfactory correlation with the test results. Too many important parameters are not considered. Therefore, the predictions can only be given for a very limited range of deck heights and do not consider the deck shape or concrete strength. Furthermore, the formulae was not calibrated to the safety concept defined in [DIN EN 1990, 2002].

The method of [Konrad, 2011] gave improved results for studs in solid slabs compared to [DIN EN 1994-1-1, 2010]. For studs in the ribs of composite slabs, the suggested $k_t$-factors showed a significantly improved coefficient of variation and correlation in comparison to the rules of [DIN EN 1994-1-1, 2010]. Nevertheless, the simpler method of [Lungershausen, 1988] showed better statistical values. A large benefit of the reduction factors by [Konrad, 2011] is their wide range of application. The given restrictions allowed the evaluation of about half of the tests in the database, while according to [DIN EN 1994-1-1, 2010] and [Lungershausen, 1988] only one third could be evaluated.

It is concluded that the presented methods are either too restrictive or too inaccurate to predict the shear stud resistance in the ribs of composite slabs. A formulae with less restrictions and a better correlation to the test results is desirable.

## 2.3 Load-displacement behaviour of composite beams

### 2.3.1 Additional requirements on the shear connection

Plastic design gives the most efficient structural design in terms of a large resistance and a simple analysis. Thereby, the assumption of plasticity is not limited to the stress distribution in the cross section, but also plastic behaviour of the shear interface, using equally spaced studs, may be assumed at ultimate limit state.

To apply this procedure, the cross section must be of class 1 or 2 in the critical section. In addition, the plastic bending resistance of the composite section must be no more than 2.5 times the plastic resistance of the pure steel section in the critical section, else additional cuts must be investigated. Furthermore, [DIN EN 1994-1-1, 2010] puts additional requirements on the shear connectors and the degree of shear connection to allow the assumption of a plastic behaviour of the shear interface.

The shear connectors are required to be 'ductile' with a sufficient deformation capacity so that the shear forces can be redistributed between the studs. [DIN EN 1994-1-1, 2010] classifies shear studs as 'ductile' if their characteristic displacement capacity, $\delta_{uk}$ is larger than 6mm. As shown in Figure 2.21, the displacement capacity of a shear connector, $\delta_u$, is defined as the slip where the load-slip curve decreases the first time to its characteristic resistance, $P_{Rk}$. [DIN EN 1994-1-1, 2010] ensures 'ductile' shear connectors by geometric requirements for the studs themselves, as shown in section 2.2.1.

Especially in solid slab cases, shear studs may reach their displacement capacity when shear failure of the stud occurs. For this brittle failure behaviour, the resulting weakening of the shear interface and redistribution of the shear force to the next stud could lead to a 'zip-like' failure. To avoid this, it must be ensured that the slip does not exceed the displacement capacity of the studs. To do so, [DIN EN 1994-1-1, 2010] requires a minimum degree of shear connection, $\min \eta$. Thereby, it is differentiated between asymmetric steel sections, as shown in equation 2.30, and symmetric steel sections, as shown in equation (2.31). An additional and slightly lower minimum degree of shear connection is required when composite

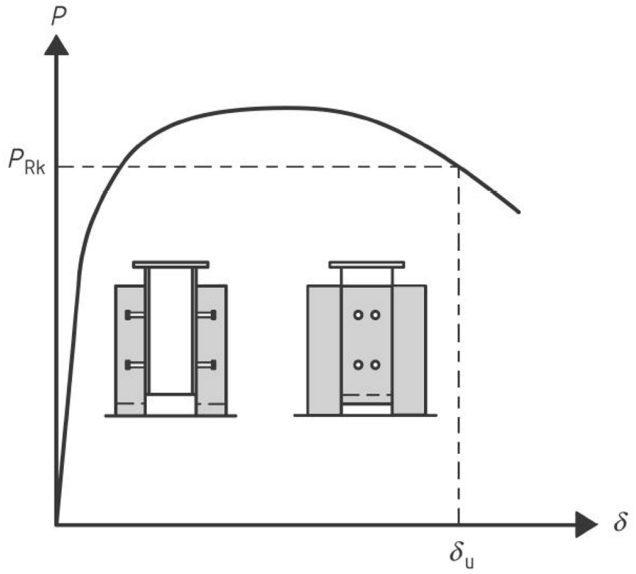


Figure 2.21: Displacement capacity, $\delta_u$, according to [DIN EN 1994-1-1, 2010].

slabs are used, as shown in equation 2.32.

$$\min \eta = \begin{cases} 1 - \dfrac{355}{f_y} \cdot (0.30 - 0.015 \cdot L_e) \geq 0.4 & \text{for } L_e \leq 20 \\ 1 & \text{for } L_e > 20 \end{cases} \tag{2.30}$$

$$\min \eta = \begin{cases} 1 - \dfrac{355}{f_y} \cdot (0.75 - 0.03 \cdot L_e) \geq 0.4 & \text{for } L_e \leq 25 \\ 1 & \text{for } L_e > 25 \end{cases} \tag{2.31}$$

$$\min \eta = \begin{cases} 1 - \dfrac{355}{f_y} \cdot (1.0 - 0.04 \cdot L_e) \geq 0.4 & \text{for } L_e \leq 25 \\ 1 & \text{for } L_e > 25 \end{cases} \tag{2.32}$$

where: $\min \eta$ Minimum degree of shear connection
$f_y$ Yield strength of the steel section
$L_e$ Length of positive moment area

However, equation (2.32) can only be applied when the following conditions are satisfied:

- The studs diameter is 19mm.
- The hight of the stud after welding must not be smaller than 76mm.
- The steel section is of double symmetry.
- The steel decking is placed transversely to the beam.
- The steel decking is continuous above the beam.
- Only one stud is welded in each deck rib.
- The height of the deck rib, $h_p$, must not be larger than 60mm.

- The width of the deck rib, $b_m$, must be at least two times the height of the deck rib, $h_p$.
- The bending resistance of the beam is determined by interpolation of the resistance, as shown in Figure 2.24.

This is rarely the case, and the other conditions for the minimum degree of shear connection must be used.

### 2.3.2 Analysis of the plastic bending resistance

If the requirements given in section 2.3.1 are satisfied, the bending resistance of a composite beam in positive bending can be determined using plastic design. The plastic bending resistance depends on the degree of shear connection. Full shear connection is achieved when the increase of the number of studs does not further increase the bending resistance. This is the case when the shear forces transferred by the studs exceed either the smaller of the compressive resistance of the concrete slab or the tensile resistance of the steel section. The bending resistance is then calculated from the plastic stress distribution. A typical example is shown in Figure 2.22.

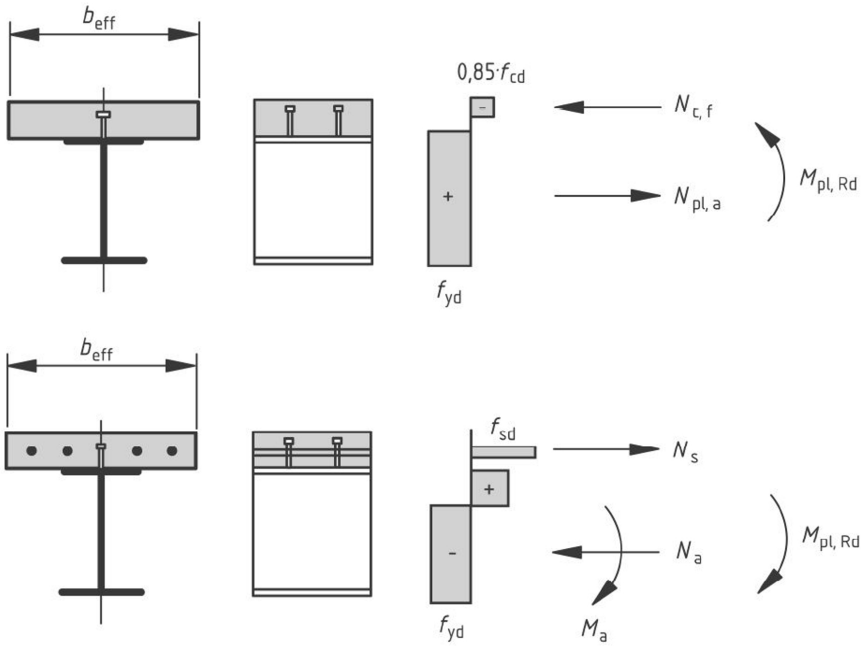


Figure 2.22: Examples of plastic stress distributions in a composite beam for full shear connection, from [DIN EN 1994-1-1, 2010].

If composite slabs are used, typically partial shear connection is achieved because of the limited number of studs along the span and the reduced shear resistance of the studs. In this case, the compression force in the concrete is determined by the shear resistance of the studs. The corresponding plastic stress distribution in the steel section is obtained from the equilibrium of axial forces. An example of a plastic stress distribution for partial shear connection is shown in Figure 2.23.

The analysis of the bending resistance using the plastic stress distribution leads to a function for the bending resistance in dependency of the degree of shear connection, as shown in Figure 2.24. Alternatively, [DIN EN 1994-1-1, 2010] allows the simplified analyse of the bending resistance by linear interpolation between the plastic bending resistance of the steel

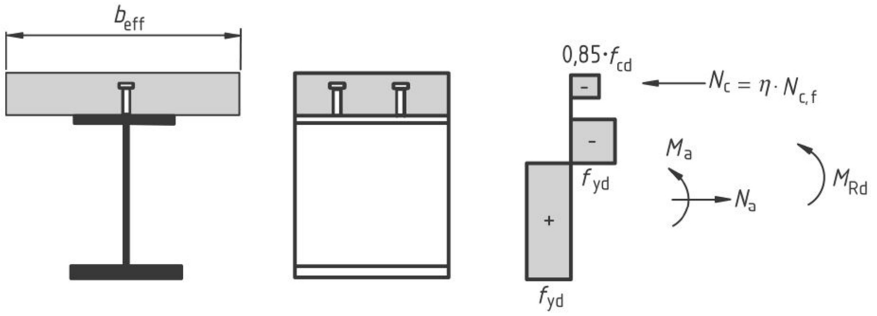


Figure 2.23: Example of a plastic stress distribution in a composite beam for partial shear connection, from [DIN EN 1994-1-1, 2010].

section and the plastic bending resistance of the composite section for full shear connection.

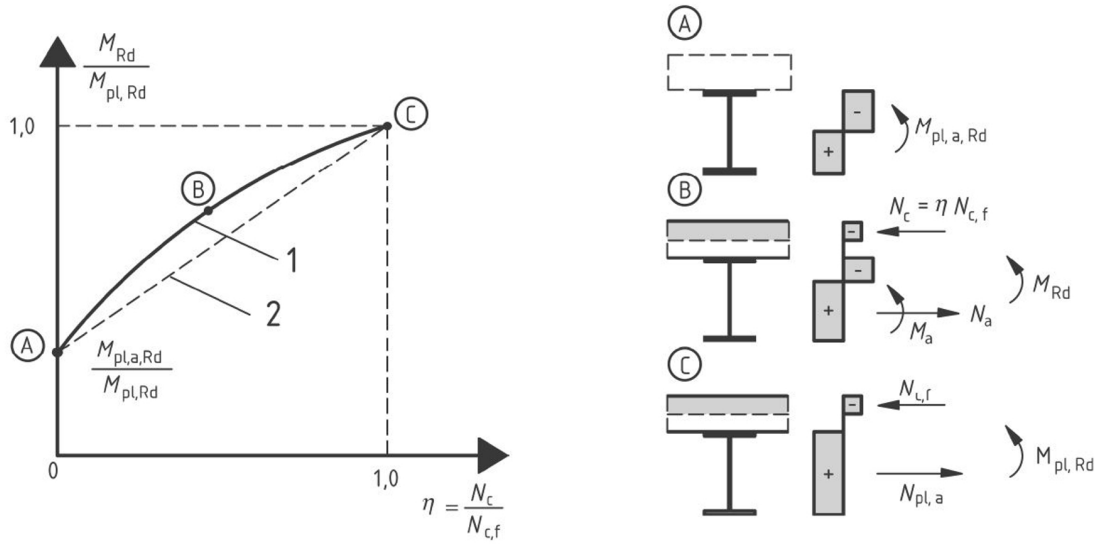


Figure 2.24: Plastic bending resistance of composite beams in dependency of the degree of shear connection, from [DIN EN 1994-1-1, 2010].

It can be concluded that the accurate prediction of the shear forces is very important for the analysis of the plastic bending resistance of composite beams.

If deep steel decking is used, and hence the shear resistance of the studs is small, it may be not possible to satisfy the required degree of shear connection, especially when long spans are required and higher steel grades are used. In such a case, [DIN EN 1994-1-1, 2010] does not allow to use plastic design. Instead the beam must be designed either by elastic analysis or non-linear analysis. Both makes the design of composite beams more complex and in some cases uneconomic or even impossible, as in elastic design it may not be possible to proof a sufficient bearing capacity of the studs. To conduct non-linear analysis, a sufficient knowledge of the behaviour of the materials and the shear connectors is required. This means that it may be necessary to conduct push-out tests in advance to obtain the load-slip behaviour of the shear connectors.

### 2.3.3 Analysis of the elastic behaviour

To analyse the behaviour of composite beam at serviceability limit state, typically the moment of inertia of the composite section transformed into steel, $I_i$, is used. In addition, the influence of shrinkage, creep and cracking of the concrete are to be considered. With respect to the evaluation of later tests and numerical analysis, only the stiffness for short time loading is discussed in this section.

$$I_{i,0} = I_a + A_a \cdot (z_a - z_{s,i})^2 + \frac{I_c}{n_0} + \frac{A_c}{n_0} \cdot (z_c - z_{s,i})^2 \tag{2.33}$$

| | | |
|---|---|---|
| where: | $I_{i,0}$ | Moment of inertia of composite section |
| | $I_a$ | Moment of inertia of steel section |
| | $I_c$ | Moment of inertia of concrete section |
| | $A_a$ | Area of steel section |
| | $A_c$ | Area of concrete section |
| | $z_a$ | Axis of steel section |
| | $z_c$ | Axis of concrete section |
| | $z_{s,i}$ | Neutral axis of composite section |
| | $n_o = \frac{E_a}{E_c}$ | Transformation factor (into steel) |
| | $E_a$ | Young's-Modulus of steel |
| | $E_c$ | Young's-Modulus of concrete |

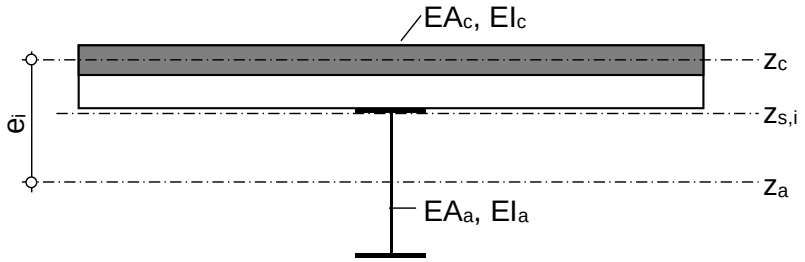


Figure 2.25: Composite section for the calculation of the bending stiffness.

According to [Yam, 1983], the bending stiffness of the composite beam can be also expressed using the composite stiffness parameter, $\alpha_i$, as shown in equation (2.34).

$$EI_{i,0} = (1 + \alpha_i) \cdot (EI_a + EI_c) \tag{2.34}$$

| | | |
|---|---|---|
| where: | $\alpha_i = \frac{e_i^2}{EI_a + EI_c} \cdot \frac{EA_a \cdot EA_c}{EA_a + EA_c}$ | Composite stiffness parameter |
| | $e_i$ | Axial spacing between steel section and concrete section |
| | $EA_a$ | Axial stiffness of steel section |
| | $EA_c$ | Axial stiffness of concrete section |
| | $EI_a$ | Bending stiffness of steel section |
| | $EI_c$ | Bending stiffness of concrete section |

The bending stiffness assumes a rigid shear connection where no end-slip occurs. However, shear connectors in composite construction are not rigid and the shear interface has a certain

flexibility. According to [Leskela et al., 2015] the flexibility of the shear connection can be considered by the flexibility parameter, $r_\delta$:

$$r_\delta = \frac{\alpha_i \cdot (EI_a + EI_c)}{\alpha_i \cdot (EI_a + EI_c) + \mu_m \cdot K_{sc,d} \cdot L_e^2 \cdot e_i^2 \cdot (\alpha_i + 1)} \begin{cases} \geq 0 \\ \leq 1 \end{cases} \tag{2.35}$$

| | | |
|---|---|---|
| Where: | $r_\delta$ | Flexibility parameter |
| | $L_e$ | Effective span between points of zero moment |
| | $K_{sc,d} = k_{s,ef}/s_c$ | Connection modulus |
| | $k_{s,ef}$ | Stiffness of shear connectors |
| | $s_c$ | Longitudinal spacing of shear connectors |
| | $\mu_m$ | Coefficient depending on the bending moment diagram<br>$\mu_m \approx 0.1$ for most common load distributions |

With the flexibility parameter, $r_\delta$, the composite action parameter can be reduced to consider the flexibility of the shear interface to give the effective composite action parameter, $\alpha_{i,eff}$:

$$\alpha_{i,eff} = \frac{1 - r_\delta}{1 + r_\delta \cdot \alpha_i} \cdot \alpha_i \tag{2.36}$$

With the effective value of the composite stiffness factor, $\alpha_{i,eff}$, the effective bending stiffness of the composite beam, $EI_{i,eff}$, can be determined, as follows:

$$EI_{i,eff} = (1 + \alpha_{i,eff}) \cdot (EI_a + EI_c) \tag{2.37}$$

The flexibility parameter, $r_\delta$, is defined as the ratio between the end-slip with flexible shear connection, $s_e$, and the maximum end-slip without shear connection, $s_{e,max}$. The end-slip with flexible shear connection then can be analysed according to equation (2.38).

$$s_e = r_\delta \cdot s_{e,max} \tag{2.38}$$

| | | |
|---|---|---|
| Where: | $s_{e,max} = \frac{A_m \cdot e_i}{EI_a + EI_c}$ | Maximum end-slip without shear connection |
| | $A_m$ | Area under the bending moment diagram<br>between maximum moment and the point of zero moment |

The presented equations will be compared to the results of composite beam tests.

# 3 Methodology and objectives

The previous sections showed, that the predicted shear resistance of headed studs in the ribs of composite slabs according to [DIN EN 1994-1-1, 2010] is not satisfactory for modern deep deck shapes. The presented alternative methods were not satisfactory, too. Because of this, the development of a new prediction formulae of the stud shear resistance is the objective of this work.

To reach this objective, the load-slip behaviour of shear connectors must be investigated. Because of the easy evaluation of the shear forces and slip, the push-out test is chosen for these investigations. Because [Hicks and Smith, 2014] reported that push-out tests may be conservative in comparison to beam tests , transverse loading is used in most of the push-out tests. The investigated parameters of the test programme are:

- The type of steel decking: 58mm or 80mm deep decking.
- The influence of different degrees of concentric transverse loading.
- The influence of eccentric transverse loading.
- The concrete strength: C20/25 or C30/37.
- The number of studs per rib: Single studs or pairs of studs per rib.
- The number of reinforcement layers: One or two layers.
- The welding procedure: Directly to the flanges of the beam or through deck welding.

The observed influences of the transverse loads on the load-slip behaviour are used to draw conclusions on an improved push-out test set-up to be used for cases with composite slaps.

To evaluate the suggested degree of transverse loading in push-out tests, two composite beam tests are conducted for comparison. The beam tests use the same decking, studs and concrete as the corresponding push-out tests. In addition, a low degree of shear connection is chosen to investigate the slip at which the plastic bending capacity is reached. Furthermore, the test results are used for the verification of numerical models.

The load-slip behaviour of the push-out tests and the observed failure modes are the basics for the development of a new prediction formulae for the shear stud resistance. The target is to describe the observed behaviour and failure modes based on simple and well known mechanical models. Statistical analysis according to [DIN EN 1990, 2002] is used to define the characteristic resistance and the design resistance for the newly developed equations.

Typically, the prediction of the shear stud resistance references only to the first maximum of the load-slip curve. The distribution of slip in a composite beams leads to an additional variability of the stud forces along the span that cannot be covered in the calibration of the stud shear resistance against push-out test results according to [DIN EN 1990, 2002]. To investigate this issue, a parametric study on composite beams is conducted using Finite Element Analysis. This analysis uses non-linear springs with the real load-slip curves from push-out tests to model the shear connection between steel beam and concrete slab.

In addition, the application of simplified load-slip curves is investigated. The target is to simplify the shear stud behaviour for the analysis of composite beams in engineering design offices.

The simplified load-slip curve is derived from the elastic stiffness of push-out specimens and assumes yielding of the spring until the displacement capacity is reached. The yield-force of the springs is derived from analysis using tested load-slip curves by averaging the forces of all studs showing plastic behaviour. This leads to a reduction factor to the first peak of the testes load-slip curve to determine the yield-force of the simplified load-slip curve.

# 4 Conducted push-out tests

Push-out tests are the common approach to investigate the behaviour of shear connectors. In section 2.1.3, different set-ups for push-out tests were shown.

Typically, the effectiveness of shear connectors in push-out tests is lower than in composite beam tests. It is explained, that this is because of the slabs vertical forces and bending moments as well as local effects that originate from the displacement or loading conditions. Even though previous research [Hicks and Smith, 2014, Rambo-Roddenberry, 2002] included concentric transverse loading, the influence of the slabs internal forces and moments is not well investigated.

A series of 33 push-out tests was conducted to investigate these influences. Furthermore, the influence of tension ties, the shape of the decking, the number of studs per rib, the number of reinforcement layers, the welding method and the concrete strength were investigated.

## 4.1 Consideration of transverse loading in push-out tests

[Hicks and Smith, 2014] investigated the transverse loading to find a value that results in a load-slip behaviour of the studs in push-out tests, which compared well with composite beam tests. The results of [Hicks and Smith, 2014] and [Rambo-Roddenberry, 2002] showed an improvement of the shear stud resistance, when concentric transverse loads were applied. However, the mechanism of how the transverse load influences the load-bearing behaviour, shown in Figures 2.1 to 2.2, was not answered. In addition, the influence of the negative bending moment of the slab was not considered. To do so, transverse loads are applied with an eccentricity to the push-out specimen, as shown in Figure 4.1.

[Hicks and Smith, 2014] proposed a transverse load of 12% of the longitudinal shear force, which was determined to calibrate the push-out test against the results of accompanying beam tests. A parametric study to investigate the ratio of the transverse load to the shear force at ultimate limit state is presented bellow. The study showed that a transverse load of 12% is not applicable for all deck shapes.

In this study, a single span composite beam as the inner support of a two span composite slab was considered, see Figure 4.2. A uniform imposed load of $q_k = 3.50$ kN/m$^2$ was assumed. The nominal material properties of steel grade S 355 and concrete grade C 30/37 were assumed. Two different deck shapes with a deck height of 58 and 80 mm were chosen. The bending resistance of the composite beam was determined for partial shear connection using the stud resistances according to the rules of [DIN EN 1994-1-1, 2010]. All configurations were designed to achieve the necessary resistance with the lowest possible number of studs.

The results of this study are shown in Figure 4.3. The ratio of the transverse load to the shear force is mostly dependent on the type of decking used. Deeper decks led to higher degrees of transverse loading because the shear force per stud is more reduced. Also longer beam spans led to lower degrees of transverse loading as the bending moment – and hence the required shear force – increased. For typical spans of the slab, the 58 mm deep decking resulted in degrees of transverse loading between 6.6% and 12.2%. The 80 mm deep decking resulted in values between 13.0% and 20.8%. Thus, the transverse load of

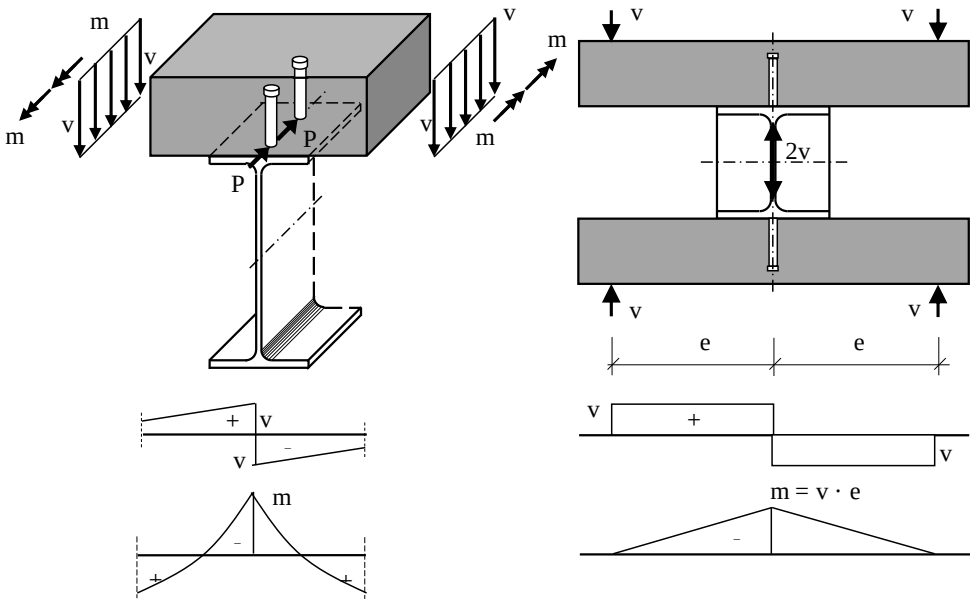


Figure 4.1: Internal forces and moments at the line of the shear studs in a composite beam and their reflection in a push-out test.

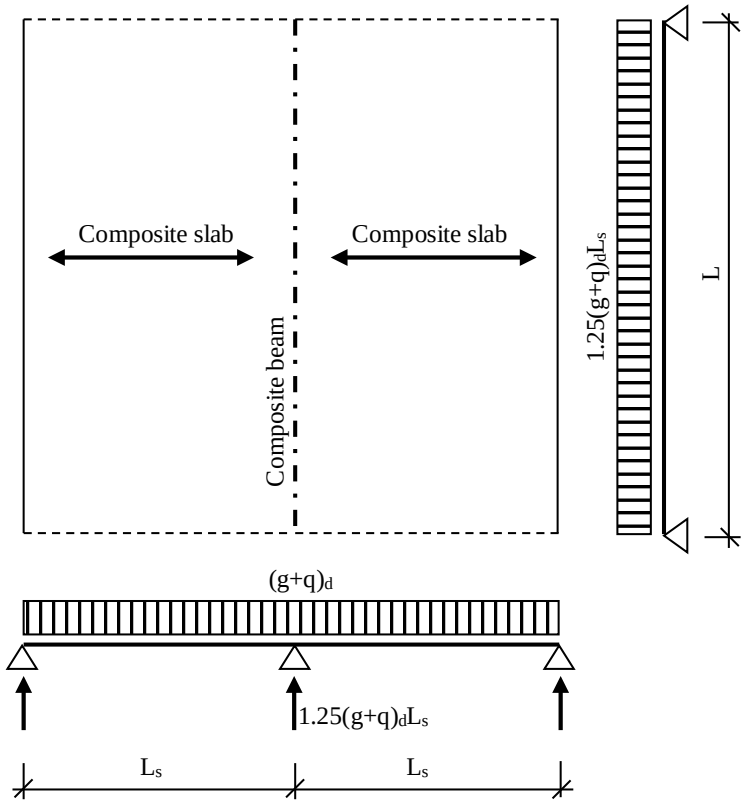


Figure 4.2: Static system used for parametric studies on the degree of transverse loading.

12% proposed by [Hicks and Smith, 2014] could not be guaranteed in all cases considering the loading conditions of the composite beam.

The transverse loads in the presented push-out test programme are chosen to reflect degrees

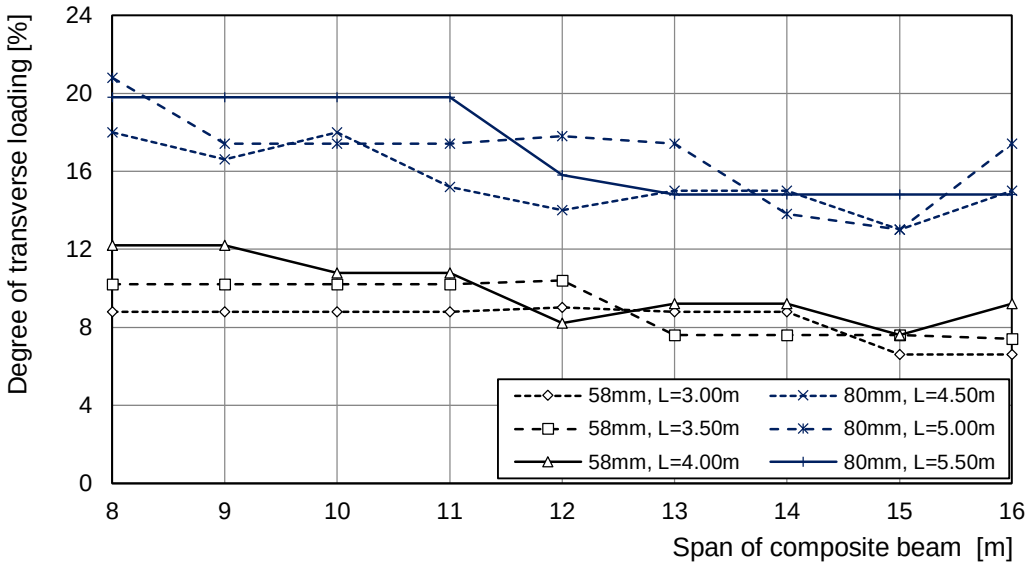


Figure 4.3: Degree of transverse loading versus span of the composite beam for different deck heights and spans of the slab, $L$.

of transverse loading of 8% and 16% of shear force. These are typical values for the two considered deck shapes. In the push-out tests concentric and eccentric transverse loads are included to investigate the influence on the load-bearing behaviour.

## 4.2 Test set-up for transverse loading

The test set-up, which was used for the application of the transverse loads, is shown in Figures 4.4 and 4.5. The clamping device consists of the three main parts HP1, HP2 and HP5. The two parts HP1 and HP2 are loaded by a horizontal hydraulic jack. The inner part HP2 pushes on the left slab and the part HP1 is pushed outwards. Because HP1 is connected to HP5 on the other side of the specimen, HP5 is pulled against the right slab to apply the transverse load.

The parts HP3 and HP4 were used to apply concentric transverse loading. The clamping device can be utilized to apply eccentric transverse loads by removing the parts HP3 and HP4.

The beams HP6 were used to compensate the differences of the height between specimens with 58 mm and 80 mm deep decking, so that the specimens were vertically centred within the device.

To ensure that only the influence the transverse loading was investigated and the bending of the slabs was not restrained, the friction at the supports of the specimen was minimized with pads of PTFE.

Some tests were conducted without transverse loading. In these tests, the slabs were placed in mortar beds to achieve a non-sliding. Tension ties, as shown in Figure 2.3, were not used. Further tests were conducted to investigate the influence of tension ties. Thereby, two different types of fixation were applied to the bars.

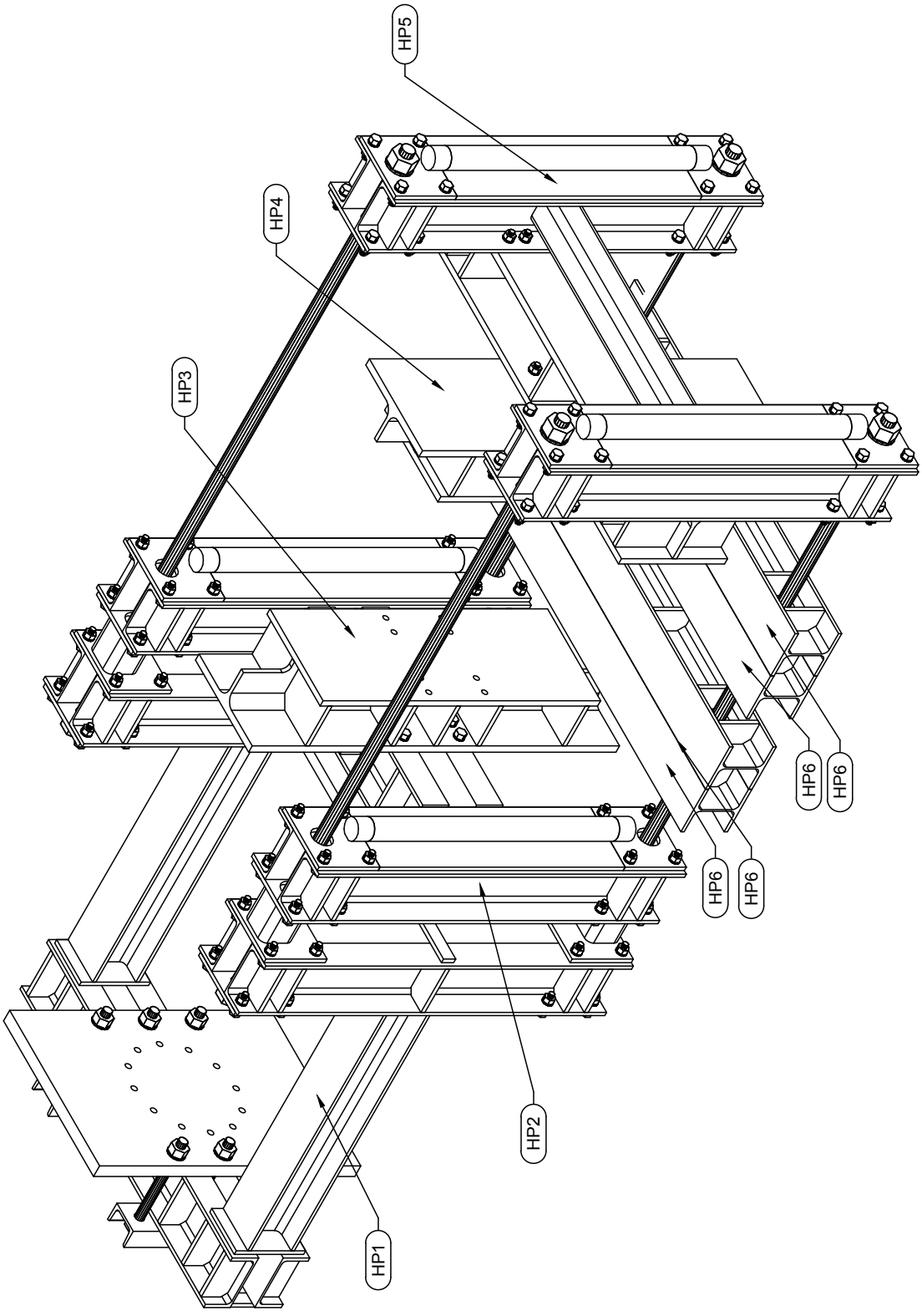


Figure 4.4: Schematic view of the clamping device for the application of transverse loads.

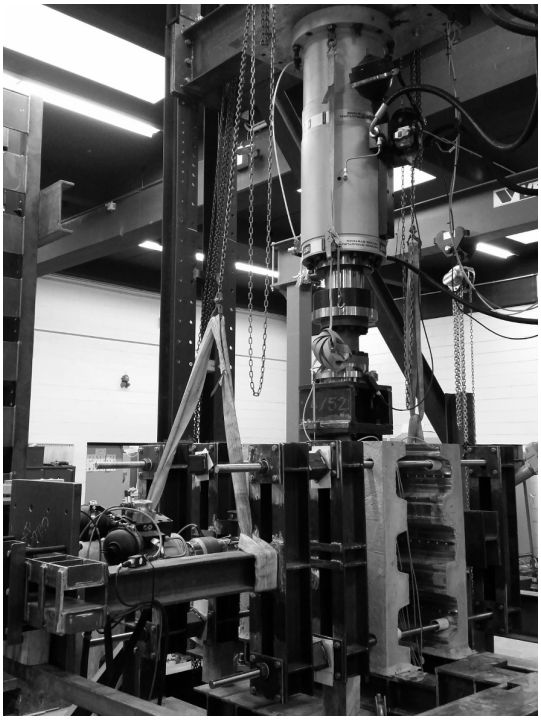

(a) Parts HP1, HP2 and HP3.

(b) Parts HP4 and HP5.

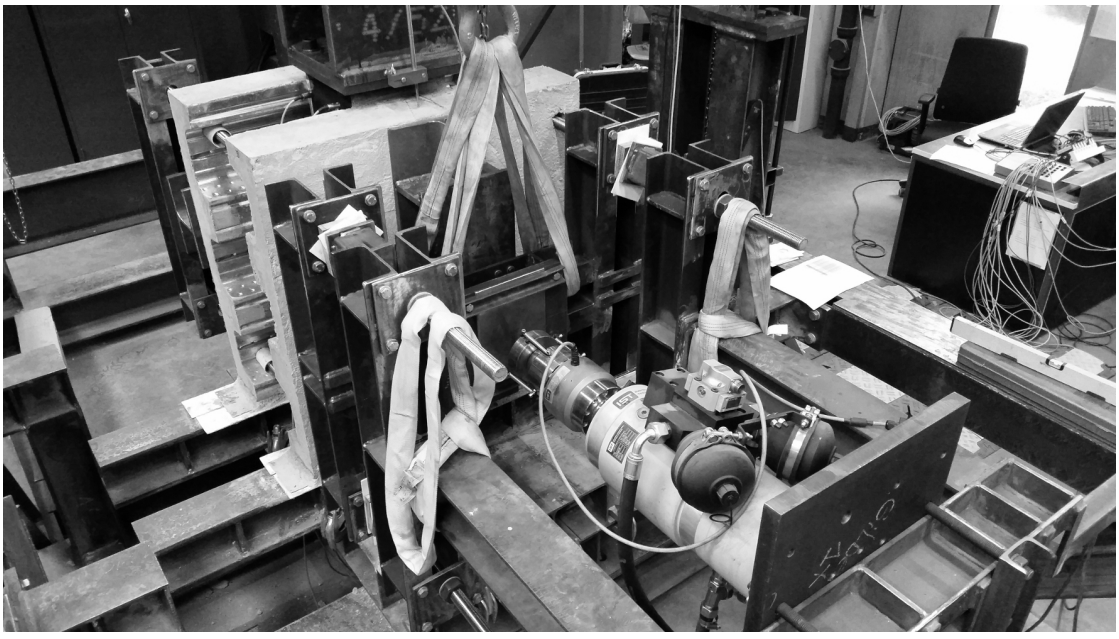

(c) Hydraulic Jack used for the load application

Figure 4.5: Test set-up for the application of transverse loading assembled for concentric loading.

## 4.3 Test programme and material properties

The push-out tests used three types of composite decking, as shown in Figure 4.6 and Table 4.1. The 80 mm deep RD80 decking was only used in early pilot testing and then was changed to CF80 decking, which has a more common shape. An overview of the conducted push-out tests is shown in Table 4.2.

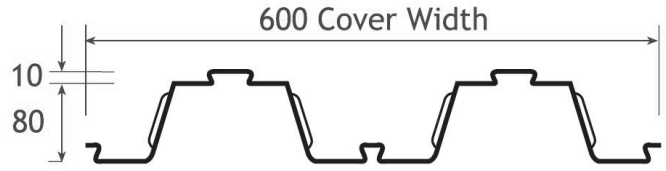


(a) RD80 decking

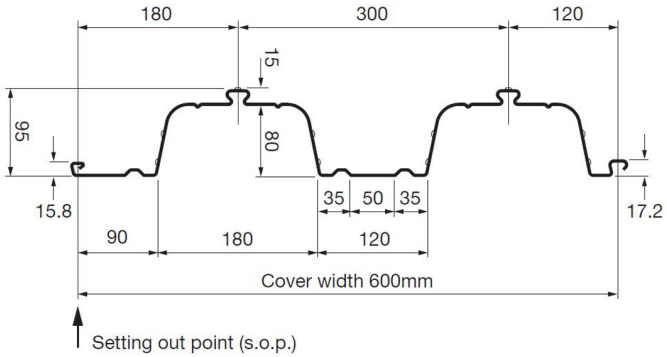


(b) CF80 decking

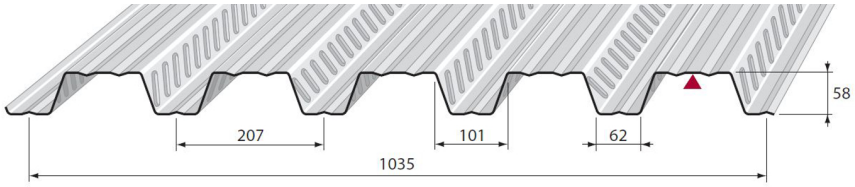


(c) CP60 decking

Figure 4.6: Composite decking used in push-out tests.

Table 4.1: Composite decking used in push-out tests.

| Decking | ID | $h_p$ [mm] | $b_u$ [mm] | $b_o$ [mm] | $a$ [mm] | $t$ [mm] |
|---|---|---|---|---|---|---|
| Ribdeck 80 | RD80 | 80 | 135 | 185 | 300 | 1.20 |
| ComFlor 80 | CF80 | 80 | 120 | 137.5 | 300 | 0.90 |
| Cofraplus 60 | CP60 | 58 | 62 | 101 | 207 | 0.885 |

$h_p$: Height of the rib
$b_u$: Width of the rib at the bottom
$b_o$: Width of the rib at the top
$a$: Spacing of the ribs
$t$: Thickness of the decking

The two tests of series PV were conducted to investigate if the clamping device, shown in section 4.2, is suitable for the application of transverse loading. The specimens had eccentric transverse loads of 10% of the vertical test load applied to each slab. RD80 decking with single shear studs of 19 mm diameter and 150 mm height were used in these tests. The

Table 4.2: Material properties, stud configuration and transverse loading of push-out tests

| Series | Test | Decking | Studs | | Concrete | Reinforcement | | Transverse load | |
|---|---|---|---|---|---|---|---|---|---|
| | | | Type | $n_r$ | | top | bottom | $P_T$ | $e$ |
| | | | [mm] | [mm] | [mm] | | | [kN/side] | [mm] |
| PV | 1, 2 | RD80 | 19x150 | 1 | C30/37 | ∅10/150 | ∅10/150 | 20%[3] | 380 |
| 1-04 | 1 | CP60[1] | 22x125 | 1 | C20/25 | Q335A | Q188A | 8.2%[3] | 0 |
| | 2, 3 | CP60[1] | 22x125 | 1 | C20/25 | Q335A | Q188A | 12.5 | 0 |
| 1-05 | 1 | CP60[1] | 22x125 | 1 | C20/25 | Q335A | Q188A | 16.4%[3] | 0 |
| | 2, 3 | CP60[1] | 22x125 | 1 | C20/25 | Q335A | Q188A | 25.0 | 0 |
| 1-06 | 1 | CP60[1] | 22x125 | 1 | C20/25 | Q335A | Q188A | 8.2%[3] | 380 |
| | 2 | CP60[1] | 22x125 | 1 | C20/25 | Q335A | Q188A | 12.5 | 380 |
| | 3 | CP60[1] | 22x125 | 1 | C30/37 | Q335A | Q188A | 12.5 | 380 |
| 1-07 | 1 | CP60[1] | 22x125 | 1 | C30/37 | Q335A | Q188A | 16.4%[3] | 380 |
| | 2, 3 | CP60[1] | 22x125 | 1 | C30/37 | Q335A | Q188A | 30.0 | 380 |
| 1-08 | 1, 2 | CF80 | 19x125 | 2[2] | C30/37 | - | Q188A | weak tie | 250 |
| | 3 | CF80 | 19x125 | 2[2] | C30/37 | - | Q188A | strong tie | 250 |
| 1-09 | 1 | CF80 | 19x125 | 2[2] | C30/37 | - | Q188A | 8.8 | 0 |
| | 2, 3 | CF80 | 19x125 | 2[2] | C30/37 | - | Q188A | 17.5 | 0 |
| 1-10 | 1 | CF80 | 19x125 | 2[2] | C30/37 | - | Q188A | 17.5 | 0 |
| | 2 | CF80 | 19x125 | 2[2] | C30/37 | - | Q188A | 13.2 | 0 |
| | 3 | CF80 | 19x125 | 2[2] | C30/37 | - | Q188A | 0 | 0 |
| 1-11 | 1 | CF80 | 19x125 | 2[2] | C30/37 | - | Q188A | 7.6%[3] | 380 |
| | 2, 3 | CF80 | 19x125 | 2[2] | C30/37 | - | Q188A | 17.5 | 380 |
| 3-01 | 1, 2 | CF80 | 19x125 | 2[2] | C30/37 | Q335A | Q188A | strong tie | 250 |
| | 3 | CF80 | 19x125 | 2[2] | C30/37 | Q335A | Q188A | 0 | 0 |
| 3-02 | 1 | CF80[1] | 19x125 | 2[2] | C30/37 | - | Q188A | 0 | 0 |
| NR1 | 1 | CF80 | 19x125 | 1 | C30/37 | - | Q188A | 0 | 0 |
| | 2 | CF80 | 19x125 | 1 | C30/37 | - | Q188A | 8.8 | 0 |
| | 3 | CF80 | 19x125 | 1 | C30/37 | - | Q188A | 17.5 | 0 |

[1] Decking was pre-punched

[2] Transverse spacing of studs was 100 mm

[3] Continuously measured and adjusted to the given percentage of the shear force per slab

studs were welded through the decking in favourable position. The specimens had no recess applied to the slabs. Apart from the deck shape and stud position, the dimensions of the specimens were the same as for specimens with CF80 decking, shown in Figure 4.8.

In test series 1-04 to 1-07, CP60 decking with single studs per rib of 22 mm diameter and 125 mm height were used. The studs were welded directly to the flange of the beam and the decking was pre-punched. All specimens had the optional recess according to [DIN EN 1994-1-1, 2010] Annex B applied to the slabs. Two layers of reinforcement were used. A typical specimen is shown in Figure 4.7.

Series 1-04 and 1-05 investigated the influence of the degree of concentric transverse loading. Series 1-06 introduced the influence of the eccentricity on the load-slip behaviour, as well as the influence of a higher concrete strength. Series 1-07 investigated the influence of larger degrees of eccentric transverse loading.

Series 1-08 to 1-11 used CF80 decking. Pairs of studs with a transverse spacing of 100 mm were welded through the decking. Headed shear studs with 19 mm diameter and 125 mm height were used. Only one layer of reinforcement was placed 30 mm above the deck rib. The reinforcement was chosen according to [DIN EN 1994-1-1, 2010] clause 9.8.1.(2). The optional recess was not used. A typical specimen is shown in Figure 4.8.

The influence of a second layer of reinforcement was investigated in series 3-01. In series

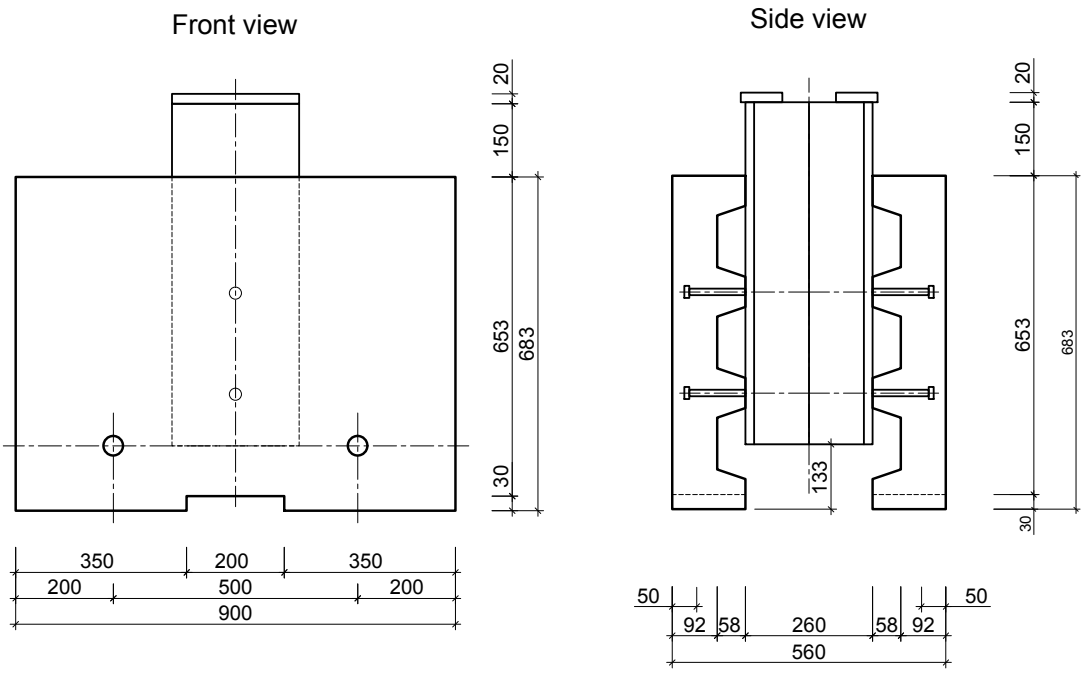


Figure 4.7: Dimensions of push-out specimens with CP60 decking.

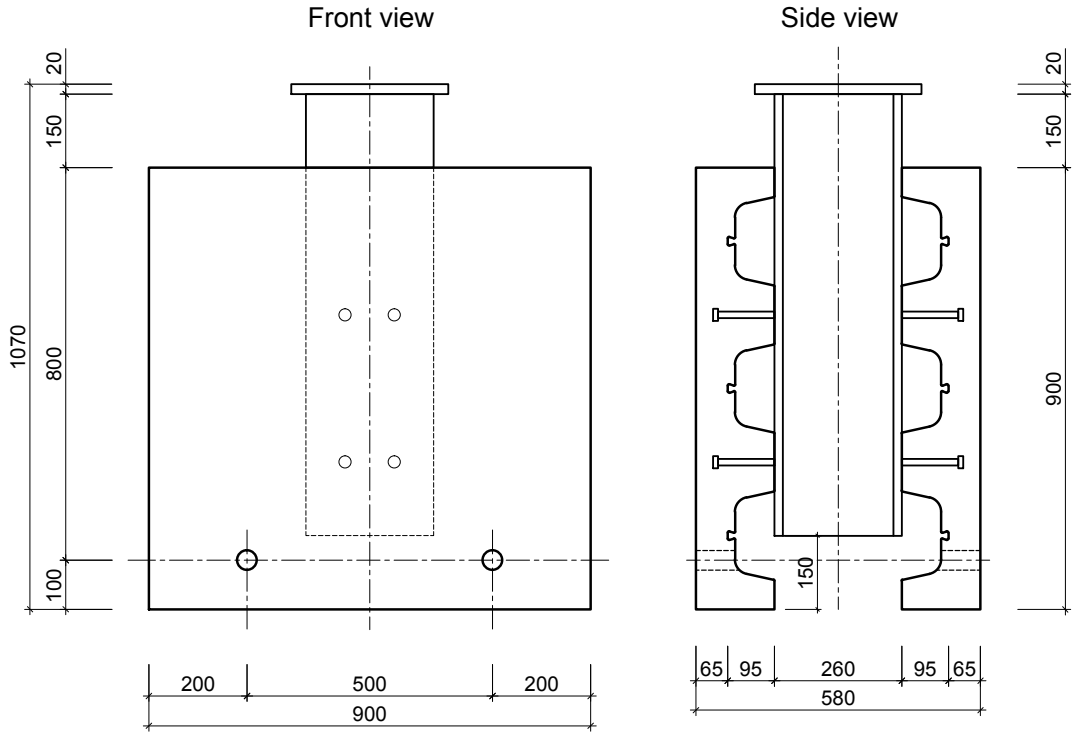


Figure 4.8: Dimensions of specimens with CF80 decking.

3-02, the influence of pre-punching the decking was investigated. Series NR1 introduces the influence of the number of studs per rib. The influence of the degree of concentric transverse loading was investigated in series 1-09, 1-10 and NR1. The influence of the eccentricity was investigated in series 1-11. Furthermore, the influence of the boundary conditions was investigated in series 1-08 and 3-01. Two types of transverse restraints were used: Tension

ties with weak fixations, as shown in Figure 4.9, and tension ties with strong fixations, as shown in Figure 4.10. The tension ties were placed close to the corners of the slabs with an horizontal eccentricity to the beam of 250 mm.

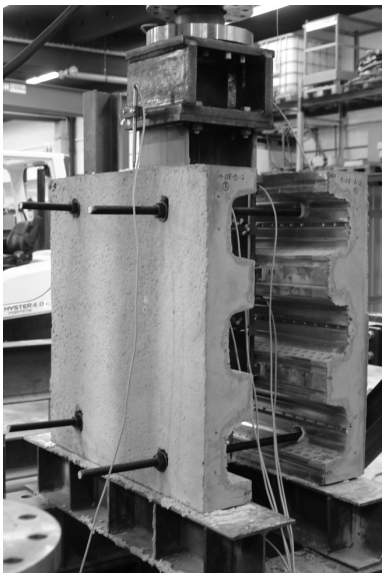

Figure 4.9: Tension ties with weak fixation.

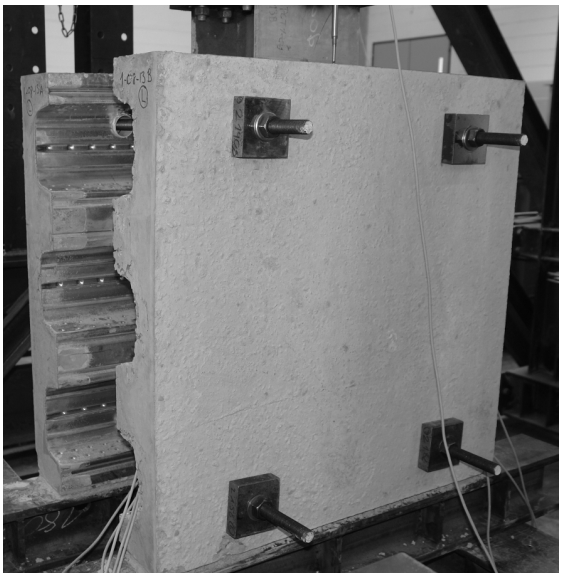

Figure 4.10: Tension ties with strong fixation.

## 4.4 Test results

### 4.4.1 General

The following sections present the conducted push-out tests. The focus lies on the presentation of the observed failure modes and load-slip curves. A detailed evaluation of the test results concerning the characteristic resistance, $P_{Rk}$, slip capacity, $\delta_{uk}$, and the influence of important testing parameters like transverse loading is given in chapter 5.

### 4.4.2 Series PV

The specimens in series PV used RD80 decking. Single shear connectors of 19 mm diameter and 150 mm height were welded through the decking. A single layer of reinforcement, made of 10 mm diameter bars at a spacing of 150 mm, was placed 30 mm above the decking. No recess was applied to the slabs.

The tests had an eccentric transverse load, $P_T$, of 10% of the vertical tests load, $P_e$, applied to each slab. This is a degree of transverse loading of 20% for each shear interface. As shown in Figure 4.3, this ratio would be valid for a span of the composite slab of 5.50 m and a span of the composite beam of up to 11.00 m.

The load-slip curves obtained from the tests are shown in Figure 4.11. The measured material properties, stud dimensions, test loads and failure modes are summarised in Table 4.3.

As shown in Figure 4.11, both specimens had a load-slip behaviour without a second load peak. Specimen PV-1 reached its maximum test load of 465.6 kN at a slip of about 2.5 mm. The maximum load of PV-2 was 426.6 kN and was reached at a slip of about 1.5 mm. The influence of relaxation was about 7% for both tests.

During the conduction of the tests, the only damage to the concrete that was observed, were diagonal cracks in the ribs, as shown in Figure 4.12. The cracks were first observed at about 50% to 60% of ultimate load. In combination with the minor plastic deformations before ultimate load was reached, it is concluded that the failure of the ribs (RF) was the decisive failure mechanism.

Further displacement then lead to stud failure (SF) in both tests, as shown in Figure 4.13. As can be seen in Figure 4.13a, the studs punched through the decking even though they were through deck welded. Furthermore, porosity was observed in the welding area, as shown in Figure 4.13b.

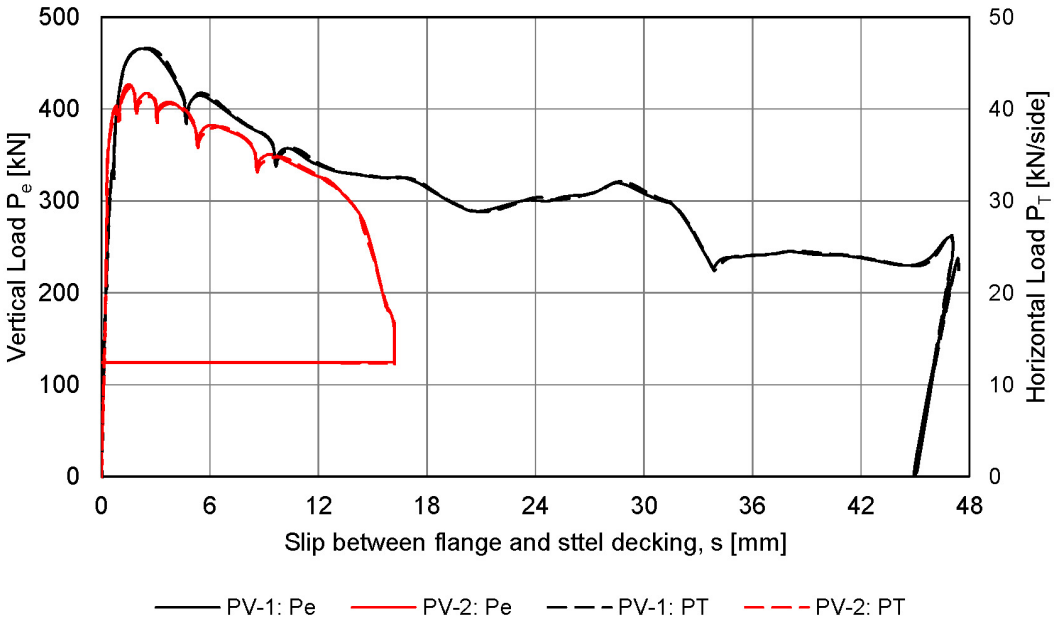


Figure 4.11: Load-slip curves for series PV.

Table 4.3: Test results for series PV.

| | | 1 | 2 | PV |
|---|---|---|---|---|
| $f_{cm}$ | [N/mm$^2$] | 45.80 | 45.80 | 45.80 |
| $E_{cm}$ | [N/mm$^2$] | 34000[1] | 34000[1] | 34000[1] |
| $f_u$ | [N/mm$^2$] | 551 | 551 | 551 |
| $n_r$ | [-] | 1 | 1 | 1 |
| $d$ | [mm] | 19.1 | 19.1 | 19.1 |
| $h_{sc}$ | [mm] | 143.75 | 143.00 | 143.38 |
| $P_e$ | [kN] | 465.64 | 426.64 | 446.14 |
| | [kN/stud] | 116.41 | 106.66 | 111.54 |
| $P_{e,static}$ | [kN] | 433.64 | 396.44 | 415.04 |
| | [kN/stud] | 108.41 | 99.11 | 103.76 |
| $P_T$ | [kN] | 10% | 10% | 10% |
| $e$ | [mm] | 380 | 380 | 380 |
| Failure | | RF,SF | RF,SF | |

[1] Calculated according to [DIN 1045-1, 2008]

Figure 4.12: Typical cracks in the ribs observed in specimens with RD80 decking.


(a) Failure surface on the slab.


(b) Failure surface on the beam.

Figure 4.13: Stud failure in RD80 decking.

To identify the displacement capacity of these tests according to [DIN EN 1994-1-1, 2010], the characteristic resistance is assumed as the 90% of the minimum resistance, which results in a test load of 384 kN. The load-slip curves drop to this load at a slip of about 8mm for specimen PV1 and about 5mm for specimen PV2. Assuming the characteristic displacement capacity as 90% of the minimum slip capacity this results in about 4.5mm, which is not ductile according to [DIN EN 1994-1-1, 2010], where a displacment capacity of 6mm is required.

However, the measured slip in this series is the relative displacement between the steel beam and the steel decking. As can be seen in Figure 4.13a, the stud punched through the decking, which means that they showed a larger displacement than measured. After testing, the difference was about 10mm, as can be seen in Figure 4.13a. To identify the total displacement of the shear studs, the following tests measured also the relative displacement between the steel beam and the support of the specimen.

### 4.4.3 Series 1-04

The specimens in series 1-04 used CP60 decking. The decking was pre-punched and single shear studs per rib with 22 mm diameter and 125 mm height were welded directly to the flange of the beam. Two layers of reinforcement were used. The bottom layer was a Q188A wire fabric and the top layer a Q335A wire fabric. The concrete cover was 15 mm. All specimens had a recess according to [DIN EN 1994-1-1, 2010], Annex B.

Specimen 1-04-1 had a concentric transverse load of 4.1% of the test load applied to each slab. Based on the results of this test, a constant transverse load of 12.5 kN was applied in the two remaining tests. The transverse load of 4.1% results in a degree of transverse loading of 8.2% per shear interface. As shown in Figure 4.3, this value is applicable in most cases for CP60 decking.

The load-slip curves obtained from the tests are shown in Figure 4.14. Table 4.4 summarises the test results and measured material properties and stud dimensions.

Table 4.4: Test results for series 1-04.

| | | 1 | 2 | 3 | 1-04 |
|---|---|---|---|---|---|
| $f_{cm}$ | [N/mm$^2$] | 30.62 | 30.89 | 30.91 | 30.62 |
| $E_{cm}$ | [N/mm$^2$] | 20900 | 21500 | 21500 | 21300 |
| $f_u$ | [N/mm$^2$] | 551 | 551 | 551 | 551 |
| $n_r$ | [-] | 1 | 1 | 1 | 1 |
| $d$ | [mm] | 22.16 | 22.24 | 22.20 | 22.20 |
| $h_{sc}$ | [mm] | 124.33 | 124.02 | 123.97 | 124.11 |
| $P_e$ | [kN] | 295.76 | 294.44 | 274.64 | 288.28 |
| | [kN/stud] | 73.94 | 73.61 | 68.66 | 72.07 |
| $P_{e,static}$ | [kN] | 281.76 | 278.52 | 260.12 | 273.47 |
| | [kN/stud] | 70.44 | 69.63 | 65.03 | 51.28 |
| $P_T$ | [kN] | 4.1% | 12.5 | 12.5 | |
| $e$ | [mm] | 0 | 0 | 0 | |
| Failure | | SF<br>CPO<br>RPT | CPO<br>RPT | SF<br>CPO<br>RPT | |

All specimens showed a load-slip behaviour with two load peaks, as shown in Figure 4.14. The load bearing behaviour matches the model according to [Lungershausen, 1988], described

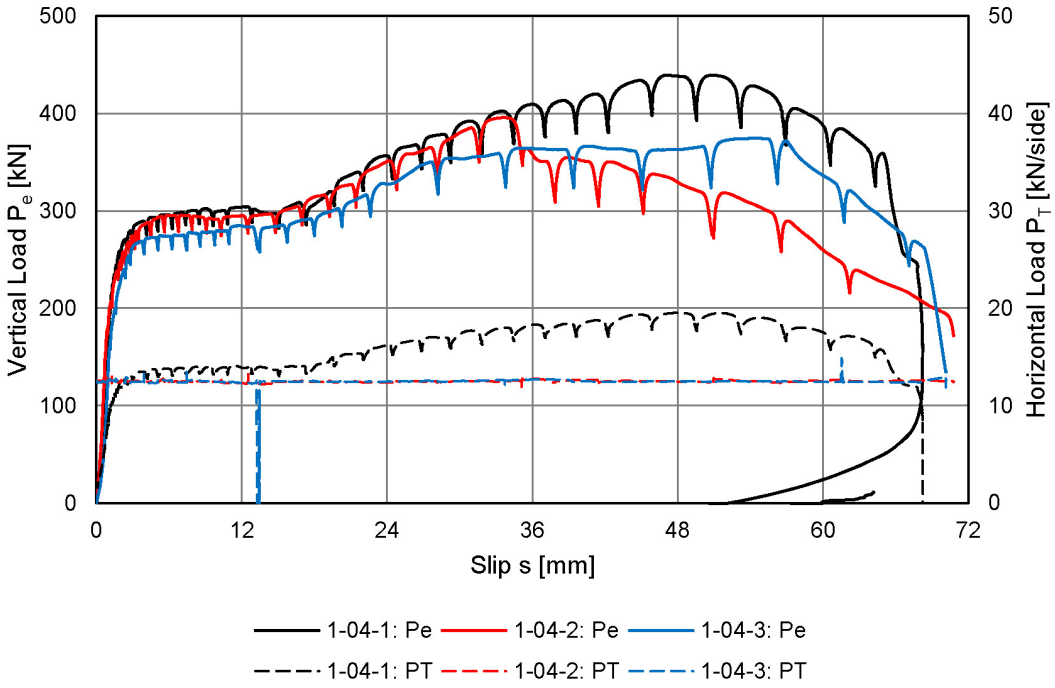


Figure 4.14: Load-slip curves for series 1-04.

in section 2.1.2. When the first peak load was reached, no damage was visible on the specimens. For further displacement, first a bulge in the decking in front of the studs occurred. Finally the studs punched through the decking, as shown in Figures 4.15 and 4.16. This is called rib punch-through failure (RPT). According to [Lungershausen, 1988], the first load peak must be characterised by the development of S-shaped stud deformation, as shown in Figure 4.18.

Further displacement lead to an increase of the test load until a second load peak was reached. This increase is because of the tension forces developing in the stud shank [Lungershausen, 1988]. The final failure modes for these tests were stud shearing (SF), shown in Figure 4.17, or concrete pull-out (CPO), shown in Figure 4.19. Failure of the shear studs was observed directly above the weld collar. Because failure occurred at large slip, it was a combined failure in tension and shear. Failed shear studs did not show any porosity in the stud shank, as shown in Figure 4.17.

As can be seen in Figure 4.14, the test loads slowly decrease after the second load peak. Especially specimen 1-04-2, which did not show stud failure, showed a very slow decrease of the test load. It is concluded that concrete pull-out is a slowly progressing failure. The damage on ribs, that did not fully fail, showed that the development of cracks started at the top corner of the rib on the tensioned side and the must have increases slowly.

The different application methods for the transverse loading did not show a significant influence on the load-slip behaviour.

Figure 4.15: Rib punch-through failure.

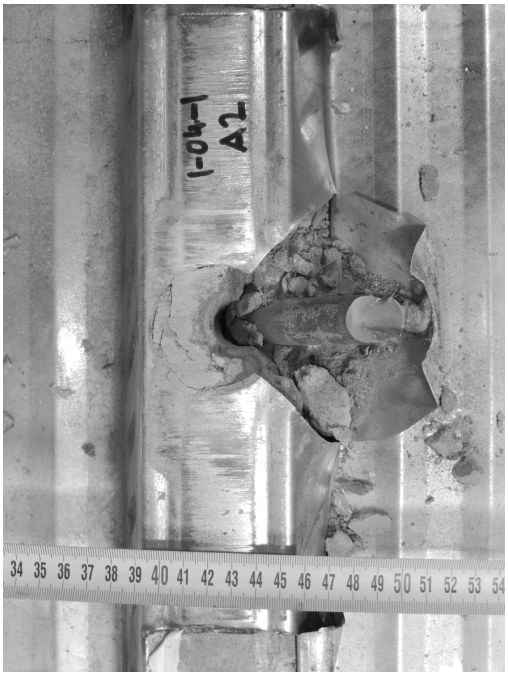


Figure 4.16: Damaged decking because of rib punch-through failure.

Figure 4.17: Failure surface of the shear studs.

Figure 4.18: Stud deformation after testing.


Figure 4.19: Concrete pull-out failure.

### 4.4.4 Series 1-05

Series 1-05 used pre-punched CP60 decking. Single studs per rib with 22 mm diameter and 125 mm height were welded directly to the flange of the beam. Two layers of reinforcement were used. The slabs had the recess according to [DIN EN 1994-1-1, 2010] Annex B applied.

The degree of concentric transverse loading was doubled to a transverse load of 8.2% of the tests load in specimen 1-05-1. For constant transverse loading, the value was also doubled to 25 kN in specimens 1-05-2 and 1-05-3.

The obtained load-slip curves are shown in Figure 4.20. Table 4.5 summarises the measured material properties, stud dimensions and test results.

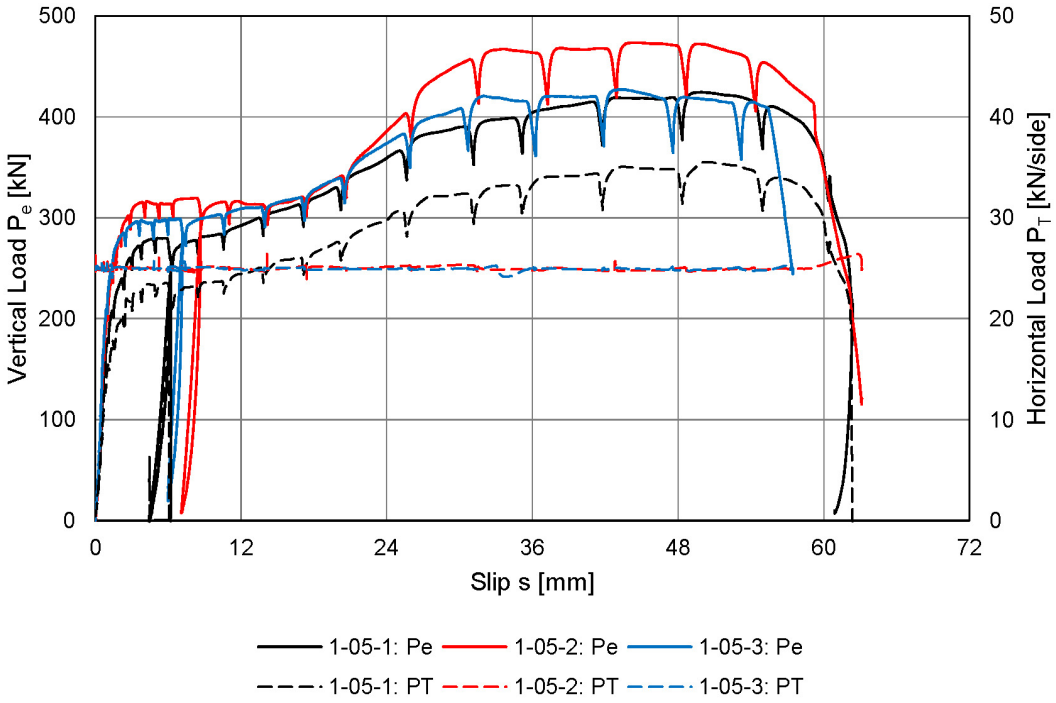


Figure 4.20: Load-slip curves for series 1-05.

In principle, the tests showed the same behaviour as series 1-04. All specimen had a load slip behaviour with two load peaks, as shown in Figure 4.20. When the first load peak was reached, rib punch-trough failure was observed. After the second load peak was reached, the specimens finally failed by stud failure or concrete pull-out.

Considering the first peak load, the observed influence of the degree of transverse loading was marginal in comparison to series 1-04. The average resistance increased by only 2.4 kN per stud. This is an increase of 3.4%. The second load peak was more pronounced and reached at a smaller slip. The test load at the second peak was about 50 kN larger than in series 1-04. The deformation capacity decreased. The maximum displacement at failure that was observed was about 60.4 mm in specimen 1-05-1. In series 1-04, the maximum displacement at failure was 68.3 mm in specimen 1-04-3.

Considering the influence of variable or constant transverse loading, specimen 1-05-1 with variable loading showed the lowest resistance in series 1-05. In series 1-04, specimen 1-04-1 with variable loading showed the highest resistance. Hence, the differences in the behaviour of tests with variable or constant are the natural variability of the shear connection.

Table 4.5: Test results for series 1-05.

| | | 1 | 2 | 3 | 1-05 |
|---|---|---|---|---|---|
| $f_{cm}$ | [N/mm$^2$] | 30.71 | 30.71 | 32.55 | 31.99 |
| $E_{cm}$ | [N/mm$^2$] | 22100 | 22100 | 22800 | 22333 |
| $f_u$ | [N/mm$^2$] | 551 | 551 | 551 | 551 |
| $n_r$ | [-] | 1 | 1 | 1 | 1 |
| $d$ | [mm] | 22.16 | 22.17 | 22.20 | 22.18 |
| $h_{sc}$ | [mm] | 124.03 | 123.80 | 123.93 | 123.92 |
| $P_e$ | [kN] | 279.80 | 316.60 | 297.72 | 298.04 |
| | [kN/stud] | 69.95 | 79.15 | 74.43 | 74.51 |
| $P_{e,static}$ | [kN] | 265.59 | 278.52 | 283.43 | 275.85 |
| | [kN] | 66.40 | 69.63 | 70.86 | 68.96 |
| $P_T$ | [kN] | 8.2% | 25.0 | 25.0 | |
| $e$ | [mm] | 0 | 0 | 0 | |
| Failure | | SF<br>CPO<br>RPT | SF<br>CPO<br>RPT | SF<br>CPO<br>RPT | |

### 4.4.5 Series 1-06

In series 1-06, pre-punched CP60 decking was used. Shear studs with 22 mm diameter and 125 mm height were welded directly onto the beam. The slabs had two layers of reinforcement and the recess according to [DIN EN 1994-1-1, 2010] Annex B.

For specimens 1-06-1 and 1-06-2, the concrete strength was about 30 N/mm$^2$, which was similar to series 1-04 and 1-05. Specimen 1-06-3 had a higher concrete strength of about 44 N/mm$^2$.

In specimen 1-06-1, a variable transverse load of 4.1% of the test load was applied eccentrically. For specimen 1-06-2, a constant transverse load of 12.5 kN was applied eccentrically. To compare the influence of the higher concrete strength in specimen 1-06-3 with these tests, the constant eccentric transverse load of 12.5 kN was maintained.

The measured material properties, stud dimensions, transverse loads and test results are summarised in Table 4.6. The obtained load-slip curves are shown in Figure 4.21.

Considering the load-slip curves of specimens 1-06-1 and 1-06-2, it was observed that the first load peak was reached at approximately the same load as in series 1-04. Rib punch through failure was observed. The second peak load was less pronounced than in series 1-04. Finally, the specimens failed by concrete pull-out. The smaller second load peak gives evidence that the tension force in the stud shank was less than in series 1-04. Because of the absence of stud failure, it is assumed that tension in the stud shank is the dominant influence on stud failure.

The concrete of specimen 1-06-3 was cast on a different date than the first two specimens and had an about 44% higher concrete strength. The first peak load increased by about 26% to 90.3 kN per stud. It was reached at an about 2 mm smaller slip.The shape of the first peak load was more pronounced. For further loading, rib punch-through failure was observed, too. The test load increased to a second peak load, which was reached at an approximately 50% lower slip than in series 1-04. Finally, specimen 1-06-3 failed by stud failure.

Comparing the results of specimens 1-06-1 and 1-06-2 to series 1-04, eccentric transverse loading decreased the second peak load. The first peak load was almost unaffected.

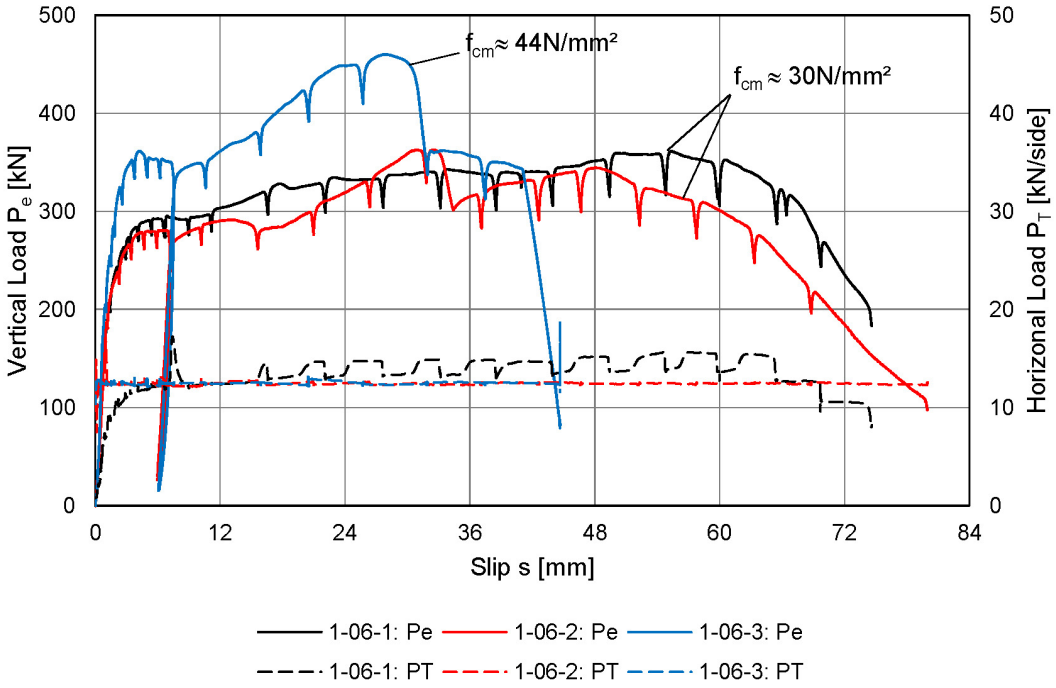


Figure 4.21: Load-slip curves for series 1-06 with two concrete strengths.

Table 4.6: Test results for series 1-06.

| | | 1 | 2 | 3 | 1-06[1] |
|---|---|---|---|---|---|
| $f_{cm}$ | [N/mm$^2$] | 29.94 | 31.06 | 43.96 | 30.50[1] |
| $E_{cm}$ | [N/mm$^2$] | 21200 | 21400 | 25900 | 21300[1] |
| $f_u$ | [N/mm$^2$] | 551 | 551 | 551 | 551 |
| $n_r$ | [-] | 1 | 1 | 1 | 1 |
| $d$ | [mm] | 22.18 | 22.16 | 22.12 | 22.17[1] |
| $h_{sc}$ | [mm] | 123.56 | 124.11 | 123.75 | 123.84[1] |
| $P_e$ | [kN] | 292.44 | 280.52 | 361.24 | 286.48[1] |
| | [kN/side] | 73.11 | 70.13 | 90.31 | 71.62[1] |
| $P_{e,ststic}$ | [kN] | 275.56 | 262.76 | 333.76 | 269.16[1] |
| | [kN] | 68.89 | 65.69 | 83.44 | 67.29[1] |
| $P_T$ | [kN] | 4.1% var. | 12.5 | 12.5 | |
| $e$ | [mm] | 380 | 380 | 380 | |
| Failure | | CPO RPT | CPO RPT | SF CPO RPT | |

[1] Average of tests 1 and 2

The increase of concrete strength in specimen 1-06-3 increased the test load, but the displacement at failure decreased. A similar but less strong effect was observed for the increase of the degree of transverse loading in series 1-05.

### 4.4.6 Series 1-07

Pre-punched CP60 decking was used in series 1-07. The shear studs of 22 mm diameter and 125 mm height were welded directly to the beam. A recess according to [DIN EN 1994-1-1, 2010] was used. The slabs were reinforced with two layers of wire fabrics. The concrete strength in series 1-07 was the same as for specimen 1-06-3.

An eccentric transverse load of 8.2% of the test load was applied in specimen 1-07-1. Based on the results of this test, a constant transverse load of 30 kN was applied to the other specimens.

The test parameters and results are summarised in Table 4.7. The obtained load-slip curves are shown in Figure 4.22.

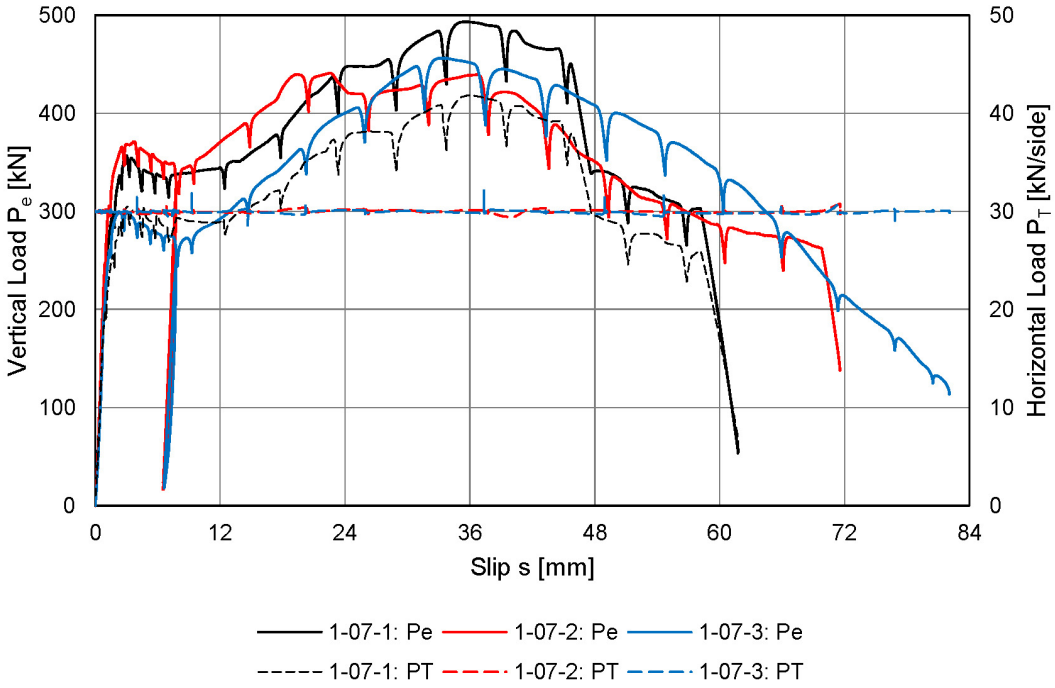


Figure 4.22: Load-slip curves for series 1-07.

All specimens showed a load-slip behaviour with two load peaks. While the specimens 1-07-1 and 1-07-2 showed a resistance similar to specimen 1-06-3, but specimen 1-07-3 had a significantly lower resistance. As the principal behaviour and failure modes of this specimen were the same as for other tests with CP60 decking, this result is assumed to be an outlier. Specimens 1-07-1 and 1-07-2 reached their first peak load at in average 85.2 kN per stud and about 2.5 mm to 4 mm slip. These values correlate well with specimen 1-06-3. Specimen 1-07-3 reached only 70.6 kN per stud at about 2.5 mm slip. Further loading lead to rib punch through failure. After the second peak load was reached, the specimens failed either by stud failure or concrete pull-out. The displacement at failure increased by more than 15mm in comparison to specimen 1-06-3. Like specimen 1-06-3, the tests in series 1-07 showed a more pronounced first load peak than tests with lower concrete strengths.

Table 4.7: Test results for series 1-07.

| | | 1 | 2 | 3 | 1-07 |
|---|---|---|---|---|---|
| $f_{cm}$ | [N/mm$^2$] | 45.09 | 40.87 | 42.59 | 42.85 |
| $E_{cm}$ | [N/mm$^2$] | 26000 | 27500 | 28000 | 27166 |
| $f_u$ | [N/mm$^2$] | 551 | 551 | 551 | 551 |
| $n_r$ | [-] | 1 | 1 | 1 | 1 |
| $d$ | [mm] | 22.12 | 22.14 | 22.14 | 22.13 |
| $h_{sc}$ | [mm] | 123.24 | 124.63 | 124.26 | 124.04 |
| $P_e$ | [kN] | 357.00 | 371.08 | 299.08 | 342.39 |
| | [kN] | 89.25 | 92.77 | 74.77 | 85.60 |
| $P_{e,static}$ | [kN] | 335.24 | 346.08 | 280.84 | 320.72 |
| | [kN/stud] | 83.81 | 86.52 | 70.21 | 80.18 |
| $P_T$ | [kN] | 8.2% var. | 30 | 30 | |
| $e$ | [mm] | 380 | 380 | 380 | |
| Failure | | SF<br>CPO<br>RPT | SF<br>CPO<br>RPT | CPO<br>RPT | |

### 4.4.7 Series 1-08

In series 1-08, CF80 decking was used. Pairs of shear studs per rib with 19 mm diameter and 125 mm hight were welded through the decking. The slabs had a single layer of reinforcement. A recess was not used in these tests. All specimens had tension ties applied. The specimens 1-08-1 and 1-08-2 had loose tension ties with low tension forces, shown in Figure 4.9. Because of the observed slip of the tension ties, a stronger preload was used in specimen 1-08-3, as shown in Figure 4.10.

The test results are summarised in Table 4.8 and Figure 4.23 shows the obtained load-slip curves.

Table 4.8: Test results for series 1-08.

| | | 1 | 2 | 3 | 1-08[1] |
|---|---|---|---|---|---|
| $f_{cm}$ | [N/mm$^2$] | 42.22 | 42.22 | 42.43 | 42.22[1] |
| $E_{cm}$ | [N/mm$^2$] | 26500 | 26500 | 26400 | 26466[1] |
| $f_u$ | [N/mm$^2$] | 551 | 551 | 551 | 551[1] |
| $n_r$ | [-] | 2 | 2 | 2 | 2[1] |
| $d$ | [mm] | 19.06 | 19.07 | 19.07 | 19.07[1] |
| $h_{sc}$ | [mm] | 117.37 | 117.50 | 117.91 | 117.44[1] |
| $P_e$ | [kN] | 364.16 | 368.72 | 386.08 | 366.44[1] |
| | [kN/stud] | 45.52 | 46.09 | 48.26 | 45.81[1] |
| $P_{e,static}$ | [kN] | 342.40 | 346.64 | 367.36 | 344.52[1] |
| | [kN/stud] | 42.80 | 43.33 | 45.92 | 43.07[1] |
| Restraint | | weak | weak | strong | |
| $e$ | [mm] | 250 | 250 | 250 | |
| Failure | | RPO | RPO | RPO | |

[1] Average of tests 1 and 2

The specimens 1-08-1 and 1-08-3 showed a similar linear stiffness even though the tension force in the tension ties was different (see Figure 4.23).

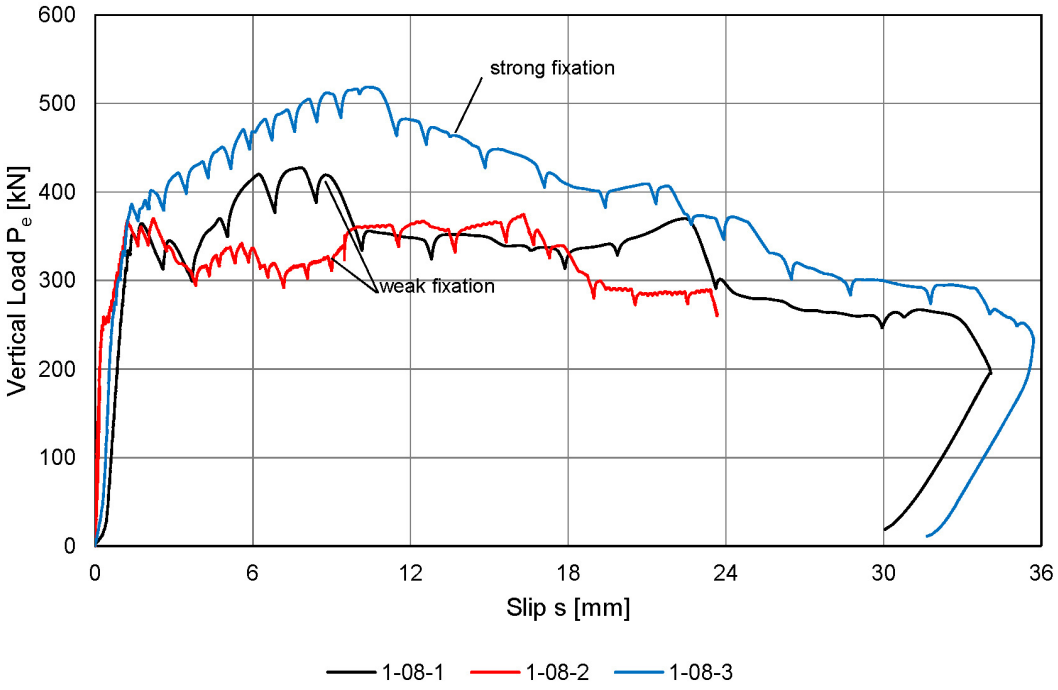


Figure 4.23: Load-slip curves for series 1-08.

Specimen 1-08-2 had an initially higher stiffness. At a load of about 270 kN, a horizontal crack in the concrete topping was observed above the bottom rib, as shown in Figure 4.24. This was a secondary failure due to the rotation of the bottom rib. For further loading, specimen 1-08-2 had a decreased stiffness and converged towards specimens 1-08-1 and 1-08-3.

With the exception of the rotational failure in specimen 1-08-2, all three specimen showed a linear behaviour until a test load of about 360 to 390 kN was reached (see Figure 4.23). At this point, all three specimens showed a sudden loss of stiffness and in case of specimens 1-08-1 and 1-08-2, a decrease of the test load was observed. Diagonal cracks at the sides of the ribs were observed, as can be seen at the upper ribs in Figure 4.25.

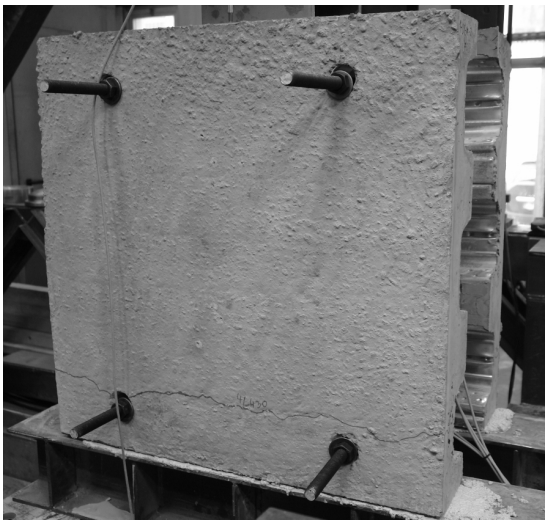

Figure 4.24: Rotation of supporting.

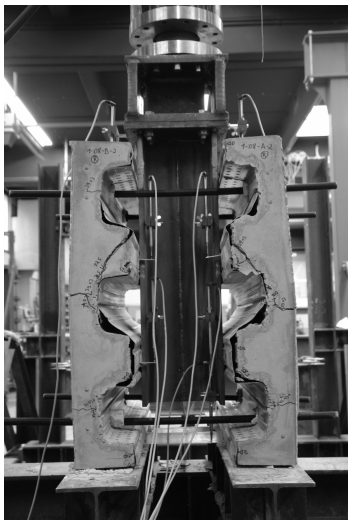

Figure 4.25: Specimen 1-08-2 after testing.

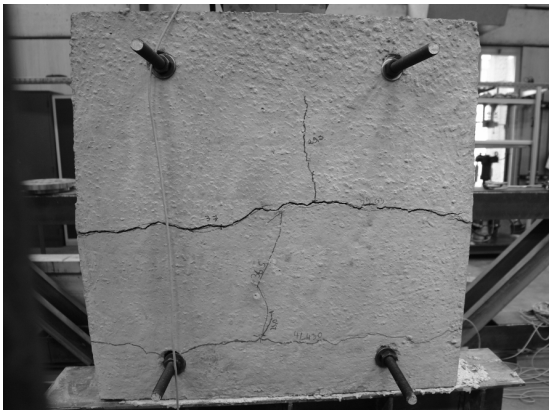

Figure 4.26: Typical crack pattern on the slabs.

Figure 4.27: Failure cone of the ribs in specimen 1-08-2.

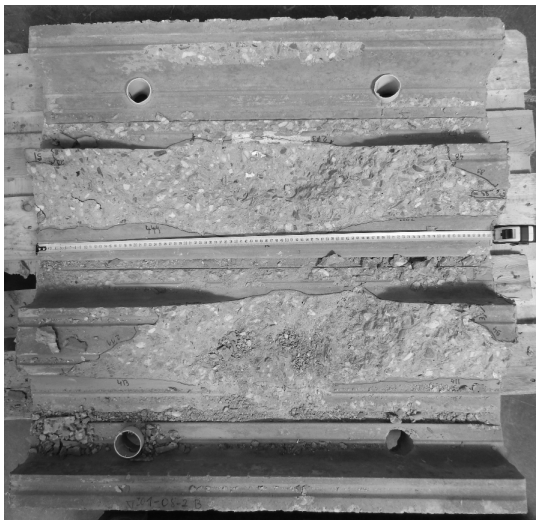

Figure 4.28: Failure cones shown on the slab.

Figure 4.29: Typical shear stud deformation.

Further displacement led to an increase of the test load in specimen 1-08-3 to about 520 kN. For specimens 1-08-1 and 1-08-2, the load-slip curves scattered around 370 kN. For all specimens, it was observed that the slabs bulged outwards at mid height of the slabs, as shown in Figure 4.25. This bending deformation lead to the development of a horizontal crack at mid-height of the slabs (see Figure 4.26). In addition, the low tension in the tension ties in specimens 1-08-1 and 1-08-2 led to a slip of the bars into the holes. This slip was prevented by the stronger tension in the ties in specimen 1-08-3.

The observed differences in the load-slip behaviour were due to the loading of the tension ties. The stronger fixations in specimen 1-08-3 increased the tension forces in the bars, which strongly improved the load-displacement behaviour. This showed, that specimens with CF80 decking were very sensitive for the boundary conditions and transverse loading.

When the specimens were demounted, it was observed that a concrete cone, as shown in Figures 4.27 and 4.28, had developed at failure. Furthermore, the shear studs showed only one plastic hinge above the weld collar, as shown in Figure 4.29.

It is assumed that the concrete cones failed, when the cracks at the side of the ribs were observed. This was the case at a load of 360 kN to 390 kN and about 1 mm to 2 mm slip. Because of the small slip, it is assumed that the tension force in the stud was too small to

cause concrete pull-out failure. The deformation of the studs indicated that the failure of the concrete cone was rather a rotational failure than a tensile failure. This failure mode is further referred to as rib pry-out failure (RPO). The test load that was reached when rib pry-out failure was observed is assumed as the resistance of the shear connection.

The failure mode explains the drop-off in the loads of specimens 1-08-1 and 1-08-2, because the load-bearing mechanism changed and the forces must be redistributed. After rib pry-out failure, friction and aggregate interlock at the failure surface bear the load. This explains the improved load-slip behaviour of specimen 1-08-3, because the frictional resistance increased with the force in the tension ties.

### 4.4.8 Series 1-09

CF80 decking was used in series 1-09. Pairs of shear connectors with 19 mm diameter and 125 mm height were welded through the decking. The slabs had a single layer of reinforcement and were cast without a recess.

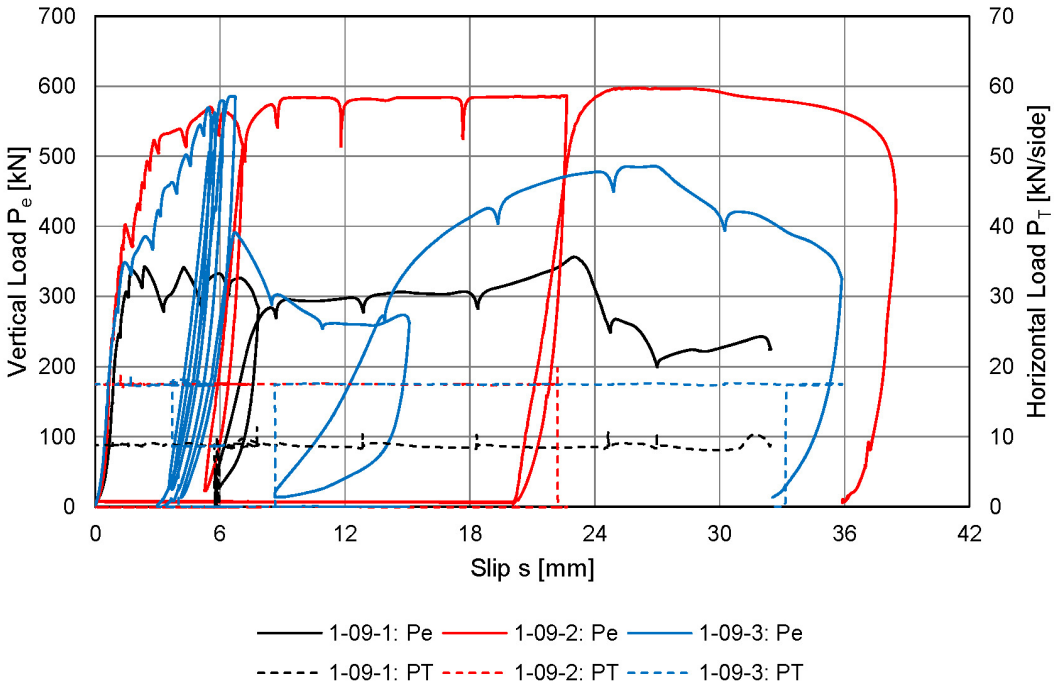


Figure 4.30: Load-slip curves for series 1-09.

Specimen 1-09-1 was loaded with a constant concentric transverse load of 8.8 kN. Rib pry-out failure occurred at a test load of 338.2 kN. The obtained load slip-curve, see Figure 4.30, was similar to specimens 1-08-1 and 1-08-2. Due to the controlled transverse loading, the load after failure was less fluctuant and remained at a value of about 300 kN until a slip of 18 mm. For further displacement, the load increased slightly and finally dropped when debonding of the stiffeners on top of the decking was observed.

Specimen 1-09-2 was scheduled to be loaded with a constant concentric transverse load of 17.5 kN. Initially, the specimen performed similar to specimen 1-09-1 and cracks in the ribs, indicating the occurrence of rib pry-out failure, were observed at a load of 402.6 kN. However, the test load further increased to about 590 kN. It was observed that the displacement

Table 4.9: Test results for series 1-09.

| | | 1 | 2 | 3 | 1-09[1] |
|---|---|---|---|---|---|
| $f_{cm}$ | [N/mm$^2$] | 42.59 | 42.59 | 42.59 | 42.59[1] |
| $E_{cm}$ | [N/mm$^2$] | 28000 | 28000 | 28000 | 28000[1] |
| $f_u$ | [N/mm$^2$] | 551 | 551 | 551 | 551[1] |
| $n_r$ | [-] | 2 | 2 | 2 | 2[1] |
| $d$ | [mm] | 19.09 | 19.12 | 19.09 | 19.10[1] |
| $h_{sc}$ | [mm] | 118.84 | 117.80 | 118.82 | 118.49[1] |
| $P_e$ | [kN] | 338.24 | 402.56 | 385.52 | 394.04[1] |
| | [kN/stud] | 42.28 | 50.32 | 48.19 | 49.26[1] |
| $P_{e,static}$ | [kN] | 312.88 | 371.20 | 367.36 | 369.28[1] |
| | [kN/stud] | 39.11 | 46.40 | 45.92 | 46.16[1] |
| $P_T$ | [kN] | 8.8 | 17.5[2] | 17.5[2] | |
| $e$ | [mm] | 0 | 0 | 0 | |
| Failure | | RPO | RPO | RPO | |

[1] Average of tests 2 and 3

[2] Unwanted clamping increased $P_T$

capacity provided in the clamping device was not sufficient. The frame restrained the bulging of the slabs. Because of this clamping, the tension ties may have taken significantly higher loads than the 17.5 kN applied to the frame by the hydraulic jack. At a displacement of about 22 mm, the specimen was unloaded and the force of the horizontal jack was removed. The specimen was then reloaded and reached again a resistance of about 600 kN. This proved that the clamping of the test frame introduced a transverse load significantly higher than 17.5 kN.

Specimen 1-09-3 was conducted to reproduce the results of specimen 1-09-2. A constant concentric transverse load of 17.5 kN was applied and the displacement capacity of the clamping device was adjusted as for test 1-09-2. Until rib pry-out failure occurred at a load of 385.5 kN, the specimen showed the same behaviour as the previous tests. As for test 1-09-2, the displacement capacity of the frame was insufficient and the test load increased up to about 590 kN because of the clamping of the frame. At a slip of about 6 mm, the specimen was unloaded and then reloaded with half of the transverse load. The test load increased again to about 590 kN. The procedure was repeated without applying a force by the horizontal jack, which still did not remove the clamping of the frame. Then the specimen was unloaded and the tension ties were loosened to allow a horizontal displacement of about 15 mm. Specimen 1-09-3 could then be reloaded to about 400 kN. The test load then dropped to about 280 kN because the clamping was removed. At a slip of about 15 mm, specimen 1-09-3 was again unloaded and reloaded with the full transverse load of 17.5 kN. The test load could then be increased to about 490 kN.

The observations during testing and when the specimens were dismounted confirmed the occurrence of rib pry-out failure for all tests.

The results of this series showed:

- The specimens with CF 80 decking are very sensible for transverse loading.
- Too high transverse loads could increase the resistance of a specimen to an unrealistic behaviour.

### 4.4.9 Series 1-10

Series 1-10 used CF80 decking with through deck welded pairs of studs. The studs had a diameter of 19 mm and a height of 125 mm. A single layer of reinforcement was used. A recess was not used.

Based on the significant influence of the transverse load in series 1-08 and 1-09, the degree of transverse loading was varied within series 1-10 to further investigate this influence. Specimen 1-10-1 was a repetition of tests 1-09-2 and 1-09-3. This means that a constant transverse load of 17.5 kN was applied to the specimen. In specimen 1-10-1 a displacement capacity of 30 mm was chosen for the clamping device. Therefore, the slabs could bulge without increasing the transverse load until a horizontal displacement of 15 mm would be reached by each slab. In specimen 1-10-2, the transverse load was reduced to 13.2 kN. Finally, test 1-10-3 was conducted without transverse loading or tension ties at all. The already presented specimen 1-09-1 completed this investigation with a transverse load of 8.8 kN.

The results of this series are summarised in Table 4.10. The obtained load-slip curves are shown in Figure 4.31 and show that there was a significant influence of the transverse loading on the shear connections behaviour.

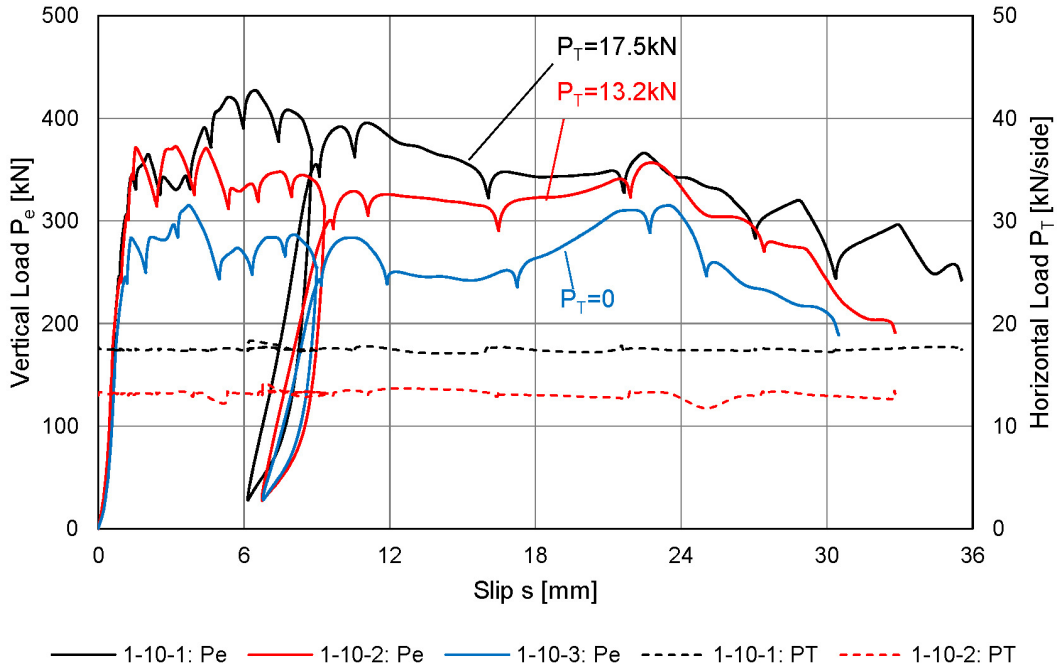


Figure 4.31: Load-slip curves for series 1-10.

All specimen exhibited rib pry-out failure at a slip of about 1.5 to 2.5 mm.

Specimen 1-10-3, without transverse loading, failed at a load of 283.7 kN. Specimen 1-10-2 with 13.2 kN transverse load reached 371.5 kN, which is an increase of about 31%. For specimen 1-10-1 with 17.5 kN transverse load, the failure load increased by about 29% to 365.1 kN. To complete this, specimen 1-09-1 with 8.8 kN transverse load reached an about 10% higher resistance of 312.9 kN compared to specimen 1-10-3.

The beneficial influence of the transverse load on the failure load, $P_e$, appeared to be limited for higher transverse loads. When tests 1-10-1 and 1-10-2 are compared, they showed

Table 4.10: Test results for series 1-10.

| | | 1 | 2 | 3 |
|---|---|---|---|---|
| $f_{cm}$ | [N/mm$^2$] | 42.59 | 42.59 | 42.59 |
| $E_{cm}$ | [N/mm$^2$] | 28000 | 28000 | 28000 |
| $f_u$ | [N/mm$^2$] | 551 | 551 | 551 |
| $n_r$ | [-] | 2 | 2 | 2 |
| $d$ | [mm] | 19.11 | 19.09 | 19.10 |
| $h_{sc}$ | [mm] | 118.64 | 118.11 | 118.24 |
| $P_e$ | [kN] | 365.12 | 371.52 | 283.68 |
| | [kN/stud] | 45.64 | 46.44 | 35.46 |
| $P_{e,static}$ | [kN] | 326.00 | 314.32 | 249.76 |
| | [kN/stud] | 40.75 | 39.29 | 31.22 |
| $P_T$ | [kN] | 17.5 | 13.2 | 0 |
| $e$ | [mm] | 0 | 0 | 0 |
| Failure | | RPO | RPO | RPO |

only a minor difference of the failure load. However, the static resistance, $P_{e,static}$, which was determined immediately after the observation of rib pry-out failure, kept increasing with transverse load.

In addition, higher transverse loads significantly improved the behaviour after rib pry-out failure in all cases. It was assumed that the shear forces were carried by frictional resistances and aggregate interlock after the occurrence of rib pry-out. Thus, the additional compression at the failure surface because of the transverse load improved the post-failure behaviour. A more in depth discussion on the influence of transverse loading will be given in section 5.3.

### 4.4.10 Series 1-11

Series 1-11 used CF80 decking with through deck welded pairs of studs of 19 mm diameter and 125 mm height. The slabs had a single layer of reinforcement and were fabricated without a recess.

In this series, the influence of an eccentricity of 380 mm of the transverse load was investigated. Eccentric transverse loading was chosen to consider the negative bending moments of the slab and reproduce more realistic stress conditions in the concrete.

For specimen 1-11-1, a variable transverse load of 3.8% of the test load was applied to each slab. This is a degree of transverse loading of 7.6% per shear interface. The specimens 1-11-2 and 1-11-3 had a constant transverse load of 17.5 kN applied to each slab.

The obtained load-slip curves are shown in Figure 4.32. Table 4.11 summarises the test results.

For all three specimens, rib pry-out failure was observed at a test load of 394.6 to 437.1 kN and a slip of 2.5 to 4.4 mm. These results correspond well with the failure of the concentric loaded specimen 1-10-1 at 365.1 kN. Likewise, the post-failure behaviour was significantly improved, as the test load could be increased up to 470 kN. Similar observations were made for specimen 1-10-1. There was no significant influence of eccentric transverse loading compared to concentric transverse loading in specimen 1-10-1. An in depth comparison of concentric and eccentric transverse loading will be given in section 5.4.

Considering the influence of applying variable or constant transverse loads, no significant difference of the behaviour was observed.

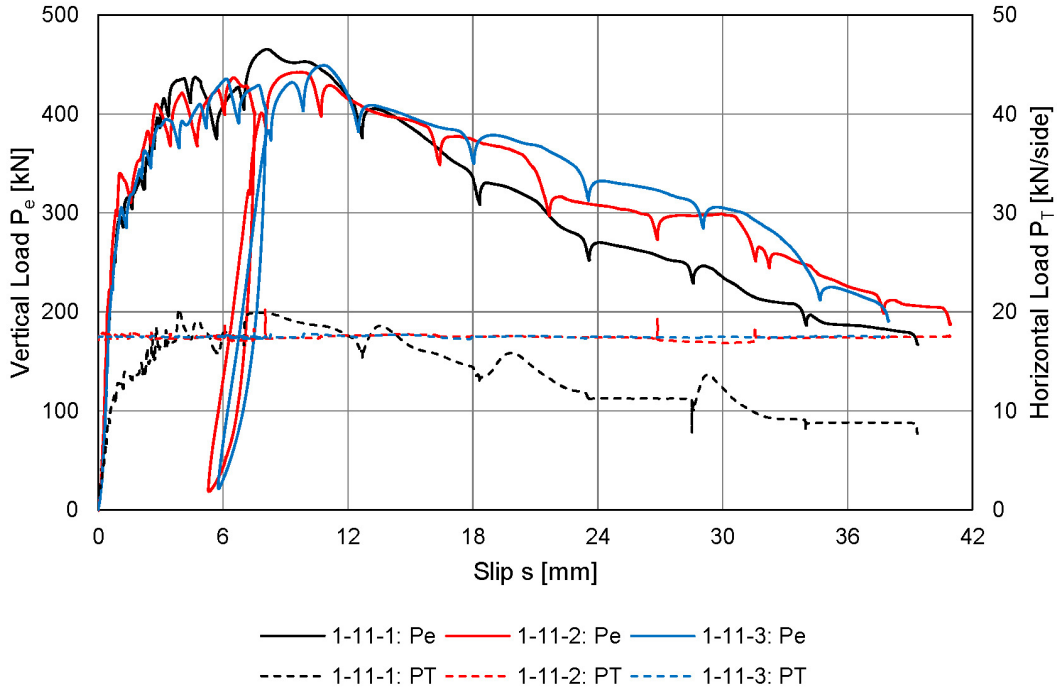


Figure 4.32: Load-slip curves for series 1-11.

Table 4.11: Test results for series 1-11.

| | | 1 | 2 | 3 | 1-11 |
|---|---|---|---|---|---|
| $f_{cm}$ | [N/mm$^2$] | 42.59 | 42.59 | 42.59 | 42.59 |
| $E_{cm}$ | [N/mm$^2$] | 28000 | 28000 | 28000 | 28000 |
| $f_u$ | [N/mm$^2$] | 551 | 551 | 551 | 551 |
| $n_r$ | [-] | 2 | 2 | 2 | 2 |
| $d$ | [mm] | 19.08 | 19.08 | 19.08 | 19.08 |
| $h_{sc}$ | [mm] | 119.40 | 118.74 | 118.57 | 118.90 |
| $P_e$ | [kN] | 437.12 | 421.44 | 394.64 | 417.73 |
| | [kN/stud] | 54.64 | 52.68 | 49.33 | 52.17 |
| $P_{e,static}$ | [kN] | 411.28 | 368.32 | 365.68 | 381.76 |
| | [kN/stud] | 51.41 | 46.04 | 45.71 | 47.72 |
| $P_T$ | [kN] | 3.8% var. | 17.5 | 17.5 | |
| $e$ | [mm] | 380 | 380 | 380 | 380 |
| Failure | | RPO | RPO | RPO | |

Because of the strong beneficial influence of the transverse loading on the post-failure behaviour of tests with CF80 decking, the reasonability of the internal forces and moments must be considered. Assuming a typical span of about 4.50 m for composite slabs with CF80 decking , the transverse load of 17.5 kN corresponds to a load of 4.42 kN/m$^2$ in a building:

$$q_{E,POT} = \frac{P_T}{H} \cdot \frac{1}{L} = \frac{17.5}{0.9 \cdot 4.50} = 4.42 \text{ kN/m}^2$$

where: $H$ Height of the slab in the push-out test
$L$ Assumed span of the real composite slab

This is close to the characteristic load for quasi-permanent loading, assuming 1.0 kN/m$^2$ surcharge, 2.0 kN/m$^2$ live load and 1.2 kN/m$^2$ for partition walls:

$$g_k + \psi_2 \cdot q_k = (0.106 \cdot 25 + 0.16 + 1.0) + 0.3 \cdot (2.0 + 1.2) = 4.77 \text{ kN/m}^2$$

Therefore, the concentric transverse load of 17.5 kN is a reasonable realistic value.

For eccentric transverse loading, the bending moment of the slab has to be considered in addition. The eccentricity of 380 mm was chosen to limit the size of the specimens and leads to a negative bending moment of 1.1 kN per rib in the push-out test:

$$M_{E,POT} = \frac{P_T}{2} \cdot e \cdot \frac{a}{H} = \frac{17.5}{2} \cdot 0.380 \cdot \frac{0.30}{0.90} = 1.1 \text{ kNm}$$

where: $e$ Eccentricity of the transverse load
$a$ Spacing of the ribs

Assuming the same load in a building, a bending moment of 3.4 kNm per rib is obtained for a slab with two spans:

$$M_{E,slab} = q_{E,POT} \cdot \frac{L^2}{8} \cdot a = 4.42 \cdot \frac{4.50^2}{8} \cdot 0.30 = 3.4 \text{ kNm}$$

This is significantly more than the bending moment applied in the push-out specimens. This is relativised by the moment-redistribution, as the specimens were designed to reflect the common practice of designing the composite slab as single span systems. For design, it is assumed that the negative (hogging) moment is completely redistributed to the positive (sagging) moment. The reinforcement layer only serves to distribute the cracks. A more realistic assumption is that the hogging moment is equal to the bending resistance of the composite slab, $M_{Pl}$, of about 3.3 kNm per rib, as follows:

$$Z = a_s \cdot f_y \cdot a = 1.88 \cdot 50 \cdot 0.300 = 28.2 \text{ kN}$$
$$x_{Pl} = \frac{Z}{f_{cm} \cdot b_u} = \frac{28.2}{4.26 \cdot 12} = 0.552 \text{ cm}$$
$$M_{PL} = Z \cdot (h_p + c_V + d_s + d_s/2 - x_{PL}/2)$$
$$M_{Pl} = 28.2 \cdot (8 + 3 + 0.6 + 0.6/2 - 0.552/2) \cdot 10^{-2} = 3.3 \text{ kNm} \begin{cases} >> & M_{E,POT} \\ < & M_{E,slab} \end{cases}$$

where: $Z$ Tensile resistance of reinforcement
$a_s$ Cross-section area of reinforcement
$f_y$ Yield strength of reinforcement
$x_{PL}$ Height of rib in compression
$b_u$ Width of the rib at the bottom
$c_V$ Concrete cover for reinforcement
$d_s$ Diameter of reinforcement bars

In a real building, the negative moment would be larger than the slabs bending resistance. Therefore, this moment would be redistributed and result in significant cracking of the slab as

well as in a large rotation of the slab along the composite beam. Eventually, the rotation could cause the cracks at the rib pry-out cone to partially open. In this case, the shear connection could not benefit from additional friction at the failure surface for the post-failure behaviour. On the other side, it could be possible that the high rotation even increases the interlock between the failure surfaces. Because the composite slabs were able to resist the too small hogging moment applied in the push-out tests the rotation of the slabs was smaller than for a real slab. Therefore, it is arguable if the load-slip behaviour, as shown in Figure 4.32, develops. Further investigation considering a realistic displacement of the composite slab would be necessary.

### 4.4.11 Series 3-01

The specimens in this series used CF80 decking with pairs of studs welded through the decking. The studs were of 19 mm diameter and 125 mm hight. The slabs had two layers of reinforcement. The bottom layer was placed directly on the decking, which is 15 mm above the rib because of the stiffener on top of the profile. The bottom layer was placed 15 mm lower than in tests with a single layer of reinforcement. A recess was not used.

Specimens 3-01-1 and 3-01-2 were conducted with tension ties using the strong type of fixation to further investigate the influence of these restraints. Therefore, the forces in the tension ties were measured. Specimen 3-01-3 the was conducted without tension ties.

The obtained load-slip curves are shown in Figure 4.33 and Table 4.12 summarises the test results.

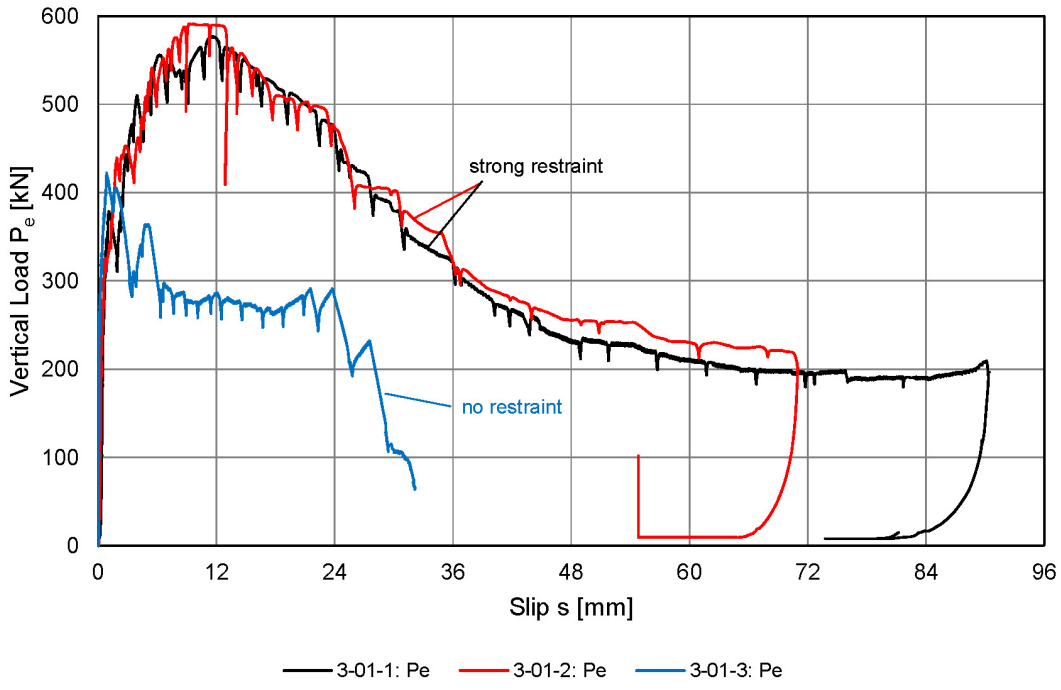


Figure 4.33: Load-slip curves for series 3-01.

For all three specimens, rib pry-out failure was observed at a load of about 380 to 440 kN. The slip was between 1.5 and 2.2 mm. After rib pry-out failure was observed, the load-slip behaviour strongly differed between the tests with tension ties and the test without tension ties.

Table 4.12: Test results for series 3-01.

| | | 1 | 2 | 3 | 3-01[1] |
|---|---|---|---|---|---|
| $f_{cm}$ | [N/mm$^2$] | 46.00 | 46.00 | 40.43 | 46.00[1] |
| $E_{cm}$ | [N/mm$^2$] | 26900 | 26800 | 26800 | 26833[1] |
| $f_u$ | [N/mm$^2$] | 551 | 551 | 551 | 551[1] |
| $n_r$ | [-] | 2 | 2 | 2 | 2[1] |
| $d$ | [mm] | 19.07 | 19.06 | 19.07 | 19.07[1] |
| $h_{sc}$ | [mm] | 118.49 | 117.38 | 118.33 | 117.94[1] |
| $P_e$ | [kN] | 378.51 | 439.36 | 422.24 | 408.94[1] |
| | [kN/stud] | 47.31 | 54.92 | 52.78 | 51.12[1] |
| $P_{e,static}$ | [kN] | 310.88 | 413.28 | 378.56 | 362.08[1] |
| | [kN/stud] | 38.86 | 51.66 | 47.32 | 45.26[1] |
| Restraint | | strong | strong | n.a. | |
| $e$ | [mm] | 250 | 250 | n.a. | |
| Failure | | RPO | RPO | RPO | |

[1] Average of tests 1 and 2

Without tension ties, the test load fell below 300 kN. Then a second peak of about 360 kN developed before the load dropped to an almost constant value between 264 to 297 kN. As the test load decreased by about one fourth of the observed maximum load before 6 mm slip were reached, the load-slip behaviour is not ductile according to [DIN EN 1994-1-1, 2010].

In the tests with tension ties, the load further increased to about 590 kN after rib pry-out failure was observed. After ultimate load was reached, the test load decreased continuously.

The measured forces in the tension ties are shown in Figures 4.34 and 4.35. It can be seen that the forces in the two tension ties at the bottom of the slabs were two to three times the force of the bars at the top.

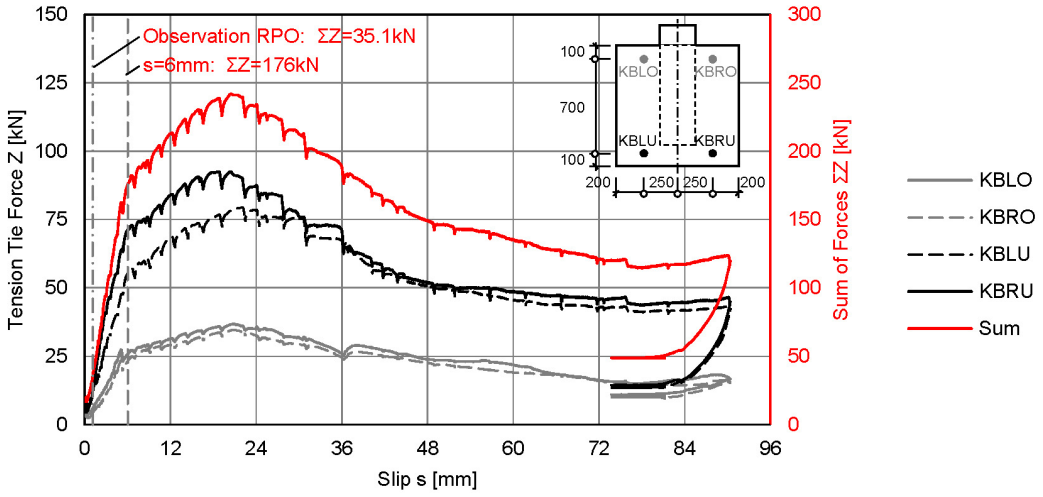


Figure 4.34: Measured forces in the tension ties for specimen 3-01-1.

For specimen 3-01-3, the sum of the tension forces was 35.1 kN when rib pry-out was observed. This was about 19% of the shear force per side. As shown in the study presented in section 4.1, this was still a reasonable value for the transverse load. For the post-failure

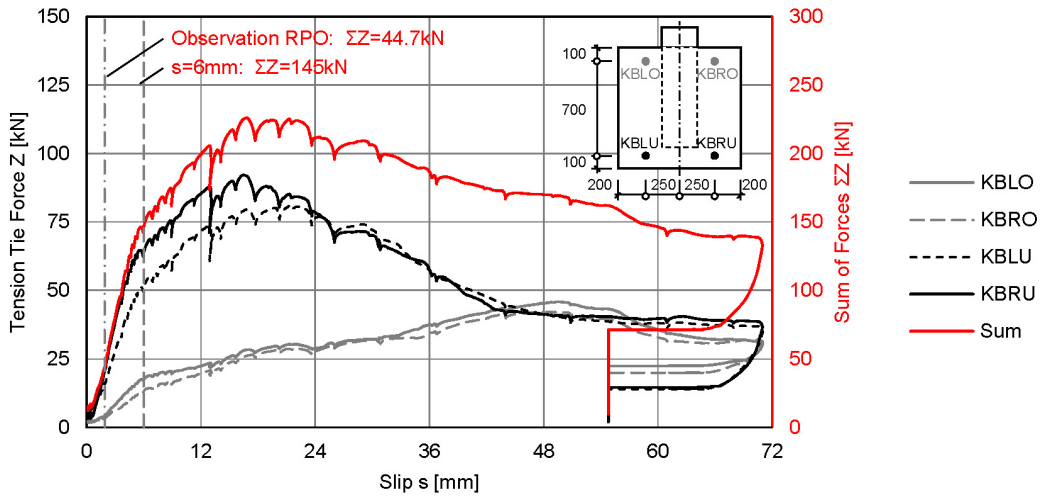


Figure 4.35: Measured forces in the tension ties for specimen 3-01-2.

behaviour the sum of the tension forces increased to about 240 kN, which is even higher than the shear force per slab. Due to this high transverse compression, the very high test loads during post-failure behaviour are not realistic. Similar observations were made for specimen 3-01-2. There the sum of the tension forces was abut 22% of the shear force per side when rib pry-out failure was observed.

The results of these tests showed that the application of tension ties strongly influenced the load-slip behaviour. The very high forces in the two bars at the bottom of the slab show that the application of a tension tie is reasonable to prevent the secondary failure of horizontal sliding of the slab at the support. Tension ties could lead to unrealistic high compression at the shear interface. It would be reasonable to include a damping element to ensure realistic forces in the bars. The use of disc springs could provide a sufficient non-linear load-displacement curve to restrain the tension forces to reasonable values even at high displacements.

### 4.4.12 Series 3-02

Specimen 3-02 used pre-punched CF 80 decking. Pairs of shear studs per rib were welded directly to the flange of the beam. The stud diameter was 19 mm and the nominal height was 125 mm. The height of the stud after welding of about 123 to 124 mm was approximately 5 mm larger than for through deck welded studs. The slabs had a single layer of reinforcement and a recess was not applied. The test was conducted without tension ties or transverse loading.

The test results are shown in Figure 4.36 and Table 4.13.

Specimen 3-02 failed by rib pry-out failure at a load of 296 kN and 1.2 mm slip. The test load then fel to about 250 kN and retained this load until about 18 mm slip were reached. For further loading, the test load continuously decreased and the test was aborted when the load had decreased to 100 kN.

As the decrease of the test load after rib pry-out failure is about 15% of the ultimate load, specimen 3-02 was not ductile according to [DIN EN 1994-1-1, 2010].

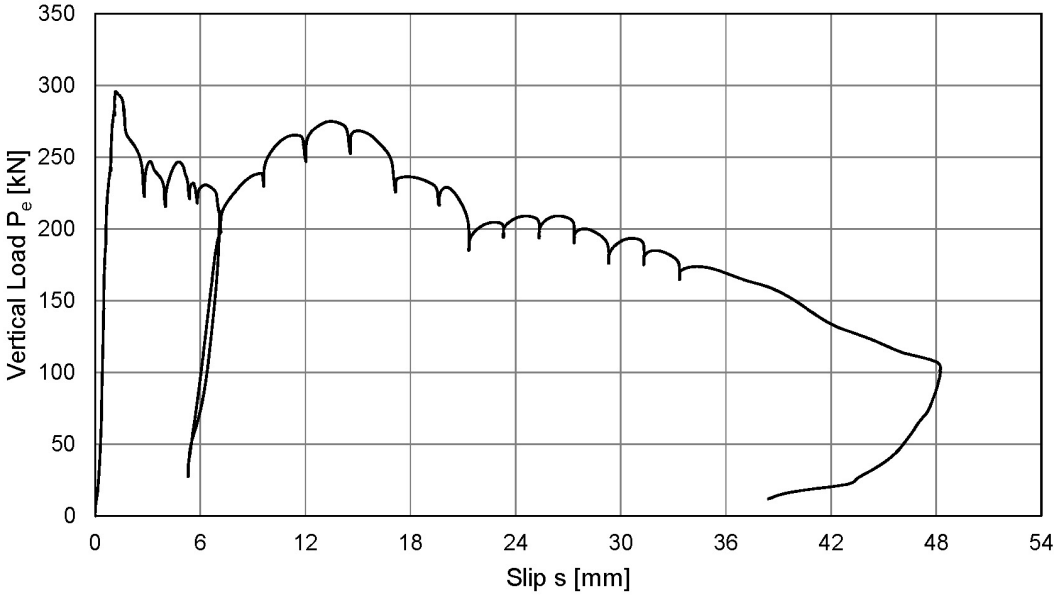


Figure 4.36: Load-slip curves for series 3-02.

Table 4.13: Test results for series 3-02.

| | | 3-02 |
|---|---|---|
| $f_{cm}$ | [N/mm$^2$] | 42.62 |
| $E_{cm}$ | [N/mm$^2$] | 28000 |
| $f_u$ | [N/mm$^2$] | 551 |
| $n_r$ | [-] | 2 |
| $d$ | [mm] | 19.08 |
| $h_{sc}$ | [mm] | 123.44 |
| $P_e$ | [kN] | 296.00 |
| | [kN/stud] | 37.00 |
| $P_{e,static}$ | [kN] | 279.20 |
| | [kN/stud] | 34.90 |
| Failure | | RPO |

### 4.4.13 Series NR1

In series NR1 , CF80 decking was used. Single stud of 19 mm diameter and 125 mm height were welded through the decking. The slabs had a single layer of reinforcement. The optional recess was not used.

This series investigated not only he number of shear studs per rib and the degree of concentric transverse loading. Test NR1-1 was conducted without tension ties or transverse loading. In specimen NR1-2, a constant concentric transverse load of 8.8 kN was applied. This was increased to 17.5 kN for specimen NR1-3.

The test results are shown in Figure 4.37 and Table 4.14.

All three specimens exhibited rib pry-out failure at about 280 to 316 kN. The observation of this failure mode was not surprising, because it was typical for all previous tests with CF80 decking. The resistance of the specimens was in average 80 kN smaller than for pairs of

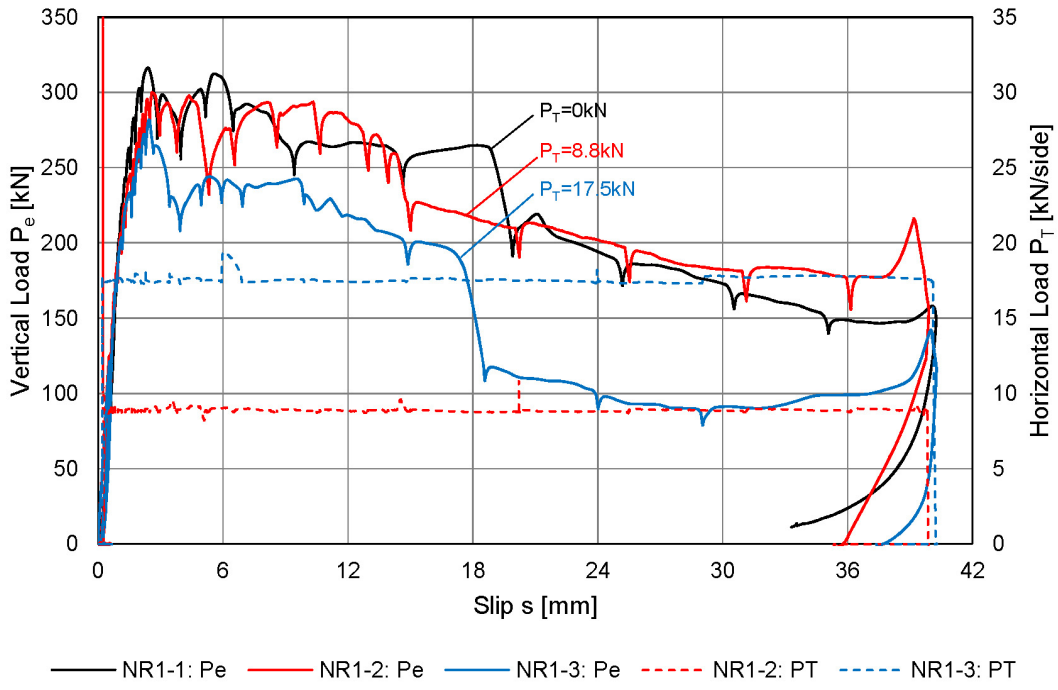


Figure 4.37: Load-slip curves for series NR1.

Table 4.14: Test results for series NR1.

| | | 1 | 2 | 3 |
|---|---|---|---|---|
| $f_{cm}$ | [N/mm$^2$] | 44.11 | 45.70 | 44.70 |
| $E_{cm}$ | [N/mm$^2$] | 25600 | 25600 | 25600 |
| $f_u$ | [N/mm$^2$] | 551 | 551 | 551 |
| $n_r$ | [-] | 1 | 1 | 1 |
| $d$ | [mm] | 19.09 | 19.09 | 19.10 |
| $h_{sc}$ | [mm] | 121.31 | 121.18 | 120.99 |
| $P_e$ | [kN] | 316.29 | 299.97 | 281.85 |
| | [kN/stud] | 79.07 | 74.99 | 70.46 |
| $P_{e,static}$ | [kN] | 287.37 | 271.70 | 259.47 |
| | [kN] | 71.84 | 67.93 | 64.87 |
| $P_T$ | [kN] | 0 | 8.8 | 17.5 |
| $e$ | [mm] | 0 | 0 | 0 |
| Failure | | RPO, SF | RPO, SF | RPO, SF |

studs per rib. This was assumable as the size of the failure cone was reduced.

For all specimens, stud failure was observed at about 15 to 20 mm slip. The studs failed inside the weld collar and showed high porosity in the welding area, as shown in Figure 4.38.

Specimen NR1-1 without transverse loading and specimen NR1-2 with 8.8 kN transverse loading showed only minor differences in their load-slip behaviour. Specimen NR1-3 with 17.5 kN transverse load showed a significantly smaller test load. The test load was about 25 to 50 kN smaller than for specimen NR1-1.

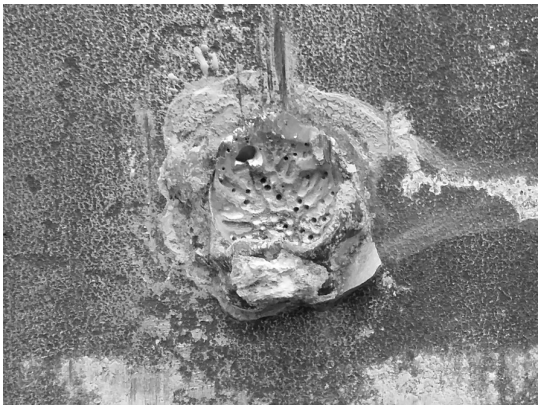

(a) Failure surface on the beam.

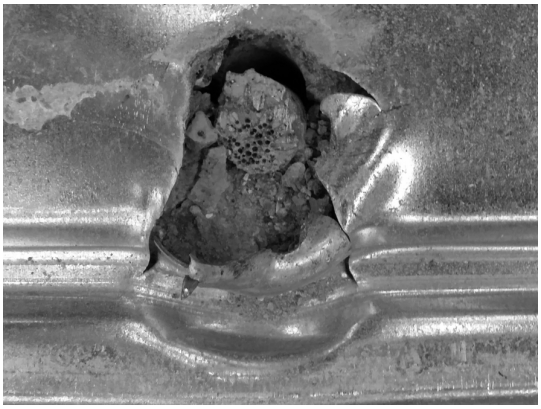

(b) Failure surface on the slab and damaged decking.

Figure 4.38: Failed studs in series NR1 with high weld porosity.

## 4.5 Concluding remarks

The conducted push-out tests used two different deck heights: 58 mm and 80 mm. For each height, typical failure modes were observed.

The shear connectors in 58 mm deep CP60 decking typically developed a load-slip behaviour with two load peaks. The first peak load was defined by the development of two yield hinges in the stud shank, as described by [Lungershausen, 1988]. Further loading lead to a second peak load, after which either concrete pull-out or stud failure were observed.

The general behaviour of shear studs with this failure mode did not change when transverse loading was applied. The first peak load did not change significantly for higher degrees of transverse loading or eccentric transverse loading. For the second load peak, higher loads were obtained and the slip at failure decreased when the degree of transverse loading was increased. Eccentric transverse loading decreased the second peak load significantly. The strongest influence on the load-slip behaviour and resistance of the shear connection in CP60 decking was observed by the increase of the concrete strength. This lead to higher resistances and significantly smaller slip at failure. In all cases, the behaviour of studs in CP60 decking can be assumed as ductile.

For shear connectors in 80 mm deep CF80 decking, typically a load-slip behaviour with one load peak developed. The typical failure mode was rib pry-out failure. This is the failure of a concrete cone at a small slip. The load-slip behaviour after rib pry-out failure strongly depends on contact forces, friction and aggregate interlock at the failure surface. Therefore, a significant influence of transverse loading on the load-slip behaviour was observed. The results of series 1-09 and 3-01 showed, that transverse loading as well as tension ties must be applied with conciousness. For series 1-09, an insufficient displacement capacity of the test frame lead to unwanted clamping and increased the transverse compression. The force measurements at the tension ties in series 3-01 showed, that clamping could lead to transverse compression forces of up to 240 kN per shear interface. This lead to unrealistic high test loads. Typically, rib pry-out failure lead to a significant decrease of the test load, as the load bearing mechanism changed. As soon as the 'frictional' mode was established, all tests with CF80 decking showed a ductile behaviour. However, it is assumable that the studs will be classified as non-ductile in some cases, because of the load drop when the load bearing mechanism changes.

# 5 Discussion of push-out test results

## 5.1 Evaluation according to EN 1994-1-1 Annex B2

Instead of performing a statistical analysis, [DIN EN 1994-1-1, 2010] Annex B2 allows a simplified method to determine the characteristic resistance, $P_{Rk}$, and slip capacity, $\delta_{uk}$, out of push-out test results.

To do this, a series of at least three tests with identical nominal properties is required. The resistance of each test must not deviate from the mean value of all tests by more than 10%. Then the characteristic resistance, $P_{Rk}$, of the test series is the minimum resistance reduced by 10%. For each specimen, the displacement capacity, $\delta_u$, is determined as the maximum slip when the test load drops below $P_{Rk}$, as shown in Figure 2.21. The characteristic value, $\delta_{uk}$, is then the minimum value reduced by 10%.

The conducted push-out test programme does not test 3 similar tests for each investigated parameter, as follows:

- The influence of using pre-punched decking instead of through deck welded studs was investigated with only one test.
- Specimen 1-06-3 had a higher concrete strength than the other two tests of series 1-06.
- In tests with CF80 decking, the transverse loading had a strong influence on the load-slip behaviour and was varied within series 1-09, 1-10 and NR1.
- The boundary conditions and application of tension ties had a large influence on the behaviour of tests with CF80 decking and were varied in series 1-08 and 3-01.
- For series 1-07, the criterion of a 10% deviation is not satisfied, because the resistance of test 1-07-3 is 12% smaller than the average resistance (although this is a small exceedance of the required 10%).

Consequently, the procedure according to [DIN EN 1994-1-1, 2010] Annex B2 is formally only applicable to series 1-04 and 1-05. For information and comparison, the procedure is also applied to the other test series.

Series 1-06 is divided into two series to consider the higher concrete strength of test 1-06-3. For the variation of transverse loading, no statement is given in [DIN EN 1994-1-1, 2010] Annex B2, because transverse loads were not considered in the development of these rules. Because transverse loading had a significant influence especially on specimen with CF80 decking, series 1-09, 1-10 and NR1 are additionally divided according to the different degree of transverse loading. Likewise, the variation of the boundary conditions in series 1-08 and 3-01 is considered by dividing these into separate series per boundary condition.

The evaluation of the characteristic resistances and displacement capacity of the conducted push-out tests is summarised in Tables 5.1 and 5.2.

Table 5.1: Characteristic resistances, $P_{Rk}$ and $P_{Rk,static}$, of the conducted push-out tests according to [DIN EN 1994-1-1, 2010] Annex B2.

| Series | i | Deck | $d$ | $n_r$ | $f_{cm}$ | Test results | | EN 1994-1-1, B2 | |
|---|---|---|---|---|---|---|---|---|---|
| | | | | | | $P_e$ | $P_{e,static}$ | $P_{Rk}$ | $P_{Rk,static}$ |
| | | | [mm] | [-] | [N/mm$^2$] | [kN/stud] | [kN/stud] | [kN/stud] | [kN/stud] |
| PV | 1 | RD80 | 19 | 1 | 45.80 | 116.41 | 108.41 | 95.99 | 89.20 |
| | 2 | RD80 | 19 | 1 | 45.80 | 106.66 | 99.11 | | |
| 1-04 | 1 | CP60 | 22 | 1 | 30.62 | 73.94 | 70.44 | 61.79 | 58.53 |
| | 2 | CP60 | 22 | 1 | 30.89 | 73.61 | 65.63 | | |
| | 3 | CP60 | 22 | 1 | 30.91 | 68.66 | 65.03 | | |
| 1-05 | 1 | CP60 | 22 | 1 | 30.71 | 69.95 | 66.40 | 62.96 | 59.76 |
| | 2 | CP60 | 22 | 1 | 30.71 | 79.15 | 69.63 | | |
| | 3 | CP60 | 22 | 1 | 32.55 | 74.43 | 70.86 | | |
| 1-06 | 1 | CP60 | 22 | 1 | 29.94 | 73.11 | 68.89 | 63.12 | 59.12 |
| | 2 | CP60 | 22 | 1 | 31.06 | 70.13 | 65.69 | | |
| 1-06 | 3 | CP60 | 22 | 1 | 43.96 | 90.31 | 83.44 | 81.28 | 75.10 |
| 1-07 | 1 | CP60 | 22 | 1 | 45.09 | 89.25 | 83.81 | 67.29 | 63.19 |
| | 2 | CP60 | 22 | 1 | 40.87 | 92.77 | 86.52 | | |
| | 3 | CP60 | 22 | 1 | 42.85 | 74.77 | 70.21 | | |
| 1-08 | 1 | CF80 | 19 | 2 | 42.22 | 45.52 | 42.80 | 40.97 | 38.52 |
| | 2 | CF80 | 19 | 2 | 42.22 | 46.09 | 43.33 | | |
| 1-08 | 3 | CF80 | 19 | 2 | 42.43 | 48.26 | 45.92 | 43.43 | 41.33 |
| 1-09 | 1 | CF80 | 19 | 2 | 42.59 | 42.28 | 39.11 | 38.05 | 35.20 |
| 1-09 | 2 | CF80 | 19 | 2 | 42.59 | 50.32 | 46.40 | 43.37 | 41.33 |
| | 3 | CF80 | 19 | 2 | 42.59 | 48.19 | 45.92 | | |
| 1-10 | 1 | CF80 | 19 | 2 | 42.59 | 45.64 | 40.75 | 41.09 | 36.68 |
| 1-10 | 2 | CF80 | 19 | 2 | 42.59 | 46.44 | 39.29 | 41.98 | 35.36 |
| 1-10 | 3 | CF80 | 19 | 2 | 42.59 | 35.46 | 31.22 | 31.91 | 28.10 |
| 1-11 | 1 | CF80 | 19 | 2 | 42.59 | 54.64 | 51.41 | 44.40 | 41.14 |
| | 2 | CF80 | 19 | 2 | 42.59 | 52.68 | 46.04 | | |
| | 3 | CF80 | 19 | 2 | 42.59 | 49.33 | 45.71 | | |
| 3-01 | 1 | CF80 | 19 | 2 | 46.00 | 47.31 | 38.86 | 42.58 | 34.97 |
| | 2 | CF80 | 19 | 2 | 46.00 | 54.92 | 51.66 | | |
| 3-01 | 3 | CF80 | 19 | 2 | 40.43 | 52.78 | 47.32 | 47.50 | 42.59 |
| 3-02 | 1 | CF80 | 19 | 2 | 42.62 | 37.00 | 34.90 | 33.30 | 31.41 |
| NR1 | 1 | CF80 | 19 | 1 | 44.11 | 79.07 | 71.84 | 71.16 | 64.66 |
| NR1 | 2 | CF80 | 19 | 1 | 45.70 | 74.99 | 67.93 | 67.49 | 61.14 |
| NR1 | 3 | CF80 | 19 | 1 | 44.70 | 70.46 | 64.87 | 63.41 | 58.38 |

Table 5.2: Characteristic displacement capacity according to [DIN EN 1994-1-1, 2010] Annex B2, $\delta_{uk}$, and second intersection, $\delta_{u2k}$, of the conducted push-out tests .

| Series | i | Deck | $d$ [mm] | $n_r$ [-] | $f_{cm}$ [N/mm$^2$] | $P_{Rk}$ [kN/stud] | $\delta_u$ [mm] | $\delta_{uk}$ [mm] | $\delta_{u2}$ [mm] | $\delta_{u2k}$ [mm] |
|---|---|---|---|---|---|---|---|---|---|---|
| PV | 1 | RD80 | 19 | 1 | 45.80 | 95.99 | 7.86 | 4.57 | - | - |
| | 2 | RD80 | 19 | 1 | 45.80 | | 5.08 | | - | |
| 1-04 | 1 | CP60 | 22 | 1 | 30.62 | 61.79 | 67.62 | 55.33 | - | - |
| | 2 | CP60 | 22 | 1 | 30.89 | | 61.48 | | - | |
| | 3 | CP60 | 22 | 1 | 30.91 | | 68.65 | | - | |
| 1-05 | 1 | CP60 | 22 | 1 | 30.71 | 62.96 | 62.08 | 51.62 | - | - |
| | 2 | CP60 | 22 | 1 | 30.71 | | 61.64 | | - | |
| | 3 | CP60 | 22 | 1 | 32.55 | | 57.35 | | - | |
| 1-06 | 1 | CP60 | 22 | 1 | 29.94 | 63.12 | 71.07 | 59.37 | - | - |
| | 2 | CP60 | 22 | 1 | 31.06 | | 65.97 | | - | |
| 1-06 | 3 | CP60 | 22 | 1 | 43.96 | 81.28 | 41.37 | 37.23 | - | - |
| 1-07 | 1 | CP60 | 22 | 1 | 45.09 | 67.29 | 58.73 | 52.86 | - | - |
| | 2 | CP60 | 22 | 1 | 40.87 | | 68.03 | | - | |
| | 3 | CP60 | 22 | 1 | 42.85 | | 67.42 | | - | |
| 1-08 | 1 | CF80 | 19 | 2 | 42.22 | 40.97 | 3.26 | 2.71 | 23.21 | 5.54 |
| | 2 | CF80 | 19 | 2 | 42.22 | | 3.01 | | 6.15 | |
| 1-08 | 3 | CF80 | 19 | 2 | 42.43 | 43.43 | 25.27 | 22.74 | - | - |
| 1-09 | 1 | CF80 | 19 | 2 | 42.59 | 38.05 | 7.59 | 6.83 | - | - |
| 1-09 | 2 | CF80 | 19 | 2 | 42.59 | 43.37 | - | - | - | - |
| | 3 | CF80 | 19 | 2 | 42.59 | | - | | - | |
| 1-10 | 1 | CF80 | 19 | 2 | 42.59 | 41.09 | 25.74 | 23.17 | - | - |
| 1-10 | 2 | CF80 | 19 | 2 | 42.59 | 41.98 | 5.11 | 4.60 | 9.05 | 8.15 |
| 1-10 | 3 | CF80 | 19 | 2 | 42.59 | 31.91 | 5.04 | 4.54 | 8.97 | 8.07 |
| 1-11 | 1 | CF80 | 19 | 2 | 42.59 | 44.40 | 16.86 | 15.17 | - | - |
| | 2 | CF80 | 19 | 2 | 42.59 | | 20.52 | | - | |
| | 3 | CF80 | 19 | 2 | 42.59 | | 22.32 | | - | |
| 3-01 | 1 | CF80 | 19 | 2 | 46.00 | 42.58 | 32.88 | 25.59 | - | - |
| | 2 | CF80 | 19 | 2 | 46.00 | | 35.31 | | - | |
| 3-01 | 3 | CF80 | 19 | 2 | 40.43 | 47.50 | 2.39 | 2.15 | - | - |
| 3-02 | 1 | CF80 | 19 | 2 | 42.62 | 33.30 | 1.80 | 1.62 | - | - |
| NR1 | 1 | CF80 | 19 | 1 | 44.11 | 71.16 | 3.68 | 3.31 | 8.22 | 7.40 |
| NR1 | 2 | CF80 | 19 | 1 | 45.70 | 67.49 | 5.00 | 4.50 | 13.53 | 12.18 |
| NR1 | 3 | CF80 | 19 | 1 | 44.70 | 63.41 | 3.27 | 2.94 | - | - |

The characteristic resistance, $P_{Rk}$, is determined as the minimum value of $P_e$ in a series reduced by 10%. The static value of the characteristic resistance, $P_{Rk,static}$, is the minimum value of $P_{e,static}$ reduced by 10%. The evaluation shows that for CP60 decking and a concrete strength of about 30 N/mm$^2$ the characteristic resistance is 61.8 to 63.1 kN. This shows that there was no significant influence of the investigated degree of transverse loading and eccentricity on the resistance of these tests. The higher concrete strength in test 1-06-3 results in a characteristic resistance of 81.3 kN. This is 18.2 kN more than for the two tests with the lower concrete strength in series 1-06. These two tests had an average concrete strength of 30.5 N/mm$^2$. The concrete strength in test 1-06-3 was 44% higher, which lead to an increase of $P_{Rk}$ of 29%. [DIN EN 1994-1-1, 2010] considers the influence of the concrete strength by $\sqrt{f_{ck} \cdot E_{cm}}$. For the measured values an increase of 32% is predicted, as follows:

$$\sqrt{\frac{43.96 \cdot 25900}{30.50 \cdot 21300}} = 1.32$$

This is reasonable close to the observed change of the characteristic resistance.

For series 1-07, a characteristic resistance, $P_{Rk}$, of only 67.3 kN is obtained, because of the low resistance of specimen 1-07-3. If only the first two tests are considered, a value for $P_{Rk}$ of 80.3 kN would be obtained, which is close to the characteristic resistance of specimen 1-06-3 of 81.3 kN. This was expectable, because of the marginal influence of transverse loading.

For the tests in series 1-08 to 3-02, which used CF80 decking and pairs of studs per rib, the characteristic resistance, $P_{Rk}$, is between 31.0 and 47.5 kN per stud. It can be observed that the presence of transverse loads, which were either directly applied or developed by tension forces, had a significant influence on the resistance. Without transverse loads and tension ties, the characteristic resistance, $P_{Rk}$, is 31.0 to 33.3 kN (see tests 1-10-3 and 3-02 in Table 5.1). This increased to between 38.0 and 44.4 kN when transverse loads or tension ties were applied. Specimen 3-01-3 with two layers of reinforcement and no tension ties had a characteristic resistance of 47.5 kN. The other two tests in series 3-01 had tension ties and reached a characteristic resistance, $P_{Rk}$, of 42.6 kN per stud. Comparing the resistance $P_e$ in series 3-01, it appears that the small value of $P_{Rk}$ in the first two tests is because of the small resistance identified for specimen 3-01-1.

For tests in series NR1 with single studs in the ribs of CF80 decking and concentric transverse compression, the characteristic resistance, $P_{Rk}$, was between 63.4 and 71.2 kN. A decrease of the resistance was observed for higher degrees of transverse loading.

Based on the characteristic resistance, $P_{Rk}$, the displacement capacity, $\delta_u$, for each specimen is determined according to Figure 2.21. The definition of $\delta_u$ was originally developed for solid slabs and may lead to a too small value for the displacement capacity when deep steel decking is used. This is especially true for the tests with CF80 decking. The change of the load bearing mechanism after the observation of rib pry-out failure typically was accompanied by a very localised drop of the test load. This drop lead to very small values of the displacement capacity, $\delta_u$, in some cases. In most cases, the test load increased again to a load that was larger than $P_{Rk}$ and a second intersection, $\delta_{u2}$, could be found at a significantly larger slip. The load-slip curve of specimen NR1-1, shown in Figure 5.1, is an example for one of this cases.

Some of the tests, for example specimen 3-01-3, did not show a second intersection of the load-slip curve with $P_{Rk}$. Nevertheless, these test showed a ductile behaviour as the load-slip curves did not show a significant decrease of the resistance. Diagrams showing the readings of the displacement capacities for all tests are presented in Appendix C. The

obtained displacement capacities $\delta_u$ and $\delta_{u2}$ are summarised in Table 5.2. The characteristic values $\delta_{uk}$ and $\delta_{u2k}$ are obtained by reducing the minimum values of $\delta_u$ and $\delta_{u2}$ by 10%.

The evaluation of the displacement capacity for specimens with CP60 decking shows a very ductile behaviour for all tests. Comparing specimen 1-06-3 to the other specimens in series 1-06 and to series 1-07, the concrete strength and the slab hogging moment can be identified as the major influences on the displacement capacity. Within series 1-06, it was observed that the higher concrete strength leads to a 37% smaller characteristic displacement capacity, $\delta_{uk}$. The increase of the eccentric transverse load in series 1-07 increased the displacement capacity by 42% in comparison to specimen 1-06-3.

Specimens with 80 mm deep steel decking show lower displacement capacities. Series PV with RD 80 decking and 150 mm long shear studs reached only a characteristic displacement capacity, $\delta_{uk}$, of only 4.6 mm. Specimens with pairs of 125 mm long studs in CF80 decking reached characteristic slip capacities, $\delta_{uk}$, of 15.2 to 25.6 mm when high transverse loads were applied. This was the case for specimens 1-08-3, 1-10-1, 3-01-1, 3-01-2 and series 1-11. Without transverse loads the characteristic slip capacity, $\delta_{uk}$, is less than 6 mm, but considering the second intersection of the load-slip curve with $P_{Rk}$ led to satisfactory slip capacities $\delta_{u2}$ in most cases.

It can be concluded that the consideration of concentric and eccentric transverse loading has a significant influence on the displacement capacity of the shear studs. Especially for deep decking, transverse loading improves the ductility of the shear connectors. For 80 mm deep decking this influence is not negligible because of the small displacement capacity without transverse loading. Therefore, the application of transverse loading is required to obtain a more realistic displacement capacity.

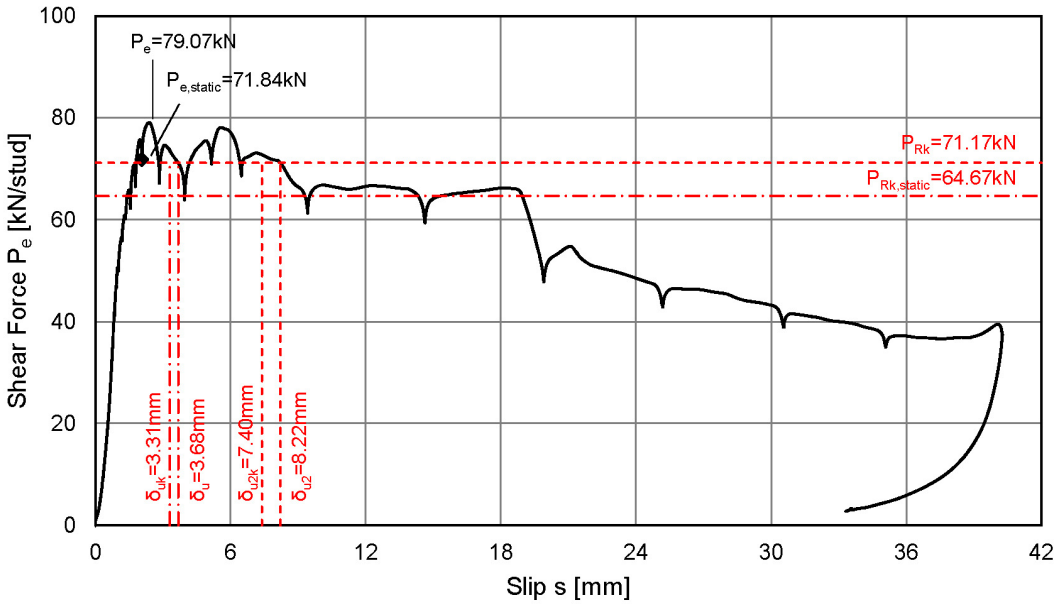


Figure 5.1: Displacement capacities $\delta_u$ and $\delta_{u2}$ for specimen NR1-1.

## 5.2 Influence of the decking and embedment depth of the stud

The type of steel decking used in the push-out tests and the resulting geometry of the shear connection was the decisive influence on the load-slip behaviour. Other influences, such as concrete strength or transverse loading, act as modifiers on the behaviour, but the geometry determines the failure modes.

Figure 5.2 shows a comparison of load-slip curves for specimens with 58 mm deep decking and 80 mm deep decking. Initially both specimens showed an identical behaviour, but when a load of about 80 kN per stud was reached, the load-slip behaviour changed completely.

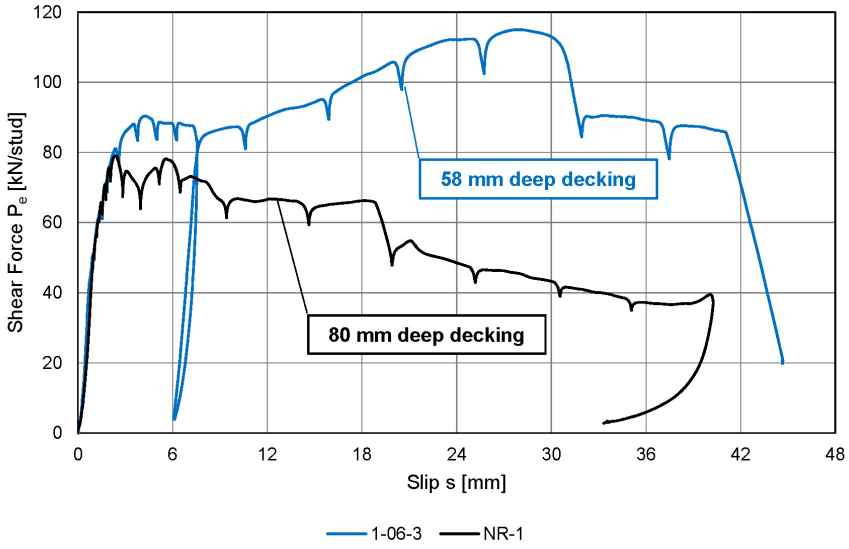


Figure 5.2: Comparison of load-slip curves for 58 mm deep decking and 80 mm deep decking.

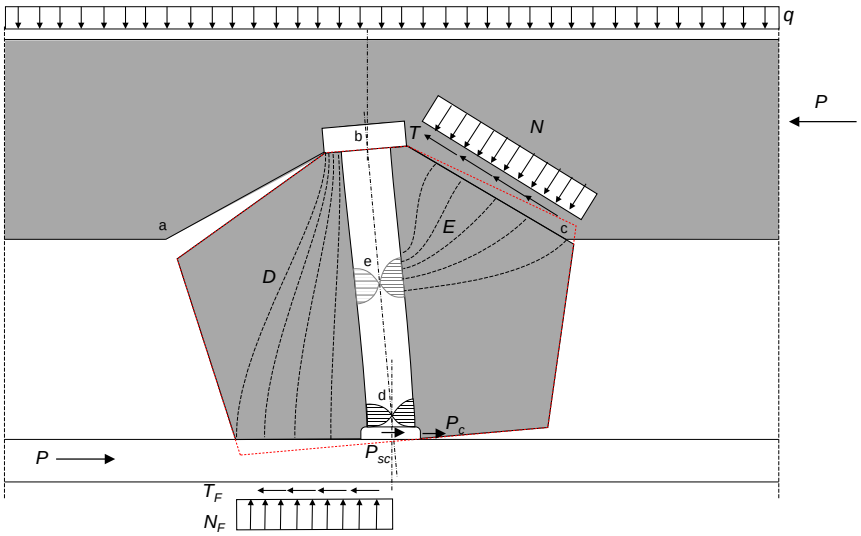


Figure 5.3: Load-bearing behaviour of studs in the ribs of composite slabs for a small embedment depth.

For the 58 mm deep decking, a load-slip behaviour with double curvature of the shear stud

developed, as was described by [Lungershausen, 1988] (see Section 2.1.2 and Figure 2.2).

In case of the 80 mm deep decking, concrete failure of the rib occurred. The load bearing-behaviour can be described according to Figure 5.3. The shear force, $P$, is divided into the components $P_c$ and $P_{sc}$. The force $P_c$ is introduced into the concrete at the weld collar and the force $P_{sc}$ remains in the stud shank and causes bending of the stud. Because of the force $P_c$, the concrete rib is subjected to a bending effect. The rib fails at point 'a', when the concrete tensile strength is reached. The failure progresses along the line $a$-$b$-$c$ until the concrete cone has separated from the topping. This leads to a drop-off in the test load. For further loading, the shear force $P$ is introduced into the slab by the forces $N$ and $T$ along the line $b$-$c$. The force $N$ is in equilibrium with compression forces $E$ that are supported by the stud shank. The rib and the stud rotate around point $d$. This leads to the development of a yield hinge in the stud. The restraint rotation of the concrete cone causes compression forces $D$ and contributes to the forces $E$ and $N$. At large slip, the forces $E$ may lead to a yield-hinge at point $e$. This behaviour is very sensitive to transverse loading. The load $q$ increases the contact force $N$ and the shear force $T$ until the resistance of the forces $D$ or $E$ in compression is reached. The increase of $T$ and $N$ develops larger shear forces $P$.

In [Lungershausen, 1988], this type of load-bearing behaviour was explained because of an insufficient embedment depth of the head of stud into the concrete above the rib. To ensure the occurrence of a failure mode according to section 2.1.2, an embedment depth of $2d\sqrt{n_r}$ was required. For single shear studs per rib, this conforms to the requirements of [DIN EN 1994-1-1, 2010]. The results of the conducted push-out tests show, that an embedment depth of $2d$ is not sufficient to prevent the occurrence of rib pry-out failure, because the embedment depth of the studs in tests with 80 mm deep decking was about $2.0d$ to $2.3d$.

The reduction factors proposed by [Konrad, 2011] require an embedment depth of $h_{sc} \geq 1.56h_p$, which was not satisfied by the stud height in tests with 80 mm deep decking. In addition, the numerical investigations in [Konrad, 2011] show a change of the correlation functions for the reduction factor, $k_t$, for $h_{sc} = 1.56h_p$ (see Figure 5.4). Considering the results of the conducted push-out tests, the change of the correlation functions can be explained by the change of the load-slip behaviour.

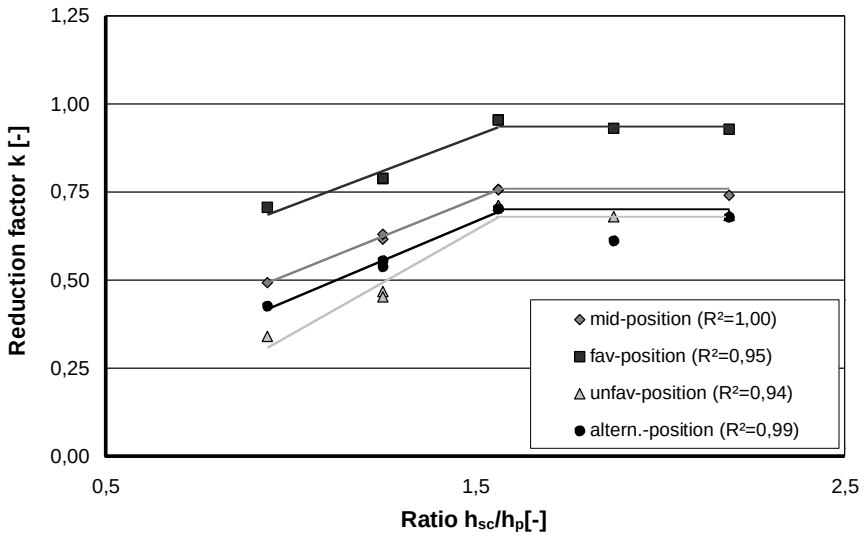


Figure 5.4: Influence of the ratio $h_{sc}/h_p$ on the reduction factor $k_t$ (from [Konrad, 2011]).

## 5.3 Influence of concentric transverse loading

The push-out tests showed two different types load-displacement behaviour:

- Tests with 58 mm deep decking showed load-slip curves with two load peaks. The failure modes were rib punch-through, concrete pull-out and stud failure.
- Tests with 80 mm deep decking showed load-slip curves with only one load peak. The failure mode was rib pry-out. Some tests with single studs per rib also showed stud failure.

Because of the different load bearing behaviour, the influence of transverse loading varied. Therefore, the influence of transverse loading will be discussed separately for each type of load-slip curve.

### 5.3.1 Influence for load-slip curves with double curvature of the stud

This type of load-slip curve was observed for specimens with 58 mm deep decking. The influence of concentric transverse loading was investigated in series 1-04 and 1-05. The concrete strength of these specimens was between 30.6 and 32.6 N/mm$^2$. In Table 5.3, the results of the tests in series 1-04 and 1-05 are summarised.

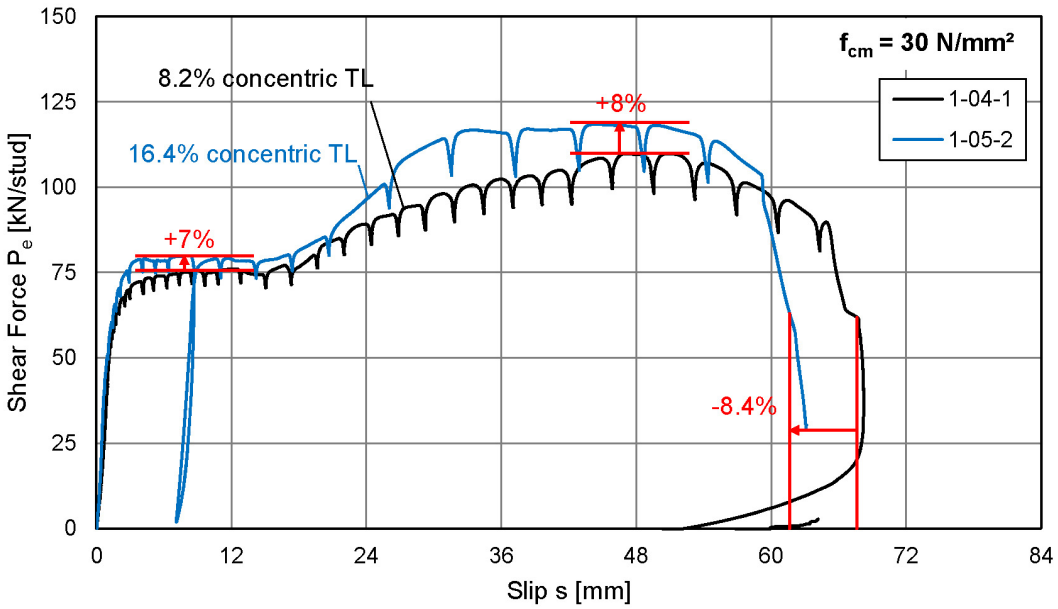


Figure 5.5: Comparison of load-slip behaviour for different degrees of concentric transverse loading.

The influence of the degree of concentric transverse loading on the first peak load is not significant, as shown in Figure 5.6 and Figure 5.5. At a degree of transverse loading of about 8% the average resistance, $P_{em}$, is 72.1 kN per stud. Doubling the degree of transverse loading to about 16% increased the average resistance, $P_{em}$, by only 3.4% to 74.2 kN per stud. For the characteristic resistance, $P_{Rk}$, the increase was only 1.9% from 61.8 to 63.0 kN per stud (see Table 5.3).

Because of the different failure modes concrete pull-out and stud failure, which were observed in tests with CP60 decking, the displacement capacities, $\delta_u$, of the tests varies by up to 7 mm

Table 5.3: Test results for specimens with CP60 decking and different degrees of concentric transverse loading.

| Series | i | $P_T$ [kN/stud] | $P_e$ [kN/stud] | $P_{em}$ [kN/stud] | $P_{Rk}$ [kN/stud] | $\delta_u$ [mm] | $\delta_{um}$ [mm] | $\delta_{uk}$ [mm] |
|---|---|---|---|---|---|---|---|---|
| | 1 | 8.2% | 73.94 | | | 67.62 | | |
| 1-04 | 2 | 6.25≙8.5% | 73.61 | 72.07 | 61.79 | 61.48 | 65.92 | 55.33 |
| | 3 | 6.25≙9.1% | 68.66 | | | 68.65 | | |
| | 1 | 16.4% | 69.95 | | | 62.08 | | |
| 1-05 | 2 | 12.5≙15.8% | 79.15 | 74.15 | 62.96 | 61.64 | 60.36 | 51.62 |
| | 3 | 12.5≙16.8% | 74.43 | | | 57.35 | | |

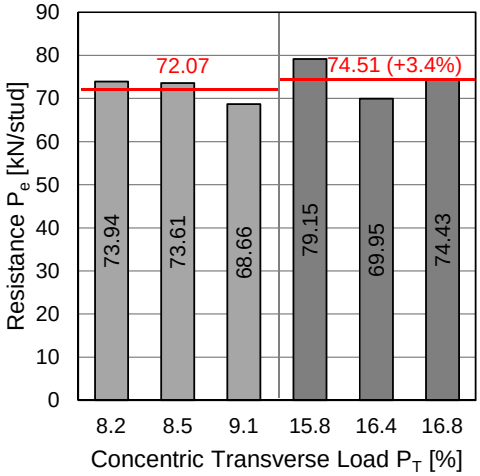


Figure 5.6: Resistance $P_e$ for different degrees of concentric transverse loading with CP60 decking.

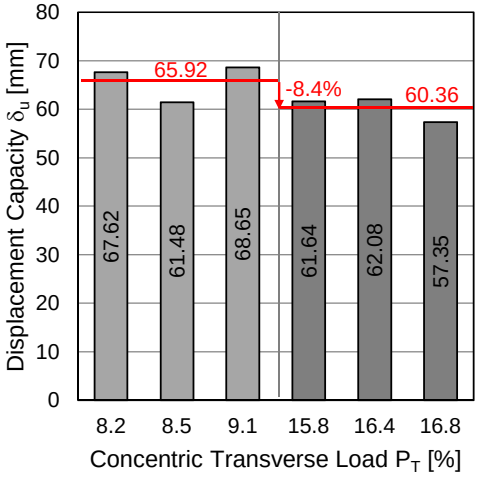


Figure 5.7: Displacement capacity $\delta_u$ for different degrees of concentric transverse loading with CP60 decking.

within a series. The displacement capacity, $\delta_u$, in series 1-04 and 1-05 was between 57.4 mm and 68.7 mm. The increase of the degree of transverse loading from 8% to 16% lead to about a 8.4% smaller displacement capacity in series 1-05, as shown in Figure 5.7. For the characteristic displacement capacity, $\delta_{uk}$, the decrease was 6.7%. Considering that the displacement capacities of the tests in series 1-04 and 1-05 was very large, the influence of the degree of transverse loading was not relevant with regards to the 6 mm ductility criterion of [DIN EN 1994-1-1, 2010].

It can be concluded that for a load-slip behaviour with two load peaks the influence of the degree of transverse loading on the resistance, $P_e$, and the displacement capacity, $\delta_u$, was not relevant for design.

### 5.3.2 Influence for load-slip curves with single curvature of the stud

This type of load-slip behaviour was observed in tests with CF80 decking. The behaviour is characterised by the occurrence of rib pry-out failure at a small slip. After the rib failed, the shear force is transferred by friction and aggregate interlock at the failure surface. Therefore, this load bearing behaviour was very sensitive to transverse loading, as can be seen in

Figures 5.8 and 5.9. The influence of concentric transverse loading for this type of load-slip behaviour was investigated in series 1-09, 1-10 and NR1. Table 5.4 gives an overview of the test results.

Table 5.4: Test results for specimens with CF80 decking and different degrees of concentric transverse loading.

| Series | i | $n_r$ [-] | $f_{cm}$ [N/mm$^2$] | $P_T$ [kN/rib] | $P_e$ [kN/rib] | $P_{6mm}$ [kN/rib] | $\delta_u$ [mm] | $\delta_{u2}$ [mm] |
|---|---|---|---|---|---|---|---|---|
| 1-09 | 1 | 2 | 42.59 | 4.4≙5.2% | 84.56 | 83.07 | 7.59 | - |
| 1-10 | 1 | 2 | 42.59 | 8.8≙10.8% | 81.50 | 106.11 | 25.74 | - |
| | 2 | 2 | 42.59 | 6.6≙8.4% | 78.58 | 82.95 | 5.11 | 9.05 |
| | 3 | 2 | 42.59 | 0 | 70.92 | 68.96 | 5.04 | 8.97 |
| NR1 | 1 | 1 | 44.11 | 0 | 71.84 | 77.16 | 3.31 | 8.22 |
| | 2 | 1 | 45.70 | 4.4≙6.4% | 67.93 | 68.33 | 4.50 | 13.53 |
| | 3 | 1 | 44.70 | 8.8≙13.6% | 64.87 | 60.56 | 2.94 | - |

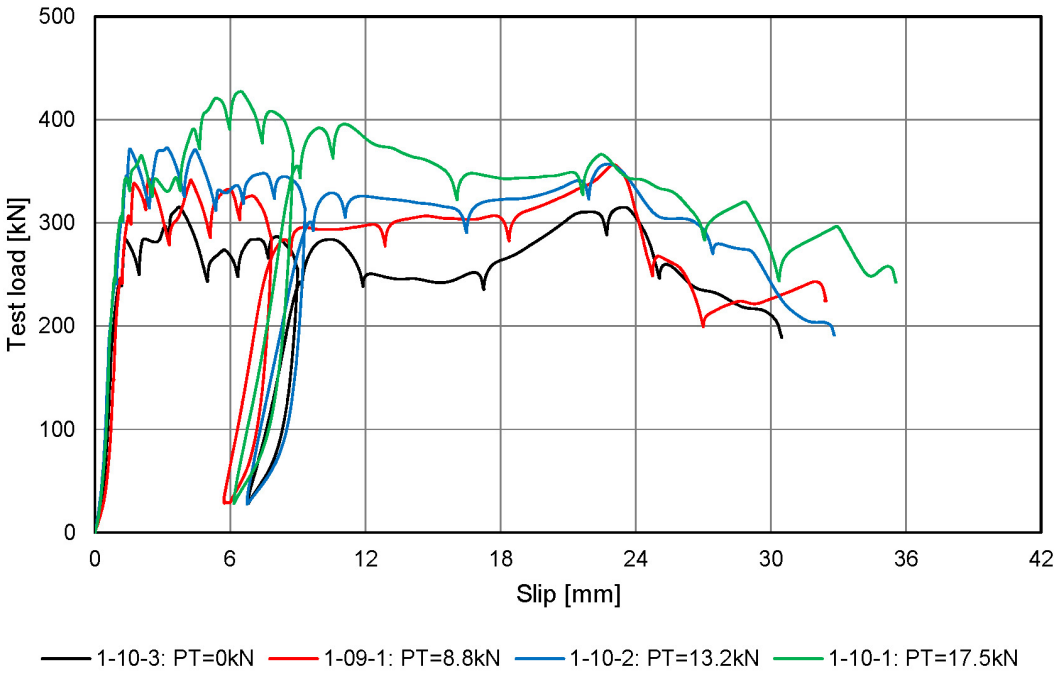


Figure 5.8: Load-slip curves at different degrees of transverse loading for CF80 decking and pairs of studs per rib.

As can be seen in Figure 5.8, the influence of transverse loading was beneficial for test with pairs of studs per through. Considering the failure load of the ribs, the shear resistance increased by about 11% to 19% when transverse loads were applied, as shown in Figure 5.10. The essential influence on the failure load appears to be the presence of transverse loading, because the failure load did not vary significantly for higher degrees of transverse loading. After the failure of the ribs was observed, the frictional load bearing mechanism establishes. Figure 5.8 shows, that the test load was significantly increased at larger slips. At 6 mm slip, the test load for specimens with transverse loading increased by up to 54% compared to a specimen without transverse loading (see Figure 5.11). The displacement capacities $\delta_u$

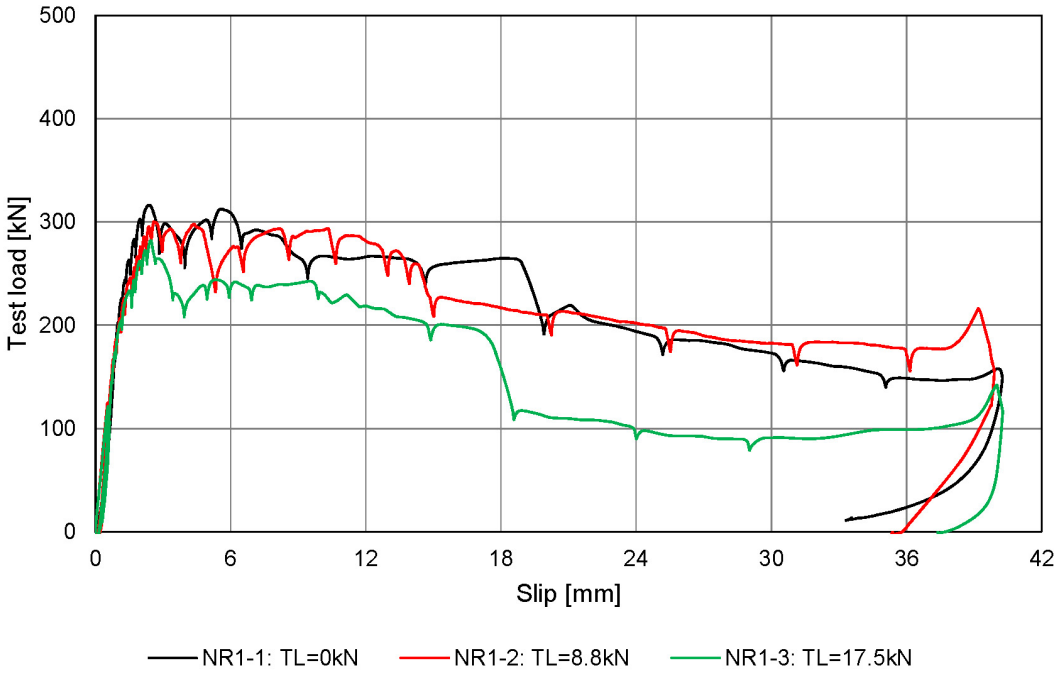


Figure 5.9: Load-slip curves at different degrees of transverse loading for CF80 decking and single studs per reb.

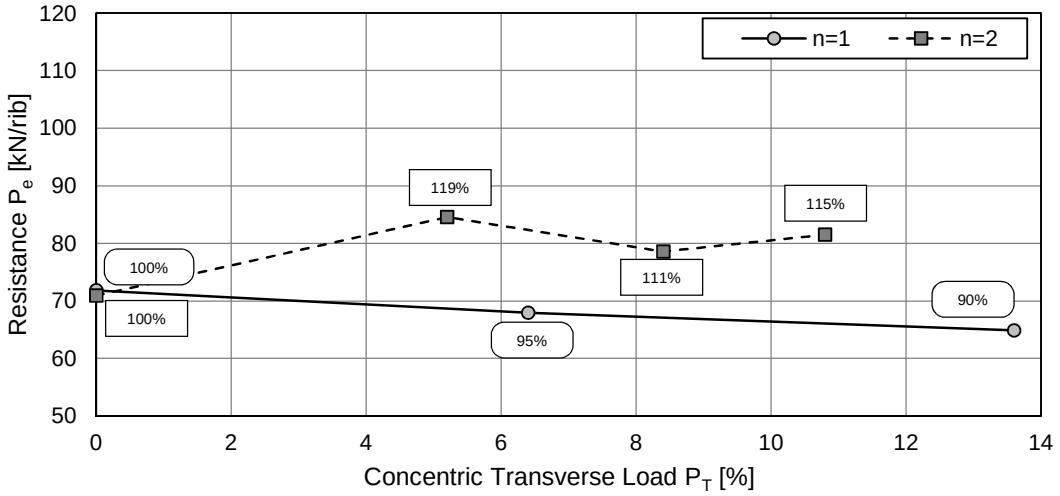


Figure 5.10: Resistance $P_e$ for different degrees of concentric transverse loading with CF80 decking.

and $\delta_{u2}$ were also increased by transverse loading because of the larger frictional resistance (see Figure 5.12). This increase was not significant for smaller degrees of transverse loading because of the fluctuation in the load-slip curves (see Figure 5.8).

In case of single studs per rib, the beneficial influence of transverse loading could not be confirmed in the tests of series NR1 (see Figure 5.9). The values for the failure load and the load at 6 mm slip showed an adverse effect of transverse loading, because the test load

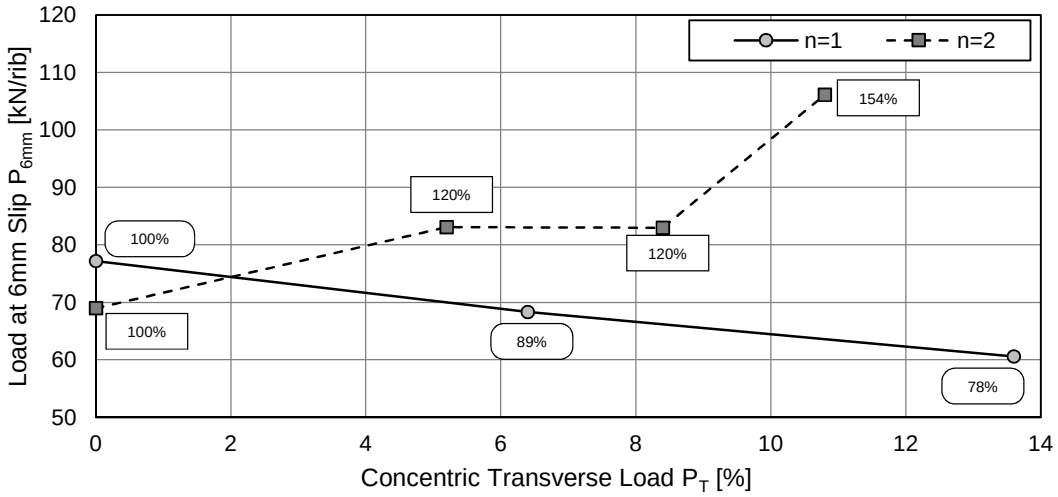


Figure 5.11: Test load at 6 mm slip for different degrees of concentric transverse loading with CF80 decking.

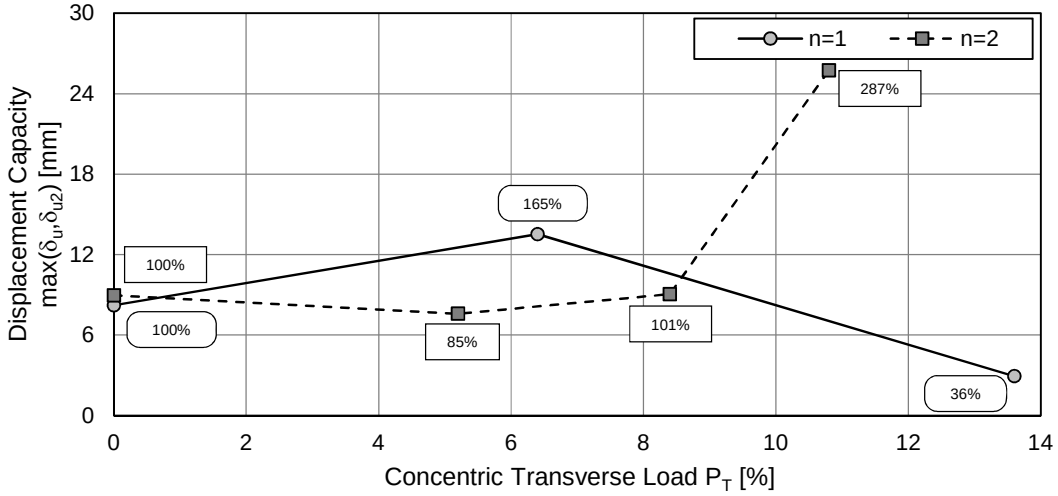


Figure 5.12: Displacement capacity $\delta_u$ for different degrees of concentric transverse loading with CF80 decking.

decreased for higher transverse loads (see Figures 5.10 and 5.11). With regards to the displacement capacity, the specimens NR1-1 and NR1-2 confirm the beneficial influence of transverse loading, because $\delta_{u2}$ increased by about 65%, as shown in Figure 5.12. But for specimen NR1-3 no second intersection of $P_{Rk}$ with the load-slip curve was found, which lead to a displacement capacity $\delta_u$ that was 64% less than without transverse loading. Considering the load-slip curves shown in Figure 5.9, the general behaviour did not change significantly because of transverse loading. The specimen without transverse loading and with 6.4% transverse load showed an almost identical behaviour. For 13.6% transverse loading, the behaviour was also almost identical until rib pry-out failure was observed.

Because the load-slip behaviour is very dependent on the failure behaviour of concrete and frictional resistances at the failure surface, there may be a large variability of the shear

resistance. Because of the large variability and small number of tests, it cannot be certainly assumed that the influence of transverse loading was adverse for single studs. More probable is, that the beneficial influence of transverse loading for specimens with single studs is not as prominent as for pairs of studs and was not observed because of the assumable large variability of the load-slip behaviour.

Because of the small number of tests in this investigation, it is not possible to give a final conclusion for the influence of the degree of transverse loading on the resistance and displacement capacity of the shear connection. However, it can be concluded that transverse loading tends to improve the load bearing behaviour. This is because of for the following points:

- Transverse loading increases the frictional resistance at the interface between steel beam and slab.
- Rib pry-out failure is governed by the behaviour of the concrete. The additional compression delays the concrete tensile failure. As a consequence, the failure load increases.
- After concrete failure, the transverse compression increases the frictional forces that can be resisted at the failure surface.

In addition, a significant influence of transverse loading was observed already at small slip and therefore transverse loading is relevant in practice. This leads to the following conclusions on the consideration of transverse loading:

1. Transverse loading must be considered in push-out tests to obtain a more realistic behaviour of the shear connection when the resistance and displacement capacity are investigated. This results in additional testing effort.
2. Alternatively, it must be ensured that rib pry-out failure does not occur and a load-slip behaviour with two load peaks develops. This allows the conduction of push-out tests without transverse loading, because the observed influence on the resistance was not relevant. On the other side, more restrictive rules e.g. for a larger embedment depth of the head of the stud would be necessary.

## 5.4 Influence of eccentric transverse loading

### 5.4.1 Influence for load-slip curves with double curvature of the stud

In series 1-06 and 1-07, push-out tests with eccentric transverse loading were conducted. The concrete strength for specimen 1-06-3 and series 1-07 was increased. Therefore, the concrete grade must be also considered in the evaluation of the influence of the eccentricity.

Figure 5.13 shows representative load-slip curves of a concentric compressed specimen (1-04-1) and an eccentric compressed specimen (1-06-1) with concrete grade C20/25. For both specimens, the degree of transverse loading was 8.2% of the shear force. It can be seen, that there was no influence on the resistance, $P_{e1}$. In this comparison, the second load peak decreased by about 18% in the test with eccentric transverse loading. The displacement capacity, $\delta_u$, increased by 5% in this example.

A comparison for different degrees of eccentric transverse loading at concrete grade C30/37 is shown in Figure 5.14. It can be seen, that a higher degree of eccentric transverse loading did not affect the resistance, $P_{e1}$, significantly. In this example, the second load peak, $P_{e2}$, increased by about 7% and the displacement capacity, $\delta_u$, increased by about 42%.

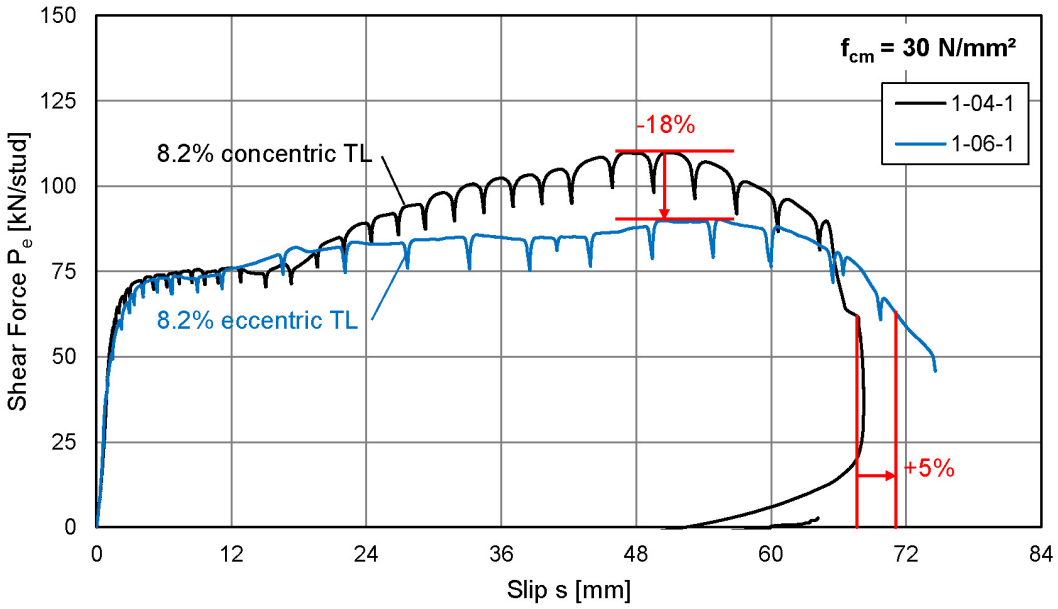


Figure 5.13: Influence of eccentric transverse loading for C20/25 and CP60 decking.

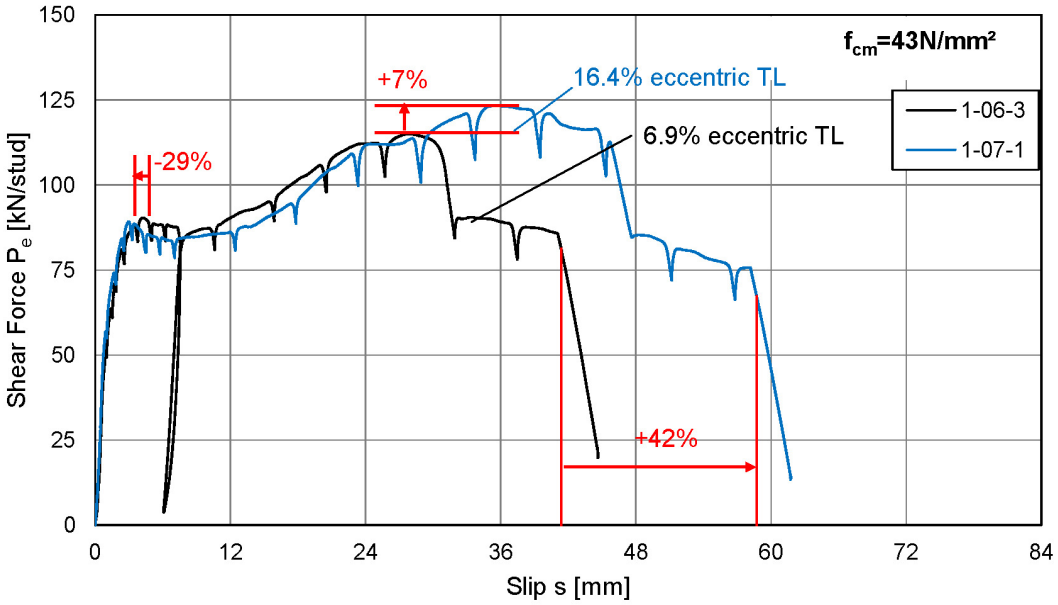


Figure 5.14: Influence of the degree of eccentric transverse loading for C30/37 and CP60 decking.

Table 5.5 shows an overview of the obtained test results for series 1-04, 1-06 and 1-07.

Considering the resistance, $P_{e1}$, there was no significant influence of eccentric transverse loading within each concrete grade, as shown in Figure 5.15. The lower resistance of specimen 1-07-3 was by tendency an outlier in comparison to other tests with C30/37. Therefore, the resistance, $P_{e1}$, was about 70 kN per stud for C20/25 and about 90 kN/stud for C30/37. The increase of $P_{e1}$ was 26% for a 41% higher concrete strength. Accord-

Table 5.5: Overview of test results with concentric and eccentric transverse loading for CP60 decking.

| Series | i | $f_{cm}$ [N/mm$^2$] | $P_T$ [kN/stud] | $P_{e1}$ [kN/stud] | $P_{e1m}$ [kN/stud] | $P_{e2}$ [kN/stud] | $P_{e2m}$ [kN/stud] | $\delta_u$ [mm] | $\delta_{um}$ [mm] |
|---|---|---|---|---|---|---|---|---|---|
| 1-04 | 1 | 30.62 | 8.2%[a] | 70.44 | 72.07 | 109.75 | 100.78 | 67.62 | 65.92 |
| | 2 | 30.89 | 6.25≙8.9%[a] | 69.63 | | 98.91 | | 61.48 | |
| | 3 | 30.91 | 6.25≙9.6%[a] | 65.03 | | 93.67 | | 68.65 | |
| 1-06 | 1 | 29.94 | 8.2% | 68.89 | 71.62 | 90.33 | 90.50 | 71.07 | 68.52 |
| | 2 | 31.06 | 6.25≙9.5% | 65.69 | | 90.67 | | 65.97 | |
| 1-06 | 3 | 43.96 | 6.25≙6.9% | 90.31 | 90.31 | 114.96 | 114.96 | 41.37 | 41.37 |
| 1-07 | 1 | 45.09 | 16.4% | 89.25 | 85.60 | 123.27 | 115.86 | 58.73 | 64.73 |
| | 2 | 40.87 | 15≙16.2% | 92.77 | | 110.28 | | 68.03 | |
| | 3 | 42.85 | 15≙20% | 74.77 | | 114.03 | | 67.42 | |

[a] Concentric transverse load

ing to [DIN EN 1994-1-1, 2010], the influence of the concrete strength can be considered according to $\sqrt{f_{ck}E_{cm}}$. If this expression is evaluated with the measured material properties, [DIN EN 1994-1-1, 2010] predicts an increase of the resistance by 33%. This is an over-estimation of the measured influence of the concrete grade.

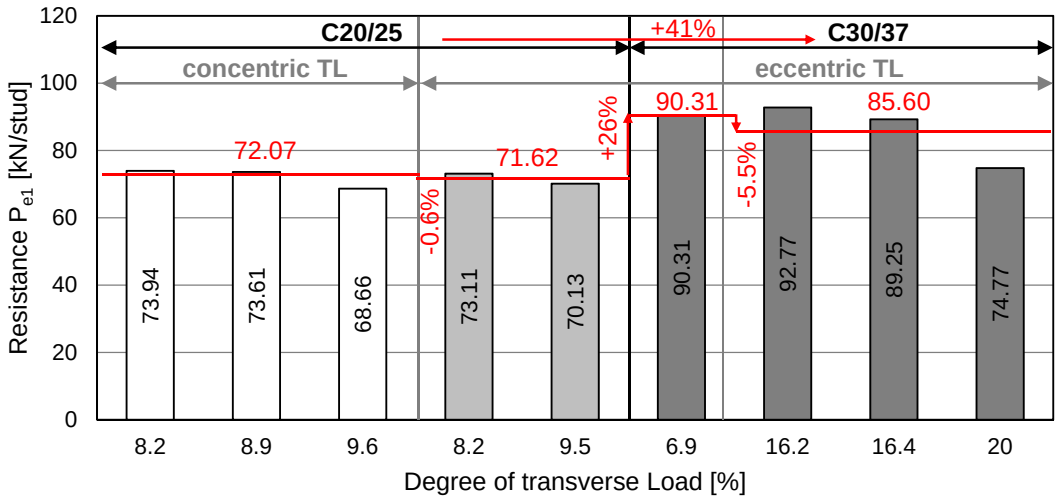


Figure 5.15: Influence of eccentric transverse loading and concrete strength on the resistance.

Figure 5.16 shows the influence of eccentric transverse loading and concrete strength on the second load peak. For concrete grade C20/25, the test results show a variation of about 20 kN per stud for the second load peak. For C30/37 concrete, the variation is about 14 kN per stud. Within each concrete grade, the scatter of the load appears to be rather because of the variation of the final failure mode between concrete pull-out and stud failure than because of the eccentric transverse load. The increase of the second load peak, $P_{e2}$, because of the higher concrete strength was 14% to 28%. Therefore, [DIN EN 1994-1-1, 2010] overestimates the influence of the concrete strength also for $P_{e2}$.

Considering the displacement capacity, $\delta_u$, a significant influence of the concrete strength and the degree of eccentric transverse loading could be identified, as shown in Figure 5.17. For C20/25 concrete displacement capacities of 62 to 71 mm were obtained. At this already high displacement capacity, the influence of eccentric transverse loading was not

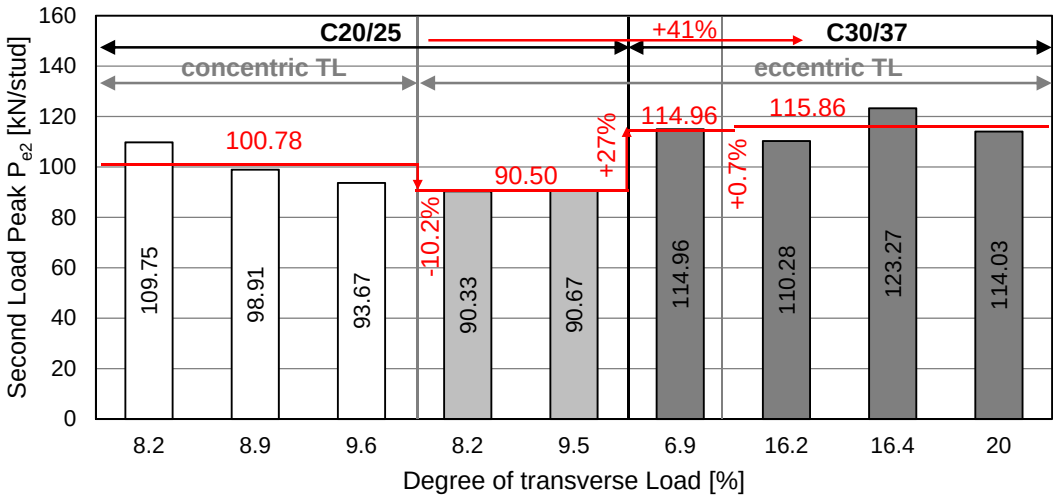


Figure 5.16: Influence of eccentric transverse loading and concrete strength on the second load peak.

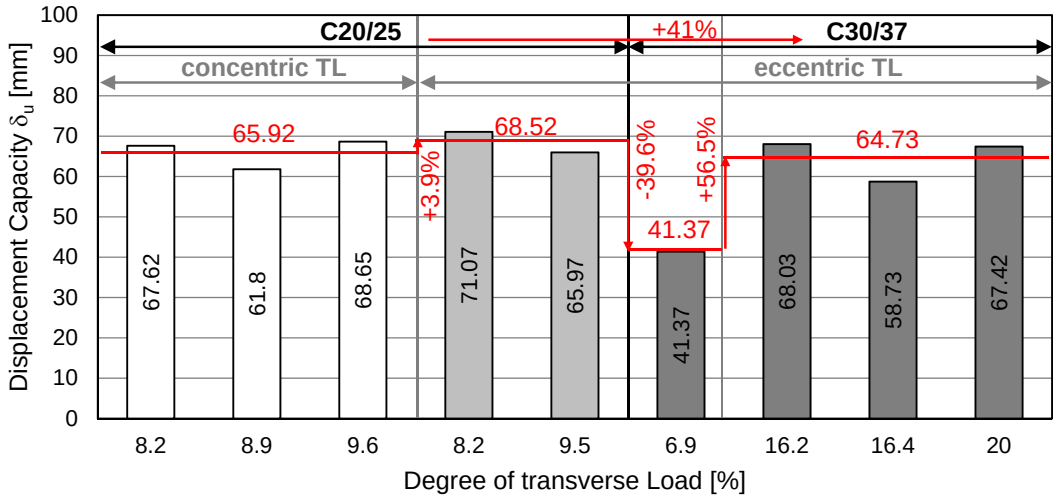


Figure 5.17: Influence of eccentric transverse loading and concrete strength on the displacement capacity.

that significant. The displacement capacity increased by only 4% comparing concentric and eccentric transverse loading. The small difference of the displacement capacities is because the plastic deformation of the stud shank is also limiting the displacement at such a large slip. The increase of the concrete strength lead to a decrease of $\delta_u$ of about 40% for a low degree of eccentric transverse loading. With C30/37 concrete, the displacement capacity increased by about 56% when the degree of eccentric transverse loading was raised from 7% to about 16%. The displacement capacity then was similar to the results for C20/25 concrete.

It can be concluded that for load bearing mechanisms with two load peaks the eccentric transverse load affects in general only the displacement capacity, $\delta_u$. The effect of eccentric loading on $\delta_u$ is beneficial and is stronger for higher concrete strengths. It is assumable that the obtained values for $\delta_u$ might become relevant in comparison to the 6 mm criterion for

high strength concrete, because the displacement capacity decreases for higher concrete strengths without eccentric transverse loading. Then the application of eccentric transverse loading is a necessity to obtain realistic displacement capacities.

### 5.4.2 Influence for load-slip curves with single curvature of the stud

This type of load-slip behaviour is characterised by rib pry-out failure. Figure 5.18 shows a comparison of load-slip curves for specimens without transverse loading, concentric and eccentric transverse loading. It can be seen that concentric and eccentric transverse loading strongly improve the resistance and displacement capacity compared to a specimen without transverse load. A significant difference of the load-slip behaviour between eccentric and concentric transverse loading could not be identified.

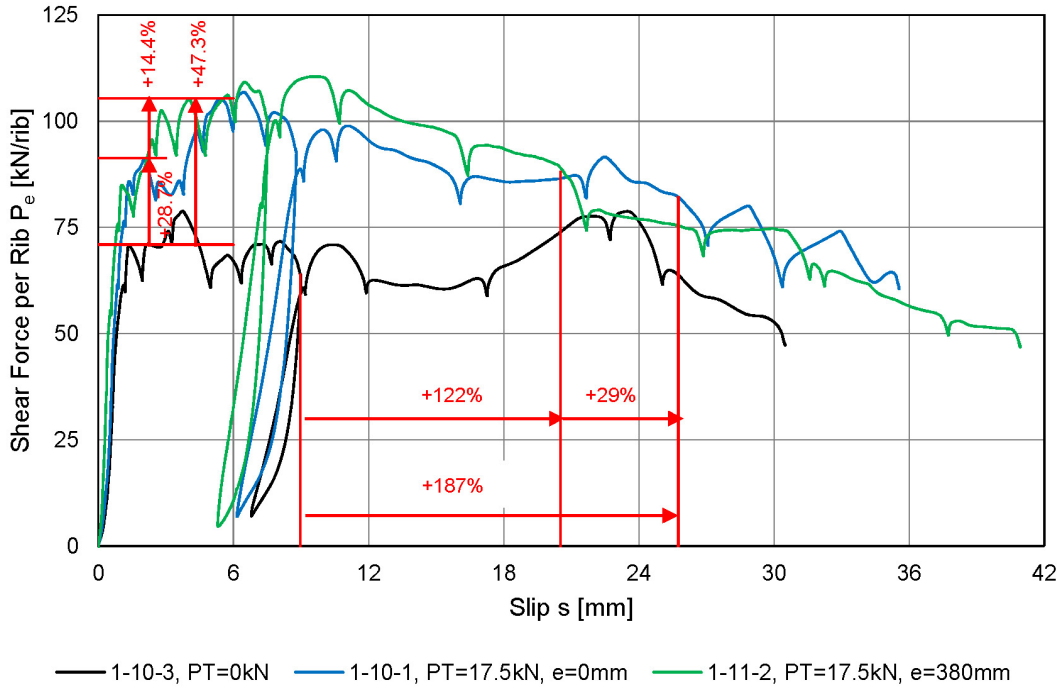


Figure 5.18: Comparison of load-slip curves for specimens without transverse load, concentric transverse load and eccentric transverse load for CF80 decking.

A comparison for the failure load $P_e$ per rib is shown in Figure 5.19. The improvement of the failure load because of the transverse load is obvious. For the eccentrically transverse loaded specimens, in average 14% higher failure loads than for the concentrically loaded specimen were identified. The failure load was identified by the observation of cracks in the ribs during the tests. However, all load slip curves (see Figure 5.18) for eccentrically and concentrically transverse loaded specimens show a significant change of the stiffness at about 80 to 90 kN per rib. This gives evidence that eccentric transverse loading does not significantly influence the failure load, $P_e$. The larger load identified in the eccentrically loaded tests was because of the improved post-failure behaviour and delayed observation of cracks.

The displacement capacity, $\delta_u$, of the specimens are compared in Figure 5.20. Determining the displacement capacity according to [DIN EN 1994-1-1, 2010] Annex B2 leads to about 23% smaller values than for concentric transverse loading. This was because of the larger failure loads identified for the eccentrically loaded specimens. However, the load-slip curves

for both types of transverse loading were very similar, as shown in Figure 5.18, and show no evidence to assume a significant difference of the displacement capacity.

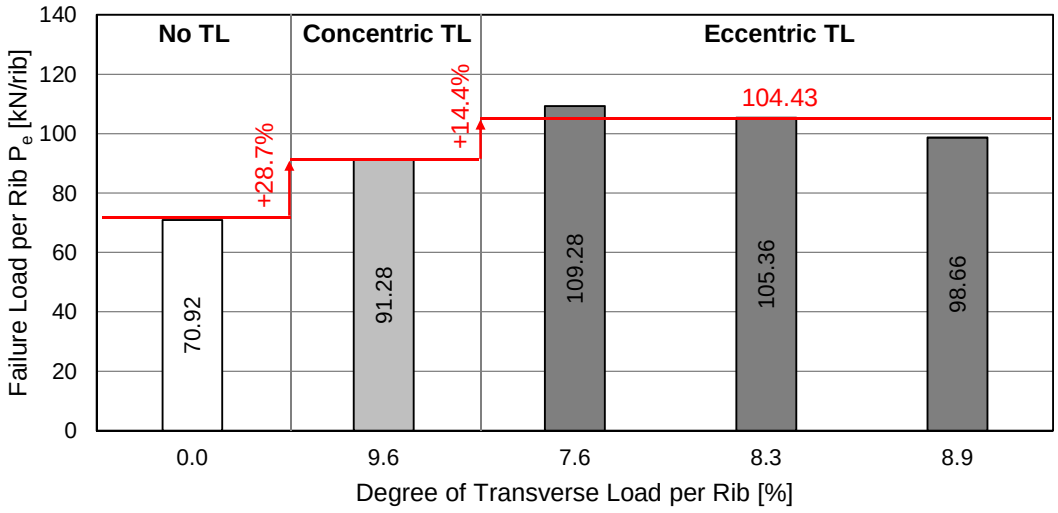


Figure 5.19: Influence of eccentric transverse loading on the failure load of the ribs.

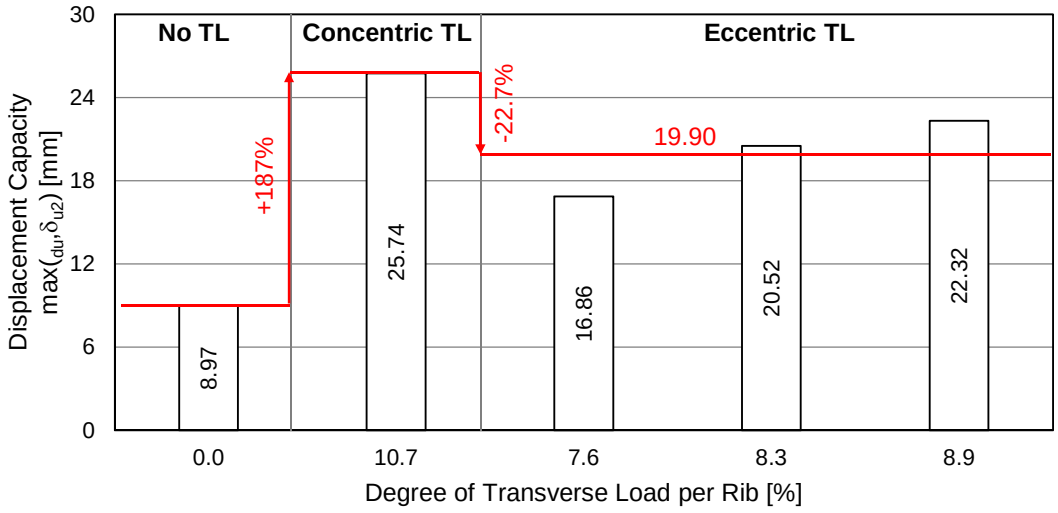


Figure 5.20: Influence of eccentric transverse loading on the displacement capacity.

## 5.5 Influence of the concrete strength

A significant change of the concrete grade was only investigated in tests using CP60 decking. For the observed rib punch-through failure in these tests, a higher concrete grade lead to an increase of the resistance and a decrease of the displacement capacity (see also Figure 4.21).

These effects were already shown in section 5.4.1. For an increase of the measured concrete strength of 41% the resistance increased by about 26%, as shown in Figure 5.15. The displacement capacity decreased by about 40%, as shown in Figure 5.17.

In section 5.4.1, it was shown that the term $\sqrt{f_{ck}E_{cm}}$ predicted an increase of the resistance of about 33% when measured material properties were used. The over-estimation of the influence of the concrete strength is the result of considering a pure concrete failure criterion.

In fact the resistance is a combination of a load-bearing component of the shear stud due to bending and a load-bearing component of the concrete. Therefore, the relative increase of the resistance is always smaller than the relative increase of the concrete strength. The consideration of the concrete strength with a correlation function as $\sqrt{f_{ck}E_{cm}}$ is not sufficient to consider this influence, because of the superposition of the two load-bearing components.

## 5.6 Influence of the welding method

The influence of using pre-punched decking or welding the shear stud through the decking was only investigated for specimens with CF80 decking. A comparison of the load-slip behaviour is given in Figure 5.21.

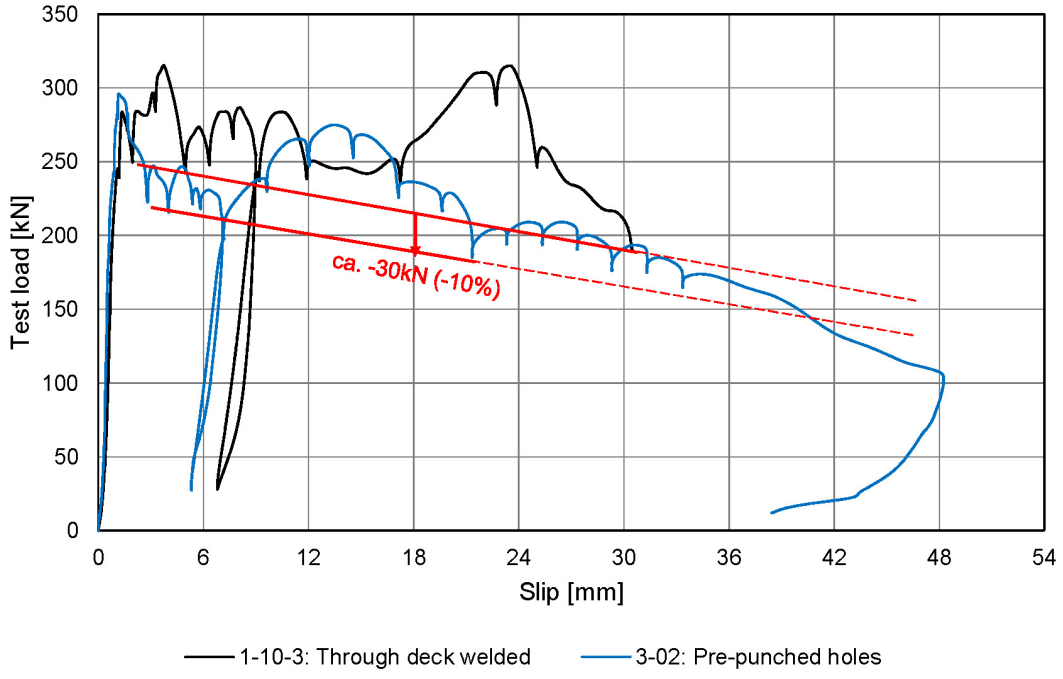


Figure 5.21: Influence of the welding procedure with CF80 decking.

The failure load of the concrete cone was not affected by the welding method. For the post-failure behaviour, studs welded through the decking showed an approximately 10% larger resistance than in the test with pre-punched decking. The additional resistance is the result of activating the decking as a tension tie. For the frictional post-failure mechanism, this effect can probably only be obtained when decking is anchored into the continuous part of the slab by a stiffener.

## 5.7 Influence of the number of reinforcement layers

Investigations on the influence of the number of reinforcement layers were conducted with CF80 decking. A comparison of the obtained load-slip behaviour is given in Figure 5.22.

Only the failure load for rib pry-out failure was significantly improved when two layers of reinforcement were used. This was because the bottom reinforcement layer overlapped the failure cone and therefore had a certain anchorage effect. After rib pry-out failure, the friction based post-failure behaviour was unaffected.

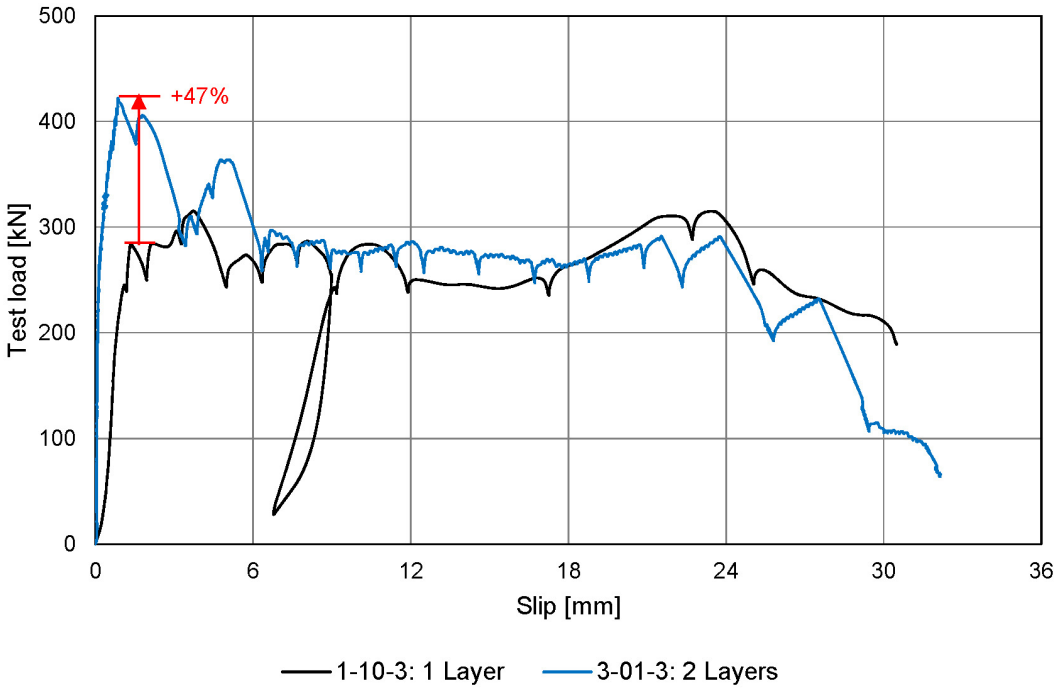


Figure 5.22: Influence of the number of reinforcement layers with CF80 decking.

## 5.8 Influence of the number of studs per rib

The influence of the number of shear studs per rib was investigated in specimens with CF80 decking. Figure 5.23 shows a comparison of the load-slip behaviour for single stud per rib and pairs of studs per rib.

An about 10% smaller failure load was identified when pairs of studs were used. This is a significantly smaller influence than the term $1/\sqrt{n_r}$ used in [DIN EN 1994-1-1, 2010] predicts. In fact, for pairs of studs a marginal increase of the resistance is assumable, because the behaviour is governed by concrete failure. The size and shape of the failure cone did not vary significantly. Hence, the resistance of the cone differs only marginally. In addition, studs with only one yield hinge have only a small contribution to the overall resistance.

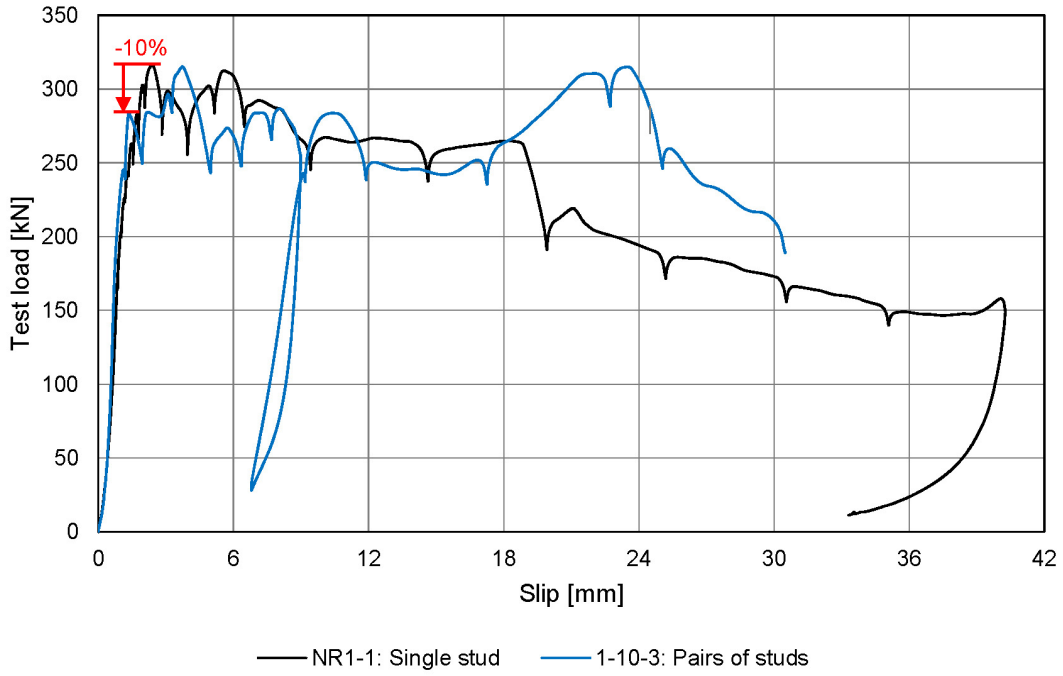


Figure 5.23: Influence of the number of studs per rib with CF80 decking.

## 5.9 Comparison with existing analytical approaches

### 5.9.1 Comparison with the resistance according to EN 1994-1-1

In this section the push-out test results are compared to their predicted average resistance, $P_{Rm}$, according to [Roik et al., 1989, DIN EN 1994-1-1, 2010]. The mean shear resistance of the stud in a solid slab according to [Roik et al., 1989] is used (see equations (2.1) and (2.2)). The resistance of the stud in a solid slab is then multiplied with the minimum of the factors $k_t$ and $k_{t,max}$ (see equation (2.6) and Table 2.1). The results of this comparison are shown in Figure 5.24 and Table 5.6. In addition, Table 5.6 shows the reduction factor, $k_{t,test}$, which is determined as the experimental resistance divided by the theoretical resistance for solid slabs.

The comparison shows that the tests reach in average only about two thirds of their predicted resistance. This is very unconservative, but the coefficients of variation and correlation both are very good for this comparison, as shown in Figure 5.24.

Series PV is over-estimated even though the studs were welded in favourable position. The $k_t$-formulae is formally restricted to studs welded in the centre of the rib or in staggert position. Thus, the $k_t$-factor may not be calibrated for studs in other positions.

Tests in series 1-04 to 1-07 also do not reach their predicted resistance, even though all requirements for the application of the $k_t$-formulae are formally satisfied. Because of the narrow ribs of the decking, the studs are in un-favourable position according to [Rambo-Roddenberry, 2002] and [Konrad, 2011].

The tests in series 1-08 to NR1 have an embedment depth of the stud which is very close and in some cases slightly below the required minimum value of $2d$. Because of this, rib pry-out failure occurred, which strongly differs from the behaviour of studs with a sufficient

Table 5.6: Comparison of push-out test results with the predicted resistance according to [Roik et al., 1989] and [DIN EN 1994-1-1, 2010].

| Test | $P_e$ [kN] | $P_{Rm,solid}$ [kN] | $k_t$ [-] | $P_{Rm}$ [kN] | $P_e/P_{Rm}$ [-] | $k_{t,test}$ [-] |
|---|---|---|---|---|---|---|
| PV1 | 116.41 | 157.87 | 1.00 | 157.87 | 0.737 | 0.74 |
| PV2 | 106.66 | 157.87 | 1.00 | 157.87 | 0.676 | 0.68 |
| 1-04-1 | 73.94 | 175.20 | 0.75 | 131.40 | 0.563 | 0.42 |
| 1-04-2 | 73.61 | 177.03 | 0.75 | 132.77 | 0.554 | 0.42 |
| 1-04-3 | 68.66 | 176.95 | 0.75 | 132.71 | 0.517 | 0.39 |
| 1-05-1 | 69.95 | 175.55 | 0.75 | 131.66 | 0.531 | 0.40 |
| 1-05-2 | 79.15 | 175.71 | 0.75 | 131.78 | 0.601 | 0.45 |
| 1-05-3 | 74.43 | 183.15 | 0.75 | 137.36 | 0.542 | 0.41 |
| 1-06-1 | 73.11 | 172.91 | 0.75 | 129.68 | 0.564 | 0.43 |
| 1-06-2 | 70.13 | 176.88 | 0.75 | 132.66 | 0.529 | 0.40 |
| 1-06-3 | 90.31 | 211.74 | 0.75 | 158.81 | 0.569 | 0.43 |
| 1-07-1 | 89.25 | 211.74 | 0.75 | 158.81 | 0.562 | 0.42 |
| 1-07-1 | 92.77 | 212.01 | 0.75 | 159.01 | 0.583 | 0.44 |
| 1-07-3 | 74.77 | 212.13 | 0.75 | 159.10 | 0.470 | 0.35 |
| 1-08-1 | 45.52 | 157.21 | 0.40 | 62.48 | 0.729 | 0.29 |
| 1-08-2 | 46.09 | 157.38 | 0.40 | 62.76 | 0.734 | 0.29 |
| 1-08-3 | 48.26 | 157.38 | 0.40 | 63.45 | 0.761 | 0.31 |
| 1-09-1 | 42.28 | 157.71 | 0.41 | 65.14 | 0.649 | 0.27 |
| 1-09-2 | 50.32 | 158.20 | 0.40 | 63.59 | 0.791 | 0.32 |
| 1-09-3 | 48.19 | 157.54 | 0.41 | 65.04 | 0.741 | 0.31 |
| 1-10-1 | 45.64 | 158.04 | 0.41 | 64.94 | 0.703 | 0.29 |
| 1-10-2 | 46.44 | 157.71 | 0.41 | 63.91 | 0.727 | 0.29 |
| 1-10-3 | 35.46 | 157.87 | 0.41 | 64.20 | 0.552 | 0.23 |
| 1-11-1 | 54.64 | 157.54 | 0.42 | 66.01 | 0.828 | 0.35 |
| 1-11-2 | 52.68 | 157.54 | 0.41 | 64.90 | 0.812 | 0.33 |
| 1-11-3 | 49.33 | 157.54 | 0.41 | 64.62 | 0.763 | 0.31 |
| 3-01-1 | 47.31 | 157.38 | 0.41 | 64.37 | 0.735 | 0.30 |
| 3-01-2 | 54.92 | 157.21 | 0.40 | 62.49 | 0.879 | 0.35 |
| 3-01-3 | 52.78 | 156.16 | 0.41 | 63.65 | 0.829 | 0.34 |
| 3-02 | 37.00 | 157.54 | 0.46 | 72.78 | 0.508 | 0.24 |
| NR1-1 | 79.07 | 157.71 | 0.62 | 97.98 | 0.807 | 0.50 |
| NR1-2 | 74.99 | 157.71 | 0.62 | 97.67 | 0.768 | 0.48 |
| NR1-3 | 70.46 | 157.87 | 0.62 | 97.32 | 0.724 | 0.45 |

embedment depth. This may be the reason why the tests do not reach the predicted resistance.

Considering the results of the comparisons in section 2.2.1, it is concluded that the reduction factor formulae according to [DIN EN 1994-1-1, 2010] gives unconservative results for the mean shear resistance, $P_{Rm}$. Especially the results obtained in section 2.2.1 show that there is no satisfactory correlation between experimental and analytical resistance, because the coefficients of correlation were between 0.55 and 0.60.

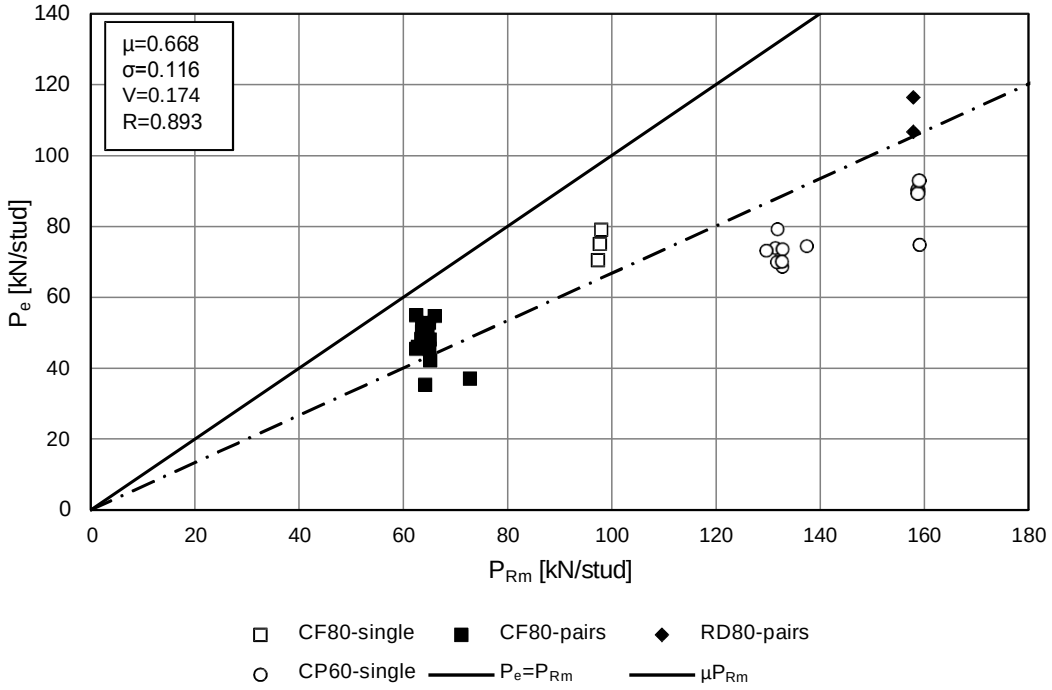


Figure 5.24: Comparison of push-out test results with the predicted resistance according to [Roik et al., 1989] and [DIN EN 1994-1-1, 2010].

### 5.9.2 Comparison with the resistance according to Lungershausen

In the following section, the push-out test results are compared to the predicted resistance according to [Lungershausen, 1988] in which the mean shear resistance according to equation (2.9) is assumed. To consider the measured strength of the studs, the plastic bending resistance, $M_{pl}$, is calculated with the measured tensile strength, $f_u$. However, assuming that the stress distribution cannot reach full plasticity a reduction of the bending resistance is considered. The reduction factor was determined by non-linear analysis of a yield-mechanism with two hinges, using the stress-strain curve described in [Lungershausen, 1988] for the shear stud. A comparison of ultimate load between non-linear analysis and calculated resistances of the yield mechanism showed, that $0.95M_{pl}$ should be used.

In addition to the comparison of the resistances, the empirical obtained distances of the yield hinges, $\varkappa \cdot d$, are compared with the values back calculated from the tests (see equation (5.1)), using:

$$a_{cal} = \frac{2 \cdot \beta \cdot (0.95 M_{pl})}{\sqrt{n_r} \cdot P_e} \tag{5.1}$$

Comparing the experimental resistance, $P_e$, to the predicted resistance, $P_{Rm}$, it can be seen that the tests reached in average only 86% of the predicted value (see Table 5.7 and Figure 5.25).

The only exceptions are the tests PV1 and PV2, which reach about 25 to 36% higher resistances than calculated. These two tests had the shear studs welded in favourable position. In addition, the concrete strength of about 46 N/mm$^2$ was significantly higher than the average strength in the tests used for the calibration of the model. The stud position as

Table 5.7: Comparison of push-out test results with the predicted resistance according to [Lungershausen, 1988].

| Test | $P_e$ [kN] | $M_{pl}$ [kNmm] | $\varkappa \cdot d$ [mm] | $P_{Rm}$ [kN] | $P_e/P_{Rm}$ [-] | $a_{cal}$ [mm] | $a_{cal}/(\varkappa \cdot d)$ [-] |
|---|---|---|---|---|---|---|---|
| PV1 | 116.41 | 607.89 | 14.32 | 85.43 | 1.363 | 9.92 | 0.693 |
| PV2 | 106.66 | 607.89 | 14.32 | 85.43 | 1.249 | 10.83 | 0.756 |
| 1-04-1 | 73.94 | 949.37 | 19.14 | 99.79 | 0.741 | 24.40 | 1.274 |
| 1-04-2 | 73.61 | 955.81 | 19.19 | 100.24 | 0.734 | 24.67 | 1.286 |
| 1-04-3 | 68.66 | 954.52 | 19.18 | 100.15 | 0.686 | 26.41 | 1.377 |
| 1-05-1 | 69.95 | 949.37 | 19.14 | 99.79 | 0.701 | 25.79 | 1.347 |
| 1-05-2 | 79.15 | 950.65 | 19.15 | 99.88 | 0.792 | 22.82 | 1.192 |
| 1-05-3 | 74.43 | 954.52 | 19.18 | 100.15 | 0.743 | 24.37 | 1.271 |
| 1-06-1 | 73.11 | 951.94 | 19.16 | 99.97 | 0.731 | 24.74 | 1.291 |
| 1-06-2 | 70.13 | 949.37 | 19.14 | 99.79 | 0.703 | 25.72 | 1.344 |
| 1-06-3 | 90.31 | 944.23 | 19.11 | 99.43 | 0.908 | 19.87 | 1.040 |
| 1-07-1 | 89.25 | 944.26 | 19.11 | 99.43 | 0.898 | 20.10 | 1.052 |
| 1-07-1 | 92.77 | 946.80 | 19.12 | 99.61 | 0.931 | 19.39 | 1.014 |
| 1-07-3 | 74.77 | 946.80 | 19.12 | 99.61 | 0.751 | 24.06 | 1.258 |
| 1-08-1 | 45.52 | 604.08 | 15.50 | 55.45 | 0.821 | 17.83 | 1.150 |
| 1-08-2 | 46.09 | 605.03 | 15.51 | 55.51 | 0.830 | 17.64 | 1.137 |
| 1-08-3 | 48.26 | 605.03 | 15.51 | 55.51 | 0.869 | 16.84 | 1.086 |
| 1-09-1 | 42.28 | 606.93 | 15.52 | 55.63 | 0.760 | 19.29 | 1.242 |
| 1-09-2 | 50.32 | 606.80 | 15.55 | 55.80 | 0.902 | 16.28 | 1.047 |
| 1-09-3 | 48.19 | 605.98 | 15.51 | 55.57 | 0.867 | 16.89 | 1.089 |
| 1-10-1 | 45.64 | 608.84 | 15.54 | 55.75 | 0.819 | 17.92 | 1.153 |
| 1-10-2 | 46.44 | 606.93 | 15.52 | 55.63 | 0.835 | 17.56 | 1.131 |
| 1-10-3 | 35.46 | 607.89 | 15.53 | 55.69 | 0.637 | 23.03 | 1.483 |
| 1-11-1 | 54.64 | 605.98 | 15.51 | 55.57 | 0.983 | 14.90 | 0.960 |
| 1-11-2 | 52.68 | 605.98 | 15.51 | 55.57 | 0.948 | 15.45 | 0.996 |
| 1-11-3 | 49.33 | 605.98 | 15.51 | 55.57 | 0.888 | 16.50 | 1.064 |
| 3-01-1 | 47.31 | 605.03 | 15.51 | 55.51 | 0.852 | 17.18 | 1.108 |
| 3-01-2 | 54.92 | 604.08 | 15.50 | 55.45 | 0.990 | 14.78 | 0.954 |
| 3-01-3 | 52.78 | 605.03 | 15.51 | 55.51 | 0.951 | 15.40 | 0.993 |
| 3-02 | 37.00 | 605.98 | 15.51 | 55.57 | 0.666 | 22.00 | 1.417 |
| NR1-1 | 79.07 | 606.93 | 15.52 | 78.67 | 1.005 | 14.58 | 0.940 |
| NR1-2 | 74.99 | 606.93 | 15.52 | 78.67 | 0.953 | 15.38 | 0.991 |
| NR1-3 | 70.46 | 607.89 | 15.53 | 78.75 | 0.895 | 16.39 | 1.055 |

well as the concrete strength might be responsible for the under-estimation of the resistance.

The tests 1-04-1 to 1-07-3, which used the CP60 decking, reach in average about 78% of their predicted resistance. This is remarkable, because all of these tests developed a load-slip curve with two load peaks and S-shaped stud deformation, as assumed in the model by [Lungershausen, 1988]. As discussed in section 2.2.2, this model does not contain the concrete strength as a parameter and was calibrated for a database of tests with an average concrete strength of 31.5 N/mm$^2$. The model predicts a resistance of about 100 kN for all tests with CP60 decking. However, the test results showed a dependency on the concrete strength, as the resistance is about 75 kN for a concrete strength of about 30 N/mm$^2$ and about 90 kN for a concrete strength of about 42 N/mm$^2$. The model assumes a distance of the yield hinges,

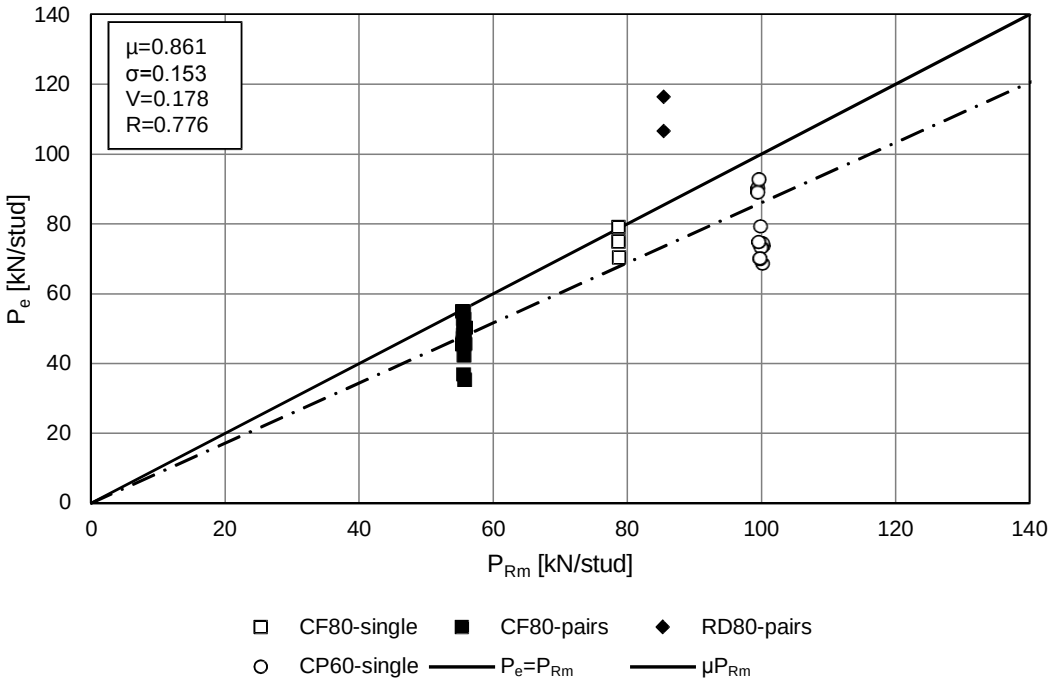


Figure 5.25: Comparison of push-out test results with the predicted resistance according to [Lungershausen, 1988].

$\varkappa \cdot d$, of about 19 mm. The distance back calculated from the test results is about 25 mm. The deformation of the shear studs (see Figure 5.26) shows that the spacing of the plastic hinges is about 45 to 57 mm and decreased for higher concrete strengths. This correlates to the observed higher resistance at a higher concrete strength. However, the consideration of the measured spacings would lead to a significant under-estimation of the resistance. In addition, because of the narrow ribs of CP60 decking, the shear studs are classified to be in unfavourable position according to [Rambo-Roddenberry, 2002] and [Konrad, 2011]. This is another not considered influence which could cause the over-estimation of the resistance.

The test 1-08-1 to 3-02 used CF80 decking and pairs of studs. They reached in average 85% of their predicted resistance. These tests did not satisfy the required embedment depth of $2d\sqrt{n_r}$. The load-slip curves showed that rib pry-out failure occurs at low slips, while the specimen still has a linear load-slip behaviour. As the load-slip behaviour and failure mode of these tests strongly differed from the assumptions of this model, it is likely that the shear resistance is not accurately predicted.

The tests in series NR1 also used CF80 decking but with single shear studs per rib. This series reached in average about 95% of the predicted resistance. However, the observed failure was rib pry-out failure which does not match the assumptions of this model.

It can be concluded that the model by [Lungershausen, 1988] is not calibrated to predict the presented push-out tests. It requires a specific mode of failure, which did not occur in all tests. In addition, important parameters like stud position and concrete strength are not considered as parameters of the model. The test results showed a significant influence of both parameters on the resistance. However, the previous comparisons (see also section 2.2.2) showed that this simple model correlates more with the tests than the formulae of [DIN EN 1994-1-1, 2010].

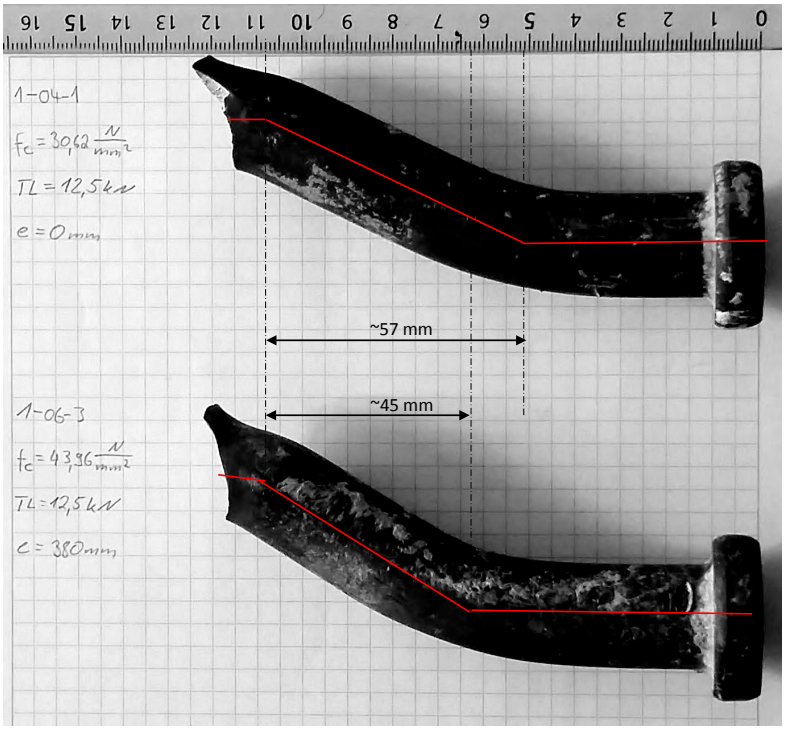


Figure 5.26: Shear stud deformation in tests 1-04-1 and 1-06-3.

### 5.9.3 Comparison with the resistance according to Konrad

In this section, the push-out test results are compared to their predicted resistances according to [Konrad, 2011]. Because the shear studs in series 1-04 to 1-07 are in unfavourable position according to this method, the reduction factor $k_{unfav,2}$ according to equation (2.26) is applied to this tests. The reduction factor was developed and calibrated for through deck welded studs. If there is an influence of the welding procedure, $k_{unfav,2}$ may over-estimate the resistance for the present case of a pre-punched decking. All other tests are predicted with the reduction factors according to equations (2.28) and (2.29). These factors require a ratio of $h_{sc}/h_p > 1.56$. For the 80 mm deep decks RD80 and CF80, this ratio results in a minimum stud height of 125 mm. This is not satisfied by the measured stud heights in tests with CF80. However, it is assumable that in practice the nominal stud height of 125 mm is considered and the reduction factors are used.

The results of the comparison are shown in Figure 5.27 and Table 5.8. In average, the tests reached about 72% of their predicted resistance. In comparison to [DIN EN 1994-1-1, 2010] and [Lungershausen, 1988], this method shows the largest coefficient of variation and the smallest coefficient of correlation. However, the accuracy of the predictions strongly differs depending on the type of decking and the stud position.

The tests in series PV, which had through deck welded studs in favourable position in the ribs of 80 mm deep decking, reached about 92% of their predicted shear resistance. As the reduction factors were developed from numerical simulation – and hence perfect welding conditions – this result may be because of imperfections of the welding or the natural variability of the tests.

The predictions for series 1-04 to 1-07, where the reduction factor $k_{unfav,2}$ was used, showed ratios $P_e/P_{Rm}$ with an average of 90%. This is the most accurate prediction for these tests considering the presented methods. Konrad assumed a reduction of the resistance due to

Table 5.8: Comparison of push-out test results with the predicted resistance according to [Konrad, 2011] using equations (2.26), (2.28) and (2.29).

| Test | $P_e$ [kN] | $P_{Rm,solid}$ [kN] | $k_t$ [-] | $P_{Rm}$ [kN] | $P_e/P_{Rm}$ [-] | $k_{t,test}$ [-] |
|---|---|---|---|---|---|---|
| PV1 | 116.41 | 147.80 | 0.82 | 121.59 | 0.957 | 0.79 |
| PV2 | 106.66 | 147.80 | 0.82 | 121.59 | 0.877 | 0.72 |
| 1-04-1 | 73.94 | 167.81 | 0.49 | 81.69 | 0.905 | 0.44 |
| 1-04-2 | 73.61 | 169.01 | 0.49 | 82.25 | 0.895 | 0.44 |
| 1-04-3 | 68.66 | 168.93 | 0.49 | 82.20 | 0.835 | 0.41 |
| 1-05-1 | 69.95 | 168.01 | 0.49 | 71.76 | 0.856 | 0.42 |
| 1-05-2 | 79.15 | 168.13 | 0.49 | 81.80 | 0.968 | 0.47 |
| 1-05-3 | 74.43 | 172.47 | 0.49 | 83.92 | 0.887 | 0.43 |
| 1-06-1 | 73.11 | 166.55 | 0.49 | 81.02 | 0.902 | 0.44 |
| 1-06-2 | 70.13 | 168.77 | 0.49 | 82.14 | 0.854 | 0.42 |
| 1-06-3 | 90.31 | 193.63 | 0.49 | 94.20 | 0.959 | 0.47 |
| 1-07-1 | 89.25 | 195.07 | 0.49 | 94.86 | 0.941 | 0.46 |
| 1-07-1 | 92.77 | 188.24 | 0.49 | 91.66 | 1.012 | 0.49 |
| 1-07-3 | 74.77 | 191.42 | 0.49 | 93.17 | 0.802 | 0.39 |
| 1-08-1 | 45.52 | 143.53 | 0.58 | 83.57 | 0.545 | 0.32 |
| 1-08-2 | 46.09 | 143.65 | 0.58 | 83.57 | 0.551 | 0.32 |
| 1-08-3 | 48.26 | 143.94 | 0.58 | 83.57 | 0.576 | 0.34 |
| 1-09-1 | 42.28 | 144.40 | 0.58 | 84.08 | 0.503 | 0.29 |
| 1-09-2 | 50.32 | 144.75 | 0.58 | 84.28 | 0.597 | 0.35 |
| 1-09-3 | 48.19 | 144.28 | 0.58 | 84.01 | 0.574 | 0.33 |
| 1-10-1 | 45.64 | 144.63 | 0.58 | 84.21 | 0.542 | 0.32 |
| 1-10-2 | 46.44 | 144.40 | 0.58 | 84.08 | 0.552 | 0.32 |
| 1-10-3 | 35.46 | 144.51 | 0.58 | 84.15 | 0.421 | 0.25 |
| 1-11-1 | 54.64 | 144.28 | 0.58 | 84.01 | 0.650 | 0.38 |
| 1-11-2 | 52.68 | 144.28 | 0.58 | 84.01 | 0.627 | 0.37 |
| 1-11-3 | 49.33 | 144.28 | 0.58 | 84.01 | 0.587 | 0.34 |
| 3-01-1 | 47.31 | 147.54 | 0.58 | 85.91 | 0.551 | 0.32 |
| 3-01-2 | 54.92 | 147.42 | 0.58 | 85.84 | 0.640 | 0.37 |
| 3-01-3 | 52.78 | 141.12 | 0.58 | 82.17 | 0.642 | 0.37 |
| 3-02 | 37.00 | 144.32 | 0.52 | 75.70 | 0.489 | 0.26 |
| NR1-1 | 79.07 | 146.49 | 0.73 | 106.62 | 0.742 | 0.54 |
| NR1-2 | 74.99 | 147.63 | 0.73 | 107.45 | 0.698 | 0.51 |
| NR1-3 | 70.46 | 147.25 | 0.73 | 107.18 | 0.657 | 0.48 |

pre-punching of the decking of about 10% in the development of equation (2.28). This value appears to be verified by the tests with CP60.

The tests with CF80 decking are strongly over-estimated and reached about 60% of the predicted resistance. The measured stud height did not satisfy the required ratio of $h_{sc}/h_p > 1.56$. The correlation curves of the reduction factor found for the influence of $h_{sc}/h_p$, see Figure 5.4, showed that the value 1.56 is a sharp change point, changing between two correlation functions [Konrad, 2011]. Thereby, a linear correlation for $h_{sc}/h_p \leq 1.56$ was shown, while for $h_{sc}/h_p > 1.56$ a constant reduction was found. Because the ratio $h_{sc}/h_p$ apparently has a large influence on the resistance, the tests with CF80 were re-evaluated with the reduction factor $k_{mid,1}$ according to equation (2.19). This factor is valid for through deck

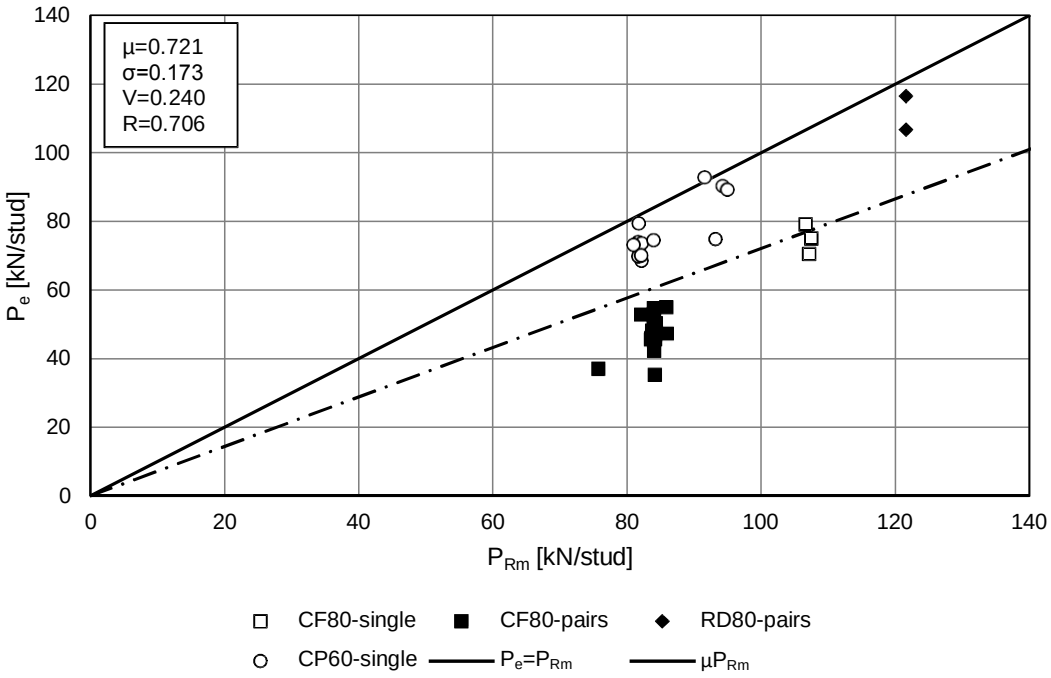


Figure 5.27: Comparison of push-out test results with the predicted resistance according to [Konrad, 2011] using equations (2.26), (2.28) and (2.29).

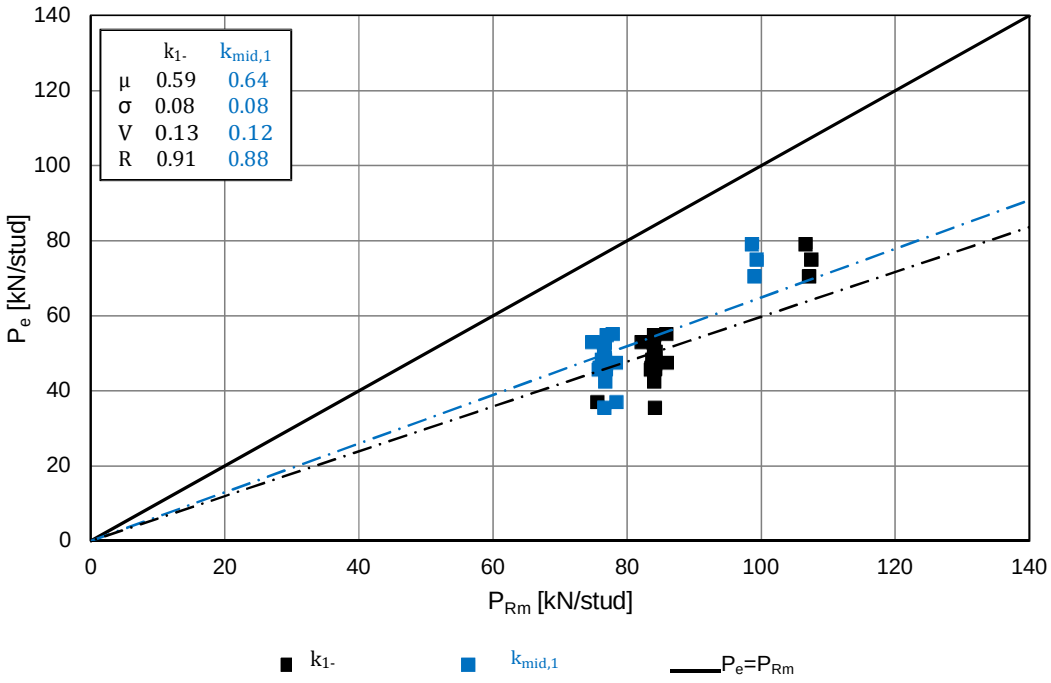


Figure 5.28: Comparison of push-out test results with CF80 with the predicted resistance using the reduction factors $k_\perp$ (2.28), (2.29) and $k_{mid,1}$ (2.19) according to [Konrad, 2011].

welded studs in mid-position with ratios $h_{sc}/h_p \leq 1.56$ and therefore should result in more realistic predictions. Figure 5.28 shows the comparison of the experimental resistance with the predictions according to equations (2.28), (2.29) and (2.19). Obviously the application of the proposed reduction factor, $k_{mid,1}$, only slightly improves the prediction of the shear resistance. It can be concluded that having ratios $h_{sc}/h_p$ of less than 1.56 is not the reason for the over-estimation of the resistance. It seams more reasonable, that the model is not able to reflect the observed rib pry-out failure.

The above comparisons showed how important the consideration of the stud position is, because using $k_{unfav,2}$ for the tests with CP60 gives the most accurate predictions for these tests. On the other side, it was also shown that this kind of statistical model is very sensitive for the observed failure mode. If the failure mode did not occur in the tests and investigations used to calibrate the model, unrealistic predictions of the resistance are obtained even though the geometry does satisfy all limitations of the model.

### 5.9.4 Concluding remarks

The previous comparisons showed that all three presented prediction methods show non-conservative results for the conducted push-out tests.

Obviously all methods had problems predicting accurately the resistance for rib pry-out failure, observed in tests with CF80 decking. The method according to [Lungershausen, 1988] showed the best accordance between experimental and predicted resistance for these cases, even though a different failure mode than in the model occurred. The predictions according to [Konrad, 2011] were the most inaccurate ones for rib pry-out failure, even though the factor $k_{mid,1}$ was valid for the geometry of the respective specimens. The application of the reduction factor $k_{unfav,2}$ according to [Konrad, 2011] for the tests with CP60 decking showed the importance of considering the stud position.

However, all presented prediction methods showed non-conservative results and unsatisfactory coefficients of correlation. Thereby, the simple mechanical model according to [Lungershausen, 1988] showed the best correlation with the test results. The mechanical approach appears to be less sensitive for the change of the failure mode and stud position than the statistical approaches according to [DIN EN 1994-1-1, 2010] and [Konrad, 2011].

Therefore, it is more reasonable to develop a mechanical based approach to predict the resistance of the studs than developing new statistically derived reduction factors. In comparison to the model by [Lungershausen, 1988], the new model will include the influence of the concrete strength and stud position. In addition, it will be based on the observed failure modes of the push-out tests.

# 6 Components of the shear connector resistance

## 6.1 General

In the calibration of a design model according to [DIN EN 1990, 2002], characteristic and design resistances are obtained by scaling the predicted results. To achieve realistic and economic design values, the focus for the development of a new design formulae must be:

1. To increase the coefficient of correlation to a value closer to 1.00.
2. To decrease the coefficient of variation to a value closer to 0.00.

Especially for the coefficient of correlation, methods which obtain the resistance of studs in the ribs of composite slabs by a reduction of the resistance for studs in solid slabs, show unsatisfactory results.

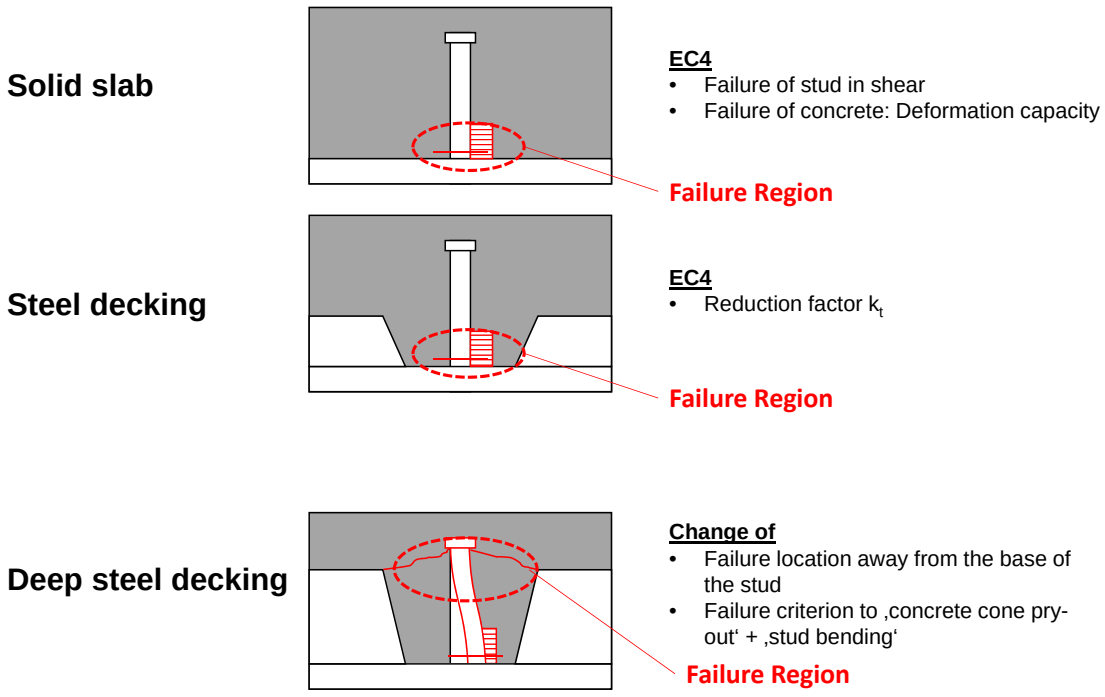


Figure 6.1: Predicted failure modes according to [DIN EN 1994-1-1, 2010] and observed failure modes in push-out tests using deep steel decking.

Figure 6.1 illustrates why no satisfactory correlation is obtained between the test results and [DIN EN 1994-1-1, 2010]. In a solid slab, either a failure of the stud shank above the weld collar or crushing of the concrete at the base of the studs are the predicted failure modes. When steel decking is used, [DIN EN 1994-1-1, 2010] reduces this resistance with a reduction factor, $k_t$, and assumes the occurrence of the same failure modes as in a solid slab. This is only reasonable for shallow decking. If deep steel decking is used, the mechanical

behaviour changes.

Failure of the stud shank typically occurs at large slip, long after the tests reached their resistance. The crushing of the concrete at the base of the studs is rather a secondary failure. It results from the plastic bending deformation of the shear stud. In addition, the failure of a concrete cone for rib pry-out and concrete pull-out occurs.

Therefore, the reduction of the resistance of a stud in a solid slab does not lead to the analysis of the correct failure modes. Unsatisfactory coefficients of correlation are the consequence.

Based on the observed failure modes and load-slip behaviour in the conducted push-out tests, the behaviour of studs in the ribs of deep steel decking can be described with the load bearing components shown in Figure 6.2.

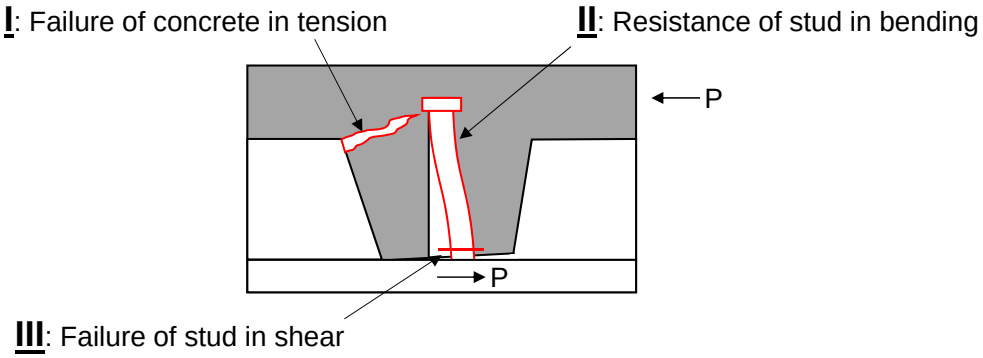


Figure 6.2: Components describing the mechanical behaviour of shear connections.

I. The first component describes the failure of the concrete cone. The forces and moments acting on the cone depend on the failure mode: Tension for concrete pull-out and bending for rib pry-out. Both failure modes have in common, that before the first load peak is reached the concrete cone starts to fail with a crack beginning at the top corner of the rib. This initial crack can be assumed as the lower bound for predicting the contribution of the concrete.

II. The second component describes the contribution of the shear stud itself. The conducted tests showed that the studs are subjected to plastic bending deformation. The type of curvature of the stud (single or double curvature) depends on the embedment depth of the head of the stud. The model by Lungershausen [Lungershausen, 1988] already showed, that calculating the plastic resistance of the stud in bending to predict the shear resistance results in higher coefficients of correlation.

III. The last component is the upper bound for the shear resistance: The plastic shear force ,that the stud shank can resist, is assumed to limit the force obtained from the first two components.

In the following sections, each component is described using simple mechanical considerations.

## 6.2 Contribution of the concrete to the shear connectors resistance

The concrete component represents a lower bound for the resulting shear force, which is valid for rib pry-out failure as well as for concrete pull-out failure.

In case of rib pry-out failure, predicting the elastic bending resistance of the concrete cone can be assumed as a conservative analysis of this failure mode. During the post-failure behaviour, it is assumed that the predicted load can be maintained by frictional resistance and aggregate interlock, because the failure cone is clamped between the slab and the steel flange.

For concrete pull-out, the crack initiation because of the bending of the rib can be assumed to occur at a small slip. For further loading, rib punch-through progresses in addition to the development of the crack. Therefore, the point of force application relocates to the upper yield hinge of the stud. The concrete cantilever shortens and the bending moment acting on the rib is reduced. Therefore, the load at crack initiation can be maintained for further loading.

Based on this considerations, the contribution of the concrete to the shear connector resistance may be calculated from the elastic bending resistance of the rib.

### 6.2.1 Elastic bending resistance of the concrete rib

To calculate the bending resistance of the rib, it is idealised as a cantilever that is fixed to concrete slab. Figure 6.3 shows the assumed forces and stresses acting on the failure cone and the static system derived for the analysis.

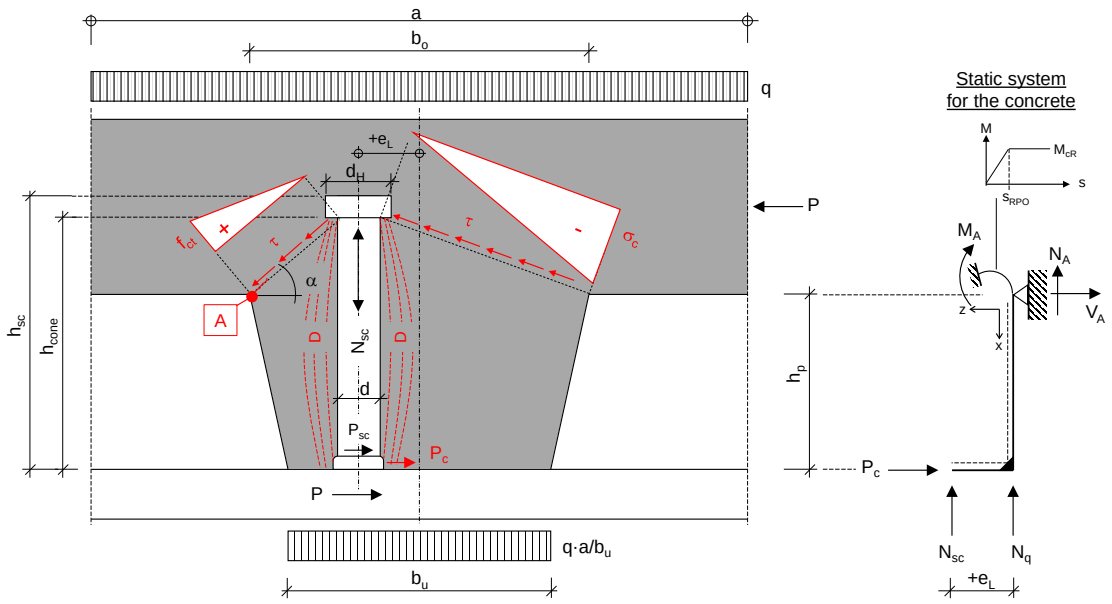


Figure 6.3: Static system, loading and stresses for the determination of the concrete bending resistance.

The concrete rib is considered as a cantilever loaded in bending an compression. The restraint of the rotation is assumed as a spring. When slip is applied to the system, the bending moment $M_A$ increases until the first crack develops at a moment equal to $M_{cR}$. This moment can be maintained, because the developing failure cone is clamped between the slab and the steel section. These assumptions lead to a simplified bi-linear moment-slip relation for the concrete bending resistance. The deformation of the shear stud itself depends strongly on the embedment depth of the head of the stud into the concrete above the rib, as explained in sections 6.3.1 and 6.3.2.

Considering the loading of the cantilever, it is assumed that a part of the shear force, $P$, is

transferred into the rib at the weld collar. This force, $P_c$, then leads to a bending moment in the rib. In addition to the force, $P_c$, the loading of the composite slab causes a compression of the concrete rib. This compression is considered by an axial force, $N_q$. Because of the embedment conditions of the head of the stud, tension forces develop in the stud shank, $N_{sc}$. This tension forces are transferred into the concrete by compression stresses $D$. They are considered by the axial force, $N_{sc}$, acting on the cantilever at an eccentricity, $e_L$, according to the welding position. This leads to an additional bending moment and influences the bending resistance of the concrete cone. Based on the static system and forces, shown in Figure 6.3, the internal forces and stresses at point $A$ can be calculated.

The internal forces at point $A$ are:

$$
\begin{aligned}
V_A &= -P_c \\
N_A &= -N_q - N_{sc} \\
M_A &= P_c \cdot h_p - N_{sc} \cdot e_L
\end{aligned}
$$

The shear stress at point $A$ is:

$$\tau = \frac{V_A \cdot S_y}{I_y \cdot t} = 0 \text{ because } S_y = 0$$

The axial stress at point $A$ is:

$$\sigma_x = \frac{N_A}{A} + \frac{M_A}{I_y} \cdot z = -\frac{N_q + N_{sc}}{A} + \frac{P_c \cdot h_p - N_{sc} \cdot e_L}{I_y} \cdot \frac{b_o}{2}$$

The failure criterion is then given by the axial stress, $\sigma_x$, reaching the tensile strength of the concrete. Considering the inclination of the failure surface, the component of the concrete tensile strength in the direction of $\sigma_x$ is:

$$f_{ctm,x} = \frac{f_{ctm}}{\cos\alpha} \text{ for: } 0° \leq \alpha \leq 90° \tag{6.1}$$

The inclination of the failure surface is derived from the geometry:

$$\alpha = \arctan \frac{h_{cone} - h_p}{b_o/2 - e_L} \tag{6.2}$$

The failure criterion is then given by equation (6.3):

$$-\frac{N_q + N_{sc}}{A} + \frac{P_c \cdot h_p - N_{sc} \cdot e_L}{I_y} \cdot \frac{b_o}{2} \leq \frac{f_{ctm}}{\cos\alpha} \tag{6.3}$$

When equation (6.3) is solved for the force $P_c$, this results in equation (6.4):

$$P_c \leq \left[\left(\frac{f_{ctm}}{\cos\alpha} + \frac{N_q + N_{sc}}{A}\right) \cdot \frac{2 \cdot I_y}{b_o} + N_{sc} \cdot e_L\right] \cdot \frac{1}{h_p} \tag{6.4}$$

To obtain the resistance per shear stud, equation (6.4) must be divided by the number of studs per rib, as follows:

$$P_c = \left[\left(\frac{f_{ctm}}{\cos\alpha} + \frac{N_q + N_{sc}}{A}\right) \cdot \frac{2 \cdot I_y}{b_o} + N_{sc} \cdot e_L\right] \cdot \frac{1}{h_p} \cdot \frac{1}{n_r} \tag{6.5}$$

with:
- $P_c$ Contribution of concrete to the shear connector resistance
- $f_{ctm}$ Tensile strength of the concrete
- $\alpha$ Inclination of the failure surface
- $N_q$ Compression of the rib because of the slabs load
- $N_{sc}$ Compression of the rib because of tension in the stud shank
- $A$ Area of the failure surface
- $I_y$ Moment of Inertia of the failure surface
- $b_o$ Width of the rib at the top
- $e_L$ Eccentricity of the stud because of the welding position
  - $e_L > 0$ for studs on the favourable side
  - $e_L < 0$ for studs on the unfavourable side
- $h_p$ Height of the rib
- $n_r$ Number of studs per rib

Considering the tensile strength, $f_{ct}$, of the concrete, it is in general not reported for push-out tests, because the formulae of [DIN EN 1994-1-1, 2010] refers to the compression strength. According to [DIN EN 1992-1-1, 2005], the tensile strength can be calculated from the compression strength, as shown in equation (6.6). In addition, the German National Annex considers a multiplication of the tensile strength with the factor $a_{ct} = 0.85$ to take the reduced load bearing capacity for static loading into account.

$$f_{ctm} = \alpha_{ct} \cdot 0.3 \cdot f_{ck}^{2/3} \tag{6.6}$$

The compression force, $N_{sc}$, develops because of the restraint displacement of the head of the stud. $N_{sc}$ is conservatively assumed according to equation (6.7). This limitation is derived from tensile force, for which the bending capacity of the stud can be calculated without considering the interaction of internal forces and moments [DIN 18800-1, 1990].

$$N_{sc} = 0.1 \cdot f_u \cdot \pi \cdot d^2/4 \tag{6.7}$$

The cross section properties, $A$ and $I_y$, are derived for the failure cones, which were observed in push-out tests.

### 6.2.2 Failure cone and cross-section properties

The conducted push-out tests showed that failure cones of a particular shape occurred for rib pry-out failure in specimens with CF80 decking and for concrete pull-out failure in CP60 decking. The geometry of the concrete cone can be assumed to be as shown in Figure 6.4. Figure 6.5 illustrates that this is an appropriate assumption by comparing the theoretical failure cone to the cone observed in a push-out test. The cross section properties of this

surface are calculated according to equations (6.8) to (6.10). The division into faces and the solutions of these equations are given in Appendix D and Appendix E.

$$A = \sum_{i=1}^{n} A_i \tag{6.8}$$

$$I_y = \sum_{i=1}^{n} I_i + \sum_{i=1}^{n} \left( A_i \cdot z_i^2 \right) \tag{6.9}$$

$$h_s = \sum_{i=1}^{n} \left( A_i \cdot h_{s,i} \right) / \sum_{i=1}^{n} A_i \tag{6.10}$$

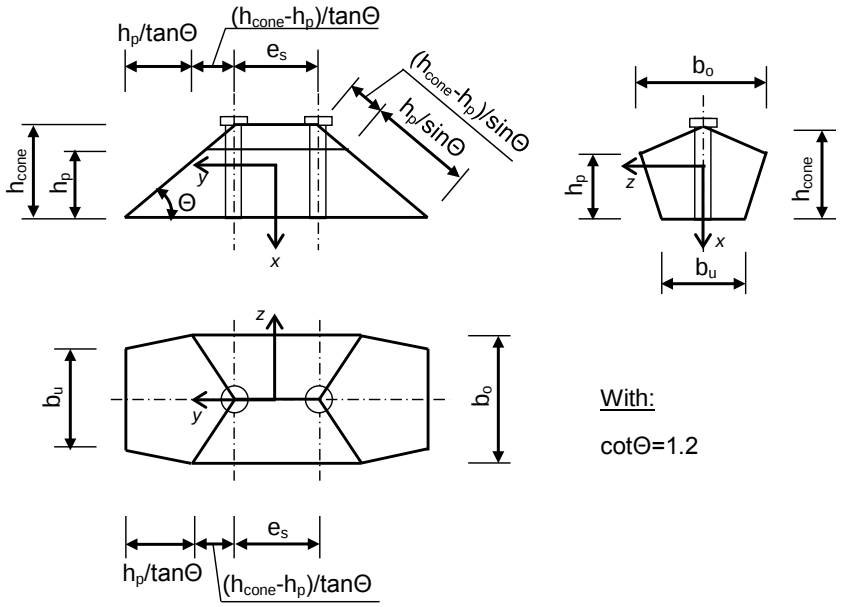


Figure 6.4: Assumed failure surface of the rib for trapezoidal decking.

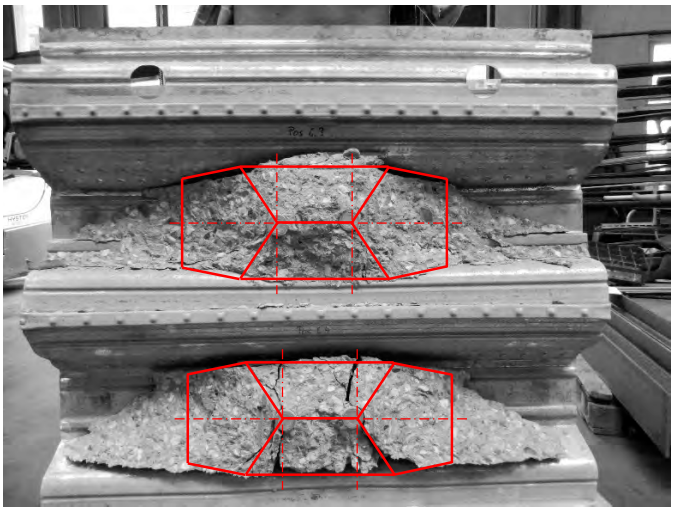

Figure 6.5: Observed failure cone in the concrete rib and idealised failure surface.

## 6.3 Contribution of the shear stud to the shear connector resistance

In many cases only the tensile strength, $f_u$, is reported for the shear connectors. Assuming the tensile strength to be reached in the determination of the shear stud resistance requires the development of plasticity in the stud. The push-out test results showed that all shear studs were exposed to plastic bending deformation.

The contribution of the shear stud to the shear resistance of the connection will be calculated from the studs plastic bending resistance. Assuming $f_u$ is the material ultimate tensile strength, the plastic bending resistance, $M_{pl}$, is obtained according to equation (6.11).

$$M_{pl} = f_u \cdot \frac{d^3}{6} \tag{6.11}$$

The plastic bending resistance considers the stress distribution shown in Figure 6.7. A typical stress-strain curve for shear stud connectors is shown in Figure 6.6. The material behaviour immediately changes from elastic to strain-hardening and does not show a yield zone. Assuming this behaviour for the stress-distribution in the stud shank, the stresses according to Figure 6.8 are obtained.

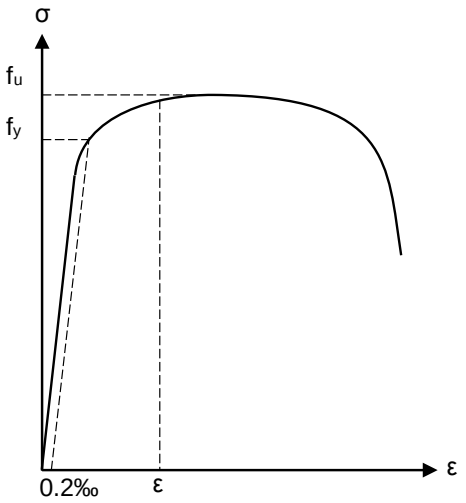


Figure 6.6: Typical stress-strain curve for cold formed steel.

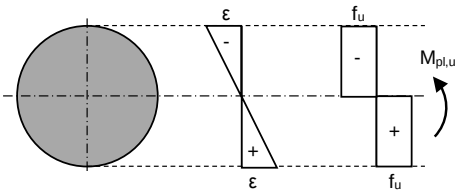


Figure 6.7: Assumed plastic stress distribution in the stud.

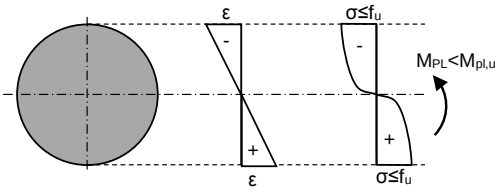


Figure 6.8: Realistic stress distribution in the stud.

The tensile strength, $f_u$, can only occur at the peaks of the stress-distribution. This means that the plastic bending resistance of the stud is smaller than the value obtained by equation (6.11). This can be considered by the application of a reduction factor to the bending resistance. The determination of a reduction is negligible, because the calibration of the model according to [DIN EN 1990, 2002] will determine scaling factors for each design criterion.

### 6.3.1 Plastic bending resistance for cases with single curvature of the stud

Figure 6.9 shows the static system assumed for this case. Single curvature of the shear stud develops for studs with a too small embedment depth of the head of the stud. The smaller the embedment depth is, the larger is the horizontal support reaction of the head of the stud, $A$,

that is required to develop the upper yield hinge. Therefore, the concrete reaches its bending resistance, $M_{cR}$, before the upper yield hinge develops in the stud shank. Because of the failure and rotation of the concrete rib, the support reaction, $A$, cannot be introduced into the slab. This is considered by assuming the horizontal support of the head of the stud as a spring that fails when the concrete resistance, $M_{cR}$, is reached. In this case, the head of the stud can move horizontally and only the bottom yield hinge develops. The loading of the pure stud is derived from the load-bearing model described in section 5.2. This results in the leaver arm as shown in Figure 6.9.

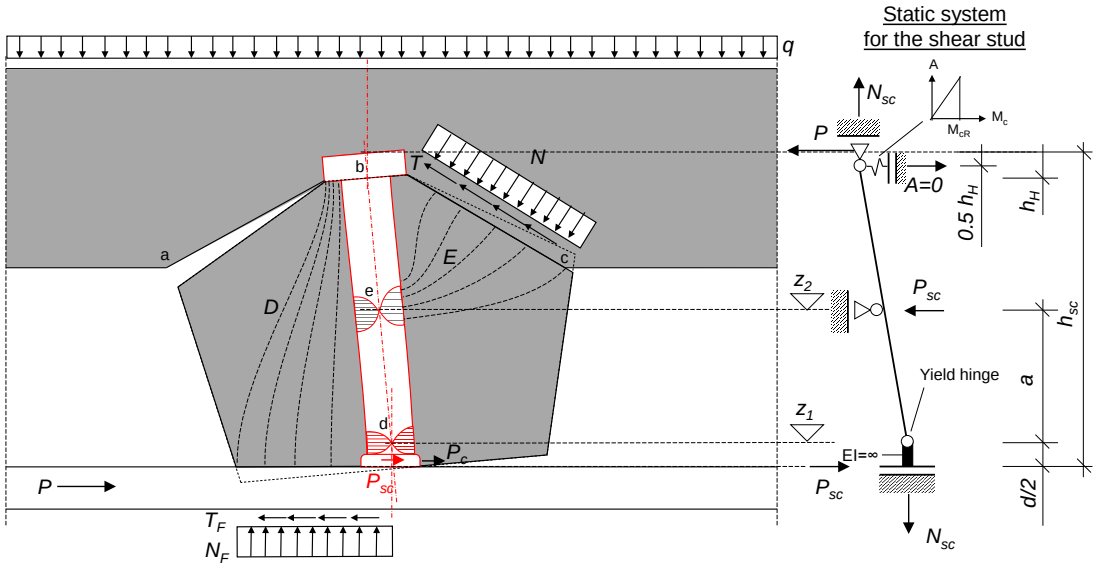


Figure 6.9: Static system and loading for shear studs with single curvature.

Using the plastic design theory, the shear force in the stud is:

$$P_{sc} = \frac{M_{pl}}{a} \tag{6.12}$$

The dimension $a$ results from the position of the yield hinge, $z_1$, and the position where the forces $E$ act on the shear stud, $z_2$. According to the observations in the push-out tests, the yield hinge develops between 0.5 diameters and 1.5 diameters above the flange of the beam. It is conservatively assumed, that the yield hinge develops 0.5 diameters above the flange of the beam. The position where the force $E$ acts on the stud, $z_2$, can be estimated from the observation of a yield hinge in the upper part of the stud in push-out tests 3-01-1 and 3-01-2 (see Figure 6.10). The two tests had very large transverse loads, because of the used tension ties and a very large slip of about 70 mm and 90 mm was applied. Because of the restraint rotation of the concrete cone, the constraining forces increased $D$ and $E$ sufficiently to develop the second yield hinge. The yield hinge was observed approximately 60 to 70 mm above the flange of the beam.

According to equation (6.10), the centre of mass of the failure surface is about 65 mm above the flange of the beam for pairs of studs and CF80 decking. This matches well with the observed position of the yield hinge. The position $z_2$, where the forces $E$ act on the stud, is therefore taken as the coordinate $h_s$ of the failure surfaces centre of mass. The dimension $a$ in equation (6.12) is then obtained as the difference between $z_2$ and $z_1$. The shear force

Figure 6.10: Two yield hinges of a stud in the rib of CF80 decking observed in specimen 3-01-1.

component in the stud is then:

$$P_{sc} = \frac{M_{pl}}{h_s - 0.5d} \tag{6.13}$$

were:

| | |
|---|---|
| $P_{sc}$ | Shear force in the stud |
| $M_{pl} = f_u \cdot \frac{d^3}{6}$ | Plastic bending resistance of the stud |
| $h_s$ | Coordinate of the centre of mass of the concrete failure surface above the flange of the beam according to equation (6.10) |
| $0.5d$ | Position of the bottom yield hinge above the flange of the beam |

### 6.3.2 Plastic bending resistance for cases with double curvature of the stud

Double curvature of the shear stud can only develop when the embedment depth of the head of the stud is sufficient to develop the support reaction, $A$, before failure of the rib occurs. The static system that is used to calculated the contribution of the stud to the shear resistance is shown in Figure 6.11.

In contrary to failure modes with single curvature of the stud, the concrete cone does not fail in bending. This is because of the large embedment depth of the head of the stud that increases the size and bending resistance of the concrete cone as well as decreases the support reaction, $A$, that is necessary to develop the yield mechanism. In addition, the force $P_c$, that is introduced into the concrete at the weld collar, decreases at high slip because of concrete crushing in front of the stud. Because the concrete cone does not fully fail in bending, the head of the stud can introduce the support reaction, $A$, into the concrete topping. The upper yield hinge develops where the stud is supported by the force $E$. The position of the force $E$ depends on the geometry of the shear connection. According to the observations in push-out tests with CP60 decking, the yield hinge develops approximately at the centre of mass of the concrete failure surface. The position of the centre of mass, $h_s$, is given by equation (6.10). The bottom hinge was observed approximately half a diameter above the flange of the beam.

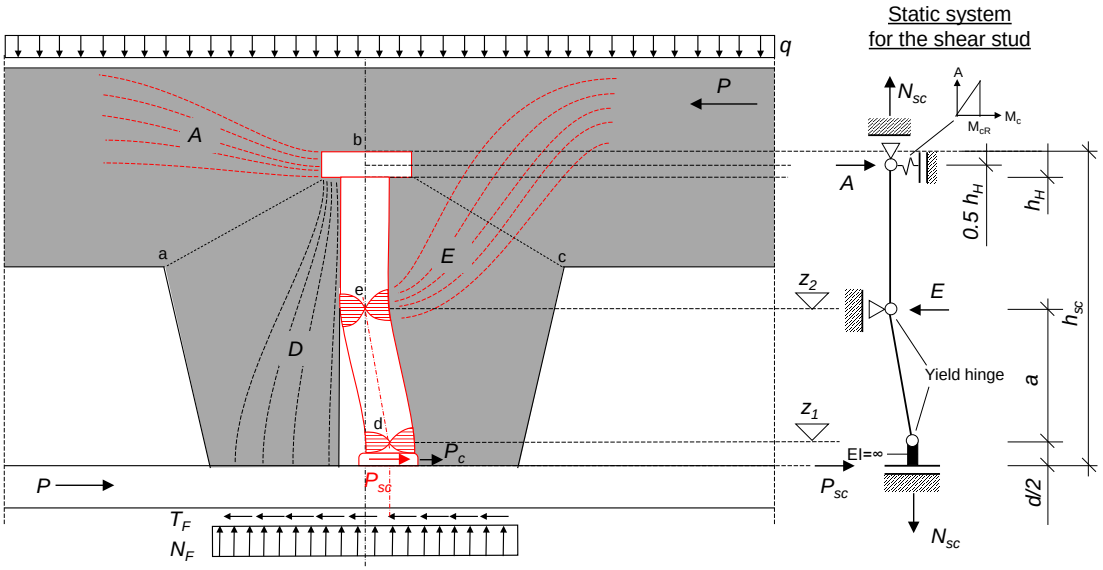


Figure 6.11: Static system and loading for studs with double curvature.

The yield mechanism shown in Figure 6.11 developed at a slip of about 2 to 4 mm. Therefore, it is assumed that the concrete contributes to the shear resistance with the force $P_c$ that leads to the first crack at point $a$ because of bending (see equation (6.5)). The contribution of the stud itself, $P_{sc}$, is obtained from the bending resistance of the stud using in plastic design:

$$P_{sc} = \frac{2 \cdot M_{pl}}{h_s - 0.5d} \tag{6.14}$$

## 6.4 Limitation for stud shear failure

As upper bound of the shear resistance, the resistance for stud shearing is assumed. Failure of the stud in pure shear occurs, when the plastic shear force, $V_{pl}$, that the stud shank can resist is reached. The resistance of the stud in shear is obtained by multiplying the cross-section area with the shear stress, $\tau$.

For a combination of axial stresses, $\sigma$, and shear stresses, $\tau$, the failure criterion is given as follows:

$$f_u = \sqrt{\sigma^2 + 3 \cdot \tau^2} \tag{6.15}$$

In pure shear, the shear stress, $\tau$, that the stud can resist is then:

$$\tau = \frac{f_u}{\sqrt{3}} \tag{6.16}$$

The resistance for stud shearing is then:

$$V_{pl} = \frac{f_u}{\sqrt{3}} \cdot \pi \cdot d^2/4 \tag{6.17}$$

## 6.5 Differentiation of the type of stud curvature

Based on the previous considerations, the resistance of the shear connector, $P$, is obtained as follows:

$$P = P_c + Psc \leq V_{pl} \tag{6.18}$$

For studs with single curvature, this leads to the shear resistance as follows:

$$P = \left[\left(\frac{f_{ctm}}{\cos\alpha} + \frac{N_q + N_{sc}}{A}\right) \cdot \frac{2 \cdot I_y}{b_o} + N_{sc} \cdot e_L\right] \cdot \frac{1}{h_p} \cdot \frac{1}{n_r} + \frac{1 \cdot M_{pl}}{h_s - 0.5d} \leq V_{pl} \tag{6.19}$$

For studs with double curvature, the shear resistance is:

$$P = \left[\left(\frac{f_{ctm}}{\cos\alpha} + \frac{N_q + N_{sc}}{A}\right) \cdot \frac{2 \cdot I_y}{b_o} + N_{sc} \cdot e_L\right] \cdot \frac{1}{h_p} \cdot \frac{1}{n_r} + \frac{2 \cdot M_{pl}}{h_s - 0.5d} \leq V_{pl} \tag{6.20}$$

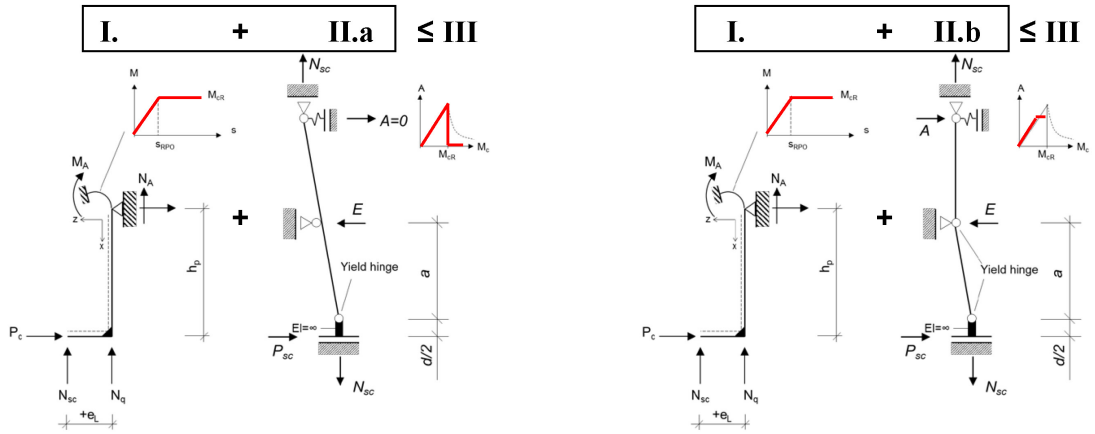


Figure 6.12: Static systems to describe the stud shear resistance for failure modes with single or double curvature of the stud.

The deformation of the stud differs only because the horizontal support of the head of the stud is either failed or not. This leads to the development of either one or two yield hinges in the stud shank. Accordingly, equations (6.19) and (6.20) only differ from each other in the factors 1 and 2 in front of the studs plastic bending resistance, $M_{pl}$. This factor is the number of yield hinges. If the numbers 1 and 2 are replaced with the factor $n_y$, a single equation for both types of curvature is obtained:

$$P = \left[\left(\frac{f_{ctm}}{\cos\alpha} + \frac{N_q + N_{sc}}{A}\right) \cdot \frac{2 \cdot I_y}{b_o} + N_{sc} \cdot e_L\right] \cdot \frac{1}{h_p} \cdot \frac{1}{n_r} + \frac{n_y \cdot M_{pl}}{h_s - 0.5d} \leq V_{pl} \tag{6.21}$$

where: $n_y$ Number of yield hinges in the stud shank

To differentiate between single or double curvature, equation (6.21) is solved for $n_y$. Then the number of yield hinges is back-calculated from push-out test results and compared against geometric parameters of the shear connection. The database of results is reduced to 191 cases in this investigation. The following cases were not considered in this model:

- Re-entrant deck profiles
- Through deck welded studs with 22 mm diameter
- Studs without a head
- Studs welded with an eccentricity to the centre line of the rib
- Test series, where the maximum or minimum resistance deviates by more than 20% of the mean resistance of the series
- tests where $V_{pl}$ is decisive

The observations in push-out tests indicate that the embedment depth of the head of the stud into the concrete above the rib is the primary criterion to differentiate between single or double curvature. [DIN EN 1994-1-1, 2010] requires an embedment depth of 2 stud diameters. Figure 6.13 shows the obtained number of yield hinges versus the embedment depth related to the stud diameter. Because of the simplified assumptions leading to equation (6.21), the results for $n_y$ show a large scatter. This makes it difficult to identify a criterion to differentiate the number of yield hinges. However, Figure 6.13 shows that it is not possible to differentiate the number of yield hinges by an embedment depth of 2 diameters.

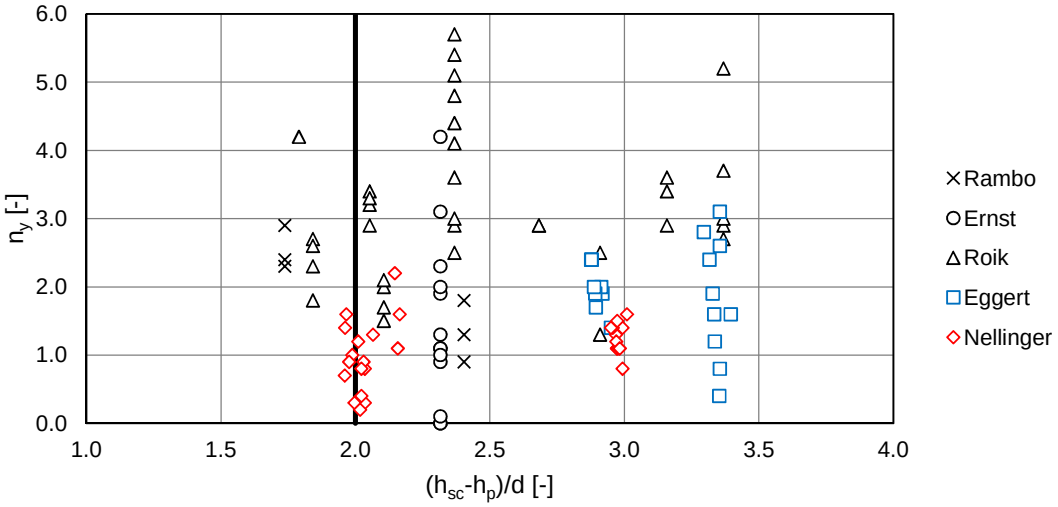


Figure 6.13: Number of yield hinges versus embedment depth related to the stud diameter.

The reduction factors in [Konrad, 2011] are differentiated for a ratio $h_{sc}/h_p = 1.56$. The numerical work in [Konrad, 2011] indicated a potential change of the failure. The comparison of the number of yield hinges against the ratio $h_{sc}/h_p$ is shown in Figure 6.14. For tests with $h_{sc}/h_p < 1.56$, the results for $n_y$ show a too large scatter to use the ratio $h_{sc}/h_p$ as a decision criterion.

In [Lungershausen, 1988] a minimum embedment depth of the stud of $2d\sqrt{n_r}$ is required, where $n_r$ is the number of studs per deck rib. Figure 6.15 shows the number of yield hinges plotted against the embedment depth relative to $d\sqrt{n_r}$. Based on the observation of 2 yield hinges in tests with CP60 decking, the required embedment depth of $2d\sqrt{n_r}$ is sufficient for the development of 2 yield hinges. Based on the results of tests with CF80 decking and pairs of studs, only one yield hinge can be assumed for an embedment depth smaller than $1.5d\sqrt{n_r}$. Considering the results shown in Figure 6.15, a linear transition between single and double curvature can be assumed. This implies a gradual transition between the failure modes, where the upper yield hinge is only partially developed. The factor $n_y$ is then given by equation (6.22).

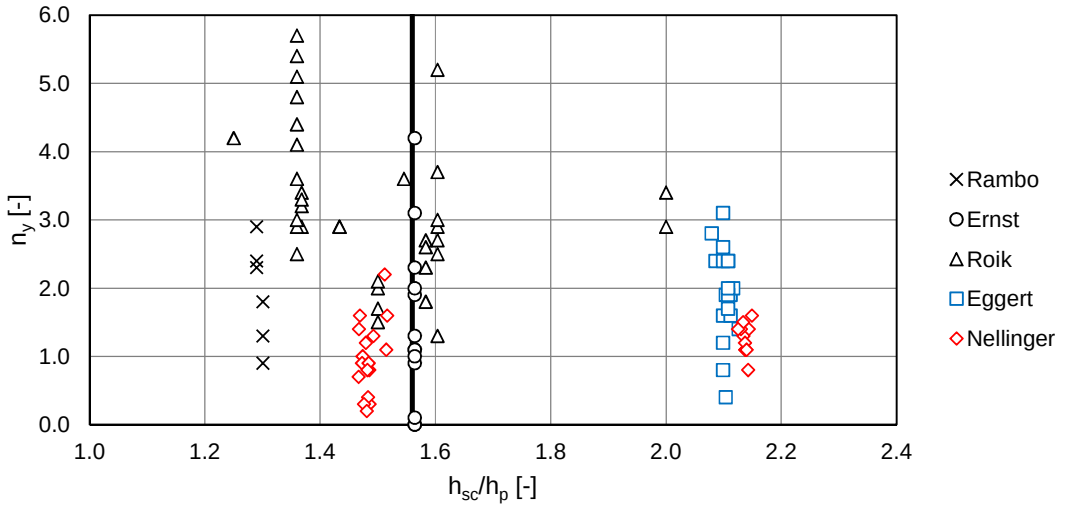


Figure 6.14: Number of yield hinges versus the ratio of stud height to deck height.

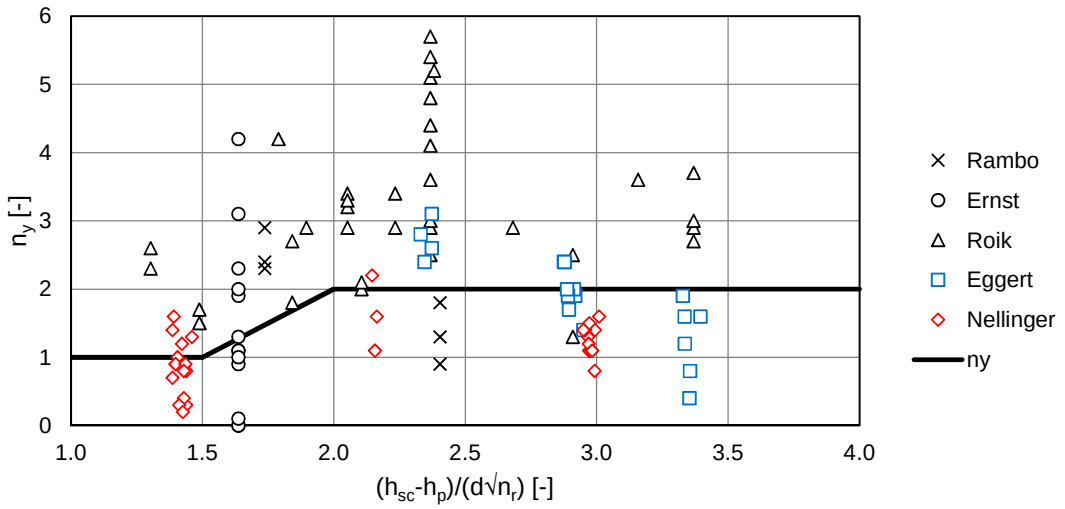


Figure 6.15: Number of yield hinges versus embedment depth related to stud diameter and number of studs per rib.

$$n_y = 2 \cdot \frac{h_{sc} - h_p}{d \cdot \sqrt{n_r}} - 2 \begin{cases} n_y \geq 1 \\ n_y \leq 2 \end{cases} \tag{6.22}$$

Considering $n_y$ according to equation (6.22), the shear resistance according to equation (6.21) is evaluated against push-out test results. The used database is reduced by the following cases:

- through deck welded studs with 22 mm diameter
- studs with the head cut-off
- test series', where the results deviate more than 30% from the mean value

The remaining database contains 291 push-out tests and considers different deck shapes,

welding methods, positions and number of studs per rib. The results of the comparison are shown in Figure 6.16 and Table 6.1. The comparisons show that the predicted shear resistances correlates well with the test results. In comparison to the analysis methods according to [DIN EN 1994-1-1, 2010], [Lungershausen, 1988] and [Konrad, 2011], the predictions are relative conservative. However, the coefficients of variation, $V$, and correlation, $R$, are significantly improved.

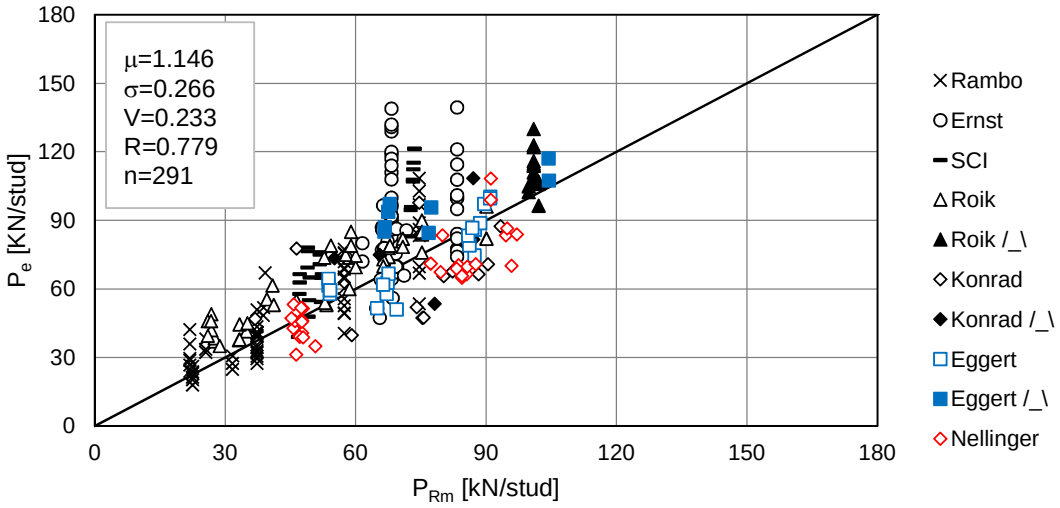


Figure 6.16: Comparison of experimental shear resistance, $P_e$, to the shear resistance according to equation (6.21), $P_{Rm}$.

Table 6.1: Comparison of analytical average shear resistance to test results for different analysis methods.

| Analysis method | $P_e/P_{Rm}$ | $\sigma$ | $V$ | $R$ |
|---|---|---|---|---|
| Equation (6.21) | 1.146 | 0.266 | 0.233 | 0.779 |
| [Roik et al., 1989, DIN EN 1994-1-1, 2010] | 0.858 | 0.259 | 0.301 | 0.623 |
| [Lungershausen, 1988] | 1.085 | 0.292 | 0.269 | 0.721 |
| [Konrad, 2011] | 0.893 | 0.255 | 0.285 | 0.616 |

## 6.6 Simplification and verification of the model

Even though equation (6.21) shows a significantly improved accordance with the test results, it is only of limited suitability in practice, because the cone properties $A$, $I_y$ and $h_s$ require a relatively large effort in calculation. In the following section, simplified equations for these properties are introduced.

The idea is to replace the three-dimensional failure cone, shown in Figure 6.4, with an equivalent rectangle. The width of the rectangle, $b_{eff}$, is taken as the horizontal width of the failure surface, and is given by the 'as-welded' height of the studs, $h_{sc}$, and the spacing between the studs, $e_s$, as follows:

$$b_{eff} = 2 \cdot h_{sc} \cdot \cot\Theta + (n_r - 1) \cdot e_s = 2.4 \cdot h_{sc} + (n_r - 1) \cdot e_s \tag{6.23}$$

The height of the rectangle, $b_{max}$, is taken as the maximum width of the concrete rib, as follows:

$$b_{max} = \max \begin{cases} b_u \\ b_o \end{cases} \tag{6.24}$$

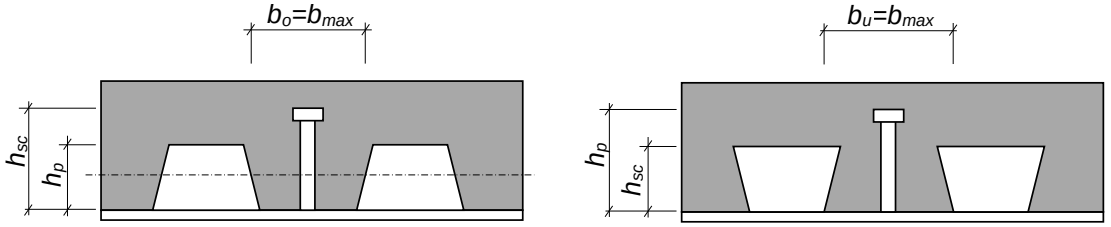


(a) Open deck shapes (b) Re-entrant deck shapes

Figure 6.17: Maximum width of the rib, $b_{max}$.

This simplifies the area of the failure surface as follows:

$$A = b_{eff} \cdot b_{max} = (2.4 \cdot h_{sc} + (n_r - 1) \cdot e_s) \cdot b_{max} \tag{6.25}$$

The moment of inertia is simplified as follows:

$$I_y = \frac{b_{eff} \cdot b_{max}^3}{12} = \frac{1}{12} \cdot (2.4 \cdot h_{sc} + (n_r - 1) \cdot e_s) \cdot b_{max}^3 \tag{6.26}$$

The position of the upper yield hinge, $h_s$, cannot be expressed by the simplified surface. Figure 6.18 shows the position of the hinge according to equation (6.10) in dependency of the stud height, when single studs per rib and different types of steel decking are used. It is shown, that for trapezoidal decking, such as CF80, RD80 and CP60, the position of the yield hinge is calculated at 0.45 times the stud height. For re-entrant decking, such as CS56 or Holorib, a value of 0.41 times the stud height is obtained.

For single studs per rib, the position of the upper yield hinge is:

$$h_{s,1} = \beta \cdot h_{sc} \tag{6.27}$$

where: $\beta = \begin{cases} 0.45 \text{ for trapezoidal deck profiles} \\ 0.41 \text{ for re-entrant deck profiles} \end{cases}$

When pairs of studs per rib are used, two additional rectangles occur between the studs in the failure surface. The area of these rectangles is given by $e_s$ and $b_{max}$. There centre of mass is located at $0.5(h_{sc} - h_p)$ above the top of the rib. Considering the position of the yield hinge found for single studs, $h_{s,1}$, and the simplifications on the area of the failure surface, $A$, this leads to a yield hinge position for multiple studs as follows:

$$\begin{aligned} h_s &= \frac{A_1 \cdot h_{s,1} + \Delta A \cdot h_{s,2}}{\sum A} \\ &= \frac{2.4 \cdot h_{sc} \cdot b_{max} \cdot \beta \cdot h_{sc} + b_{max} \cdot (n_r - 1) \cdot e_s \cdot (h_p + 0.5 \cdot (h_{sc} - h_p))}{2.4 \cdot h_{sc} \cdot b_{max} + (n_r - 1) \cdot e_s \cdot b_{max}} \end{aligned}$$

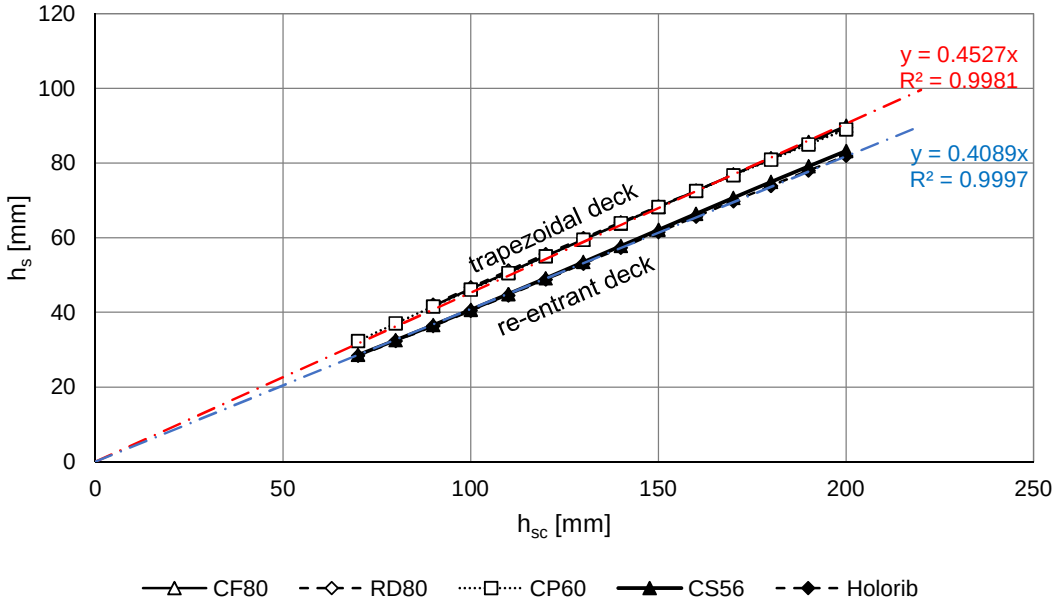


Figure 6.18: Position of the upper yield hinge, $h_s$, versus stud height, $h_{sc}$, for single studs and different steel decks.

This results in the position of the upper yield hinge for single studs per rib or multiple studs per rib as follows:

$$h_s = \frac{\beta \cdot h_{sc} + \frac{(n_r - 1) \cdot e_s}{4.8 \cdot h_{sc}} \cdot (h_p + h_{sc})}{1 + \frac{(n_r - 1) \cdot e_s}{2.4 \cdot h_{sc}}} \tag{6.28}$$

Because of the simplifications on the cone properties $A$ and $I_y$, the consideration of the failure surfaces inclination, $\alpha$, is no longer necessary. Therefore, equation (6.21) can be simplified to:

$$P = \left[\left(f_{ctm} + \frac{N_q + N_{sc}}{A}\right) \cdot \frac{2 \cdot I_y}{b_o} + N_{sc} \cdot e_L\right] \cdot \frac{1}{h_p} \cdot \frac{1}{n_r} + \frac{n_y \cdot M_{pl}}{h_s - 0.5d} \leq V_{pl} \tag{6.29}$$

The evaluation of equation (6.29) with the simplifications on $A$, $I_y$ and $h_s$ is shown in Figure 6.19. The simplifications did not only reduce the calculation effort, but even improved the accuracy of the predicted shear resistances in comparison to the results of equation (6.21), shown in Figure 6.16.

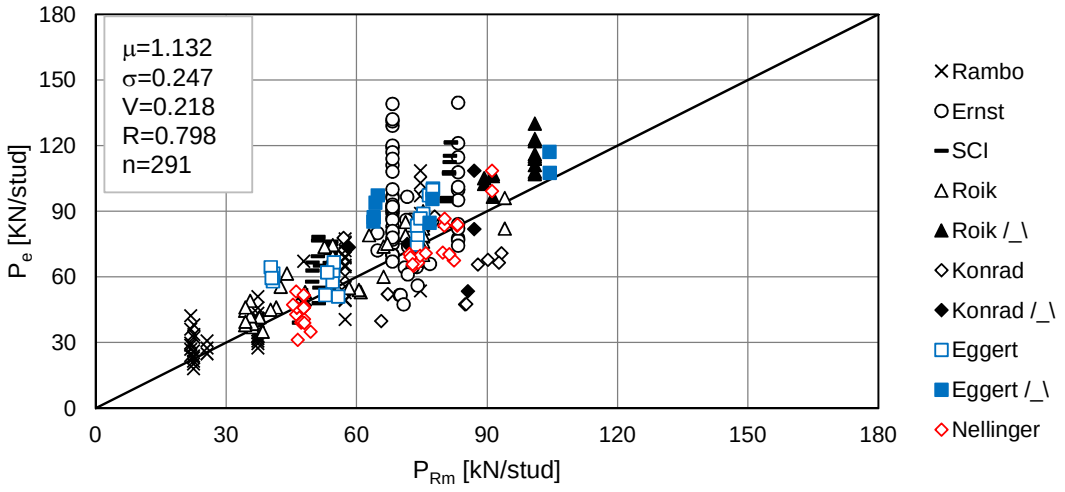


Figure 6.19: Comparison of push-out test results to simplified analytical shear resistances, $P_{Rm}$ according to equation (6.29).

## 6.7 Calibration according to EN 1990

In the following section the equation for the shear connection resistance (see equation (6.29)) is calibrated statistically against the test results. The standardised evaluation method according to [DIN EN 1990, 2002] Appendices D.8.2 and D.8.3 is used. This method derives scaling factors to identify the characteristic value and design value for equation (6.29). This linear scaling of the resistance is the reason why previously special attention was paid on improving the coefficient of correlation rather than the ratio $P_e/P_t$. The characteristic resistance is derived for a 5%-fractile (see Table D.1 in [DIN EN 1990, 2002]) and the design value for a probability of failure of 0.1% (see Table D.2 in [DIN EN 1990, 2002]).

For details on the evaluation method refer to the standard. Here, only additional considerations on the evaluation of equation (6.29) and the assumed input parameters are discussed.

[DIN EN 1990, 2002] requires a comparison between experimental resistance and theoretical resistance calculated with measured properties to verify the accuracy of the design model. This was already shown in Figure 6.19.

The final equations contain the characteristic material properties. [DIN EN 1990, 2002] assumes the use of measured properties in the calibration. Therefore, [Roik et al., 1989] and [Konrad, 2011] multiplied the finally calibrated equations with further conversion factors. Because the present design model is a complex function, such a conversion factor cannot be used and the characteristic material properties are used. The characteristic material properties are obtained according to equations (6.30) and (6.31).

$$f_{ck} = f_{cm} - 8 \tag{6.30}$$

$$f_{uk} = f_{um} \cdot (1 - k_{\infty} \cdot V_{fu}) \tag{6.31}$$

The theoretical resistance, $r_t$, of the shear connection is then the minimum of equations (6.32) and (6.33).

$$r_{t,1} = \left[\left(f_{ctm} + \frac{N_q + N_{sc}}{A}\right) \cdot \frac{2 \cdot I_y}{b_o} + N_{sc} \cdot e_L\right] \cdot \frac{1}{h_p \cdot n_r} + \frac{n_y \cdot M_{pl}}{h_s - 0.5d} \tag{6.32}$$

$$r_{t,2} = \frac{f_{uk}}{\sqrt{3}} \cdot \pi \cdot d^2/4 \tag{6.33}$$

| | | |
|---|---|---|
| Where: | $f_{ctm} = 0.3\alpha_{ct} f_{ck}^{2/3}$ | Concrete tensile strength with $f_{ck} \leq 50$ N/mm$^2$ |
| | $N_{sc} = 0.1 n_r f_{uk} \pi d^2/4$ | Compression applied below the head of the stud |
| | $M_{pl} = f_{uk} d^3/6$ | Plastic bending resistance of the stud |

For the reduced test database, equation (6.32) becomes decisive for 182 tests and equation (6.33) is decisive for 111 tests. For both equations, further investigations are conducted for through deck welded studs and tests with pre-punched deck profiles, as shown in Table 6.2. Because for some of these cases the number of samples is small, all cases are evaluated assuming a finite number of samples. The fractile-factors $k_n$ according to [DIN EN 1990, 2002] Table D.1 and $k_{d,n}$ according to Table D.2 are chosen for the number of samples in each case to consider the statistical uncertainty of a small number of samples.

Table 6.2: Case differentiations for the calibration of the theoretical resistance $r_t$

| ID | Description | No. of tests | |
|---|---|---|---|
| | | Bending Eq. (6.32) | Stud shearing Eq. (6.33) |
| A | All tests with headed studs and a variation of the results $\leq$ 30% | 182 | 111 |
| B | As A, but only tests with studs in mid-, staggert- or favourable position and $16\text{mm} \leq d \leq \begin{cases} 20\text{mm when through-welded} \\ 22\text{mm with pre-punched decking} \end{cases}$ | 143 | 41 |
| C | As B, but only through deck welded studs | 72 | 21 |
| D | As B, but only with pre-punched decking | 71 | 20 |

For a finite number of samples, the coefficient of variation, $V_{rt}$, of the theoretical resistance function is given by equation (6.34). Because the theoretical resistance according to equation (6.32) is not a product, the partial derivatives cannot be expressed as a factor of $g_{rt}$. Therefore, $g_{rt}$ cannot be cancelled and $V_{rt}$ is dependent on the average values of the variables $\underline{X}_m$. For this reason, equation (6.34) is evaluated for each test and the mean value of $V_{rt}$ is used in the further progress.

$$V_{rt}^2 = \frac{1}{g_{rt}^2(\underline{X}_m)} \times \sum_{i=1}^{j} \left(\frac{\partial g_{rt}}{\partial X_i} \times \sigma_i\right)^2 \tag{6.34}$$

The partial derivatives, $\frac{\partial g_{rt}}{\partial X_i}$, are given in Appendix F. The used coefficients of variation, $V_{xi}$, for each variable are summarised in Table 6.3. According to [Roik et al., 1989], a variability of 15% of the concrete compressive strength, $f_{ck}$, 5% of the studs tensile strength, $f_u$, and 3% of the stud diameter, $d$, are assumed. Measurements of the welded height of the stud, $h_{sc}$, (see Appendix C) led to the assumption of a variation of 1%. For the dimension of the steel

decking, $h_p$, $b_o$, $b_u$, a variability of 5% is assumed, considering the limiting sizes according to [DIN 18807-1, 1987]. This assumption is relatively conservative, but more realistic than assuming a variation of at least 10%, which [DIN EN 1990, 2002] requires for unknown coefficients of variation. Furthermore, it was observed that the steel decking, which was received for the push-out and beam tests, was strongly deformed after transport, in some cases. In those cases, the assumed variation of 5% can be assumed reasonable, at least for the width of the rib at the top, $b_o$. For the welding position of the stud, $e_s$ and $e_L$, no coefficients of variation are known. According to [DIN EN 1990, 2002], a minimum variability of 10% is assumed. This can be assumed as a relatively conservative estimation of the variability, because an inaccuracy of up to about 3 mm is considered for the eccentricity, $e_s$, and up to 10 mm for the transverse spacing of the studs, $e_L$. The variation of the number of yield hinges, $n_y$, is assumed to be considered within the coefficient of variation, $V_\delta$, of the average correction factor, $b$. A variation for the number of studs is not needed. The variation of the transverse load, $N_q$, is assumed to be considered in the loading assumptions according to [DIN EN 1991-1-1, 2010].

Table 6.3: Coefficients of variation $V_{xi}$ for the variables $X_i$.

| $f_{ck}$ | $f_{uk}$ | $d$ | $h_{sc}$ | $h_p$ | $b_u$ | $b_o$ | $e_s$ | $e_L$ | $n_y$ | $n_r$ | $N_q$ |
|---|---|---|---|---|---|---|---|---|---|---|---|
| 15% | 5% | 3% | 1% | 5% | 5% | 5% | 10% | 10% | - | - | - |

The calibration is conducted separately for each equation. The results for the shear resistance due to bending, $r_{t,1}$ according to equation (6.32), are summarised in Table 6.4. Considering all 182 test results, a safety factor of $\gamma_M = 1.34$ is obtained. This improves to $\gamma_M = 1.31$ when the position of the stud in the rib is restricted and the limitations for the stud diameter according to [DIN EN 1994-1-1, 2010] are considered (case B). In addition, the restricted field of application leads to about 4% higher characteristic and design resistances. A further improvement of the resistances and safety factor is obtained for cases with pre-punched deck profile, but the results significantly worsen for through deck welded studs. However, the database of tests with pre-punched decking consists to 69% of single studs per deck rib, while the database for through deck welded studs consists only to 36% of single studs. Hence, from this comparison it cannot be finally concluded if the larger variation is because of the welding method or the number of studs per deck rib.

For the stud shear resistance, $r_{t,2}$ according to equation (6.33), a safety factor of $\gamma_M = 1.42$ is required for all 111 tests results, as shown in Table 6.5. The high safety factor results from the small resistance for studs with small diameters or studs in unfavourable position used in [Rambo-Roddenberry, 2002]. This is proven, as the safety factor improves to $\gamma_M = 1.25$ when the field of application is restricted (Case B). For the shear resistance due to bending, the safety factor further improves when the deck profile is pre-punched. A significantly higher safety factor is obtained for through deck welded shear studs. All tests with pre-punched decking used single studs per deck rib. For tests with through deck welded studs, 85% of the tests also used single studs per deck rib. This leads to the conclusion that through deck welded studs require higher safety factors than studs where the deck profile is pre-punched. When the stud is welded through the decking, a certain amount of zinc evaporation is enclosed in the welding area. This weakens the cross-section of the shear studs and causes a larger variation of the stud shear resistance. This variation is so large that through deck welded studs may not benefit from the contribution of the decking for their design resistance.

A further differentiation of the cases C, through-welded studs, and D, pre-punched deck profiles, according to the number of studs per deck rib is shown in Table 6.6. Comparing the

average correction factor $b$ for single studs per deck rib, a higher resistance can be confirmed for through deck welded studs (C-1 vs. D1), but it appears that the resistance decreases for pairs of studs when through deck welding is used (C-2+ vs. D-2+). A comparison with respect to the characteristic resistance, design resistance and safety factor is not possible between these cases, because the number of samples is too different. This means, that for a smaller number of samples a larger statistical uncertainty is considered (see $k_n$ and $k_{d,n}$ in Table 6.6). This makes it impossible to identify if the different values result from the number of studs, the welding method or the number of samples. Therefore, the influence of the number of studs per deck rib and the welding method should be further assessed.

Based on these results, the design resistance of the shear connection is proposed without any further considerations on the welding method or number of studs per deck rib. Only the limitations on the shear stud diameter according to [DIN EN 1994-1-1, 2010] and on the stud position are considered. The obtained design resistances are then shown as case B in Tables 6.4, 6.5 and 6.6. Figures 6.20 and 6.21 visualise these results.

For the combined bending failure of the concrete rib and the shear stud, $r_{t,1}$ according to equation (6.32), a safety factor of $\gamma_M = 1.31$ is obtained. If the characteristic resistance $r_{k,1}$ is further reduced, the safety factor $\gamma_M = 1.25$ can be used to be in line with [DIN EN 1994-1-1, 2010], according to:

$$r_{k,1}^{*} = \frac{1.25}{1.306} \cdot 0.882 \cdot r_{t,1} = 0.84 \cdot r_{t,1}$$

For stud shearing, $r_{t,2}$ according to equation (6.33), the required safety factor is very close to $\gamma_M = 1.25$ and further conversions are not necessary. The design resistances are then shown in equations (6.35) and (6.36).

Table 6.4: Calibration of the shear resistance due to bending, $r_{t,1}$, according to [DIN EN 1990, 2002].

| Case | A | B | C | D |
|---|---|---|---|---|
| $n$ | 182 | 143 | 72 | 71 |
| $b = \sum(r_e r_t)/\sum r_t^2$ | 1.208 | 1.228 | 1.255 | 1.206 |
| $\delta_i = r_{ei}/(b r_{ti})$ | - | - | - | - |
| $\Delta_i = \ln \delta_i$ | - | - | - | - |
| $\bar{\Delta} = 1/n \sum_{i=1}^{n} \Delta_i$ | 0.008 | 0.008 | -0.001 | 0.013 |
| $s_\delta^2 = 1/(n-1) \sum_{i=1}^{n} (\Delta_i - \bar{\Delta})^2$ | 0.043 | 0.036 | 0.045 | 0.026 |
| $V_\delta^2 = \exp(s_\delta^2) - 1$ | 0.044 | 0.037 | 0.046 | 0.027 |
| $V_{rt}^2 = 1/g_{rt}^2(\underline{X}_m) \times \sum_{i=1}^{j} \left(\frac{\partial g_{rt}}{\partial X_i} \times \sigma_i\right)^2$ | 0.000 | 0.001 | 0.001 | 0.001 |
| $V_r^2 = V_\delta^2 + V_{rt}^2$ | 0.044 | 0.037 | 0.047 | 0.027 |
| $Q_{rt} = \sqrt{\ln(V_{rt}^2 + 1)}$ | 0.022 | 0.023 | 0.023 | 0.024 |
| $Q_\delta = \sqrt{\ln(V_\delta^2 + 1)}$ | 0.207 | 0.189 | 0.213 | 0.163 |
| $Q = \sqrt{\ln(V_r^2 + 1)}$ | 0.208 | 0.191 | 0.214 | 0.164 |
| $\alpha_{rt} = Q_{rt}/Q$ | 0.105 | 0.122 | 0.106 | 0.145 |
| $\alpha_\delta = Q_\delta/Q$ | 0.995 | 0.993 | 0.995 | 0.990 |
| $k_n$ | 1.64 | 1.64 | 1.672 | 1.673 |
| $k_\infty$ | 1.64 | 1.64 | 1.64 | 1.64 |
| $r_k/r_t = b \exp(-k_\infty \alpha_{rt} Q_{rt} - k_n \alpha_\delta Q_\delta - 0.5Q^2)$ | 0.840 | 0.882 | 0.858 | 0.904 |
| $k_{d,n}$ | 3.04 | 3.04 | 3.200 | 3.206 |
| $k_{d,\infty}$ | 3.04 | 3.04 | 3.04 | 3.04 |
| $r_d/r_t = b \exp(-k_{d,\infty} \alpha_{rt} Q_{rt} - k_{d,n} \alpha_\delta Q_\delta - 0.5Q^2)$ | 0.628 | 0.675 | 0.619 | 0.703 |
| $\gamma_M = r_k/r_d$ | 1.338 | 1.306 | 1.387 | 1.286 |

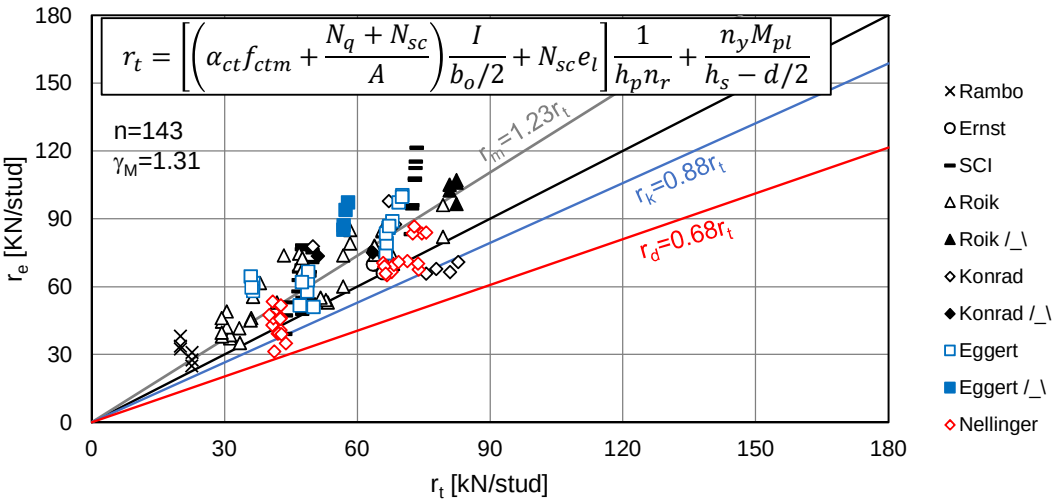


Figure 6.20: Results of the calibration according to [DIN EN 1990, 2002] for the shear resistance due to bending with the restricted field of application.

Table 6.5: Calibration of the shear resistance due to stud shearing, $r_{t,2}$, according [DIN EN 1990, 2002].

| Case | A | B | C | D |
|---|---|---|---|---|
| $n$ | 111 | 41 | 20 | 21 |
| $b = \sum(r_e r_t)/\sum r_t^2$ | 1.313 | 1.257 | 1.294 | 1.236 |
| $\delta_i = r_{ei}/(b r_{ti})$ | - | - | - | - |
| $\Delta_i = \ln \delta_i$ | - | - | - | - |
| $\bar{\Delta} = 1/n \sum_{i=1}^{n} \Delta_i$ | -0.033 | 0.003 | 0.000 | -0.004 |
| $s_\delta^2 = 1/(n-1) \sum_{i=1}^{n} (\Delta_i - \bar{\Delta})^2$ | 0.048 | 0.009 | 0.013 | 0.004 |
| $V_\delta^2 = \exp(s_\delta^2) - 1$ | 0.050 | 0.009 | 0.013 | 0.004 |
| $V_{rt}^2 = 1/g_{rt}^2(\underline{X}_m) \times \sum_{i=1}^{j} \left(\frac{\partial g_{rt}}{\partial X_i} \times \sigma_i\right)^2$ | 0.013 | 0.013 | 0.012 | 0.014 |
| $V_r^2 = V_\delta^2 + V_{rt}^2$ | 0.063 | 0.022 | 0.026 | 0.018 |
| $Q_{rt} = \sqrt{\ln(V_{rt}^2 + 1)}$ | 0.114 | 0.114 | 0.111 | 0.117 |
| $Q_\delta = \sqrt{\ln(V_\delta^2 + 1)}$ | 0.220 | 0.095 | 0.114 | 0.067 |
| $Q = \sqrt{\ln(V_r^2 + 1)}$ | 0.247 | 0.148 | 0.159 | 0.134 |
| $\alpha_{rt} = Q_{rt}/Q$ | 0.464 | 0.770 | 0.699 | 0.870 |
| $\alpha_\delta = Q_\delta/Q$ | 0.892 | 0.642 | 0.720 | 0.496 |
| $k_n$ | 1.64 | 1.707 | 1.760 | 1.756 |
| $k_\infty$ | 1.64 | 1.64 | 1.64 | 1.64 |
| $r_k/r_t = b \exp(-k_\infty \alpha_{rt} Q_{rt} - k_n \alpha_\delta Q_\delta - 0.5Q^2)$ | 0.846 | 0.970 | 0.974 | 0.979 |
| $k_{d,n}$ | 3.04 | 3.377 | 3.640 | 3.620 |
| $k_{d,\infty}$ | 3.04 | 3.04 | 3.04 | 3.04 |
| $r_d/r_t = b \exp(-k_{d,\infty} \alpha_{rt} Q_{rt} - k_{d,n} \alpha_\delta Q_\delta - 0.5Q^2)$ | 0.597 | 0.775 | 0.748 | 0.798 |
| $\gamma_M = r_k/r_d$ | 1.418 | 1.252 | 1.301 | 1.226 |

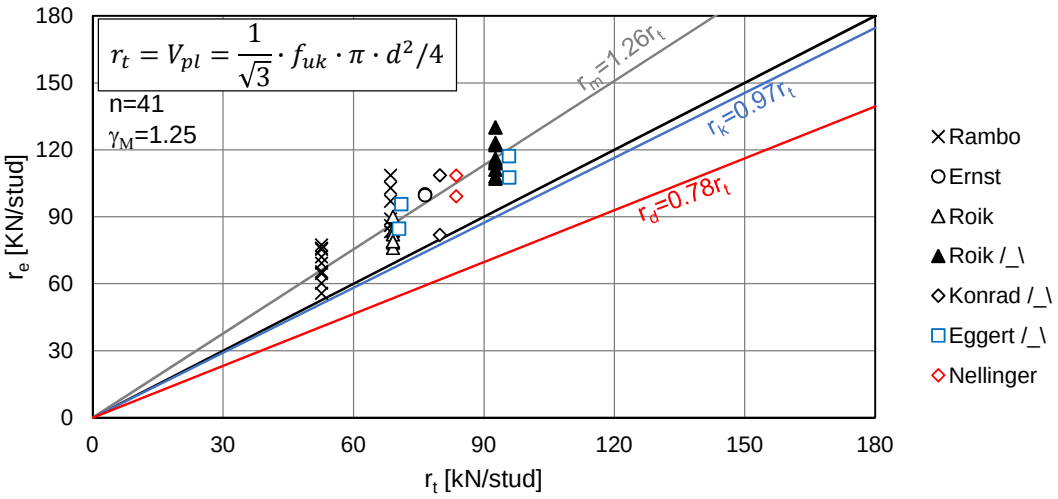


Figure 6.21: Results of the calibration according to [DIN EN 1990, 2002] for the stud shear resistance with the restricted field of application.

Table 6.6: Comparison of the statistical evaluation for different welding methods and single or pairs of studs per deck rib.

| | | B | C | C-1 | C-2+ | D | D-1 | D-2+ |
|---|---|---|---|---|---|---|---|---|
| $r_{t,1}$ | $n$ | 143 | 72 | 26 | 46 | 71 | 49 | 22 |
| | $b$ | 1.228 | 1.255 | 1.345 | 1.181 | 1.206 | 1.166 | 1.298 |
| | $k_n$ | 1.64 | 1.672 | 1.736 | 1.702 | 1.673 | 1.698 | 1.754 |
| | $k_{d,n}$ | 3.04 | 3.200 | 3.520 | 3.349 | 3.206 | 3.331 | 3.600 |
| | $r_k/r_t$ | 0.882 | 0.858 | 0.975 | 0.788 | 0.904 | 0.906 | 0.915 |
| | $r_d/r_t$ | 0.675 | 0.619 | 0.713 | 0.545 | 0.703 | 0.719 | 0.645 |
| | $\gamma_M$ | 1.306 | 1.387 | 1.368 | 1.445 | 1.286 | 1.261 | 1.418 |
| $r_{t,2}$ | $n$ | 41 | 20 | 17 | 3 | 21 | 21 | 0 |
| | $b$ | 1.257 | 1.294 | 1.285 | 1.382 | 1.236 | 1.236 | - |
| | $k_n$ | 1.707 | 1.760 | 1.780 | n.a. | 1.756 | 1.756 | - |
| | $k_{d,n}$ | 3.377 | 3.640 | 3.901 | n.a. | 3.620 | 3.620 | - |
| | $r_k/r_t$ | 0.970 | 0.974 | 0.961 | n.a. | 0.979 | 0.979 | - |
| | $r_d/r_t$ | 0.775 | 0.748 | 0.721 | n.a. | 0.798 | 0.798 | - |
| | $\gamma_M$ | 1.252 | 1.301 | 1.333 | n.a. | 1.226 | 1.226 | - |

C-1: Single studs, through-welded C-2+: Two or three studs, through-welded

D-1: Single studs, pre-punched deck D-2+: Two or three studs, pre-punched deck

## 6.8 Design resistance of shear connectors

$$P_{Rd,1} = 0.84 \cdot \left[ \frac{\left( f_{ctm} + \frac{N_q + N_{sc}}{A} \right) \cdot W + N_{sc} \cdot e_L}{h_p \cdot n_r} + \frac{n_y \cdot M_{pl}}{h_s - d/2} \right] \cdot \frac{1}{\gamma_V} \tag{6.35}$$

$$P_{Rd,2} = 0.56 \cdot f_{uk} \cdot \pi \cdot \frac{d^2}{4} \cdot \frac{1}{\gamma_V} \tag{6.36}$$

Where:

| | |
|---|---|
| $\gamma_V = 1.25$ | Safety factor |
| $f_{ctm} = 0.3\alpha_{ct} f_{ck}^{2/3}$ | Concrete tensile strength with $f_{ck} \leq 50$ N/mm$^2$ |
| $\alpha_{ct}$ | Factor for static loading: $\alpha_{ct} = 0.85$ |
| $f_{uk} \leq 500$ N/mm$^2$ | Stud tensile strength |
| $N_q$ | Transverse load per deck rib |
| $N_{sc} = 0.1 n_r f_{uk} \pi d^2/4$ | Compression applied below the head of the stud |
| $A = (2.4h_{sc} + (n_r - 1)e_s) b_{max}$ | Area of the concrete failure surface |
| $W = (2.4h_{sc} + (n_r - 1)e_s) b_{max}^3/(6 \cdot b_o)$ | Section modulus of the concrete failure surface |
| $h_s = \dfrac{\beta h_{sc} + \dfrac{(n_r - 1)(h_p + h_{sc})e_s}{4.8h_{sc}}}{1 + \dfrac{(n_r - 1)e_s}{2.4h_{sc}}}$ | Position of upper yield hinge |
| $1 \leq n_y = 2\dfrac{h_{sc} - h_p}{d\sqrt{n_r}} - 2 \leq 2$ | Number of yield hinges |
| $M_{pl} = f_{uk} d^3/6$ | Bending resistance of the stud |
| $h_p \leq 155$mm | Height of the deck rib |
| $b_o$ | Width of the deck rib at the top |
| $b_{max}$ | Maximum width of the deck rib |
| $n_r \leq 3$ | Number of studs per rib |
| $e_s$ | Transverse spacing between studs |
| $e_L \begin{cases} > 0 \text{ for favourable position} \\ = 0 \text{ for mid- and staggert position} \end{cases}$ | Eccentricity of the stud |
| $16\text{mm} \leq d \leq \begin{cases} 22\text{mm pre-punched deck} \\ 20\text{mm through-welded} \end{cases}$ | Diameter of the shear stud |
| $h_{sc} = h_{sc,nom} - 5$ | As-welded stud height |
| $h_{sc,nom}$ | Nominal stud height |
| $h_{sc} - h_p \geq d$ | Minimum embedment depth |
| $\beta = \begin{cases} 0.45 \text{ for trapezoidal decking} \\ 0.41 \text{ for re-entrant decking} \end{cases}$ | Shape factor for the decking |

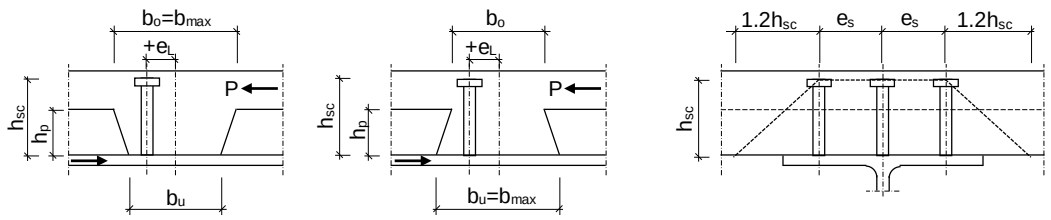

## 6.9 Discussion of the new shear resistances in comparison to EN 1994-1-1

### 6.9.1 Discussion on the limitations onto geometry and material properties

During the development of the new design formulae for the stud shear resistance, the improvement of the coefficients of correlation and variation was already highlighted. After the calibration according to [DIN EN 1990, 2002], it is now discussed how the field of application and shear resistance change in comparison to [DIN EN 1994-1-1, 2010]. A comparison of the limitations on the analytical resistances according to the new model and [DIN EN 1994-1-1, 2010] is shown in Table 6.7.

Table 6.7: Comparison of the limitations on the analytical stud shear resistance in [DIN EN 1994-1-1, 2010] and the new model.

| Restriction | [DIN EN 1994-1-1, 2010] | New model | Relative to EC4 |
|---|---|---|---|
| Embedment depth | $h_{sc} - h_p \geq 2d$ | $h_{sc} - h_p \geq d$ | -50% |
| Stud diameter | $16\text{mm} \leq d \leq \begin{cases} 22\text{mm pre-punched} \\ 20\text{mm through welded} \end{cases}$ | | unchanged |
| Rib height | $h_p \leq 85\text{mm}$ | $h_p \leq 155\text{mm}$ | +82% |
| Rib width | $b_m \geq h_p$<br>$\min b \geq 50\text{mm}$ | No restrictions | N.A. |
| Number of studs | $n_r \leq 2$ | $n_r \leq 3$ | +50% |
| Stud position | Mid, Staggered, (Favourable) | Mid, Staggered, Favourable | N.A. |
| Concrete strength | $f_{ck} \leq 60\text{N/mm}^2$ | $f_{ck} \leq 50\text{N/mm}^2$ | -17% |
| Tensile strength | $f_{uk} \leq 450\text{N/mm}^2$ | $f_{uk} \leq 500\text{N/mm}^2$ | +11% |
| No. of tests in limitations | 115 | 184 | +60% |

The required embedment depth of the stud into the concrete topping is reduced by 50% from two diameters to one diameter. This reduction is possible, because the new model was developed and calibrated considering tests with a small embedment depth, as for example tests with CF80 decking or tests in [Hicks and Smith, 2014]. It is not considered that this new limitation will lead to smaller studs in practice, because of the standardised dimensions of shear connectors, but it will clarify limit cases, as in [Hicks and Smith, 2014] or the presented CF80 tests. However, it is strongly recommended to not minimize the stud height, because of the rather brittle concrete failure that occurs and the high sensitivity to transverse loading for studs with a small embedment depth.

Considering the shear connector diameter, the same rules as in [DIN EN 1994-1-1, 2010] apply to the new model.

The biggest changes come with the more relaxed limitations on the deck geometry. The maximum deck height is increased by 82% to 155 mm. Steel decking with such a depth is used for slim floor applications rather than being placed on top of the steel beam. However, many manufacturers already provide decking with a height of 80mm. It is considered that deeper decking will be developed if the reduced self weight of the slab is of sufficient economical and ecological benefit. This development is further supported as no limitations on the width of the deck rib are required, which allows the use of deck profiles with very slender ribs.

The number of studs per deck rib that can be taken into account is increased from two to

three. However, tests with CF80 decking showed that an increase of the number of studs does not necessarily increase the total resistance of the shear connection. The more studs are welded per deck rib, the larger the embedment depth becomes that is necessary to avoid local concrete failure. If the embedment depth is too small, rib pry-out failure occurs. Then the shear studs contribute only with one yield hinge.

In [DIN EN 1994-1-1, 2010], the shear stud position is limited to mid- or staggered position according to clause 6.6.5.8 (3). Studs in favourable or unfavourable positions are formally not allowed and no benefit of an increased resistance for studs in a favourable position is made. For further comparisons, studs in favourable position are considered to be within the limitations of [DIN EN 1994-1-1, 2010], because they can be assumed as conservatively predicted. The new model allows studs in mid-, staggered- and favourable positions. Thereby, an increase of the resistance for studs in favourable position is considered by the term $N_{sc}e_L$. This term may also consider a reduced resistance for studs in unfavourable position, but it is strongly recommended not to use studs in unfavourable position. The new model is not well calibrated for this stud position, because of the small number of available test results. Should the resistance of studs in unfavourable position be required, the calibration according to [DIN EN 1990, 2002] led to the following reduced resistances:

- For the bending resistance, $P_{Rd,1}$ according to equation (6.35), a reduction of 75% , based on 11 results.
- For the shear failure of the stud, $P_{Rd,2}$ according to equation (6.36), a reduction by 47%,based on the evaluation of 6 tests.

The concrete compressive strength is limited to 50 N/mm$^2$ in the new model. This is smaller than in [DIN EN 1994-1-1, 2010]. However, the current limitation results from the definition of the concrete tensile strength in [DIN EN 1992-1-1, 2005] and the available test data. For a compressive strength larger than 50 N/mm$^2$, the used equation for $f_{ctm}$ is not valid and the test database, see Appendix C, does not contain tests with high strength concrete to verify the use of the respective equation for $f_{ctm}$ in [DIN EN 1992-1-1, 2005]. Considering the mechanical behaviour and its reflection in the component model, there is no need to restrain the concrete strength, but the model should be evaluated by tests with high strength concrete.

In [DIN EN 1994-1-1, 2010] the tensile strength of the stud is limited to 450 N/mm$^2$, when the studs are placed in the ribs of steel decking, whereas in solid slabs 500 N/mm$^2$ are permitted. Especially for the case of pre-punched deck profiles, a reduction of the tensile strength is not reasonable. The limitation must be the result of the available test data for the calibration. Based on the available data, the tensile strength is limited to 500 N/mm$^2$ in the new model. This gives a uniform definition for studs in solid slabs and studs in the ribs of steel decking. There is no mechanical reason to prohibit higher tensile strengths, but the validity of the new model must then be proven by further tests.

In all, the number of available tests fitting the given limitations of the new increased by 60% compared to [DIN EN 1994-1-1, 2010]. Thereby, the new model gives deck manufacturers a larger range for future developments.

### 6.9.2 Comparison of the design resistances

Finally, the design resistances according to [DIN EN 1994-1-1, 2010] and equations (6.35) and (6.36) are compared to experimental results. Considered are only tests that satisfied the limitations of each model. The results of this comparison are shown in Figure 6.22.

The most important finding of this comparison is that the design resistances according to

[DIN EN 1994-1-1, 2010] are not safe for all tests. This is the case for tests with CF80 and CP60 decking reported in this thesis and [Odenbreit et al., 2015]. In case of the tests with CF80 decking, the embedment depth of the head of the stud was too small in many cases. This lead to the failure of a concrete cone around the shear studs. This type of failure must be avoided according to [DIN EN 1994-1-1, 2010]. Therefore, these tests are not covered by the rules of [DIN EN 1994-1-1, 2010]. However, without knowledge of the measured stud height after welding, the studs might not be identified as too short in practice. In case of tests with CP60 decking, the narrow ribs led to an unfavourable position of the studs according to [Konrad, 2011]. This position cannot be considered as covered by [DIN EN 1994-1-1, 2010], but the current limitations do not exclude these tests.

The new design resistances according to equations (6.35) and (6.36) are safe for all tests. In addition, the new model shows significantly improved coefficients of variation and correlation.

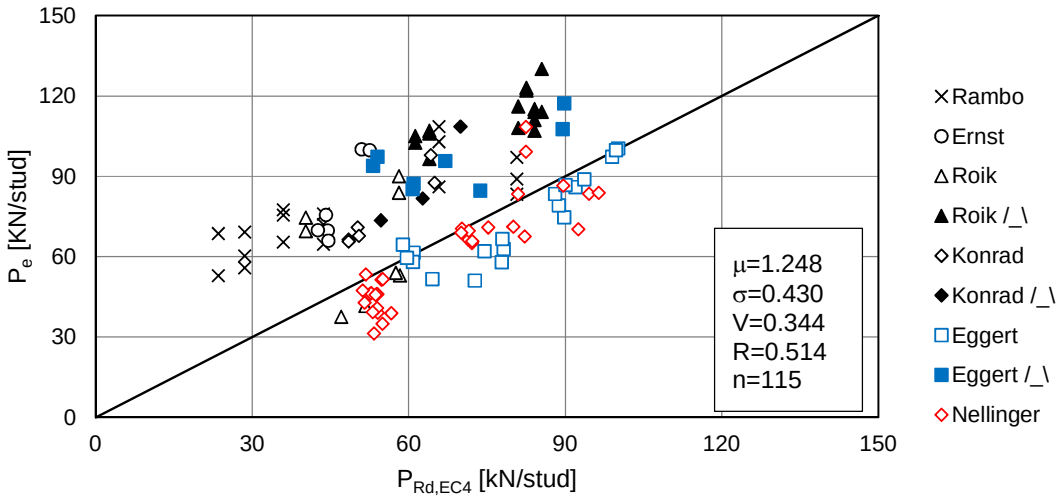


(a) Design resistance according to [DIN EN 1994-1-1, 2010].

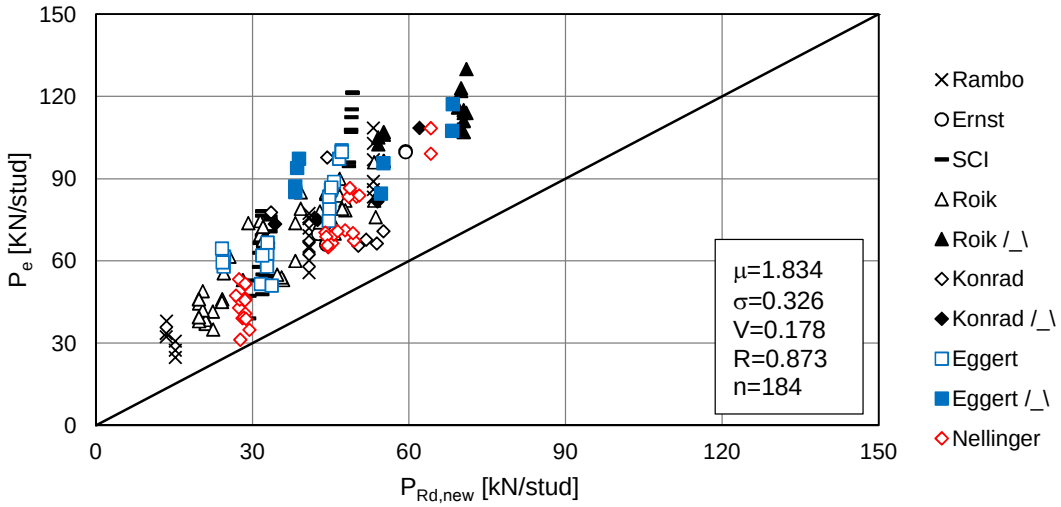


(b) Design resistance according to equations (6.35) and (6.36).

Figure 6.22: Comparison of experimental resistance, $P_e$, to design resistance, $P_{Rd}$.

The downside of introducing the safe resistances according to equations (6.35) and (6.36)

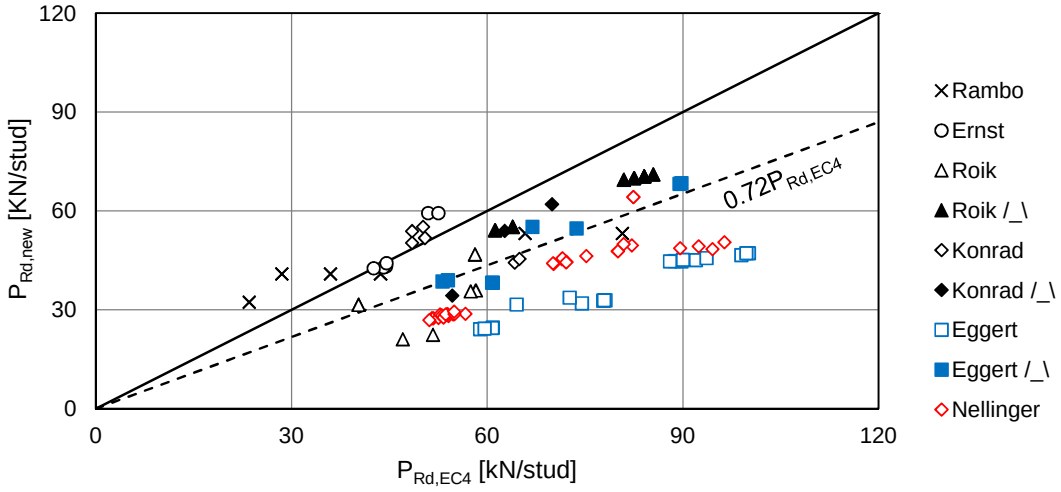


Figure 6.23: Comparison of the design resistance according to equations (6.35) and (6.36) to [DIN EN 1994-1-1, 2010] in the common field of application.

is that lower resistances are obtained. Figure 6.23 shows a comparison of the new design resistances, $P_{Rd,new}$, to the design resistances of [DIN EN 1994-1-1, 2010], $P_{Rd,EC4}$, for the common field of application. It is shown, that for the majority of tests a smaller resistance is obtained with the new model. In average the new resistances are about 30% smaller than in [DIN EN 1994-1-1, 2010]. However, this is a consequence of the fact that [DIN EN 1994-1-1, 2010] is unsafe for some tests, while they are safely predicted with the new model.

### 6.9.3 Concluding remarks

It can be concluded that the newly developed model shows an improved correlation with push-out test results compared to [DIN EN 1994-1-1, 2010], but the result of a 'safe' prediction of the shear resistance is a lower resistance.

The new resistances according to equations (6.35) and (6.36) may appear more complex than the $k_t$-formulae of [DIN EN 1994-1-1, 2010], but they are based on simple mechanical considerations of the shear connector behaviour. This is beneficial for future extensions and improvements of the model, because the mechanical assumptions can be modified according to new applications. Examples where the model can be extended are the consideration of the welding procedure or reinforced concrete ribs. The complexity of equation (6.35) is further increased by the additional consideration of beneficial influences, like welding studs in the favourable position and transverse loading. In addition, the model has a significantly wider field of application that allows a much larger range of shapes for the steel decking.

Furthermore, the new model allows a certain classification of the expected load-slip behaviour. For cases where equation (6.35) is decisive with $n_y = 2$, double curvature of the stud and a load bearing behaviour as observed in tests with CP60 decking may be assumed. Cases with $n_y = 1$ lead to a behaviour with single curvature of the stud as observed in tests with CF80 decking. The shear resistance according to equation (6.36) results in a load-slip behaviour as observed in tests with RD80 decking, which was similar to CF80, but allowed the development of plasticity in the stud before the peak load was reached. This information is helpful for identifying the need of applying transverse loads to push-out tests.

# 7 Conducted composite beam tests

## 7.1 Test set-up, test programme and material properties

Two composite beam tests were conducted using CF80 decking and configurations of the shear connection system known from the push-out tests. The objectives of the beam tests were:

- To compare the load-slip behaviour of the shear connectors in push-out tests and beam tests
- To investigate the load-displacement behaviour of beams with low degrees of shear connection
- To gather the information for the verification of later FE-Models

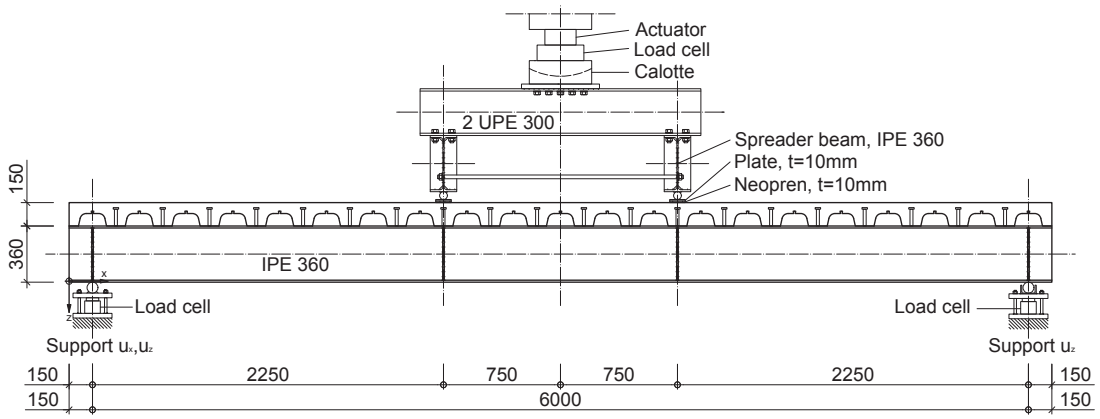


Figure 7.1: Test set-up of 6m span composite beam tests.

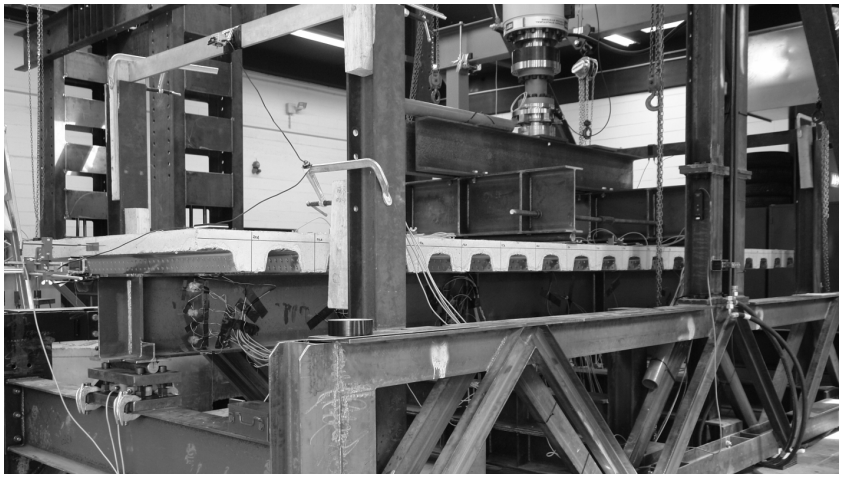

Figure 7.2: Specimen 2-10 at the beginning of the test.

Both tests were conducted as 4-point bending tests, as shown in Figures 7.1and 7.2. The span of the beams was 6m and the steel section was an IPE 360. The composite slab had a width of 1.50m and a thickness of 150mm. As in the push-out specimens, a Q188 A reinforcement mesh was placed 30 mm above the top of the deck rib. The same concrete as for the push-out tests was used. Both beam tests used headed studs of 19 mm diameter and 125 mm nominal length that were welded through the decking. The tests differed only in the number of shear studs per deck rib. Specimen 2-09 used single studs per deck rib, as the push-tests in series NR1, and specimen 2-10 used pairs of studs per deck rib, as for example the push-tests in series 1-10.

Table 7.1: Parameters of composite beam tests.

| | Steel profile | | | Composite slab | | | Shear connectors | | | |
|---|---|---|---|---|---|---|---|---|---|---|
| Test | Section | $f_y$ [N/mm$^2$] | Decking | $h_c$ [mm] | $b$ [m] | $f_c$ [N/mm$^2$] | $\varnothing$ [mm] | $h_{sc,nom}$ [mm] | $f_u$ [N/mm$^2$] | $n_r$ |
| 2-09 | IPE 360 | 382 | CF80 | 150 | 1.50 | 48.62 | 19 | 125 | 550 | 1 |
| 2-10 | IPE 360 | 382 | CF80 | 150 | 1.50 | 49.02 | 19 | 125 | 550 | 2 |

In addition to the force applied by the actuator, the support reactions were measured, as shown in Figure 7.1. Furthermore, extensive displacement and strain measurements were taken, as shown in Figures 7.3 and 7.4. The deflection of the beam was measured at the positions D-D-1 to D-D-7. The concrete strain was measured at two cross sections with displacement sensors, E-W-10 to E-W-24, to obtain information on the distribution of stresses across the width of the slab. The longitudinal strain in the flanges of the steel section was measured at seven sections, S-SD-10 to S-SD-71. This extensive strain measurement allows the evaluation of the internal forces and moments of the steel section.

From those results, various conclusions on the introduced shear forces can be drawn. This allows to compare the shear resistance per stud at ultimate load to the push-out test results. Additionally, the strains in the web were measured at 0° (longitudinal) , 45° and 90° (vertical) with strain gauges, R-L-10 to R-L-72. The purpose was to evaluate the direction of principle strains close to the supports and loading points. The slip was measured at 13 positions, D-S-1 to D-S-13. However, the measurements D-S-2 to D-S-12 were taken between the decking and the flange of the beam and did not show accurate results because of the through deck welded studs. Therefore, only the measured end-slips are assumed to be accurate.

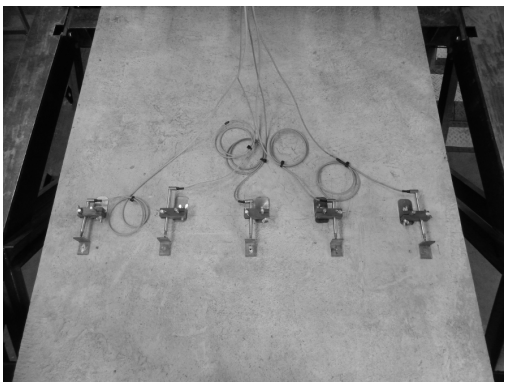

(a) Measurement of concrete strains.

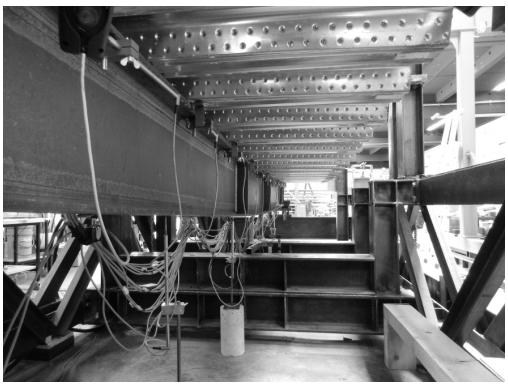

(b) Deflection and slip measurements.

Figure 7.3: Measurement of slip, deflection and concrete strain.

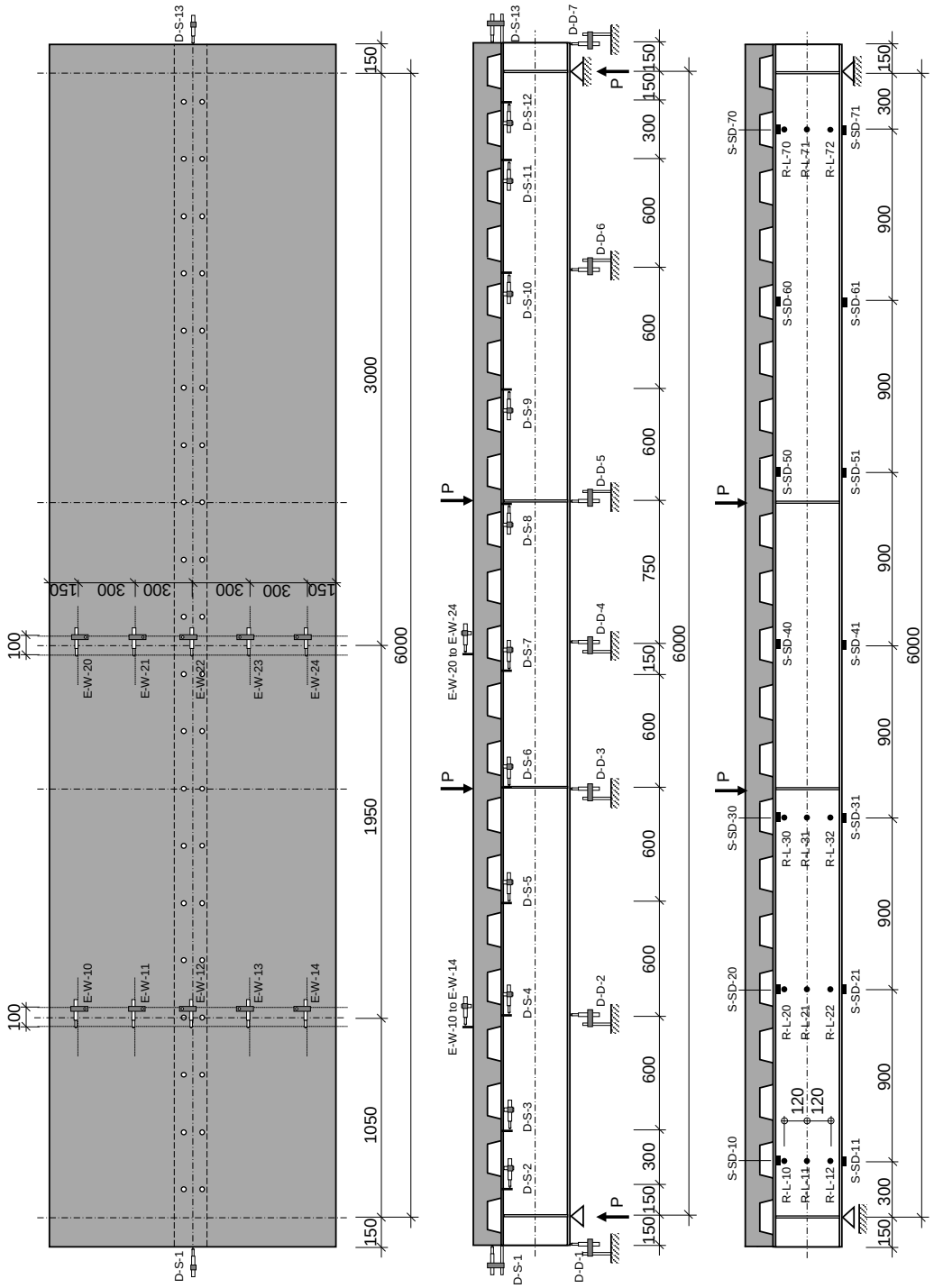


Figure 7.4: Measurement set-up of composite beam tests.

## 7.2 Prediction of bending resistance and stiffness

In the following section, the plastic load bearing capacity of the test specimens is predicted. Besides the specimen dimensions and material properties, the shear connector resistance is of major influence. To verify the new equations for the shear stud resistance, the bending resistance of the beams is predicted assuming the average shear resistance of the studs according to [DIN EN 1994-1-1, 2010] and the newly developed formulae. The stud resistances are calculated assuming measured material properties. Thereby, the correction factor $b$ is not considered in the evaluation of equation (6.32), as it can be seen in Figure 6.20 that the equation was satisfactory for the push-out tests presented in chapter 4.

[DIN EN 1994-1-1, 2010] allows two methods to calculate the plastic bending resistance of a composite beam with partial shear connection:

1. A plastic stress distribution is assumed, based on the shear force that the studs can transfer. This is the accurate method.
2. The bending resistance is linearly interpolated between the plastic resistance of the steel section, $\eta = 0$, and the plastic bending resistance of the composite beam for full shear connection, $\eta = 1$. This is a conservative approximation.

Thus, the bending resistance of the beams is predicted for four cases, as summarised in Table 7.2.

Table 7.2: Predicted bending resistance using measured material properties and average stud resistances according to [DIN EN 1994-1-1, 2010] and the new model.

| Test | | | [DIN EN 1994-1-1, 2010] Interpolation $0 \leq \eta \leq 1$ | [DIN EN 1994-1-1, 2010] Plastic stresses | New model Interpolation $0 \leq \eta \leq 1$ | New model Plastic stresses |
|---|---|---|---|---|---|---|
| 2-09 | $P_{Rm}$ | [kN/stud] | 88.9 | 88.9 | 67.5 | 67.5 |
| | $n$ | [-] | 7 | 7 | 7 | 7 |
| | $N_c$ | [kN] | 622.3 | 622.3 | 472.5 | 472.5 |
| | $N_{pl}$ | [kN] | 2777.1 | 2777.1 | 2777.1 | 2777.1 |
| | $\eta$ | [-] | 0.224 | 0.224 | 0.170 | 0.170 |
| | $\min \eta$ | [-] | 0.47 | 0.47 | 0.47 | 0.47 |
| | $M_{pl,Rm}$ | [kNm] | 493.5 | 560.2 | 468.4 | 525.5 |
| 2-10 | $P_{Rm}$ | [kN/stud] | 62.8 | 62.8 | 42.7 | 42.7 |
| | $n$ | [-] | 14 | 14 | 14 | 14 |
| | $N_c$ | [kN] | 879.2 | 879.2 | 597.8 | 597.8 |
| | $N_{pl}$ | [kN] | 2777.1 | 2777.1 | 2777.1 | 2777.1 |
| | $\eta$ | [-] | 0.317 | 0.317 | 0.215 | 0.215 |
| | $\min \eta$ | [-] | 0.47 | 0.47 | 0.47 | 0.47 |
| | $M_{pl,Rm}$ | [kNm] | 536.5 | 610.3 | 489.4 | 554.8 |

For test specimen 2-09 with single studs per deck rib, [DIN EN 1994-1-1, 2010] predicts an average shear resistance of 89kN per stud. This leads to a degree of shear connection of 22%, which is smaller than the required minimum degree of shear connection of 47%. The bending resistance obtained from the plastic stress distribution is 561kNm and for the simplified interpolation of the resistance, it is 496kNm.

The new formulae for the stud resistance results in a shear resistance of 68kN per stud. This is 79% of the prediction according to [DIN EN 1994-1-1, 2010]. For the degree of shear connection of only 17%, a bending resistance of 526kNm is obtained from the plastic

stress distribution, which is 94% of the case with the stud resistance assumed according to [DIN EN 1994-1-1, 2010]. For the interpolated resistance, 95% of the prediction according to [DIN EN 1994-1-1, 2010] is reached with 470kNm.

For specimen 2-10, an average shear stud resistance of 63kN per stud is predicted according to [DIN EN 1994-1-1, 2010]. This leads to a degree of shear connection of 32%, which is 42% higher than for specimen 2-09. The bending resistance according to the plastic stress distributions is 611kNm. The bending resistance obtained by interpolation is 540kNm. Thus, [DIN EN 1994-1-1, 2010] predicts a 9% higher bending resistance of the composite beam when pairs of studs per deck rib are used.

The new model for the stud shear resistance leads to an average resistance per shear stud of 43kN, which is 68% of the stud resistance according to [DIN EN 1994-1-1, 2010]. The bending resistance calculated from the plastic stress distribution is 555kNm and using interpolation it is 492kNm. These are about 91% of the prediction according to [DIN EN 1994-1-1, 2010]. With the stud resistance according to the new formulae, the increase of the bending resistance for pairs of studs compared to single studs per deck rib is only 4% to 6%.

The elastic bending stiffness and slip are predicted according to [Leskela et al., 2015]. The Young's Modulus of the steel section is taken as 210 GPa and for the concrete it is calculated according to [DIN EN 1992-1-1, 2005]. For the determination of the stiffness, the stiffeners on top of the steel decking are ignored, because it can be assumed that they do not significantly reduce the stiffness. The stiffness of the shear connectors is determined from push-out tests. Because the self weight of the slab is relatively small, the results of tests without transverse loading are considered. Accordingly, specimen 1-10-3 is considered for pairs of studs and specimen NR1-1 for single studs per deck rib. To determine the stiffness of the shear connectors, the secant-modulus through the points at 10% and 80% of the shear resistance are considered, as shown in Figure 7.5, which corresponds to the normal application range.

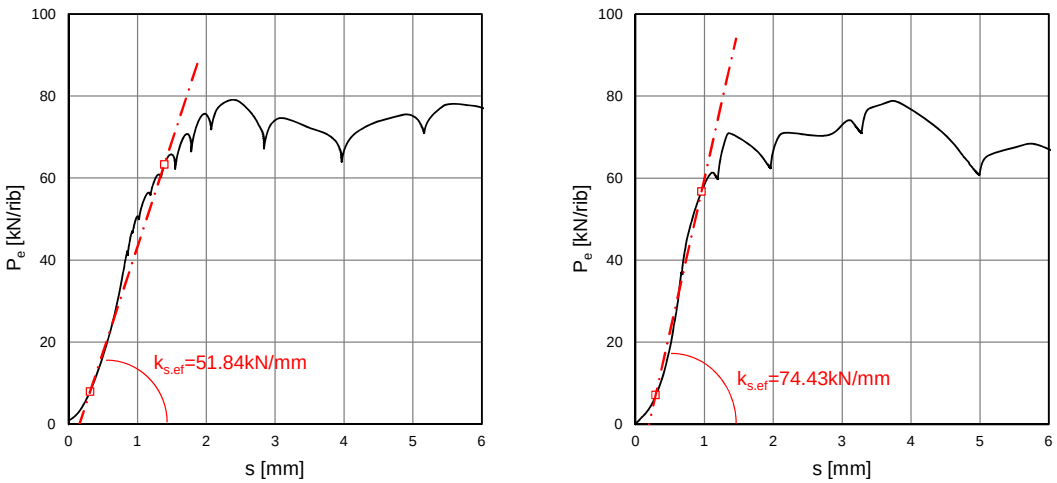


(a) Stiffness for single studs per deck rib from push-out specimen NR1-1.

(b) Stiffness for pairs of studs per deck rib from push-out specimen 1-10-3.

Figure 7.5: Assumed stiffness of shear connectors to predict the elastic behaviour of composite beam specimens.

It can be seen that the use of pairs of studs increases the stiffness of the shear connection only by about 45%. The predictions of the composite beams bending stiffness are summarised in

Table 7.3. The consideration of a flexible shear connection reduces the bending stiffness by about 39% to 45% compared to the stiffness for a rigid shear connection. The bending stiffness of the composite beam with pairs of studs benefits only by 12% from the higher shear connector stiffness.

Table 7.3: Predicted stiffness and deformation according to [Leskela et al., 2015] at 70% of the assumed ultimate load.

| Beam | $\alpha_i$ [-] | $EI_{i,0}$[a] [MNm$^2$] | $K_{sc.d}$ [MN/m$^2$] | $r_\delta$ [-] | $\alpha_{i.eff}$ [-] | $EI_{i,0,eff}$[b] [MNm$^2$] |
|---|---|---|---|---|---|---|
| 2-09 | 2.63 | 126.65 | 171.1 | 0.24 | 1.00 | 69.78 |
| 2-10 | 2.63 | 126.65 | 248.1 | 0.31 | 1.24 | 78.13 |

[a] Assuming rigid shear connection
[b] Assuming flexible shear connection

## 7.3 Test results

For both specimens, the record of measurement data started after the assembly of the test set-up. This means that the self weight is not covered by the measured data. The self weight of the composite beams is about 4.9 kN/m. Accordingly, the bending moment at the loading points because of self weight is 20.6 kNm. The loading rig had a self-weigth of 4 kN in total. Accordingly, a point load of 2kN contributes to the tests bending moment. Figure 7.6 illustrates the assumed distribution of the bending moments for each load case.

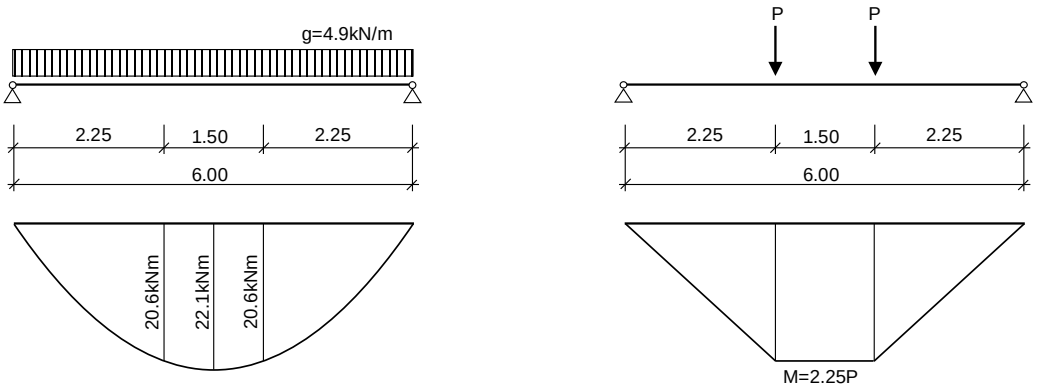


(a) Moment distribution due to self weight.

(b) Moment distribution due to point loads.

Figure 7.6: Assumed distribution of bending moments because of self weight and point loads.

### 7.3.1 Specimen 2-09

Figure 7.7 shows the applied load plotted versus the deflection at mid span. The specimen reached its ultimate load at 212.5kN at a deflection of 54.8mm. Accordingly, the bending resistance of the specimen was 503.3kNm.

$$M_{Test} = (212.5 + 2 + 4.9 \cdot \frac{6.00}{2}) \cdot 2.25 - 4.9 \cdot \frac{2.25^2}{2} = 503.3 \text{ kNm}$$

Independently of how the shear stud resistance was determined, the test did not reach the bending resistance predicted from the plastic stress distribution. The calculation of the deflection using the bending stiffness according to [Leskela et al., 2015] gives accurate results up to about 70% of ultimate load.

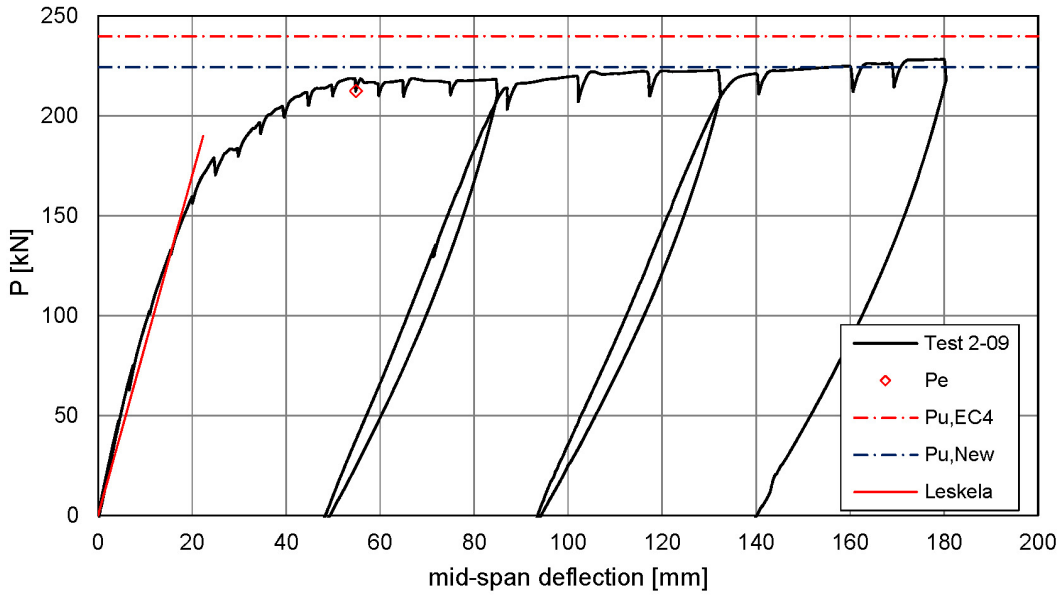


Figure 7.7: Applied point load, $P$, versus mid span deflection for specimen 2-09 (self-weight not included).

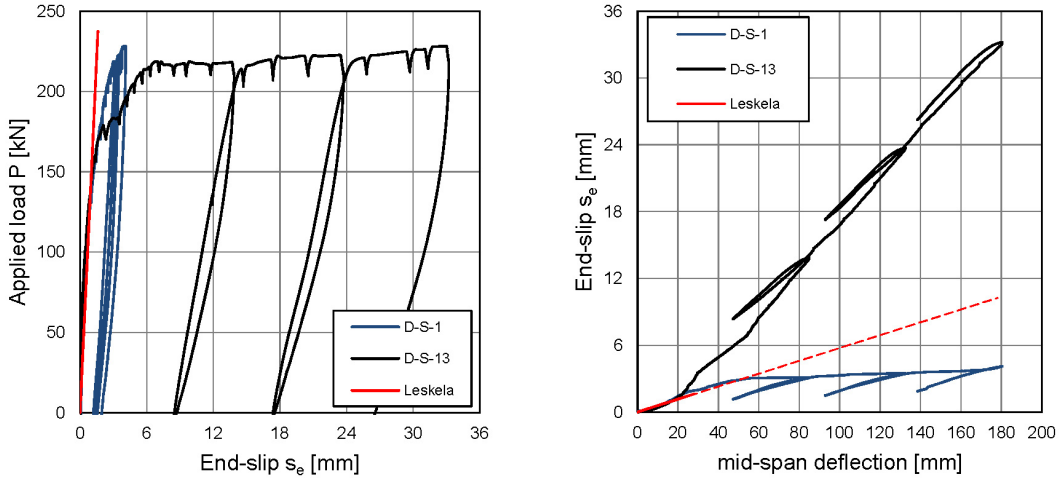


(a) Applied load versus end-slip.

(b) End-slip versus mid-span deflection.

Figure 7.8: Dependencies of applied point load, $P$ and deflection to end-slip.

Figure 7.8 shows the measured end-slips in comparison to the applied load and the mid-span deflection. It can be seen that the predicted end-slip according to [Leskela et al., 2015] corresponds well with the measurements up to about 70% of ultimate load. The end-slip

was symmetrical up to a deflection of about 23mm. This corresponds to the point of the load deflection curve, shown in Figure 7.7, where the first significant non-linear displacement occurred. After that, the end-slip almost completely was shifted to one side of the beam. This indicates that at about 23 mm deflection an asymmetric failure must have occurred in the shear interface. The end-slips at ultimate load are 3.0mm and 7.1mm. For higher loading stages, the asymmetric behaviour can be also found in the measured deflection of the specimen, shown in Figure 7.9.

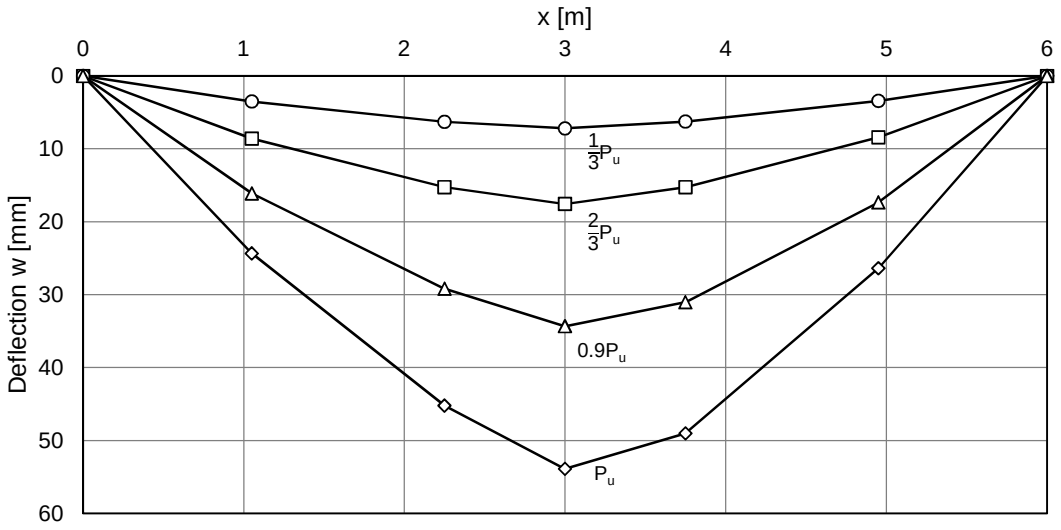


Figure 7.9: Deflection of specimen 2-09 for selected load stages.

The evaluation of measured strains confirms the asymmetric failure of the shear interface. The strains were evaluated using the assumptions shown in Figure 7.10. Between the measured strains in top and bottom flange of the steel section, a linear strain distribution was assumed. Considering a typical simplified stress-strain relation the stress distribution was obtained. The integration of stresses then lead to the axial force and bending moment of the steel section. The axial force is equal to the introduced shear force.

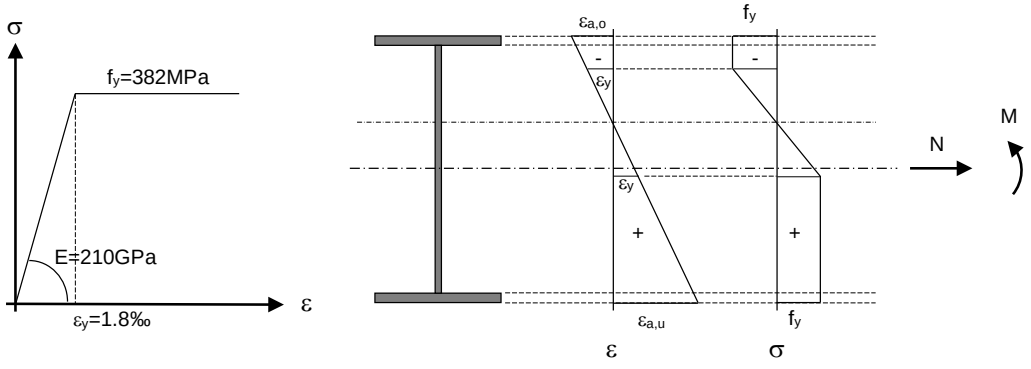


Figure 7.10: Assumptions for the evaluation of strain measurements.

Figure 7.11 shows the obtained shear forces in the measuring points for selected loading stages. It can be seen that up to about 70% of the test load the shear forces were distributed symmetrical. This corresponds to the elastic part of the load-displacement plot.

Furthermore, it is shown that at about 90% of ultimate load, the shear connectors between $x = 4.80$m and $x = 5.70$m must have failed. During testing, lifting of the rib at $x = 4.95$m was observed at a deflection of around 25 to 30mm. When the concrete was removed, a poor quality of the welding was identified for this stud, see Figure 7.12. The same failure was identified for the stud at $x = 5.55$m. For the stud at the end of the beam and below or directly besides the loading points, double curvature of the stud was observed. At the loading points, the large local transverse compression allowed the development of two yield hinges in the stud. This leads to the conclusion that also the stud at the end of the beam must have been subjected to transverse compression forces. The wavelike displacement of the concrete slab, see Figure 7.13, supports this assumption. For the remaining studs between loading point and end of the beam, rib pry-out failure with single curvature of the studs was identified.

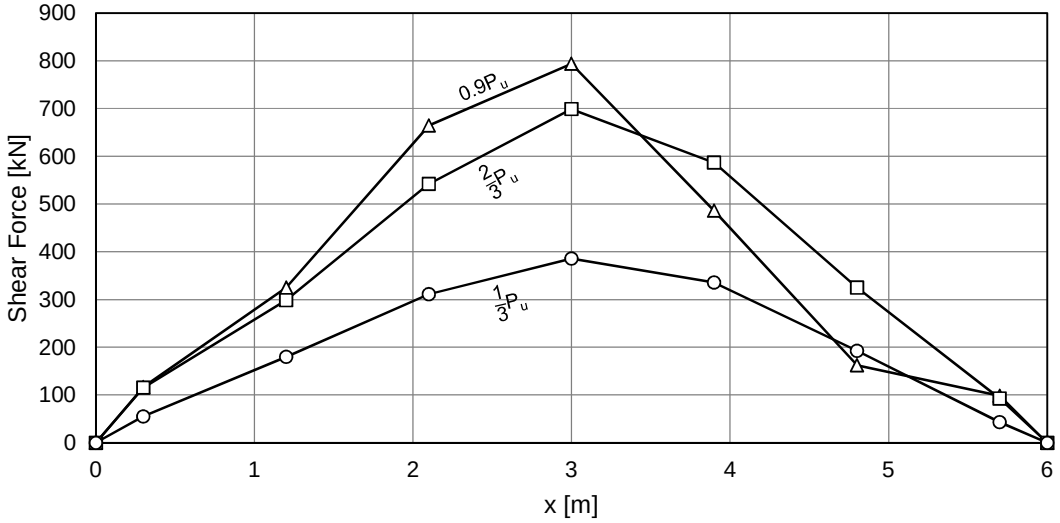


Figure 7.11: Introduced shear forces along the span of the beam for selected load stages.

Evaluating the shear forces between each section, where strain measurements were taken, the average force per stud in each interval was obtained. Figure 7.14 shows these forces plotted against the end-slips of the beam. It can be observed that the studs at the end of the beam, $P_{s,10}$ and $P_{s,70}$, reached a shear force of about 105kN to 120kN at end-slips of about 1.5mm. The shear connectors in front of the loading points, $P_{s,30-20}$ and $P_{s,50-60}$, also reached about 120kN at end-slips of 2.5mm to 3mm. Between the loading points, $P_{s,40-30}$ and $P_{s,40-50}$, smaller shear forces were transferred because of the small slip at mid-span. However, on the weak side of the shear interface up to 115kN were reached at an end-slip of about 4.3mm. All these studs had a significantly larger shear resistance than observed in the corresponding push-out specimen NR1-1. Considering the deformation of the concrete slab, as shown in Figure 7.13, these studs are assumed to be subjected to significant transverse compression. The remaining studs, which were 0.45m to 1.05m away from the supports, reached a shear force of about 80kN. This corresponds well with the accompanying push-out test. As shown in Figure 7.13, a lift of the concrete slab in this region of the beam occurred. Accordingly, the studs welded there did not benefit from transverse compression. They may even have suffered from transverse tension, which could have caused the weld failure of two studs. Considering the studs on the weak side of the beam, $P_{s,60-70}$, it can be seen that the first stud must have failed at an end-slip of about 2.1mm. The second stud must have failed at an end-slip of about 3.2mm.

(a) Concrete failure and deformed stud.

(b) Weld porosity of the stud.

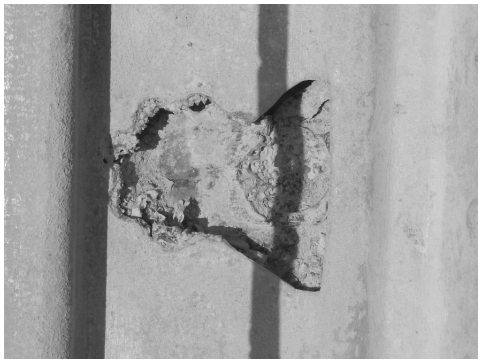

(c) Failure surface on the beam.

Figure 7.12: Weld failure of stud at $x = 4.95$m.

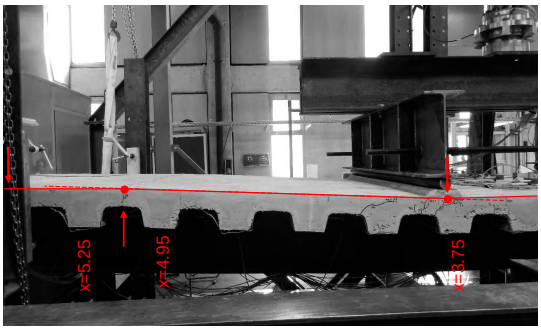


(a) Wavelike deformation of the concrete slab.

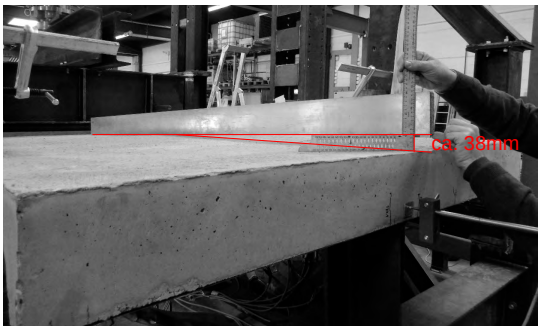


(b) Local rotation in slab.

Figure 7.13: Local deformation of concrete slab.

The re-assessment of the beams bending resistance shows a significantly improved accordance to the test, when two studs are assumed to have failed at ultimate load, as shown in Table 7.4. Shown are the results that were obtained from the analysis of the plastic stress distribution. Using the stud resistance according to [Roik et al., 1989, DIN EN 1994-1-1, 2010], which was 89kN, the static resistance of the beam is still over-estimated by 3%. If the shear stud resistance according to Chapter 6, which was 67.5kN, is applied, then the bending resistance of the beam is predicted by 2.5% on the safe side.

The results of this beam test showed, that the behaviour of composite beams at serviceability limit sate corresponds well with the equations by [Leskela et al., 2015]. The asymmetric failure of the shear interface made it difficult to draw conclusions on the resistance of the shear connectors. In addition, the deformation of the concrete slab itself lead to effects

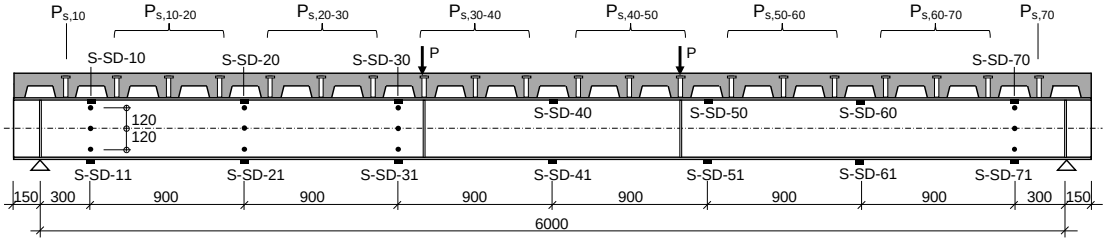


(a) Position of studs.

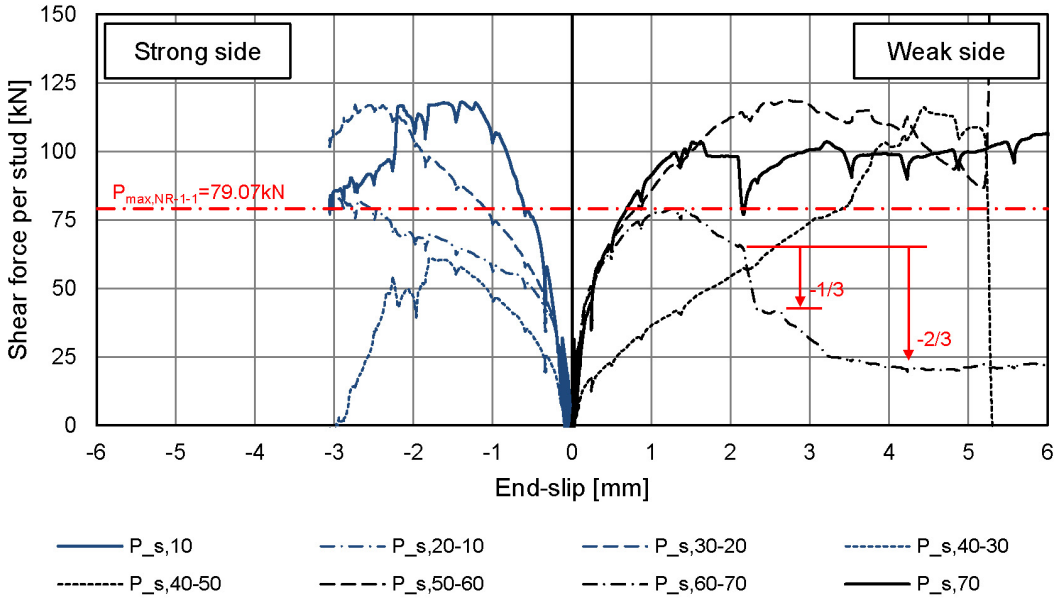


(b) Load-slip curves.

Figure 7.14: Shear forces per stud versus end-slip in beam test 2-09.

Table 7.4: Comparison of test resistance to theoretical resistance calculated from plastic stress distributions, assuming $n = 7$ or $n = 5$ studs in the shear length.

| Studs according to | | | $n = 7$ | $n = 5$ |
|---|---|---|---|---|
| [DIN EN 1994-1-1, 2010] | $\eta$ | [-] | 0.224 | 0.160 |
| | $M_{Pl,Rm}$ | [kNm] | 560.2 | 518.6 |
| | $M_{Test}$ | [kNm] | 503.3 | 503.3 |
| | $M_{Test}/M_{Pl,Rm}$ | [-] | 0.898 | 0.970 |
| New model | $\eta$ | [-] | 0.170 | 0.121 |
| | $M_{Pl,Rm}$ | [kNm] | 525.5 | 490.8 |
| | $M_{Test}$ | [kNm] | 503.3 | 503.3 |
| | $M_{Test}/M_{Pl,Rm}$ | [-] | 0.958 | 1.025 |

of transverse loading that locally influence the shear connector resistance. However, the analysis of the bending resistance of the beam showed good accordance to the test result using the stud resistance according to Chapter 6.

The ultimate load was reached at a deflection of around span/100 with end-slips of 3mm and 7mm. It can be assumed that for a symmetric behaviour of the shear interface, the end-slip

would have been between these two values. This leads to the conclusion, that the specimen could have develop its plastic bending capacity without exceeding a limiting slip of 6mm, even though the degree of shear connection was very small. Considering the preliminary failure of the studs, the degree of shear connection was only 12% assuming the stud shear resistance according to equation (6.29) and 16% according to [DIN EN 1994-1-1, 2010].

### 7.3.2 Specimen 2-10

Specimen 2-10 did show a symmetrical behaviour up to a deflection of about 130mm. The beam reached its static ultimate load of 233.4kN at a deflection of 68.8mm, as shown in Figure 7.15. The corresponding test moment was 550.3 kNm.

$$M_{Test} = (233.4 + 2 + 4.9 \cdot \frac{6.00}{2}) \cdot 2.25 - 4.9 \cdot \frac{2.25^2}{2} = 550.3\text{kNm}$$

The analysis of the plastic bending resistance for the stud shear resistance according to equation (6.29) predicted a plastic bending resistance of 554.8kNm. This is an over-estimation of only 0.8%. Assuming the stud resistance according to [DIN EN 1994-1-1, 2010] over-predicts the bending resistance by 9.8%. The elastic part of the load deflection curve, shown in Figure 7.15, can be accurately analysed by application of the bending stiffness according to [Leskela et al., 2015].

Table 7.5: Comparison of test resistance to theoretical resistance calculated from plastic stress distributions.

| Studs according to | | | $n = 14$ |
|---|---|---|---|
| [DIN EN 1994-1-1, 2010] | $\eta$ | [-] | 0.317 |
| | $M_{Pl,Rm}$ | [kNm] | 610.3 |
| | $M_{Test}$ | [kNm] | 550.3 |
| | $M_{Test}/M_{Pl,Rm}$ | [-] | 0.902 |
| New model | $\eta$ | [-] | 0.215 |
| | $M_{Pl,Rm}$ | [kNm] | 554.8 |
| | $M_{Test}$ | [kNm] | 550.3 |
| | $M_{Test}/M_{Pl,Rm}$ | [-] | 0.992 |

At a point load of about 205 kN was applied, the elastic behaviour abruptly ended and the deflection increased by about 10mm. At the same time the end-slips increased by about 1.3mm, as shown in Figure 7.16. It was assumed that rib pry-out failure had occurred, which was confirmed during the later removal of the concrete slab. Rib pry-out must have shown a significant drop in the shear resistance, as observed in push-out test 3-01-3. The predicted end-slip according to [Leskela et al., 2015] was quite conservative up to this point. At ultimate load the end-slips were 6.4mm and 6.6mm.

The deflection of the beam, shown in Figure 7.17, and introduced shear force, shown in Figure 7.18, were almost symmetrical. From the shear forces, it can bee seen that the shear interface weakened between the supports and loading points at higher loading stages. This shows that the shear resistance of the studs must have decreased at some point, because of rib pry-out failure of the shear connectors.

As can be seen in Figure 7.19, the concrete slab itself showed a wavelike deformation. Accordingly, it can be assumed that the shear connectors at the end of the beam and close

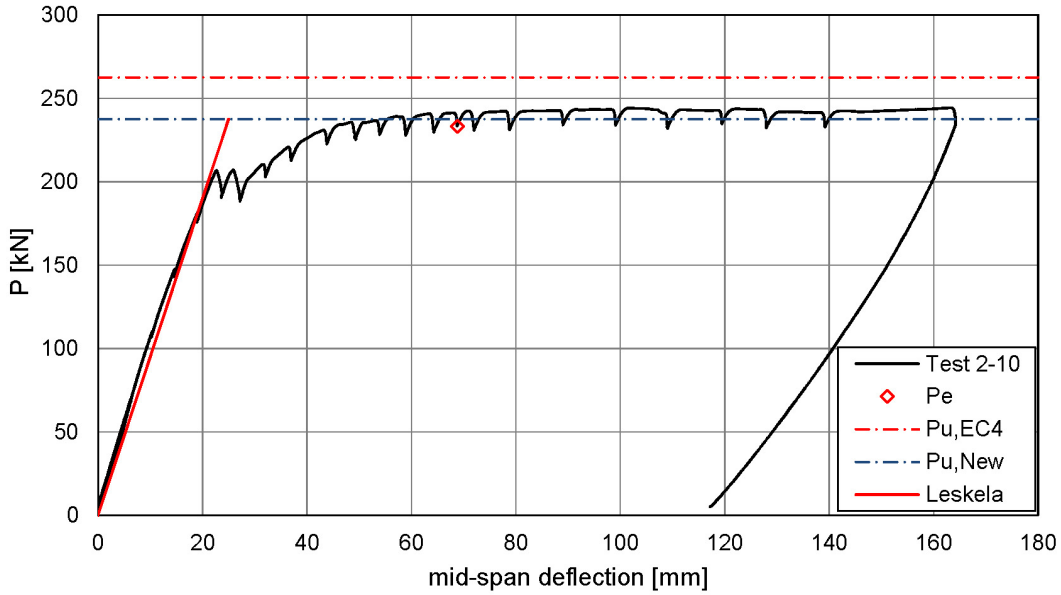


Figure 7.15: Applied point load, $P$, versus mid span deflection for specimen 2-10 (self-weight not included).

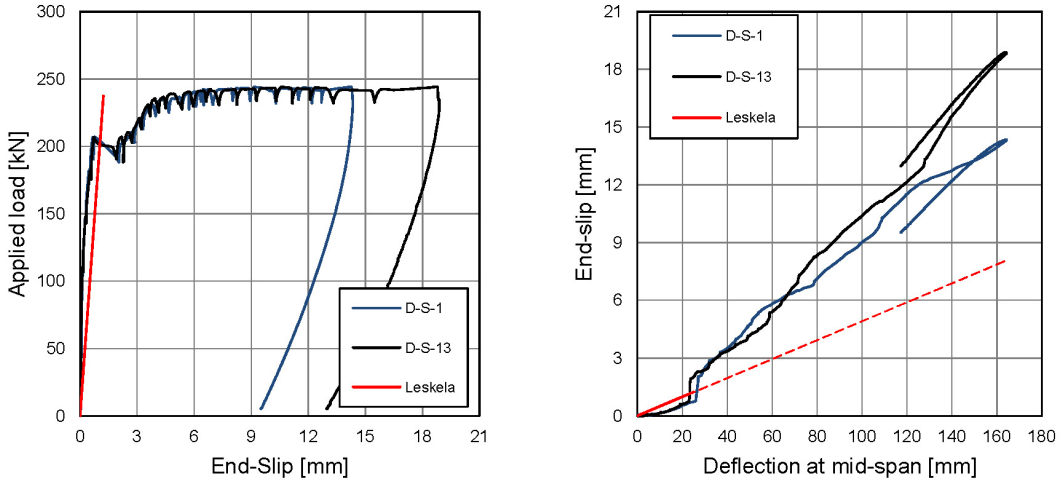


(a) Applied load versus end-slip.

(b) End-slip versus mid-span deflection.

Figure 7.16: Dependencies of applied load and deflection to end-slip.

to the loading points were influenced by transverse compression forces, which resulted from the deformation of the beam. Therefore, the load-slip behaviour of the studs was evaluated in the regions of the beam, where a lift of the slab was observed, as highlighted in Figure 7.19. In these regions, the deformation of the concrete slab is similar to push-out tests. The shear forces per stud are plotted against the end-slip in Figure 7.20.

It can be seen that rib pry-out failure occurred at a shear force of about 75kN per stud. This value is exceptionally high and was previously not observed in push-out test. Afterwards the

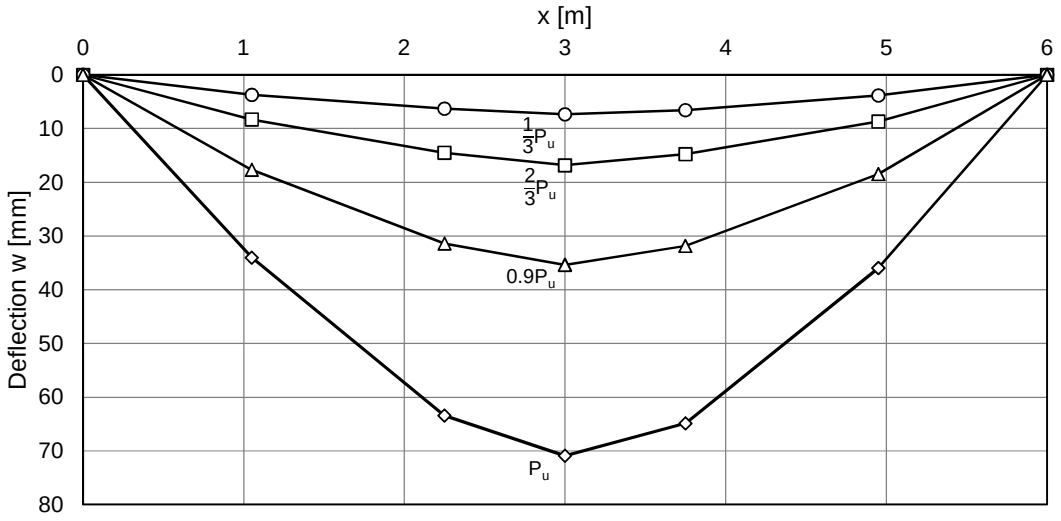


Figure 7.17: Deflection of specimen 2-10 for selected load stages.

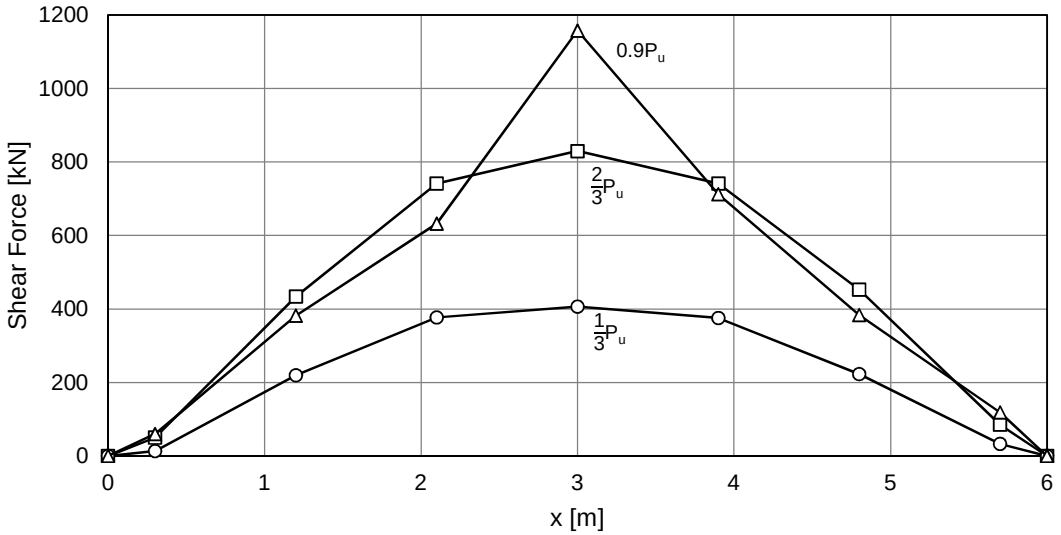


Figure 7.18: Introduced shear forces along the span of the beam for selected load stages.

shear force dropped to about 40kN to 50 kN per stud. This is larger than the shear resistance of push-out specimen 1-10-3 without transverse loading. However, the behaviour of push-out specimen 1-10-2 with about 8% transverse load matches well the post-failure resistance of the studs in beam 2-10. In addition, equation (6.29) gives a good estimation of the shear forces in the considered part of the shear interface.

It can be concluded that the equations for the shear stud resistance developed in Chapter 6 accurately predicted the resistance of the studs in beam test 2-10. Accordingly, the analysis of the plastic bending resistance matches well the test result. The bending resistance was reached at an end slip of only 6.6mm, even though the degree of shear connection was only 22%. The elastic behaviour of the beam can be accurately analysed using the equations in [Leskela et al., 2015].

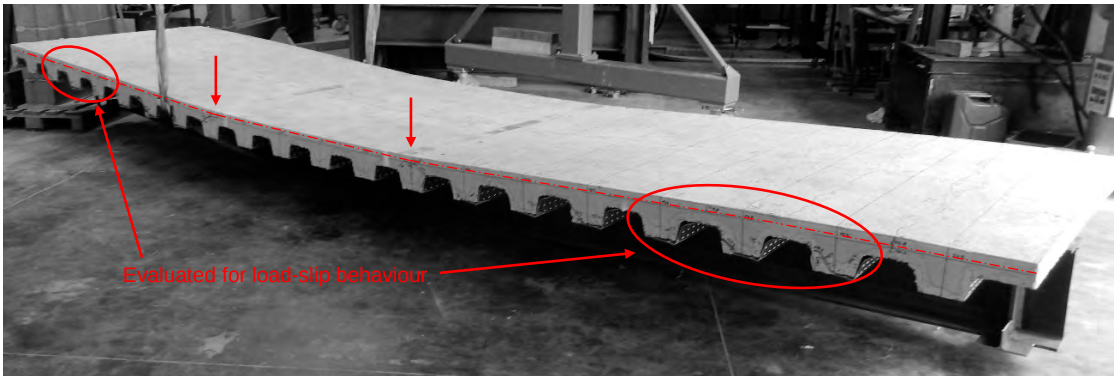


Figure 7.19: Deformation of specimen 2-10 after testing.

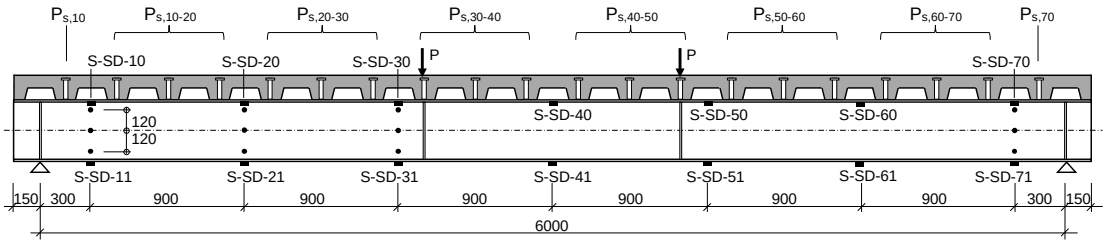


(a) Position of studs.

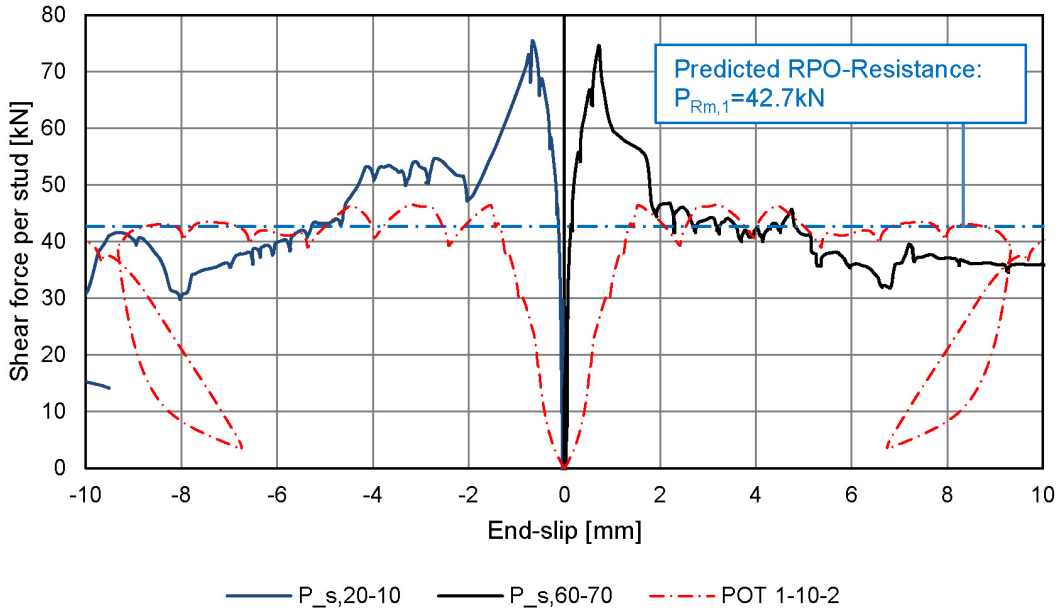


(b) Load-slip curves.

Figure 7.20: Shear forces per stud versus end-slip in beam test 2-10.

## 7.4 Concluding remarks

Table 7.6 summarises the results of the conducted beam tests. The two tests showed that the shear stud resistance according to Chapter 6 results in reasonable accurate predictions of the shear force in the beam. The analytical bending resistance obtained with these shear

forces matched the test results with an accuracy of $\pm$3%.

The test specimens reached their ultimate load at a deflection of about L/87 to L/109 . In practice, this means that the beams may be designed for serviceability limit state, rather than for ultimate limit state. The beams remained elastic up to 83% to 88% of their ultimate load. The corresponding defection was about L/230 to L/240. The behaviour of the beams at serviceability limit state can be accurately analysed according to [Leskela et al., 2015].

Both specimens had very low degrees of shear connection. For specimen 2-09, it was only 12% for a shear connector resistance of 67.5kN determined according to Chapter 6. For specimen 2-10, the degree of shear connection was 22%, assuming a resistance of 42.7kN per shear connector, determined according to 6. The end-slips at ultimate load were 7.1mm and 6.6mm. This means that the limiting slip of 6mm was exceeded by less than 20%, even though the required minimum degree of shear connection was much higher at 47%. Assuming that the plastic stress distribution in the cross-section cannot be reached with finite strains, the end-slip may be assessed at a smaller load stage. At 95% of the plastic bending resistance, the end-slips were only 4.2mm and 4.7mm. This satisfies the limiting slip of [DIN EN 1994-1-1, 2010].

Table 7.6: Test results at ultimate load and at 95% of the calculated plastic bending resistance.

| Test | $\eta$ [-] | $M$ [kNm] | $M/M_{pl}$ [-] | $L/w_m$ [-] | $s_e$ [mm] | $\epsilon_m/\epsilon_y$ [-] |
|---|---|---|---|---|---|---|
| 2-09 | 0.12 | 503.3=$M_{Test}$ | 1.025 | 109 | 7.1 | 1.6 |
| | | 466.3=$0.95M_{pl}$ | 0.95 | 158 | 4.7 | 1.3 |
| 2-10 | 0.22 | 550.3=$M_{Test}$ | 0.992 | 87 | 6.6 | 1.8 |
| | | 527.1=$0.95M_{pl}$ | 0.95 | 130 | 4.2 | 1.7 |

$P$: Static test load — $M$: Applied test moment (static value)

$M_{pl}$: Plastic bending resistance — $L$: Span of beam $L = 6.00$m

$w_m$: Mid-span deflection — $s_e$: Maximum end-slip

$\epsilon_m$: Strain in axis of bottom flange at mid span — $\epsilon_y$=1.82‰: Yield strain

$\eta$: Degree of shear connection with shear resistance according to equation (6.29)

Based on the results of two composite beam tests, where one showed a strongly asymmetric behaviour at ultimate load, the degree of shear connection of both tests was less then half of the required degree of shear connection and the exceedance of the limiting slip at ultimate load was relatively small. Considering the slip at a smaller percentage of the bending resistance to account for finite strains, the limiting slip was satisfied. This is reasonable evidence that the required minimum degree of shear connection could be reduced for short span composite beams. The test with single shear connectors reached 102% of its plastic bending resistance using the mean shear resistance according to Chapter 6, and the test with pairs with pairs of shear connectors reached 99% of its plastic bending resistance. Both results confirm that the plastic bending resistance may be reached for 12% and 22% degree of shear connection.

# 8 Numerical investigations on composite beams

Push-out tests are suitable to investigate the influence of parameters, as for example material strength or welding position on the shear connector behaviour. However, push-out tests can only give an idea of what happens in the shear interface of a composite beam. Because a push-out specimen represents only a small part of the shear interface, it can not show the influence of the transferred shear force on:

- The variability of slip along the shear interface.
- Transverse forces that, independently from the loading of the system, originate from the local deformation of the concrete slab itself.

The results of full scale beam tests include such effects, but they can hardly be quantified in the back-analysis of the tests. This is because of limited measurements and the variability of important input parameters. Furthermore, beam tests are typically conducted with point loads. The conditions of real beams with distributed loading cannot easily be reproduced in testing.

Therefore, finite element analysis is necessary to investigate the behaviour of the full shear interface. All numerical investigations in this work were conducted with the finite element software SOFiSTiK.

## 8.1 Finite Element Model of composite beams

The level of complexity of the used finite element model always depends on the problem it has to solve. In the following investigations, a simple model is defined that is able to:

- Predict the ultimate load of the composite beam.
- Predict the deformation behaviour at the serviceability limit state.
- Investigate the influence of varying slip along the shear interface on the shear force for a known load-slip behaviour of the studs.

Because all these questions are rather global considerations of the composite beams behaviour, it is not necessary to conduct detailed modelling of the shear interface. Instead, the shear connectors can be defined by springs that reflect the non-linear behaviour of the studs. The simplest assumable model would utilise BEAM elements to model the steel section and concrete slab and connect those with the springs. Furthermore, symmetry conditions may be used to reduce the size of the system and safe on calculation time.

To consider the imperfect stud welding and asymmetric failure of beam test 2-09, a more complex model must be chosen because of the software limitations. To model the preliminary failure of the studs in beam test 2-09, it is necessary to remove the springs for the failed studs from the model at the respective load stage. SOFiSTiK allows to explicitly enable or disable the stiffness of grouped elements for each calculation of a load-case. The additional use of a so called primary load cases allows to consider a redistribution of internal forces and moments that result from the modification of the system. This procedure is illustrated

in example 5.6 in [ASE, 2013]. However, it is currently not possible to consider non-linear material properties with this method, when BEAM elements are used. For this reason, the model utilised QUAD elements to model the steel section and concrete slab. Consequently, the full span of the beams is modelled to reproduce the asymmetry of specimen 2-09. Figure 8.1 illustrates the details of the model.

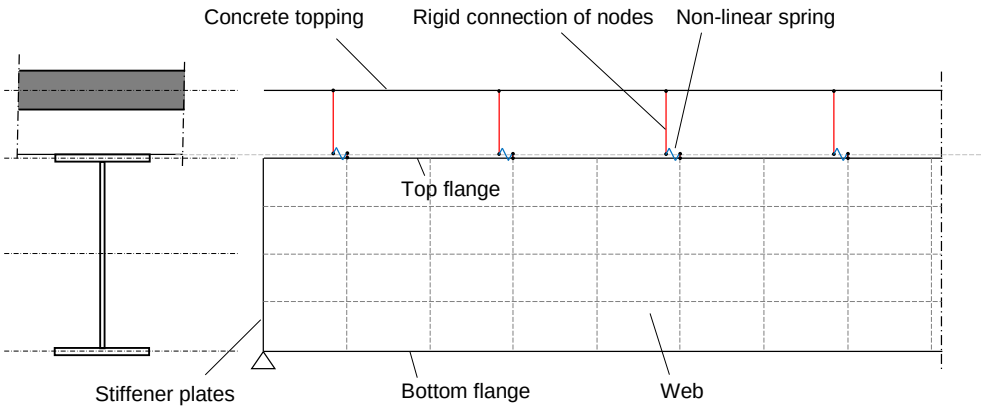


Figure 8.1: Schematic representation of the used Finite Element Model.

Modelling the beam with QUAD elements requires a three-dimensional structure. The steel beam consists of the flanges and the web. They are modelled from QUAD elements centred to the axis of the respective plate. In addition, stiffeners must be placed at the supports. For the concrete slab, only the continuous part is modelled.

Rigid connections between nodes are used to connect the top flange to the shear interface. Likewise, the concrete slab is rigidly connected to nodes at the shear interface. This gives a pair of nodes that is connected with non-linear springs, which mimic the load-slip behaviour of the shear connectors. The stiffness of these springs in directions transversely to the beam has to be quasi-rigid. In addition, a rigid connection of the rotation around the axis of the beam is used.

To each QUAD element, non-linear material properties for steel or concrete are assigned. The reinforcement is modelled as a parameter of the QUAD elements. This parameter assigns the amount of surface reinforcement. The reinforcement also considers non-linear material properties. All material properties are defined using uni-axial stress-strain curves.

Considering the application of loads, it is necessary to prevent bending moments in the concrete slab transversely to the beam. Because the ribs of the slab are not modelled, it has not the realistic bending stiffness in this direction. Loading situations that lead to bending moments in the slab transversely to the beam would therefore cause an unwanted concrete failure. For this reason, the self-weight of the concrete is set to zero and applied as line load at the axis of the slab.

The model described above can also be used with BEAM elements. This simplifies the model into a two-dimensional structure. The elements of the concrete slab and steel section are centred to the respective axis. Each axis is rigidly connected to the shear interface, where the springs mimic the behaviour of the studs. Furthermore, no problems with the load application occur, because there is no transverse bending of the concrete slab.

## 8.2 Verification against conducted beam tests

To verify the described finite element model, its results are compared to the conducted beam tests. The geometry of the test specimen is modelled, including the extension of the beam at the supports. The web of the steel section is divided into 10 elements. This is equal to the number of layers over the thickness of the QUAD elements of the slab. The support conditions are chosen to be symmetric. Thus, the composite beam is only vertically supported and the horizontal fixations are placed at the axis of symmetry and where the hydraulic jack was attached to the loading structure. The load introduction is modelled with beam elements for the longitudinal load distribution beam. The transverse load distribution beams are modelled by fixing the vertical displacement of the longitudinal load distribution beam to the slab. Figure 8.2 shows the used model.

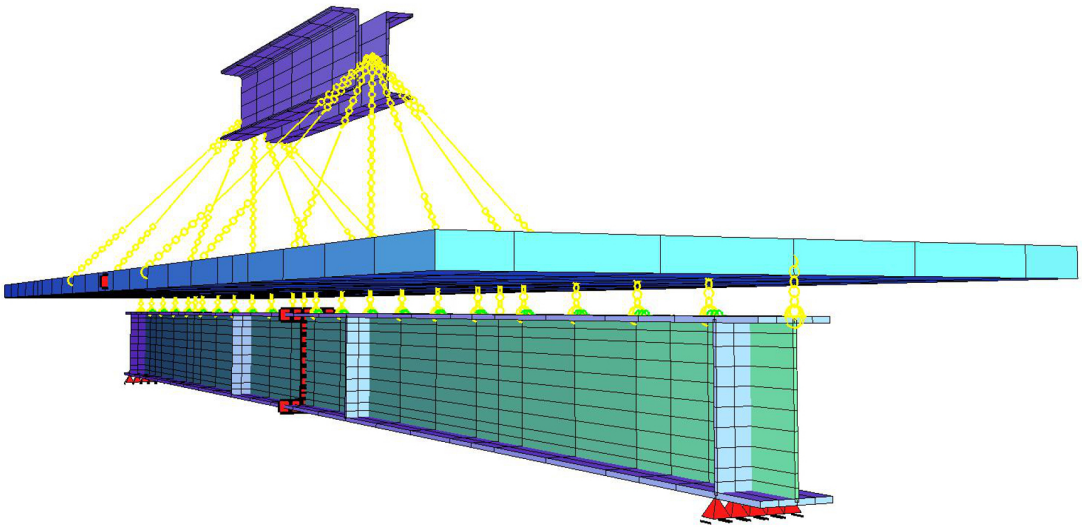

Figure 8.2: Finite Element Model used to recalculate the beam test results.

To take account of softening at high strains, the stress-strain curve for concrete in compression is modelled according to [DIN EN 1992-1-2, 2006], see equation (8.1). The stress-strain curve is derived for 20°C. Then the concrete strength $f_{c,\Theta}$ is equal to the measured concrete strength, which is multiplied with the factor $\alpha_{cc} = 0.85$ to consider static loading. The peak of the stress-strain curve occurs at a strain $\epsilon_{c1,\Theta}$ of 2.5‰.

$$\sigma_c = \frac{3\epsilon f_{c,\Theta}}{\epsilon_{c1,\Theta}\left[2 + \left(\frac{\epsilon}{\epsilon_{c1,\Theta}}\right)^3\right]} \tag{8.1}$$

The tensile strength of the concrete was not measured. According to the measured compressive strength, the concrete grade was between C30/37 and C35/45. Conservatively, the tensile strength of C30/37 according to [DIN EN 1992-1-1, 2005] is assigned.

The material properties of the reinforcement were not measured. Therefore, it is defined according to [DIN EN 1992-1-1, 2005], as shown in Figure 8.4.

The properties of the steel beam are modelled according to the results of tensile tests that were conducted on samples which were cut from the flanges and web of the beams. The used stress-strain curves for the steel section are shown in Figure 8.5

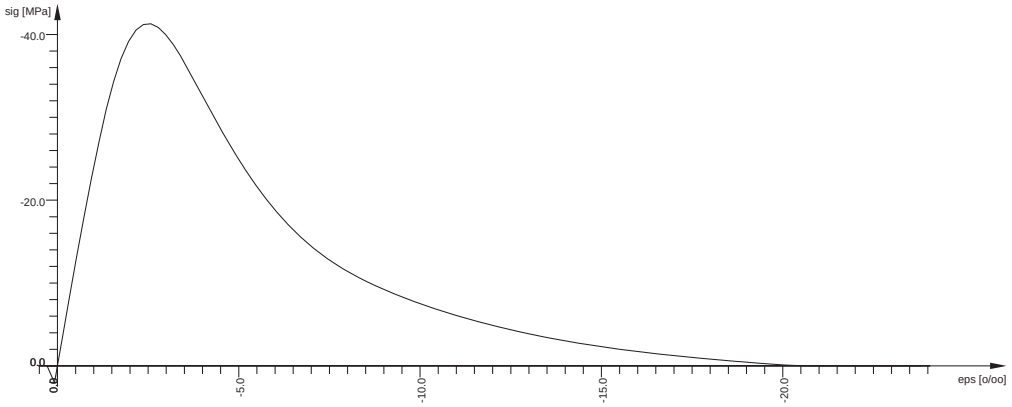


Figure 8.3: Stress-strain curve for concrete.

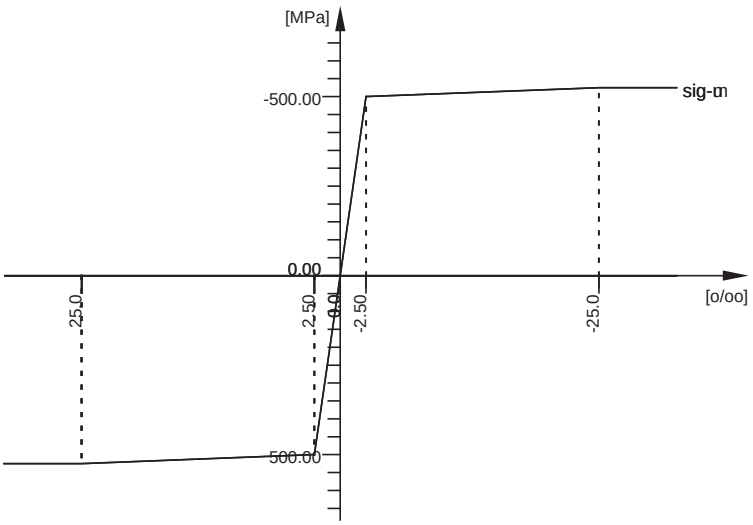


Figure 8.4: Stress-strain curve for reinforcement.

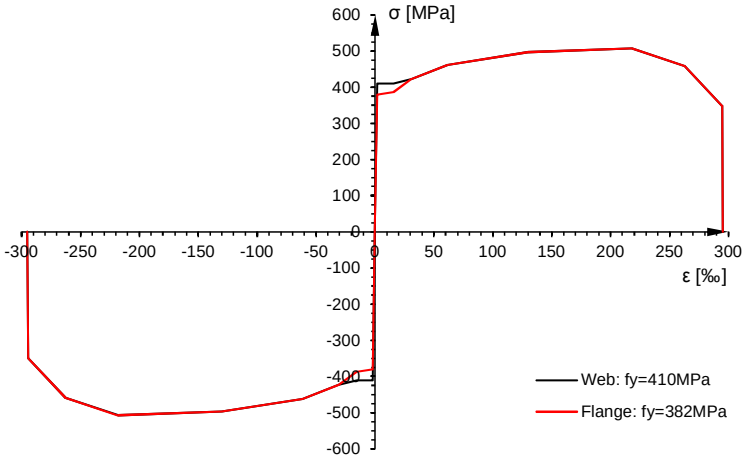


Figure 8.5: Stress-strain curves for the steel section.

The properties of the shear connectors were different for the two beams. They are shown together with the analysis of the respective beam.

### 8.2.1 Specimen 2-10

At first the finite element model is compared to the results of specimen 2-10, because there was no significantly asymmetric failure of the shear interface observed. Specimen 2-10 used through deck welded pairs of shear connectors in CF80 decking. To avoid the influence of local transverse compression when determining the spring properties, the 2nd, 3rd and 4th rib are considered. These were the ribs, where a lift of the slab was observed. The respective average shear force per stud is shown in Figure 8.6a. For the finite element analysis, a rather conservative static load slip curve for both sides of the beam is determined. According to the measured values a failure load of about 68 kN per stud is obtained. In comparison to push-out test results this value appears exceptionally large. After rib pry-out, the load drops to between 40 and 35 kN per stud, which corresponds well with push-out test results. In the finite element model, the pair of studs is combined in a single spring. Thus the loads in the spring properties, shown in Figure 8.6b, are doubled. When the slip is larger than 10mm, linear softening up to 40mm is assumed.

Using the above shear connector and material properties, the finite element model results in the load-displacement plot shown in Figure 8.7. In comparison to the test results, the model matches very well the elastic behaviour of the beam up to an applied load of about 200kN. Alos the static resistance of the test is matched very well for deflections larger than 45mm. Only for the transition between elastic and plastic behaviour, at deflections between about 22mm and 45mm, the model strongly differs from the test result. This can be because of the very high load assumed for rib pry-out failure.

A comparison to the test results for slip versus deflection is shown in Figure 8.8. As long as the beam behaviour was elastic, the slip is well predicted. When the first non-linear displacements occurred, test results and finite element model strongly differ. However, the model predicts a sudden increase of slip when rib pry-out occurs, as it was observed in the test, just that this increase happens at an about 20mm larger deflection. After rib pry-out the curves from the test and from the model are parallel. Therefore, it can be assumed that the post-failure behaviour of the studs was modelled accurately. Accordingly, the spring properties need to be modified for a smaller rib pry-out resistance.

To modify the resistance for rib pry-out of the spring properties, all studs between support and loading point are averaged. This leads to the load-slip curves shown in Figure 8.9

Because the elastic behaviour and post-failure behaviour were assumed as well predicted, only the peak for rib pry-out failure is modified. The load peak is decreased from 68kN to 60kN per stud. This is a reduction of the stud shear resistance of about 12%. Repeating the analysis with the modified spring properties lead to the results shown in Figures 8.10 and 8.11. The accordance with the test results improved, but the transition between elastic and plastic behaviour is too smooth. Considering the development of the slip, it can be assumed that the drop-off in the load is considered too soft in the spring properties.

As the next modification of the spring properties, the drop-off in the load after rib pry-out failure is sharpened by reducing the slip by 50%. The model then gives the results shown in Figures 8.13 and 8.14. The accordance between numerical results and measured results is very well for the elastic and plastic behaviour. Also the characteristics of the transition between elastic and plastic behaviour are now predicted more accurate. It can be concluded that with sufficient knowledge of the shear connectors load-slip behaviour the finite element model accurately predicts the behaviour of the composite beam test.

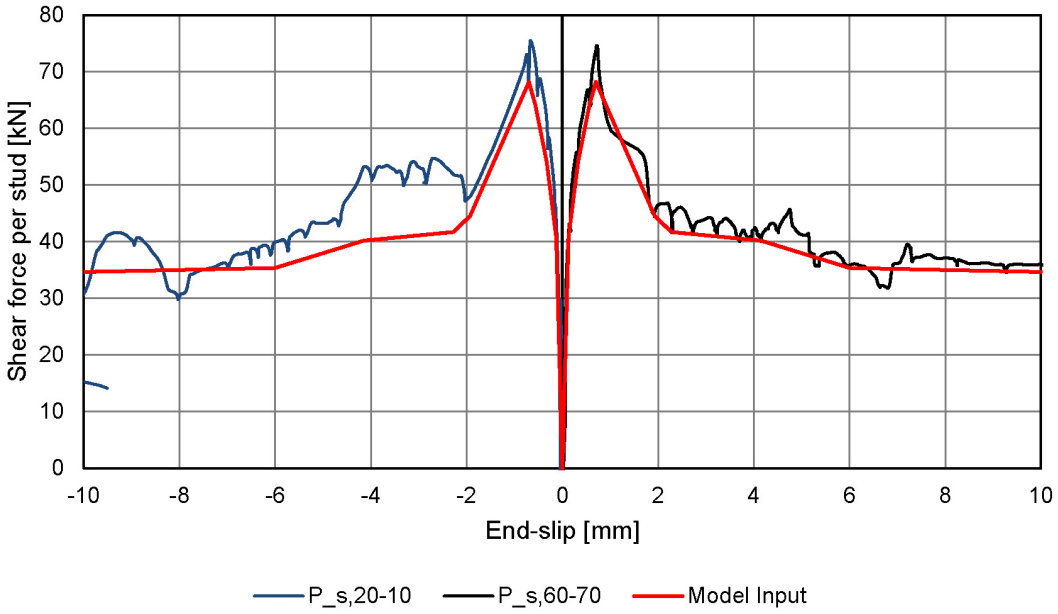


(a) Behaviour per stud derived as average of the 2nd, 3rd and 4th row of studs.

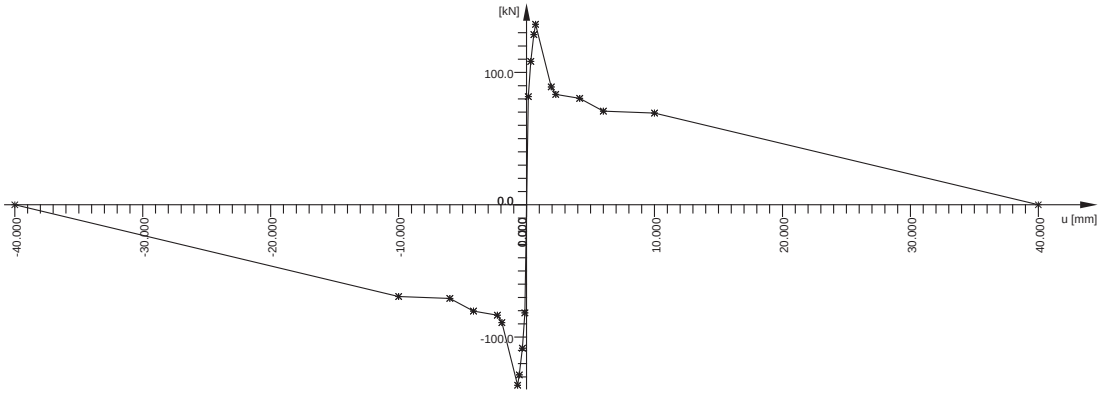


(b) Load-displacement curve applied to the springs.

Figure 8.6: Initial assumption for the load-slip behaviour of shear connectors.

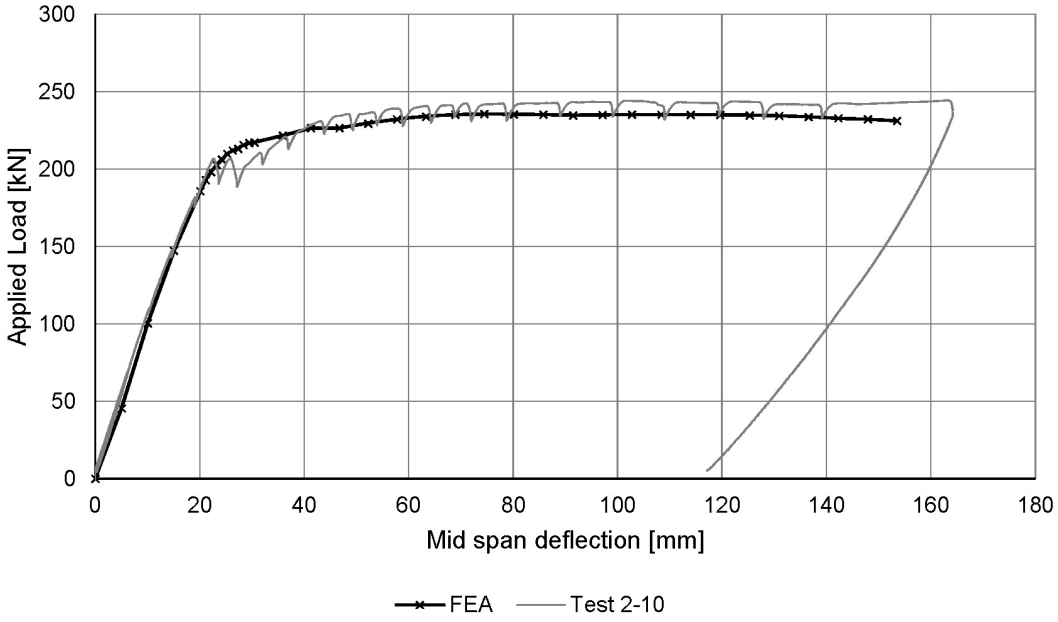


Figure 8.7: Comparison of load-displacement plot from FEA to the test result.

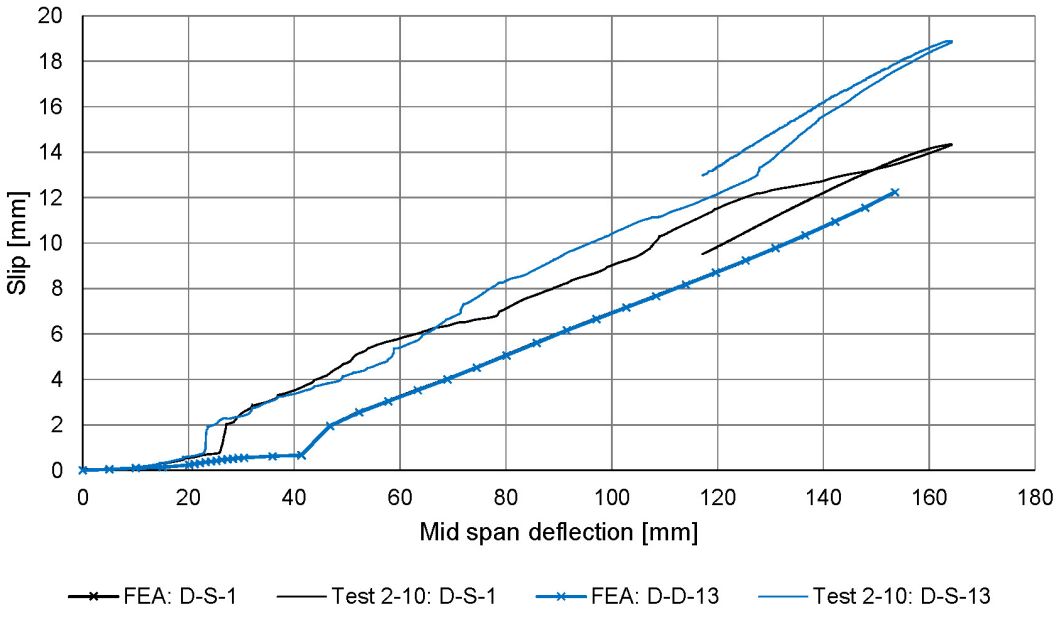


Figure 8.8: Comparison of slip-displacement plot from FEA to the test result.

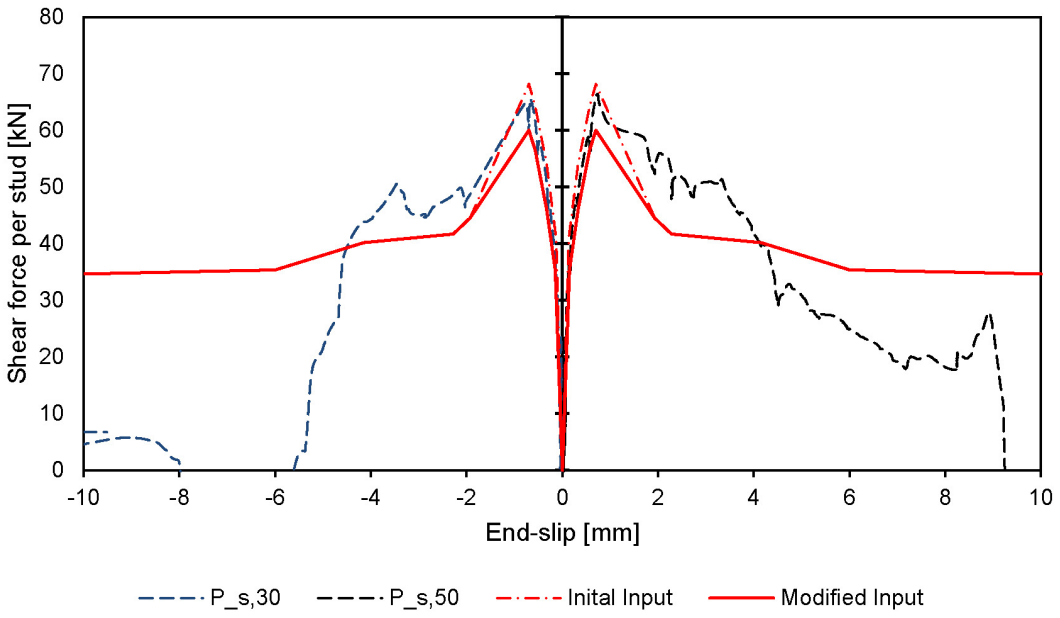


Figure 8.9: Modification of the spring properties by averaging all studs between support and loading point.

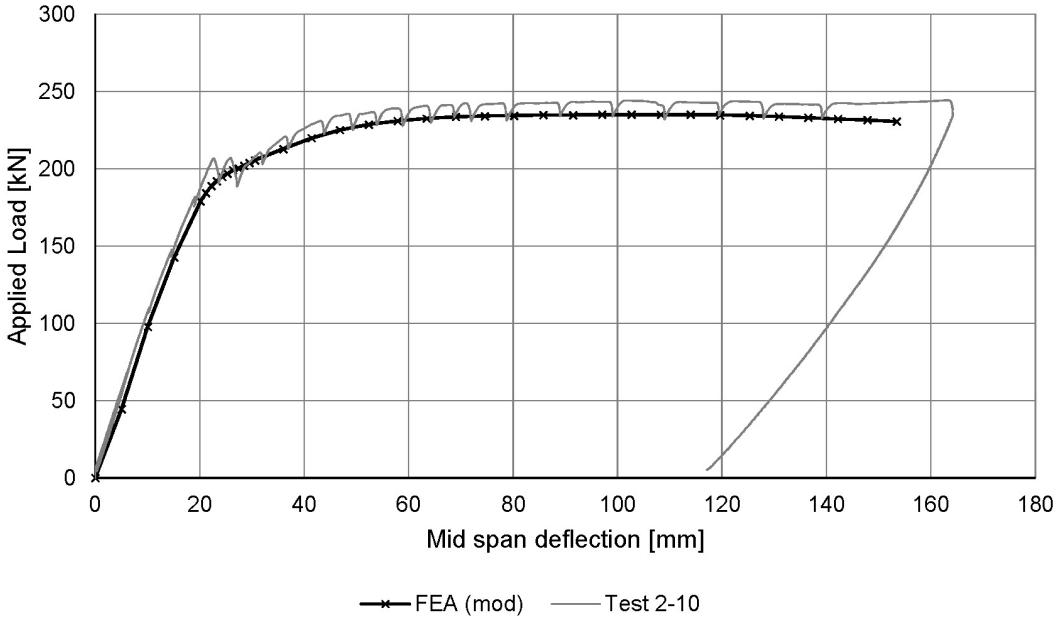


Figure 8.10: Comparison of load-displacement plots after reduction of the stud resistance.

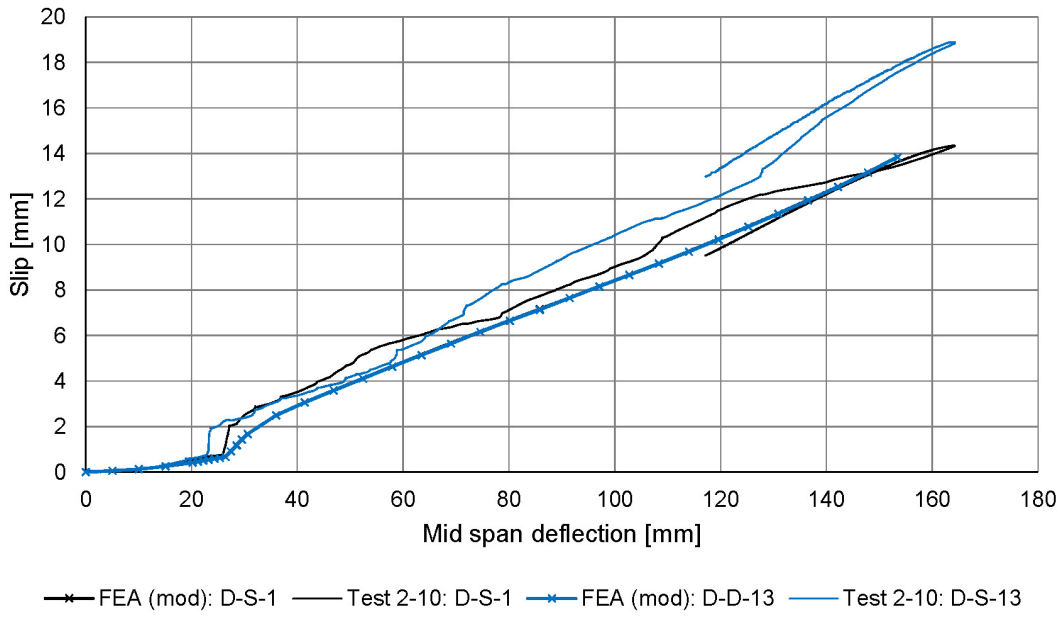


Figure 8.11: Comparison of the slip-displacement plots after reduction of the stud resistance.

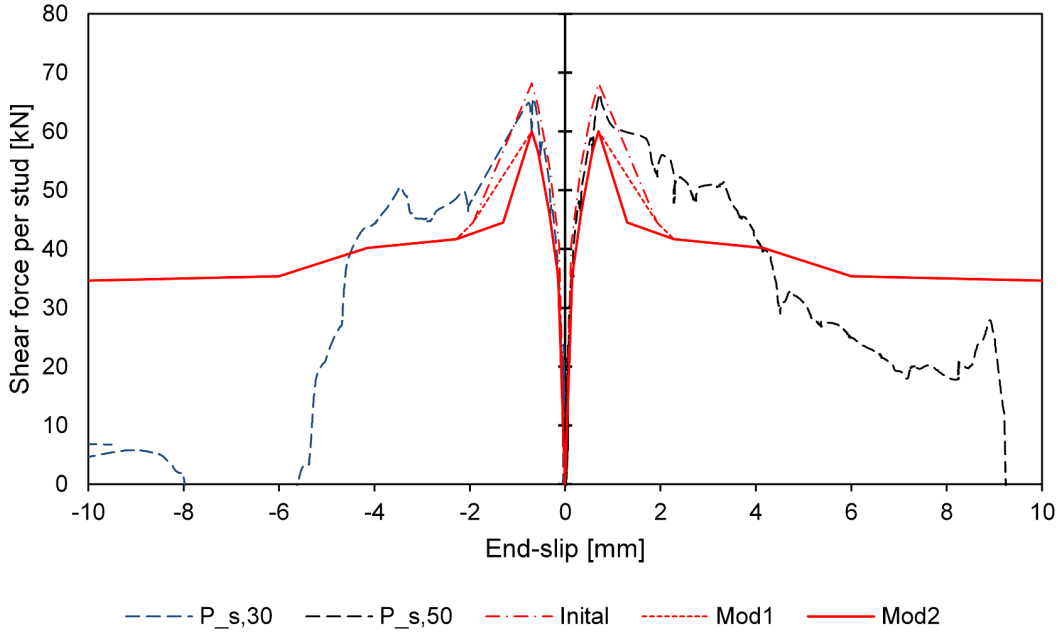


Figure 8.12: Sharpening of the drop-off in the stud shear resistance.

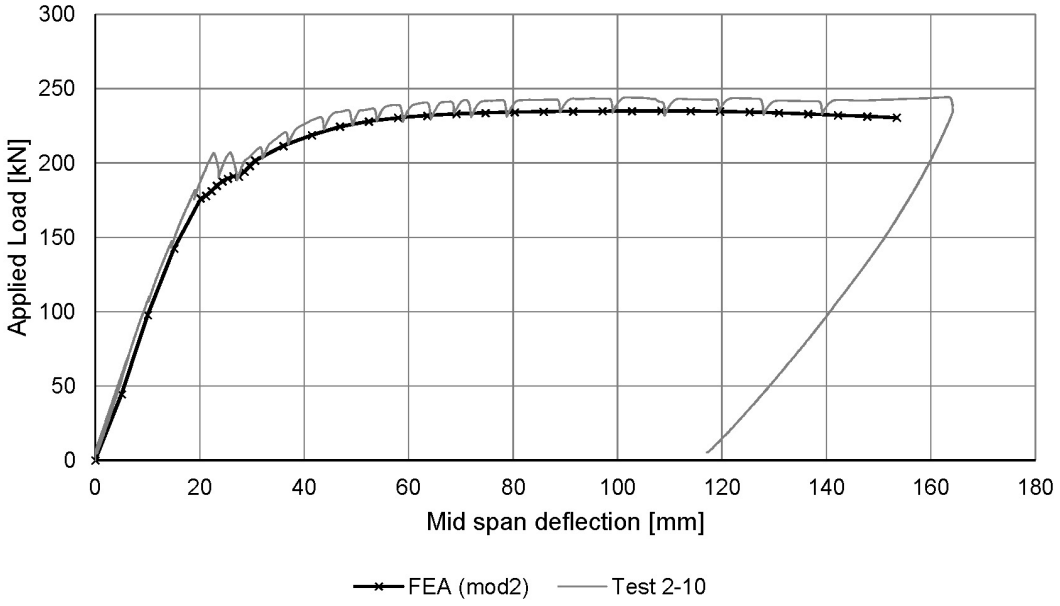


Figure 8.13: Comparison of load-displacement plots after sharpening the drop-off in the stud resistance.

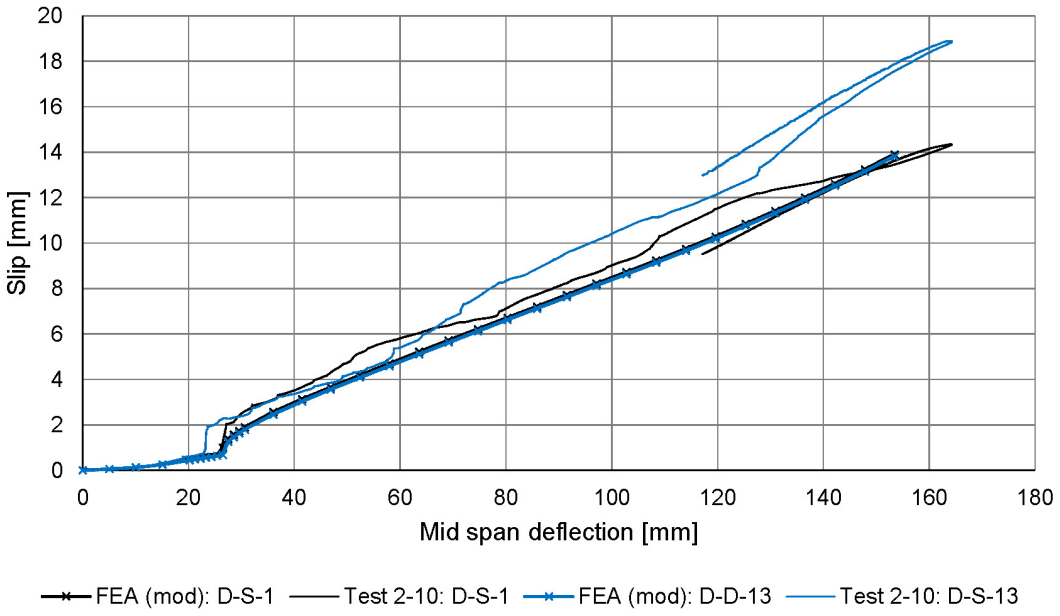


Figure 8.14: Comparison of the slip-displacement plots after sharpening the drop-off in the stud resistance.

### 8.2.2 Specimen 2-09

For the analysis of specimen 2-09, the concretes stress-strain curve in compression is modified by applying the measured concrete strength to equation (8.1). The material properties for steel and reinforcement are maintained as for specimen 2-10. For the shear connectors, the load-displacement behaviour is determined from the average shear force of the 4 studs closest to the supports. This has shown to be a good estimation of the behaviour of the shear interface in the analysis of specimen 2-10. The load-slip behaviour for the first 5mm of slip is determined from the measurements during the test, as shown in Figure 8.15a. After 5mm slip, linear softening is assumed until 40mm slip. This leads to the spring properties shown in Figure 8.15b.

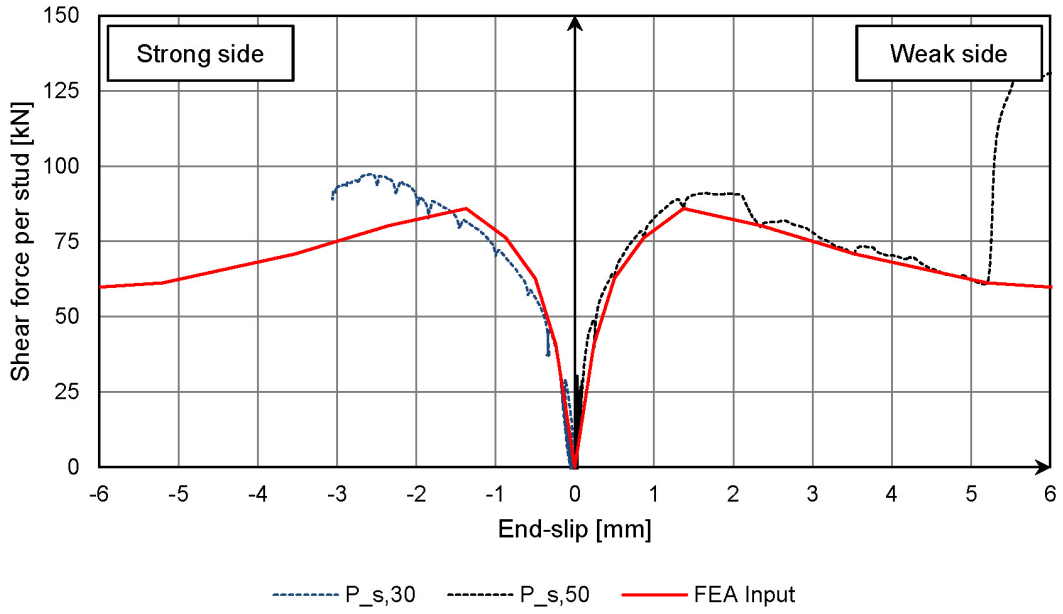


(a) Behaviour per stud derived as average of the 4 outermost studs.

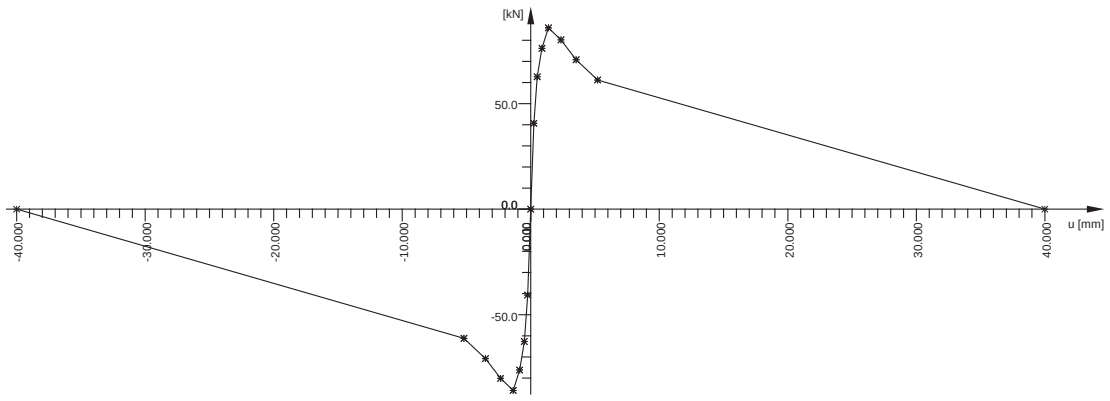


(b) Load-displacement curve applied to the springs.

Figure 8.15: Assumption for the load-slip behaviour of shear connectors.

The support reactions are still modelled considering symmetry. However, to allow an asymmetric distribution of slip between steel beam and concrete slab, the horizontal fixations of the

slab at mid-span are removed. The other boundary conditions are modelled as for specimen 2-10.

To consider the preliminary failure of studs because of imperfect welding, some springs are removed from the system at a given load case. During testing, failure of the 4th stud, counted from the support, was observed by an up-lift of the rib at about 25mm deflection. Failure of the 2nd stud was confirmed after the concrete was removed. To model this behaviour, the corresponding two springs are removed for load cases with applied displacements of more than 25mm.

This analysis lead to the load-displacement plot shown in Figure 8.16 and the slip-displacement plot shown in Figure 8.17. The asymmetric development of slip is well analysed and the load-displacement plot is also accurate up to a deflection of about 100mm. The analysis reached ultimate load of 214.0kN at a deflection of 64.3mm. In the test ultimate load was 212.5kN at 54.8mm deflection. At this deflection a load of about 211kN was analysed. The continuous decrease of the applied load results from the assumed softening of the springs. On one side, this shows that unloading properties of shear connectors can be analysed if the structure is loaded with displacements. On the other sides, the load-displacement behaviour of the test specimen indicates, that the studs did not show a significant unloading and must have maintained a shear force of about 60kN per stud. Figure 8.18 shows the displacement and forces of the springs at ultimate load of the analysis.

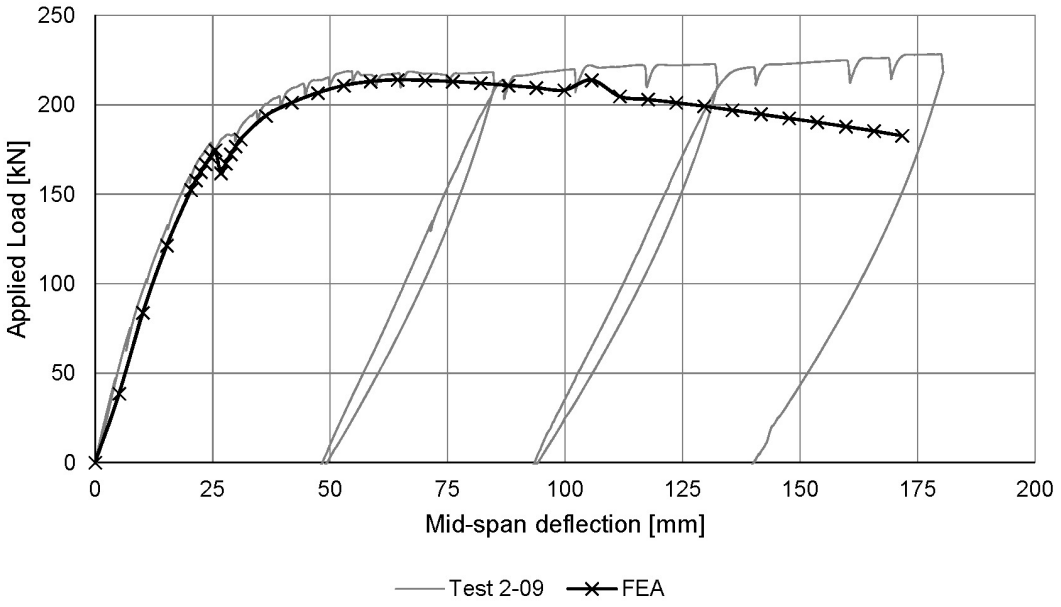


Figure 8.16: Comparison of load-displacement plot from FEA to the test result.

It can be concluded that the behaviour of specimen 2-09 could be accurately analysed using measured material and spring properties from the test. Also the asymmetric behaviour of the specimen could be modelled by removing the failed studs from the system at higher loading stages. The asymmetry in slip was very well analysed, even though instantly removing the springs can be assumed as a quite rough approximation of the real local failure of the studs. These results confirm that the presented finite element model can be used to analyse the load-displacement behaviour of composite beams.

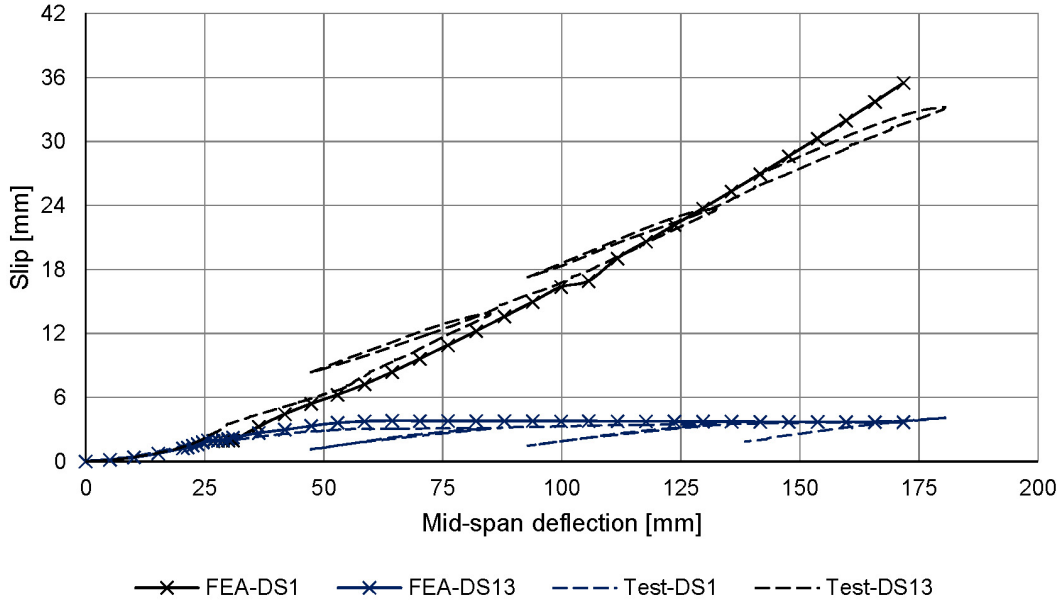


Figure 8.17: Comparison of slip-displacement plot from FEA to the test result.

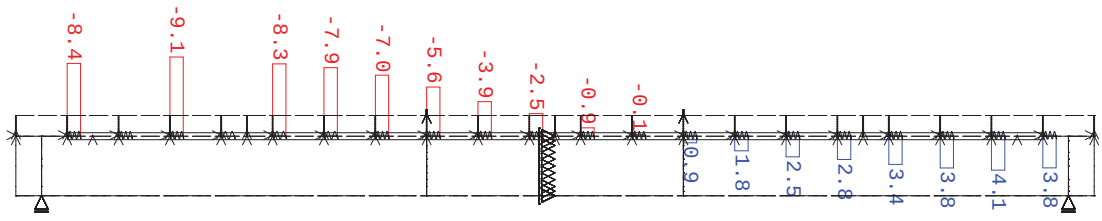


(a) Displacement of springs in mm.

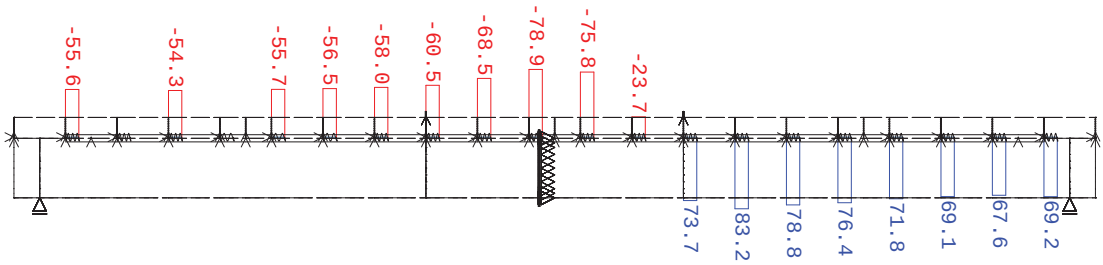


(b) Forces of springs in kN.

Figure 8.18: Displacement, in [mm], and forces, in [kN], of springs at ultimate load of analysis.

## 8.3 Parametric studies

After the verification of the finite element model against the conducted composite beam tests, the model is now utilised for parametric studies. The studies aim on answering following questions:

- What is the influence of the variation of slip along the span of the beam on the shear

force?

- How can the load-slip behaviour be simplified for structural analysis in engineering offices or parametric studies?

To investigate these questions, the behaviour of composite beams with spans from 6.00m to 12.00m was analysed. For each span, the steel section was chosen to satisfy a typical span-depth ratio of 22, as shown in Figure 8.19.

To consider different types of load-slip curves, the beams were modelled once assuming CF80 decking and once assuming CP60 decking. For both types of decking, a total thickness of the concrete slab of 150mm is assumed. This was also the case in the push-out and beam tests. The load-slip curve for the case of CF80 decking is taken from push-out specimen NR1-1. The results of specimen 1-03-3, reported in [Odenbreit et al., 2015], are used for CP60 decking, because there was a similar concrete strength and no transverse loading was used.

The whole steel section is modelled in S355 steel grade with the stress-strain curve according to [DIN EN 1993-1-1, 2005]. The stress-strain curve of the reinforcement is modelled according to [DIN EN 1992-1-1, 2005]. For concrete in compression, the stress-strain curve according to [DIN EN 1992-1-2, 2006] is assumed for a compressive strength of 44.1N/mm$^2$.

In these studies, the more common type of uniform loaded beams is investigated. Therefore, the concrete slab is loaded with a distributed load at its centreline, as shown in Figure 8.21, to avoid transverse bending. SOFiSTiK is utilized to iterate the ultimate load of the beams by increasing the applied line load. The iteration is stopped when no equilibrium can be found for larger load factors.

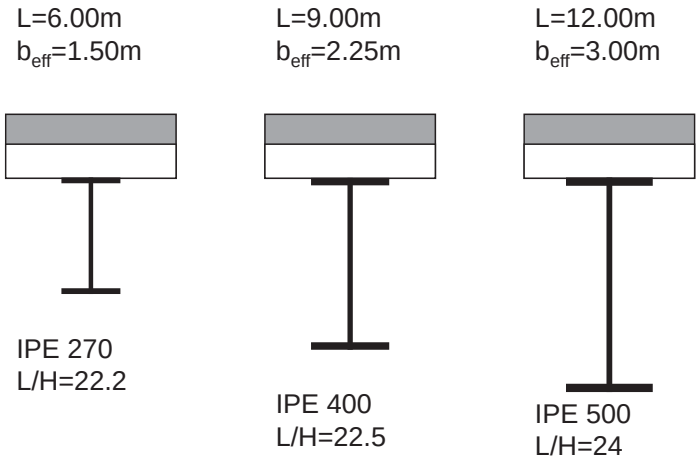


Figure 8.19: Analysed cross-sections for composite beams between 6.00m and 12.00m span.

### 8.3.1 Influence of the slip distribution on the shear force

The first investigation considers the determination of the shear force, $N_c$, in composite beams. Typically, the shear force is determined by multiplication of the stud shear resistance with the number of studs between support and the considered cross-section. Thereby, the stud shear resistance is obtained either by calculation or by push-out tests. This means, that in general the first load-peak of the studs load-slip curve is used.

The reason for the following investigations is that in a composite beam every stud has an

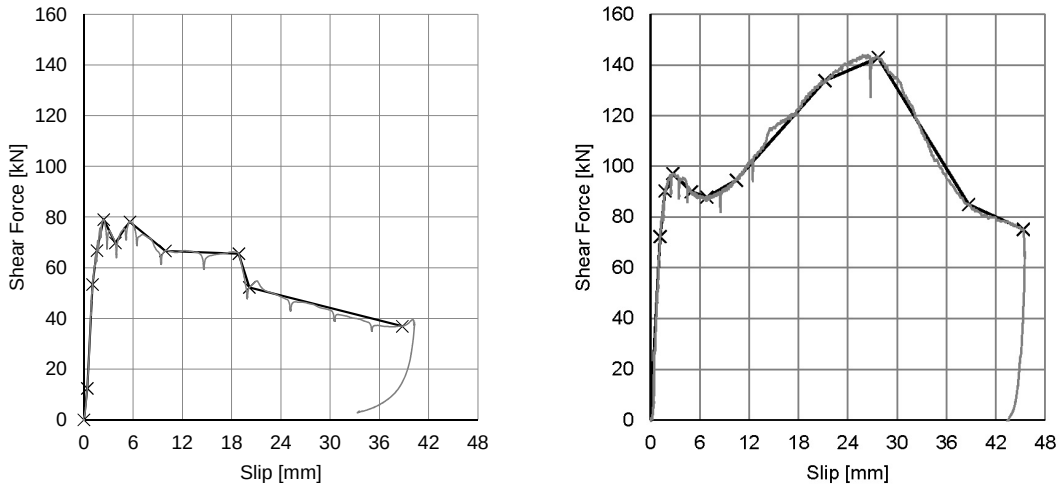


(a) Cases with CF80 decking.

(b) Cases with CP60 decking.

Figure 8.20: Spring properties for the parametric study.

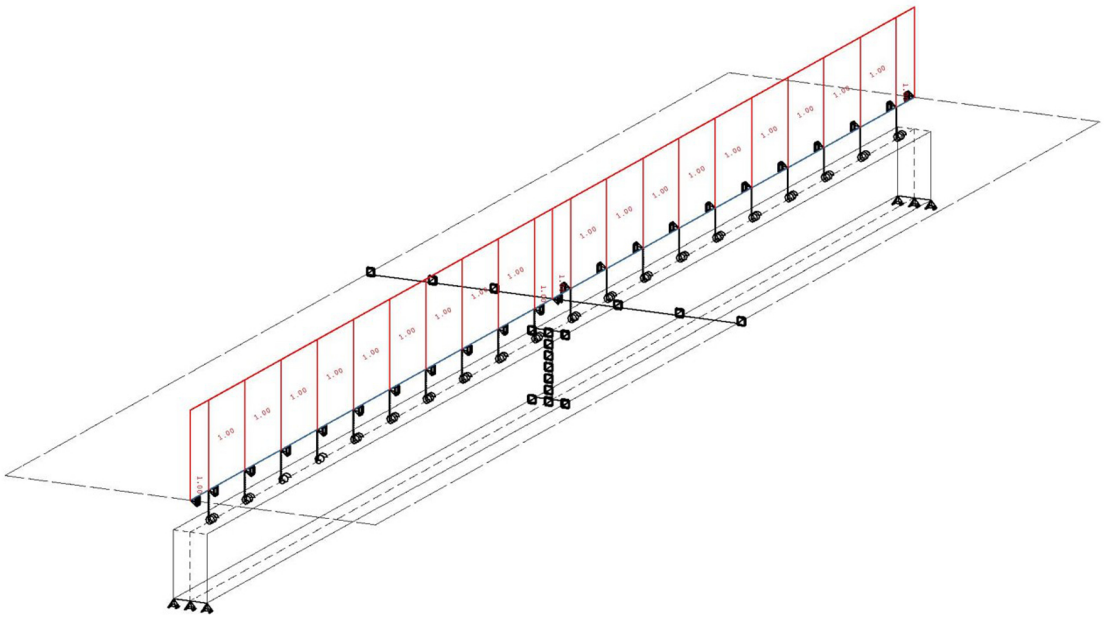

Figure 8.21: Structure and applied loading for parametric studies.

individual slip. Hence, every stud has an individual load according to the studs load-slip curve. This means that studs close to mid-span have a small slip and hence transfer a small shear force, but they are assumed as fully charged. Studs close to the end of the beam have a large slip, but when the load-slip curve decreases they also transfer smaller forces than assumed. In consequence, the sum of the shear forces of each stud must be smaller than the assumed shear force, $N_c$. Accordingly, the bending resistance of the composite beam is overestimated.

To investigate this effect, the bending resistance, $M_{R,pl}$, of the beams is calculated from a plastic stress distribution. Thereby, the shear force, $N_c$, is calculated from the load peaks

of the used load-slip curves, shown in Figure 8.20. This leads to the forces and moments shown in Table 8.1. The shear force and bending resistance are than compared to the results of the finite element analysis.

Table 8.1: Comparison of shear force, $N_c$, and bending resistance, $M_{R,pl}$, to results of finite element analysis.

| | | | CF80 cases | | | CP60 cases | | |
|---|---|---|---|---|---|---|---|---|
| Calculated | $L$ | [m] | 6.00 | 9.00 | 12.00 | 6.00 | 9.00 | 12.00 |
| | $n$ | [-] | 10 | 14 | 19 | 14 | 21 | 28 |
| | $P_{e1}$ | [kN] | 79.07 | 79.07 | 79.07 | 97.13 | 97.13 | 97.13 |
| | $n \cdot P_{e1}$ | [kN] | 790.7 | 1107 | 1502.3 | 1359.8 | 2039.7 | 2719.6 |
| | $\eta$ | [-] | 0.49 | 0.37 | 0.36 | 0.83 | 0.68 | 0.66 |
| | $M_{R,pl}$ | [kNm] | 330.2 | 745.3 | 1217.6 | 409.6 | 881.3 | 1402.6 |
| FEA: L/50 | $M_E$ | [kNm] | 299.7 | 686.7 | 1118.9 | 358.9 | 794.1 | 1256.7 |
| | $\frac{M_E}{M_{R,pl}}$ | [-] | 0.91 | 0.92 | 0.92 | 0.88 | 0.90 | 0.90 |
| | $\sum_{i=1}^{n} P_i$ | [kN] | 677.6 | 968.2 | 1297.4 | 1116.7 | 1786.7 | 2414.8 |
| | $\eta$ | [-] | 0.42 | 0.32 | 0.32 | 0.69 | 0.60 | 0.59 |
| | $\frac{\sum_{i=1}^{n} P_i}{n \cdot P_{e1}}$ | [-] | 0.86 | 0.87 | 0.86 | 0.82 | 0.88 | 0.89 |

Figure 8.22 shows the obtained ratio of the applied bending moment, $M_E$, to the calculated bending resistance, $M_{R,pl}$, plotted against the relative displacement. It is shown, that none of the beams reached the predicted bending resistance. In average, only 90% of the predicted resistance were reached.Furthermore, it can be seen that the load-displacement behaviour is elastic up to a deflection of span/200.

The reason for the over-estimation of the bending resistance is that the assumed shear force, $N_c$, was not reached. The sum of the spring forces was in average only 86% of the predicted shear force, as shown in Figure 8.23. As shown in Figure 8.24 for the case of 9m span and CF80 decking, the shear forces in the studs are significantly smaller than the peak value of the load-slip curve.

According to these results, the shear force, $N_c$, should be reduced by about 15%. A recalculation of the bending resistance, assuming a reduction factor of 0.85 on the shear force, leads to the results shown in Table 8.2. Even though the shear force is now assumed more conservative, only about 95% of the predicted bending resistance can be achieved. This is because infinite strains would be required to develop the assumed plastic stress distribution in the composite cross-section. For the finite displacements of a real beam, or non-linear analysis of beams, the cross- section cannot develop full plasticity.

On the other side, the conducted composite beam tests, presented in Chapter 7, could be analysed using the shear stud resistance developed in Chapter 6 without further reduction of the concrete compression force, $N_c$. It was found, that the behaviour of the studs could strongly vary along the span of the beam, as can be seen in Figure 7.14. It was concluded that the shear connectors were affected by transverse loads, which originated from the observed displacement of the concrete slabs. The results from the analysis of the beam tests show the occurrence of transverse forces acting on the studs, even though the beams were point loaded, see Figure 8.25. Likewise, transverse loads occur for the beams with distributed loading, as shown in Figure 8.26. These forces are mostly larger than the theoretical value

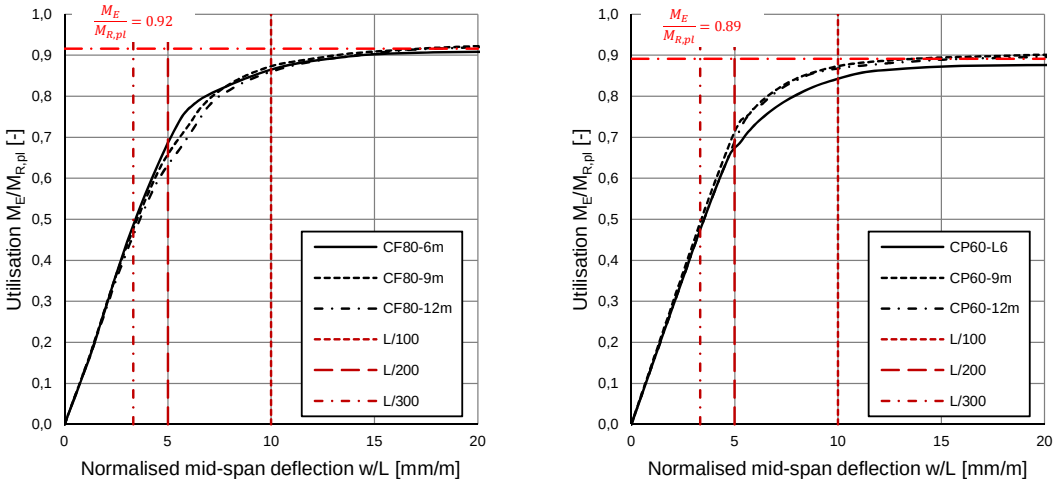


(a) Cases with CF80 decking.

(b) Cases with CP60 decking.

Figure 8.22: Utilization of bending resistance versus relative deflection.

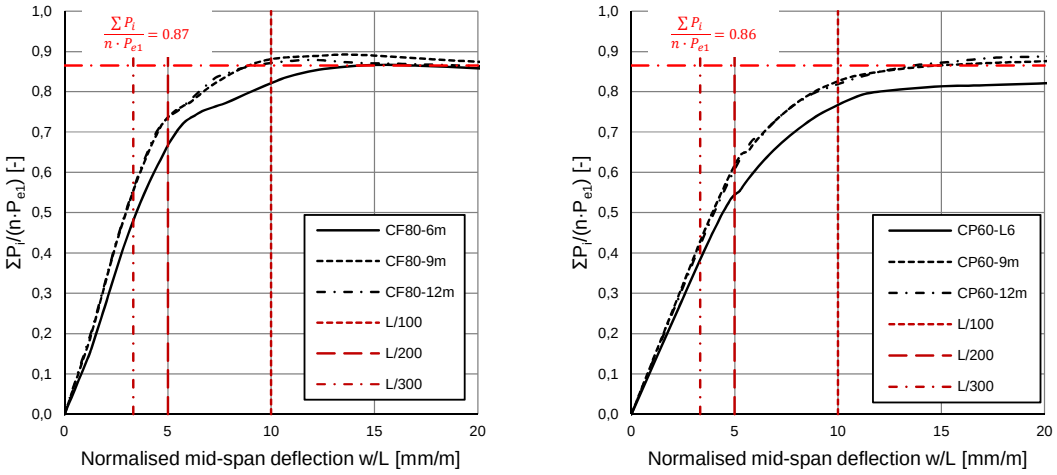


(a) Cases with CF80 decking.

(b) Cases with CP60 decking.

Figure 8.23: Utilization of shear force versus relative deflection.

obtained from the vertical loading of the system. This means that the transverse force, $N_q$, used in the calculation of the stud resistance according to equation (6.35) can be conservatively obtained from the vertical loading of the beam.

The conducted push-out tests with CF80 decking showed that the shear resistance of the studs strongly benefited from transverse loads. This explains why the conducted beam tests could be accurately predicted without a reduction of the concrete compression force, $N_c$.

In consequence, the shear resistance of a push-out tests is only an approximation of the real shear interface. The introduced concrete compression force, $N_c$, is also dependent on

- the transverse forces at the shear interface, which depend on the load case.

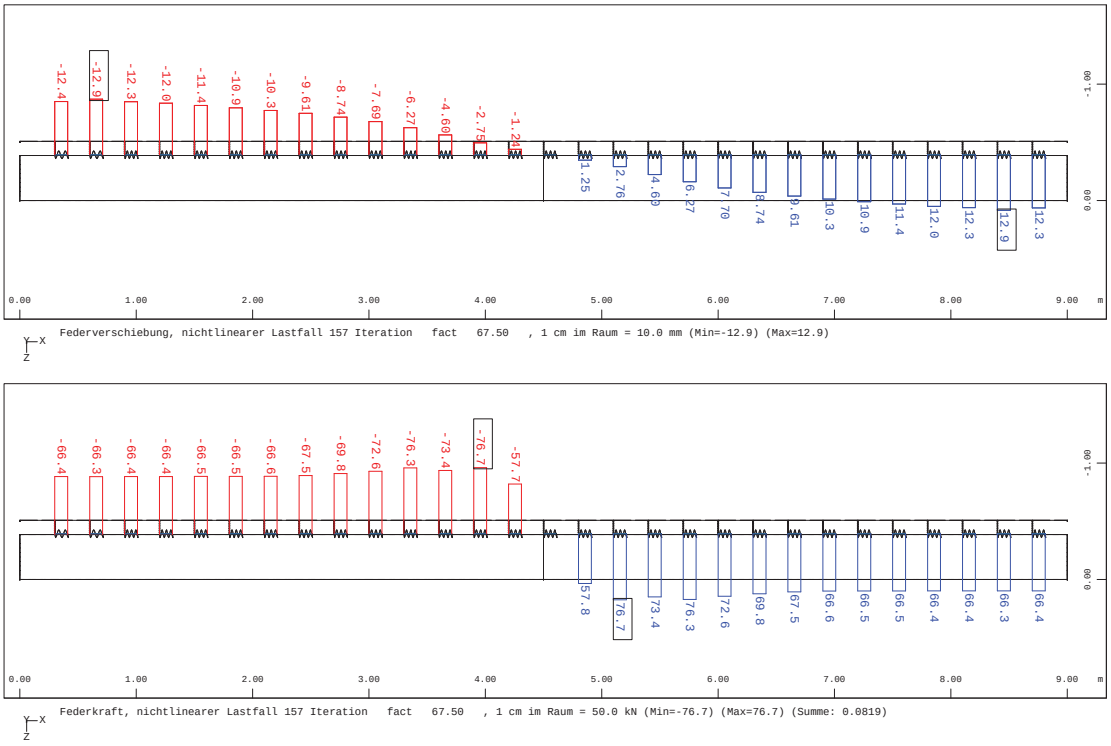


Figure 8.24: Slip and forces of springs at ultimate load for the case CF80-9m.

Table 8.2: Recalculated bending resistance, $M_{R,pl}$, for a reduced shear force, $N_{c,red}$, compared to results of finite element analysis.

| | | | CF80 cases | | | CP60 cases | | |
|---|---|---|---|---|---|---|---|---|
| Calculated | $L$ | [m] | 6.00 | 9.00 | 12.00 | 6.00 | 9.00 | 12.00 |
| | $n$ | [-] | 10 | 14 | 19 | 14 | 21 | 28 |
| | $P_{e1}$ | [kN] | 79.07 | 79.07 | 79.07 | 97.13 | 97.13 | 97.13 |
| | $0.85 \cdot n \cdot P_{e1}$ | [kN] | 672.1 | 940.9 | 1277.0 | 1155.8 | 1733.8 | 2311.7 |
| | $M_{R,pl}$ | [kNm] | 312.6 | 716.7 | 1173.0 | 382.1 | 838.6 | 1344.6 |
| FEA: L/50 | $M_E$ | [kNm] | 299.7 | 686.7 | 1118.9 | 358.9 | 794.1 | 1256.7 |
| | $\frac{M_E}{M_{R,pl}}$ | [-] | 0.96 | 0.96 | 0.95 | 0.94 | 0.95 | 0.93 |
| | $\sum_{i=1}^{n} P_i$ | [kN] | 677.6 | 968.2 | 1297.4 | 1116.7 | 1786.7 | 2414.8 |
| | $\frac{\sum_{i=1}^{n} P_i}{0.85 \cdot n \cdot P_{e1}}$ | [-] | 1.01 | 1.03 | 1.02 | 0.97 | 1.03 | 1.04 |

- the sensitivity of the shear connection for transverse loading.
- the individual force per stud resulting from the distribution of the slip.

Therefore, only for the type of load-slip behaviour used in CP60 cases, see Figure 8.20, which has only a marginal sensibility for transverse loading, a reduction of the compression force by 15% can be assumed. For CF80 cases, no conclusion can be drawn because of the sensibility of the shear connectors for transverse loading.

In addition, the aim is to determine the design value of the composite beams plastic bending re-

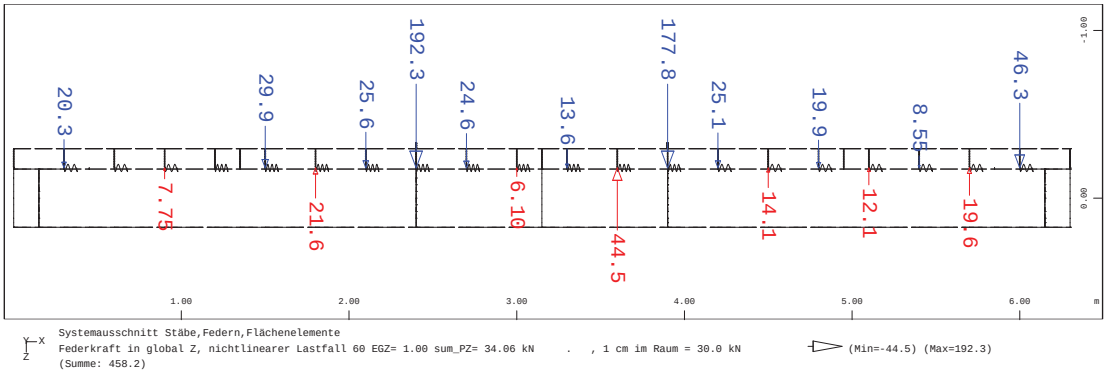


(a) Specimen 2-09

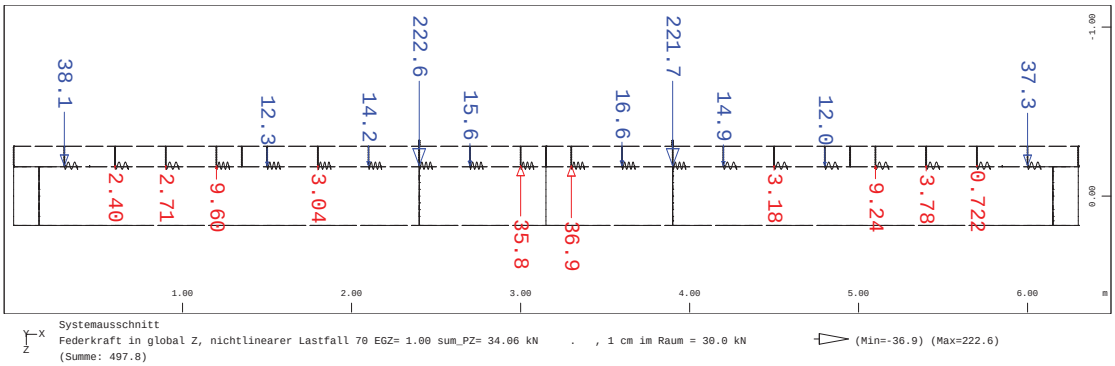


(b) Specimen 2-10

Figure 8.25: Transverse forces acting on shear connectors at ultimate load in conducted beam tests with point loading, obtained from non-linear analysis.

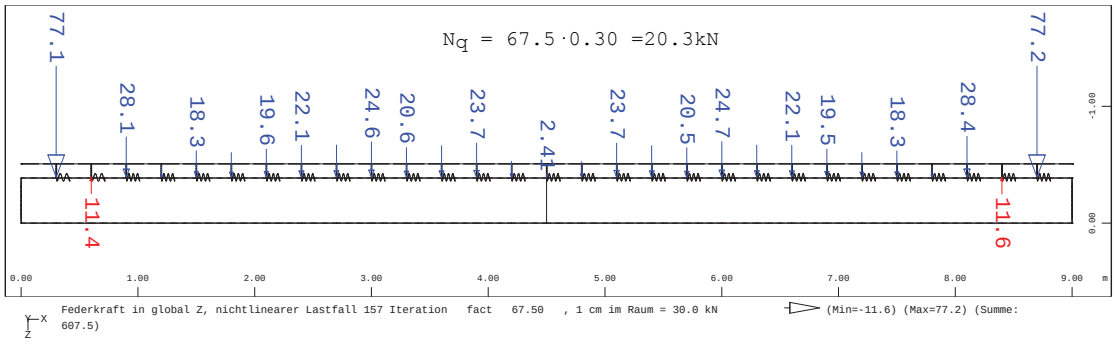


Figure 8.26: Transverse forces acting on shear connectors at ultimate load for the case CF80-9m with uniform distributed loading.

sistance. At ultimate limit state, all materials and the shear connectors are considered by there design resistances to calculate the bending resistance. According to [DIN EN 1990, 2002], each of this components contributing to the beams bending resistance has a probability of failure of less than 0.1%. This automatically leads to a certain level of safety for the bending resistance of the beam. It should be further investigated if the probability of failure of the bending resistance is satisfactory small so that the additional influences described above can be neglected.

### 8.3.2 Application of simplified springs to model the shear stud behaviour

In section 8.2 it was shown that the presented finite element model is suitable to analyse the behaviour of composite beams. However, the relatively complex load-displacement behaviour of the shear connection, see for example Figure 8.20, that was used so far is not suitable for parametric studies or the use in engineering offices. Therefore, the use of a simplified shear connector behaviour, as shown in Figure 8.27, is investigated in this section.

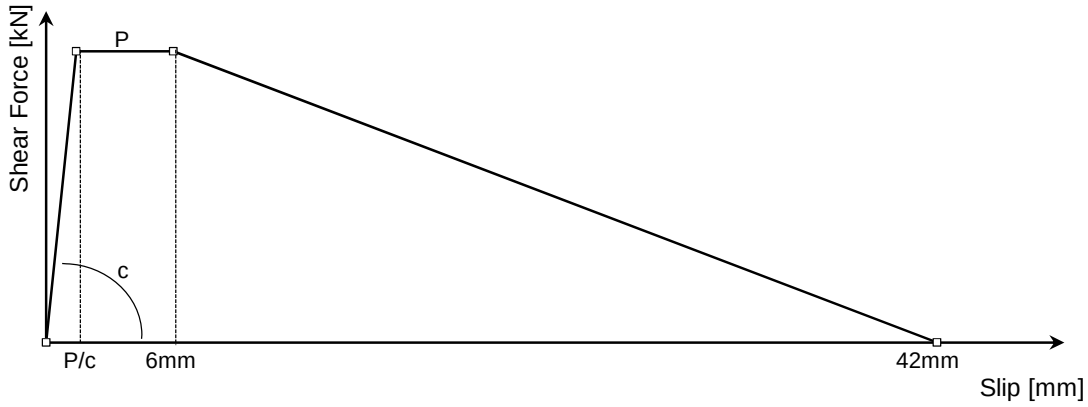


Figure 8.27: Simplified load-displacement behaviur for shear connectors.

The shown load-displacement curve is characterised by the elastic stiffness, $c$, and the shear resistance, $P$. Currently, [DIN EN 1994-1-1, 2010] requires a slip capacity of 6mm. It is assumed that the stud can maintain its shear resistance until this slip is exceeded. Then an unloading of the studs is assumed until 42mm slip are reached. This unloading characteristic has shown good results for the analysis of the beam tests in section 8.2. This type of curve is most suitable for failure modes of the stud with only one yield hinge. For failure modes with 2 yield hinges it may be conservative when 6mm slip are exceeded.

The resistance, $P$, of this curve can be determined using equations (6.35) and (6.36). To determine the elastic stiffness, $c$, the results of the push-out tests are investigated. For each test, the secant modulus between 10% and 70% of the resistance is determined. This way, it is ensured that the stiffness is not under-estimated because of plastic deformation at high loads or slip in the test frame at small loads. An overview of the results is shown in Table 8.3.

Because the elastic part of the load-slip behaviour was not significantly affected by transverse loading, the tests can be grouped according to the deck shape, number of studs per rib and concrete strength. Table 8.4 shows the mean values of the elastic stiffness, $c_m$, for each group. It can be seen, that for single shear connectors the stiffness is approximately the same for both types of decking. Therefore it is assumed that the elastic stiffness is not significantly dependent on the deck shape and stud diameter. Pairs of studs per deck rib,result in approximately the same stiffness per shear connector as single studs. Thus, doubling the number of studs, should double the stiffness of the shear connection. A significant influence on the stiffness is observed for the concrete strength. The stiffness, $c_m$, varies approximately as the term $\sqrt{f_{cm}E_{cm}}$:

$$\frac{57.45}{46.18} = 1.244 \hat{\approx} \sqrt{\frac{43.1 \cdot 34107}{30.9 \cdot 30868}} = 1.241$$

Referencing to a concrete strength of 30N/mm$^2$, a reference value for the stiffness, $c_{ref}$, of

Table 8.3: Elastic stiffness of shear connectors in push-out tests.

| Test | $f_{cm}$ | $n_r$ | $0.1P$ | $s(0.1P)$ | $0.7P$ | $s(0.7P)$ | $\Delta P$ | $\Delta s$ | $c$ |
|---|---|---|---|---|---|---|---|---|---|
| | [N/mm$^2$] | [-] | [kN] | [mm] | [kN] | [mm] | [kN] | [mm] | [kN/(mm·stud)] |
| 1-04-1 | 30.6 | 1 | 7.81 | 0.29 | 52.92 | 1.21 | 45.11 | 0.93 | 48.77 |
| 1-04-2 | 30.9 | 1 | 7.24 | 0.24 | 51.72 | 1.2 | 44.48 | 0.97 | 46.09 |
| 1-04-3 | 30.9 | 1 | 6.01 | 0.38 | 47.86 | 1.41 | 41.85 | 1.03 | 40.75 |
| 1-05-1 | 30.7 | 1 | 7.66 | 0.22 | 48.93 | 1.21 | 41.27 | 0.99 | 41.60 |
| 1-05-2 | 30.7 | 1 | 8 | 0.22 | 55.67 | 1.14 | 47.67 | 0.92 | 52.04 |
| 1-05-3 | 32.6 | 1 | 7.61 | 0.18 | 51.76 | 0.89 | 44.16 | 0.71 | 62.63 |
| 1-06-1 | 29.9 | 1 | 7.54 | 0.27 | 52.07 | 1.48 | 44.54 | 1.21 | 36.72 |
| 1-06-2 | 31.1 | 1 | 7.22 | 0.23 | 48.8 | 1.25 | 41.58 | 1.02 | 40.84 |
| 1-06-3 | 44.0 | 1 | 9.34 | 0.27 | 63.38 | 1.39 | 54.05 | 1.12 | 48.38 |
| 1-07-1 | 45.1 | 1 | 9.03 | 0.2 | 62.49 | 1.14 | 53.46 | 0.94 | 56.75 |
| 1-07-2 | 40.9 | 1 | 9.19 | 0.21 | 64.87 | 1.03 | 55.68 | 0.82 | 67.57 |
| 1-07-3 | 42.6 | 1 | 7.39 | 0.2 | 53.08 | 1 | 45.69 | 0.8 | 57.11 |
| 1-08-1 | 42.2 | 2 | 4.64 | 0.46 | 31.75 | 0.97 | 27.11 | 0.52 | 52.54 |
| 1-08-2 | 42.2 | 2 | 4.02 | 0.01 | 32.29 | 0.31 | 28.27 | 0.3 | 94.22 |
| 1-08-3 | 42.4 | 2 | 5.15 | 0.26 | 33.79 | 0.72 | 28.64 | 0.47 | 61.46 |
| 1-09-1 | 42.6 | 2 | 4.27 | 0.43 | 29.4 | 1.06 | 25.14 | 0.63 | 39.90 |
| 1-09-2 | 42.6 | 2 | 5.09 | 0.39 | 35.05 | 0.96 | 29.96 | 0.57 | 52.55 |
| 1-09-3 | 42.6 | 2 | 4.8 | 0.28 | 30.59 | 0.89 | 25.79 | 0.61 | 42.63 |
| 1-10-1 | 42.6 | 2 | 4.61 | 0.28 | 31.9 | 0.91 | 27.29 | 0.63 | 43.67 |
| 1-10-2 | 42.6 | 2 | 4.77 | 0.26 | 32.6 | 0.99 | 27.83 | 0.73 | 38.12 |
| 1-10-3 | 42.6 | 2 | 3.61 | 0.3 | 24.81 | 0.82 | 21.2 | 0.52 | 40.77 |
| 1-11-1 | 42.6 | 2 | 5.55 | 0.18 | 36.14 | 0.95 | 30.59 | 0.77 | 39.62 |
| 1-11-2 | 42.6 | 2 | 5.17 | 0.18 | 35.8 | 0.77 | 30.63 | 0.58 | 52.46 |
| 1-11-3 | 42.6 | 2 | 5.06 | 0.21 | 34.48 | 0.92 | 29.42 | 0.71 | 41.49 |
| 3-01-1 | 46.0 | 2 | 4.85 | 0.1 | 33.08 | 0.59 | 28.23 | 0.49 | 57.73 |
| 3-01-2 | 46.0 | 2 | 5.35 | 0.07 | 37.75 | 0.59 | 32.41 | 0.52 | 62.08 |
| 3-01-3 | 40.4 | 2 | 5.61 | 0.05 | 36.56 | 0.24 | 30.95 | 0.19 | 162.89 |
| 3-02 | 42.6 | 2 | 3.7 | 0.23 | 25.9 | 0.65 | 22.19 | 0.42 | 53.47 |
| NR1-1 | 44.1 | 1 | 7.97 | 0.31 | 55.09 | 1.1 | 47.12 | 0.79 | 59.80 |
| NR1-3 | 44.7 | 1 | 7.17 | 0.3 | 49.39 | 1.04 | 42.22 | 0.74 | 56.90 |
| NR1-2 | 45.7 | 1 | 7.46 | 0.28 | 51.61 | 1.08 | 44.15 | 0.8 | 55.46 |

Table 8.4: Mean values of the elastic stiffness of shear connectors.

| Decking | $n_r$ | $f_{cm}$ | $E_{cm}$ | $c_m$ |
|---|---|---|---|---|
| | [-] | [N/mm$^2$] | [N/mm$^2$] | [kN/(mm · stud)] |
| CP60 | 1 | 30.9 | 30868 | 46.18 |
| | 1 | 43.1 | 34107 | 57.45 |
| CF80 | 2 | 42.8 | 34036 | 58.48 |
| | 1 | 44.8 | 34507 | 57.39 |

45.3kN/mm is obtained:

$$c_{ref} = 46.18 \cdot \sqrt{\frac{30 \cdot 30589}{30.9 \cdot 30868}} = 45.3 \text{ [kN/mm]}$$

The stiffness of each shear connection can then be assumed according to equation (8.2).

$$c = n_r \cdot c_{ref} \cdot \sqrt{f_{cm} E_{cm}} \cdot 10^{-3} \tag{8.2}$$

| | | |
|---|---|---|
| Where: | $c$ | Elastic stiffness of shear connection in [kN/mm] |
| | $n_r$ | Number of studs per deck rib |
| | $c_{ref} = 45.3$ kN/mm | Reference stiffness |
| | $f_{cm}$ | Concrete strength in [N/mm$^2$] |
| | $E_{cm}$ | Young's modulus in [N/mm$^2$] |

The simplified load-displacement curve, shown in Figure 8.27, is then fully described by the resistance, $P$, according to equations (6.35) and (6.36) and the stiffness, $c$, according to equation (8.2). Therefore, it is suitable for the use in engineering offices and for parametric studies. In the following, it is investigated how accurate the analysis with the simplified behaviour is in comparison to more realistic load-slip curves.

Performing the analysis with the simplified spring law utilising the full resistance of the push-out result, $P_{e1}$, would over-estimate the shear resistance in the comparison study. The resistance for the simplified law is slightly reduced to smooth the peak value. Considering the analysis using the push-out behaviour, it was found that all studs exceeding the elastic slip bear in average about 92% of the peak load, $P_{e1}$, as shown in Table 8.5.

Table 8.5: Average shear forces of studs in the plastic part of the load-slip curve using realistic stud behaviour.

| $\frac{1}{n}\sum_{i=1}^{n} P_i/P_{e1}$ | $L = 6.00$ m | $L = 9.00$ m | $L = 12.00$ m |
|---|---|---|---|
| CF80 | 0.94 | 0.88 | 0.89 |
| CP60 | 0.93 | 0.93 | 0.94 |

Figure 8.28 shows the comparison of the results for the analysis with realistic and simplified spring properties for CF80 cases. In these cases, the simplified spring is a conservative estimation of the push test result, but the general characteristics of the two load-slip curves are similar. The results of the analysis show, that the load-displacement behaviour is well approximated with the parametric load-slip curve and is slightly conservative. The slip is accurate until about 5 mm end-slip are reached. This is sufficient to analyse the behaviour of the beam at serviceability limit state. For larger slip at ultimate limit state, the simplified spring leads to slightly conservative values of the end-slip. The concrete compression forces are also slightly conservative for ultimate limit state.

Figure 8.29 shows the comparison of the analysis with simplified and realistic load-slip curves of the studs for CP60 cases. In this case, the simplified spring properties are a very conservative approximation of the push test result and do not benefit from the second load peak. However, the simplified shear connector behaviour is accurate enough to analyse the slip and displacement at serviceability limit state as well as ultimate load of the beams. Only the end slip is very conservative for long span beams.

It can be concluded that the proposed load-slip curve is suitable for the analysis of composite beams in engineering offices. The deflection at serviceability limit state and ultimate load of the composite beam can be analysed. The elastic stiffness of the springs is determined according to equation (8.2). For serviceability limit state, the characteristic shear resistance has to be used and at ultimate limit state the design resistance has to be used. The shear resistance of the stud is given by equations (6.35) and (6.36).

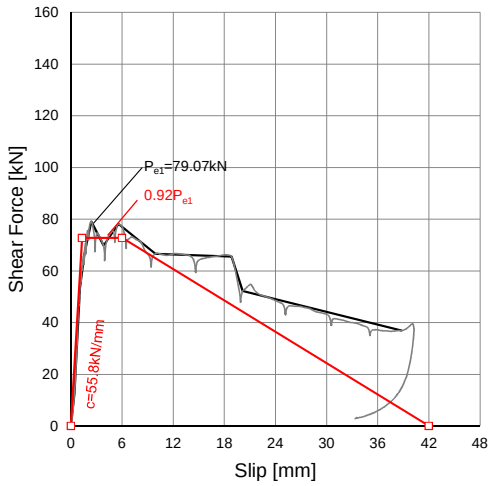


(a) Used spring properties.

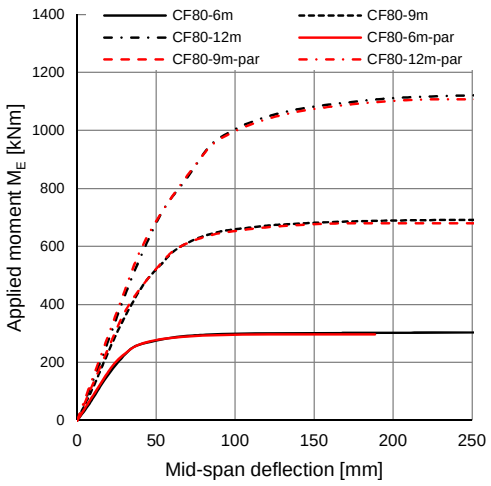


(b) Moment-displacement plot.

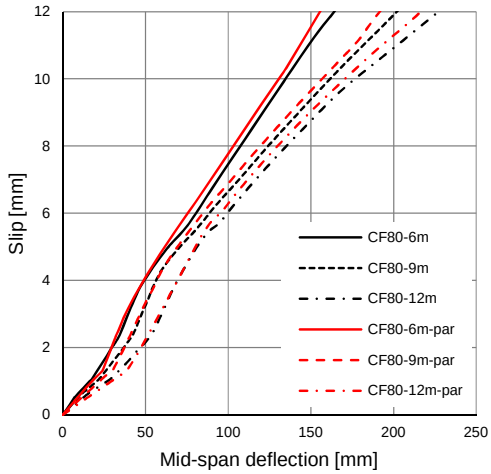


(c) Slip-displacement plot.

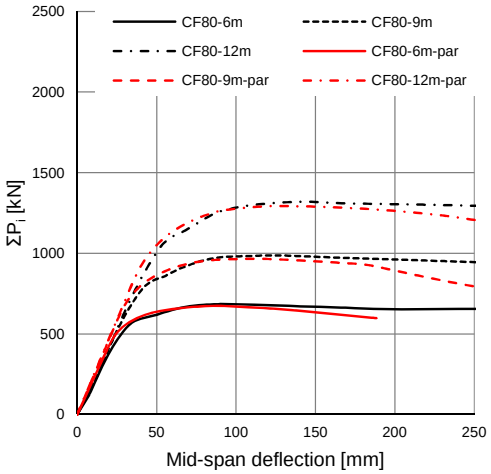


(d) Shear force versus displacement.

Figure 8.28: Comparison of analysis with realistic and simplified load-slip curves for CF80 cases.

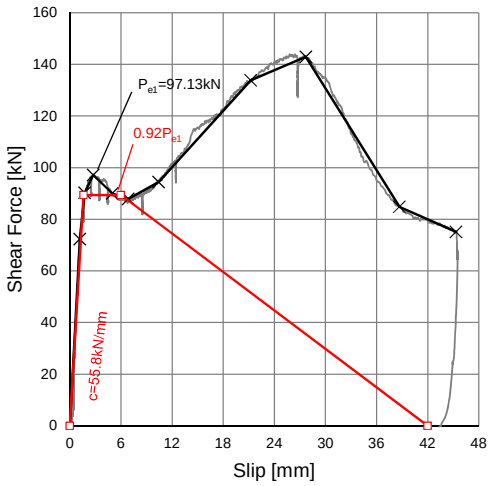


(a) Used spring properties.

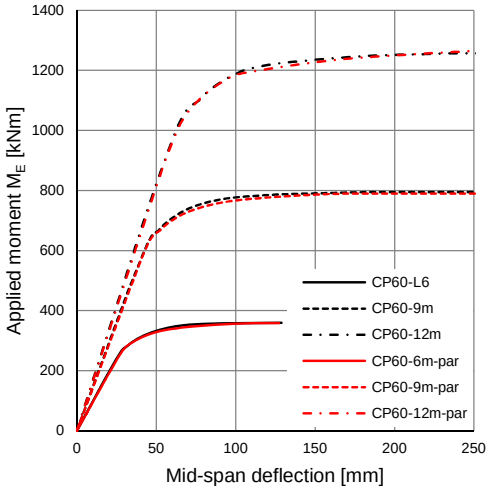


(b) Moment-displacement plot.

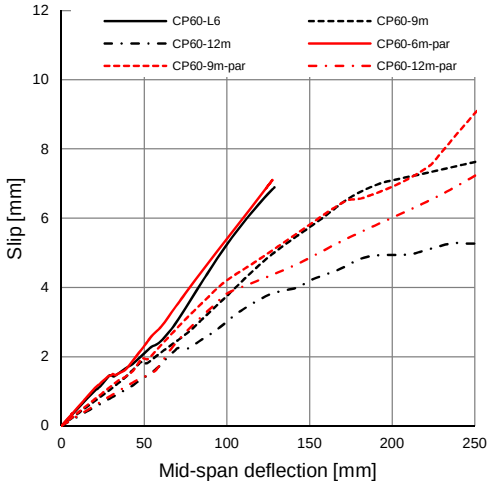


(c) Slip-displacement plot.

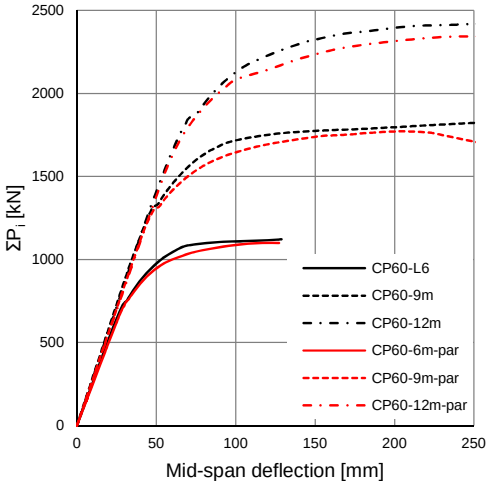


(d) Shear force versus displacement.

Figure 8.29: Comparison of analysis with realistic and simplified load-slip curves for CP60 cases.

# 9 Conclusions

| | |
|---|---|
| Chapter 1 | - Introduction |
| Chapter 2 | - Load-Bearing behaviour of headed shear studs<br>- Test set-ups to investigate the shear connector behaviour<br>- Investigations of the accuracy of existing methods to analyse the shear connector resistance<br>- No method showed a satisfactory correlation with test results<br>- Analysis and design of composite beams |
| Chapter 3 | - Methodology and objectives |
| Chapter 4 | - Degree of transverse loading in ULS analysis<br>- Test set-up for concentric and eccentric transverse loading<br>- Push-out test results<br>- New failure mode of shear connectors: Rib pry-out |
| Chapter 5 | - Characteristic resistance and displacement capacity according to EN 1994-1-1 Annex B<br>- Failure modes depend on geometry of the shear connection<br>- Influence of transverse loading depends on failure modes<br>- Rib pry-out: General improved behaviour<br>- 'Classic' failure modes: Increased displacement capacity<br>- Unsafe analysis of the resistance by existing models |
| Chapter 6 | - Mechanical analysis of shear connector resistance<br>- Bending failure of concrete rib and shear stud<br>- Pure shear failure of the stud shank<br>- Safe resistances and increased field of application |
| Chapter 7 | - Composite beam test results<br>- Analysis of plastic bending resistance verified with new shear connector resistances<br>- Analysis of elastic behaviour verified<br>- Minor exceedance of the limiting slip, even with very low degrees of shear connection |
| Chapter 8 | - Simple model to analyse composite beams with non-linear material and shear connector behaviour<br>- Simple load-slip curve for shear connectors in non-linear analysis<br>- Eventually needed reduction of the shear forces to consider the variability of slip |
| Chapter 9 | - Conclusions |

Figure 9.1: Summary of the presented work and major outcomes.

First qualitative descriptions of the load-bearing behaviour and load-bearing components of shear connectors were developed in the late 1980s. Up to date, they are used to describe the mechanical behaviour of headed shear studs. These simple models already showed, that the load-displacement behaviour strongly differs between studs embedded in solid slabs or in the ribs of composite slabs.

For shear connectors in solid slabs, the load-bearing capacity is well predicted by the rules of [DIN EN 1994-1-1, 2010] or [Konrad, 2011]. When the studs are placed in the ribs of composite slabs, the shear resistance is reduced by an empirical reduction factor. In comparison to experimental results, the analysed resistances are unsafe in many cases. In addition, the coefficients of correlation are unsatisfactory. This is the case, because the really occurring failure modes are not analysed. The mechanical approach on the shear stud resistance according to [Lungershausen, 1988] shows significantly improved results. However, this model is quite restrictive and does not consider important influences like concrete strength or stud position.

The predicted resistances for the newly conducted push-out tests were in general non-conservative. The empirical reduction factors of [DIN EN 1994-1-1, 2010] and [Konrad, 2011] are not well calibrated for the used types of modern steel decking and the mechanical model of [Lungershausen, 1988] is missing important test parameters. Developments in modern steel decking show the tendency to use narrower ribs or deeper decking. The use of very narrow deck ribs leads to the classification of the shear studs as welded in unfavourable position. [Konrad, 2011] investigated the influence of the stud position, but finally proposed reduction factors, where the unfavourable position is not allowed. This puts additional limitations on the geometry of the decking. The rules of [DIN EN 1994-1-1, 2010] and [Lungershausen, 1988] do not consider the stud position at all. The use of deeper decking increases the bending moments acting on the concrete ribs. For shear studs with a small embedment depth of the head of the stud, this resulted in the newly identified failure mode of the shear connection: Rib pry-out failure. All discussed design equations are unsafe for this failure mode.

One major outcome of the conducted push-out tests was that the load-slip behaviour and failure modes depend on the geometry of the shear connection. Furthermore, the investigations on concentric and eccentric transverse loading showed that the observed influence depends on the failure modes. For shear connectors with a 'classic' load-slip behaviour, as described in [Lungershausen, 1988], it was observed that transverse loading has no significant influence on the design resistance. The application of concentric transverse loads decreased the displacement capacity while the more realistic case of eccentric transverse loading strongly increased the displacement capacity of the shear connectors. This effect is especially beneficial when high strength concrete is used. When the new failure mode rib pry-out occurred, the load-displacement behaviour was generally improved. For larger degrees of transverse loading, the shear forces could be increased even after the observation of rib pry-out failure. This is because the post failure behaviour largely relies on friction and aggregate interlock at the concrete failure surface. Because of the increased shear resistance, no influence on the displacement capacity, as defined in [DIN EN 1994-1-1, 2010], was observed. A difference between concentric and eccentric transverse loading was not observed.

Because the shear resistances according to [DIN EN 1994-1-1, 2010], [Konrad, 2011] and [Lungershausen, 1988] were unsafe for the conducted push-out tests, new equations for the shear resistance were developed. Based on the failure modes and shear stud deformation in the push-out tests, mechanical equations were derived. They consider the shear resistance either as a combined bending failure of the concrete rib and stud or as a pure shear failure of the stud. The new equations show improved coefficients of correlation and variation and a significantly increased field of application in comparison to the other methods. The

new equations consider the material properties of the concrete and the shear stud as well as the stud position, but the unfavourable position. Further work on the shear stud resistance could extend the model for the unfavourable position, higher concrete grades or enhanced shear connections, like reinforced ribs. Also, parametric studies on a more accurate differentiation of the yield-chain mechanism may be worth further investigations. The developed equations were calibrated according to [DIN EN 1990, 2002] to analyse the design resistance of the shear connectors. The obtained safety factors of 1.25 and 1.31 are significantly smaller than the safety factor 1.76 that [Roik et al., 1989] determined for the rules of [DIN EN 1994-1-1, 2010]. According to [Roik et al., 1989], the required safety factor for the model in [Lungershausen, 1988] was 1.30, which is similar to the new equations, but with a significantly smaller field of application. The formulae by [Konrad, 2011] required a safety factor of 1.21, but it is more restrictive for the embedment depth of the stud and the width of the deck rib, because of the required welding positions.

The application of the new stud resistances to calculate the plastic bending resistance of the conducted beam tests showed an accuracy of about 2%. The use of the elastic stiffness of the shear connectors obtained in push-out tests led to an accurate analysis of the elastic behaviour of the tests when the flexibility of the shear connection was considered according to [Leskela et al., 2015]. The degrees of shear connection of 0.12 and 0.22 in these tests were much smaller than the minimum degree of shear connection of 0.47. However, the maximum measured end-slip at ultimate load was only 7.1mm. The limiting slip of 6mm was exceeded by only 18%. At 95% of the theoretical bending resistance, the limiting slip was satisfied. Therefore, it is assumable that the minimum degree of shear connection could be reduced.

Future work on the development of new rules for the minimum degree of shear connection will require extensive numerical investigations. This work presented a simple finite element model, that can be utilised for this. The model considers the non-linear behaviour of the materials and shear connection. Therefore, the shear connection is modelled by non-linear springs and a simplified load-displacement curve for the studs was introduced.

Numerical investigations of composite beams using load-slip curves of push-out tests showed that the concrete compression force is over-predicted by about 15%, when it is calculated from the ultimate load of the shear studs. The reason is that every stud has an individual slip. For each slip, a shear force is assigned according to the load-slip curve. This leads to an average value of the shear forces, that is smaller than the studs ultimate load. The consequence of reduced shear forces is a smaller bending resistance. This was not observed in the conducted beam tests. However, the shear connectors used in the tests were very sensitive for transverse loading and may have strongly benefited from local compression close to the supports and loading points. The determination of the concrete compression force therefore needs further investigation. The reduction of the compression force may be influenced by the sensitivity of the studs for transverse loading, the loading conditions of the beam and the slip distribution at the shear interface. In addition, it has to be considered that the concept of partial safety factors already reduces the resistance of the shear connectors. The calibration of the new stud resistances according to [DIN EN 1990, 2002] led to design values which are 38% to 45% smaller than the average resistance. Future work needs to verify if this already leads to a satisfactory safety of the bending resistance of composite beams, or if the shear forces must be further reduced to account for the influence of slip.

# Bibliography


[ASE, 2013] (2013). *ASE General Static Analysis of Finite Element Structures*. SOFiSTiK AG.

[An and Cederwall, 1991] An, L. and Cederwall, K. (1991). Push-out tests on stud connectors in normal and high strength concrete. Technical report, Chalmers University of Technology, Göteborg.

[Bode and Künzel, 1988] Bode, H. and Künzel, R. (1988). Zur Traglast von Verbundträgern unter besonderer Beücksichtigung einer nachgiebigen Verdübelung. Technical report, Universität Kaiserslautern.

[Bullo and Di MArco, 1995] Bullo, S. and Di MArco, R. (1995). Effects of high-performance concrete on shear connector behavior. In *Nordic Steel Concstruction Conference*.

[DIN 1045-1, 2008] DIN 1045-1 (2008). *Tragwerke aus Beton, Stahlbeton und Spannbeton - Teil 1: Bemessung und Konstruktion*.

[DIN 18800-1, 1990] DIN 18800-1 (1990). *Stahlbauten - Teil 1: Bemessung und Konstruktion*.

[DIN 18800-5, 1999] DIN 18800-5 (1999). *Stahlbauten - Teil 5: Verbundtragwerke aus Stahl und Beton. Bemessung und Konstruktion*.

[DIN 18807-1, 1987] DIN 18807-1 (1987). *Trapezprofile im Hochbau; Stahltrapezprofile; Allgemeine Anforderungen, Ermittlung der tragfähigkeitswerte durch Berechnung*.

[DIN EN 1990, 2002] DIN EN 1990 (2002). *Eurocode: Grundlagen der Tragwerksplanung; Deutsche Fassung EN 1990:2002*.

[DIN EN 1991-1-1, 2010] DIN EN 1991-1-1 (2010). *Eurocode 1:Einwirkungen auf Tragwerke - Teil 1-1: Allgemeine Einwirkungen auf Tragwerke - Wichten, Eigengewicht und Nutzlasten im Hochbau; Deutsche Fassung EN 1991-1-1:2002 + AC: 2009*.

[DIN EN 1992-1-1, 2005] DIN EN 1992-1-1 (2005). *Eurocode 2: Bemessung und Konstruktion von Stahlbeton- und Spannbetontragwerken - Teil 1-1: Allgemeine Bemessungsregeln und Regeln für den Hochbau; Deutsche Fassung EN 1992-1-1:2004*.

[DIN EN 1992-1-2, 2006] DIN EN 1992-1-2 (2006). *Eurocode 2: Bemessung und Konstruktion von Stahlbeton- und Spannbetontragwerken - Teil 1-2: Tragwerksbemessung für den Brandfall; Deutsche Fassung EN 1992-1-2:2004*.

[DIN EN 1993-1-1, 2005] DIN EN 1993-1-1 (2005). *Eurocode 3: Bemessung und Konstruktion von Stahlbauten - Teil 1-1: Allgemeine Bemessungsregeln und Regeln für den Hochbau; Deutsche Fassung EN 1993-1-1:2005*.

[DIN EN 1994-1-1, 2010] DIN EN 1994-1-1 (2010). *Eurocode 4: Bemessung und Konstruktion von Verbundtragwerken aus Stahl und Beton - Teil 1-1: Allgemeine Bemessungsregeln und Anwendungsregeln für den Hochbau; Deutsche Fassung EN 1994-1-1:2004 + AC:2009*.

[Döinghaus, 2001] Döinghaus, P. (2001). *Zum Zusammenwirken hochfester Baustoffe in Verbundträgern*. PhD thesis, RWTH Aachen.

[Ernst, 2006] Ernst, S. (2006). *Factors Affecting the Behaviour of the Shear Connection of*

*Steel-Concrete Composite Beams*. PhD thesis, University of Western Sydney.

[Feldmann et al., 2007] Feldmann, M., Hegger, J., Hechler, O., and Rauscher, S. (2007). Untersuchungen zum Trag- und Verformungsverhalten von Verbundmitteln unter ruhender und nichtruhender Belastung bei Verwendung hochfester Werkstoffe. Technical report, RWTH Aachen.

[Hanswille et al., 1998] Hanswille, G., Jost, K., Trillmich, R., and Schmit, C. (1998). Experimentelle Untersuchungen zur Tragfähigkeit von Kopfbolzendübeln mit großen Schaftdurchmessern. *Stahlbau 67*, (7):555–560.

[Hanswille et al., 2006] Hanswille, G., Jost, K., and Üstündag, C. (2006). Versuchsbericht über die Durchführung von 77 Push-Out-Versuchen (Förderzeitraum 2002-2004), Forschungsprojekt: Modellierung von Schädigungsmechanismen zur Beurteilung der Lebensdauer von Verbundkonstruktionen aus Stahl und Beton. Technical report, Bergische Universität Wuppertal.

[Hicks and Smith, 2014] Hicks, S. and Smith, A. (2014). Stud shear connectors in composite beams that support slabs with profiled steel sheeting. *Structural Engineering International*, (2/2014):246–253.

[Hiragi et al., 1981] Hiragi, H., Miyoshi, E., Kurita, A., Ugai, M., and Akao, S. (1981). Static strength of shear stud connectors in src structures. *Transactions of the Japan Concrete Institute*, 3:453–460.

[Konrad, 2011] Konrad, M. (2011). *Tragverhalten von Kopfbolzen in Verbundträgern bei senkrecht spannenden Trapezblechen*. PhD thesis, Institut für Konstruktion und Entwurf, Stahl- Holz- und Verbundbau, Universität Stuttgart.

[Lam, 1998] Lam, D. (1998). *Composite Steel Beams Using Precast Concrete Hollow Core Floor Slabs*. PhD thesis, University of Nottingham.

[Lam et al., 2011] Lam, D., Qureshi, J., and Ye, J. (2011). Effect of shear connector spacing and layout on the shear connector capacity in composite beams. *Journal of Constructional Steel Research*, 67:706–719.

[Leskela et al., 2015] Leskela, M. V., Peltonen, S., and Obiala, R. (2015). Composite action in shallow floor beams with different shear connections. *Steel Construction*, 8(2):90–95.

[Lungershausen, 1988] Lungershausen, H. (1988). *Zur Schubtragfähigkeit von Kopfbolzendübeln*. PhD thesis, Institut für konstruktiven Ingenieurbau, Ruhr-Universität Bochum.

[Mainstone and Menzies, 1967] Mainstone, R. and Menzies, J. B. (1967). Shear connectors in steel-concrete beams for bridges. *Concrete*, 1(9):291–302.

[Menzies, 1971] Menzies, J. B. (1971). Cp117 and shear connectors in steel-concrete composite beams mad with normaldensity or lightweight concrete. *The Structural Engineer*, 49(3):137–154.

[Nellinger et al., 2014] Nellinger, S., Odenbreit, C., and Lawson, M. (May 28-30, 2014). Push-out tests with modern deck sheeting and realistic transverse loading. In *12th International Conference on Steel, Space and Composite Structures: Conference proceedings*.

[Odenbreit et al., 2015] Odenbreit, C., Kuhlman, U., Nellinger, S., and Eggert, F. (2015). Development of Improved Shear Connection Rules in Composite Beams (DISCCO) - Deliverable 1.3: Report on push-out tests.

[Oehlers, 1981] Oehlers, D. J. (1981). Results on 101 push-specimens and composite beams, resear report ce 8. Technical report, University of Warwick.

[Ollgaard and Slutter, 1967] Ollgaard, J. G. and Slutter, R. G. (1967). Shear strength of stud

connectors in lightweight and normal-weight-concrete. *Enginerin Journal, AISC*, pages 55–64.

[Rambo-Roddenberry, 2002] Rambo-Roddenberry, M. D. (2002). *Behaviour and strength of welded stud shear connectors*. PhD thesis, Virginia Polytechnic Institute and State University.

[Roik and Bürkner, 1980] Roik, K. and Bürkner, K.-E. (1980). Untersuchungen des Trägerverbundes unter Verwendung von Stahltrapezprofilblechen mit einer Höhe > 80 mm. Technical report, Studiengesellschaft für Anwendungstechnik von Eisen und Stahl e.V.

[Roik and Bürkner, 1981] Roik, K. and Bürkner, K.-E. (1981). Beitrag zur Tragfähigkeit von Kopfbolzendübeln in Verbundträgern mit Stahlprofilblechen. *Bauingenieur*, 56:97–101.

[Roik and Hanswille, 1983] Roik, K. and Hanswille, G. (1983). Beitrag zur Tragfähigkeit von Kopfbolzendübeln. *Der Stahlbau*, 10:301–308.

[Roik and Hanswille, 1987] Roik, K. and Hanswille, G. (1987). Zur Dauerfestigkeit von Kopfbolzendübeln bei Verbundträgern. *Bauingenieur*, 62:273–285.

[Roik and Hanswille, 1988] Roik, K. and Hanswille, G. (1988). Gutachten für die Holorib GmbH zur Frage der Tragfähigkeit von Kopfbolzendübeln bei auf dem Verbundträger gestoßenen Profilblechen.

[Roik et al., 1989] Roik, K., Hanswille, G., Cunze, O., and Lanna, O. (1989). Report on eurocode 4 - clause 6.3.2: Stud connectors, report ec4/8/88. Technical report, Ruhr-Universität Bochum.

[Roik and Lungershausen, 1988] Roik, K. and Lungershausen, H. (1988). Verbundträger mit Stahltrapezprofilblechen mit Rippenhöhen größer 80 mm. Technical report, Studiengesellschaft für Anwendungstechnik von Eisen und Stahl e.V.

[Smith, 2009] Smith, A. (2009). Effect of key varaibles on shear connector performance using new push rig; report to bcsa task group for long-span composite beams; document rt1236 version 02. Technical report, The Steel Construction Institute.

[Yam, 1983] Yam, L. C. P. (1983). Design of composite steel-concrete structures. *Surrey University Press*.

[Yamato and Nakamura, 1962] Yamato, M. and Nakamura, S. (1962). The study on shear connectors. Technical report, The Public Works Research Institute, Construction Ministry Japan.

# A Push-Out test results with solid slabs

Table A.1: Database of push-out tests with solid slabs

| Nr. | Lit. | ID | Studs $d$ [mm] | Studs $h_{sc}$ [mm] | Studs $f_u$ [N/mm$^2$] | Concrete $f_{cm}$ [N/mm$^2$] | Concrete $E_{c0m}$ [N/mm$^2$] | Concrete $E_{cm}$ [N/mm$^2$] | Results $P_e$ [kN/stud] |
|---|---|---|---|---|---|---|---|---|---|
| 1 | [Ollgaard and Slutter, 1967] | SA1 | 16 | 76 | 493 | 28.2 | 28916[a] | 25200 | 88.5 |
| 2 | [Ollgaard and Slutter, 1967] | SA2 | 16 | 76 | 493 | 28.2 | 28916[a] | 25200 | 94.4 |
| 3 | [Ollgaard and Slutter, 1967] | SA3 | 16 | 76 | 493 | 28.2 | 28916[a] | 25200 | 90.3 |
| 4 | [Ollgaard and Slutter, 1967] | SB1 | 16 | 76 | 493 | 28.3 | 28950[a] | 22300 | 82.6 |
| 5 | [Ollgaard and Slutter, 1967] | SB2 | 16 | 76 | 493 | 28.3 | 28950[a] | 22300 | 76.7 |
| 6 | [Ollgaard and Slutter, 1967] | SB3 | 16 | 76 | 493 | 28.3 | 28950[a] | 22300 | 85.3 |
| 7 | [Ollgaard and Slutter, 1967] | A1 | 19 | 76 | 499 | 35.7 | 31281[a] | 26300 | 132.9 |
| 8 | [Ollgaard and Slutter, 1967] | A2 | 19 | 76 | 499 | 35.7 | 31281[a] | 26300 | 147.4 |
| 9 | [Ollgaard and Slutter, 1967] | A3 | 19 | 76 | 499 | 35.7 | 31281[a] | 26300 | 138.8 |
| 10 | [Ollgaard and Slutter, 1967] | LA1 | 19 | 76 | 499 | 25.6 | 27999[a] | 24700 | 111.1 |
| 11 | [Ollgaard and Slutter, 1967] | LA2 | 19 | 76 | 499 | 25.6 | 27999[a] | 24700 | 120.2 |
| 12 | [Ollgaard and Slutter, 1967] | LA3 | 19 | 76 | 499 | 25.6 | 27999[a] | 24700 | 112.0 |
| 13 | [Ollgaard and Slutter, 1967] | B1 | 19 | 76 | 499 | 33.6 | 30655[a] | 22400 | 124.3 |
| 14 | [Ollgaard and Slutter, 1967] | B2 | 19 | 76 | 499 | 33.6 | 30655[a] | 22400 | 115.2 |
| 15 | [Ollgaard and Slutter, 1967] | B3 | 19 | 76 | 499 | 33.6 | 30655[a] | 22400 | 115.2 |
| 16 | [Ollgaard and Slutter, 1967] | LB1 | 19 | 76 | 499 | 18.8 | 25261[a] | 15400 | 83.0 |
| 17 | [Ollgaard and Slutter, 1967] | LB2 | 19 | 76 | 499 | 18.8 | 25261[a] | 15400 | 82.1 |
| 18 | [Ollgaard and Slutter, 1967] | LB3 | 19 | 76 | 499 | 18.8 | 25261[a] | 15400 | 78.5 |
| 19 | [Ollgaard and Slutter, 1967] | 2B1 | 19 | 76 | 499 | 33.6 | 30655[a] | 22400 | 118.4 |
| 20 | [Ollgaard and Slutter, 1967] | 2B2 | 19 | 76 | 499 | 33.6 | 30655[a] | 22400 | 115.7 |
| 21 | [Ollgaard and Slutter, 1967] | 2B3 | 19 | 76 | 499 | 33.6 | 30655[a] | 22400 | 113.4 |
| 22 | [Mainstone and Menzies, 1967] | S3 | 19 | 100 | 600 | 29.0 | 29187[a] | 25273[a] | 96.2 |
| 23 | [Mainstone and Menzies, 1967] | S4 | 19 | 100 | 600 | 28.3 | 28950[a] | 25022[a] | 100.1 |
| 24 | [Mainstone and Menzies, 1967] | S5 | 19 | 100 | 600 | 27.7 | 28744[a] | 24805[a] | 106.7 |
| 25 | [Mainstone and Menzies, 1967] | S6 | 19 | 100 | 600 | 29.1 | 29221[a] | 25309[a] | 126.2 |
| 26 | [Mainstone and Menzies, 1967] | S8 | 19 | 100 | 600 | 30.7 | 29747[a] | 25873[a] | 121.4 |
| 27 | [Mainstone and Menzies, 1967] | S11 | 19 | 100 | 600 | 29.6 | 29387[a] | 25486[a] | 112.7 |
| 28 | [Mainstone and Menzies, 1967] | S16 | 19 | 100 | 600 | 31.3 | 29939[a] | 26081[a] | 115.0 |
| 29 | [Mainstone and Menzies, 1967] | S19 | 19 | 100 | 600 | 32.0 | 30161[a] | 26322[a] | 115.0 |
| 30 | [Mainstone and Menzies, 1967] | S22 | 19 | 100 | 600 | 34.7 | 30986[a] | 27233[a] | 106.9 |
| 31 | [Mainstone and Menzies, 1967] | S26 | 19 | 100 | 600 | 24.9 | 27741[a] | 23763[a] | 99.1 |
| 32 | [Mainstone and Menzies, 1967] | S29 | 19 | 100 | 600 | 27.1 | 28535[a] | 24586[a] | 104.1 |
| 33 | [Menzies, 1971] | P1 | 19 | 100 | 600 | 16.6 | 24234[a] | 20302[a] | 97.5 |
| 34 | [Menzies, 1971] | P2 | 19 | 100 | 600 | 16.6 | 24234[a] | 20302[a] | 96.5 |
| 35 | [Menzies, 1971] | P3 | 19 | 100 | 600 | 16.6 | 24234[a] | 20302[a] | 97.0 |
| 36 | [Menzies, 1971] | P4 | 19 | 100 | 600 | 40.8 | 32705[a] | 29196[a] | 127.0 |
| 37 | [Menzies, 1971] | P5 | 19 | 100 | 600 | 40.8 | 32705[a] | 29196[a] | 127.0 |
| 38 | [Menzies, 1971] | P6 | 19 | 100 | 600 | 40.8 | 32705[a] | 29196[a] | 127.0 |
| 39 | [Roik and Hanswille, 1983] | T1/1 | 19 | 100 | 460 | 36.7 | 31570[a] | 27890[a] | 144.5 |
| 40 | [Roik and Hanswille, 1983] | T1/2 | 19 | 100 | 460 | 36.7 | 31570[a] | 27890[a] | 147.8 |
| 41 | [Roik and Hanswille, 1983] | T1/3 | 19 | 100 | 460 | 36.7 | 31570[a] | 27890[a] | 135.5 |
| 42 | [Roik and Hanswille, 1983] | T1/4 | 19 | 100 | 460 | 38.3 | 32023[a] | 28405[a] | 148.9 |
| 43 | [Roik and Hanswille, 1983] | T1/5 | 19 | 100 | 460 | 38.3 | 32023[a] | 28405[a] | 137.8 |
| 44 | [Roik and Hanswille, 1983] | T3/1 | 19 | 100 | 460 | 44.7 | 33715[a] | 30397[a] | 140.1 |
| 45 | [Roik and Hanswille, 1983] | T3/2 | 19 | 100 | 460 | 44.7 | 33715[a] | 30397[a] | 154.1 |
| 46 | [Roik and Hanswille, 1983] | T4/1 | 19 | 100 | 460 | 44.7 | 33715[a] | 30397[a] | 137.3 |
| 47 | [Roik and Hanswille, 1983] | T4/2 | 19 | 100 | 460 | 44.7 | 33715[a] | 30397[a] | 133.7 |
| 48 | [Roik and Hanswille, 1983] | T4/3 | 19 | 100 | 460 | 44.7 | 33715[a] | 30397[a] | 137.7 |
| 49 | [Roik and Hanswille, 1983] | T2/1 | 22 | 100 | 471 | 36.3 | 31455[a] | 27759[a] | 170.1 |
| 50 | [Roik and Hanswille, 1983] | T2/2 | 22 | 100 | 471 | 36.3 | 31455[a] | 27759[a] | 168.1 |
| 51 | [Roik and Hanswille, 1983] | T2/3 | 22 | 100 | 471 | 36.3 | 31455[a] | 27759[a] | 165.9 |
| 52 | [Roik and Hanswille, 1983] | T2/4 | 22 | 100 | 471 | 36.3 | 31455[a] | 27759[a] | 170.6 |
| 53 | [Roik and Hanswille, 1983] | T2/5 | 22 | 100 | 471 | 36.3 | 31455[a] | 27759[a] | 168.8 |
| 54 | [Roik and Hanswille, 1983] | T5/1 | 22 | 100 | 471 | 59.0 | 36983[a] | 34546[a] | 176.3 |
| 55 | [Roik and Hanswille, 1983] | T5/2 | 22 | 100 | 471 | 59.0 | 36983[a] | 34546[a] | 177.5 |

[a] According to [DIN 1045-1, 2008]

*Continued on next page*

Table A.1 – *Continued from previous page*

| Nr. | Lit. | ID | Studs $d$ [mm] | Studs $h_{sc}$ [mm] | Studs $f_u$ [N/mm$^2$] | Concrete $f_{cm}$ [N/mm$^2$] | Concrete $E_{c0m}$ [N/mm$^2$] | Concrete $E_{cm}$ [N/mm$^2$] | Results $P_e$ [kN/stud] |
|---|---|---|---|---|---|---|---|---|---|
| 56 | [Roik and Hanswille, 1983] | T6/1 | 22 | 100 | 471 | 57.3 | 36625[a] | 34069[a] | 166.1 |
| 57 | [Roik and Hanswille, 1983] | T6/2 | 22 | 100 | 471 | 57.3 | 36625[a] | 34069[a] | 159.9 |
| 58 | [Roik and Hanswille, 1983] | T6/3 | 22 | 100 | 471 | 57.3 | 36625[a] | 34069[a] | 177.9 |
| 59 | [Yamato and Nakamura, 1962] | D1/1 | 16 | 100 | 580 | 30.2 | 29584[a] | 25698[a] | 99.0 |
| 60 | [Yamato and Nakamura, 1962] | D1/2 | 16 | 100 | 580 | 30.2 | 29584[a] | 25698[a] | 94.0 |
| 61 | [Yamato and Nakamura, 1962] | D2/1 | 19 | 100 | 500 | 30.2 | 29584[a] | 25698[a] | 123.0 |
| 62 | [Yamato and Nakamura, 1962] | D2/2 | 19 | 100 | 500 | 30.2 | 29584[a] | 25698[a] | 128.8 |
| 63 | [Yamato and Nakamura, 1962] | D2/3 | 19 | 100 | 500 | 30.2 | 29584[a] | 25698[a] | 126.5 |
| 64 | [Yamato and Nakamura, 1962] | D3/1 | 22 | 120 | 548 | 30.2 | 29584[a] | 25698[a] | 148.5 |
| 65 | [Yamato and Nakamura, 1962] | D3/2 | 22 | 120 | 548 | 30.2 | 29584[a] | 25698[a] | 148.0 |
| 66 | [Yamato and Nakamura, 1962] | D3/3 | 22 | 120 | 548 | 30.2 | 29584[a] | 25698[a] | 146.8 |
| 67 | [Hiragi et al., 1981] | 2A | 19 | 70 | 485 | 40.3 | 32571[a] | 29040[a] | 141.0 |
| 68 | [Hiragi et al., 1981] | 3A | 19 | 100 | 485 | 39.1 | 32244[a] | 28661[a] | 166.0 |
| 69 | [Hiragi et al., 1981] | 4A | 19 | 100 | 485 | 47.1 | 34308[a] | 31119[a] | 160.0 |
| 70 | [Hiragi et al., 1981] | 5A | 19 | 100 | 485 | 57.5 | 36667[a] | 34126[a] | 172.0 |
| 71 | [Feldmann et al., 2007] | K-22.1 | 22 | 98.2 | 546 | 109.5 | 45449[a] | 39800 | 253.4 |
| 72 | [Feldmann et al., 2007] | K-22.2 | 22 | 97.9 | 546 | 110.0 | 45518[a] | 40800 | 243.3 |
| 73 | [Feldmann et al., 2007] | K-22.3 | 22 | 97.9 | 546 | 110.0 | 45518[a] | 40800 | 249.4 |
| 74 | [Feldmann et al., 2007] | RK-22.1 | 22 | 98.3 | 546 | 107.6 | 45185[a] | 46500 | 239.8 |
| 75 | [Feldmann et al., 2007] | A0-22.1 | 22 | 97.9 | 546 | 101.1 | 44256[a] | 38500 | 269.9 |
| 76 | [Feldmann et al., 2007] | A0-22.2 | 22 | 97.4 | 546 | 104.6 | 44761[a] | 38900 | 247.8 |
| 77 | [Feldmann et al., 2007] | A0-22.3 | 22 | 98.6 | 546 | 104.6 | 44761[a] | 38900 | 252.5 |
| 78 | [Feldmann et al., 2007] | A3-25.1 | 25 | 99.6 | 554 | 103.3 | 44575[a] | 42600 | 318.9 |
| 79 | [Feldmann et al., 2007] | A3-25.2 | 25 | 99.7 | 554 | 103.3 | 44575[a] | 42600 | 312.8 |
| 80 | [Feldmann et al., 2007] | A3-25.3 | 25 | 99.7 | 554 | 102.7 | 44488[a] | 44488[a] | 310.2 |
| 81 | [Feldmann et al., 2007] | S-19.1 | 19 | 76.6 | 537 | 106.8 | 45073[a] | 40150 | 133.8 |
| 82 | [Feldmann et al., 2007] | S-19.2 | 19 | 76.6 | 537 | 106.8 | 45073[a] | 40150 | 138.3 |
| 83 | [Feldmann et al., 2007] | S-19.3 | 19 | 75.3 | 537 | 106.8 | 45073[a] | 40150 | 143.3 |
| 84 | [Feldmann et al., 2007] | S-22.1 | 22 | 98.6 | 546 | 106.8 | 45073[a] | 40150 | 201.3 |
| 85 | [Feldmann et al., 2007] | S-22.2 | 22 | 99.4 | 546 | 106.8 | 45073[a] | 40150 | 188.5 |
| 86 | [Feldmann et al., 2007] | S-22.3 | 22 | 98.3 | 546 | 106.8 | 45073[a] | 40150 | 207.0 |
| 87 | [Feldmann et al., 2007] | A2-19-W.1 | 19 | 77.5 | 537 | 101.6 | 44329[a] | 39800 | 211.2 |
| 88 | [Feldmann et al., 2007] | A2-19-W.2 | 19 | 77.2 | 537 | 107.0 | 45101[a] | 41700 | 208.7 |
| 89 | [Feldmann et al., 2007] | A2-19-W.3 | 19 | 77.3 | 537 | 107.0 | 45101[a] | 41700 | 200.8 |
| 90 | [Feldmann et al., 2007] | S-19-W.1 | 19 | 76.6 | 537 | 106.8 | 45073[a] | 40150 | 160.3 |
| 91 | [Feldmann et al., 2007] | S-19-W.2 | 19 | 76.6 | 537 | 106.8 | 45073[a] | 40150 | 149.1 |
| 92 | [Feldmann et al., 2007] | S-19-W.3 | 19 | 75.3 | 537 | 106.8 | 45073[a] | 40150 | 150.8 |
| 93 | [Feldmann et al., 2007] | S-22-oW.1 | 22 | 98.3 | 546 | 94.9 | 43332[a] | 40150 | 185.7 |
| 94 | [Feldmann et al., 2007] | S-22-oW.2 | 22 | 98.3 | 546 | 94.9 | 43332[a] | 40150 | 178.5 |
| 95 | [Feldmann et al., 2007] | S-22-oW.3 | 22 | 98.3 | 546 | 94.9 | 43332[a] | 40150 | 184.1 |
| 96 | [Feldmann et al., 2007] | U-22.1 | 22 | 98.5 | 546 | 100.7 | 44198[a] | 38800 | 256.6 |
| 97 | [Feldmann et al., 2007] | U-22.2 | 22 | 98.9 | 546 | 96.2 | 43529[a] | 38500 | 252.4 |
| 98 | [Feldmann et al., 2007] | U-22.3 | 22 | 97.7 | 546 | 101.1 | 44256[a] | 38500 | 264.4 |
| 99 | [Feldmann et al., 2007] | A460 | 22 | 96 | 764 | 108.4 | 45297[a] | 42800 | 272.2 |
| 100 | [Feldmann et al., 2007] | A690.1 | 22 | 96 | 823 | 119.4 | 46780[a] | 43200 | 250.7 |
| 101 | [Feldmann et al., 2007] | A690.2 | 22 | 96.1 | 823 | 119.4 | 46780[a] | 43200 | 287.0 |
| 102 | [Feldmann et al., 2007] | A690.3 | 22 | 96 | 823 | 119.4 | 46780[a] | 43200 | 290.1 |
| 103 | [Feldmann et al., 2007] | DDS-22.1 | 22 | 97.8 | 546 | 107.6 | 45185[a] | 45600 | 236.4 |
| 104 | [Feldmann et al., 2007] | DDS-22.2 | 22 | 98.1 | 546 | 118.4 | 46649[a] | 42500 | 230.9 |
| 105 | [Feldmann et al., 2007] | DDS-22.3 | 22 | 98.4 | 546 | 118.4 | 46649[a] | 42500 | 222.3 |
| 106 | [Feldmann et al., 2007] | DDF-22.1 | 22 | 98 | 546 | 107.6 | 45185[a] | 45600 | 192.2 |
| 107 | [Feldmann et al., 2007] | DDF-22.2 | 22 | 97.6 | 546 | 107.9 | 45227[a] | 45600 | 196.7 |
| 108 | [Feldmann et al., 2007] | DDF-22.3 | 22 | 98.3 | 546 | 118.4 | 46649[a] | 42500 | 208.4 |
| 109 | [Rambo-Roddenberry, 2002] | 1.1 | 19 | 101.6 | 447.5 | 23.7 | 27288[a] | 23300[a] | 114.6 |
| 110 | [Rambo-Roddenberry, 2002] | 1.2 | 19 | 101.6 | 447.5 | 23.7 | 27288[a] | 23300[a] | 128.2 |
| 111 | [Rambo-Roddenberry, 2002] | 1.3 | 19 | 101.6 | 447.5 | 23.7 | 27288[a] | 23300[a] | 113.7 |
| 112 | [Rambo-Roddenberry, 2002] | 2.4 | 19 | 101.6 | 447.5 | 23.7 | 27288[a] | 23300[a] | 126.4 |
| 113 | [Rambo-Roddenberry, 2002] | 2.5 | 19 | 101.6 | 447.5 | 23.7 | 27288[a] | 23300[a] | 112.1 |
| 114 | [Rambo-Roddenberry, 2002] | 2.6 | 19 | 101.6 | 447.5 | 23.7 | 27288[a] | 23300[a] | 115.0 |
| 115 | [Rambo-Roddenberry, 2002] | 3.7 | 19 | 101.6 | 447.5 | 23.7 | 27288[a] | 23300[a] | 101.8 |
| 116 | [Rambo-Roddenberry, 2002] | 3.8 | 19 | 101.6 | 447.5 | 23.7 | 27288[a] | 23300[a] | 118.6 |
| 117 | [Rambo-Roddenberry, 2002] | 3.9 | 19 | 101.6 | 447.5 | 23.7 | 27288[a] | 23300[a] | 114.4 |
| 118 | [Rambo-Roddenberry, 2002] | 4.10 | 19 | 101.6 | 447.5 | 23.7 | 27288[a] | 23300[a] | 115.8 |
| 119 | [Rambo-Roddenberry, 2002] | 4.11 | 19 | 101.6 | 447.5 | 23.7 | 27288[a] | 23300[a] | 113.0 |
| 120 | [Rambo-Roddenberry, 2002] | 4.12 | 19 | 101.6 | 447.5 | 23.7 | 27288[a] | 23300[a] | 108.5 |
| 121 | [Rambo-Roddenberry, 2002] | 5.13 | 19 | 101.6 | 447.5 | 32.2 | 30223[a] | 26390[a] | 106.9 |
| 122 | [Rambo-Roddenberry, 2002] | 5.14 | 19 | 101.6 | 447.5 | 32.2 | 30223[a] | 26390[a] | 109.4 |

[a] According to [DIN 1045-1, 2008]

*Continued on next page*

Table A.1 – *Continued from previous page*

| Nr. | Lit. | ID | Studs $d$ [mm] | $h_{sc}$ [mm] | $f_u$ [N/mm$^2$] | Concrete $f_{cm}$ [N/mm$^2$] | $E_{c0m}$ [N/mm$^2$] | $E_{cm}$ [N/mm$^2$] | Results $P_e$ [kN/stud] |
|---|---|---|---|---|---|---|---|---|---|
| 123 | [Rambo-Roddenberry, 2002] | 5.15 | 19 | 101.6 | 447.5 | 32.2 | 30223[a] | 26390[a] | 101.2 |
| 124 | [Rambo-Roddenberry, 2002] | 6.16 | 19 | 101.6 | 447.5 | 32.2 | 30223[a] | 26390[a] | 109.4 |
| 125 | [Rambo-Roddenberry, 2002] | 6.17 | 19 | 101.6 | 447.5 | 32.2 | 30223[a] | 26390[a] | 106.9 |
| 126 | [Rambo-Roddenberry, 2002] | 6.18 | 19 | 101.6 | 447.5 | 32.2 | 30223[a] | 26390[a] | 114.6 |
| 127 | [Rambo-Roddenberry, 2002] | 7.19 | 19 | 101.6 | 447.5 | 33.6 | 30655[a] | 26865[a] | 132.2 |
| 128 | [Rambo-Roddenberry, 2002] | 7.20 | 19 | 101.6 | 447.5 | 33.6 | 30655[a] | 26865[a] | 127.4 |
| 129 | [Rambo-Roddenberry, 2002] | 7.21 | 19 | 101.6 | 447.5 | 33.6 | 30655[a] | 26865[a] | 132.2 |
| 130 | [Rambo-Roddenberry, 2002] | 8.22 | 19 | 101.6 | 447.5 | 33.6 | 30655[a] | 26865[a] | 104.9 |
| 131 | [Rambo-Roddenberry, 2002] | 8.23 | 19 | 101.6 | 447.5 | 33.6 | 30655[a] | 26865[a] | 118.6 |
| 132 | [Rambo-Roddenberry, 2002] | 8.24 | 19 | 101.6 | 447.5 | 33.6 | 30655[a] | 26865[a] | 119.2 |
| 133 | [Döinghaus, 2001] | 1/1 | 19 | 80 | 550 | 93.6 | 43134[a] | 43134[a] | 140.4 |
| 134 | [Döinghaus, 2001] | 1/2 | 19 | 80 | 550 | 93.6 | 43134[a] | 43134[a] | 139.8 |
| 135 | [Döinghaus, 2001] | 1/3 | 19 | 80 | 550 | 93.6 | 43134[a] | 43134[a] | 146.9 |
| 136 | [Döinghaus, 2001] | 2/1 | 22 | 100 | 530 | 95.7 | 43454[a] | 43454[a] | 197.2 |
| 137 | [Döinghaus, 2001] | 2/2 | 22 | 100 | 530 | 95.7 | 43454[a] | 43454[a] | 190.9 |
| 138 | [Döinghaus, 2001] | 2/3 | 22 | 100 | 530 | 95.7 | 43454[a] | 43454[a] | 200.7 |
| 139 | [Döinghaus, 2001] | 3/1 | 25 | 120 | 450 | 96.7 | 43605[a] | 43605[a] | 226.0 |
| 140 | [Döinghaus, 2001] | 3/2 | 25 | 120 | 450 | 96.7 | 43605[a] | 43605[a] | 237.3 |
| 141 | [Döinghaus, 2001] | 3/3 | 25 | 120 | 450 | 96.7 | 43605[a] | 43605[a] | 226.9 |
| 142 | [Döinghaus, 2001] | 9/1 | 19 | 80 | 557 | 98.1 | 43814[a] | 43814[a] | 183.9 |
| 143 | [Döinghaus, 2001] | 9/2 | 19 | 80 | 557 | 98.1 | 43814[a] | 43814[a] | 168.2 |
| 144 | [Döinghaus, 2001] | 10/1 | 22 | 100 | 531 | 98.4 | 43859[a] | 43859[a] | 246.6 |
| 145 | [Döinghaus, 2001] | 10/2 | 22 | 100 | 531 | 98.4 | 43859[a] | 43859[a] | 244.0 |
| 146 | [Döinghaus, 2001] | 10/3 | 22 | 100 | 531 | 98.4 | 43859[a] | 43859[a] | 235.5 |
| 147 | [Döinghaus, 2001] | 11/1 | 19 | 80 | 557 | 68.6 | 38889[a] | 37175[a] | 171.2 |
| 148 | [Döinghaus, 2001] | 11/2 | 19 | 80 | 557 | 68.6 | 38889[a] | 37175[a] | 162.5 |
| 149 | [Döinghaus, 2001] | 11/3 | 19 | 80 | 557 | 68.6 | 38889[a] | 37175[a] | 155.2 |
| 150 | [Döinghaus, 2001] | 12/1 | 22 | 100 | 531 | 68.6 | 38889[a] | 37175[a] | 216.1 |
| 151 | [Döinghaus, 2001] | 12/2 | 22 | 100 | 531 | 68.6 | 38889[a] | 37175[a] | 211.0 |
| 152 | [Döinghaus, 2001] | 12/3 | 22 | 100 | 531 | 68.6 | 38889[a] | 37175[a] | 218.2 |
| 153 | [Döinghaus, 2001] | 13/1 | 25 | 120 | 452 | 73.1 | 39722[a] | 38377[a] | 210.9 |
| 154 | [Döinghaus, 2001] | 13/2 | 25 | 120 | 452 | 73.1 | 39722[a] | 38377[a] | 225.1 |
| 155 | [Döinghaus, 2001] | 13/4 | 25 | 120 | 452 | 73.1 | 39722[a] | 38377[a] | 254.4 |
| 156 | [Döinghaus, 2001] | 14/1 | 19 | 80 | 557 | 73.1 | 39722[a] | 38377[a] | 147.0 |
| 157 | [Döinghaus, 2001] | 14/2 | 19 | 80 | 557 | 73.1 | 39722[a] | 38377[a] | 156.6 |
| 158 | [Döinghaus, 2001] | 14/3 | 19 | 80 | 557 | 73.1 | 39722[a] | 38377[a] | 161.7 |
| 159 | [Döinghaus, 2001] | 27/1 | 19 | 80 | 557 | 75.7 | 40187[a] | 39064[a] | 157.0 |
| 160 | [Döinghaus, 2001] | 27/2 | 19 | 80 | 557 | 75.7 | 40187[a] | 39064[a] | 159.8 |
| 161 | [Döinghaus, 2001] | 27/3 | 19 | 80 | 557 | 75.7 | 40187[a] | 39064[a] | 138.5 |
| 162 | [Döinghaus, 2001] | 25/1 | 22 | 100 | 554 | 91.0 | 42730[a] | 42730[a] | 240.5 |
| 163 | [Döinghaus, 2001] | 25/2 | 22 | 100 | 554 | 91.0 | 42730[a] | 42730[a] | 235.0 |
| 164 | [Döinghaus, 2001] | 25/3 | 22 | 100 | 554 | 91.0 | 42730[a] | 42730[a] | 216.3 |
| 165 | [Döinghaus, 2001] | 34/1 | 19 | 80 | 721 | 75.9 | 40223[a] | 39117[a] | 180.6 |
| 166 | [Döinghaus, 2001] | 34/2 | 19 | 80 | 721 | 75.9 | 40223[a] | 39117[a] | 176.8 |
| 167 | [Döinghaus, 2001] | 34/3 | 19 | 80 | 721 | 75.9 | 40223[a] | 39117[a] | 179.8 |
| 168 | [Döinghaus, 2001] | 35/1 | 19 | 80 | 721 | 80.7 | 41053[a] | 40372[a] | 191.6 |
| 169 | [Döinghaus, 2001] | 35/2 | 19 | 80 | 721 | 80.7 | 41053[a] | 40372[a] | 201.0 |
| 170 | [Döinghaus, 2001] | 35/3 | 19 | 80 | 721 | 80.7 | 41053[a] | 40372[a] | 195.0 |
| 171 | [Oehlers, 1981] | RSs1 | 19 | 100 | 620 | 27.0 | 28500[a] | 24549[a] | 135.0 |
| 172 | [Oehlers, 1981] | RSs2 | 19 | 100 | 620 | 27.0 | 28500[a] | 24549[a] | 133.0 |
| 173 | [Oehlers, 1981] | RSs3 | 19 | 100 | 620 | 21.8 | 26538[a] | 22546[a] | 122.0 |
| 174 | [Oehlers, 1981] | RSs4 | 19 | 100 | 620 | 21.8 | 26538[a] | 22546[a] | 131.0 |
| 175 | [Oehlers, 1981] | RSs5 | 19 | 100 | 620 | 25.5 | 27962[a] | 23990[a] | 133.0 |
| 176 | [Oehlers, 1981] | RSs6 | 19 | 100 | 620 | 25.5 | 27962[a] | 23990[a] | 142.0 |
| 177 | [Hanswille et al., 1998] | I/1 | 25 | 125 | 468.2 | 23.7 | 27288[a] | 29445 | 179.5 |
| 178 | [Hanswille et al., 1998] | I/2 | 25 | 125 | 468.2 | 23.7 | 27288[a] | 29445 | 183.0 |
| 179 | [Hanswille et al., 1998] | I/3 | 25 | 125 | 468.2 | 23.7 | 27288[a] | 29445 | 180.4 |
| 180 | [Hanswille et al., 1998] | I/4 | 25 | 125 | 468.2 | 23.7 | 27288[a] | 29445 | 183.1 |
| 181 | [Hanswille et al., 1998] | I/5 | 25 | 125 | 468.2 | 23.7 | 27288[a] | 29445 | 178.6 |
| 182 | [Hanswille et al., 1998] | II/1 | 25 | 125 | 468.2 | 41.3 | 32838[a] | 34687 | 233.0 |
| 183 | [Hanswille et al., 1998] | II/2 | 25 | 125 | 468.2 | 41.3 | 32838[a] | 34687 | 238.0 |
| 184 | [Hanswille et al., 1998] | II/3 | 25 | 125 | 468.2 | 41.3 | 32838[a] | 34687 | 234.9 |
| 185 | [Hanswille et al., 1998] | II/4 | 25 | 125 | 468.2 | 41.3 | 32838[a] | 34687 | 243.5 |
| 186 | [Hanswille et al., 1998] | II/5 | 25 | 125 | 468.2 | 41.3 | 32838[a] | 34687 | 232.8 |
| 187 | [Hanswille et al., 2006] | S1-1a | 22 | 125 | 528 | 44.2 | 33589[a] | 36400 | 191.3 |
| 188 | [Hanswille et al., 2006] | S1-1b | 22 | 125 | 528 | 49.0 | 34763[a] | 36400 | 211.3 |
| 189 | [Hanswille et al., 2006] | S1-1c | 22 | 125 | 528 | 49.7 | 34928[a] | 36400 | 213.0 |

[a] According to [DIN 1045-1, 2008]

*Continued on next page*

Table A.1 – *Continued from previous page*

| Nr. | Lit. | ID | Studs $d$ [mm] | Studs $h_{sc}$ [mm] | Studs $f_u$ [N/mm$^2$] | Concrete $f_{cm}$ [N/mm$^2$] | Concrete $E_{c0m}$ [N/mm$^2$] | Concrete $E_{cm}$ [N/mm$^2$] | Results $P_e$ [kN/stud] |
|---|---|---|---|---|---|---|---|---|---|
| 190 | [Hanswille et al., 2006] | S2-1a | 22 | 125 | 528 | 44.7 | 33715[a] | 33800 | 201.3 |
| 191 | [Hanswille et al., 2006] | S2-1b | 22 | 125 | 528 | 42.8 | 33231[a] | 33800 | 173.3 |
| 192 | [Hanswille et al., 2006] | S2-1c | 22 | 125 | 528 | 42.8 | 33231[a] | 33800 | 175.3 |
| 193 | [Hanswille et al., 2006] | S3-1a | 22 | 125 | 528 | 56.2 | 36389[a] | 39000 | 216.0 |
| 194 | [Hanswille et al., 2006] | S3-1b | 22 | 125 | 528 | 53.9 | 35886[a] | 39000 | 200.6 |
| 195 | [Hanswille et al., 2006] | S3-1c | 22 | 125 | 528 | 53.9 | 35886[a] | 39000 | 201.0 |
| 196 | [Hanswille et al., 2006] | S4-1a | 22 | 125 | 528 | 43.4 | 33385[a] | 33900 | 186.8 |
| 197 | [Hanswille et al., 2006] | S4-1b | 22 | 125 | 528 | 43.4 | 33385[a] | 33900 | 176.5 |
| 198 | [Hanswille et al., 2006] | S4-1c | 22 | 125 | 528 | 43.4 | 33385[a] | 33900 | 179.1 |
| 199 | [Hanswille et al., 2006] | S5-1a | 22 | 125 | 528 | 42.9 | 33256[a] | 33050 | 184.6 |
| 200 | [Hanswille et al., 2006] | S5-1b | 22 | 125 | 528 | 42.9 | 33256[a] | 33050 | 186.8 |
| 201 | [Hanswille et al., 2006] | S5-1c | 22 | 125 | 528 | 45.8 | 33990[a] | 33050 | 196.0 |
| 202 | [An and Cederwall, 1991] | HSC11 | 19 | 75 | 519 | 86.1 | 41951[a] | 34080 | 156.8 |
| 203 | [An and Cederwall, 1991] | HSC12 | 19 | 75 | 519 | 81.3 | 41148[a] | 34080 | 158.6 |
| 204 | [An and Cederwall, 1991] | HSC21 | 19 | 75 | 519 | 81.3 | 41148[a] | 34080 | 151.9 |
| 205 | [An and Cederwall, 1991] | HSC22 | 19 | 75 | 519 | 91.2 | 42768[a] | 34080 | 161.0 |
| 206 | [Bullo and Di MArco, 1995] | 6019A | 19 | 75 | 495 | 48.6 | 34659[a] | 43110 | 148.3 |
| 207 | [Bullo and Di MArco, 1995] | 6019B | 19 | 75 | 495 | 48.6 | 34659[a] | 43110 | 147.6 |
| 208 | [Bullo and Di MArco, 1995] | 6019C | 19 | 75 | 495 | 48.6 | 34659[a] | 43110 | 163.1 |
| 209 | [Bullo and Di MArco, 1995] | 6025A | 25 | 125 | 495 | 48.6 | 34659[a] | 43110 | 189.1 |
| 210 | [Bullo and Di MArco, 1995] | 6025B | 25 | 125 | 495 | 48.6 | 34659[a] | 43110 | 256.2 |
| 211 | [Bullo and Di MArco, 1995] | 6025C | 25 | 125 | 495 | 48.6 | 34659[a] | 43110 | 252.7 |
| 212 | [Bullo and Di MArco, 1995] | 8019A | 19 | 75 | 495 | 79.9 | 40922[a] | 45644 | 203.6 |
| 213 | [Bullo and Di MArco, 1995] | 8019B | 19 | 75 | 495 | 79.9 | 40922[a] | 45644 | 191.0 |
| 214 | [Bullo and Di MArco, 1995] | 8019C | 19 | 75 | 495 | 79.9 | 40922[a] | 45644 | 180.9 |
| 215 | [Bullo and Di MArco, 1995] | 8025A | 25 | 120 | 495 | 79.9 | 40922[a] | 45644 | 250.0 |
| 216 | [Bullo and Di MArco, 1995] | 8025B | 25 | 120 | 495 | 79.9 | 40922[a] | 45644 | 293.2 |
| 217 | [Bullo and Di MArco, 1995] | 8025C | 25 | 120 | 495 | 79.9 | 40922[a] | 45644 | 199.7 |

[a] According to [DIN 1045-1, 2008]

*Continued on next page*

# B Push-out tests with composite slabs reported in literature

Table B.1: Database of push-out tests with composite slabs

| | | | | Composite Deck | | | | | | Shear Connectors | | | Concrete | | Transv. load | | |
|---|---|---|---|---|---|---|---|---|---|---|---|---|---|---|---|---|---|
| No. | Lit | Test | Sheet | $h_p$ | $b_u$ | $b_o$ | $a$ | $t$ | $d$ | $h_{sc}$ | $n_R$ | $f_{um}$ | $f_{cm}$ | $E_{cm}$ | $P_T$ | $e$ | $P_e$ |
| | | | | [mm] | [mm] | [mm] | [mm] | [mm] | [mm] | [mm] | [-] | $\left[\frac{N}{mm^2}\right]$ | $\left[\frac{N}{mm^2}\right]$ | $\left[\frac{N}{mm^2}\right]$ | [%] | [mm] | [kN] |
| 1 | [Konrad, 2011] | V1-TK-2f | T85.1 | 83 | 40 | 161 | 280 | 0.75 | 19.0 | 150.0 | $2^{F,T}$ | 570.0 | 31.6 | 26253[c] | n.a. | n.a. | 70.88 |
| 2 | [Konrad, 2011] | V2-TK-2f | T85.1 | 83 | 40 | 161 | 280 | 0.75 | 19.0 | 150.0 | $2^{F,T}$ | 570.0 | 30.3 | 25733[c] | n.a. | n.a. | 66.38 |
| 3 | [Konrad, 2011] | V3-TK-2u | T85.1 | 83 | 40 | 161 | 280 | 0.75 | 19.0 | 150.0 | $2^{U,T}$ | 570.0 | 31.6 | 26185[c] | n.a. | n.a. | 47.38 |
| 4 | [Konrad, 2011] | V4-TK-2u | T85.1 | 83 | 40 | 161 | 280 | 0.75 | 19.0 | 150.0 | $2^{U,T}$ | 570.0 | 31.6 | 26185[c] | n.a. | n.a. | 47.50 |
| 5 | [Konrad, 2011] | V5-TK-2a | T85.1 | 83 | 40 | 161 | 280 | 0.75 | 19.0 | 150.0 | $2^{S,T}$ | 570.0 | 30.8 | 25733[c] | n.a. | n.a. | 65.63 |
| 6 | [Konrad, 2011] | V6-TK-2a | T85.1 | 83 | 40 | 161 | 280 | 0.75 | 19.0 | 150.0 | $2^{S,T}$ | 570.0 | 31.8 | 26253[c] | n.a. | n.a. | 67.75 |
| 7 | [Konrad, 2011] | V7-Co-1f | Cofrastra 70 | 71 | 87 | 143 | 183 | 1.00 | 19.0 | 100.0 | $1^{F,T}$ | 532.0 | 33.7 | 26899[c] | n.a. | n.a. | 77.75 |
| 8 | [Konrad, 2011] | V8-Co-1f | Cofrastra 70 | 71 | 87 | 143 | 183 | 1.00 | 19.0 | 125.0 | $1^{F,T}$ | 570.0 | 33.7 | 26899[c] | n.a. | n.a. | 97.75 |
| 9 | [Konrad, 2011] | V9-Co-1f | Cofrastra 70 | 71 | 87 | 143 | 183 | 1.00 | 19.0 | 150.0 | $1^{F,T}$ | 570.0 | 34.2 | 27066[c] | n.a. | n.a. | 87.50 |
| 10 | [Konrad, 2011] | V10-Co-1u | Cofrastra 70 | 71 | 87 | 143 | 183 | 1.00 | 19.0 | 100.0 | $1^{U,T}$ | 532.0 | 34.2 | 27066[c] | n.a. | n.a. | 47.00 |
| 11 | [Konrad, 2011] | V11-Co-1u | Cofrastra 70 | 71 | 87 | 143 | 183 | 1.00 | 19.0 | 125.0 | $1^{U,T}$ | 570.0 | 32.5 | 26493[c] | n.a. | n.a. | 39.75 |
| 12 | [Konrad, 2011] | V12-Co-1u | Cofrastra 70 | 71 | 87 | 143 | 183 | 1.00 | 19.0 | 150.0 | $1^{U,T}$ | 570.0 | 32.5 | 26493[c] | n.a. | n.a. | 52.00 |
| 13 | [Konrad, 2011] | V13-Hoe-1m | HR51/150 | 51 | 135 | 113 | 150 | 0.75 | 19.0 | 75.0 | $1^{M,T}$ | 551.0 | 32.7 | 26561[c] | n.a. | n.a. | 75.00 |
| 14 | [Konrad, 2011] | V14-Hoe-1m | HR51/150 | 51 | 135 | 113 | 150 | 0.75 | 19.0 | 100.0 | $1^{M,T}$ | 532.0 | 32.7 | 26561[c] | n.a. | n.a. | 81.75 |
| 15 | [Konrad, 2011] | V14-Hoe-1u | HR51/150 | 51 | 135 | 113 | 150 | 0.75 | 19.0 | 100.0 | $1^{U,T}$ | 532.0 | 37.5 | 28149[c] | n.a. | n.a. | 53.50 |
| 16 | [Konrad, 2011] | V14-Hoe-1f | HR51/150 | 51 | 135 | 113 | 150 | 0.75 | 19.0 | 100.0 | $1^{F,T}$ | 532.0 | 37.5 | 28149[c] | n.a. | n.a. | 108.50 |
| 17 | [Konrad, 2011] | V14-Hoe-1a | HR51/150 | 51 | 135 | 113 | 150 | 0.75 | 19.0 | 100.0 | $1^{S,T}$ | 532.0 | 35.1 | 27365[c] | n.a. | n.a. | 73.50 |
| 18 | [Rambo-Roddenberry, 2002] | D1 | 2" | 50.8 | 127 | 177.8 | 305 | 0.95 | 12.7 | 101.6 | $1^{F,T}$ | 510.2 | 30.5 | 25803[c] | 10 | n.a. | 43.46 |
| 19 | [Rambo-Roddenberry, 2002] | D2 | 2" | 50.8 | 127 | 177.8 | 305 | 0.95 | 12.7 | 101.6 | $1^{F,T}$ | 510.2 | 30.5 | 25803[c] | 10 | n.a. | 34.43 |
| 20 | [Rambo-Roddenberry, 2002] | D3 | 2" | 50.8 | 127 | 177.8 | 305 | 0.95 | 12.7 | 101.6 | $1^{F,T}$ | 510.2 | 30.5 | 25803[c] | 10 | n.a. | 41.06 |
| 21 | [Rambo-Roddenberry, 2002] | D4 | 2" | 50.8 | 127 | 177.8 | 305 | 0.95 | 12.7 | 101.6 | $2^{F,T}$ | 510.2 | 30.5 | 25803[c] | 10 | n.a. | 39.81 |
| 22 | [Rambo-Roddenberry, 2002] | D5 | 2" | 50.8 | 127 | 177.8 | 305 | 0.95 | 12.7 | 101.6 | $2^{F,T}$ | 510.2 | 30.5 | 25803[c] | 10 | n.a. | 38.97 |
| 23 | [Rambo-Roddenberry, 2002] | D6 | 2" | 50.8 | 127 | 177.8 | 305 | 0.95 | 12.7 | 101.6 | $2^{F,T}$ | 510.2 | 30.5 | 25803[c] | 10 | n.a. | 31.85 |
| 24 | [Rambo-Roddenberry, 2002] | D7 | 2" | 50.8 | 127 | 177.8 | 305 | 0.95 | 12.7 | 101.6 | $2^{U,T}$ | 510.2 | 30.5 | 25803[c] | 10 | n.a. | 27.40 |
| 25 | [Rambo-Roddenberry, 2002] | D8 | 2" | 50.8 | 127 | 177.8 | 305 | 0.95 | 12.7 | 101.6 | $2^{U,T}$ | 510.2 | 30.5 | 25803[c] | 10 | n.a. | 35.63 |
| 26 | [Rambo-Roddenberry, 2002] | D9 | 2" | 50.8 | 127 | 177.8 | 305 | 0.95 | 12.7 | 101.6 | $2^{U,T}$ | 510.2 | 30.5 | 25803[c] | 10 | n.a. | 33.09 |
| 27 | [Rambo-Roddenberry, 2002] | D10 | 2" | 50.8 | 127 | 177.8 | 305 | 0.95 | 15.9 | 101.6 | $1^{F,T}$ | 500.6 | 20.1 | 21844[c] | 10 | n.a. | 55.74 |
| 28 | [Rambo-Roddenberry, 2002] | D11 | 2" | 50.8 | 127 | 177.8 | 305 | 0.95 | 15.9 | 101.6 | $1^{F,T}$ | 500.6 | 20.1 | 21844[c] | 10 | n.a. | 60.23 |
| 29 | [Rambo-Roddenberry, 2002] | D12 | 2" | 50.8 | 127 | 177.8 | 305 | 0.95 | 15.9 | 101.6 | $1^{F,T}$ | 500.6 | 20.1 | 21844[c] | 10 | n.a. | 69.20 |
| 30 | [Rambo-Roddenberry, 2002] | D13 | 2" | 50.8 | 127 | 177.8 | 305 | 0.95 | 15.9 | 101.6 | $1^{U,T}$ | 500.6 | 20.1 | 21844[c] | 10 | n.a. | 67.08 |
| 31 | [Rambo-Roddenberry, 2002] | D14 | 2" | 50.8 | 127 | 177.8 | 305 | 0.95 | 15.9 | 101.6 | $1^{U,T}$ | 500.6 | 20.1 | 21844[c] | 10 | n.a. | 41.82 |
| 32 | [Rambo-Roddenberry, 2002] | D15 | 2" | 50.8 | 127 | 177.8 | 305 | 0.95 | 15.9 | 101.6 | $1^{U,T}$ | 500.6 | 20.1 | 21844[c] | 10 | n.a. | 48.49 |
| 33 | [Rambo-Roddenberry, 2002] | D16 | 2" | 50.8 | 127 | 177.8 | 305 | 0.95 | 15.9 | 101.6 | $2^{F,T}$ | 500.6 | 20.1 | 21844[c] | 10 | n.a. | 52.80 |
| 34 | [Rambo-Roddenberry, 2002] | D17 | 2" | 50.8 | 127 | 177.8 | 305 | 0.95 | 15.9 | 101.6 | $2^{F,T}$ | 500.6 | 20.1 | 21844[c] | 10 | n.a. | 68.59 |
| 35 | [Rambo-Roddenberry, 2002] | D19 | 2" | 50.8 | 127 | 177.8 | 305 | 0.95 | 12.7 | 101.6 | $1^{F,T}$ | 510.2 | 40.6 | 29134[c] | 10 | n.a. | 39.41 |

M: Mid Position, F: Favourable Position, U: Unfavourable Position, S: Staggered Position, T: Through deck welded, nh: No head, ehd: Stud enhancement device

c: According to DIN 1045-1 [DIN 1045-1, 2008]: $E_{cm} = \alpha_i \cdot 9500 \cdot f_{cm}^{1/3}$ with $\alpha_i = 0.8 + 0.2 \cdot (f_{cm}/88) \leq 1.0$ d: No static results

*Continued on next page*

Table B.1 – *Continued from previous page*

| No. | Lit | Test | Sheet | Composite Deck | | | | | | Shear Connectors | | | Concrete | | Transv. load | | |
|---|---|---|---|---|---|---|---|---|---|---|---|---|---|---|---|---|---|
| | | | | $h_p$ | $b_u$ | $b_o$ | $a$ | $t$ | $d$ | $h_{sc}$ | $n_R$ | $f_{um}$ | $f_{cm}$ | $E_{cm}$ | $P_T$ | $e$ | $P_e$ |
| | | | | [mm] | [mm] | [mm] | [mm] | [mm] | [mm] | [mm] | [-] | $\left[\frac{N}{mm^2}\right]$ | $\left[\frac{N}{mm^2}\right]$ | $\left[\frac{N}{mm^2}\right]$ | [%] | [mm] | [kN] |
| 36 | [Rambo-Roddenberry, 2002] | D20 | 2" | 50.8 | 127 | 177.8 | 305 | 0.95 | 12.7 | 101.6 | 1[F,T] | 510.2 | 40.6 | 29134[c] | 10 | n.a. | 40.66 |
| 37 | [Rambo-Roddenberry, 2002] | D21 | 2" | 50.8 | 127 | 177.8 | 305 | 0.95 | 12.7 | 101.6 | 1[F,T] | 510.2 | 40.6 | 29134[c] | 10 | n.a. | 29.49 |
| 38 | [Rambo-Roddenberry, 2002] | D22 | 2" | 50.8 | 127 | 177.8 | 305 | 0.95 | 12.7 | 101.6 | 2[F,T] | 510.2 | 40.6 | 29134[c] | 10 | n.a. | 41.06 |
| 39 | [Rambo-Roddenberry, 2002] | D23 | 2" | 50.8 | 127 | 177.8 | 305 | 0.95 | 12.7 | 101.6 | 2[F,T] | 510.2 | 40.6 | 29134[c] | 10 | n.a. | 45.82 |
| 40 | [Rambo-Roddenberry, 2002] | D24 | 2" | 50.8 | 127 | 177.8 | 305 | 0.95 | 12.7 | 101.6 | 2[F,T] | 510.2 | 40.6 | 29134[c] | 10 | n.a. | 50.98 |
| 41 | [Rambo-Roddenberry, 2002] | D25 | 2" | 50.8 | 127 | 177.8 | 305 | 0.95 | 12.7 | 101.6 | 1[U,T] | 510.2 | 40.6 | 29134[c] | 10 | n.a. | 40.79 |
| 42 | [Rambo-Roddenberry, 2002] | D26 | 2" | 50.8 | 127 | 177.8 | 305 | 0.95 | 12.7 | 101.6 | 1[U,T] | 510.2 | 40.6 | 29134[c] | 10 | n.a. | 32.56 |
| 43 | [Rambo-Roddenberry, 2002] | D27 | 2" | 50.8 | 127 | 177.8 | 305 | 0.95 | 12.7 | 101.6 | 1[U,T] | 510.2 | 40.6 | 29134[c] | 10 | n.a. | 30.60 |
| 44 | [Rambo-Roddenberry, 2002] | D28 | 2" | 50.8 | 127 | 177.8 | 305 | 0.95 | 19.1 | 101.6 | 1[F,T] | 453.7 | 48.8 | 31623[c] | 10 | n.a. | 89.01 |
| 45 | [Rambo-Roddenberry, 2002] | D29 | 2" | 50.8 | 127 | 177.8 | 305 | 0.95 | 19.1 | 101.6 | 1[F,T] | 453.7 | 48.8 | 31623[c] | 10 | n.a. | 83.27 |
| 46 | [Rambo-Roddenberry, 2002] | D30 | 2" | 50.8 | 127 | 177.8 | 305 | 0.95 | 19.1 | 101.6 | 1[F,T] | 453.7 | 48.8 | 31623[c] | 10 | n.a. | 96.97 |
| 47 | [Rambo-Roddenberry, 2002] | D31 | 2" | 50.8 | 127 | 177.8 | 305 | 0.95 | 19.1 | 101.6 | 2[F,T] | 453.7 | 48.8 | 31623[c] | 10 | n.a. | 34.52 |
| 48 | [Rambo-Roddenberry, 2002] | D32 | 2" | 50.8 | 127 | 177.8 | 305 | 0.95 | 19.1 | 101.6 | 2[F,T] | 453.7 | 48.8 | 31623[c] | 10 | n.a. | 77.80 |
| 49 | [Rambo-Roddenberry, 2002] | D33 | 2" | 50.8 | 127 | 177.8 | 305 | 0.95 | 19.1 | 101.6 | 2[F,T] | 453.7 | 48.8 | 31623[c] | 10 | n.a. | 92.92 |
| 50 | [Rambo-Roddenberry, 2002] | D34 | 2" | 50.8 | 127 | 177.8 | 305 | 0.95 | 19.1 | 101.6 | 1[U,T] | 453.7 | 48.8 | 31623[c] | 10 | n.a. | 66.95 |
| 51 | [Rambo-Roddenberry, 2002] | D35 | 2" | 50.8 | 127 | 177.8 | 305 | 0.95 | 19.1 | 101.6 | 1[U,T] | 453.7 | 48.8 | 31623[c] | 10 | n.a. | 53.51 |
| 52 | [Rambo-Roddenberry, 2002] | D36 | 2" | 50.8 | 127 | 177.8 | 305 | 0.95 | 19.1 | 101.6 | 1[U,T] | 453.7 | 48.8 | 31623[c] | 10 | n.a. | 69.70 |
| 53 | [Rambo-Roddenberry, 2002] | D37 | 2" | 50.8 | 127 | 177.8 | 305 | 0.95 | 15.9 | 101.6 | 1[F,T] | 500.6 | 32.5 | 26493[c] | 10 | n.a. | 71.97 |
| 54 | [Rambo-Roddenberry, 2002] | D38 | 2" | 50.8 | 127 | 177.8 | 305 | 0.95 | 15.9 | 101.6 | 1[F,T] | 500.6 | 32.5 | 26493[c] | 10 | n.a. | 75.93 |
| 55 | [Rambo-Roddenberry, 2002] | D39 | 2" | 50.8 | 127 | 177.8 | 305 | 0.95 | 15.9 | 101.6 | 1[F,T] | 500.6 | 32.5 | 26493[c] | 10 | n.a. | 64.63 |
| 56 | [Rambo-Roddenberry, 2002] | D40 | 2" | 50.8 | 127 | 177.8 | 305 | 0.95 | 15.9 | 101.6 | 2[F,T] | 500.6 | 32.5 | 26493[c] | 10 | n.a. | 65.39 |
| 57 | [Rambo-Roddenberry, 2002] | D41 | 2" | 50.8 | 127 | 177.8 | 305 | 0.95 | 15.9 | 101.6 | 2[F,T] | 500.6 | 32.5 | 26493[c] | 10 | n.a. | 75.40 |
| 58 | [Rambo-Roddenberry, 2002] | D42 | 2" | 50.8 | 127 | 177.8 | 305 | 0.95 | 15.9 | 101.6 | 2[F,T] | 500.6 | 32.5 | 26493[c] | 10 | n.a. | 77.43 |
| 59 | [Rambo-Roddenberry, 2002] | D43 | 2" | 50.8 | 127 | 177.8 | 305 | 0.95 | 15.9 | 101.6 | 1[U,T] | 500.6 | 32.5 | 26493[c] | 10 | n.a. | 40.57 |
| 60 | [Rambo-Roddenberry, 2002] | D44 | 2" | 50.8 | 127 | 177.8 | 305 | 0.95 | 15.9 | 101.6 | 1[U,T] | 500.6 | 32.5 | 26493[c] | 10 | n.a. | 49.55 |
| 61 | [Rambo-Roddenberry, 2002] | D45 | 2" | 50.8 | 127 | 177.8 | 305 | 0.95 | 15.9 | 101.6 | 1[U,T] | 500.6 | 32.5 | 26493[c] | 10 | n.a. | 49.24 |
| 62 | [Rambo-Roddenberry, 2002] | D46 | 2" | 50.8 | 127 | 177.8 | 305 | 0.95 | 9.5 | 101.6 | 1[F,T] | 546.1 | 27.1 | 24586[c] | 10 | n.a. | 26.20 |
| 63 | [Rambo-Roddenberry, 2002] | D47 | 2" | 50.8 | 127 | 177.8 | 305 | 0.95 | 9.5 | 101.6 | 1[F,T] | 546.1 | 27.1 | 24586[c] | 10 | n.a. | 23.04 |
| 64 | [Rambo-Roddenberry, 2002] | D48 | 2" | 50.8 | 127 | 177.8 | 305 | 0.95 | 9.5 | 101.6 | 1[F,T] | 546.1 | 27.1 | 24586[c] | 10 | n.a. | 23.84 |
| 65 | [Rambo-Roddenberry, 2002] | D49 | 2" | 50.8 | 127 | 177.8 | 305 | 0.95 | 22.2 | 101.6 | 1[F,T] | 444.7 | 27.1 | 24586[c] | 10 | n.a. | 84.92 |
| 66 | [Rambo-Roddenberry, 2002] | D50 | 2" | 50.8 | 127 | 177.8 | 305 | 0.95 | 22.2 | 101.6 | 1[F,T] | 444.7 | 27.1 | 24586[c] | 10 | n.a. | 42.75 |
| 67 | [Rambo-Roddenberry, 2002] | D51 | 2" | 50.8 | 127 | 177.8 | 305 | 0.95 | 22.2 | 101.6 | 1[F,T] | 444.7 | 27.1 | 24586[c] | 10 | n.a. | 58.27 |
| 68 | [Rambo-Roddenberry, 2002] | D52 | 2" | 50.8 | 127 | 177.8 | 305 | 0.95 | 9.5 | 101.6 | 1[U,T] | 546.1 | 27.1 | 24586[c] | 10 | n.a. | 18.02 |
| 69 | [Rambo-Roddenberry, 2002] | D53 | 2" | 50.8 | 127 | 177.8 | 305 | 0.95 | 9.5 | 101.6 | 1[U,T] | 546.1 | 27.1 | 24586[c] | 10 | n.a. | 20.19 |
| 70 | [Rambo-Roddenberry, 2002] | D54 | 2" | 50.8 | 127 | 177.8 | 305 | 0.95 | 9.5 | 101.6 | 1[U,T] | 546.1 | 27.1 | 24586[c] | 10 | n.a. | 21.40 |
| 71 | [Rambo-Roddenberry, 2002] | D55 | 2" | 50.8 | 127 | 177.8 | 305 | 0.95 | 22.2 | 101.6 | 1[U,T] | 444.7 | 27.1 | 24586[c] | 10 | n.a. | 65.17 |

M: Mid Position, F: Favourable Position, U: Unfavourable Position, S: Staggered Position, T: Through deck welded, nh: No head, ehd: Stud enhancement device

c: According to DIN 1045-1 [DIN 1045-1, 2008]: $E_{cm} = \alpha_i \cdot 9500 \cdot f_{cm}^{1/3}$ with $\alpha_i = 0.8 + 0.2 \cdot (f_{cm}/88) \leq 1.0$ d: No static results

*Continued on next page*

Table B.1 – *Continued from previous page*

| No. | Lit | Test | Sheet | Composite Deck | | | | | Shear Connectors | | | | Concrete | | Transv. load | | |
|---|---|---|---|---|---|---|---|---|---|---|---|---|---|---|---|---|---|
| | | | | $h_p$ | $b_u$ | $b_o$ | $a$ | $t$ | $d$ | $h_{sc}$ | $n_R$ | $f_{um}$ | $f_{cm}$ | $E_{cm}$ | $P_T$ | $e$ | $P_e$ |
| | | | | [mm] | [mm] | [mm] | [mm] | [mm] | [mm] | [mm] | [-] | $\left[\frac{\text{N}}{\text{mm}^2}\right]$ | $\left[\frac{\text{N}}{\text{mm}^2}\right]$ | $\left[\frac{\text{N}}{\text{mm}^2}\right]$ | [%] | [mm] | [kN] |
| 72 | [Rambo-Roddenberry, 2002] | D56 | 2" | 50.8 | 127 | 177.8 | 305 | 0.95 | 22.2 | 101.6 | 1[U,T] | 444.7 | 27.1 | 24586[c] | 10 | n.a. | 52.76 |
| 73 | [Rambo-Roddenberry, 2002] | D57 | 2" | 50.8 | 127 | 177.8 | 305 | 0.95 | 22.2 | 101.6 | 1[U,T] | 444.7 | 27.1 | 24586[c] | 10 | n.a. | 56.85 |
| 74 | [Rambo-Roddenberry, 2002] | D58 | 3" | 76.2 | 127 | 177.8 | 305 | 0.95 | 9.5 | 127.0 | 1[F,T] | 532.3 | 36.1 | 27694[c] | 10 | n.a. | 26.82 |
| 75 | [Rambo-Roddenberry, 2002] | D59 | 3" | 76.2 | 127 | 177.8 | 305 | 0.95 | 9.5 | 127.0 | 1[F,T] | 532.3 | 36.1 | 27694[c] | 10 | n.a. | 36.03 |
| 76 | [Rambo-Roddenberry, 2002] | D60 | 3" | 76.2 | 127 | 177.8 | 305 | 0.95 | 9.5 | 127.0 | 1[F,T] | 532.3 | 36.1 | 27694[c] | 10 | n.a. | 42.26 |
| 77 | [Rambo-Roddenberry, 2002] | D61 | 3" | 76.2 | 127 | 177.8 | 305 | 0.95 | 22.2 | 127.0 | 1[F,T] | 439.9 | 36.1 | 27694[c] | 10 | n.a. | 58.81 |
| 78 | [Rambo-Roddenberry, 2002] | D62 | 3" | 76.2 | 127 | 177.8 | 305 | 0.95 | 22.2 | 127.0 | 1[F,T] | 439.9 | 36.1 | 27694[c] | 10 | n.a. | 53.25 |
| 79 | [Rambo-Roddenberry, 2002] | D63 | 3" | 76.2 | 127 | 177.8 | 305 | 0.95 | 22.2 | 127.0 | 1[F,T] | 439.9 | 36.1 | 27694[c] | 10 | n.a. | 69.44 |
| 80 | [Rambo-Roddenberry, 2002] | D64 | 3" | 76.2 | 127 | 177.8 | 305 | 0.95 | 9.5 | 127.0 | 1[U,T] | 532.3 | 36.1 | 27694[c] | 10 | n.a. | 24.02 |
| 81 | [Rambo-Roddenberry, 2002] | D65 | 3" | 76.2 | 127 | 177.8 | 305 | 0.95 | 9.5 | 127.0 | 1[U,T] | 532.3 | 36.1 | 27694[c] | 10 | n.a. | 29.71 |
| 82 | [Rambo-Roddenberry, 2002] | D66 | 3" | 76.2 | 127 | 177.8 | 305 | 0.95 | 9.5 | 127.0 | 1[U,T] | 532.3 | 36.1 | 27694[c] | 10 | n.a. | 28.73 |
| 83 | [Rambo-Roddenberry, 2002] | D67 | 3" | 76.2 | 127 | 177.8 | 305 | 0.95 | 22.2 | 127.0 | 1[U,T] | 439.9 | 36.1 | 27694[c] | 10 | n.a. | 50.22 |
| 84 | [Rambo-Roddenberry, 2002] | D68 | 3" | 76.2 | 127 | 177.8 | 305 | 0.95 | 22.2 | 127.0 | 1[U,T] | 439.9 | 36.1 | 27694[c] | 10 | n.a. | 83.98 |
| 85 | [Rambo-Roddenberry, 2002] | D69 | 3" | 76.2 | 127 | 177.8 | 305 | 0.95 | 22.2 | 127.0 | 1[U,T] | 439.9 | 36.1 | 27694[c] | 10 | n.a. | 76.87 |
| 86 | [Rambo-Roddenberry, 2002] | D70 | 4.5" | 114.3 | 76.2 | 76.2 | 305 | 0.95 | 19.1 | 152.4 | 1[M,T] | 430.9 | 34.5 | 27166[c] | 10 | n.a. | 38.08 |
| 87 | [Rambo-Roddenberry, 2002] | D71 | 4.5" | 114.3 | 76.2 | 76.2 | 305 | 0.95 | 19.1 | 152.4 | 1[M,T] | 430.9 | 34.5 | 27166[c] | 10 | n.a. | 33.58 |
| 88 | [Rambo-Roddenberry, 2002] | D72 | 4.5" | 114.3 | 76.2 | 76.2 | 305 | 0.95 | 19.1 | 152.4 | 1[M,T] | 430.9 | 34.5 | 27166[c] | 10 | n.a. | 32.34 |
| 89 | [Rambo-Roddenberry, 2002] | D73 | 6" | 152.4 | 88.9 | 88.9 | 318 | 0.95 | 19.1 | 203.2 | 1[M,T] | 452.3 | 34.5 | 27166[c] | 10 | n.a. | 30.74 |
| 90 | [Rambo-Roddenberry, 2002] | D74 | 6" | 152.4 | 88.9 | 88.9 | 318 | 0.95 | 19.1 | 203.2 | 1[M,T] | 452.3 | 34.5 | 27166[c] | 10 | n.a. | 27.45 |
| 91 | [Rambo-Roddenberry, 2002] | D75 | 6" | 152.4 | 88.9 | 88.9 | 318 | 0.95 | 19.1 | 203.2 | 1[M,T] | 452.3 | 34.5 | 27166[c] | 10 | n.a. | 24.82 |
| 92 | [Rambo-Roddenberry, 2002] | D76 | 2" | 50.8 | 127 | 177.8 | 305 | 0.95 | 19.1 | 101.6 | 1[F,T] | 453.7 | 34.5 | 27166[c] | 5 | n.a. | 43.46 |
| 93 | [Rambo-Roddenberry, 2002] | D77 | 2" | 50.8 | 127 | 177.8 | 305 | 0.95 | 19.1 | 101.6 | 1[F,T] | 453.7 | 34.5 | 27166[c] | 5 | n.a. | 100.26 |
| 94 | [Rambo-Roddenberry, 2002] | D78 | 2" | 50.8 | 127 | 177.8 | 305 | 0.95 | 19.1 | 101.6 | 1[F,T] | 453.7 | 34.5 | 27166[c] | 5 | n.a. | 56.67 |
| 95 | [Rambo-Roddenberry, 2002] | D79 | 2" | 50.8 | 127 | 177.8 | 305 | 0.95 | 19.1 | 101.6 | 1[F,T] | 453.7 | 34.5 | 27166[c] | 20 | n.a. | 102.84 |
| 96 | [Rambo-Roddenberry, 2002] | D80 | 2" | 50.8 | 127 | 177.8 | 305 | 0.95 | 19.1 | 101.6 | 1[F,T] | 453.7 | 34.5 | 27166[c] | 20 | n.a. | 86.07 |
| 97 | [Rambo-Roddenberry, 2002] | D81 | 2" | 50.8 | 127 | 177.8 | 305 | 0.95 | 19.1 | 101.6 | 1[F,T] | 453.7 | 34.5 | 27166[c] | 20 | n.a. | 108.49 |
| 98 | [Rambo-Roddenberry, 2002] | D82 | 2" | 50.8 | 127 | 177.8 | 305 | 0.95 | 19.1 | 101.6 | 1[U,T] | 453.7 | 32.3 | 26425[c] | 5 | n.a. | 61.83 |
| 99 | [Rambo-Roddenberry, 2002] | D83 | 2" | 50.8 | 127 | 177.8 | 305 | 0.95 | 19.1 | 101.6 | 1[U,T] | 453.7 | 32.3 | 26425[c] | 5 | n.a. | 83.85 |
| 100 | [Rambo-Roddenberry, 2002] | D84 | 2" | 50.8 | 127 | 177.8 | 305 | 0.95 | 19.1 | 101.6 | 1[U,T] | 453.7 | 32.3 | 26425[c] | 5 | n.a. | 44.92 |
| 101 | [Rambo-Roddenberry, 2002] | D85 | 2" | 50.8 | 127 | 177.8 | 305 | 0.95 | 19.1 | 101.6 | 1[U,T] | 453.7 | 32.3 | 26425[c] | 20 | n.a. | 48.00 |
| 102 | [Rambo-Roddenberry, 2002] | D86 | 2" | 50.8 | 127 | 177.8 | 305 | 0.95 | 19.1 | 101.6 | 1[U,T] | 453.7 | 32.3 | 26425[c] | 20 | n.a. | 92.12 |
| 103 | [Rambo-Roddenberry, 2002] | D87 | 2" | 50.8 | 127 | 177.8 | 305 | 0.95 | 19.1 | 101.6 | 1[U,T] | 453.7 | 32.3 | 26425[c] | 20 | n.a. | 88.56 |
| 104 | [Rambo-Roddenberry, 2002] | D88 | 2" | 50.8 | 127 | 177.8 | 305 | 0.95 | 19.1[nh] | 76.2 | 1[F,T] | 453.7 | 34.5 | 27166[c] | 10 | n.a. | 77.00 |
| 105 | [Rambo-Roddenberry, 2002] | D89 | 2" | 50.8 | 127 | 177.8 | 305 | 0.95 | 19.1[nh] | 76.2 | 1[F,T] | 453.7 | 34.5 | 27166[c] | 10 | n.a. | 77.18 |
| 106 | [Rambo-Roddenberry, 2002] | D90 | 2" | 50.8 | 127 | 177.8 | 305 | 0.95 | 19.1[nh] | 76.2 | 1[F,T] | 453.7 | 34.5 | 27166[c] | 10 | n.a. | 82.38 |
| 107 | [Rambo-Roddenberry, 2002] | D91 | 2" | 50.8 | 127 | 177.8 | 305 | 0.95 | 19.1[nh] | 76.2 | 1[U,T] | 453.7 | 34.5 | 27166[c] | 10 | n.a. | 48.13 |

M: Mid Position, F: Favourable Position, U: Unfavourable Position, S: Staggered Position, T: Through deck welded, nh: No head, ehd: Stud enhancement device

c: According to DIN 1045-1 [DIN 1045-1, 2008]: $E_{cm} = \alpha_i \cdot 9500 \cdot f_{cm}^{1/3}$ with $\alpha_i = 0.8 + 0.2 \cdot (f_{cm}/88) \leq 1.0$ d: No static results

*Continued on next page*

Table B.1 – *Continued from previous page*

| No. | Lit | Test | Sheet | Composite Deck | | | | | Shear Connectors | | | | Concrete | | Transv. load | | |
|---|---|---|---|---|---|---|---|---|---|---|---|---|---|---|---|---|---|
| | | | | $h_p$ | $b_u$ | $b_o$ | $a$ | $t$ | $d$ | $h_{sc}$ | $n_R$ | $f_{um}$ | $f_{cm}$ | $E_{cm}$ | $P_T$ | $e$ | $P_e$ |
| | | | | [mm] | [mm] | [mm] | [mm] | [mm] | [mm] | [mm] | [-] | $\left[\frac{N}{mm^2}\right]$ | $\left[\frac{N}{mm^2}\right]$ | $\left[\frac{N}{mm^2}\right]$ | [%] | [mm] | [kN] |
| 108 | [Rambo-Roddenberry, 2002] | D92 | 2" | 50.8 | 127 | 177.8 | 305 | 0.95 | 19.1[nh] | 76.2 | 1[U,T] | 453.7 | 34.5 | 27166[c] | 10 | n.a. | 50.49 |
| 109 | [Rambo-Roddenberry, 2002] | D93 | 2" | 50.8 | 127 | 177.8 | 305 | 0.95 | 19.1[nh] | 76.2 | 1[U,T] | 453.7 | 34.5 | 27166[c] | 10 | n.a. | 47.73 |
| 110 | [Roik and Bürkner, 1981] | 1.1 | T60/200 | 60 | 101 | 153 | 200 | 0.75 | 19 | 125 | 1[M] | 460 | 34.8 | 27266[c] | n.a. | n.a. | 83.80 |
| 111 | [Roik and Bürkner, 1981] | 1.2 | T60/200 | 60 | 101 | 153 | 200 | 0.75 | 19 | 125 | 1[M] | 460 | 34.8 | 27266[c] | n.a. | n.a. | 90.00 |
| 112 | [Roik and Bürkner, 1981] | 2.1 | T60/200 | 60 | 101 | 153 | 200 | 0.75 | 19 | 100 | 1[M] | 460 | 27.4 | 24696[c] | n.a. | n.a. | 73.80 |
| 113 | [Roik and Bürkner, 1981] | 2.2 | T60/200 | 60 | 101 | 153 | 200 | 0.75 | 19 | 100 | 1[M] | 460 | 27.4 | 24696[c] | n.a. | n.a. | 60.00 |
| 114 | [Roik and Bürkner, 1981] | 3.1 | T80/183 | 80 | 89 | 143 | 183 | 0.75 | 19 | 125 | 1[M] | 460 | 34.9 | 27299[c] | n.a. | n.a. | 53.00 |
| 115 | [Roik and Bürkner, 1981] | 3.2 | T80/183 | 80 | 89 | 143 | 183 | 0.75 | 19 | 125 | 1[M] | 460 | 34.3 | 27099[c] | n.a. | n.a. | 54.00 |
| 116 | [Roik and Bürkner, 1981] | 4.1 | T60/200 | 60 | 101 | 153 | 200 | 0.75 | 19 | 125 | 2[M] | 460 | 29.2 | 25345[c] | n.a. | n.a. | 69.50 |
| 117 | [Roik and Bürkner, 1981] | 4.2 | T60/200 | 60 | 101 | 153 | 200 | 0.75 | 19 | 125 | 2[M] | 460 | 29.2 | 25345[c] | n.a. | n.a. | 74.50 |
| 118 | [Roik and Bürkner, 1981] | 5.1 | T60/200 | 60 | 101 | 153 | 200 | 0.75 | 19 | 100 | 2[S] | 460 | 32.5 | 26493[c] | n.a. | n.a. | 61.50 |
| 119 | [Roik and Bürkner, 1981] | 5.2 | T60/200 | 60 | 101 | 153 | 200 | 0.75 | 19 | 100 | 2[S] | 460 | 29.8 | 25557[c] | n.a. | n.a. | 55.50 |
| 120 | [Roik and Bürkner, 1981] | 6.1 | T80/183 | 80 | 89 | 143 | 183 | 0.75 | 19 | 125 | 2[S] | 460 | 41.9 | 29539[c] | n.a. | n.a. | 41.50 |
| 121 | [Roik and Bürkner, 1981] | 6.2 | T80/183 | 80 | 89 | 143 | 183 | 0.75 | 19 | 125 | 2[S] | 460 | 37.1 | 28019[c] | n.a. | n.a. | 37.50 |
| 122 | [Roik and Bürkner, 1981] | 7.1 | T60/200 | 60 | 101 | 153 | 200 | 0.75 | 19 | 100 | 1[F] | 460 | 29.6 | 25486[c] | n.a. | n.a. | 74.00 |
| 123 | [Roik and Bürkner, 1981] | 7.2 | T60/200 | 60 | 101 | 153 | 200 | 0.75 | 19 | 100 | 1[F] | 460 | 29.6 | 25486[c] | n.a. | n.a. | 78.00 |
| 124 | [Roik and Bürkner, 1981] | 8.1 | T60/200 | 60 | 101 | 153 | 200 | 0.75 | 19 | 100 | 1[U] | 460 | 29.6 | 25486[c] | n.a. | n.a. | 79.00 |
| 125 | [Roik and Bürkner, 1981] | 8.2 | T60/200 | 60 | 101 | 153 | 200 | 0.75 | 19 | 100 | 1[U] | 460 | 34.9 | 27299[c] | n.a. | n.a. | 75.00 |
| 126 | [Roik and Bürkner, 1980] | 1.1 | n.a. | 106 | 40 | 110 | 250 | 0.75 | 19 | 150 | 1[M] | 460 | 26.8 | 24475[c] | n.a. | n.a. | 37.00 |
| 127 | [Roik and Bürkner, 1980] | 1.2 | n.a. | 106 | 40 | 110 | 250 | 0.75 | 19 | 150 | 1[M] | 460 | 26.8 | 24475[c] | n.a. | n.a. | 38.50 |
| 128 | [Roik and Bürkner, 1980] | 2.1 | n.a. | 106 | 40 | 110 | 250 | 0.75 | 19 | 175 | 1[M] | 460 | 24.7 | 23686[c] | n.a. | n.a. | 44.50 |
| 129 | [Roik and Bürkner, 1980] | 2.2 | n.a. | 106 | 40 | 110 | 250 | 0.75 | 19 | 175 | 1[M] | 460 | 24.7 | 23686[c] | n.a. | n.a. | 38.00 |
| 130 | [Roik and Bürkner, 1980] | 3.1 | n.a. | 106 | 140 | 210 | 250 | 0.75 | 19 | 150 | 1[M] | 460 | 31.1 | 26012[c] | n.a. | n.a. | 82.00 |
| 131 | [Roik and Bürkner, 1980] | 3.2 | n.a. | 106 | 140 | 210 | 250 | 0.75 | 19 | 150 | 1[M] | 460 | 31.1 | 26012[c] | n.a. | n.a. | 78.50 |
| 132 | [Roik and Bürkner, 1980] | 4.2 | n.a. | 106 | 140 | 210 | 250 | 0.75 | 19 | 175 | 1[M] | 460 | 33.4 | 26798[c] | n.a. | n.a. | 76.00 |
| 133 | [Roik and Bürkner, 1980] | 5.1 | n.a. | 125 | 40 | 120 | 250 | 0.75 | 19 | 175 | 1[M] | 460 | 26.9 | 24512[c] | n.a. | n.a. | 42.00 |
| 134 | [Roik and Bürkner, 1980] | 5.2 | n.a. | 125 | 40 | 120 | 250 | 0.75 | 19 | 175 | 1[M] | 460 | 26.9 | 24512[c] | n.a. | n.a. | 49.00 |
| 135 | [Roik and Bürkner, 1980] | 6.1 | n.a. | 125 | 40 | 120 | 250 | 0.75 | 19 | 175 | 1[M] | 460 | 24.7 | 23686[c] | n.a. | n.a. | 39.50 |
| 136 | [Roik and Bürkner, 1980] | 6.2 | n.a. | 125 | 40 | 120 | 250 | 0.75 | 19 | 175 | 1[M] | 460 | 24.7 | 23686[c] | n.a. | n.a. | 46.00 |
| 137 | [Roik and Bürkner, 1980] | 7.1 | n.a. | 125 | 130 | 210 | 250 | 0.75 | 19 | 175 | 1[M] | 460 | 31.6 | 26185[c] | n.a. | n.a. | 73.00 |
| 138 | [Roik and Bürkner, 1980] | 7.2 | n.a. | 125 | 130 | 210 | 250 | 0.75 | 19 | 175 | 1[M] | 460 | 31.6 | 26185[c] | n.a. | n.a. | 70.00 |
| 139 | [Roik and Bürkner, 1980] | 8.1 | n.a. | 125 | 130 | 210 | 250 | 0.75 | 19 | 175 | 1[M] | 460 | 25.1 | 23839[c] | n.a. | n.a. | 79.00 |
| 140 | [Roik and Bürkner, 1980] | 8.2 | n.a. | 125 | 130 | 210 | 250 | 0.75 | 19 | 175 | 1[M] | 460 | 25.1 | 23839[c] | n.a. | n.a. | 85.00 |
| 141 | [Roik and Bürkner, 1980] | 11.1 | n.a. | 106 | 140 | 210 | 250 | 0.75 | 19 | 175 | 1[M] | 460 | 24.8 | 23725[c] | n.a. | n.a. | 84.50 |
| 142 | [Roik and Bürkner, 1980] | 11.2 | n.a. | 106 | 140 | 210 | 250 | 0.75 | 19 | 175 | 1[M] | 460 | 24.8 | 23725[c] | n.a. | n.a. | 85.00 |
| 143 | [Roik and Bürkner, 1980] | 12.1 | n.a. | 106 | 140 | 210 | 250 | 0.75 | 19 | 175 | 2[M] | 460 | 23.6 | 23261[c] | n.a. | n.a. | 73.75 |

M: Mid Position, F: Favourable Position, U: Unfavourable Position, S: Staggered Position, T: Through deck welded, nh: No head, ehd: Stud enhancement device

c: According to DIN 1045-1 [DIN 1045-1, 2008]: $E_{cm} = \alpha_i \cdot 9500 \cdot f_{cm}^{1/3}$ with $\alpha_i = 0.8 + 0.2 \cdot (f_{cm}/88) \leq 1.0$ d: No static results

*Continued on next page*

Table B.1 – *Continued from previous page*

| No. | Lit | Test | Sheet | Composite Deck | | | | | | Shear Connectors | | | Concrete | | Transv. load | | |
|---|---|---|---|---|---|---|---|---|---|---|---|---|---|---|---|---|---|
| | | | | $h_p$ | $b_u$ | $b_o$ | $a$ | $t$ | $d$ | $h_{sc}$ | $n_R$ | $f_{um}$ | $f_{cm}$ | $E_{cm}$ | $P_T$ | $e$ | $P_e$ |
| | | | | [mm] | [mm] | [mm] | [mm] | [mm] | [mm] | [mm] | [-] | $\left[\frac{\text{N}}{\text{mm}^2}\right]$ | $\left[\frac{\text{N}}{\text{mm}^2}\right]$ | $\left[\frac{\text{N}}{\text{mm}^2}\right]$ | [%] | [mm] | [kN] |
| 144 | [Roik and Bürkner, 1980] | 13.1 | n.a. | 106 | 140 | 210 | 250 | 0.75 | 22 | 175 | $1^{M}$ | 460 | 26.9 | 24512[c] | n.a. | n.a. | 82.00 |
| 145 | [Roik and Bürkner, 1980] | 13.2 | n.a. | 106 | 140 | 210 | 250 | 0.75 | 22 | 175 | $1^{M}$ | 460 | 26.9 | 24512[c] | n.a. | n.a. | 96.00 |
| 146 | [Roik and Bürkner, 1980] | 16.1 | n.a. | 125 | 130 | 210 | 250 | 0.75 | 19 | 175 | $1^{M}$ | 460 | 33.1 | 26696[c] | n.a. | n.a. | 79.00 |
| 147 | [Roik and Bürkner, 1980] | 16.2 | n.a. | 125 | 40 | 120 | 250 | 0.75 | 19 | 175 | $1^{M}$ | 460 | 33.1 | 26696[c] | n.a. | n.a. | 35.00 |
| 148 | [Roik and Lungershausen, 1988] | B11 | n.a. | 110 | 40 | 129 | 275 | 0.75 | 19 | 175 | $1^{M}$ | 530 | 33.3 | 26764[c] | n.a. | n.a. | 53.00 |
| 149 | [Roik and Lungershausen, 1988] | B12 | n.a. | 136 | 40 | 137 | 292 | 0.75 | 19 | 175 | $1^{M}$ | 530 | 33.3 | 26764[c] | n.a. | n.a. | 46.00 |
| 150 | [Roik and Lungershausen, 1988] | A1 | n.a. | 136 | 40 | 137 | 292 | 0.75 | 22 | 200 | $1^{M}$ | 530 | 37.3 | 28084[c] | n.a. | n.a. | 55.00 |
| 151 | [Roik and Lungershausen, 1988] | A2 | n.a. | 136 | 40 | 137 | 292 | 0.75 | 22 | 200 | $2^{M}$ | 530 | 37.3 | 28084[c] | n.a. | n.a. | 45.00 |
| 152 | [Bode and Künzel, 1988] | H1 | Holorib | 51 | 138 | 114 | 150 | 0.75 | 22 | 100 | $1^{M}$ | 460 | 38.3 | 28405[c] | n.a. | n.a. | 114.00 |
| 153 | [Bode and Künzel, 1988] | H2 | Holorib | 51 | 138 | 114 | 150 | 0.75 | 22 | 100 | $1^{M}$ | 460 | 38.3 | 28405[c] | n.a. | n.a. | 107.00 |
| 154 | [Bode and Künzel, 1988] | H3 | Holorib | 51 | 138 | 114 | 150 | 0.75 | 22 | 100 | $1^{M}$ | 460 | 39.1 | 28661[c] | n.a. | n.a. | 114.00 |
| 155 | [Bode and Künzel, 1988] | H4 | Holorib | 51 | 138 | 114 | 150 | 0.75 | 22 | 100 | $1^{M}$ | 460 | 39.1 | 28661[c] | n.a. | n.a. | 130.00 |
| 156 | [Bode and Künzel, 1988] | H5 | Holorib | 51 | 138 | 114 | 150 | 0.75 | 22 | 100 | $1^{M}$ | 460 | 38.3 | 28405[c] | n.a. | n.a. | 111.00 |
| 157 | [Bode and Künzel, 1988] | H6 | Holorib | 51 | 138 | 114 | 150 | 0.75 | 22 | 100 | $1^{M}$ | 460 | 38.3 | 28405[c] | n.a. | n.a. | 115.00 |
| 158 | [Bode and Künzel, 1988] | H7 | Holorib | 51 | 138 | 114 | 150 | 0.75 | 22 | 100 | $1^{M}$ | 460 | 37.4 | 28116[c] | n.a. | n.a. | 122.00 |
| 159 | [Bode and Künzel, 1988] | H8 | Holorib | 51 | 138 | 114 | 150 | 0.75 | 22 | 100 | $1^{M}$ | 460 | 37.4 | 28116[c] | n.a. | n.a. | 123.00 |
| 160 | [Bode and Künzel, 1988] | H11 | Holorib | 51 | 138 | 114 | 150 | 0.75 | 22 | 100 | $1^{M}$ | 460 | 36.5 | 27824[c] | n.a. | n.a. | 108.00 |
| 161 | [Bode and Künzel, 1988] | H13 | Holorib | 51 | 138 | 114 | 150 | 0.75 | 22 | 100 | $1^{M}$ | 460 | 36.5 | 27824[c] | n.a. | n.a. | 116.00 |
| 162 | [Roik and Hanswille, 1988] | D1 | Holorib | 51 | 138 | 114 | 150 | 1.00 | 22 | 125 | $2^{M}$ | 550 | 35.9 | 27628[c] | n.a. | n.a. | 214.00 |
| 163 | [Roik and Hanswille, 1988] | D2 | Holorib | 51 | 138 | 114 | 150 | 1.00 | 22 | 125 | $2^{M}$ | 550 | 35.9 | 27628[c] | n.a. | n.a. | 193.00 |
| 164 | [Roik and Hanswille, 1988] | D3 | Holorib | 51 | 138 | 114 | 150 | 1.00 | 22 | 125 | $2^{M}$ | 550 | 35.9 | 27628[c] | n.a. | n.a. | 212.00 |
| 165 | [Roik and Hanswille, 1988] | D4 | Holorib | 51 | 138 | 114 | 150 | 0.75 | 22 | 125 | $2^{M}$ | 550 | 34.0 | 26999[c] | n.a. | n.a. | 205.00 |
| 166 | [Roik and Hanswille, 1988] | D5 | Holorib | 51 | 138 | 114 | 150 | 0.75 | 22 | 125 | $2^{M}$ | 550 | 34.0 | 26999[c] | n.a. | n.a. | 210.00 |
| 167 | [Ernst, 2006] | S3 | KF70 | 55 | 136 | 193 | 300 | 0.60 | $19^{ehd}$ | 100 | $1^{M,F,T}$ | 460 | 23.5 | 23222[c] | n.a. | n.a. | 90.00[d] |
| 168 | [Ernst, 2006] | S4 | KF70 | 55 | 136 | 193 | 300 | 0.60 | $19^{ehd}$ | 100 | $1^{M,U,T}$ | 460 | 23.1 | 23065[c] | n.a. | n.a. | 80.00[d] |
| 169 | [Ernst, 2006] | S1 | KF70 | 55 | 136 | 193 | 300 | 0.60 | $19^{ehd}$ | 100 | $2^{M,S,T}$ | 460 | 32.9 | 26629[c] | n.a. | n.a. | 75.00[d] |
| 170 | [Ernst, 2006] | S2 | KF70 | 55 | 136 | 193 | 300 | 0.60 | $19^{ehd}$ | 100 | $2^{M,S,T}$ | 460 | 32.9 | 26629[c] | n.a. | n.a. | 70.00[d] |
| 171 | [Ernst, 2006] | S3 | KF70 | 55 | 136 | 193 | 300 | 0.60 | 19 | 100 | $2^{M,S,T}$ | 460 | 33.9 | 26966[c] | n.a. | n.a. | 75.00[d] |
| 172 | [Ernst, 2006] | S4 | KF70 | 55 | 136 | 193 | 300 | 0.60 | $19^{ehd}$ | 100 | $2^{M,S,T}$ | 460 | 33.9 | 26966[c] | n.a. | n.a. | 70.00[d] |
| 173 | [Ernst, 2006] | S5 | KF70 | 55 | 136 | 193 | 300 | 0.60 | 19 | 100 | $2^{M,F,T}$ | 460 | 36.2 | 27727[c] | n.a. | n.a. | 68.00[d] |
| 174 | [Ernst, 2006] | S6 | KF70 | 55 | 136 | 193 | 300 | 0.60 | $19^{ehd}$ | 100 | $2^{M,F,T}$ | 460 | 37.9 | 28277[c] | n.a. | n.a. | 83.00[d] |
| 175 | [Ernst, 2006] | SR1 | KF70 | 55 | 136 | 193 | 300 | 1.00 | 19 | 100 | $1^{M,F,T}$ | 460 | 28.4 | 25058[c] | n.a. | n.a. | 92.00[d] |
| 176 | [Ernst, 2006] | SR2 | KF70 | 55 | 136 | 193 | 300 | 0.60 | 19 | 100 | $1^{M,F,T}$ | 460 | 41.0 | 29259[c] | n.a. | n.a. | 89.00[d] |
| 177 | [Ernst, 2006] | SR3 | KF70 | 55 | 136 | 193 | 300 | 1.00 | 19 | 100 | $1^{M,F,T}$ | 460 | 41.0 | 29259[c] | n.a. | n.a. | 119.00[d] |
| 178 | [Ernst, 2006] | SR4 | KF70 | 55 | 136 | 193 | 300 | 1.00 | $19^{ehd}$ | 100 | $1^{M,F,T}$ | 460 | 32.7 | 26561[c] | n.a. | n.a. | 120.00[d] |
| 179 | [Ernst, 2006] | SR5 | KF70 | 55 | 136 | 193 | 300 | 1.00 | 19 | 100 | $2^{M,S,T}$ | 460 | 38.2 | 28373[c] | n.a. | n.a. | 91.00[d] |

M: Mid Position, F: Favourable Position, U: Unfavourable Position, S: Staggered Position, T: Through deck welded, nh: No head, ehd: Stud enhancement device

c: According to DIN 1045-1 [DIN 1045-1, 2008]: $E_{cm} = \alpha_i \cdot 9500 \cdot f_{cm}^{1/3}$ with $\alpha_i = 0.8 + 0.2 \cdot (f_{cm}/88) \leq 1.0$ d: No static results

*Continued on next page*

Table B.1 – *Continued from previous page*

| No. | Lit | Test | Sheet | Composite Deck | | | | | Shear Connectors | | | | Concrete | | Transv. load | | |
|---|---|---|---|---|---|---|---|---|---|---|---|---|---|---|---|---|---|
| | | | | $h_p$ | $b_u$ | $b_o$ | $a$ | $t$ | $d$ | $h_{sc}$ | $n_R$ | $f_{um}$ | $f_{cm}$ | $E_{cm}$ | $P_T$ | $e$ | $P_e$ |
| | | | | [mm] | [mm] | [mm] | [mm] | [mm] | [mm] | [mm] | [-] | $\left[\frac{N}{mm^2}\right]$ | $\left[\frac{N}{mm^2}\right]$ | $\left[\frac{N}{mm^2}\right]$ | [%] | [mm] | [kN] |
| 180 | [Ernst, 2006] | SR6 | KF70 | 55 | 136 | 193 | 300 | 1.00 | 19 | 100 | $2^{M,F,T}$ | 460 | 30.8 | 25908[c] | n.a. | n.a. | 87.00[d] |
| 181 | [Ernst, 2006] | SR7 | KF70 | 55 | 136 | 193 | 300 | 1.00 | 19 | 100 | $2^{M,F,T}$ | 460 | 30.8 | 25908[c] | n.a. | n.a. | 77.00[d] |
| 182 | [Ernst, 2006] | SR8 | KF70 | 55 | 136 | 193 | 300 | 1.00 | $19^{ehd}$ | 100 | $2^{M,S,T}$ | 460 | 39.2 | 28692[c] | n.a. | n.a. | 97.00[d] |
| 183 | [Ernst, 2006] | SR9 | KF70 | 55 | 136 | 193 | 300 | 1.00 | $19^{ehd}$ | 100 | $2^{M,F,T}$ | 460 | 34.4 | 27133[c] | n.a. | n.a. | 96.00[d] |
| 184 | [Ernst, 2006] | SR10 | KF70 | 55 | 136 | 193 | 300 | 1.00 | $19^{ehd}$ | 100 | $2^{M,F,T}$ | 460 | 34.4 | 27133[c] | n.a. | n.a. | 86.00[d] |
| 185 | [Ernst, 2006] | SR13 | KF70 | 55 | 136 | 193 | 300 | 1.00 | 19 | 130 | $2^{M,F}$ | 460 | 38.2 | 28373[c] | n.a. | n.a. | 70.00[d] |
| 186 | [Ernst, 2006] | S01 | KF70 | 55 | 136 | 193 | 300 | 1.00 | 19 | 100 | $2^{M,S,T}$ | 460 | 26.6 | 24401[c] | n.a. | n.a. | 80.00[d] |
| 187 | [Ernst, 2006] | S02 | KF70 | 55 | 136 | 193 | 300 | 1.00 | 19 | 100 | $2^{M,S,T}$ | 460 | 32.8 | 26595[c] | n.a. | n.a. | 93.00[d] |
| 188 | [Ernst, 2006] | S03 | KF70 | 55 | 136 | 193 | 300 | 1.00 | 19 | 100 | $2^{M,S,T}$ | 460 | 32.1 | 26356[c] | n.a. | n.a. | 81.00[d] |
| 189 | [Ernst, 2006] | S04 | KF70 | 55 | 136 | 193 | 300 | 1.00 | 19 | 100 | $2^{M,S,T}$ | 460 | 26.6 | 24401[c] | n.a. | n.a. | 72.00[d] |
| 190 | [Ernst, 2006] | S05 | KF70 | 55 | 136 | 193 | 300 | 1.00 | 19 | 100 | $2^{M,S,T}$ | 460 | 31.3 | 26081[c] | n.a. | n.a. | 78.00[d] |
| 191 | [Ernst, 2006] | S06 | KF70 | 55 | 136 | 193 | 300 | 1.00 | 19 | 100 | $2^{M,S,T}$ | 460 | 32.3 | 26425[c] | n.a. | n.a. | 67.00[d] |
| 192 | [Ernst, 2006] | S07 | KF70 | 55 | 136 | 193 | 300 | 1.00 | 19 | 100 | $1^{M,F,T}$ | 460 | 30.2 | 25698[c] | n.a. | n.a. | 129.00[d] |
| 193 | [Ernst, 2006] | S08 | KF70 | 55 | 136 | 193 | 300 | 1.00 | 19 | 100 | $1^{M,F,T}$ | 460 | 32.2 | 26390[c] | n.a. | n.a. | 131.00[d] |
| 194 | [Ernst, 2006] | S09 | KF70 | 55 | 136 | 193 | 300 | 1.00 | 19 | 100 | $1^{M,F,T}$ | 460 | 35.3 | 27431[c] | n.a. | n.a. | 139.00[d] |
| 195 | [Ernst, 2006] | S10 | KF70 | 55 | 136 | 193 | 300 | 1.00 | 19 | 100 | $1^{M,F,T}$ | 460 | 29.6 | 27431[c] | n.a. | n.a. | 92.00[d] |
| 196 | [Ernst, 2006] | S11 | KF70 | 55 | 136 | 193 | 300 | 1.00 | 19 | 100 | $1^{M,F,T}$ | 460 | 31.9 | 26288[c] | n.a. | n.a. | 100.00[d] |
| 197 | [Ernst, 2006] | S12 | KF70 | 55 | 136 | 193 | 300 | 1.00 | 19 | 100 | $1^{M,F,T}$ | 460 | 39.8 | 28882[c] | n.a. | n.a. | 117.00[d] |
| 198 | [Ernst, 2006] | S01 | KF70 | 55 | 136 | 193 | 300 | 0.75 | 19 | 125 | $1^{M,F,T}$ | 417 | 48.2 | 31446[c] | n.a. | n.a. | 111.00[d] |
| 199 | [Ernst, 2006] | S02 | KF70 | 55 | 136 | 193 | 300 | 0.75 | 19 | 125 | $1^{M,U,T}$ | 417 | 48.5 | 31535[c] | n.a. | n.a. | 108.00[d] |
| 200 | [Ernst, 2006] | S03 | KF70 | 55 | 136 | 193 | 300 | 0.75 | $19^{ehd}$ | 125 | $1^{M,F,T}$ | 417 | 48.5 | 31535[c] | n.a. | n.a. | 114.00[d] |
| 201 | [Ernst, 2006] | S04 | KF70 | 55 | 136 | 193 | 300 | 0.75 | $19^{ehd}$ | 125 | $1^{M,U,T}$ | 417 | 49.1 | 31712[c] | n.a. | n.a. | 132.00[d] |
| 202 | [Ernst, 2006] | SW1 | W-Dek | 78 | 143 | 212 | 350 | 0.75 | 19 | 127 | $1^{M}$ | 509 | 29.6 | 25486[c] | n.a. | n.a. | 100.00[d] |
| 203 | [Ernst, 2006] | SW2 | W-Dek | 78 | 143 | 212 | 350 | 0.75 | 19 | 127 | $1^{M}$ | 509 | 30.7 | 25873[c] | n.a. | n.a. | 99.70[d] |
| 204 | [Ernst, 2006] | SW3 | n.a. | 78 | 143 | 212 | 350 | n.a. | 19 | 127 | $1^{M}$ | 509 | 29.8 | 25557[c] | n.a. | n.a. | 84.10[d] |
| 205 | [Ernst, 2006] | SW4 | n.a. | 78 | 143 | 212 | 350 | n.a. | 19 | 127 | $1^{M}$ | 509 | 30.9 | 25942[c] | n.a. | n.a. | 77.60[d] |
| 206 | [Ernst, 2006] | SW5 | n.a. | 78 | 143 | 212 | 350 | n.a. | 19 | 127 | $1^{M}$ | 509 | 41.4 | 29384[c] | n.a. | n.a. | 95.00[d] |
| 207 | [Ernst, 2006] | SW6 | n.a. | 78 | 143 | 212 | 350 | n.a. | 19 | 127 | $1^{M}$ | 509 | 34.3 | 27099[c] | n.a. | n.a. | 76.70[d] |
| 208 | [Ernst, 2006] | SW7 | n.a. | 78 | 143 | 212 | 350 | n.a. | 19 | 127 | $1^{M}$ | 509 | 33.8 | 26932[c] | n.a. | n.a. | 74.20[d] |
| 209 | [Ernst, 2006] | SWP1 | n.a. | 78 | 143 | 212 | 350 | n.a. | 19 | 127 | $2^{M}$ | 509 | 28.3 | 25022[c] | n.a. | n.a. | 51.60[d] |
| 210 | [Ernst, 2006] | SWP2 | n.a. | 78 | 143 | 212 | 350 | n.a. | 19 | 127 | $2^{M}$ | 509 | 28.5 | 25094[c] | n.a. | n.a. | 51.60[d] |
| 211 | [Ernst, 2006] | SWP3 | n.a. | 78 | 143 | 212 | 350 | n.a. | 19 | 127 | $2^{M}$ | 509 | 29.1 | 25309[c] | n.a. | n.a. | 47.40[d] |
| 212 | [Ernst, 2006] | SWR1 | n.a. | 78 | 143 | 212 | 350 | n.a. | 19 | 127 | $2^{M}$ | 509 | 31.9 | 26288[c] | n.a. | n.a. | 56.00[d] |
| 213 | [Ernst, 2006] | SWR2 | n.a. | 78 | 143 | 212 | 350 | n.a. | 19 | 127 | $2^{M}$ | 509 | 29.3 | 25380[c] | n.a. | n.a. | 64.20[d] |
| 214 | [Ernst, 2006] | SWR3 | n.a. | 78 | 143 | 212 | 350 | n.a. | $19^{ehd}$ | 127 | $2^{M}$ | 509 | 31.7 | 26219[c] | n.a. | n.a. | 64.50[d] |
| 215 | [Ernst, 2006] | SWR4 | n.a. | 78 | 143 | 212 | 350 | n.a. | $19^{ehd}$ | 127 | $2^{M}$ | 509 | 32.3 | 26425[c] | n.a. | n.a. | 67.20[d] |

M: Mid Position, F: Favourable Position, U: Unfavourable Position, S: Staggered Position, T: Through deck welded, nh: No head, ehd: Stud enhancement device

c: According to DIN 1045-1 [DIN 1045-1, 2008]: $E_{cm} = \alpha_i \cdot 9500 \cdot f_{cm}^{1/3}$ with $\alpha_i = 0.8 + 0.2 \cdot (f_{cm}/88) \leq 1.0$ d: No static results

*Continued on next page*

Table B.1 – *Continued from previous page*

| No. | Lit | Test | Sheet | Composite Deck | | | | | Shear Connectors | | | | Concrete | | Transv. load | | |
|---|---|---|---|---|---|---|---|---|---|---|---|---|---|---|---|---|---|
| | | | | $h_p$ | $b_u$ | $b_o$ | $a$ | $t$ | $d$ | $h_{sc}$ | $n_R$ | $f_{um}$ | $f_{cm}$ | $E_{cm}$ | $P_T$ | $e$ | $P_e$ |
| | | | | [mm] | [mm] | [mm] | [mm] | [mm] | [mm] | [mm] | [-] | $\left[\frac{\text{N}}{\text{mm}^2}\right]$ | $\left[\frac{\text{N}}{\text{mm}^2}\right]$ | $\left[\frac{\text{N}}{\text{mm}^2}\right]$ | [%] | [mm] | [kN] |
| 216 | [Ernst, 2006] | SWR5 | n.a. | 78 | 143 | 212 | 350 | n.a. | 19[ehd] | 127 | 2[M] | 509 | 30.1 | 25663[c] | n.a. | n.a. | 77.80[d] |
| 217 | [Ernst, 2006] | SWR6 | W-Dek | 78 | 143 | 212 | 350 | 1.00 | 19 | 127 | 2[M] | 509 | 32.9 | 26629[c] | n.a. | n.a. | 69.70[d] |
| 218 | [Ernst, 2006] | SWR7 | W-Dek | 78 | 143 | 212 | 350 | 1.00 | 19 | 127 | 2[M] | 509 | 32.9 | 26629[c] | n.a. | n.a. | 69.70[d] |
| 219 | [Ernst, 2006] | SWR8 | n.a. | 78 | 143 | 212 | 350 | n.a. | 19[ehd] | 127 | 2[M] | 509 | 33.4 | 26798[c] | n.a. | n.a. | 82.10[d] |
| 220 | [Ernst, 2006] | SWR9 | n.a. | 78 | 143 | 212 | 350 | n.a. | 19[ehd] | 127 | 1[M] | 509 | 32.0 | 26322[c] | n.a. | n.a. | 107.80[d] |
| 221 | [Ernst, 2006] | SWD1 | W-Dek | 78 | 143 | 212 | 350 | 0.75 | 19[ehd] | 127 | 1[M] | 509 | 33.9 | 26966[c] | n.a. | n.a. | 101.10[d] |
| 222 | [Ernst, 2006] | SWD2 | W-Dek | 78 | 143 | 212 | 350 | 0.75 | 19[ehd] | 127 | 1[M] | 509 | 33.2 | 26730[c] | n.a. | n.a. | 114.60[d] |
| 223 | [Ernst, 2006] | SWD3 | W-Dek | 78 | 143 | 212 | 350 | 0.75 | 19[ehd] | 127 | 1[M] | 509 | 33.6 | 26865[c] | n.a. | n.a. | 121.00[d] |
| 224 | [Ernst, 2006] | SWD4 | W-Dek | 78 | 143 | 212 | 350 | 0.75 | 19[ehd] | 127 | 1[M] | 509 | 32.8 | 26595[c] | n.a. | n.a. | 139.50[d] |
| 225 | [Ernst, 2006] | SWD5 | W-Dek | 78 | 143 | 212 | 350 | 0.75 | 19[ehd] | 127 | 2[M] | 509 | 30.9 | 25942[c] | n.a. | n.a. | 64.40[d] |
| 226 | [Ernst, 2006] | SWD6 | W-Dek | 78 | 143 | 212 | 350 | 0.75 | 19[ehd] | 127 | 2[M] | 509 | 30.0 | 25628[c] | n.a. | n.a. | 73.80[d] |
| 227 | [Ernst, 2006] | SWD7 | W-Dek | 78 | 143 | 212 | 350 | 0.75 | 19[ehd] | 127 | 2[M] | 509 | 30.5 | 25803[c] | n.a. | n.a. | 86.10[d] |
| 228 | [Ernst, 2006] | SWD8 | W-Dek | 78 | 143 | 212 | 350 | 0.75 | 19[ehd] | 127 | 2[M] | 509 | 29.8 | 25557[c] | n.a. | n.a. | 96.60[d] |
| 229 | [Ernst, 2006] | SDM1 | W-Dek | 78 | 143 | 212 | 350 | 0.75 | 19 | 127 | 2[S] | 550 | 31.2 | 26046[c] | n.a. | n.a. | 69.80[d] |
| 230 | [Ernst, 2006] | SDM2 | W-Dek | 78 | 143 | 212 | 350 | 0.75 | 19 | 127 | 2[S] | 550 | 31.3 | 26081[c] | n.a. | n.a. | 86.40[d] |
| 231 | [Ernst, 2006] | SDM3 | W-Dek | 78 | 143 | 212 | 350 | 0.75 | 19 | 127 | 2[S] | 550 | 33.0 | 26663[c] | n.a. | n.a. | 65.90[d] |
| 232 | [Ernst, 2006] | SDM4 | W-Dek | 78 | 143 | 212 | 350 | 0.75 | 19 | 127 | 2[S] | 550 | 33.5 | 26831[c] | n.a. | n.a. | 85.70[d] |
| 233 | [Ernst, 2006] | SDM5 | W-Dek | 78 | 143 | 212 | 350 | 0.75 | 19 | 127 | 2[M] | 509 | 29.9 | 25592[c] | n.a. | n.a. | 61.10[d] |
| 234 | [Ernst, 2006] | SDM6 | W-Dek | 78 | 143 | 212 | 350 | 0.75 | 19 | 127 | 2[M] | 509 | 29.6 | 25486[c] | n.a. | n.a. | 86.00[d] |
| 235 | [Smith, 2009] | A1U-1 | MD60 | 60 | 119 | 181 | 323 | 0.90 | 19 | 100 | 1[F,T] | 550 | 18.9 | 24110 | 12 | n.a. | 94.56 |
| 236 | [Smith, 2009] | A1U-2 | MD60 | 60 | 119 | 181 | 323 | 0.90 | 19 | 100 | 1[F,T] | 550 | 18.9 | 24110 | 12 | n.a. | 83.09 |
| 237 | [Smith, 2009] | A1U-3 | MD60 | 60 | 119 | 181 | 323 | 0.90 | 19 | 100 | 1[F,T] | 550 | 18.9 | 24110 | 12 | n.a. | 95.98 |
| 238 | [Smith, 2009] | A1D-1 | MD60 | 60 | 119 | 181 | 323 | 0.90 | 19 | 100 | 1[F,T] | 550 | 19.0 | 21392[c] | 12 | n.a. | 115.28 |
| 239 | [Smith, 2009] | A1D-2 | MD60 | 60 | 119 | 181 | 323 | 0.90 | 19 | 100 | 1[F,T] | 550 | 19.0 | 21392[c] | 12 | n.a. | 112.49 |
| 240 | [Smith, 2009] | A1D-3 | MD60 | 60 | 119 | 181 | 323 | 0.90 | 19 | 100 | 1[F,T] | 550 | 19.0 | 21392[c] | 12 | n.a. | 121.49 |
| 241 | [Smith, 2009] | B1U-1 | MD60 | 60 | 119 | 181 | 323 | 0.90 | 19 | 100 | 1[F,T] | 550 | 19.1 | 23920 | 12 | n.a. | 121.32 |
| 242 | [Smith, 2009] | B1U-2 | MD60 | 60 | 119 | 181 | 323 | 0.90 | 19 | 100 | 1[F,T] | 550 | 19.1 | 23920 | 12 | n.a. | 107.32 |
| 243 | [Smith, 2009] | B1U-3 | MD60 | 60 | 119 | 181 | 323 | 0.90 | 19 | 100 | 1[F,T] | 550 | 19.0 | 23920 | 12 | n.a. | 107.14 |
| 244 | [Smith, 2009] | A2DX-1 | MD60 | 60 | 119 | 181 | 323 | 0.90 | 19 | 100 | 2[F,T] | 550 | 19.3 | 23550 | 12 | n.a. | 57.85 |
| 245 | [Smith, 2009] | A2DX-2 | MD60 | 60 | 119 | 181 | 323 | 0.90 | 19 | 100 | 2[F,T] | 550 | 19.3 | 23550 | 12 | n.a. | 63.93 |
| 246 | [Smith, 2009] | A2DX-3 | MD60 | 60 | 119 | 181 | 323 | 0.90 | 19 | 100 | 2[F,T] | 550 | 19.3 | 23550 | 12 | n.a. | 66.60 |
| 247 | [Smith, 2009] | A2UY-1 | MD60 | 60 | 119 | 181 | 323 | 0.90 | 19 | 100 | 2[F,T] | 550 | 19.3 | 23550 | 12 | n.a. | 55.10 |
| 248 | [Smith, 2009] | A2UY-2 | MD60 | 60 | 119 | 181 | 323 | 0.90 | 19 | 100 | 2[F,T] | 550 | 19.3 | 23550 | 12 | n.a. | 47.90 |
| 249 | [Smith, 2009] | A2UY-3 | MD60 | 60 | 119 | 181 | 323 | 0.90 | 19 | 100 | 2[F,T] | 550 | 19.3 | 23550 | 12 | n.a. | 65.10 |
| 250 | [Smith, 2009] | A2DY-1 | MD60 | 60 | 119 | 181 | 323 | 0.90 | 19 | 100 | 2[F,T] | 550 | 21.1 | 22248[c] | 12 | n.a. | 76.15 |
| 251 | [Smith, 2009] | A2DY-2 | MD60 | 60 | 119 | 181 | 323 | 0.90 | 19 | 100 | 2[F,T] | 550 | 21.1 | 22248[c] | 12 | n.a. | 70.88 |

M: Mid Position, F: Favourable Position, U: Unfavourable Position, S: Staggered Position, T: Through deck welded, nh: No head, ehd: Stud enhancement device

c: According to DIN 1045-1 [DIN 1045-1, 2008]: $E_{cm} = \alpha_i \cdot 9500 \cdot f_{cm}^{1/3}$ with $\alpha_i = 0.8 + 0.2 \cdot (f_{cm}/88) \leq 1.0$ d: No static results

*Continued on next page*

Table B.1 – *Continued from previous page*

| No. | Lit | Test | Sheet | Composite Deck | | | | | | Shear Connectors | | | Concrete | | Transv. load | | |
|---|---|---|---|---|---|---|---|---|---|---|---|---|---|---|---|---|---|
| | | | | $h_p$ | $b_u$ | $b_o$ | $a$ | $t$ | $d$ | $h_{sc}$ | $n_R$ | $f_{um}$ | $f_{cm}$ | $E_{cm}$ | $P_T$ | $e$ | $P_e$ |
| | | | | [mm] | [mm] | [mm] | [mm] | [mm] | [mm] | [mm] | [-] | $\left[\frac{N}{mm^2}\right]$ | $\left[\frac{N}{mm^2}\right]$ | $\left[\frac{N}{mm^2}\right]$ | [%] | [mm] | [kN] |
| 252 | [Smith, 2009] | A2DY-3 | MD60 | 60 | 119 | 181 | 323 | 0.90 | 19 | 100 | $2^{F,T}$ | 550 | 21.1 | 22248[c] | 12 | n.a. | 75.04 |
| 253 | [Smith, 2009] | A2DZ-1 | MD60 | 60 | 119 | 181 | 323 | 0.90 | 19 | 100 | $2^{F,T}$ | 550 | 19.3 | 23550 | 12 | n.a. | 54.4 |
| 254 | [Smith, 2009] | A2DZ-2 | MD60 | 60 | 119 | 181 | 323 | 0.90 | 19 | 100 | $2^{F,T}$ | 550 | 19.3 | 23550 | 12 | n.a. | 64.90 |
| 255 | [Smith, 2009] | A2DZ-3 | MD60 | 60 | 119 | 181 | 323 | 0.90 | 19 | 100 | $2^{F,T}$ | 550 | 19.3 | 23550 | 12 | n.a. | 66.50 |
| 256 | [Smith, 2009] | B2U-1 | MD60 | 60 | 119 | 181 | 323 | 0.90 | 19 | 100 | $2^{F,T}$ | 550 | 18.9 | 24110 | 12 | n.a. | 76.50 |
| 257 | [Smith, 2009] | B2U-2 | MD60 | 60 | 119 | 181 | 323 | 0.90 | 19 | 100 | $2^{F,T}$ | 550 | 18.9 | 24110 | 12 | n.a. | 69.40 |
| 258 | [Smith, 2009] | B2U-3 | MD60 | 60 | 119 | 181 | 323 | 0.90 | 19 | 100 | $2^{F,T}$ | 550 | 18.9 | 24110 | 12 | n.a. | 78.20 |
| 259 | [Smith, 2009] | A3D-1 | MD60 | 60 | 119 | 181 | 323 | 0.90 | 19 | 100 | $3^{F,T}$ | 550 | 18.9 | 24110 | 12 | n.a. | 52.90 |
| 260 | [Smith, 2009] | A3D-2 | MD60 | 60 | 119 | 181 | 323 | 0.90 | 19 | 100 | $3^{F,T}$ | 550 | 18.9 | 24110 | 12 | n.a. | 47.30 |
| 261 | [Smith, 2009] | A3D-3 | MD60 | 60 | 119 | 181 | 323 | 0.90 | 19 | 100 | $3^{F,T}$ | 550 | 18.9 | 24110 | 12 | n.a. | 39.00 |
| 262 | [Odenbreit et al., 2015] | 1-03-1 | Cofraplus 60 | 58 | 62 | 101 | 207 | 0.885 | 22.1 | 123.3 | $1^{M}$ | 514 | 41.0 | 29259[c] | n.a. | n.a. | 74.63 |
| 263 | [Odenbreit et al., 2015] | 1-03-2 | Cofraplus 60 | 58 | 62 | 101 | 207 | 0.885 | 22.1 | 122.5 | $1^{M}$ | 514 | 42.5 | 29724[c] | n.a. | n.a. | 86.00 |
| 264 | [Odenbreit et al., 2015] | 1-03-3 | Cofraplus 60 | 58 | 62 | 101 | 207 | 0.885 | 22.2 | 122.8 | $1^{M}$ | 514 | 42.9 | 29848[c] | n.a. | n.a. | 88.88 |
| 265 | [Odenbreit et al., 2015] | 2-01-1 | Cofraplus 60 | 58 | 62 | 101 | 207 | 0.885 | 19.1 | 121.8 | $1^{M,T}$ | 467 | 42.4 | 29694[c] | n.a. | n.a. | 57.88 |
| 266 | [Odenbreit et al., 2015] | 2-01-2 | Cofraplus 60 | 58 | 62 | 101 | 207 | 0.885 | 19.1 | 121.8 | $1^{M,T}$ | 467 | 42.6 | 29755[c] | n.a. | n.a. | 62.75 |
| 267 | [Odenbreit et al., 2015] | 2-01-3 | Cofraplus 60 | 58 | 62 | 101 | 207 | 0.885 | 19.2 | 122.0 | $1^{M,T}$ | 467 | 41.8 | 29508[c] | n.a. | n.a. | 66.63 |
| 268 | [Odenbreit et al., 2015] | 2-02 | Cofraplus 60 | 58 | 62 | 101 | 207 | 0.885 | 19 | 122.5 | $1^{M,T}$ | 467 | 40.7 | 29165[c] | n.a. | n.a. | 62.00 |
| 269 | [Odenbreit et al., 2015] | 2-03 | Cofraplus 60 | 58 | 62 | 101 | 207 | 0.885 | 19 | 121.8 | $1^{M}$ | 467 | 39.7 | 28851[c] | n.a. | n.a. | 51.63 |
| 270 | [Odenbreit et al., 2015] | 2-04 | Cofraplus 60 | 58 | 62 | 101 | 207 | 0.885 | 19 | 120.6 | $2^{M}$ | 467 | 40.3 | 29040[c] | n.a. | n.a. | 61.50 |
| 271 | [Odenbreit et al., 2015] | 2-05-1 | Cofraplus 60 | 58 | 62 | 101 | 207 | 0.885 | 19 | 121.0 | $2^{M,T}$ | 467 | 40.2 | 29008[c] | n.a. | n.a. | 57.94 |
| 272 | [Odenbreit et al., 2015] | 2-05-2 | Cofraplus 60 | 58 | 62 | 101 | 207 | 0.885 | 19 | 121.8 | $2^{M,T}$ | 467 | 38.6 | 28501[c] | n.a. | n.a. | 64.44 |
| 273 | [Odenbreit et al., 2015] | 2-05-3 | Cofraplus 60 | 58 | 62 | 101 | 207 | 0.885 | 19 | 121.8 | $2^{M,T}$ | 467 | 39.2 | 28692[c] | n.a. | n.a. | 59.50 |
| 274 | [Odenbreit et al., 2015] | 2-06-1 | Cofraplus 60 | 58 | 62 | 101 | 207 | 0.885 | 22.2 | 122.3 | $1^{M}$ | 514 | 40.1 | 28977[c] | n.a. | n.a. | 79.13 |
| 275 | [Odenbreit et al., 2015] | 2-06-2 | Cofraplus 60 | 58 | 62 | 101 | 207 | 0.885 | 22.2 | 122.3 | $1^{M}$ | 514 | 39.6 | 28819[c] | n.a. | n.a. | 83.38 |
| 276 | [Odenbreit et al., 2015] | 2-06-3 | Cofraplus 60 | 58 | 62 | 101 | 207 | 0.885 | 22.3 | 122.3 | $1^{M}$ | 514 | 40.6 | 29134[c] | n.a. | n.a. | 86.75 |
| 277 | [Odenbreit et al., 2015] | 2-07-1 | Cofraplus 60 | 58 | 62 | 101 | 207 | 0.885 | 22.2 | 121.8 | $1^{M}$ | 514 | 46.4 | 30910[c] | n.a. | n.a. | 97.25 |
| 278 | [Odenbreit et al., 2015] | 2-07-2 | Cofraplus 60 | 58 | 62 | 101 | 207 | 0.885 | 22.3 | 122.3 | $1^{M}$ | 514 | 46.3 | 30880[c] | n.a. | n.a. | 100.38 |
| 279 | [Odenbreit et al., 2015] | 2-07-3 | Cofraplus 60 | 58 | 62 | 101 | 207 | 0.885 | 22.3 | 122.3 | $1^{M}$ | 514 | 46.0 | 30790[c] | n.a. | n.a. | 99.75 |
| 280 | [Odenbreit et al., 2015] | 2-08 | Cofraplus 60 | 58 | 62 | 101 | 207 | 0.885 | 19.1 | 122.0 | $1^{M}$ | 467 | 45.8 | 30790[c] | n.a. | n.a. | 51.00 |
| 281 | [Odenbreit et al., 2015] | 3-03 | Cofrastra 56 | 56 | 137 | 110 | 150 | 1.00 | 19.0 | 122.0 | $1^{M,T}$ | 467 | 39.9 | 28914[c] | n.a. | n.a. | 84.63 |
| 282 | [Odenbreit et al., 2015] | 3-04 | Cofrastra 56 | 56 | 137 | 110 | 150 | 1.00 | 19.1 | 122.3 | $1^{M}$ | 467 | 41.0 | 29259[c] | n.a. | n.a. | 95.63 |
| 283 | [Odenbreit et al., 2015] | 3-05 | Cofrastra 56 | 56 | 137 | 110 | 150 | 1.00 | 19.1 | 121.9 | $2^{M,T}$ | 467 | 39.7 | 28851[c] | n.a. | n.a. | 87.19 |
| 284 | [Odenbreit et al., 2015] | 3-06 | Cofrastra 56 | 56 | 137 | 110 | 150 | 1.00 | 19.1 | 121.8 | $2^{M,T}$ | 467 | 39.5 | 28787[c] | n.a. | n.a. | 85.13 |
| 285 | [Odenbreit et al., 2015] | 3-07 | Cofrastra 56 | 56 | 137 | 110 | 150 | 1.00 | 19.1 | 122.4 | $2^{M}$ | 467 | 40.7 | 29165[c] | n.a. | n.a. | 93.88 |
| 286 | [Odenbreit et al., 2015] | 3-08 | Cofrastra 56 | 56 | 137 | 110 | 150 | 1.00 | 19.1 | 122.0 | $2^{M}$ | 467 | 41.3 | 29352[c] | n.a. | n.a. | 97.25 |
| 287 | [Odenbreit et al., 2015] | 3-09 | Cofrastra 56 | 56 | 137 | 110 | 150 | 1.00 | 22.2 | 123.3 | $1^{M}$ | 467 | 40.7 | 29165[c] | n.a. | n.a. | 117.13 |

M: Mid Position, F: Favourable Position, U: Unfavourable Position, S: Staggered Position, T: Through deck welded, nh: No head, ehd: Stud enhancement device

c: According to DIN 1045-1 [DIN 1045-1, 2008]: $E_{cm} = \alpha_i \cdot 9500 \cdot f_{cm}^{1/3}$ with $\alpha_i = 0.8 + 0.2 \cdot (f_{cm}/88) \leq 1.0$ d: No static results

*Continued on next page*

Table B.1 – *Continued from previous page*

| No. | Lit | Test | Sheet | Composite Deck | | | | | | Shear Connectors | | | Concrete | | | Transv. load | | |
|---|---|---|---|---|---|---|---|---|---|---|---|---|---|---|---|---|---|---|
| | | | | $h_p$ | $b_u$ | $b_o$ | $a$ | $t$ | $d$ | $h_{sc}$ | $n_R$ | $f_{um}$ | $f_{cm}$ | $E_{cm}$ | $P_T$ | $e$ | $P_e$ |
| | | | | [mm] | [mm] | [mm] | [mm] | [mm] | [mm] | [mm] | [-] | $\left[\frac{\text{N}}{\text{mm}^2}\right]$ | $\left[\frac{\text{N}}{\text{mm}^2}\right]$ | $\left[\frac{\text{N}}{\text{mm}^2}\right]$ | [%] | [mm] | [kN] |
| 288 | [Odenbreit et al., 2015] | 3-10 | Cofrastra 56 | 56 | 137 | 110 | 150 | 1.00 | 22.2 | 122.3 | 1[M] | 467 | 40.5 | 29102[c] | n.a. | n.a. | 107.50 |

M: Mid Position, F: Favourable Position, U: Unfavourable Position, S: Staggered Position, T: Through deck welded, nh: No head, ehd: Stud enhancement device

c: According to DIN 1045-1 [DIN 1045-1, 2008]: $E_{cm} = \alpha_i \cdot 9500 \cdot f_{cm}^{1/3}$ with $\alpha_i = 0.8 + 0.2 \cdot (f_{cm}/88) \leq 1.0$ d: No static results

# C Data sheets of conducted push-out tests

## Specimen PV-1

### STEEL PROFILE

| | | | |
|---|---|---|---|
| HEB 260 | $L = 700$mm | $f_y = 424$N/mm$^2$ | $f_u = 525$N/mm$^2$ |

### COMPOSITE DECKING

| | | | |
|---|---|---|---|
| RD80 | $t = 1.2$mm | through welded | |
| $h_p = 80$mm | $b_u = 135$mm | $b_o = 185$mm | $a = 300$mm |

### CONCRETE SLABS

| | | | |
|---|---|---|---|
| $B = 900$ mm | $H = 900$ mm | $D = 160$ mm | No recess |
| $f_{cm} = 45.80$ N/mm$^2$ | $E_c$ not measured | | |

### REINFORCEMENT

| | | |
|---|---|---|
| BSt 500 A | Top: n.a. | Bottom: ∅10/150 |
| | Edge: ∅8/150 | Recess: n.a. |

### SHEAR STUDS

| | | |
|---|---|---|
| 4 Köco SD 19x150 | favourable-position | $f_u = 550.7$N/mm$^2$ |

| | | A1 | A2 | B1 | B2 | $\mu$ | $\sigma$ |
|---|---|---|---|---|---|---|---|
| $d$ | [mm] | | 19mm nominal | | | | |
| $h_{sc}$ | [mm] | | 150mm nominal | | | | |

### TEST RESULTS

$P_{e1} = 116.41$ kN/stud $P_{e1,static} = 108.41$ kN/stud $s_{e1} = 2.40$ mm
Stud failure

### LOAD-SLIP CURVE

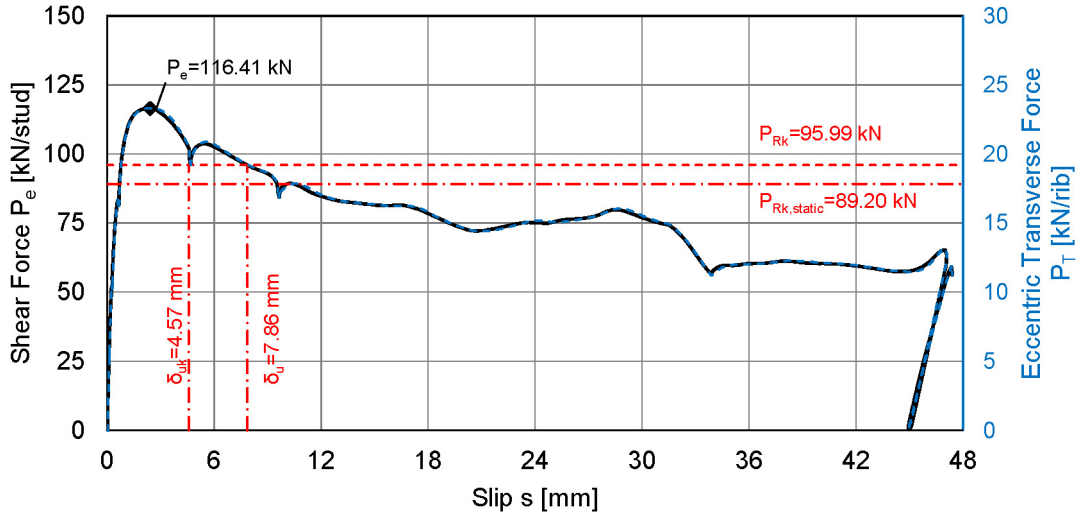

## Specimen PV-1

### STEEL PROFILE

| | | | |
|---|---|---|---|
| HEB 260 | $L = 700$mm | $f_y = 424$N/mm$^2$ | $f_u = 525$N/mm$^2$ |

### COMPOSITE DECKING

| | | | |
|---|---|---|---|
| RD80 | $t = 1.2$mm | through welded | |
| $h_p = 80$mm | $b_u = 135$mm | $b_o = 185$mm | $a = 300$mm |

### CONCRETE SLABS

| | | | |
|---|---|---|---|
| $B = 900$ mm | $H = 900$ mm | $D = 160$ mm | No recess |
| $f_{cm} = 45.80$ N/mm$^2$ | $E_c$ not measured | | |

### REINFORCEMENT

| | | |
|---|---|---|
| BSt 500 A | Top: n.a. | Bottom: ∅10/150 |
| | Edge: ∅8/150 | Recess: n.a. |

### SHEAR STUDS

| | | |
|---|---|---|
| 4 Köco SD 19x150 | favourable-position | $f_u = 550.7$N/mm$^2$ |

| | | A1 | A2 | B1 | B2 | $\mu$ | $\sigma$ |
|---|---|---|---|---|---|---|---|
| $d$ | [mm] | 19mm nominal | | | | | |
| $h_{sc}$ | [mm] | 150mm nominal | | | | | |

### TEST RESULTS

$P_{e1} = 106.66$ kN/stud $P_{e1,static} = 99.11$ kN/stud $s_{e1} = 1.53$ mm
Stud failure

### LOAD-SLIP CURVE

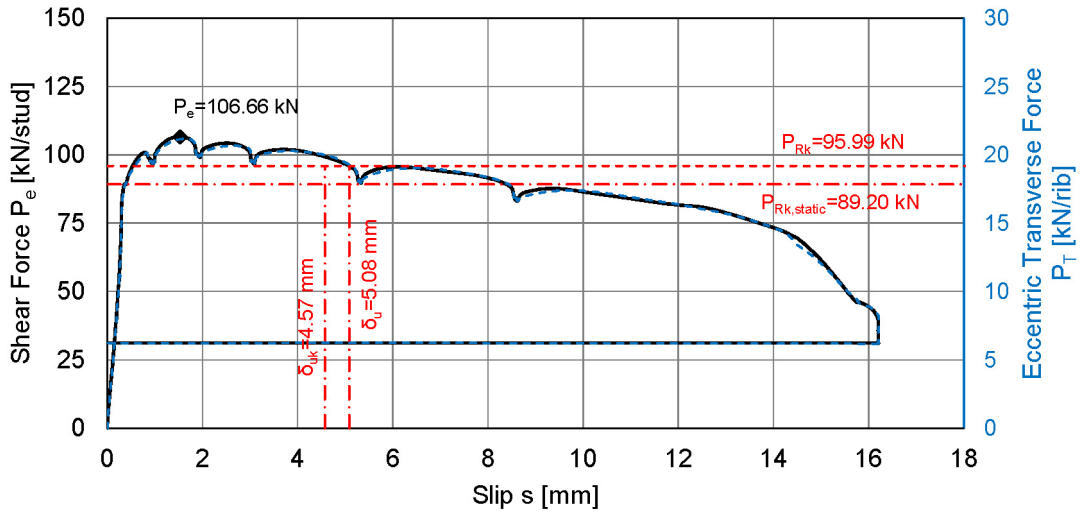

## Specimen 1-04-1

### STEEL PROFILE

| | | | |
|---|---|---|---|
| HEB 260 | $L = 700$mm | $f_y = 424$N/mm$^2$ | $f_u = 525$N/mm$^2$ |

### COMPOSITE DECKING

| | | | |
|---|---|---|---|
| CP60 | $t = 0.88$mm | pre-punched | |
| $h_p = 58$mm | $b_u = 62$mm | $b_o = 101$mm | $a = 207$mm |

### CONCRETE SLABS

| | | | |
|---|---|---|---|
| $B = 900$ mm | $H = 683$ mm | $D = 160$ mm | Recess $200x30$ mm |
| $f_{cm} = 30.06$ N/mm$^2$ | $E_c = 20900$ N/mm$^2$ | | |

### REINFORCEMENT

| | | |
|---|---|---|
| BSt 500 A | Top: Q335A | Bottom: Q188A |
| | Edge: ∅8/150 | Recess: 1∅20 |

### SHEAR STUDS

| | | |
|---|---|---|
| 4 Köco SD 22x125 | mid-position | $f_u = 550.7$N/mm$^2$ |

| | | A1 | A2 | B1 | B2 | $\mu$ | $\sigma$ |
|---|---|---|---|---|---|---|---|
| $d$ | [mm] | 22.17 | 22.15 | 22.16 | 22.16 | 22.16 | 0.008 |
| $h_{sc}$ | [mm] | 124.37 | 124.72 | 123.63 | 124.58 | 124.33 | 0.485 |

### TEST RESULTS

| | | |
|---|---|---|
| $P_{e1} = 73.91$ kN/stud | $P_{e1,static} = 70.44$ kN/stud | $s_{e1} = 8.49$ mm |
| $P_{e2} = 109.75$ kN/stud | $P_{e2,static} = 99.51$ kN/stud | $s_{e2} = 45.88$ mm |
| Rib punch-through | Concrete pull-out | Stud failure |

### LOAD-SLIP CURVE

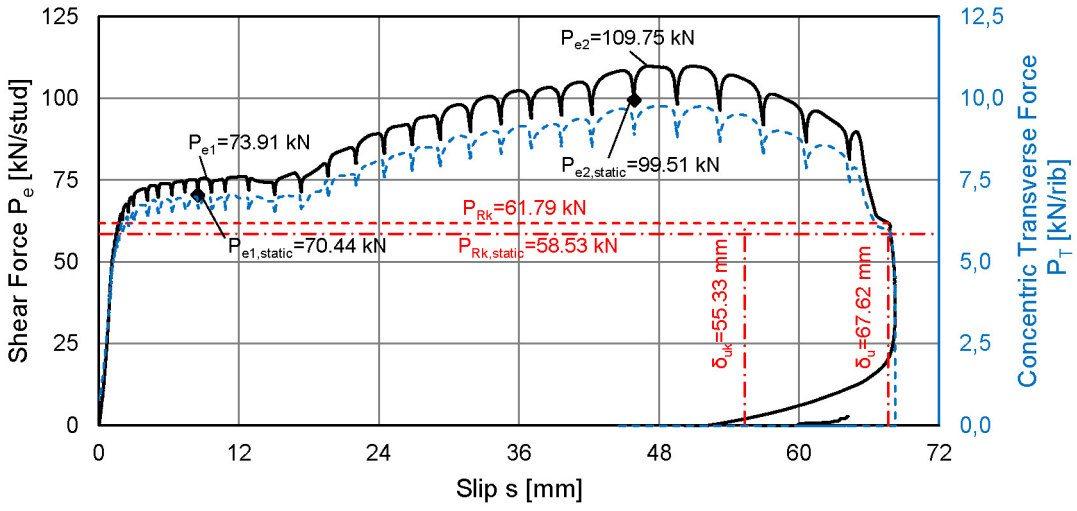

## Specimen 1-04-2

### STEEL PROFILE

| | | | |
|---|---|---|---|
| HEB 260 | $L = 700$mm | $f_y = 424$N/mm$^2$ | $f_u = 525$N/mm$^2$ |

### COMPOSITE DECKING

| | | | |
|---|---|---|---|
| CP60 | $t = 0.88$mm | pre-punched | |
| $h_p = 58$mm | $b_u = 62$mm | $b_o = 101$mm | $a = 207$mm |

### CONCRETE SLABS

| | | | |
|---|---|---|---|
| $B = 900$ mm | $H = 683$ mm | $D = 160$ mm | Recess $200x30$ mm |
| $f_{cm} = 30.89$ N/mm$^2$ | $E_c = 21500$ N/mm$^2$ | | |

### REINFORCEMENT

| | | |
|---|---|---|
| BSt 500 A | Top: Q335A | Bottom: Q188A |
| | Edge: ∅8/150 | Recess: 1∅20 |

### SHEAR STUDS

| | | |
|---|---|---|
| 4 Köco SD 22x125 | mid-position | $f_u = 550.7$N/mm$^2$ |

| | | A1 | A2 | B1 | B2 | $\mu$ | $\sigma$ |
|---|---|---|---|---|---|---|---|
| $d$ | [mm] | 22.25 | 22.23 | 22.27 | 22.20 | 22.24 | 0.030 |
| $h_{sc}$ | [mm] | 124.36 | 124.79 | 124.35 | 124.58 | 123.58 | 0.396 |

### TEST RESULTS

| | | |
|---|---|---|
| $P_{e1} = 73.61$ kN/stud | $P_{e1,static} = 69.63$ kN/stud | $s_{e1} = 5.63$ mm |
| $P_{e2} = 98.91$ kN/stud | $P_{e2,static} = 87.47$ kN/stud | $s_{e2} = 31.61$ mm |
| Rib punch-through | Concrete pull-out | |

### LOAD-SLIP CURVE

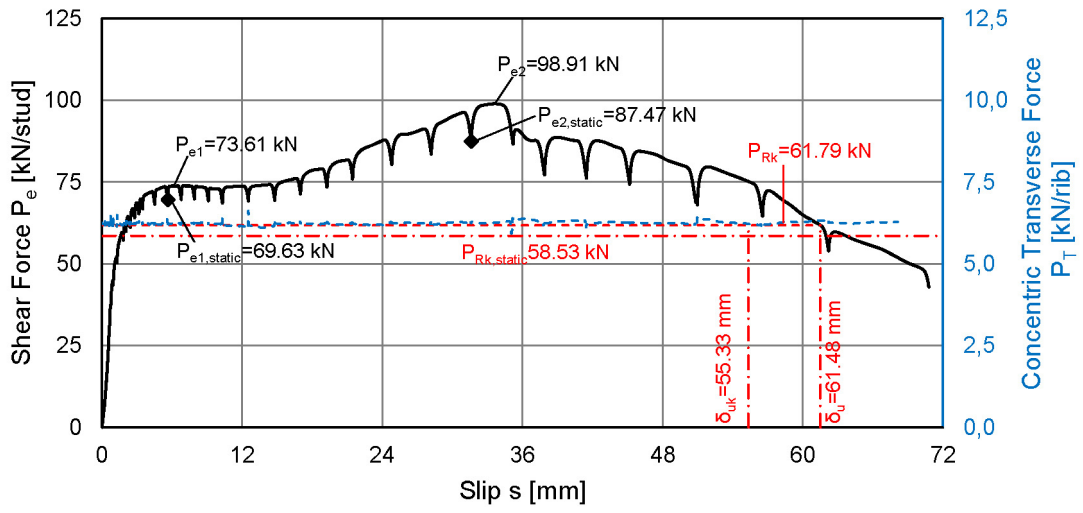

## Specimen 1-04-3

### STEEL PROFILE

| | | | |
|---|---|---|---|
| HEB 260 | $L = 700$mm | $f_y = 424$N/mm$^2$ | $f_u = 525$N/mm$^2$ |

### COMPOSITE DECKING

| | | | |
|---|---|---|---|
| CP60 | $t = 0.88$mm | pre-punched | |
| $h_p = 58$mm | $b_u = 62$mm | $b_o = 101$mm | $a = 207$mm |

### CONCRETE SLABS

| | | | |
|---|---|---|---|
| $B = 900$ mm | $H = 683$ mm | $D = 160$ mm | Recess $200x30$ mm |
| $f_{cm} = 30.91$ N/mm$^2$ | $E_c = 21500$ N/mm$^2$ | | |

### REINFORCEMENT

| | | |
|---|---|---|
| BSt 500 A | Top: Q335A | Bottom: Q188A |
| | Edge: ∅8/150 | Recess: 1∅20 |

### SHEAR STUDS

| | | |
|---|---|---|
| 4 Köco SD 22x125 | mid-position | $f_u = 550.7$N/mm$^2$ |

| | | A1 | A2 | B1 | B2 | $\mu$ | $\sigma$ |
|---|---|---|---|---|---|---|---|
| $d$ | [mm] | 22.18 | 22.24 | 22.16 | 22.23 | 22.20 | 0.039 |
| $h_{sc}$ | [mm] | 123.71 | 123.66 | 124.34 | 124.17 | 123.97 | 0.337 |

### TEST RESULTS

| | | |
|---|---|---|
| $P_{e1} = 68.66$ kN/stud | $P_{e1,static} = 65.06$ kN/stud | $s_{e1} = 5.09$ mm |
| $P_{e2} = 93.67$ kN/stud | $P_{e2,static} = 81.94$ kN/stud | $s_{e2} = 56.24$ mm |
| Rib punch-through | Concrete pull-out | Stud failure |

### LOAD-SLIP CURVE

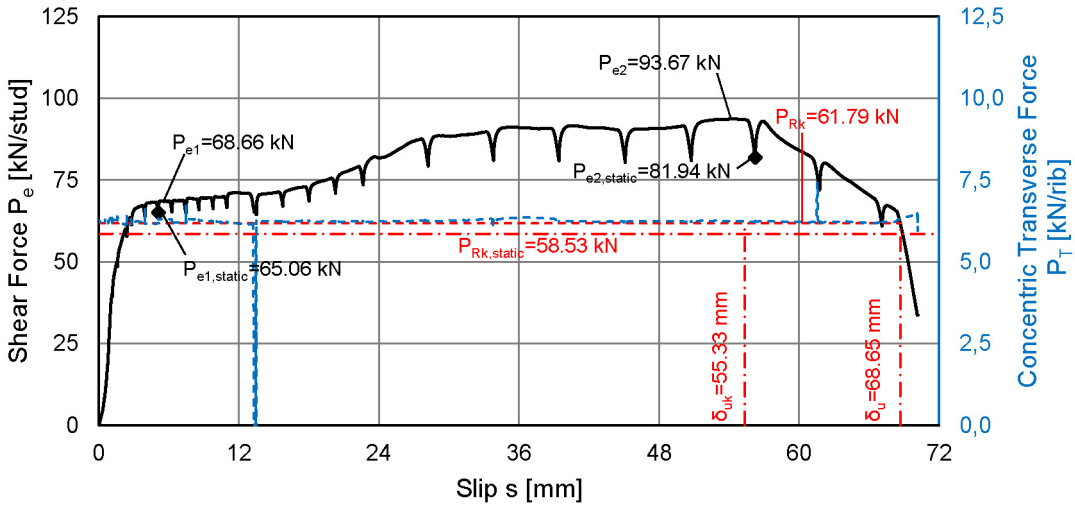

## Specimen 1-05-1

### STEEL PROFILE

| | | | |
|---|---|---|---|
| HEB 260 | $L = 700$mm | $f_y = 424$N/mm$^2$ | $f_u = 525$N/mm$^2$ |

### COMPOSITE DECKING

| | | | |
|---|---|---|---|
| CP60 | $t = 0.88$mm | pre-punched | |
| $h_p = 58$mm | $b_u = 62$mm | $b_o = 101$mm | $a = 207$mm |

### CONCRETE SLABS

| | | | |
|---|---|---|---|
| $B = 900$ mm | $H = 683$ mm | $D = 160$ mm | Recess $200x30$ mm |
| $f_{cm} = 31.71$ N/mm$^2$ | $E_c = 22100$ N/mm$^2$ | | |

### REINFORCEMENT

| | | |
|---|---|---|
| BSt 500 A | Top: Q335A | Bottom: Q188A |
| | Edge: ∅8/150 | Recess: 1∅20 |

### SHEAR STUDS

| | | |
|---|---|---|
| 4 Köco SD 22x125 | mid-position | $f_u = 550.7$N/mm$^2$ |

| | | A1 | A2 | B1 | B2 | $\mu$ | $\sigma$ |
|---|---|---|---|---|---|---|---|
| $d$ | [mm] | 22.16 | 22.16 | 22.16 | 22.17 | 22.16 | 0.005 |
| $h_{sc}$ | [mm] | 123.62 | 123.78 | 124.06 | 124.64 | 124.03 | 0.449 |

### TEST RESULTS

| | | |
|---|---|---|
| $P_{e1} = 69.95$ kN/stud | $P_{e1,static} = 66.48$ kN/stud | $s_{e1} = 4.96$ mm |
| $P_{e2} = 106.11$ kN/stud | $P_{e2,static} = 94.30$ kN/stud | $s_{e2} = 48.36$ mm |
| Rib punch-through | Concrete pull-out | Stud failure |

### LOAD-SLIP CURVE

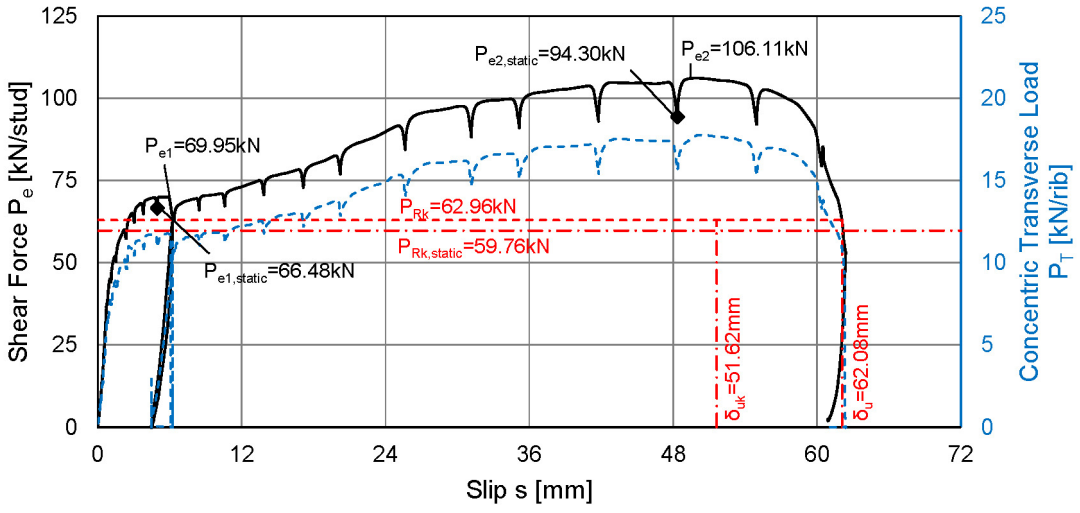

## Specimen 1-05-2

### STEEL PROFILE

| | | | |
|---|---|---|---|
| HEB 260 | $L = 700$mm | $f_y = 424$N/mm$^2$ | $f_u = 525$N/mm$^2$ |

### COMPOSITE DECKING

| | | | |
|---|---|---|---|
| CP60 | $t = 0.88$mm | pre-punched | |
| $h_p = 58$mm | $b_u = 62$mm | $b_o = 101$mm | $a = 207$mm |

### CONCRETE SLABS

| | | | |
|---|---|---|---|
| $B = 900$ mm | $H = 683$ mm | $D = 160$ mm | Recess $200x30$ mm |
| $f_{cm} = 31.71$ N/mm$^2$ | $E_c = 22100$ N/mm$^2$ | | |

### REINFORCEMENT

| | | |
|---|---|---|
| BSt 500 A | Top: Q335A | Bottom Q188A |
| | Edge ∅8/150 | Recess 1∅20 |

### SHEAR STUDS

| | | |
|---|---|---|
| 4 Köco SD 22x125 | mid-position | $f_u = 550.7$N/mm$^2$ |

| | | A1 | A2 | B1 | B2 | $\mu$ | $\sigma$ |
|---|---|---|---|---|---|---|---|
| $d$ | [mm] | 22.16 | 22.22 | 22.15 | 22.15 | 22.17 | 0.034 |
| $h_{sc}$ | [mm] | 124.15 | 123.80 | 123.70 | 123.55 | 123.80 | 0.255 |

### TEST RESULTS

| | | |
|---|---|---|
| $P_{e1} = 79.15$ kN/stud | $P_{e1,static} = 75.23$ kN/stud | $s_{e1} = 4.11$ mm |
| $P_{e2} = 118.33$ kN/stud | $P_{e2,static} = 104.89$ kN/stud | $s_{e2} = 42.94$ mm |
| Rib punch-through | Concrete pull-out | Stud failure |

### LOAD-SLIP CURVE

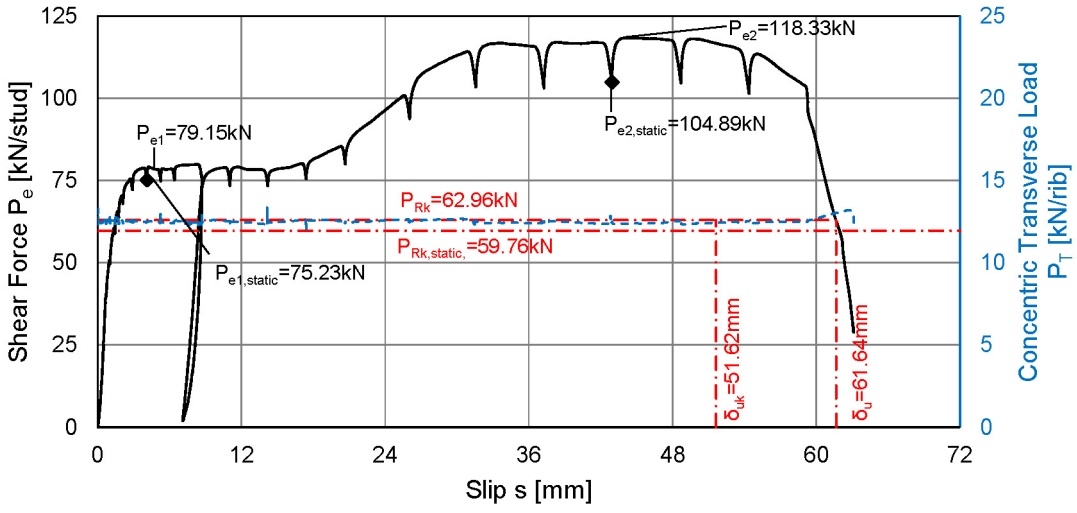

## Specimen 1-05-3

### STEEL PROFILE

| | | | |
|---|---|---|---|
| HEB 260 | $L = 700$mm | $f_y = 424$N/mm$^2$ | $f_u = 525$N/mm$^2$ |

### COMPOSITE DECKING

| | | | |
|---|---|---|---|
| CP60 | $t = 0.88$mm | pre-punched | |
| $h_p = 58$mm | $b_u = 62$mm | $b_o = 101$mm | $a = 207$mm |

### CONCRETE SLABS

| | | | |
|---|---|---|---|
| $B = 900$ mm | $H = 683$ mm | $D = 160$ mm | Recess $200x30$ mm |
| $f_{cm} = 32.55$ N/mm$^2$ | $E_c = 22900$ N/mm$^2$ | | |

### REINFORCEMENT

| | | |
|---|---|---|
| BSt 500 A | Top: Q335A | Bottom: Q188A |
| | Edge: ∅8/150 | Recess: 1∅20 |

### SHEAR STUDS

| | | |
|---|---|---|
| 4 Köco SD 22x125 | mid-position | $f_u = 550.7$N/mm$^2$ |

| | | A1 | A2 | B1 | B2 | $\mu$ | $\sigma$ |
|---|---|---|---|---|---|---|---|
| $d$ | [mm] | 22.17 | 22.21 | 22.24 | 22.16 | 22.20 | 0.037 |
| $h_{sc}$ | [mm] | 123.80 | 124.65 | 123.80 | 123.45 | 123.93 | 0.511 |

### TEST RESULTS

| | | |
|---|---|---|
| $P_{e1} = 74.43$ kN/stud | $P_{e1,static} = 70.68$ kN/stud | $s_{e1} = 3.66$ mm |
| $P_{e2} = 106.79$ kN/stud | $P_{e2,static} = 92.77$ kN/stud | $s_{e2} = 41.89$ mm |
| Rib punch-through | Concrete pull-out | Stud failure |

### LOAD-SLIP CURVE

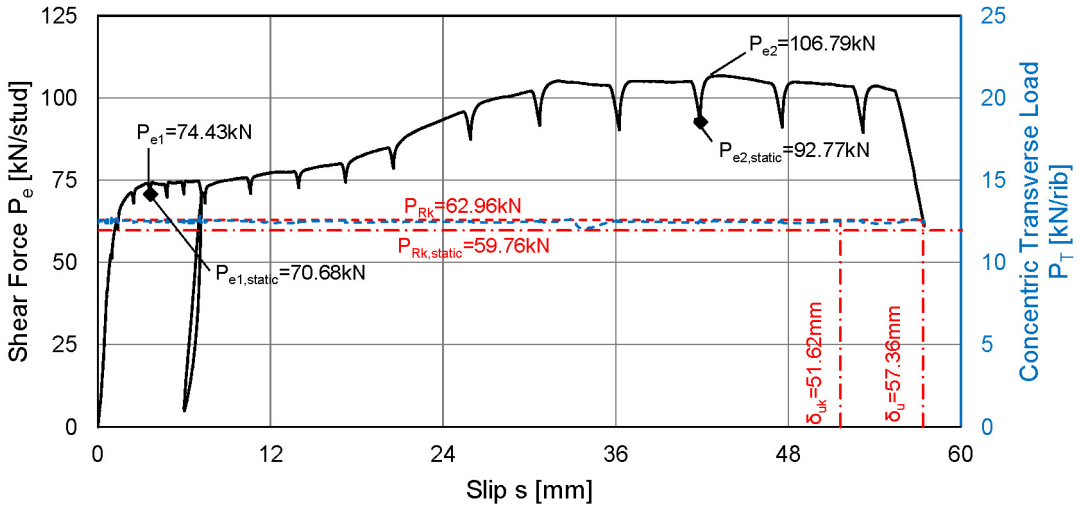

## Specimen 1-06-1

### STEEL PROFILE

| | | | |
|---|---|---|---|
| HEB 260 | $L = 700$mm | $f_y = 424$N/mm$^2$ | $f_u = 525$N/mm$^2$ |

### COMPOSITE DECKING

| | | | |
|---|---|---|---|
| CP60 | $t = 0.88$mm | pre-punched | |
| $h_p = 58$mm | $b_u = 62$mm | $b_o = 101$mm | $a = 207$mm |

### CONCRETE SLABS

| | | | |
|---|---|---|---|
| $B = 900$ mm | $H = 683$ mm | $D = 160$ mm | Recess $200x30$ mm |
| $f_{cm} = 29.94$ N/mm$^2$ | $E_c = 21200$ N/mm$^2$ | | |

### REINFORCEMENT

| | | |
|---|---|---|
| BSt 500 A | Top: Q335A | Bottom: Q188A |
| | Edge: ∅8/150 | Recess: 1∅20 |

### SHEAR STUDS

| | | |
|---|---|---|
| 4 Köco SD 22x125 | mid-position | $f_u = 550.7$N/mm$^2$ |

| | | A1 | A2 | B1 | B2 | $\mu$ | $\sigma$ |
|---|---|---|---|---|---|---|---|
| $d$ | [mm] | 22.17 | 22.18 | 22.18 | 22.17 | 22.18 | 0.006 |
| $h_{sc}$ | [mm] | 123.36 | 123.55 | 123.66 | 123.65 | 123.56 | 0.139 |

### TEST RESULTS

| | | |
|---|---|---|
| $P_{e1} = 73.11$ kN/stud | $P_{e1,static} = 68.89$ kN/stud | $s_{e1} = 5.43$ mm |
| $P_{e2} = 90.33$ kN/stud | $P_{e2,static} = 79.28$ kN/stud | $s_{e2} = 54.85$ mm |
| Rib punch-through | Concrete pull-out | |

### LOAD-SLIP CURVE

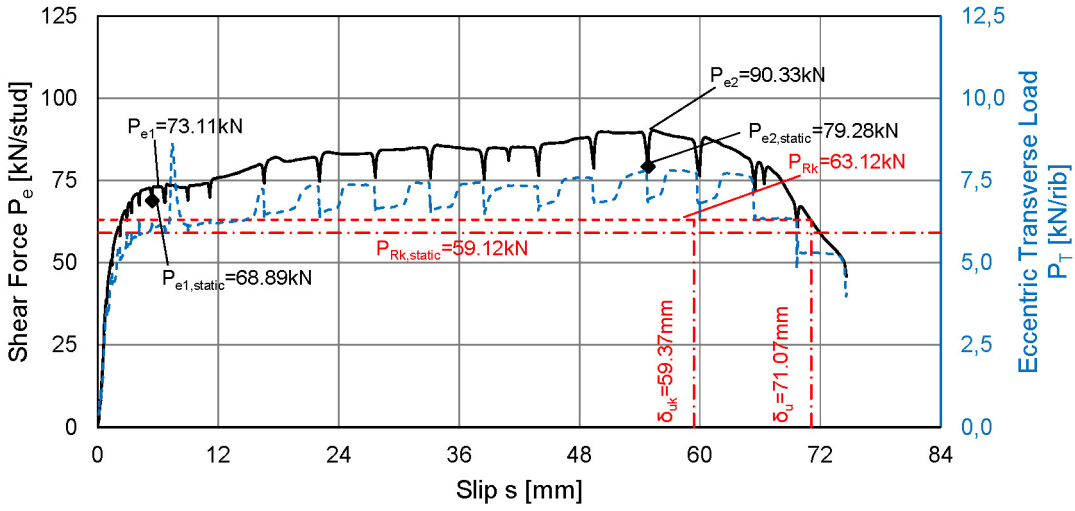

## Specimen 1-06-2

### STEEL PROFILE

| | | | |
|---|---|---|---|
| HEB 260 | $L = 700$mm | $f_y = 424$N/mm$^2$ | $f_u = 525$N/mm$^2$ |

### COMPOSITE DECKING

| | | | |
|---|---|---|---|
| CP60 | $t = 0.88$mm | pre-punched | |
| $h_p = 58$mm | $b_u = 62$mm | $b_o = 101$mm | $a = 207$mm |

### CONCRETE SLABS

| | | | |
|---|---|---|---|
| $B = 900$ mm | $H = 683$ mm | $D = 160$ mm | Recess $200x30$ mm |
| $f_{cm} = 31.06$ N/mm$^2$ | $E_c = 21400$ N/mm$^2$ | | |

### REINFORCEMENT

| | | |
|---|---|---|
| BSt 500 A | Top: Q335A | Bottom: Q188A |
| | Edge: ∅8/150 | Recess: 1∅20 |

### SHEAR STUDS

| | | |
|---|---|---|
| 4 Köco SD 22x125 | mid-position | $f_u = 550.7$N/mm$^2$ |

| | | A1 | A2 | B1 | B2 | $\mu$ | $\sigma$ |
|---|---|---|---|---|---|---|---|
| $d$ | [mm] | 22.17 | 22.14 | 22.15 | 22.16 | 22.16 | 0.013 |
| $h_{sc}$ | [mm] | 124.65 | 124.44 | 123.51 | 123.85 | 124.11 | 0.525 |

### TEST RESULTS

| | | |
|---|---|---|
| $P_{e1} = 70.13$ kN/stud | $P_{e1,static} = 65.69$ kN/stud | $s_{e1} = 5.94$ mm |
| $P_{e2} = 90.67$ kN/stud | $P_{e2,static} = 82.27$ kN/stud | $s_{e2} = 31.83$ mm |
| Rib punch-through | Concrete pull-out | |

### LOAD-SLIP CURVE

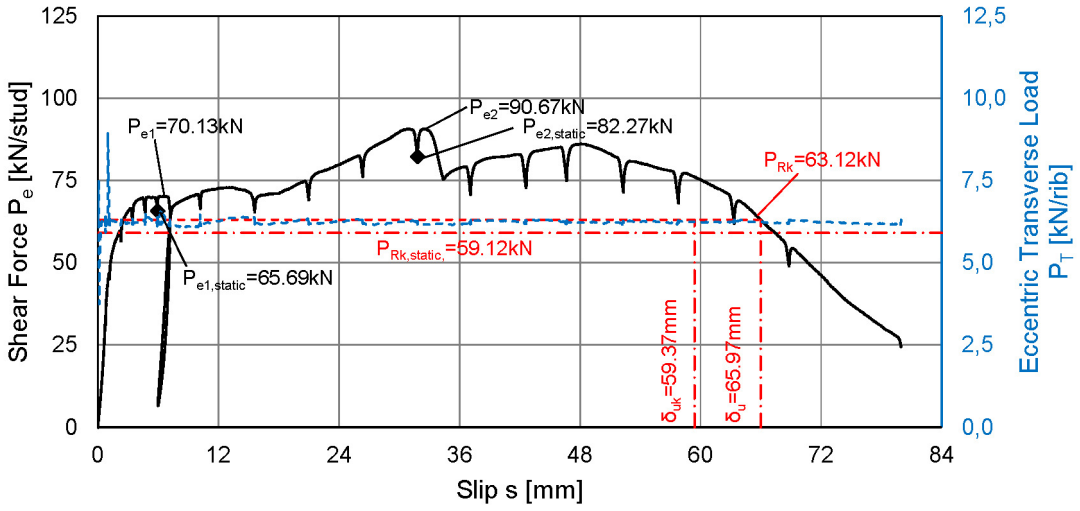

## Specimen 1-06-3

### STEEL PROFILE

| | | | |
|---|---|---|---|
| HEB 260 | $L = 700$mm | $f_y = 424$N/mm$^2$ | $f_u = 525$N/mm$^2$ |

### COMPOSITE DECKING

| | | | |
|---|---|---|---|
| CP60 | $t = 0.88$mm | pre-punched | |
| $h_p = 58$mm | $b_u = 62$mm | $b_o = 101$mm | $a = 207$mm |

### CONCRETE SLABS

| | | | |
|---|---|---|---|
| $B = 900$ mm | $H = 683$ mm | $D = 160$ mm | Recess $200x30$ mm |
| $f_{cm} = 43.96$ N/mm$^2$ | $E_c = 25900$ N/mm$^2$ | | |

### REINFORCEMENT

| | | |
|---|---|---|
| BSt 500 A | Top: Q335A | Bottom: Q188A |
| | Edge: ∅8/150 | Recess: 1∅20 |

### SHEAR STUDS

| | | |
|---|---|---|
| 4 Köco SD 22x125 | mid-position | $f_u = 550.7$N/mm$^2$ |

| | | A1 | A2 | B1 | B2 | $\mu$ | $\sigma$ |
|---|---|---|---|---|---|---|---|
| $d$ | [mm] | 22.11 | 22.12 | 22.13 | 22.12 | 22.12 | 0.008 |
| $h_{sc}$ | [mm] | 123.63 | 123.51 | 123.94 | 123.90 | 124.75 | 0.209 |

### TEST RESULTS

| | | |
|---|---|---|
| $P_{e1} = 90.31$ kN/stud | $P_{e1,static} = 83.44$ kN/stud | $s_{e1} = 3.80$ mm |
| $P_{e2} = 114.96$ kN/stud | $P_{e2,static} = 102.53$ kN/stud | $s_{e2} = 25.75$ mm |
| Rib punch-through | Concrete pull-out | Stud failure |

### LOAD-SLIP CURVE

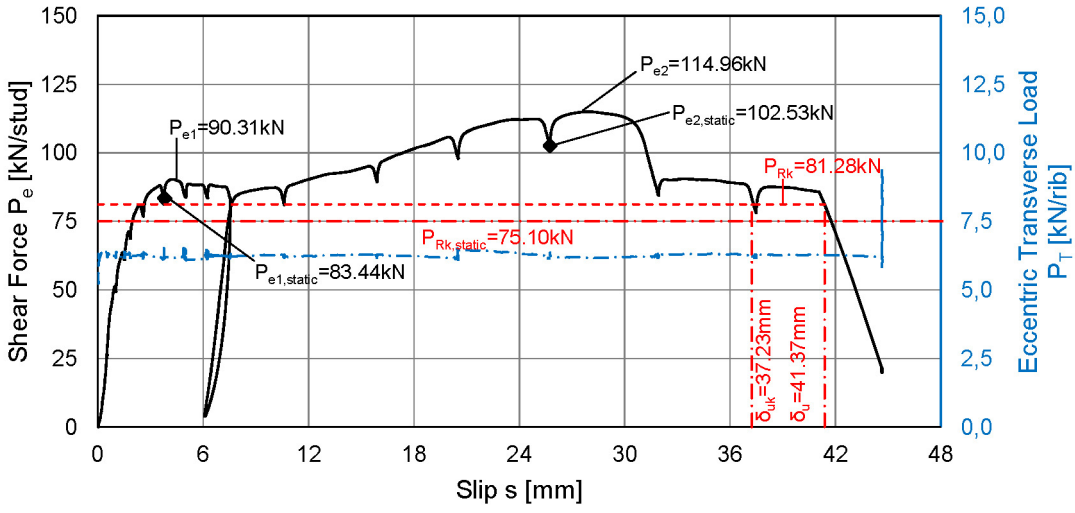

## Specimen 1-07-1

### STEEL PROFILE

| | | | |
|---|---|---|---|
| HEB 260 | $L = 700$mm | $f_y = 424$N/mm$^2$ | $f_u = 525$N/mm$^2$ |

### COMPOSITE DECKING

| | | | |
|---|---|---|---|
| CP60 | $t = 0.88$mm | pre-punched | |
| $h_p = 58$mm | $b_u = 62$mm | $b_o = 101$mm | $a = 207$mm |

### CONCRETE SLABS

| | | | |
|---|---|---|---|
| $B = 900$ mm | $H = 683$ mm | $D = 160$ mm | Recess $200x30$ mm |
| $f_{cm} = 45.09$ N/mm$^2$ | $E_c = 26000$ N/mm$^2$ | | |

### REINFORCEMENT

| | | |
|---|---|---|
| BSt 500 A | Top: Q335A | Bottom: Q188A |
| | Edge: ∅8/150 | Recess: 1∅20 |

### SHEAR STUDS

| | | |
|---|---|---|
| 4 Köco SD 22x125 | mid-position | $f_u = 550.7$N/mm$^2$ |

| | | A1 | A2 | B1 | B2 | $\mu$ | $\sigma$ |
|---|---|---|---|---|---|---|---|
| $d$ | [mm] | 22.12 | 22.11 | 22.12 | 22.12 | 22.12 | 0.008 |
| $h_{sc}$ | [mm] | 123.50 | 123.14 | 123.17 | 123.15 | 124.24 | 0.174 |

### TEST RESULTS

| | | |
|---|---|---|
| $P_{e1} = 89.25$ kN/stud | $P_{e1,static} = 83.81$ kN/stud | $s_{e1} = 3.30$ mm |
| $P_{e2} = 123.27$ kN/stud | $P_{e2,static} = 108.25$ kN/stud | $s_{e2} = 39.52$ mm |
| Rib punch-through | Concrete pull-out | Stud failure |

### LOAD-SLIP CURVE

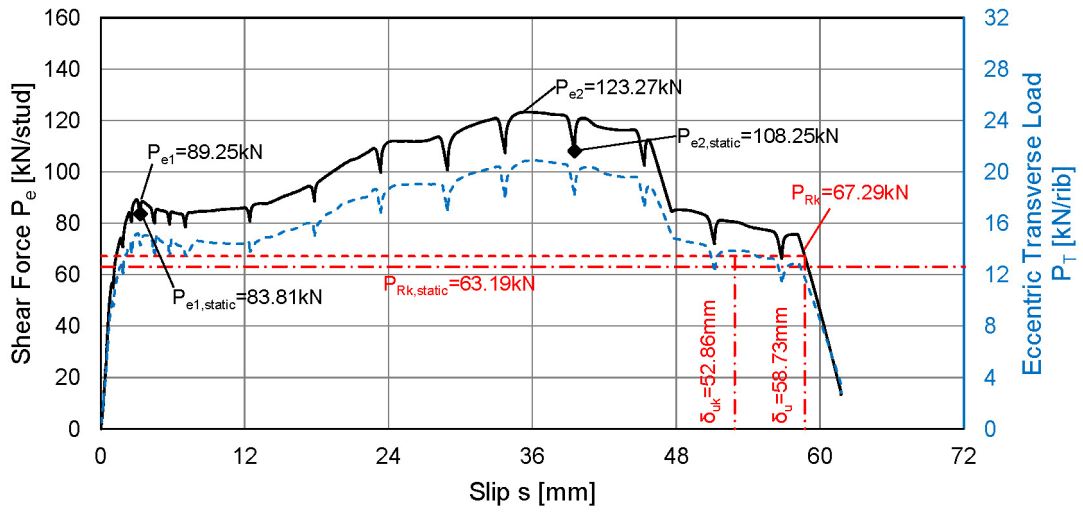

## Specimen 1-07-2

### STEEL PROFILE

| | | | |
|---|---|---|---|
| HEB 260 | $L = 700$mm | $f_y = 424$N/mm$^2$ | $f_u = 525$N/mm$^2$ |

### COMPOSITE DECKING

| | | | |
|---|---|---|---|
| CP60 | $t = 0.88$mm | pre-punched | |
| $h_p = 58$mm | $b_u = 62$mm | $b_o = 101$mm | $a = 207$mm |

### CONCRETE SLABS

| | | | |
|---|---|---|---|
| $B = 900$ mm | $H = 683$ mm | $D = 160$ mm | Recess $200x30$ mm |
| $f_{cm} = 40.87$ N/mm$^2$ | $E_c = 27461$ N/mm$^2$ | | |

### REINFORCEMENT

| | | |
|---|---|---|
| BSt 500 A | Top: Q335A | Bottom: Q188A |
| | Edge: ∅8/150 | Recess: 1∅20 |

### SHEAR STUDS

| | | |
|---|---|---|
| 4 Köco SD 22x125 | mid-position | $f_u = 550.7$N/mm$^2$ |

| | | A1 | A2 | B1 | B2 | $\mu$ | $\sigma$ |
|---|---|---|---|---|---|---|---|
| $d$ | [mm] | 22.15 | 22.15 | 22.10 | 22.15 | 22.14 | 0.025 |
| $h_{sc}$ | [mm] | 124.65 | 124.35 | 124.60 | 124.90 | 124.63 | 0.225 |

### TEST RESULTS

| | | |
|---|---|---|
| $P_{e1} = 92.77$ kN/stud | $P_{e1,static} = 86.52$ kN/stud | $s_{e1} = 2.80$ mm |
| $P_{e2} = 110.28$ kN/stud | $P_{e2,static} = 100.65$ kN/stud | $s_{e2} = 20.50$ mm |
| Rib punch-through | Concrete pull-out | Stud failure |

### LOAD-SLIP CURVE

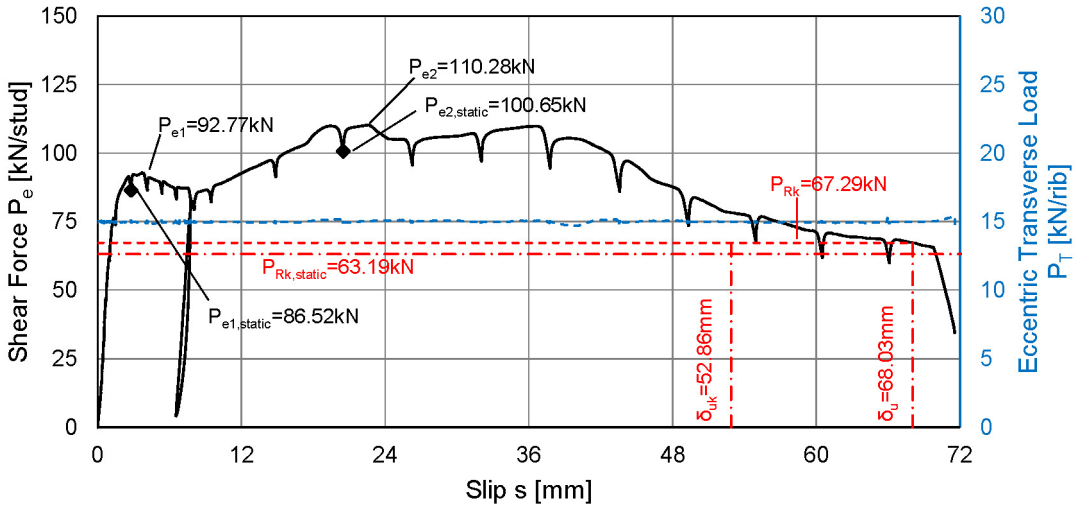

## Specimen 1-07-3

### STEEL PROFILE

HEB 260 | $L = 700$mm | $f_y = 424$N/mm$^2$ | $f_u = 525$N/mm$^2$

### COMPOSITE DECKING

CP60 | $t = 0.88$mm | pre-punched
$h_p = 58$mm | $b_u = 62$mm | $b_o = 101$mm | $a = 207$mm

### CONCRETE SLABS

$B = 900$ mm | $H = 683$ mm | $D = 160$ mm | Recess $200x30$ mm
$f_{cm} = 42.59$ N/mm$^2$ | $E_c = 28000$ N/mm$^2$

### REINFORCEMENT

BSt 500 A | Top: Q335A | Bottom: Q188A
Edge: ∅8/150 | Recess: 1∅20

### SHEAR STUDS

4 Köco SD 22x125 | mid-position | $f_u = 550.7$N/mm$^2$

| | | A1 | A2 | B1 | B2 | $\mu$ | $\sigma$ |
|---|---|---|---|---|---|---|---|
| $d$ | [mm] | 22.10 | 22.10 | 22.15 | 22.20 | 22.14 | 0.048 |
| $h_{sc}$ | [mm] | 124.10 | 124.15 | 124.40 | 124.40 | 124.26 | 0.160 |

### TEST RESULTS

$P_{e1} = 74.77$ kN/stud | $P_{e1,static} = 70.21$ kN/stud | $s_{e1} = 2.77$ mm
$P_{e2} = 114.03$ kN/stud | $P_{e2,static} = 100.70$ kN/stud | $s_{e2} = 31.67$ mm
Rib punch-through | Concrete pull-out

### LOAD-SLIP CURVE

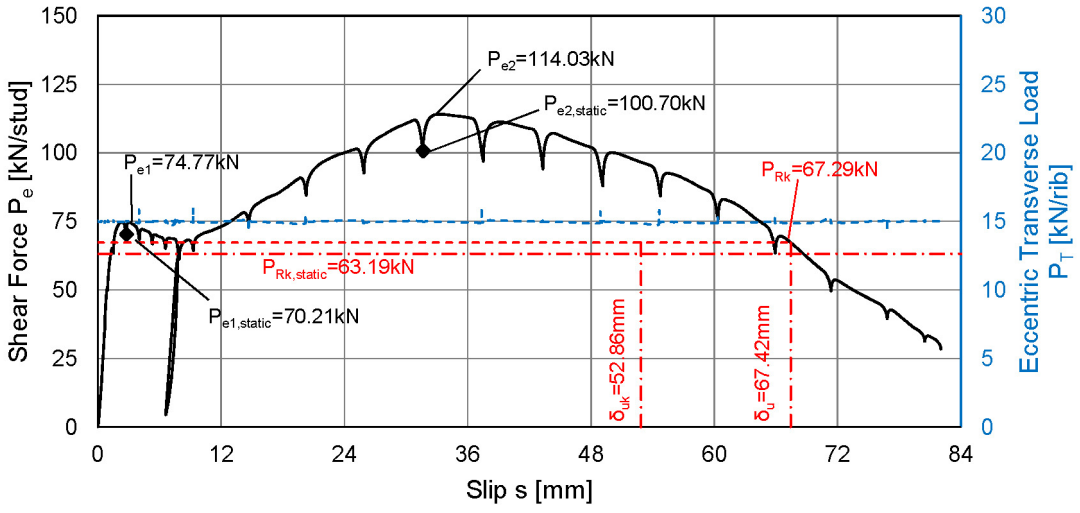

## Specimen 1-08-1

### STEEL PROFILE

HEB 260 $L = 900$mm $f_y = 424$N/mm$^2$ $f_u = 525$N/mm$^2$

### COMPOSITE DECKING

CF860 $t = 0.90$mm through deck welded
$h_p = 80$mm $b_u = 120$mm $b_o = 155$mm $a = 300$mm

### CONCRETE SLABS

$B = 900$ mm $H = 900$ mm $D = 160$ mm No recess
$f_{cm} = 42.22$ N/mm$^2$ $E_c = 26500$ N/mm$^2$

### REINFORCEMENT

BSt 500 A Top: n.a. Bottom: Q188A
Edge: ∅8/150 Recess: n.a.

### SHEAR STUDS

8 Köco SD 19x125 mid-position $f_u = 550.7$N/mm$^2$

| | | A1-1 | A1-2 | A2-1 | A2-2 | B1-1 | B1-2 | B2-1 | B2-2 | $\mu$ | $\sigma$ |
|---|---|---|---|---|---|---|---|---|---|---|---|
| $d$ | [mm] | 19.06 | 19.05 | 19.09 | 19.09 | 19.04 | 19.04 | 19.04 | 19.04 | 19.06 | 0.002 |
| $h_{sc}$ | [mm] | 116.65 | 115.97 | 117.67 | 117.65 | 117.53 | 117.19 | 118.19 | 118.12 | 117.37 | 0.750 |

### TEST RESULTS

$P_{e1} = 45.52$ kN/stud $P_{e1,static} = 42.80$ kN/stud $s_{e1} = 1.63$ mm
$P_{e2} =$ n.a. $P_{e2,static} =$ n.a. $s_{e2} =$ n.a.
Rib pry-out

### LOAD-SLIP CURVE

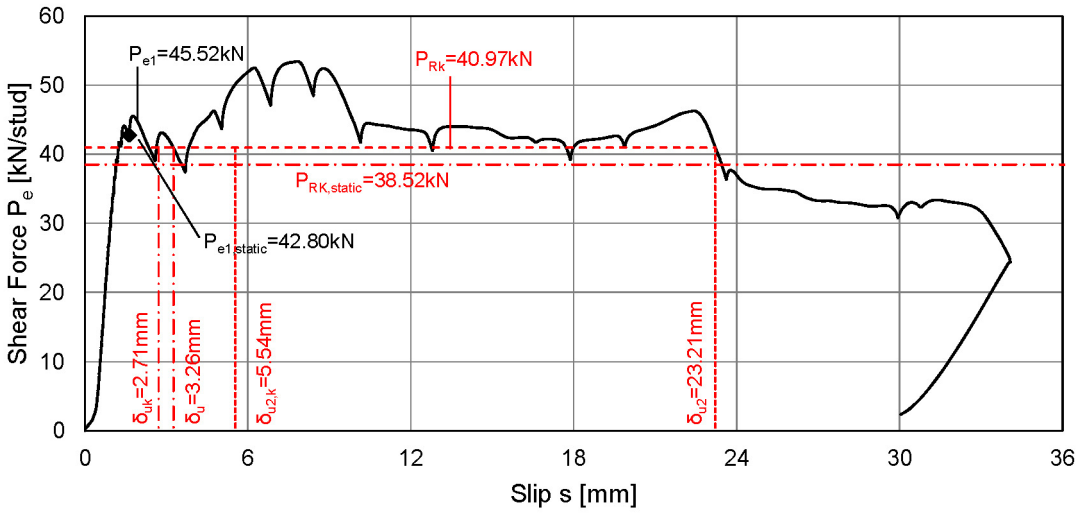

## Specimen 1-08-2

### STEEL PROFILE

| | | | |
|---|---|---|---|
| HEB 260 | $L = 900$mm | $f_y = 424$N/mm$^2$ | $f_u = 525$N/mm$^2$ |

### COMPOSITE DECKING

| | | | |
|---|---|---|---|
| CF80 | $t = 0.90$mm | through deck welded | |
| $h_p = 80$mm | $b_u = 120$mm | $b_o = 155$mm | $a = 300$mm |

### CONCRETE SLABS

| | | | |
|---|---|---|---|
| $B = 900$ mm | $H = 900$ mm | $D = 160$ mm | No recess |
| $f_{cm} = 42.22$ N/mm$^2$ | $E_c = 26500$ N/mm$^2$ | | |

### REINFORCEMENT

| | | |
|---|---|---|
| BSt 500 A | Top: n.a. | Bottom: Q188A |
| | Edge: ∅8/150 | Recess: n.a. |

### SHEAR STUDS

| | | |
|---|---|---|
| 8 Köco SD 19x125 | mid-position | $f_u = 550.7$N/mm$^2$ |

| | | A1-1 | A1-2 | A2-1 | A2-2 | B1-1 | B1-2 | B2-1 | B2-2 | $\mu$ | $\sigma$ |
|---|---|---|---|---|---|---|---|---|---|---|---|
| $d$ | [mm] | 19.08 | 19.11 | 19.09 | 19.08 | 19.02 | 19.06 | 19.04 | 19.05 | 19.07 | 0.029 |
| $h_{sc}$ | [mm] | 117.20 | 117.71 | 116.69 | 117.08 | 117.12 | 118.14 | 118.60 | 117.50 | 117.51 | 0.625 |

### TEST RESULTS

| | | |
|---|---|---|
| $P_{e1} = 46.09$ kN/stud | $P_{e1,static} = 43.33$ kN/stud | $s_{e1} = 1.13$ mm |
| $P_{e2} =$ n.a. | $P_{e2,static} =$ n.a. | $s_{e2} =$ n.a. |
| Rib pry-out | | |

### LOAD-SLIP CURVE

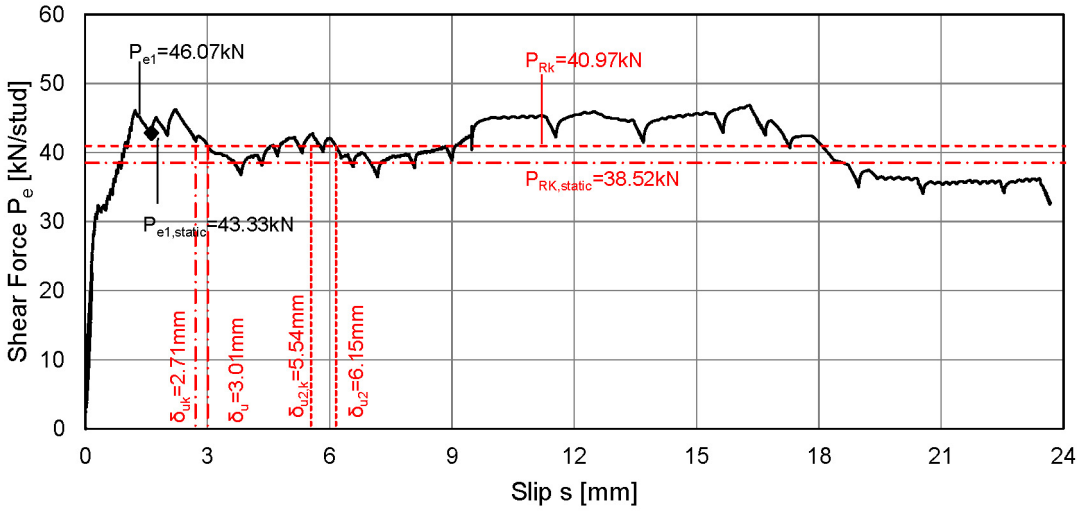

## Specimen 1-08-3

### STEEL PROFILE

HEB 260 $L = 900$mm $f_y = 424$N/mm$^2$ $f_u = 525$N/mm$^2$

### COMPOSITE DECKING

CF80 $t = 0.90$mm through deck welded
$h_p = 80$mm $b_u = 120$mm $b_o = 155$mm $a = 300$mm

### CONCRETE SLABS

$B = 900$ mm $H = 900$ mm $D = 160$ mm No recess
$f_{cm} = 42.22$ N/mm$^2$ $E_c = 26500$ N/mm$^2$

### REINFORCEMENT

BSt 500 A Top: n.a. Bottom: Q188A
Edge: ∅8/150 Recess: n.a.

### SHEAR STUDS

8 Köco SD 19x125 mid-position $f_u = 550.7$N/mm$^2$

| | | A1-1 | A1-2 | A2-1 | A2-2 | B1-1 | B1-2 | B2-1 | B2-2 | $\mu$ | $\sigma$ |
|---|---|---|---|---|---|---|---|---|---|---|---|
| $d$ | [mm] | 19.05 | 19.05 | 19.07 | 19.07 | 19.07 | 19.06 | 19.09 | 19.08 | 19.07 | 0.014 |
| $h_{sc}$ | [mm] | 117.15 | 117.86 | 118.20 | 118.18 | 118.10 | 118.62 | 117.77 | 117.37 | 117.91 | 0.476 |

### TEST RESULTS

$P_{e1} = 48.26$ kN/stud $P_{e1,static} = 45.92$ kN/stud $s_{e1} = 1.64$ mm
$P_{e2} = 64.79$ kN/stud $P_{e2,static} = 60.48$ kN/stud $s_{e2} = 9.36$ mm
Rib pry-out

### LOAD-SLIP CURVE

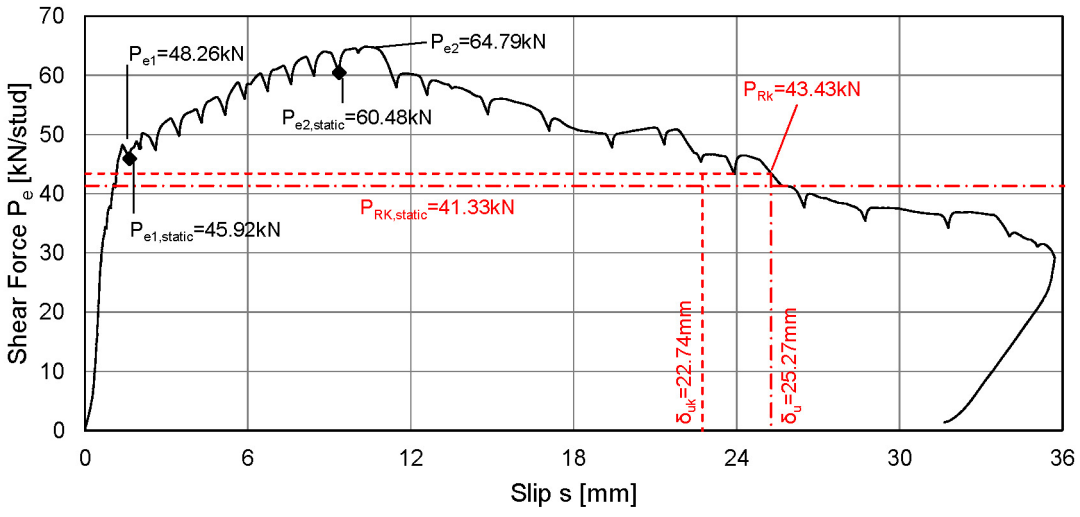

## Specimen 1-09-1

### STEEL PROFILE

HEB 260 | $L = 900$mm | $f_y = 424$N/mm$^2$ | $f_u = 525$N/mm$^2$

### COMPOSITE DECKING

CF80 | $t = 0.90$mm | through deck welded
$h_p = 80$mm | $b_u = 120$mm | $b_o = 155$mm | $a = 300$mm

### CONCRETE SLABS

$B = 900$ mm | $H = 900$ mm | $D = 160$ mm | No recess
$f_{cm} = 42.59$ N/mm$^2$ | $E_c = 28000$ N/mm$^2$

### REINFORCEMENT

BSt 500 A | Top: n.a. | Bottom: Q188A
Edge: ∅8/150 | Recess: n.a.

### SHEAR STUDS

8 Köco SD 19x125 | mid-position | $f_u = 550.7$N/mm$^2$

| | | A1-1 | A1-2 | A2-1 | A2-2 | B1-1 | B1-2 | B2-1 | B2-2 | $\mu$ | $\sigma$ |
|---|---|---|---|---|---|---|---|---|---|---|---|
| $d$ | [mm] | 19.10 | 19.10 | 19.10 | 19.10 | 19.10 | 19.10 | 19.05 | 19.05 | 19.09 | 0.023 |
| $h_{sc}$ | [mm] | 119.20 | 119.00 | 118.90 | 119.30 | 118.15 | 118.05 | 118.65 | 119.50 | 118.84 | 0.527 |

### TEST RESULTS

$P_{e1} = 42.28$ kN/stud | $P_{e1,static} = 39.11$ kN/stud | $s_{e1} = 2.26$ mm
$P_{e2} =$ n.a. | $P_{e2,static} =$ n.a. | $s_{e2} =$ n.a.
Rib pry-out

### LOAD-SLIP CURVE

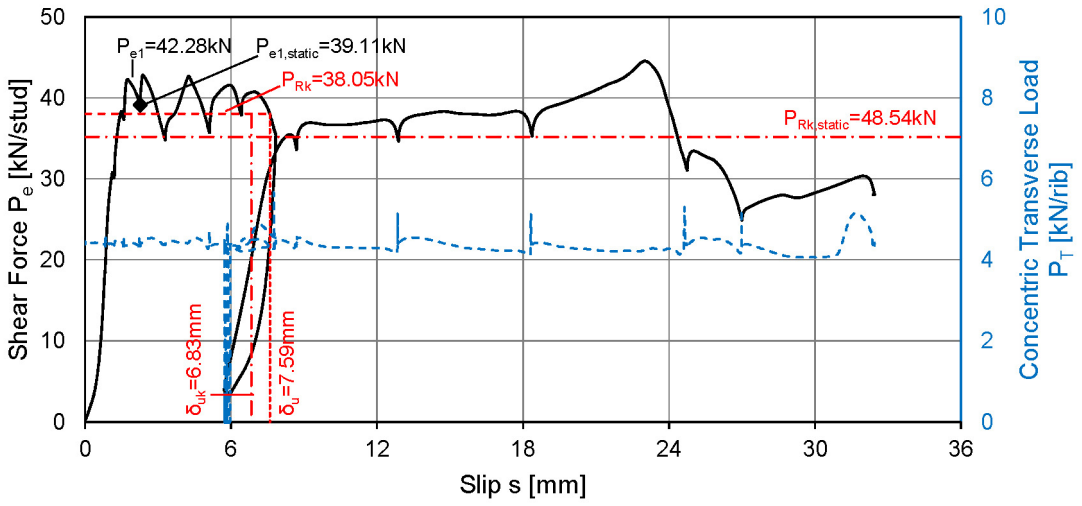

## Specimen 1-09-2

### STEEL PROFILE

HEB 260 $L = 900$mm $f_y = 424$N/mm$^2$ $f_u = 525$N/mm$^2$

### COMPOSITE DECKING

CF80 $t = 0.90$mm through deck welded
$h_p = 80$mm $b_u = 120$mm $b_o = 155$mm $a = 300$mm

### CONCRETE SLABS

$B = 900$ mm $H = 900$ mm $D = 160$ mm No recess
$f_{cm} = 42.59$ N/mm$^2$ $E_c = 28000$ N/mm$^2$

### REINFORCEMENT

BSt 500 A Top: n.a. Bottom: Q188A
Edge: ∅8/150 Recess: n.a.

### SHEAR STUDS

8 Köco SD 19x125 mid-position $f_u = 550.7$N/mm$^2$

| | | A1-1 | A1-2 | A2-1 | A2-2 | B1-1 | B1-2 | B2-1 | B2-2 | $\mu$ | $\sigma$ |
|---|---|---|---|---|---|---|---|---|---|---|---|
| $d$ | [mm] | 19.10 | 19.10 | 19.15 | 19.20 | 19.05 | 19.10 | 19.15 | 19.10 | 19.12 | 0.046 |
| $h_{sc}$ | [mm] | 117.30 | 116.25 | 117.65 | 119.15 | 117.45 | 117.00 | 119.20 | 118.00 | 117.75 | 1.017 |

### TEST RESULTS

$P_{e1} = 50.32$ kN/stud $P_{e1,static} = 46.40$ kN/stud $s_{e1} = 1.81$ mm
$P_{e2} =$ n.a. $P_{e2,static} =$ n.a. $s_{e2} =$ n.a.
Rib pry-out Clamping

### LOAD-SLIP CURVE

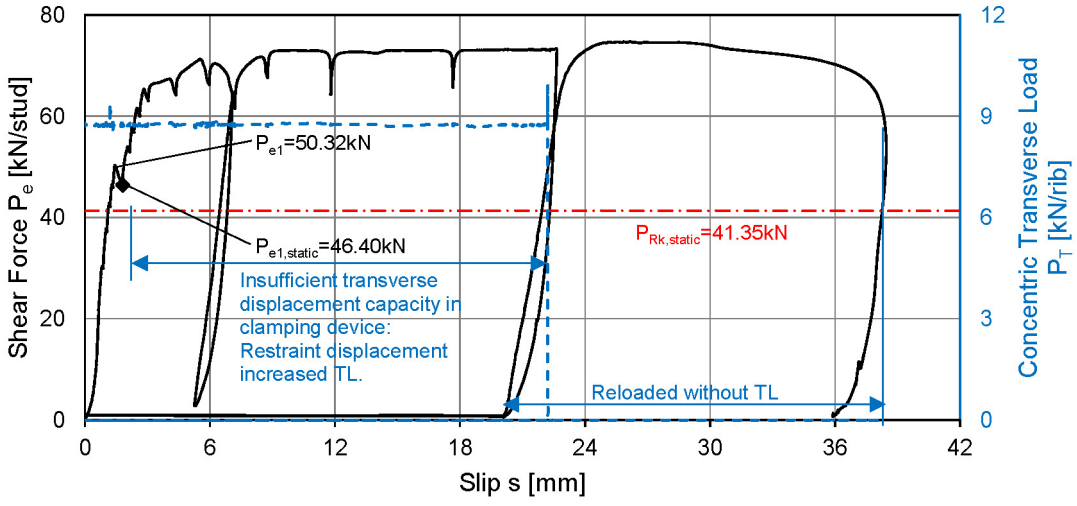

## Specimen 1-09-3

### STEEL PROFILE

| | | | |
|---|---|---|---|
| HEB 260 | $L = 900$mm | $f_y = 424$N/mm$^2$ | $f_u = 525$N/mm$^2$ |

### COMPOSITE DECKING

| | | | |
|---|---|---|---|
| CF80 | $t = 0.90$mm | through deck welded | |
| $h_p = 80$mm | $b_u = 120$mm | $b_o = 155$mm | $a = 300$mm |

### CONCRETE SLABS

| | | | |
|---|---|---|---|
| $B = 900$ mm | $H = 900$ mm | $D = 160$ mm | No recess |
| $f_{cm} = 42.59$ N/mm$^2$ | $E_c = 28000$ N/mm$^2$ | | |

### REINFORCEMENT

| | | |
|---|---|---|
| BSt 500 A | Top: n.a. | Bottom: Q188A |
| | Edge: ∅8/150 | Recess: n.a. |

### SHEAR STUDS

| | | |
|---|---|---|
| 8 Köco SD 19x125 | mid-position | $f_u = 550.7$N/mm$^2$ |

| | | A1-1 | A1-2 | A2-1 | A2-2 | B1-1 | B1-2 | B2-1 | B2-2 | $\mu$ | $\sigma$ |
|---|---|---|---|---|---|---|---|---|---|---|---|
| $d$ | [mm] | 19.10 | 19.05 | 19.10 | 19.10 | 19.10 | 19.10 | 19.10 | 19.10 | 19.09 | 0.018 |
| $h_{sc}$ | [mm] | 117.30 | 119.50 | 119.55 | 120.15 | 117.05 | 118.05 | 120.05 | 119.70 | 118.92 | 1.254 |

### TEST RESULTS

| | | |
|---|---|---|
| $P_{e1} = 48.19$ kN/stud | $P_{e1,static} = 45.98$ kN/stud | $s_{e1} = 2.76$ mm |
| $P_{e2} =$ n.a. | $P_{e2,static} =$ n.a. | $s_{e2} =$ n.a. |
| Rib pry-out | Clamping | |

### LOAD-SLIP CURVE

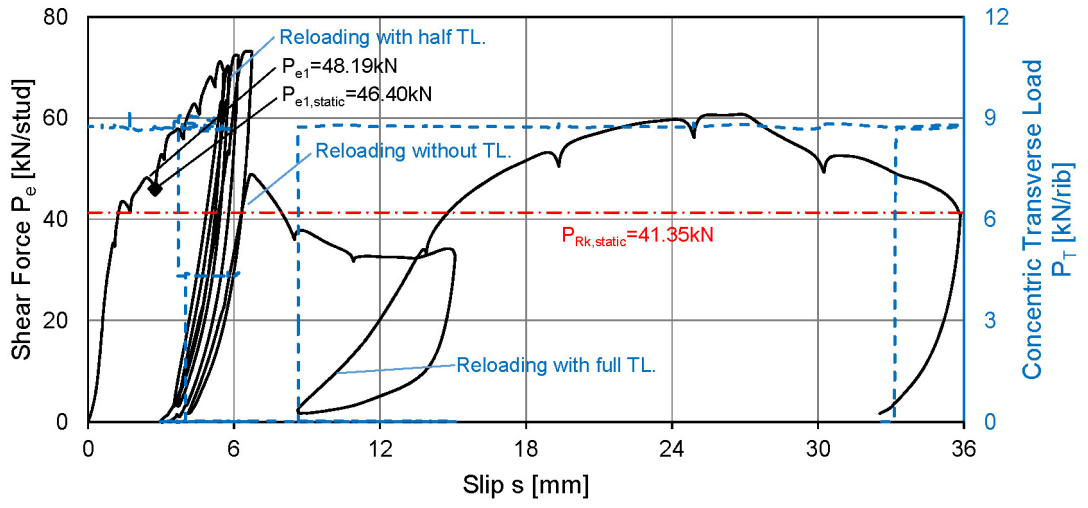

## Specimen 1-10-1

### STEEL PROFILE

HEB 260 $L = 900$mm $f_y = 424$N/mm$^2$ $f_u = 525$N/mm$^2$

### COMPOSITE DECKING

CF80 $t = 0.90$mm through deck welded
$h_p = 80$mm $b_u = 120$mm $b_o = 155$mm $a = 300$mm

### CONCRETE SLABS

$B = 900$ mm $H = 900$ mm $D = 160$ mm No recess
$f_{cm} = 42.59$ N/mm$^2$ $E_c = 28000$ N/mm$^2$

### REINFORCEMENT

BSt 500 A Top: n.a. Bottom: Q188A
Edge: ∅8/150 Recess: n.a.

### SHEAR STUDS

8 Köco SD 19x125 mid-position $f_u = 550.7$N/mm$^2$

| | | A1-1 | A1-2 | A2-1 | A2-2 | B1-1 | B1-2 | B2-1 | B2-2 | $\mu$ | $\sigma$ |
|---|---|---|---|---|---|---|---|---|---|---|---|
| $d$ | [mm] | 19.10 | 19.10 | 19.15 | 19.15 | 19.10 | 19.05 | 19.15 | 19.10 | 19.11 | 0.035 |
| $h_{sc}$ | [mm] | 118.15 | 119.20 | 117.70 | 119.15 | 119.05 | 118.20 | 118.85 | 118.80 | 118.64 | 0.551 |

### TEST RESULTS

$P_{e1} = 45.64$ kN/stud $P_{e1,static} = 40.57$ kN/stud $s_{e1} = 1.55$ mm
$P_{e2} = 53.38$ kN/stud $P_{e2,static} = 48.80$ KN/stud $s_{e2} = 5.98$ mm
Rib pry-out

### LOAD-SLIP CURVE

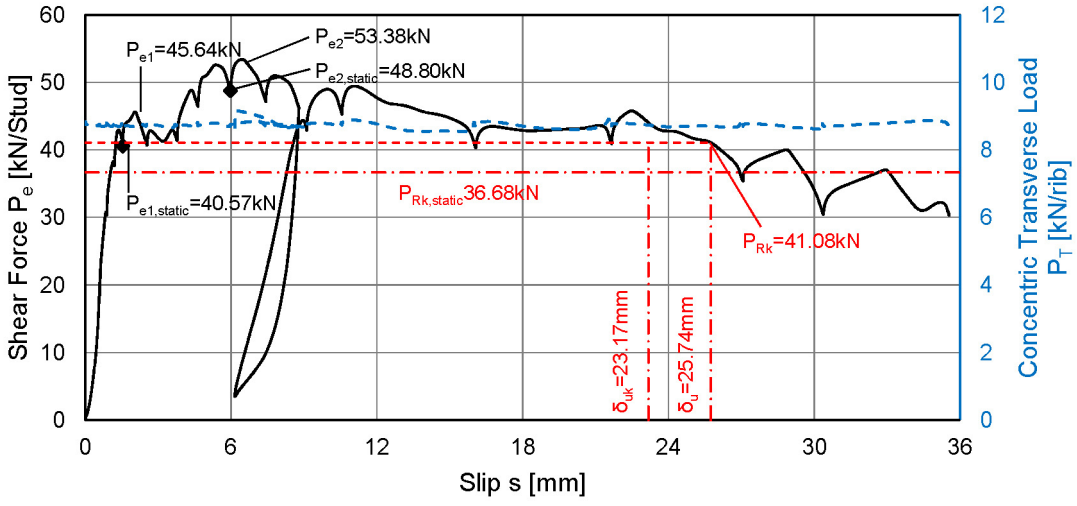

## Specimen 1-10-2

### STEEL PROFILE

HEB 260 | $L = 900$mm | $f_y = 424$N/mm$^2$ | $f_u = 525$N/mm$^2$

### COMPOSITE DECKING

CF80 | $t = 0.90$mm | through deck welded
$h_p = 80$mm | $b_u = 120$mm | $b_o = 155$mm | $a = 300$mm

### CONCRETE SLABS

$B = 900$ mm | $H = 900$ mm | $D = 160$ mm | No recess
$f_{cm} = 42.59$ N/mm$^2$ | $E_c = 28000$ N/mm$^2$

### REINFORCEMENT

BSt 500 A | Top: n.a. | Bottom: Q188A
Edge: ∅8/150 | Recess: n.a.

### SHEAR STUDS

8 Köco SD 19x125 | mid-position | $f_u = 550.7$N/mm$^2$

| | | A1-1 | A1-2 | A2-1 | A2-2 | B1-1 | B1-2 | B2-1 | B2-2 | $\mu$ | $\sigma$ |
|---|---|---|---|---|---|---|---|---|---|---|---|
| $d$ | [mm] | 19.10 | 19.10 | 19.10 | 19.15 | 19.05 | 19.10 | 19.10 | 19.05 | 19.09 | 0.032 |
| $h_{sc}$ | [mm] | 117.20 | 118.60 | 119.15 | 119.30 | 116.75 | 116.50 | 118.20 | 119.20 | 118.15 | 1.156 |

### TEST RESULTS

$P_{e1} = 46.44$ kN/stud | $P_{e1,static} = 39.29$ kN/stud | $s_{e1} = 2.41$ mm
$P_{e2} =$ n.a. | $P_{e2,static} =$ n.a. | $s_{e2} =$ n.a.
Rib pry-out

### LOAD-SLIP CURVE

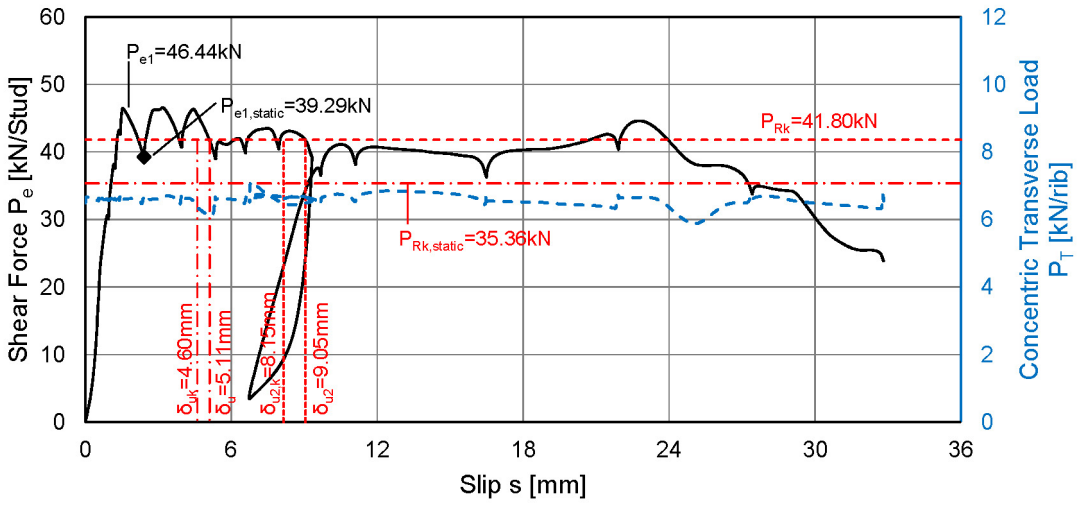

## Specimen 1-10-3

### STEEL PROFILE

HEB 260 | $L = 900$mm | $f_y = 424$N/mm$^2$ | $f_u = 525$N/mm$^2$

### COMPOSITE DECKING

CF80 | $t = 0.90$mm | through deck welded
$h_p = 80$mm | $b_u = 120$mm | $b_o = 155$mm | $a = 300$mm

### CONCRETE SLABS

$B = 900$ mm | $H = 900$ mm | $D = 160$ mm | No recess
$f_{cm} = 42.59$ N/mm$^2$ | $E_c = 28000$ N/mm$^2$

### REINFORCEMENT

BSt 500 A | Top: n.a. | Bottom: Q188A
Edge: ∅8/150 | Recess: n.a.

### SHEAR STUDS

8 Köco SD 19x125 | mid-position | $f_u = 550.7$N/mm$^2$

| | | A1-1 | A1-2 | A2-1 | A2-2 | B1-1 | B1-2 | B2-1 | B2-2 | $\mu$ | $\sigma$ |
|---|---|---|---|---|---|---|---|---|---|---|---|
| $d$ | [mm] | 19.10 | 19.10 | 19.10 | 19.10 | 19.10 | 19.10 | 19.10 | 19.10 | 19.10 | 0 |
| $h_{sc}$ | [mm] | 117.50 | 118.45 | 116.75 | 119.15 | 119.25 | 118.35 | 118.35 | 118.10 | 118.24 | 0.820 |

### TEST RESULTS

$P_{e1} = 35.46$ kN/stud | $P_{e1,static} = 31.22$ kN/stud | $s_{e1} = 1.96$ mm
$P_{e2} =$ n.a. | $P_{e2,static} =$ n.a. | $s_{e2} =$ n.a.
Rib pry-out

### LOAD-SLIP CURVE

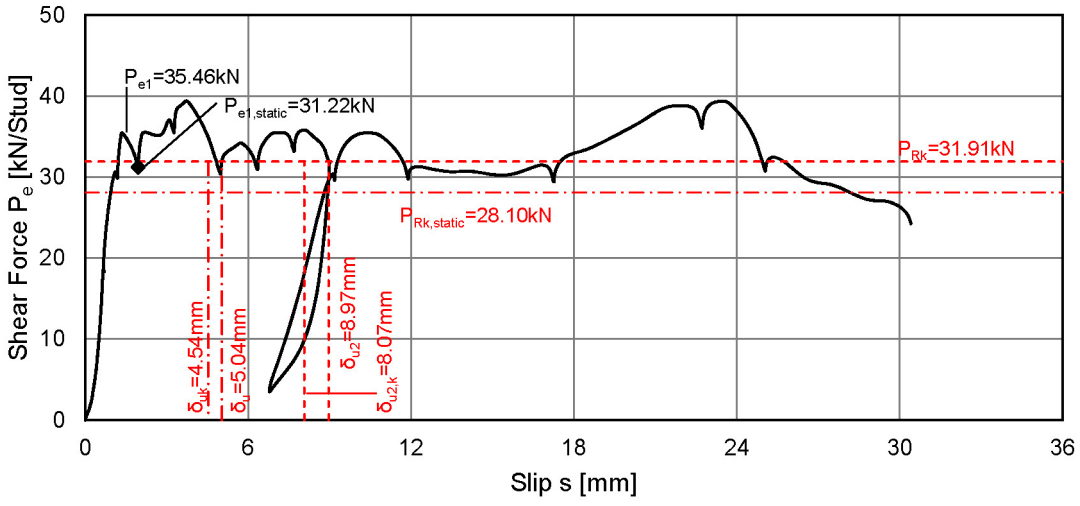

## Specimen 1-11-1

### STEEL PROFILE

HEB 260 | $L = 900$mm | $f_y = 424$N/mm$^2$ | $f_u = 525$N/mm$^2$

### COMPOSITE DECKING

CF80 | $t = 0.90$mm | through deck welded
$h_p = 80$mm | $b_u = 120$mm | $b_o = 155$mm | $a = 300$mm

### CONCRETE SLABS

$B = 900$ mm | $H = 900$ mm | $D = 160$ mm | No recess
$f_{cm} = 42.59$ N/mm$^2$ | $E_c = 28000$ N/mm$^2$

### REINFORCEMENT

BSt 500 A | Top: n.a. | Bottom: Q188A
Edge: ∅8/150 | Recess: n.a.

### SHEAR STUDS

8 Köco SD 19x125 | mid-position | $f_u = 550.7$N/mm$^2$

| | | A1-1 | A1-2 | A2-1 | A2-2 | B1-1 | B1-2 | B2-1 | B2-2 | $\mu$ | $\sigma$ |
|---|---|---|---|---|---|---|---|---|---|---|---|
| $d$ | [mm] | 19.05 | 19.10 | 19.10 | 19.05 | 19.05 | 19.10 | 19.10 | 19.05 | 19.08 | 0.027 |
| $h_{sc}$ | [mm] | 119.15 | 119.40 | 118.60 | 118.75 | 119.05 | 119.40 | 119.55 | 119.40 | 119.16 | 0.342 |

### TEST RESULTS

$P_{e1} = 54.64$ kN/stud | $P_{e1,static} = 51.41$ kN/stud | $s_{e1} = 4.44$ mm
$P_{e2} =$ n.a. | $P_{e2,static} =$ n.a. | $s_{e2} =$ n.a.
Rib pry-out

### LOAD-SLIP CURVE

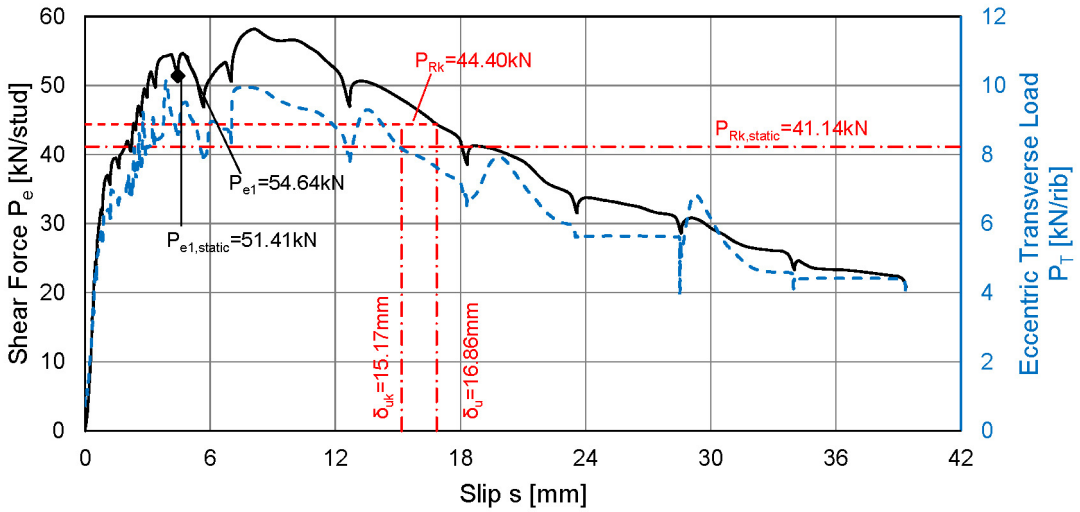

## Specimen 1-11-2

### STEEL PROFILE

| | | | |
|---|---|---|---|
| HEB 260 | $L = 900$mm | $f_y = 424$N/mm$^2$ | $f_u = 525$N/mm$^2$ |

### COMPOSITE DECKING

| | | | |
|---|---|---|---|
| CF80 | $t = 0.90$mm | through deck welded | |
| $h_p = 80$mm | $b_u = 120$mm | $b_o = 155$mm | $a = 300$mm |

### CONCRETE SLABS

| | | | |
|---|---|---|---|
| $B = 900$ mm | $H = 900$ mm | $D = 160$ mm | No recess |
| $f_{cm} = 42.59$ N/mm$^2$ | $E_c = 28000$ N/mm$^2$ | | |

### REINFORCEMENT

| | | |
|---|---|---|
| BSt 500 A | Top: n.a. | Bottom: Q188A |
| | Edge: ∅8/150 | Recess: n.a. |

### SHEAR STUDS

| | | |
|---|---|---|
| 8 Köco SD 19x125 | mid-position | $f_u = 550.7$N/mm$^2$ |

| | | A1-1 | A1-2 | A2-1 | A2-2 | B1-1 | B1-2 | B2-1 | B2-2 | $\mu$ | $\sigma$ |
|---|---|---|---|---|---|---|---|---|---|---|---|
| $d$ | [mm] | 19.10 | 19.07 | 19.07 | 19.07 | 19.10 | 19.10 | 19.10 | 19.05 | 19.08 | 0.020 |
| $h_{sc}$ | [mm] | 117.40 | 118.75 | 120.60 | 119.00 | 116.85 | 117.65 | 120.40 | 119.25 | 118.74 | 1.368 |

### TEST RESULTS

| | | |
|---|---|---|
| $P_{e1} = 52.68$ kN/stud | $P_{e1,static} = 46.04$ kN/stud | $s_{e1} = 2.57$ mm |
| $P_{e2}$ = n.a. | $P_{e2,static}$ = n.a. | $s_{e2}$ = n.a. |
| Rib pry-out | Rotation of bottom rib | |

### LOAD-SLIP CURVE

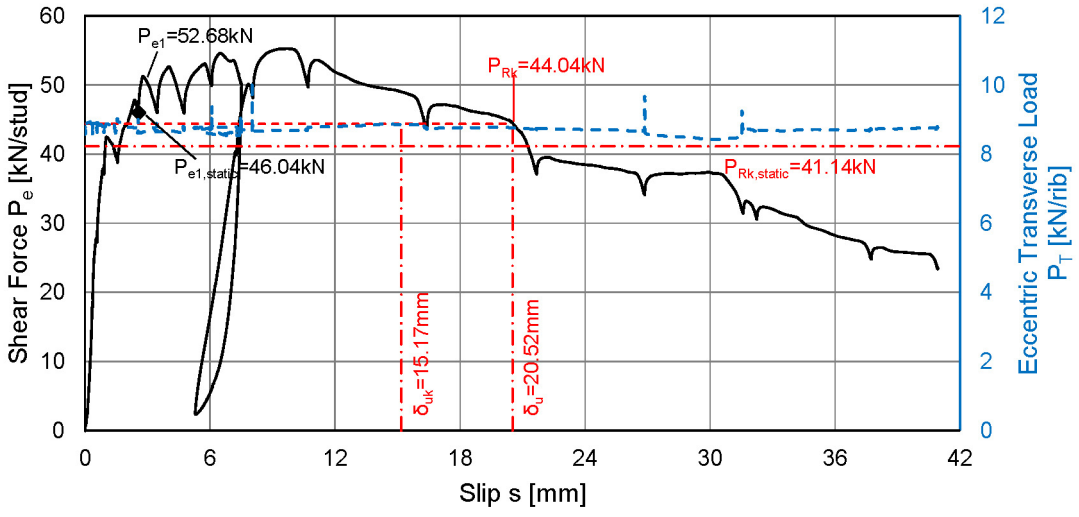

## Specimen 1-11-3

### STEEL PROFILE

| | | | |
|---|---|---|---|
| HEB 260 | $L = 900$mm | $f_y = 424$N/mm$^2$ | $f_u = 525$N/mm$^2$ |

### COMPOSITE DECKING

| | | | |
|---|---|---|---|
| CF80 | $t = 0.90$mm | through deck welded | |
| $h_p = 80$mm | $b_u = 120$mm | $b_o = 155$mm | $a = 300$mm |

### CONCRETE SLABS

| | | | |
|---|---|---|---|
| $B = 900$ mm | $H = 900$ mm | $D = 160$ mm | No recess |
| $f_{cm} = 42.59$ N/mm$^2$ | $E_c = 28000$ N/mm$^2$ | | |

### REINFORCEMENT

| | | |
|---|---|---|
| BSt 500 A | Top: n.a. | Bottom: Q188A |
| | Edge: ∅8/150 | Recess: n.a. |

### SHEAR STUDS

| | | |
|---|---|---|
| 8 Köco SD 19x125 | mid-position | $f_u = 550.7$N/mm$^2$ |

| | | A1-1 | A1-2 | A2-1 | A2-2 | B1-1 | B1-2 | B2-1 | B2-2 | $\mu$ | $\sigma$ |
|---|---|---|---|---|---|---|---|---|---|---|---|
| $d$ | [mm] | 19.05 | 19.05 | 19.15 | 19.10 | 19.05 | 19.05 | 19.10 | 19.05 | 19.08 | 0.038 |
| $h_{sc}$ | [mm] | 117.25 | 118.60 | 120.40 | 119.70 | 117.45 | 117.15 | 119.60 | 118.40 | 118.57 | 1.238 |

### TEST RESULTS

| | | |
|---|---|---|
| $P_{e1} = 49.33$ kN/stud | $P_{e1,static} = 45.71$ kN/stud | $s_{e1} = 3.89$ mm |
| $P_{e2} =$ n.a. | $P_{e2,static} =$ n.a. | $s_{e2} =$ n.a. |
| Rib pry-out | Rotation of bottom rib | |

### LOAD-SLIP CURVE

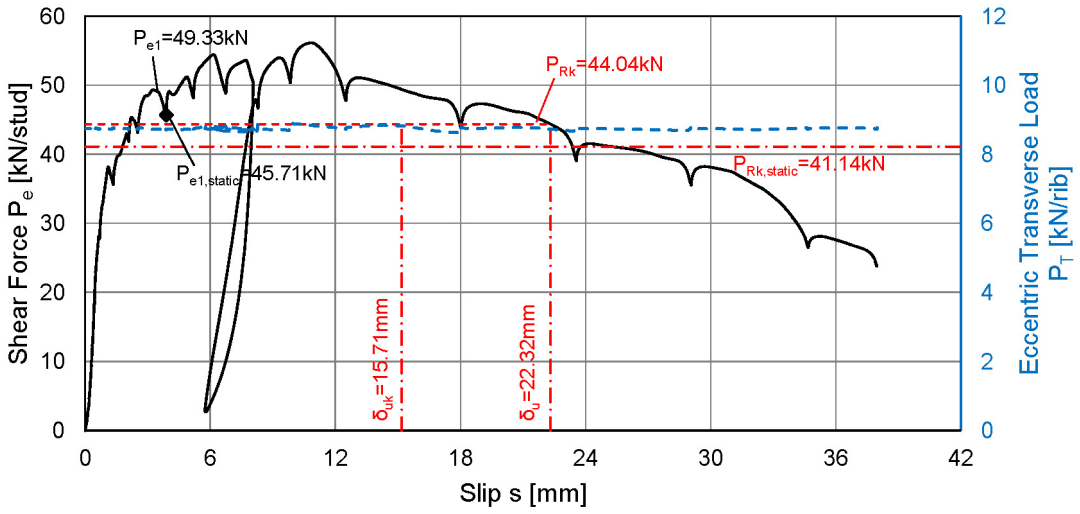

## Specimen 3-01-1

### STEEL PROFILE

| | | | |
|---|---|---|---|
| HEB 260 | $L = 900$mm | $f_y = 424$N/mm$^2$ | $f_u = 525$N/mm$^2$ |

### COMPOSITE DECKING

| | | | |
|---|---|---|---|
| CF80 | $t = 0.90$mm | through deck welded | |
| $h_p = 80$mm | $b_u = 120$mm | $b_o = 155$mm | $a = 300$mm |

### CONCRETE SLABS

| | | | |
|---|---|---|---|
| $B = 900$ mm | $H = 900$ mm | $D = 160$ mm | No recess |
| $f_{cm} = 46.00$ N/mm$^2$ | $E_c = 26900$ N/mm$^2$ | | |

### REINFORCEMENT

| | | |
|---|---|---|
| BSt 500 A | Top: Q335A | Bottom: Q188A |
| | Edge: ∅8/150 | Recess: n.a. |

### SHEAR STUDS

| | | |
|---|---|---|
| 8 Köco SD 19x125 | mid-position | $f_u = 550.7$N/mm$^2$ |

| | | A1-1 | A1-2 | A2-1 | A2-2 | B1-1 | B1-2 | B2-1 | B2-2 | $\mu$ | $\sigma$ |
|---|---|---|---|---|---|---|---|---|---|---|---|
| $d$ | [mm] | 19.07 | 19.04 | 19.05 | 19.05 | 19.07 | 19.08 | 19.07 | 19.09 | 19.07 | 0.017 |
| $h_{sc}$ | [mm] | 117.51 | 119.16 | 118.01 | 119.16 | 118.61 | 118.69 | 118.45 | 118.33 | 118.49 | 0.557 |

### TEST RESULTS

| | | |
|---|---|---|
| $P_{e1} = 47.31$ kN/stud | $P_{e1,static} = 38.86$ kN/stud | $s_{e1} = 1.95$ mm |
| $P_{e2} =$ n.a. | $P_{e2,static} =$ n.a. | $s_{e2} =$ n.a. |
| Rib pry-out | Rotation of bottom rib | |

### LOAD-SLIP CURVE

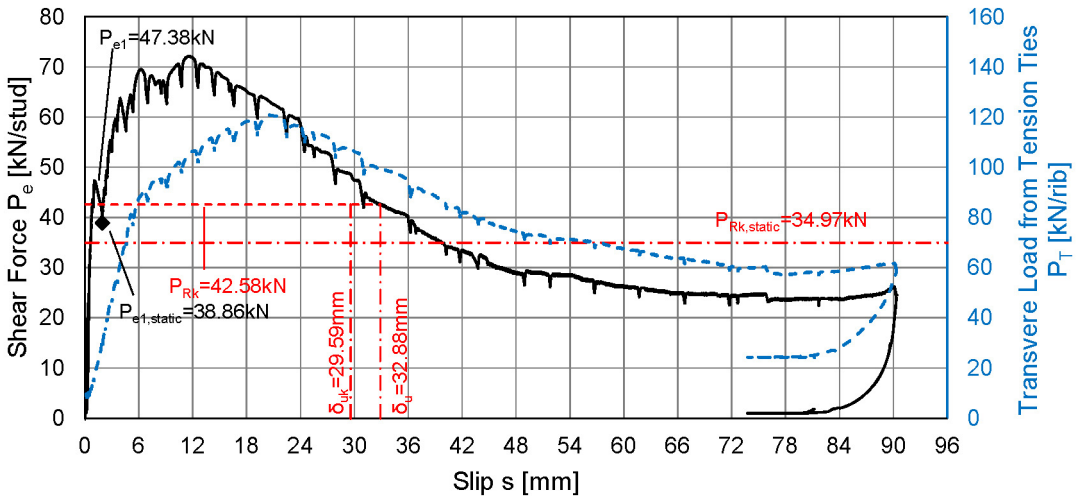

## TENSION TIES

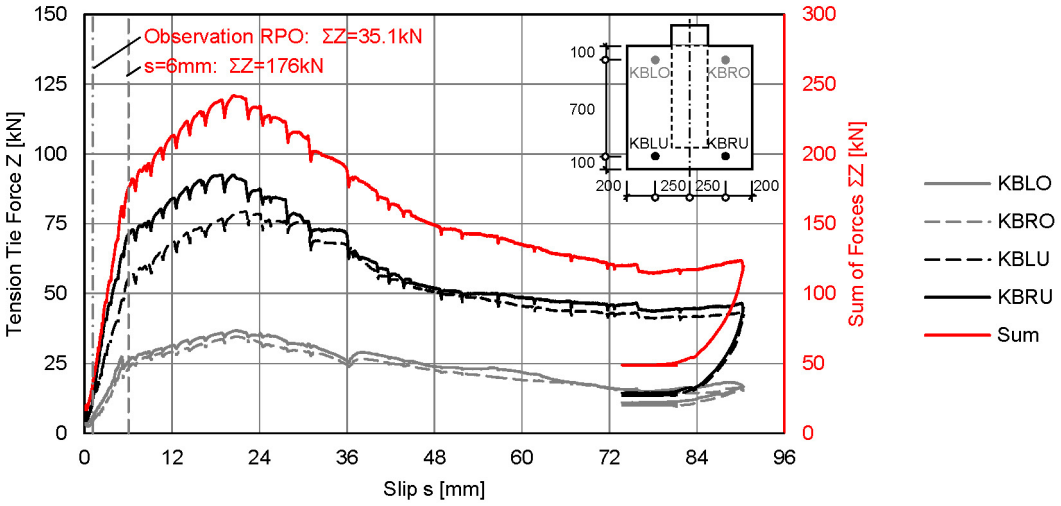

## Specimen 3-01-2

### STEEL PROFILE

HEB 260 | $L = 900$mm | $f_y = 424$N/mm$^2$ | $f_u = 525$N/mm$^2$

### COMPOSITE DECKING

CF80 | $t = 0.90$mm | through deck welded
$h_p = 80$mm | $b_u = 120$mm | $b_o = 155$mm | $a = 300$mm

### CONCRETE SLABS

$B = 900$ mm | $H = 900$ mm | $D = 160$ mm | No recess
$f_{cm} = 46.00$ N/mm$^2$ | $E_c = 26800$ N/mm$^2$

### REINFORCEMENT

BSt 500 A | Top: Q335A | Bottom: Q188A
Edge: ∅8/150 | Recess: n.a.

### SHEAR STUDS

8 Köco SD 19x125 | mid-position | $f_u = 550.7$N/mm$^2$

| | | A1-1 | A1-2 | A2-1 | A2-2 | B1-1 | B1-2 | B2-1 | B2-2 | $\mu$ | $\sigma$ |
|---|---|---|---|---|---|---|---|---|---|---|---|
| $d$ | [mm] | 19.08 | 19.04 | 19.06 | 19.06 | 19.07 | 19.04 | 19.05 | 19.06 | 19.06 | 0.014 |
| $h_{sc}$ | [mm] | 116.43 | 117.45 | 117.14 | 117.71 | 117.29 | 117.41 | 117.77 | 117.84 | 117.38 | 0.455 |

### TEST RESULTS

$P_{e1} = 54.92$ kN/stud | $P_{e1,static} = 51.66$ kN/stud | $s_{e1} = 2.21$ mm
$P_{e2} =$ n.a. | $P_{e2,static} =$ n.a. | $s_{e2} =$ n.a.
Rib pry-out

### LOAD-SLIP CURVE

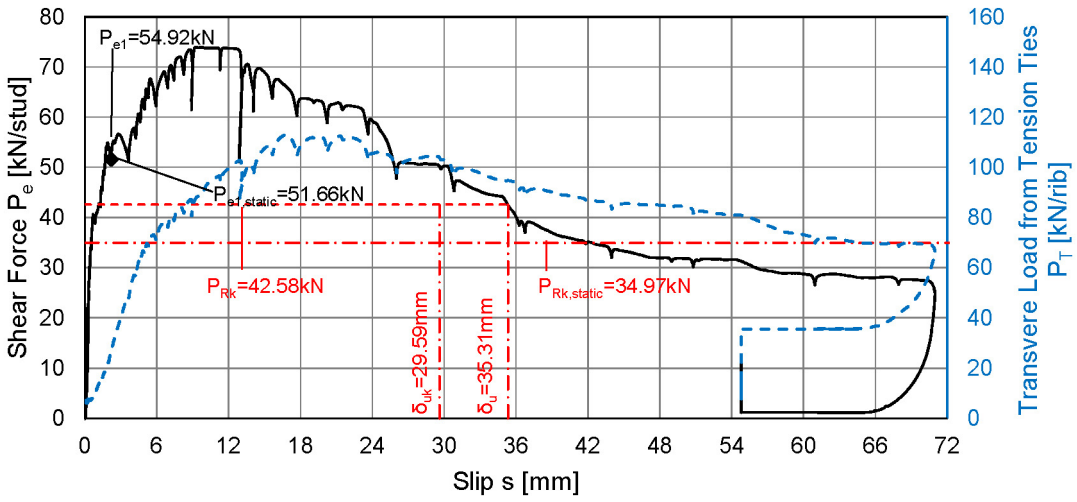

## TENSION TIES

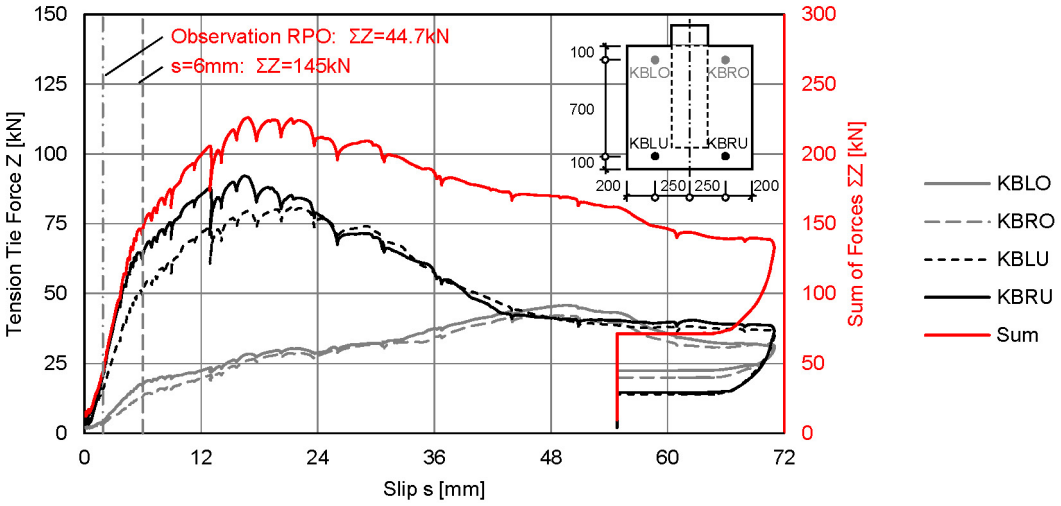

## Specimen 3-01-3

### STEEL PROFILE

HEB 260 $L = 900$mm $f_y = 424$N/mm$^2$ $f_u = 525$N/mm$^2$

### COMPOSITE DECKING

CF80 $t = 0.90$mm through deck welded
$h_p = 80$mm $b_u = 120$mm $b_o = 155$mm $a = 300$mm

### CONCRETE SLABS

$B = 900$ mm $H = 900$ mm $D = 160$ mm No recess
$f_{cm} = 40.43$ N/mm$^2$ $E_c = 26900$ N/mm$^2$

### REINFORCEMENT

BSt 500 A Top: Q335A Bottom: Q188A
Edge: ∅8/150 Recess: n.a.

### SHEAR STUDS

8 Köco SD 19x125 mid-position $f_u = 550.7$N/mm$^2$

| | | A1-1 | A1-2 | A2-1 | A2-2 | B1-1 | B1-2 | B2-1 | B2-2 | $\mu$ | $\sigma$ |
|---|---|---|---|---|---|---|---|---|---|---|---|
| $d$ | [mm] | 19.09 | 19.05 | 19.07 | 19.08 | 19.05 | 19.06 | 19.05 | 19.05 | 19.07 | 0.014 |
| $h_{sc}$ | [mm] | 118.32 | 110.62 | 119.61 | 118.71 | 116.44 | 117.52 | 116.70 | 118.75 | 118.33 | 1.419 |

### TEST RESULTS

$P_{e1} = 52.78$ kN/stud $P_{e1,static} = 47.32$ kN/stud $s_{e1} = 1.54$ mm
$P_{e2} =$ n.a. $P_{e2,static} =$ n.a. $s_{e2} =$ n.a.
Rib pry-out

### LOAD-SLIP CURVE

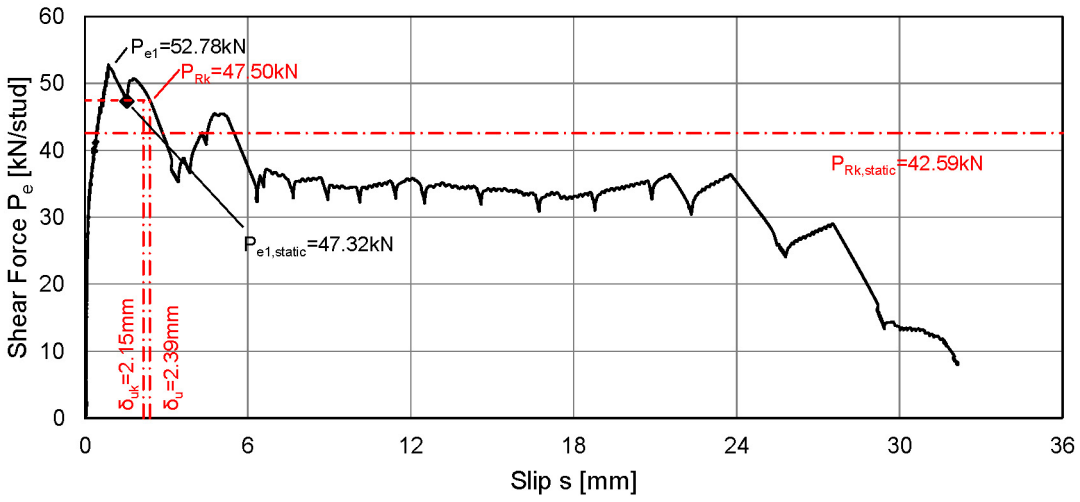

## Specimen 3-02

### STEEL PROFILE

HEB 260 $L = 900$mm $f_y = 424$N/mm$^2$ $f_u = 525$N/mm$^2$

### COMPOSITE DECKING

CF80 $t = 0.90$mm pre-punched
$h_p = 80$mm $b_u = 120$mm $b_o = 155$mm $a = 300$mm

### CONCRETE SLABS

$B = 900$ mm $H = 900$ mm $D = 160$ mm No recess
$f_{cm} = 42.62$ N/mm$^2$ $E_c = 28000$ N/mm$^2$

### REINFORCEMENT

BSt 500 A Top: Q335A Bottom: Q188A
Edge: ∅8/150 Recess: n.a.

### SHEAR STUDS

8 Köco SD 19x125 mid-position $f_u = 550.7$N/mm$^2$

| | | A1-1 | A1-2 | A2-1 | A2-2 | B1-1 | B1-2 | B2-1 | B2-2 | $\mu$ | $\sigma$ |
|---|---|---|---|---|---|---|---|---|---|---|---|
| $d$ | [mm] | 19.11 | 19.11 | 19.05 | 19.11 | 19.05 | 19.10 | 19.05 | 19.10 | 19.09 | 0.029 |
| $h_{sc}$ | [mm] | 123.05 | 123.40 | 123.75 | 123.30 | 123.50 | 123.40 | 123.50 | 123.60 | 123.44 | 0.208 |

### TEST RESULTS

$P_{e1} = 37.00$ kN/stud $P_{e1,static} = 34.90$ kN/stud $s_{e1} = 1.12$ mm
Rib pry-out

### LOAD-SLIP CURVE

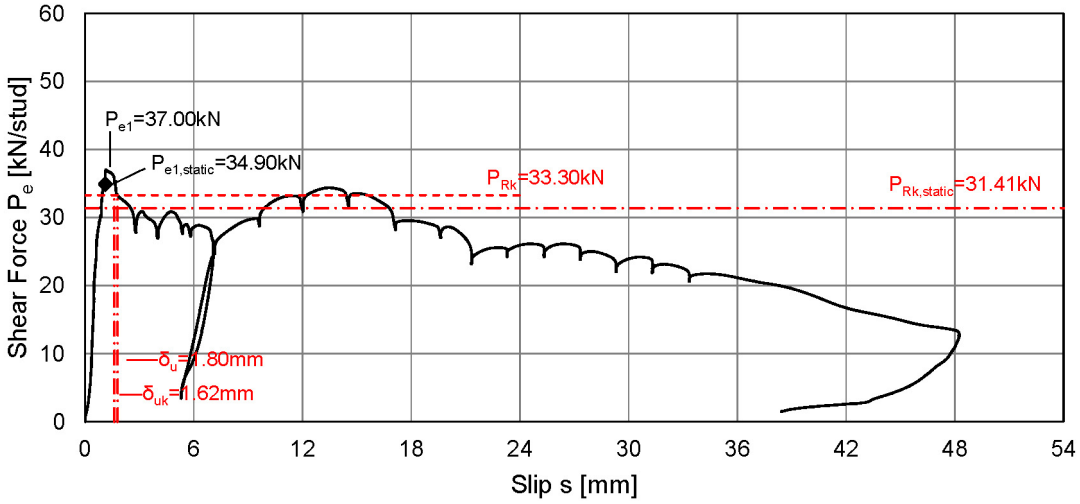

## Specimen NR1-1

### STEEL PROFILE

HEB 260 $L = 900$mm $f_y = 424$N/mm$^2$ $f_u = 525$N/mm$^2$

### COMPOSITE DECKING

CF80 $t = 0.90$mm through deck welded
$h_p = 80$mm $b_u = 120$mm $b_o = 155$mm $a = 300$mm

### CONCRETE SLABS

$B = 900$ mm $H = 900$ mm $D = 150$ mm No recess
$f_{cm} = 44.11$ N/mm$^2$ $E_c = 25600$ N/mm$^2$

### REINFORCEMENT

BSt 500 A Top: n.a. Bottom: Q188A
Edge: ∅8/150 Recess: n.a.

### SHEAR STUDS

4 Köco SD 19x125 mid-position $f_u = 550.7$N/mm$^2$

| | | A1 | A2 | B1 | B2 | $\mu$ | $\sigma$ |
|---|---|---|---|---|---|---|---|
| $d$ | [mm] | 19.10 | 19.10 | 19.05 | 19.10 | 19.09 | 0.025 |
| $h_{sc}$ | [mm] | 120.75 | 120.50 | 121.40 | 122.60 | 121.31 | 0.938 |

### TEST RESULTS

$P_{e1} = 79.07$ kN/stud $P_{e1,static} = 71.84$ kN/stud $s_{e1} = 2.07$ mm
Rib pry-out Stud failure

### LOAD-SLIP CURVE

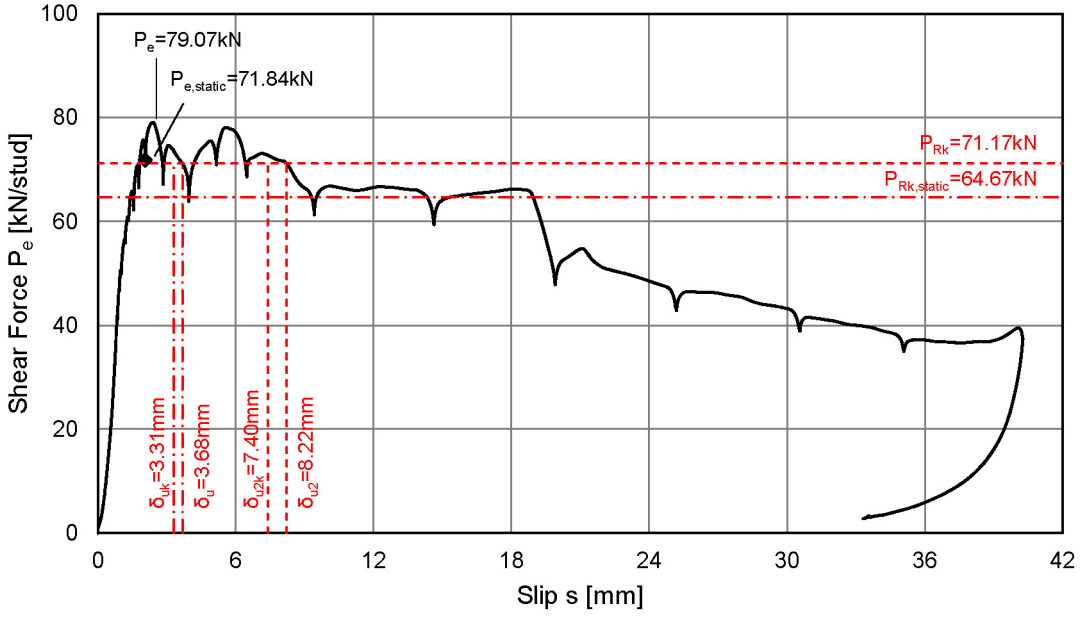

## Specimen NR1-2

### STEEL PROFILE

HEB 260 | $L = 900$mm | $f_y = 424$N/mm$^2$ | $f_u = 525$N/mm$^2$

### COMPOSITE DECKING

CF80 | $t = 0.90$mm | through deck welded
$h_p = 80$mm | $b_u = 120$mm | $b_o = 155$mm | $a = 300$mm

### CONCRETE SLABS

$B = 900$ mm | $H = 900$ mm | $D = 150$ mm | No recess
$f_{cm} = 45.70$ N/mm$^2$ | $E_c = 25600$ N/mm$^2$

### REINFORCEMENT

BSt 500 A | Top: n.a. | Bottom: Q188A
Edge: ∅8/150 | Recess: n.a.

### SHEAR STUDS

4 Köco SD 19x125 | mid-position | $f_u = 550.7$N/mm$^2$

| | | A1 | A2 | B1 | B2 | $\mu$ | $\sigma$ |
|---|---|---|---|---|---|---|---|
| $d$ | [mm] | 19.15 | 19.10 | 19.05 | 19.05 | 19.09 | 0.048 |
| $h_{sc}$ | [mm] | 122.15 | 121.70 | 120.25 | 120.60 | 121.18 | 0.897 |

### TEST RESULTS

$P_{e1} = 74.93$ kN/stud | $P_{e1,static} = 67.93$ kN/stud | $s_{e1} = 2.48$ mm
Rib pry-out | Stud failure

### LOAD-SLIP CURVE

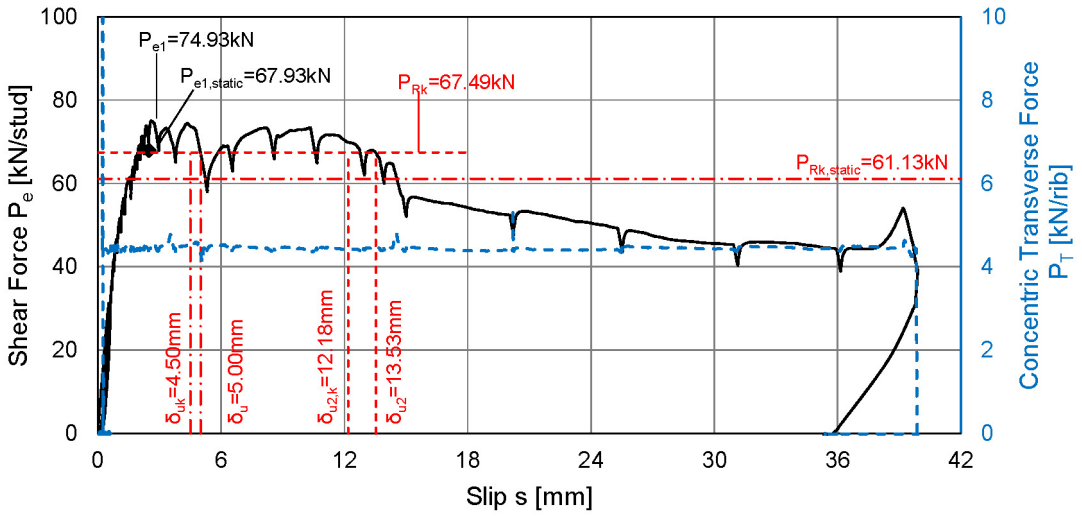

## Specimen NR1-3

### STEEL PROFILE

| | | | |
|---|---|---|---|
| HEB 260 | $L = 900$mm | $f_y = 424$N/mm$^2$ | $f_u = 525$N/mm$^2$ |

### COMPOSITE DECKING

| | | | |
|---|---|---|---|
| CF80 | $t = 0.90$mm | through deck welded | |
| $h_p = 80$mm | $b_u = 120$mm | $b_o = 155$mm | $a = 300$mm |

### CONCRETE SLABS

| | | | |
|---|---|---|---|
| $B = 900$ mm | $H = 900$ mm | $D = 150$ mm | No recess |
| $f_{cm} = 44.70$ N/mm$^2$ | $E_c = 25600$ N/mm$^2$ | | |

### REINFORCEMENT

| | | |
|---|---|---|
| BSt 500 A | Top: n.a. | Bottom: Q188A |
| | Edge: ∅8/150 | Recess: n.a. |

### SHEAR STUDS

| | | |
|---|---|---|
| 4 Köco SD 19x125 | mid-position | $f_u = 550.7$N/mm$^2$ |

| | | A1 | A2 | B1 | B2 | $\mu$ | $\sigma$ |
|---|---|---|---|---|---|---|---|
| $d$ | [mm] | 19.10 | 19.05 | 19.20 | 19.05 | 19.10 | 0.071 |
| $h_{sc}$ | [mm] | 120.20 | 120.40 | 121.55 | 121.80 | 120.99 | 0.805 |

### TEST RESULTS

| | | |
|---|---|---|
| $P_{e1} = 70.46$ kN/stud | $P_{e1,static} = 64.87$ kN/stud | $s_{e1} = 2.66$ mm |
| Rib pry-out | Stud failure | |

### LOAD-SLIP CURVE

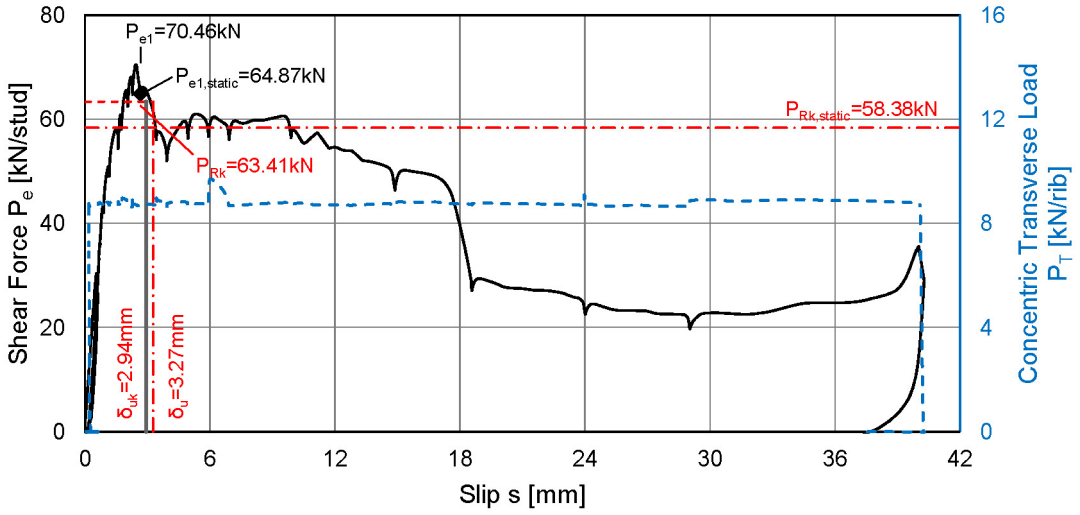

# D Failure surface for open deck shapes

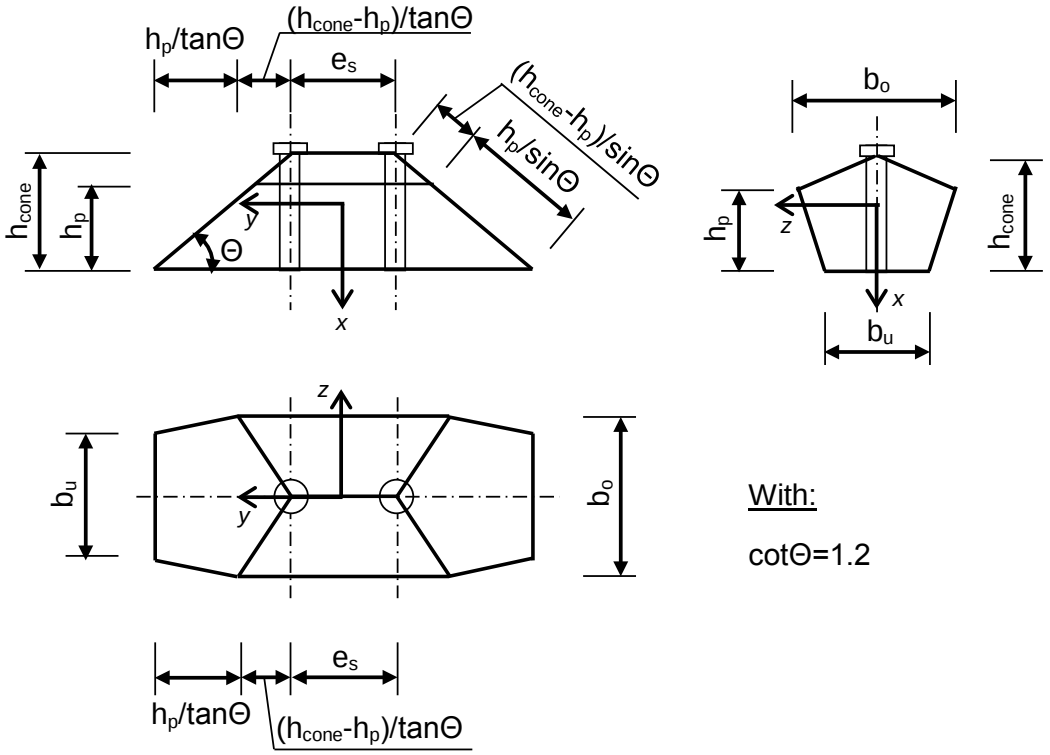


Figure D.1: Shape and dimensions of the failure cone for studs welded in mid and staggert position in open deck shapes.

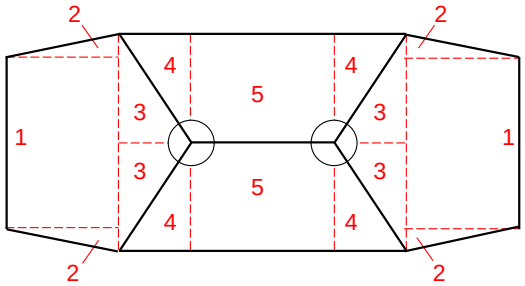


Figure D.2: Divison of the failure cone into sub-faces for the calculation of cross-section properties.

Height of the cone:

$$h_{cone} = h_{sc,nom} - 5 - h_{head} \tag{D.1}$$

Surface of the failure cone:

$$A_{cone} = \sum_{i=1}^{5} A_i \tag{D.2}$$

with:

$$\sum A_1 = 2 \cdot \frac{b_u \cdot h_p}{\sin\Theta}$$

$$\sum A_2 = 4 \cdot \frac{1}{2} \cdot \frac{\frac{b_o - b_u}{2} \cdot h_p}{\sin\Theta} = \frac{(b_o - b_u) \cdot h_p}{\sin\Theta}$$

$$\sum A_3 = 4 \cdot \frac{1}{2} \cdot \frac{\frac{b_o}{2} \cdot (h_{cone} - h_p)}{\sin\Theta} = \frac{b_0 \cdot (h_{cone} - h_p)}{\sin\Theta}$$

$$\sum A_4 = 4 \cdot \frac{1}{2} \cdot \frac{\sqrt{(h_{cone} - h_p)^2 + \left(\frac{b_o}{2}\right)^2} \cdot (h_{cone} - h_p)}{\tan\Theta}$$

$$= 2 \cdot \frac{\sqrt{(h_{cone} - h_p)^2 + \left(\frac{b_o}{2}\right)^2} \cdot (h_{cone} - h_p)}{\tan\Theta}$$

$$\sum A_5 = 2 \cdot (n_r - 1) \cdot e_s \cdot \sqrt{(h_{cone} - h_p)^2 + \left(\frac{b_o}{2}\right)^2}$$

Height of the centre of mass above the flange:

$$h_{s,cone} = \frac{\sum_{i=1}^{5} A_i h_{s,i}}{\sum_{i=1}^{5} A_i} \tag{D.3}$$

with:

$$h_{s,1} = \frac{h_p}{2}$$

$$h_{s,2} = \frac{2}{3} \cdot h_p$$

$$h_{s,3} = h_p + \frac{1}{3} \cdot (h_{cone} - h_p) = \frac{2h_p + h_{cone}}{3}$$

$$h_{s,4} = h_{s,3} = \frac{2h_p + h_{cone}}{3}$$

$$h_{s,5} = h_p + \frac{h_{cone} - h_p}{2} = \frac{h_p + h_{cone}}{2}$$

Moment of Inertia for the cone:

$$I_y = \sum_{i=1}^{5} I_i + \sum_{i=1}^{5} A_i z_i^2 \tag{D.4}$$

with:

$$\sum I_1 = 2 \cdot \frac{b_u^3 \cdot h_p}{12 \sin \Theta} = \frac{b_u^3 \cdot h_p}{6 \cdot \sin \Theta}$$

$$\sum I_2 = 4 \cdot \frac{\left(\frac{b_o - b_u}{2}\right)^3 \cdot h_p}{36 \cdot \sin \Theta} = \frac{(b_o - b_u)^3 \cdot h_p}{72 \cdot \sin \Theta}$$

$$\sum I_3 = 4 \cdot \frac{\left(\frac{b_o}{2}\right)^3 \cdot (h_{cone} - h_p)}{36 \cdot \sin \Theta} = \frac{b_o^3 \cdot (h_{cone} - h_p)}{72 \cdot \sin \Theta}$$

$$\sum I_4 = 4 \cdot \frac{\left((h_{cone} - h_p)^2 + \left(\frac{b_o}{2}\right)^2\right)^{3/2} \cdot (h_{cone} - h_p)}{36 \cdot \tan \Theta}$$

$$= \frac{\left((h_{cone} - h_p)^2 + \left(\frac{b_o}{2}\right)^2\right)^{3/2} \cdot (h_{cone} - h_p)}{9 \cdot \tan \Theta}$$

$$\sum I_5 = 2 \cdot \frac{\left((h_{cone} - h_p)^2 + \left(\frac{b_o}{2}\right)^2\right)^{3/2} \cdot e_s \cdot (n_r - 1)}{12}$$

$$= \frac{\left((h_{cone} - h_p)^2 + \left(\frac{b_o}{2}\right)^2\right)^{3/2} \cdot e_s \cdot (n_r - 1)}{6}$$

and:

$$z_1 = 0$$

$$z_2 = \frac{b_u}{2} + \frac{1}{3} \cdot \frac{b_o - b_u}{2} = \frac{2b_u + b_o}{6}$$

$$z_3 = \frac{1}{3} \cdot \frac{b_o}{2} = \frac{b_o}{6}$$

$$z_4 = \frac{2}{3} \cdot \frac{b_o}{2} = \frac{b_o}{3}$$

$$z_5 = \frac{1}{2} \cdot \frac{b_o}{2} = \frac{b_o}{4}$$

# E Failure surface for re-entrant deck shapes

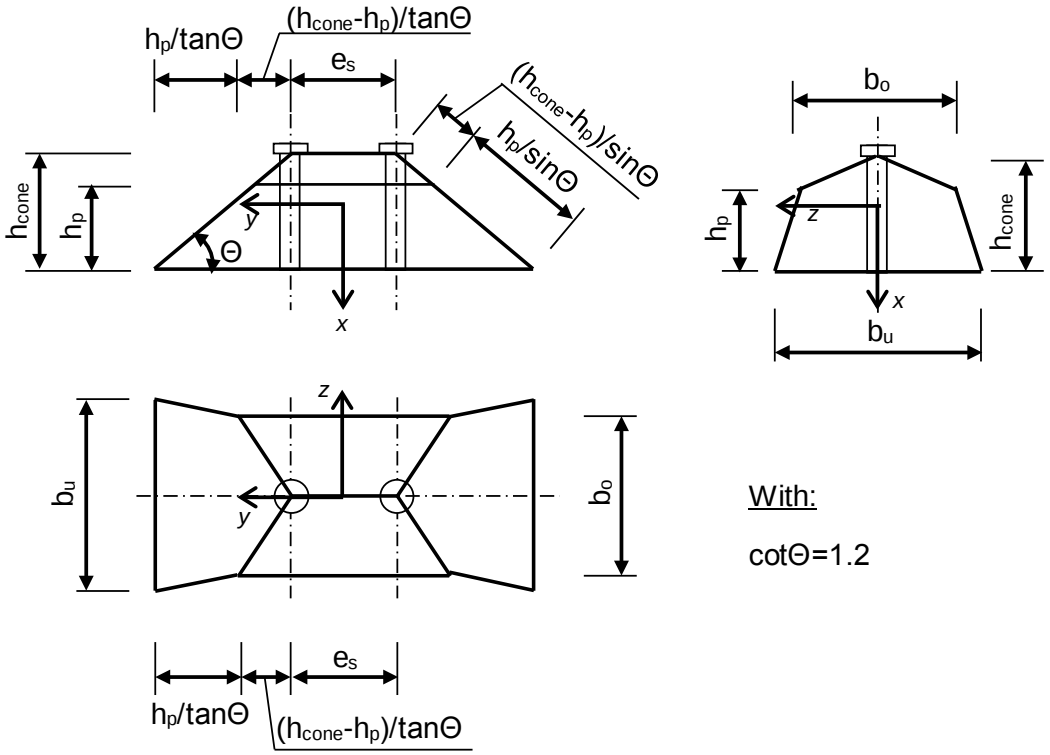


Figure E.1: Shape and dimensions of the failure cone for studs welded in mid and staggert position in re-entrant decking.

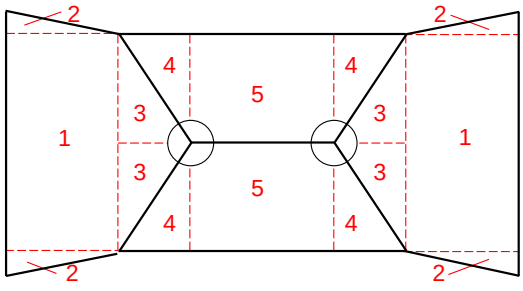


Figure E.2: Division of the failure cone into sub-faces for the calculation of cross-section properties.

Height of the cone:

$$h_{cone} = h_{sc,nom} - 5 - h_{head} \tag{E.1}$$

Surface of the failure cone:

$$A_{cone} = \sum_{i=1}^{5} A_i \tag{E.2}$$

with:

$$\sum A_1 = 2 \cdot \frac{b_o \cdot h_p}{\sin\Theta}$$

$$\sum A_2 = 4 \cdot \frac{1}{2} \cdot \frac{\frac{b_u - b_o}{2} \cdot h_p}{\sin\Theta} = \frac{(b_o - b_u) \cdot h_p}{\sin\Theta}$$

$$\sum A_3 = 4 \cdot \frac{1}{2} \cdot \frac{\frac{b_o}{2} \cdot (h_{cone} - h_p)}{\sin\Theta} = \frac{b_0 \cdot (h_{cone} - h_p)}{\sin\Theta}$$

$$\sum A_4 = 4 \cdot \frac{1}{2} \cdot \frac{\sqrt{(h_{cone} - h_p)^2 + \left(\frac{b_o}{2}\right)^2} \cdot (h_{cone} - h_p)}{\tan\Theta}$$

$$= 2 \cdot \frac{\sqrt{(h_{cone} - h_p)^2 + \left(\frac{b_o}{2}\right)^2} \cdot (h_{cone} - h_p)}{\tan\Theta}$$

$$\sum A_5 = 2 \cdot (n_r - 1) \cdot e_s \cdot \sqrt{(h_{cone} - h_p)^2 + \left(\frac{b_o}{2}\right)^2}$$

Height of the centre of mass above the flange:

$$h_{s,cone} = \frac{\sum_{i=1}^{5} A_i h_{s,i}}{\sum_{i=1}^{5} A_i} \tag{E.3}$$

with:

$$h_{s,1} = \frac{h_p}{2}$$

$$h_{s,2} = \frac{2}{3} \cdot h_p$$

$$h_{s,3} = h_p + \frac{1}{3} \cdot (h_{cone} - h_p) = \frac{2h_p + h_{cone}}{3}$$

$$h_{s,4} = h_{s,3} = \frac{2h_p + h_{cone}}{3}$$

$$h_{s,5} = h_p + \frac{h_{cone} - h_p}{2} = \frac{h_p + h_{cone}}{2}$$

Moment of Inertia for the cone:

$$I_y = \sum_{i=1}^{5} I_i + \sum_{i=1}^{5} A_i z_i^2 \tag{E.4}$$

with:

$$\sum I_1 = 2 \cdot \frac{b_o^3 \cdot h_p}{12 \sin \Theta} = \frac{b_u^3 \cdot h_p}{6 \cdot \sin \Theta}$$

$$\sum I_2 = 4 \cdot \frac{\left(\frac{b_u - b_o}{2}\right)^3 \cdot h_p}{36 \cdot \sin \Theta} = \frac{(b_u - b_o)^3 \cdot h_p}{72 \cdot \sin \Theta}$$

$$\sum I_3 = 4 \cdot \frac{\left(\frac{b_o}{2}\right)^3 \cdot (h_{cone} - h_p)}{36 \cdot \sin \Theta} = \frac{b_o^3 \cdot (h_{cone} - h_p)}{72 \cdot \sin \Theta}$$

$$\sum I_4 = 4 \cdot \frac{\left((h_{cone} - h_p)^2 + \left(\frac{b_o}{2}\right)^2\right)^{3/2} \cdot (h_{cone} - h_p)}{36 \cdot \tan \Theta}$$

$$= \frac{\left((h_{cone} - h_p)^2 + \left(\frac{b_o}{2}\right)^2\right)^{3/2} \cdot (h_{cone} - h_p)}{9 \cdot \tan \Theta}$$

$$\sum I_5 = 2 \cdot \frac{\left((h_{cone} - h_p)^2 + \left(\frac{b_o}{2}\right)^2\right)^{3/2} \cdot e_s \cdot (n_r - 1)}{12}$$

$$= \frac{\left((h_{cone} - h_p)^2 + \left(\frac{b_o}{2}\right)^2\right)^{3/2} \cdot e_s \cdot (n_r - 1)}{6}$$

and:

$$z_1 = 0$$

$$z_2 = \frac{b_u}{2} + \frac{1}{3} \cdot \frac{b_u - b_o}{2} = \frac{2b_o + b_u}{6}$$

$$z_3 = \frac{1}{3} \cdot \frac{b_o}{2} = \frac{b_o}{6}$$

$$z_4 = \frac{2}{3} \cdot \frac{b_o}{2} = \frac{b_o}{3}$$

$$z_5 = \frac{1}{2} \cdot \frac{b_o}{2} = \frac{b_o}{4}$$

# F Partial derivatives of the resistance functions

Rib bending failure:

$$r_{t,1} = \left[\left(f_{ctm} + \frac{N_q + N_{sc}}{A}\right) \cdot \frac{2 \cdot I_y}{b_o} + N_{sc} \cdot e_L\right] \cdot \frac{1}{h_p \cdot n_r} + \frac{n_y \cdot M_{pl}}{h_s - 0.5d} \tag{F.1}$$

Partial derivatives:

$$\frac{\partial r_{t,1}}{\partial f_{ck}} = \frac{\alpha_{ct} \cdot [2.4 \cdot h_{sc} + (n_r - 1) \cdot e_s] \cdot b_{max}^3}{30 \cdot f_{ck}^{1/3} \cdot b_o \cdot h_p \cdot n_r} \tag{F.2}$$

$$\frac{\partial r_{t,1}}{\partial f_u} = \frac{\pi \cdot d^2 \cdot b_{max}^2}{240 \cdot b_o \cdot h_p} + \frac{\pi \cdot d^2 \cdot e_L}{40 \cdot h_p} + \frac{n_y \cdot d^3}{6 \cdot (h_s - d/2)} \tag{F.3}$$

$$\frac{\partial r_{t,1}}{\partial d} = \frac{f_u \cdot \pi \cdot b_{max}^2}{120 \cdot b_o \cdot h_p} + \frac{f_u \cdot \pi \cdot d \cdot e_l}{20 \cdot h_p} + \frac{n_y \cdot f_u \cdot d^2}{2 \cdot (h_s - d/2)} + \frac{n_y \cdot f_u \cdot d^3}{12 \cdot (h_s - d/2)^2} \tag{F.4}$$

$$\begin{aligned}\frac{\partial r_{t,1}}{\partial h_{sc}} = {} & \frac{3}{25} \cdot \frac{\alpha_{ct} \cdot f_{ck}^{2/3} \cdot b_{max}^3}{b_o \cdot h_p \cdot n_r} \\ & - \frac{n_y \cdot f_u \cdot d^3}{6 \cdot (h_s - d/2)^2} \cdot \frac{\beta + \dfrac{(n_r - 1) \cdot e_s}{4.8 \cdot h_{sc}} - \dfrac{(n_r - 1) \cdot e_s (h_p + h_{sc})}{4.8 \cdot h_{sc}^2}}{1 + \dfrac{(n_r - 1) \cdot e_s}{2.4 \cdot h_{sc}}} \\ & - \frac{n_y \cdot f_u \cdot d^3}{6 \cdot (h_s - d/2)^2} \cdot \frac{\left(\beta \cdot h_{sc} + \dfrac{(n_r - 1) \cdot e_s \cdot (h_p + h_{sc})}{4.8 \cdot h_{sc}}\right) \cdot (n_r - 1) \cdot e_s}{2.4 \cdot \left(1 + \dfrac{(n_r - 1) \cdot e_s}{2.4 \cdot h_{sc}}\right)^2 \cdot h_{sc}^2}\end{aligned} \tag{F.5}$$

$$\begin{aligned}\frac{\partial r_{t,1}}{\partial h_p} = {} & - \frac{\alpha_{ct} \cdot f_{ck}^{2/3} \cdot [2.4 \cdot h_{sc} + (n_r - 1) \cdot e_s] \cdot b_{max}^3}{20 \cdot b_o \cdot h_p^2 \cdot n_r} \\ & - \frac{N_q \cdot b_{max}^2}{6 \cdot b_o \cdot h_p^2 \cdot n_r} - \frac{f_u \cdot \pi \cdot d^2 \cdot b_{max}^2}{240 \cdot b_o \cdot h_p^2} - \frac{f_u \cdot \pi \cdot d^2 \cdot e_L}{40 \cdot h_p^2} \\ & - \frac{5 \cdot n_y \cdot f_u \cdot d^3 \cdot (n_r - 1) \cdot e_s}{144 \cdot \left[(h_s - d/2)^2 \cdot h_{sc} \cdot \left(1 + \dfrac{(n_r - 1) \cdot e_s}{2.4 \cdot h_{sc}}\right)\right]}\end{aligned} \tag{F.6}$$

$$\begin{aligned}\frac{\partial r_{t,1}}{\partial b_o} = {} & - \frac{\alpha_{ct} \cdot f_{ck}^{2/3} \cdot [2.4 \cdot h_{sc} + (n_r - 1) \cdot e_s] \cdot b_{max}^3}{20 \cdot b_o^2 \cdot h_p \cdot n_r} \\ & - \frac{N_q \cdot b_{max}^2}{6 \cdot b_o^2 \cdot h_p \cdot n_r} - \frac{f_u \cdot \pi \cdot d^2 \cdot b_{max}^2}{240 \cdot b_o^2 \cdot h_p}\end{aligned} \tag{F.7}$$

$$\frac{\partial r_{t,1}}{\partial b_{max}} = \frac{3 \cdot \alpha_{ct} \cdot f_{ck}^{2/3} \cdot [2.4 \cdot h_{sc} + (n_r - 1) \cdot e_s] \cdot b_{max}^2}{20 \cdot b_o \cdot h_p \cdot n_r} + \frac{N_q \cdot b_{max}}{3 \cdot b_o \cdot h_p \cdot n_r} + \frac{f_u \cdot \pi \cdot d^2 \cdot b_{max}}{120 \cdot b_o \cdot h_p} \tag{F.8}$$

$$\frac{\partial r_{t,1}}{\partial e_L} = \frac{f_u \cdot \pi \cdot d^2}{40 \cdot h_p} \tag{F.9}$$

$$\frac{\partial r_{t,1}}{\partial e_s} = \frac{\alpha_{ct} \cdot f_{ck}^{2/3} \cdot (n_r - 1) b_{max}^3}{20 \cdot b_o \cdot h_p \cdot n_r} - \frac{n_y \cdot f_u \cdot d^3}{6 \cdot (h_s - d/2)^2} \cdot \frac{(n_r - 1) \cdot (h_p + h_{sc})}{4.8 \cdot h_{sc} \left(1 + \frac{(n_r - 1) \cdot e_s}{2.4 \cdot h_{sc}}\right)} + \frac{n_y \cdot f_u \cdot d^3}{6 \cdot (h_s - d/2)^2} \cdot \frac{\beta \cdot h_{sc} + \frac{(n_r - 1) \cdot e_s \cdot (h_p + h_{sc})}{4.8 \cdot h_{sc}} \cdot (n_r - 1)}{2.4 \cdot \left(1 + \frac{(n_r - 1) \cdot e_s}{2.4 \cdot h_{sc}}\right)^2 \cdot h_{sc}} \tag{F.10}$$

Resistance for stud shearing:

$$r_{t,2} = \frac{1}{\sqrt{3}} \cdot f_u \cdot \pi \cdot d^2/4 \tag{F.11}$$

Partial derivatives:

$$\frac{\partial r_{t,2}}{\partial d} = \frac{2}{d} \cdot r_{t,2} \tag{F.12}$$

$$\frac{\partial r_{t,2}}{\partial f_u} = \frac{1}{f_u} \cdot r_{t,2} \tag{F.13}$$